VOL. 547 NOS. 1 + 2 JUNE 28, 1991

RNAL OF CHROMATOGRAPHY

LUDING ELECTROPHORESIS AND OTHER SEPARATION METHODS

ELSEVIER

Scope. The *Journal of Chromatography* publishes papers on all aspects of chromatography, electrophoresis and related methods. Contributions consist mainly of research papers dealing with chromatographic theory, instrumental development and their applications. The section *Biomedical Applications*, which is under separate editorship, deals with the following aspects: developments in and applications of chromatographic and electrophoretic techniques related to clinical diagnosis or alterations during medical treatment; screening and profiling of body fluids or tissues with special reference to metabolic disorders; results from basic medical research with direct consequences in clinical practice; drug level monitoring and pharmacokinetic studies; clinical toxicology; analytical studies in occupational medicine.

Submission of Papers. Manuscripts (in English; *four* copies are required) should be submitted to: Editorial Office of *Journal of Chromatography*, P.O. Box 681, 1000 AR Amsterdam, The Netherlands, Telefax (+31-20) 5862 304, or to: The Editor of *Journal of Chromatography, Biomedical Applications*, P.O. Box 681, 1000 AR Amsterdam, The Netherlands. Review articles are invited or proposed by letter to the Editors. An outline of the proposed review should first be forwarded to the Editors for preliminary discussion prior to preparation. Submission of an article is understood to imply that the article is original and unpublished and is not being considered for publication elsewhere. For copyright regulations, see below.

Publication. The *Journal of Chromatography* (incl. *Biomedical Applications*) has 38 volumes in 1991. The subscription prices for 1991 are:

J. Chromatogr. (incl. *Cum. Indexes, Vols. 501–550*) + *Biomed. Appl.* (Vols. 535–572):
Dfl. 7220.00 plus Dfl. 1140.00 (p.p.h.) (total *ca.* US$ 4519.00)

J. Chromatogr. (incl. *Cum. Indexes, Vols. 501–550*) only (Vols. 535–561):
Dfl. 5859.00 plus Dfl. 810.00 (p.p.h.) (total *ca.* US$ 3604.75)

Biomed. Appl. only (Vols. 562–572):
Dfl. 2387.00 plus Dfl. 330.00 (p.p.h.) (total *ca.* US$ 1468.75).

Subscription Orders. The Dutch guilder price is definitive. The US$ price is subject to exchange-rate fluctuations and is given as a guide. Subscriptions are accepted on a prepaid basis only, unless different terms have been previously agreed upon. Subscriptions orders can be entered only by calender year (Jan.–Dec.) and should be sent to Elsevier Science Publishers, Journal Department, P.O. Box 211, 1000 AE Amsterdam, The Netherlands, Tel. (+31-20) 5803 642, Telefax (+31-20) 5803 598, or to your usual subscription agent. Postage and handling charges include surface delivery except to the following countries where air delivery via SAL (Surface Air Lift) mail is ensured: Argentina, Australia, Brazil, Canada, Hong Kong, India, Israel, Japan*, Malaysia, Mexico, New Zealand, Pakistan, PR CHina, Singapore, South Africa, South Korea, Taiwan, Thailand, USA. * For Japan air delivery (SAL) requires 50% additional charge of the normal postage and handling charge. For all other countries airmail rates are available upon request. Claims for missing issues must be made within three months of our publication (mailing) date, otherwise such claims cannot be honoured free of charge. Back volumes of the *Journal of Chromatography* (Vols. 1–534) are available at Dfl. 208.00 (plus postage). Customers in the USA and Canada wishing information on this and other Elsevier journals, please contact Journal Information Center, Elsevier Science Publishing Co. Inc., 655 Avenue of the Americas, New York, NY 10010, USA, Tel. (+1-212) 633 3750, Telefax (+1-212) 633 3990.

Abstracts/Contents Lists published in Analytical Abstracts, Biochemical Abstracts, Biological Abstracts, Chemical Abstracts, Chemical Titles, Chromatography Abstracts, Clinical Chemistry Lookout, Current Contents/Life Sciences, Current Contents/Physical, Chemical & Earth Sciences, Deep-Sea Research/Part B: Oceanographic Literature Review, Excerpta Medica, Index Medicus, Mass Spectrometry Bulletin, PASCAL-CNRS, Pharmaceutical Abstracts, Referativnyi Zhurnal, Research Alert, Science Citation Index and Trends in Biotechnology.

See inside back cover for Publication Schedule, Information for Authors and information on Advertisements.

0021-9673/91/$03.50

Printed in The Netherlands

CONTENTS

(*Abstracts/Contents Lists published in Analytical Abstracts, Biochemical Abstracts, Biological Abstracts, Chemical Abstracts, Chemical Titles, Chromatography Abstracts, Current Contents/Life Sciences, Current Contents/Physical, Chemical & Earth Sciences, Deep-Sea Research/Part B: Oceanographic Literature Review, Excerpta Medica, Index Medicus, Mass Spectrometry Bulletin, PASCAL-CNRS, Referativnyi Zhurnal, Research Alert and Science Citation Index*)

REGULAR PAPERS

Column Liquid Chromatography

Gas Chromatography

(Continued overleaf)

(Continued overleaf)

Contents (continued)

In articles with more than one author, the name of the author to whom correspondence should be addressed is indicated in the article heading by a 6-pointed asterisk (*)

FOR ADVERTISING INFORMATION PLEASE CONTACT OUR ADVERTISING REPRESENTATIVES

USA/CANADA

Weston Media Associates

Mr. Daniel S. Lipner
P.O. Box 1110, GREENS FARMS, CT 06436-1110
Tel: (203) 261-2500, Fax: (203) 261-0101

GREAT BRITAIN

T.G. Scott & Son Ltd.

Tim Blake
Portland House, 21 Narborough Road
COSBY, Leicestershire LE9 5TA
Tel: (0533) 753-333, Fax: (0533) 750-522

Mr. M. White or Mrs. A. Curtis
30-32 Southampton Street, LONDON WC2E 7HR
Tel: (071) 240 2032, Fax: (071) 379 7155,
Telex: 299181 adsale/g

JAPAN

ESP - Tokyo Branch

Mr. S. Onoda
20-12 Yushima, 3 chome, Bunkyo-Ku
TOKYO 113
Tel: (03) 3836 0810, Fax: (03) 3839-4344
Telex: 02657617

REST OF WORLD

ELSEVIER SCIENCE PUBLISHERS

Ms. W. van Cattenburch
P.O. Box 211, 1000 AE AMSTERDAM,
The Netherlands
Tel: (20) 515.3220/21/22, Telex: 16479 els vi nl
Fax: (20) 683.3041

JOURNAL OF CHROMATOGRAPHY

VOL. 547 (1991)

JOURNAL of CHROMATOGRAPHY

INCLUDING ELECTROPHORESIS AND OTHER SEPARATION METHODS

ELSEVIER
AMSTERDAM — OXFORD — NEW YORK — TOKYO

J. Chromatogr., Vol. 547 (1991)

0021-9673/91/$03.50

Printed in The Netherlands

Journal of Chromatography, 547 (1991) 1–10
Elsevier Science Publishers B.V., Amsterdam

CHROM. 23 246

Optimization of Nafion-coated electrodes for selective detection in high-performance liquid chromatography

A. J. TÜDŐS, W. J. J. OZINGA and W. Th. KOK*

Laboratory of Analytical Chemistry, University of Amsterdam, Nieuwe Achtergracht 166, 1018 WV Amsterdam (Netherlands)

(First received December 7th, 1990; revised manuscript received February 22nd, 1991)

ABSTRACT

The performance of Nafion-coated electrodes for detection in liquid chromatography was optimized. The effect of the composition of the mobile phase and the film thickness on the selectivity of the detection of catecholamines was investigated. The stability and the response of the coated electrodes were also determined. From the results, general guidelines were formulated for the optimum use of Nafion-coated electrodes in high-performance liquid chromatography. The increase in the selectivity when using the Nafion-coated electrode was demonstrated by analyzing urine samples.

INTRODUCTION

The determination of catecholamines in biological samples has long been a challenge. In the 1970s, the early radioenzymatic assay method [1–4] was gradually replaced with the less laborious high-performance liquid chromatography (HPLC). Among the various detection techniques in HPLC, electrochemical detection became very popular for catecholamine assay owing to its high sensitivity and relatively low cost. Owing to the low concentration of catecholamines in biological samples and the complexity of the matrix, an extra precolumn extraction or clean-up step in the sample preparation is unavoidable [4–7]. However, it has been shown recently that with urine samples precolumn separation can be omitted when the selectivity of the detector is enhanced by modifying the surface of the working electrode [8—10].

Chemically modified electrodes have been at the focus of attention since the early 1970s, when the first electrode surfaces were chemically functionalized [11]. These electrodes, modified with compounds that incorporate electrochemical catalysts, can be used to achieve more sensitive or selective detection owing to the enhanced electron exchange rate [10–12]. Electrodes have also been modified with permselective coatings to achieve protection against high-molecular-weight compounds, or (as in our work) to provide shielding from anions or cations [8–10]. Recent reviews on chemically modified electrodes give a systematic summary of the state of art [11,12]. Modified electrodes for electrochemical detection in flowing streams have also been reviewed recently [13].

0021-9673/91/$03.50

Chemically modified electrodes with permselective, shielding coatings can provide enhanced selectivity and stability in electrochemical detection. Nafion, a polymeric cation exchanger, has proved to be suitable for the preparation of shielded electrodes. Nafion-modified electrodes have been used in various research projects ranging from fundamental studies on transport processes [14–17] through research on the electrocatalytic activity of incorporated particles [18,19] to analytical applications in flowing liquids [20–24]. Nafion coatings on microvoltammetric electrodes have provided sufficient shielding to be able to monitor the concentration of catecholamines *in vivo* [25,26].

Several groups have published results on the detection of catecholamines with Nafion-modified electrodes in flow systems. Matsue *et al.* [20] demonstrated that a detector cell containing indium–tin oxide microelectrode arrays coated with Nafion is suitable for the selective detection of catecholamines. The same group published another paper on catecholamine detection with Nafion-coated glassy carbon electrodes [21].

Wang *et al.* [22] demonstrated the usefulness of Nafion coating on a carbon working electrode for the detection of neurotransmitters in flow streams. A rapid loss of detector activity showed that Nafion did not provide the desired protection. A second, cellulose acetate, film had to be cast on top of the electrode to prevent it from passivation. Ji and Wang [23] found, however, that a single Nafion coating was sufficient to protect an electrode from anions (ascorbic acid) and that the electrode was highly stable even in the presence of bovine serum albumin [23].

Here, we report on the optimization of detection in HPLC using a Nafion-modified glassy carbon electrode. First, the reproducibility of the film preparation and the optimum film thickness were determined. Second, the effect of the composition of the mobile phase was studied; the influence of the methanol concentration on the film stability was clarified, and also the effects of pH and the type and concentration of buffer cations on the selectivity. The response of the coated electrodes was determined from the peak broadening. Finally, the applicability of the electrode under the determined optimum conditions was demonstrated by detecting catecholamines in urine samples.

EXPERIMENTAL

Apparatus and reagents

The HPLC system consisted of a Gilson (Villiers-le-Bel, France) pump, a 150 × 4.6 mm I.D. column packed with 5-μm Hypersil ODS (Shandon Scientific, Astmoor, UK) and an AMOR (Spark Holland, Emmen, Netherlands) detector cell equipped with a glassy carbon working electrode. The detector potential was set at 0.5 V *vs.* an Ag/AgCl reference electrode. Unless stated otherwise, the mobile phase contained $5 \cdot 10^{-3}$ *M* hexanesulphonic acid (HSA), 10^{-4} *M* EDTA and 10% methanol in phosphate buffer (pH 7).

All chemicals were of analytical-reagent grade and were used without further purification. Dopamine · HCl (DA), *dl*-norepinephrine (NE), 3,4-dihydroxyphenylacetic acid (DOPAC) and catechol (C) were obtained from Janssen Chimica (Beerse, Belgium) and *dl*-epinephrine (E) and *dl*-dihydroxyphenylalanine (DOPA) from Sigma (St. Louis, MO, USA). Concentrated stock solutions were stored at 4°C.

Nafion solution was obtained from Aldrich (Brussels, Belgium) (5%, w/w, equivalent weight = 1100); dilutions were prepared in methanol. The concentrations of these solutions were determined by titration with sodium hydroxide.

Urine samples were filtered (0.8-μm AA filter), diluted 1:1 with the mobile phase and 10^{-3} mol l^{-1} of ascorbic acid was added. The mobile phase was buffered with 0.02 mol l^{-1} lithium phosphate.

Preparation of Nafion-coated electrodes

The glassy carbon surface of the working electrode was completely covered with 12.5 μl of the dilute Nafion solution. After about 15 min the methanol had evaporated and the modified electrode was ready for use. The thickness of the film was calculated from the mass of Nafion applied to the electrode. After a day's work the Nafion coating was removed from the electrode by wiping it off with a tissue soaked in methanol.

RESULTS

Film preparation and stability

The reproducibility of the film preparation was assessed by measuring the permeability of several 4-μm films. The permeability of the film towards the tested compounds was calculated by comparing the chromatographic peak heights at coated and at uncoated electrodes, measured under otherwise identical conditions. The permeability (P) is defined as the ratio of the responses at a coated and bare electrode; P ranges from 0 (impermeable film) to 1 (completely permeable film).

The results of the reproducibility measurements are given in Table I for norepinephrine, epinephrine and dopamine. The differences among the individual films are reflected in the permeabilities for all three tested compounds.

Nafion-type shielding films can be considered as a selective resistance to mass transport on the electrode surface, providing especially low resistance against certain compounds and high resistance for others. The resistance of the film against mass transport (R) can be defined as

$$R = (1 - P)/P \tag{1}$$

TABLE I

REPRODUCIBILITY OF FILM PREPARATION

Permeability of 4-μm Nafion films for N, E and DA in 0.2 M potassium phosphate buffer at pH 7.

Film No.	Permeability		
	N	E	DA
1	0.079	0.146	0.198
2	0.094	0.166	0.214
3	0.075	0.134	0.169
4	0.083	0.152	0.181
5	0.070	0.136	0.137
Relative standard deviation (%)	11	9	16

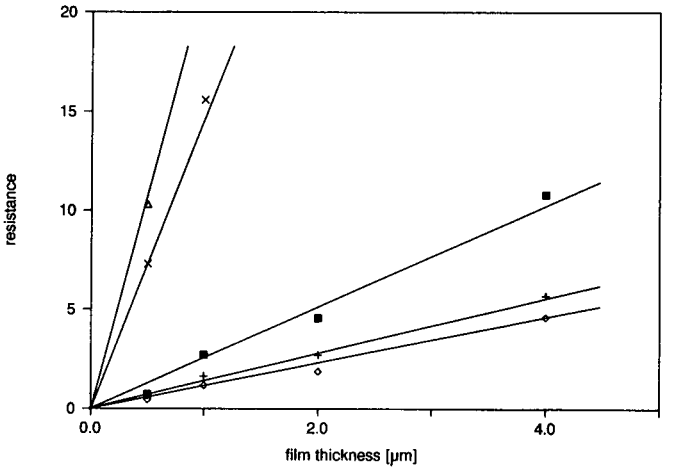

Fig. 1. Effect of the film thickness. Resistance of Nafion films for (■) NE, (+) E, (◇) DA, (△) DOPA and (×) catechol in potassium phosphate buffer at pH 7.

Fig. 1 shows the results of the resistance measurements for NE, E, DA, DOPA and C. The resistance of the Nafion-coated electrode was found to increase linearly with the calculated film thickness. As expected, the slope is low for cationic compounds, indicating a small resistance towards positively charged particles. Neutral and especially anionic species, however, experience higher resistance. The resistance of 4-μm Nafion films was found to be sufficiently low towards the cationic catecholamines (below 10), whereas they provided sufficient shielding towards non-cationic compounds.

Nafion films cast on the electrode do not undergo further chemical reaction (*e.g.*, cross-linking), and remain soluble in alcohol. Therefore, the influence of the methanol content of the mobile phase on the long-term stability of the film was investigated. A 4-μm thick Nafion film was cast on the electrode and the permeability for NE, E and DA was measured immediately after preparation. Then the mobile phase was continuously pumped through the cell, and the permeability was measured again after 2 and 16 h. The decrease in the film thickness was calculated from the increase of the permeability.

The stability of the film was evaluated at four methanol concentrations, ranging from 5% to 30%. As shown in Table II, the film was stable in 5% methanol. When

TABLE II

INFLUENCE OF METHANOL CONTENT OF MOBILE PHASE ON FILM STABILITY

Methanol content (%, v/v)	Loss of film after 2 h (%)	Loss of film after 16 h (%)
5	0	1
10	2	3
20	5	13
30	10	–

using mobile phases of 10–20% methanol content the film thickness should be checked after a few hours' work. Higher methanol contents cannot be applied without considerable loss of the Nafion film.

Influence of pH

The influence of the pH of the mobile phase on the permeability of the Nafion film was studied on acidic, neutral and basic catechols (Fig. 2). In the pH range studied, the permeability of the film for basic catecholamines did not change significantly with the pH (Fig. 2a); DA, E and NE are cationic in this pH range. The permeability for neutral species (catechol in Fig. 2b) shows almost no change with the pH, because their transport in the film is not an ionic process and it is not influenced by the pH.

The pH can be a determining factor, however, in the permeability of the film

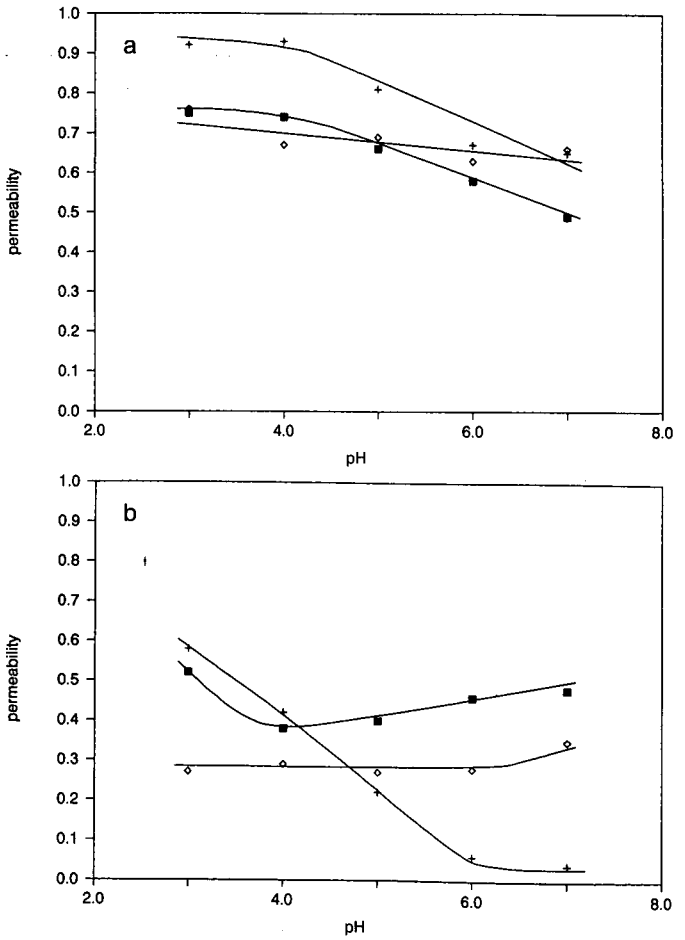

Fig. 2. Effect of the pH on the permeability of the Nafion film. (a) 4-μm Nafion film: (■) NE; (+) E; (◇) DA. (b) 0.2-μm Nafion film: (◇) catechol; (■) DOPA; (+) DOPAC.

towards acidic and zwitterionic analytes. The weak acid DOPAC is transported more rapidly through the film below pH 4, as a neutral molecule, than above pH 5 in its anionic form. The permeability is clearly higher for the amino acid DOPA at pH 3, when it is partly cationic, than at higher pH values, when it is in the zwitterionic form. Hence the detection of DOPA is possible at a Nafion-coated electrode below pH 4. The conclusion from the pH measurement is that a suitable choice of pH is essential if Nafion-coated electrodes are used for electrochemical detection.

Influence of buffer cations

As demonstrated in a previous study [24], the resistance of Nafion films towards cationic analytes is influenced by all cations present in the system. The competitive effect of the buffer cations is determined by two factors: the affinity of the ion exchanger towards the various cations and the cation concentration in the solution.

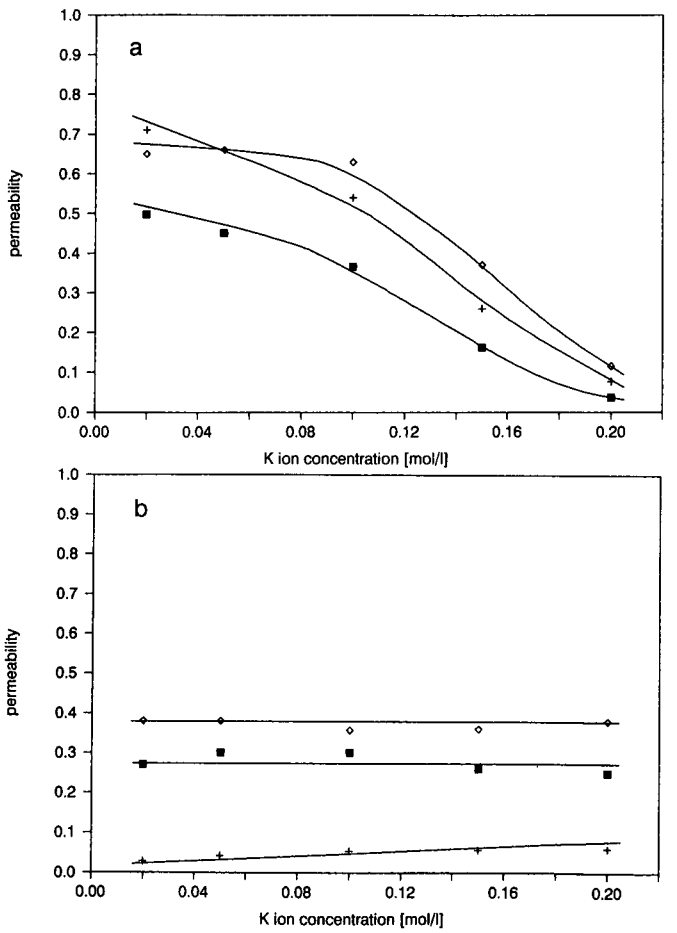

Fig. 3. Influence of buffer cation concentration on the permeability of Nafion films in potassium phosphate buffer at pH 7. (a) Film thickness 4 μm; (■) NE; (+) E; (◇) DA. (b) Film thickness 0.2 μm; (■) DOPA; (◇) catechol; (+) DOPAC.

The effect of the cation concentration was studied with potassium phosphate buffers at pH 7. The results are shown in Fig. 3. The permeability of the film for the cationic compounds decreases at high buffer concentrations, indicating that the majority of the exchange sites will be occupied by the buffer cations (Fig. 3a).

Fig. 3b shows the measured permeability values for the neutral analytes (DOPA and catechol). The only means of transport in the film for these particles is diffusion. As diffusion is not influenced by the ionic state of the film, the buffer concentration has no influence on the permeability towards neutral compounds. The permeability for DOPAC, however, shows some increase with increasing cation concentration. This may be an effect of a reduced zeta potential of the ionic groups in the Nafion film, which causes a decrease in the repulsion against the anionic DOPAC particles.

The ion-exchange characteristics of the Nafion-modified electrode were determined by studying the competition of epinephrine and three different buffer cations (Li^+, Na^+ and K^+). Fig. 4 shows the permeability of a 4-μm Nafion layer for epinephrine at different buffer concentrations. The permeability is highest in the lithium buffer and lower in the sodium buffer. With increasing buffer concentration the permeability decreases at approximately the same rate in both lithium and sodium buffers. The most drastic drop in the permeability of the film is observed with the potassium buffer, indicating that the affinity of the film is the strongest towards potassium ions.

Response of coated electrodes

The use of chemically modified electrodes for detection in HPLC can result in increased peak broadening owing to retarded diffusion of the analytes in the film. A recent theoretical study was devoted to the description of the response of film-coated electrodes, including computer simulations of the transport processes [27].

The response of a coated electrode is determined by the diffusion coefficient of the analyte in the film and by its distribution between the film and the solution. The contribution of the film coating to the peak broadening (σ_{film}) is theoretically

$$\sigma^2_{film} = \lambda(f^4/D_f^2) \tag{2}$$

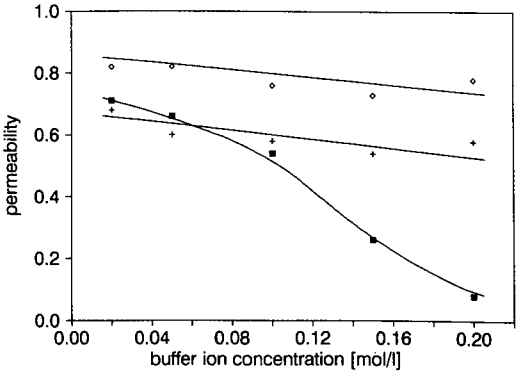

Fig. 4. Permeability of the Nafion-coated electrode for epinephrine in (■) potassium, (+) sodium and (◇) lithium phosphate buffers. Film thickness, 4 μm.

TABLE III

PERMEABILITY OF NAFION FILM IN THE MOBILE PHASE USED FOR URINE SAMPLES.

Conditions as in Fig. 5.

Analyte	Permeability[a]	Analyte	Permeability[a]
Epinephrine	0.99 ± 0.02	Catechol	0.35 ± 0.01
Norepinephrine	0.90 ± 0.01	DOPA	0.28 ± 0.005
Dopamine	0.93 ± 0.03	DOPAC	0.05 ± 0.01

[a] Mean ± S.D. (n = 3).

where f is the film thickness, D_f is the diffusion coefficient in the film and λ is a factor that depends on the distribution constant (K_d) of the analyte. The calculated value of this factor ranges from 1/90 at small K_d to 1/6 at high K_d values. In theory, peak broadening can be reduced by increasing the diffusion coefficient or by decreasing the distribution coefficient. The diffusion coefficient cannot be influenced easily, and it also is not advantageous to decrease K_d; in the latter instance the competitive effect of the buffer cation would be increased.

The changes in the peak broadening were studied on analytes having high (NE, E) and low (C) distribution constants in 0.1 M potassium phosphate buffer at pH 7

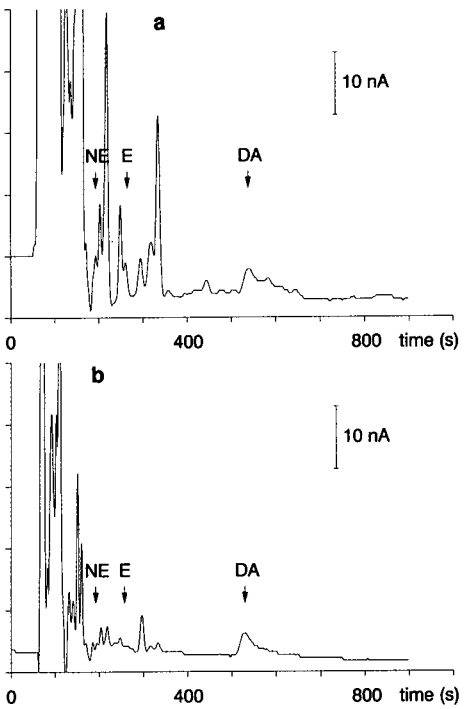

Fig. 5. Chromatograms of a urine sample measured at (a) bare and (b) 4-μm Nafion-coated electrodes. Mobile phase: 0.02 M lithium phosphate (pH 7)–10% methanol–5 · 10^{-3} M HSA–10^{-4} M EDTA.

containing 5% of methanol. The contribution of the film to peak broadening was calculated from

$$\sigma_{film}^2 = \sigma_c^2 - \sigma_b^2 \quad (3)$$

where σ_b and σ_c are halves of the measured peak widths at 0.61 of the peak height at bare and coated electrodes, respectively, under the same chromatographic conditions. The peak broadening measured at a 4-μm Nafion film was 0.5 ± 0.5 for norepinephrine, 1.3 ± 0.6 for epinephrine and 1.1 ± 0.4 s for catechol.

Measurements in urine samples

The permeabilities of the film towards some analytes are given in Table III, determined under the chromatographic conditions used for the analysis of urine samples. As can be seen, under optimum conditions the permeability towards catecholamines approaches 100%, whereas it is below 10% towards negatively charged particles.

Fig. 5 shows the results of measurements in urine samples at (a) bare and (b) Nafion-coated electrodes. In order to achieve optimum selectivity the mobile phase was buffered with 0.02 mol l^{-1} lithium phosphate. Owing to interferences, the peaks of norepinephrine, epinephrine and dopamine cannot be identified at the bare electrode. At coated electrodes the interfering peaks are strongly reduced. Endogenous DA concentrations can be directly determined, and also elevated NE and E concentrations can be detected without sample clean-up.

CONCLUSIONS

From this systematic study to determine the optimum conditions for the use of Nafion-modified electrodes in HPLC, the following guidelines were formulated. The pH should be kept as high as possible in order to convert the weakly acidic interferents into their anionic form, thus preventing them from reaching the electrode. To keep the competitive effect of the buffer cations to the minimum, the buffer concentration must be as low as possible, and lithium or sodium buffers are preferred to potassium buffers. The methanol concentration of the mobile phase is limited to *ca.* 20%. Films of 4 μm can be used without serious deterioration of the peak shape.

REFERENCES

1 M. Da Prada and G. Zucher, *Life Sci.*, 19 (1976) 1161.
2 J. D. Peuler and G. A. Johnson, *Life Sci.*, 21 (1977) 625.
3 E. Endert, *Clin. Chim. Acta*, 96 (1979) 233.
4 B. L. Lee, K. S. Chia and C. N. Ong, *J. Chromatogr.*, 494 (1989) 303.
5 A. A. Descombes and W. Haerdi, *Chromatographia*, 28 (1989) 459.
6 I. N. Mefford, M. Ota, M. Stipetic and W. Singleton, *J. Chromatogr.*, 420 (1987) 241.
7 G. Schuddinck, C. Dewaele and M. Verzele, *J. High Resolut. Chromatogr.*, 12 (1989) 697.
8 H. Gunasingham, C.-B. Tan, C.-H. Tan and T.-C. Aw, *J. Chromatogr. Sci.*, 27 (1989) 672.
9 J. Wang, G. D. Rayson, Z. Lu and H. Wu, *Anal. Chem.*, 62 (1990) 1924.
10 L. A. Coury, Jr, E. W. Huber, E. M. Birch and W. R. Heineman, *J. Electrochem. Soc.*, 136 (1989) 1044.
11 A. Merz, *Top. Curr. Chem.*, 152 (1990) 49.
12 R. W. Murray, A. G. Ewing and R. A. Durst, *Anal. Chem.*, 59 (1987) 379A.

13 J. Wang, *Anal. Chim. Acta*, 234 (1990) 41.
14 L. D. Whiteley and C. R. Martin, *J. Phys. Chem.*, 93 (1989) 4650.
15 J. Ye and K. Doblhofer, *Ber. Bunsenges. Phys. Chem.*, 92 (1988) 1271.
16 K. Shimazu, H. Kita and T. Kuwana, *J. Electroanal. Chem.*, 258 (1989) 49.
17 H.-L. Li, J. Q. Chambers and D. T. Hobbs, *J. Electroanal. Chem.*, 256 (1988) 447.
18 G. Nagy, G. A. Gerhardt, A. F. Oke, M. E. Rice, R. N. Adams, R. B. Moore, III, M. N. Szentirmay and C. R. Martin, *J. Electroanal. Chem.*, 188 (1985) 85.
19 H. Gunasingham and C. B. Tan, *Analyst*, 114 (1989) 695.
20 T. Matsue, A. Aoki, T. Abe and I. Uchida, *Chem. Lett.*, (1989) 133.
21 A. Aoki, T. Matsue and I. Uchida, *Denki Kagaku*, 56 (1988) 1120; *C.A.*, 110 (1989) 108323m.
22 J. Wang, P. Tuzhi and T. Golden, *Anal. Chim. Acta*, 194 (1987) 129.
23 H. Ji, E. Wang, *J. Chromatogr.*, 410 (1987) 111.
24 A. J. Tüdős, W. J. J. Ozinga, H. Poppe and W. Th. Kok, *Anal. Chem.*, 62 (1990) 367.
25 R. N. Adams, *Ann. N. Y. Acad. Sci.*, 473 (1986) 42.
26 R. M. Wightman, L. J. May and A. C. Michael, *Anal. Chem.*, 60 (1988) 769A.
27 W. Th. Kok, A. J. Tüdős and H. Poppe, *Anal. Chim. Acta*, 228 (1990) 39.

Journal of Chromatography, 547 (1991) 11–19
Elsevier Science Publishers B.V., Amsterdam

CHROM. 23 303

Low-capacity latex-coated resins for anion chromatography

ROY F. STRASBURG and JAMES S. FRITZ*
Ames Laboratory and Department of Chemistry, Iowa State University, Ames, IA 50011 (USA)
and
JOHN O. NAPLES
The Rohm and Haas Company, 727 Norristown Road, Spring House, PA 19477 (USA)
(First received August 15th, 1990; revised manuscript received March 14th, 1991)

ABSTRACT

Methods are described for coating latexes bearing a quaternary ammonium group onto spherical, non-porous polymeric resins. Exchange capacity of the coated resins is controlled by the amount of acetonitrile in the coating slurry and on the amount of latex in the slurry. A capacity range of 11–85 μequiv./g was obtained. Excellent chromatographic separations were obtained with columns packed with the coated resins. Sulfate is shown to elute before bromide and nitrate. As much as 40% methanol can be incorporated into the eluent without damaging the chromatographic column.

INTRODUCTION

Efficient anion-exchange resins for ion chromatography can be prepared by coating an unfunctionalized resin with a monomer or polymer containing a quaternary ammonium group. Cassidy and Elchuk [1] have developed both dynamic and permanent procedures for coating resins with long-chain quaternary ammonium compounds. DuVal and Fritz [2] demonstrated the successful use of permanently coated resin columns. Several other authors [3–5] have also used coated resins for ion chromatography.

As early as 1975 it was shown that efficient materials for anion chromatography can be prepared by coating resins that have been surface-sulfonated with a quaternized latex [6,7]. The positive charge of the latex is apparently attracted to the negatively charged sulfonate group on the resin surface.

Warth *et al.* [8] described the preparation and use of resins made by hydrophobically coating an anion-exchange latex onto unfunctionalized spherical resins. In the present study new latexes have been prepared and the method of coating has been altered in an attempt to obtain a more even coating and increase chromatographic efficiency. A latex that is only 54% quaternized was used to coat spherical polystrene beads. This material has very good chromatographic efficiency and can be used in conjunction with eluents containing up to 40% methanol.

0021-9673/91/$03.50

EXPERIMENTAL

Apparatus

The chromatographic systems consist of the following components. The first system consisted of a Milton-Roy mini-pump (Laboratory Data Control, Rivera Beach, FL, USA); a Rheodyne Model 7000 injection valve (Rainin, Woburn, MA, USA), equipped with a 10-μl sample loop; and a Milton-Roy pulse dampener (Laboratory Data Control) placed between the pump and the sample injector; a Spectroflow 783 (Kratos) variable-wavelength detector. This system was used for the indirect UV detection of the analytes. Various wavelengths were used and are noted in the text.

The second system consisted of an LKB 2150 high-performance liquid chromatography (HPLC) pump (Pharmacia), Wescan ICM II ion analyzer with conductivity detector (Alltech, CA, USA) and a Rheodyne Model 7125 injection valve fitted with a 10-μl sample loop.

A Shimadzu HPLC column packer (Phenomenex, CA, USA) was used to pack the column at a packing pressure ranging from 3000 to 6000 p.s.i. The columns used were 4.6 mm I.D., glass-lined, stainless-steel columns (Scientific Glass Engineering, Austin, TX, USA). Column lengths ranged from 5.0 to 15.0 cm in length and are noted in the text.

Resins

A 4.5-μm, spherical, non-porous, polystyrene resin with 10% divinyl benzene (DVB) cross-linking was prepared by expansion of monodisperse emulsion seed particles [9].

The latexes, which were 0.1 μm in diameter, were prepared by emulsifier-free terpolymerization of styrene, vinylbenzyl chloride and 5.5% DVB, followed by treatment with trimethylamine. The different levels of functionalization were obtained by varying the relative amounts of styrene and vinylbenzyl chloride.

Anion-exchange resins were produced by coating the 4.5-μm resin substrate with quaternized latex. Prior to the coating process, 10 ml of 4.5-μm resin was filtered in a medium, fritted-glass crucible, rinsed with 60 ml water and 30 ml of acetonitrile to remove adsorbed emulsifiers, and finally rinsed with deionized water. Then the rinsed resin was placed in a 100-ml beaker containing 45 ml of deionized water. In some cases acetonitrile was added at this point. The desired amount of latex was added dropwise with continuous magnetic stirring, and the total volume was brought to 50 ml by addition of water.

Coating experiments with varying percentages of acetonitrile were performed with 1 ml of latex suspension and 1 ml of polystyrene resin. Experiments on the effect of increasing amounts of latex suspension were performed in a slurry containing 1% (v/v) acetonitrile and 10 ml of polystyrene resin, with a final dilution to 25 ml. Resin exchange capacities were determined by a nitrate–sulfate displacement method. The coated resin [8] was packed using the upward packing method.

Reagents and solution

1,3,5-Benzenetricarboxylic acid (BTA) (97%, Aldrich) was purified by recrystallization from boiling, distilled, deionized water (Millipore). The precipitate was

filtered by suction and washed. All other chemicals were of reagent grade or better, and were used without further purification. Distilled, deionized water was used throughout.

Eluents of phthalate and BTA were prepared by dissolving the acids in water and adjusting the pH with 0.1 *M* lithium hydroxide. Eluents were vacuum filtered through a 0.2-μm membrane filter and vacuum degassed. Stock solutions of sample anions were prepared from their sodium salts. Dicarboxylic acids were prepared from the acid and deprotonated with lithium hydroxide. Stock solutions of 1000 ppm were used and samples prepared by diluting aliquots of the stock solutions as necessary.

RESULTS AND DISCUSSION

Coating methods

Warth *et al.* [8] showed that efficient columns for anion chromatography could be produced by coating a spherical polystyrene resin with quaternized polymeric latex particles. They found that latexes 76% functionalized with quaternary ammonium groups adhered more tightly to the resin substrate and gave better separations than those that were 100% functionalized (one quaternary ammonium group per benzene ring).

It was felt that latexes with still lower percentages of funtionalization might provide even better coverage and ion-exchange efficiency. Accordingly, latexes were prepared that 76, 54, 47, 35 and 20% functionalized with quaternary ammonium groups. These were coated on to 4.5-μm non-porous polystyrene beads by the coating method used by Warth *et al.* [8]. The column efficiency of ion-chromatographic columns packed with 35 or 20% quaternized latex was very poor. Microscopic examination showed that these two latexes have a strong tendency to agglomerate and thereby give a very uneven coating. Some difficulty was also encountered with the 47% quaternized material. However, the 54% quaternized latex (like the 76%) showed much less tendency to agglomerate and was therefore used in all of the present research.

The first procedure used to prepare coated resins involved filtering the 4.5-μm resin substrate and washing with water before coating with the 54% latex. While this produced resins that gave good chromatographic separations, the resin capacity was unpredictable. Variations in capacity were caused by the presence of adsorbed emulsifiers that competed with the latex for adsorption sites on the resin surface. This situation was corrected by first washing the filtered resin substrate with acetonitrile and then with water before the coating step. The rinsed resin temporarily agglomerated during the coating step, but the aggregates dispersed as the substrate became coated with the quaternized latex. Continuous stirring of the mixing slurry also facilitated breaking up the aggregates. The resulting anion-exchange resin produced excellent separations. It was also possible to alter the capacity in a predictable manner.

Previous work involving latex that had 76 and 100% functionalization demonstrated that the capacity of the coated resin was dependent on the length of time the slurry was mixed, on the concentration of NaCl and on the amount of functionalized latex present in the slurry [8]. In each case, capacity increased as one or more of these three parameters increased. In the present work with 54% functionalized latex, it was found that the final resin capacity was independent of the concentration of NaCl or

the length of time the latex and substrate were mixed together. For example, after 1, 2 and 4 h of continuous mixing, the resin had a capacity of 27.3, 26.7 and 27.7 μequiv./g, respectively. This is probably due to the more hydrophobic nature of this latex which causes the latex to reach equilibrium quickly between the resin and the aqueous slurry.

The presence of sodium chloride in the aqueous slurry actually had a deleterious effect when 54% functionalized latex was used. Increasing the ionic strength of the slurry resulted in formation of latex aggreates that could be observed with an optical microscope (21 ×). This produced an unevenly coated resin and inefficient chromatographic columns. By having 1% (v/v) acetonitrile in the slurry, the problem of latex aggregation was alleviated and no aggregates could be seen with the microscope. A marked improvement in column efficiency was observed when this resin was tested chromatographically. Efficiencies as high as 19 500 theoretical plates per meter were obtained at a flow-rate of 1 ml/min. Increasing the percentage of acetonitrile in the slurry to greater than 1% did not further improve the chromatographic efficiency when the slurry contained a 1:10 latex-to-substrate ratio.

Capacity

The capacity of the coated resin can be controlled by the percentage of acetonitrile present in the slurry and the amount of latex used. Fig. 1 shows that, as expected, the capacity decreases as the percentage of acetonitrile increases. As the slurry becomes more hydrophobic, the latex is less readily adsorbed onto the hydrophobic substrate. It is interesting to note that while previous work indicated that

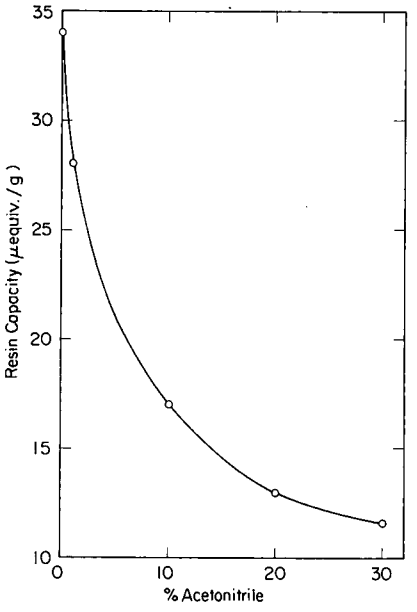

Fig. 1. Relationship between resin capacity (μequiv./g) and percent acetonitrile present in slurry. Each slurry contained 1 ml of latex suspension and 1 ml of washed polystyrene substrate, diluted to 25 ml and stirred for 1 h.

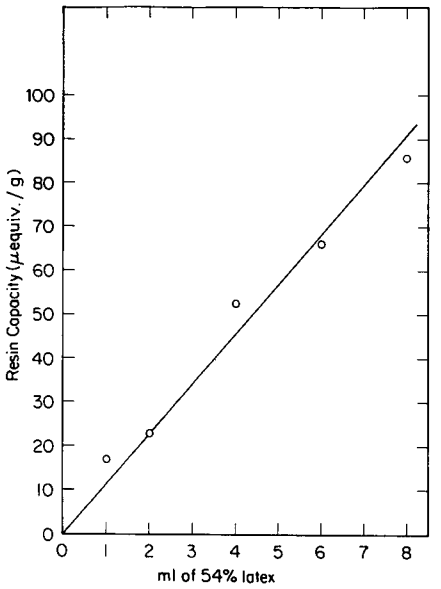

Fig. 2. Relationship between resin capacity and volume of latex added to slurry. Each slurry contained 10 ml of polystyrene substrate and 1% (v/v) acetonitrile. Other conditions as in Fig. 1.

organic modifiers washed the higher-functionalized latexes off the substrate, anion-exchange resins were able to be prepared in the presence of acetonitrile using the 54% functionalized latex.

Fig. 2 shows a nearly linear increase in capacity as the volume of latex used to coat the substrate was increased. Since this latex is more hydrophobic, a heavier coating was possible than with previous latexes. By varying the percentage of acetonitrile and the volume of latex used in the slurry, the capacity can be varied from 11.5 to 85 μequiv./g.

Selectivity

Fig. 3 shows the separation of seven common anions in less than 7 min. The column is 50 × 4.6 mm I.D. Even though a short column was used, a nearly baseline separation was possible in a short analysis time. The eluent was 0.8 m*M* dilithium phthalate at pH 9.50. It is interesting to note that SO_4^{2-} and $C_2O_4^{2-}$ elute before Br^-. This is unexpected, since resins made with 76% functionalized latex of identical capacity did not show this elution order using a phthalate eluent [10].

Effect of methanol

The effect of adding methanol to the eluent was studied next. The presence of methanol affects some anions more than others, as illustrated by the retention times in Table I. There is a substantial change in the retention times of sulfate, bromide and nitrate, while the retention time sof chloride and nitrite are less affected.

A commercial column (Wescan 269-029) was also used to investigate the effect of methanol on the retention times of these anions. The retention times of Cl^-, NO_2^-,

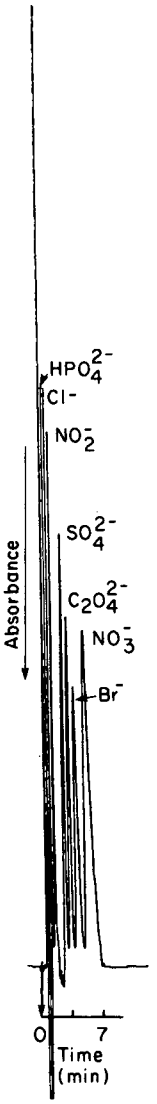

Fig. 3. Separation of 5 ppm HPO_4^{2-}, 2.5 ppm Cl^-, 5 ppm NO_2^-, 10 ppm SO_4^{2-}, 10 ppm $C_2O_4^{2-}$, 20 ppm Br^- and 30 ppm NO_3^- on a 5.0 cm × 4.6 mm I.D. column (capacity = 27 μequiv./g). Eluent, 0.8 m*M* dilithium phthalate at pH 9.50; flow-rate, 1 ml/min; wavelength λ = 250 nm; 0.025 a.u.f.s.

Br^- and NO_3^- were unaffected and SO_4^{2-} increased only slightly. The ability to alter selectivity by using an organic modifier in the eluent provides a novel dimension to latex-coated resins.

The stability of 54% functionalized latex in the presence of methanol was also investigated. After using 40% methanol in the eluent, aqueous phthalate was again used. The retention times of the anions and the elution order were essentially the same as before the use of methanol. We do not claim that 40% methanol can be used

TABLE I

EFFECT OF METHANOL AS ELUENT MODIFIER ON THE ADJUSTED RETENTION TIMES OF FIVE COMMON ANIONS

CH_3OH in eluent (%)	Average adjusted retention time (min, $n = 3$)				
	Cl^-	NO_2^-	SO_4^{2-}	Br^-	NO_3^-
0	0.62	0.99	2.93	3.64	4.60
10	0.67	1.02	3.82	3.82	4.72
20	0.66	0.96	4.53	3.57	4.53
30	0.64	0.86	5.48	3.20	3.81
40	0.61	0.76	6.47	2.78	3.22

indefinitely, although use for 8 h had no effect on analyte retention times. Fig. 4 shows a very nice separation of eight anions after using 40% methanol in the eluent. The two dicarboxylic acids were not resolved.

Applications

The analysis of dicarboxylic acids is important in industries such as the wine

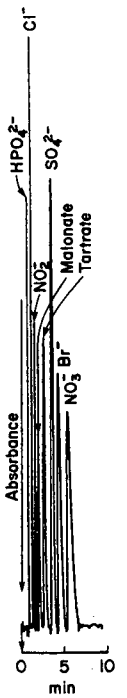

Fig. 4. Separation of 10 ppm HPO_4^{2-}, 5 ppm Cl^-, 5 ppm NO_2^-, 10 ppm malonate, 20 ppm tartrate, 25 ppm SO_4^{2-}, 30 ppm Br^- and 30 ppm NO_3^-, after 40% methanol was used as eluent modifier. Eluent, 0.5 m*M* dilithium phthalate at pH 8.25; flow-rate, 1 ml/min; column, 10 cm × 4.6 mm I.D. with a capacity of 35 μequiv./g, $\lambda = 270$ nm; 0.025 a.u.f.s.

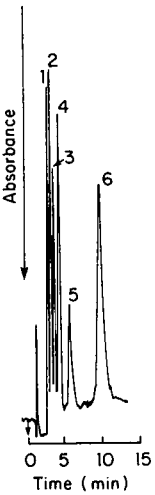

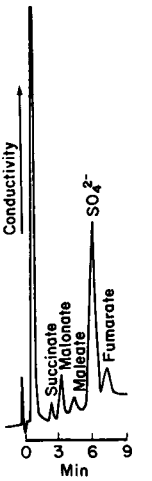

Fig. 5. Separation of 10 ppm glutarate, 10 ppm succinate, 10 ppm malate, 10 ppm malonate, 5 ppm tartrate and 20 ppm oxalate using indirect UV detection on a 10 cm × 4.6 mm I.D. column (capacity = 28 μequiv./g). Eluent, 0.2 m*M* dilithium phthalate at pH 8.40; λ = 245 nm; 0.025 a.u.f.s.

Fig. 6. Separation of 10 ppm each succinate, malonate, maleate, sulfate and fumarate using conductivity detection (1 μS f.s.). Eluent, 0.25 m*M* dilithium phthalate at pH 8.50, column same as in Fig. 5.

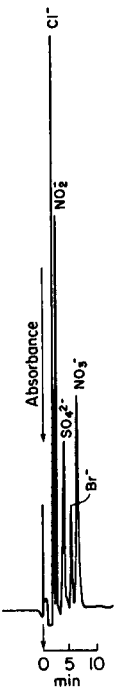

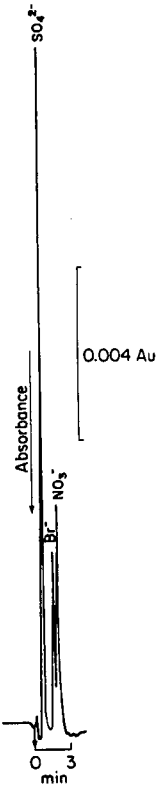

Fig. 7. Separation of 10 ppm Cl^-, 10 ppm NO_2^-, 10 ppm SO_4^{2-}, 10 ppm Br^- and 20 ppm NO_3^- on a 5 cm × 4.6 mm I.D. column (capacity = 27 μequiv./g). Eluent, 0.05 m*M* BTA at pH 4.3, flow-rate, 1 ml/min, λ = 250 nm; 0.025 a.u.f.s.

Fig. 8. Rapid separation of 5 ppm each SO_4^{2-}, Br^- and NO_3^- on a 5.0 cm × 4.6 mm I.D. column (capacity = 15 μequiv./g). Eluent, 0.05 m*M* BTA at pH = 4.6; flow-rate 1 ml/min; λ = 240 nm; 0.025 a.u.f.s.

industry. Fig. 5 shows a nice separation of six dicarboxylic acids in 10 min. As the alkyl chain length of the dicarboxylic acids increases, the retention times of the acids decrease. As the carboxylic acid moieties are farther apart, the molecule behaves chromatographically more like a monovalent anion.

Indirect UV detection is the detection method of choice for analyzing dicarboxylic acids. Fig. 6 shows a separation of 10-ppm each succinate, malonate, maleate, sulfate and fumarate, using 0.25 m*M* dilithium phthalate at pH 8.5 as the eluent with conductivity detection. A comparison between Fig. 5 and Fig. 6 demonstrates that indirect UV detection is much more sensitive.

Very low exchange capacities can be obtained readily with latex-coated resins. This makes it possible to obtain excellent sensitivity in the analysis of low concentrations of anions. The effect of capacity on sensitivity is illustrated by the chromatograms in Figs. 7 and 8. The chromatographic conditions are almost the same except that the resin capacity is 27 μequiv./g in Fig. 7 and 15 μequiv./g in Fig. 8. The retention times of sulfate, bromide and nitrate are all smaller on the lower capacity column (Fig. 8) and the peak heights per 1 ppm of anion are 4–8 times larger on the column of lower capacity. Excellent calibration curves were also obtained. For example, linear calibration curves were obtained from 0.5 to 50 ppm chloride and sulfate, and from 1.5 to 75 ppm nitrate with correlation coefficients of 0.9997 or better.

ACKNOWLEDGEMENTS

R.F.S. and J.S.F. gratefully acknowledge financial support of the Rohm and Haas Co. This research was performed at the Ames Laboratory, which is operated for the US Department of Energy at Iowa State University.

REFERENCES

1 R. M. Cassidy and S. Elchuk, *J. Chromatogr.*, 262 (1983) 311.
2 D. L. DuVal and J. S. Fritz, *J. Chromatogr.*, 295 (1984) 89.
3 B. B. Wheals, *J. Chromatogr.*, 402 (1987) 115.
4 A. S. Al-Omair and S. J. Lyle, *Talanta*, 34 (1987) 361.
5 P. K. Dasgupta, *Anal. Chem.*, 56 (1984) 769.
6 H. Small, T. S. Stevens and W. C. Bauman, *Anal. Chem.*, 47 (1975) 1801.
7 H. Small and T. S. Stevens, *US Pat.* 4 101 460 (1978).
8 L. M. Warth, J. S. Fritz and J. O. Naples, *J. Chromatogr.*, 462 (1989) 165; J. O. Naples, J. S. Fritz and L. M. Warth, *Eur. Pat. Appl.* 346 037 (1989).
9 M. S. Frazza (The Rohm & Haas Company, Philadelphia, PA) US patent pending.
10 Y. Miura and J. S. Fritz, *J. Chromatogr.*, 482 (1989) 155.

Journal of Chromatography, 547 (1991) 21–30
Elsevier Science Publishers B.V., Amsterdam

CHROM. 23 227

Stability of Superdex 75 prep grade and Superdex 200 prep grade under different chromatographic conditions

INGRID DREVIN and BO-LENNART JOHANSSON*
Pharmacia LKB Biotechnology AB, S-751 82 Uppsala 1 (Sweden)
(First received September 6th, 1990; revised manuscript received February 19th, 1991)

ABSTRACT

The chemical stability of two gel filtration media, Superdex 75 prep grade and Superdex 200 prep grade, was studied in bulk and column experiments. The release of agarose and dextran from these two composite media was measured by three different methods: a specific nephelometric method based on the use of antidextran antiserum, an anthrone method and a gel filtration chromatographic method with a light-scattering detector. Dextran fragments were released from Superdex 75 and 200 prep grade under extreme basic and acidic conditions. However, Superdex withstands many short-term incubations (contact time *ca.* 4 h each time) at pH 14 and 1 without any influence on the chromatographic behaviour. Equilibration of a Superdex column with a neutral buffer after these short-term treatments lowered the concentration of dextran in the eluate to an undetectable level after about three bed volumes. The ability of Superdex columns to withstand practical mistakes such as pumping air into the column was also investigated.

INTRODUCTION

Superdex 75 prep grade and Superdex 200 prep grade are new composite high-performance preparative gel filtration media [1] made by binding dextran covalently to cross-linked agarose beads. The selectivities of the Superdex gels are designed to give separation ranges for proteins similar to those of the corresponding Sephadex media. Thus, Superdex 75 prep grade has the same selectivity as Sephadex G-75 (3–80 kilodalton) and Superdex 200 prep grade has the same selectivity as Sephadex G-200 (5–600 kilodalton) [2]. The mean particle size of the Superdex prep grade matrix is *ca.* 34 μm. The chromatographic properties of these gels have been described in more detail elsewhere [1,3].

It is high important from many points of view that preparative liquid chromatographic (LC) media are chemically stable. The decomposition of such media in different mobile phase buffer solutions is of crucial interest to those involved in purifying pharmacological products. Significant contamination in this area would severely limit the general adoption of the media to process-scale purification. Several studies concerned with the stability of silica-based packings for reversed-phase chromatography have been reported [4–7].

The main aim of this work was to produce quantitative data to demonstrate the

0021-9673/91/$03.50

chemical stability of Superdex 75 prep grade and Superdex 200 prep grade in different solvents. Previously we observed [3] that the K_{av} values of proteins increased slightly on Superdex 75 prep grade treated with solutions of high pH (13–14) and low pH (1–2) for long periods. An increased volume of the agarose pores because of hydrolysis of dextran was assumed to cause this effect. To verify this interpretation, the leakage of polysaccharides from the two media was studied at extreme pH values under static and chromatographic conditions. In addition, the functional resistance to 1.0 *M* NaOH, 0.1 *M* HCl and air pumped into columns packed with Superdex 200 prep grade was studied.

EXPERIMENTAL

Chemicals and apparatus

Superdex 75 prep grade, Superdex 200 prep grade, dextran 70, cross-linked agarose beads (semi-product in the production of Superdex gels) and the dextran used for Superdex were obtained from Pharmacia LKB Biotechnology. Dextran standards with different molecular weights (see Table III) were purchased from Pharmacosmos. The proteins used are listed in Table I and all inorganic compounds were of analytical-reagent grade. The antidextran antiserum was obtained from Pharmacia. The production of antiserum has been described earlier [8]. Tween 20 and polyethylene glycol (PEG) 6000 were provided by KEBO Lab.

Chromatographic measurements were performed on fast protein (FPLC) systems from Pharmacia. Two systems were used, each consisting of an LCC-500 control unit, two P-500 precision pumps, a UV-1 monitor (280 nm, HR 10 cell), an MV-7 sample injector with a 500-μl loop, an MV-8 sample holder, a P-1 peristaltic pump and a REC-481 recorder. A Shimadzu C-R3A integrator was used to store chromatographic results.

A Shimadzu RF-540 spectrofluorimeter with a DR-3 data recorder and a 10 × 2 mm cell as used for nephelometric measurements.

Determination of polysaccharides with anthrone was carried out with a Technicon AutoAnalyzer II system.

TABLE I

PROTEINS USED FOR STUDYING CHROMATOGRAPHIC PROPERTIES OF SUPERDEX 200 PREP GRADE DURING CLEANING-IN-PLACE EXPERIMENTS

Substance		Source	Concentration (mg/ml)	Molecular weight
A	Cytidine		0.10	323
B	Lysozyme	Egg white	0.62	13 900
C	Cytochrome *c*	Horse heart	1.25	12 400
D	Myoglobin	Horse heart	1.25	17 800
E	α-Chymotrypsinogen	Bovine pancrease	1.25	25 000
F	β-Lactoglobulin	Bovine milk	1.25	35 000
G	Ovalbumin	Egg white	2.50	45 000
H	Serum albumin	Bovine	1.25	67 000
I	Immunoglobulin G	Human	1.25	160 000
J	Ferritin	Horse spleen	0.20	440 000

Analysis of the molecular size distribution of the polysaccharides released from Superdex was performed by using an FPLC solvent delivery system. The separation was performed on three serially coupled columns. The column combination was one TSK G2000PW, one TSK G3000PW and one TSK G5000PW (30 cm × 0.8 cm I.D. (Tokyo Soda, Tokyo, Japan). Column effluents were monitored by using an OPTI-LAB Multiref 901 detector.

Functional stability of Superdex 200 prep grade under different treatments

Treatment with 1.0 M NaOH and 0.1 M HCl. The functional stability of Superdex 200 prep grade was studied by making on-column treatments of the gel with 1.0 *M* NaOH and 0.1 *M* HCl at ambient temperature (22°C). Superdex 200 prep grade was packed in two HR 16/50 columns (50 cm × 1.6 cm I.D.), one for each solution. The solutions were pumped into the columns at a flow-rate of 0.33 ml/min. When the columns were filled with either of the solutions, the flow was stopped. After a specified time (stated below), the gels were equilibrated with three bed volumes of the mobile phase (0.02 *M* phosphate buffer, pH 7.0, containing 0.3 *M* sodium chloride). A series of proteins, listed in Table I, were then injected onto the columns, and the chromatographic behaviour was evaluated by individual injections of the proteins to avoid interactions between the proteins. The total time of exposure to 1.0 *M* NaOH or 0.1 *M* HCl was 2 weeks, divided into *ca.* nineteen treatments of 8 h each and eleven treatments of 16 h. The chromatographic behaviour was tested after each treatment. The flow-rate was 0.5 ml/min and the injection volume was 500 μl. The resulting retention volumes (V_e) of the proteins were used to calculate the distribution coefficient (K_{av}) from the equation

$$K_{av} = (V_e - V_o/(V_t - V_o)$$

where V_o and V_t represent the void volume and the total bed volume of fluid and gel combined, respectively. Blue Dextran 2000 (1.0 mg/ml) was employed as a V_o marker and V_t was calculated from the bed height and the inside diameter of the column. V_t was 103 ml and the void fraction V_o/V_t was 0.36 for both columns. The number of theoretical plates (N) was determined by injection of 500 μl of 1% (v/v) acetone at the start and at the end of the experiments for both columns. The retention volume (V_e) and the peak width at half-height ($W_{0.5}$) were used to calculate N [$N = 5.54(v_e/W_{0.5})^2$].

Resistance to air. A column (HR 16/50) packed with Superdex 200 prep grade was treated with air several times. After each treatment the column was regenerated and the performance evaluated. The amounts of air and buffer for regeneration are given in Table V. The performance of the column was determined in two ways, measuring the plate number and the K_{av} values of β-lactoglobulin and lysozyme.

Determination of leakage from Superdex 75 and 200 prep grade

Leakage in bulk experiments. About 50 ml of homogenized suspension of Superdex 75 or 200 prep grade were transferred to a glass filter-funnel (pore size G3). The gels were washed with about 1 l of distilled water and then sucked dry with a water pump. Portions of 2.00 g gel were transferred to 25-ml conical flasks, 10 ml of the incubation solution were added and the flasks were sealed with a piece of Para-

film. The incubation solutions were hydrochloric acid (pH 1, 2 and 3) and sodium hydroxide (pH 12, 13 and 14) solutions. After an incubation time of 2 weeks at 22°C the supernatant was removed and filtered through a 0.45-μm filter and then analysed for its polysaccharide content (see below). Samples with a high polysaccharide content were diluted with distilled water prior to analysis.

Leakage in on-column experiments. The gels were packed in Pharmacia K 16/10 columns (10 cm × 1.6 cm I.D.) at a flow-rate of 2 ml/min to settle the gel. After the end adaptor had been inserted the gel bed was stabilized by pumping water through the column at a flow-rate of 7 ml/min for 1 h. Sodium hydroxide solution (1 *M*) was then pumped into the columns at a flow-rate of 1 ml/min. The flow was stopped after passage of 40 ml of 1.0 *M* NaOH. After a contact time of 4 h the columns were equilibrated with ten bed volumes of 0.02 *M* sodium phosphate buffer (pH 7.0) at a flow-rate of 1 ml/min. Fractions of the eluate were continuously sampled during the equilibration of the columns and analysed with the nephelometric method (see below) to determine any released amount of dextran. The treatment of the columns with sodium hydroxide solution was then repeated twice. All experiments were performed at room temperature (22°C).

Nephelometric determination of dextran. The antidextran antiserum was diluted 50-fold with 0.05 *M* phosphate buffer containing 0.1 *M* NaCl, 0.15 ml/l of Tween 20 and 100 g/l PEG 6000 [8]. After 20 min at room temperature, the solution was filtered through a 0.22-μm Millipore filter. A 360-μl volume of this antiserum–polymer solution was mixed with 30 μl of the sample solution in a 600-μl quartz cuvette. After a reaction time of 4 min the light scattering was measured at 312 nm by scanning the excitation and emission monochromators in a synchronous manner ($\Delta\lambda$ = 0 nm) between 250 and 350 nm. Dextran used in the production of Superdex was used as a standard and gave linear calibration graphs in all incubation solutions in the range 0–10 μg/ml.

Determination of dextran and agarose with anthrone. The selection of sulphuric acid concentration, reaction time, reaction temperature and anthrone concentration was made in accordance with the conditions recommended by Scott and Melvin [9]. The wavelength for the absorption measurements was adjusted to 620 nm. Dextran 70 was used as the calibration substance and linear calibration graphs were obtained for all incubation solutions in the working range 0–30 μg/ml.

RESULTS AND DISCUSSION

The exact lifetime of Superdex columns will depend on the nature of the sample and the stability of the matrix with respect to the elution and cleaning conditions. The stability of gel filtration packings in typical FPLC separations is often not considered to be an important problem [10,11]. Relatively mild conditions are often met in many analytical applications. However, separation media for preparative applications must be periodically renewed after exposures to large amounts of protein. A common approach for cleaning or regeneration of contaminated preparative media is to wash them with acidic or alkaline solutions [12]. It is therefore important that gel filtration media for preparative separation can withstand extreme pH conditions to ensure a long column lifetime.

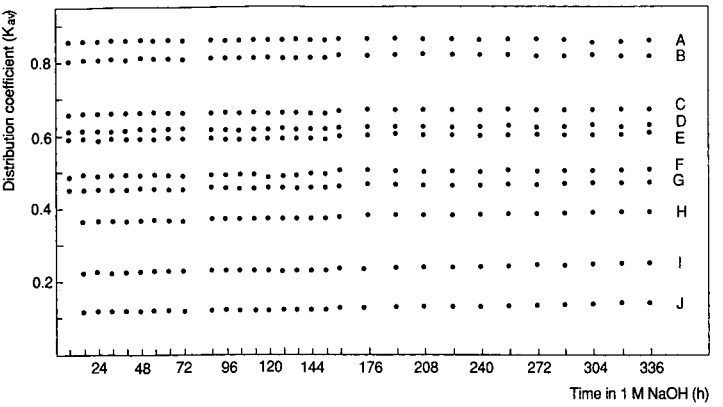

Fig. 1. Influence of repeated CIP treatments with 1.0 *M* NaOH on the distribution coefficients of a series of proteins (Table I) on Superdex 200 prep grade in an HR 16/50 column.

Chemical stability of Superdex 200 prep grade on repeated column washes at pH 1 and 14

Recently, we showed that Superdex 75 prep grade withstands at least 25 short-term treatments (exposure time 4 h each time) with 1.0 *M* NaOH or 0.1 *M* HCl without any changes in chromatographic behaviour [3]. Figs. 1 and 2 show that Superdex 200 prep grade was also functionally stable during all cleaning-in-place cycles with 1.0 *M* NaOH or 0.1 *M* HCl with a contact time of 8 h per cycle. These results demonstrate that Superdex 75 and 200 prep grade may be cleaned with solutions that effectively regenerate and purify the matrix. No effect on the efficiency of the columns was observed during the tests. However, a small increase in retention volumes was observed for the proteins, but not for cytidine, when the cleaning time was prolonged to 16 h (Figs. 1 and 2). This behaviour was also observed with Superdex 75 prep grade [3]. We previously suggested [3] that hydrolysis of dextran in the

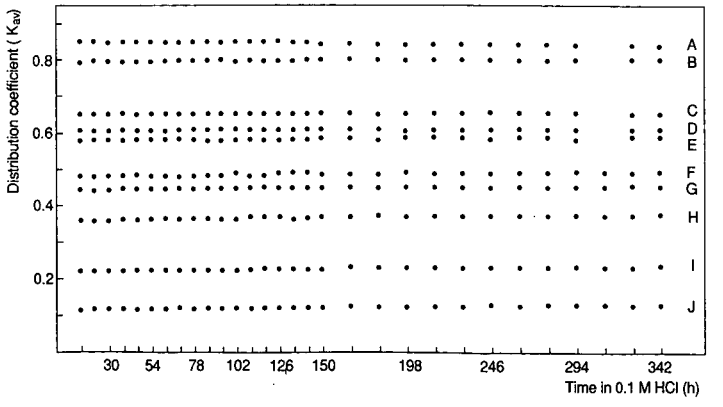

Fig. 2. Influence of repeated CIP treatments with 0.1 *M* HCl on the distribution coefficients of a series of proteins (Table I) on Superdex 200 prep grade in an HR 16/50 column.

agarose pores can give rise to increased K_{av} values. To verify this hypothesis and to investigate the risk of contamination of fractionated proteins with polysaccharide fragments, a study of possible leakage products from Superdex media was undertaken.

Leakage of polysaccharides from Superdex 75 and 200 prep grade

To determine the amount of dextran and agarose released from Superdex 75 and 200 prep grade, a specific nephelometric method for dextran [8], based on the use of antidextran antiserum, and the well documented anthrone method [9] were used.

Static experiments. From the agarose base matrix, to which dextran is coupled in the production of Superdex 75 and 200 prep grade, only small amounts of agarose were released during static experiments at pH 1 (Table II). However, polysaccharides were released from the Superdex gels at all pHs investigated (Table II). These results show that the polysaccharide leakage from Superdex mainly originated from the dectran structures of the gel. The dextran leakage was highest at extremely high pH (14) and low pH (1) (and decreased when the incubation pH was changed towards neutral values). Also, the leakage of dextran was higher from Superdex 75 than Superdex 200 prep grade. The results from the antrone and the nephelometric measurements were in good accord (Table II) and also support the suggestion that dextran is the main leakage product.

The leakage of dextran is probably caused by base- and acid-promoted hydrolysis of glycosidic linkages between glucose units. This means that the molecular weight–size distribution curve of the dextran fragments released ought to be displaced

TABLE II

POLYSACCHARIDE LEAKAGE FROM SUPERDEX 75 AND 200 PREP GRADE AND SEMI-PRODUCT TO SUPERDEX IN STATIC EXPERIMENTS DURING 2 WEEKS IN DIFFERENT SOLUTIONS

Incubation medium	Method[a]	Superdex 75 prep grade (μg/ml)	Superdex 200 prep grade (μg/ml)	Sepharose[b] (μg/ml)
1 *M* NaOH	ANT	1500	150	<2
0.1 *M* NaOH	ANT	740	86	<2
0.01 *M* NaOH	ANT	80	31	<2
0.001 *M* HCl	ANT	41	4	<2
0.01 *M* HCl	ANT	43	16	<2
0.1 *M* HCl	ANT	295	70	5
1 *M* NaOH	NEP	960	540	n.a.[c]
0.1 *M* NaOH	NEP	850	208	n.a.
0.01 *M* NaOH	NEP	2	5	n.a.
0.001 *M* HCl	NEP	3	5	n.a.
0.01 *M* HCl	NEP	55	48	n.a.
0.1 *M* HCl	NEP	220	152	n.a.

[a] The leakage was analysed using two different methods: ANT = anthrone method; NEP = nephelometry.

[b] Sepharose is the agarose bead on which Superdex 75 and 200 prep grade are based.

[c] n.a. = Not analysed.

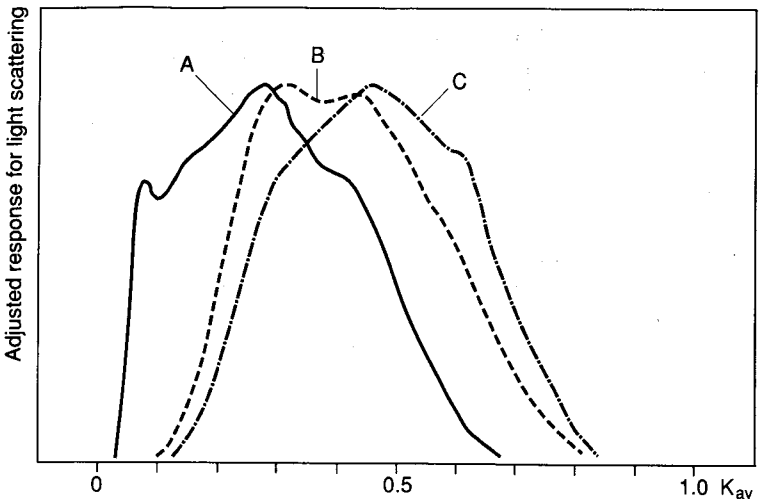

Fig. 3. Gel filtration elution pattern of (A) dextran used in the production of Superdex, and polysaccharides released from Superdex 75 prep grade incubated for 2 weeks in (B) 0.1 *M* HCl and (C) 1.0 *M* NaOH.

towards lower molecular weights compared with the dextran used in the production of Superdex. This was also verified when the dextran leakage was analysed by gel filtration chromatography after incubation of the gels in 1.0 *M* NaOH or 0.1 *M* HCl (Fig. 3). Fig. 3 also shows that the size distribution of released dextran fragments covered the range from $2.4 \cdot 10^6$ ($K_{av} = 0.1$) to $2.0 \cdot 10^3$ ($K_{av} = 0.80$).

To study the effect of the molecular size of dextran on the results from the nephelometric and the spectrophotometric (anthrone) methods, different dextran standards were analysed (Table III). The results of the anthrone method were not

TABLE III

COMPARISON BETWEEN NEPHELOMETRIC (NEP) AND ANTHRONE (ANT) ANALYSIS OF DEXTRANS WITH DIFFERENT MOLECULAR WEIGHTS IN 0.1 *M* NaOH

Molecular weight of dextran standard	True dextran concentration (μg/ml)	Found dextran concentration (μg/ml)	
		NEP[b]	ANT[b]
1080	5.1	0.2 (0.04)	4.9 (0.96)
4440	5.3	3.1 (0.58)	4.9 (0.92)
9890	5.0	4.9 (0.98)	n.a.
21 400	5.0	6.7 (1.34)	4.5 (0.90)
43 500	5.1	6.4 (1.25)	4.9 (0.96)
66 700	5.0	6.3 (1.26)	n.a.
123 600	5.0	5.7 (1.14)	n.a.
196 300	5.0	5.5 (1.10)	n.a.
276 500	5.1	5.2 (1.02)	4.6 (0.90)
401 300	5.0	5.0 (1.00)	n.a.
Dextran[a]	5.0	5.0 (1.00	4.7 (0.94)

[a] Dextran used in the production of Superdex 75 and 200 prep grade.
[b] Values in parentheses show the ratio between found and true dextran concentration; n.a. = not analysed.

influenced by the size of the dextran fragments. On the other hand, the nephelometric method gave too low results at molecular weights below $1.0 \cdot 10^3$ and slightly too high values between $2 \cdot 10^4$ and $2 \cdot 10^5$ (Table III). Although the results from the anthrone and the nephelometric measurements were in good accord (Table II), these findings indicate that the most reliable results for determination of the dextran leakage were achieved with the anthrone method.

It can also be noted that the released amounts of dextran reported in Table II are low compared with the total amount of dextran in Superdex media. This conclusion is verified by the small K_{av} effects observed for Superdex 200 prep grade after treatment with 1.0 *M* NaOH or 0.1 *M* HCl for 2 weeks (Figs. 1 and 2).

On-column experiments. Chromatographic separations of proteins are normally not performed at pH 14 and 1. However, solutions with high or low pH values are usually used to clean packed chromatographic columns contaminated with proteins, endotoxins or microorganisms [13]. In cleaning-in-place (CIP) experiments with 1.0 *M* NaOH, the leakage level of dextran at the column outlet was lower for Superdex 200 prep grade than for Superdex 75 prep grade (Table IV). This was also observed in the static bulk experiments (see above) and is probably related to the fact that the amount of dextran in the two gels is highest for Superdex 75 prep grade. Also, for both gels the dextran leakage decreased with the number of CIP cycles (Table IV). The dextran released in a CIP procedure must be thoroughly washed out if eluates are not to be contaminated with dextran. From Table IV it can be seen that after passage of three bed volumes of mobile phase buffer through the column no dextran fragments can be observed in the eluate.

Further, as the sodium hydroxide solution was stagnant in the column for 4 h, the concentration of released dextran obtained was higher than that in a typical CIP

TABLE IV

LEAKAGE OF DEXTRAN FROM SUPERDEX 75 AND 200 PREP GRADE COLUMNS (K 16/10) AFTER CLEANING-IN-PLACE (CIP) WITH 1.0 *M* NaOH

CIP cycle	Equilibration fraction[a]	Dextran leakage (μg/ml)	
		Superdex 75 prep grade[b]	Superdex 200 prep grade[c]
First	1st	193	51
	3rd	7.8	n.a.
	4th	3.9	n.a.
	5th	n.d.	n.a.
Second	1st	132	23
	3rd	5.2	n.a.
	4th	3.0	n.a.
	5th	n.d.	n.a.
Third	1st	110	17
	3rd	4.3	n.a.
	4th	n.d.	n.a.

[a] After treatment for 4 h with 1 *M* NaOH the columns were equilibrated with phosphate buffer (pH 7.0) where the first fraction corresponded to one bed volume (20 ml) and the other fractions to 10 ml.
[b] n.d. = Not detected.
[c] n.a. = Not analysed.

TABLE V

VARIATION OF EFFICIENCY WITH VOLUME OF AIR PUMPED THROUGH AN HR 16/50 COLUMN PACKED WITH 100 ml OF SUPERDEX 200 PREP GRADE

Volume of air pumped through the column (ml)	Equilibration volume of buffer[a] (ml)	Plate number (m^{-1})
New packing	100	11 500
1	100	11 600
1	100	12 100
30	100	10 450
30	100	9800
90	100	9000
90	750	8800
	1250	10 500
720	500	6600
	1500	8900

[a] After each air treatment the column was treated with different amounts of buffer before the efficiency test.

procedure with continuous flow through the column. It has been shown for other media that the concentration of leakage products in the eluate is inversely proportional to the flow-rate [14].

Functional stability of a Superdex 200 prep grade column after pumping air through the column

A common mistake in chromatographic experiments is to pump air into the column because the mobile phase in the eluent reservoir has been used up. To study how this influences the column efficiency and the retention properties of Superdex 200 prep grade, a column was treated with different amounts of air. Table V shows that when small amounts of air (1 ml) were pumped into the column no significant effect on the column efficiency was observed. However, when 30 ml or more of air were applied the N value decreased (Table V). The magnitude of this decrease was related to the volume of equilibration buffer pumped through the column after air exposure. The bed height after equilibration and the K_{av} values of the proteins (Table V) remained unchanged during the test.

In conclusion it has been shown that Superdex 75 prep grade and Superdex 200 prep grade are functionally stable to short-term treatments with 1.0 M NaOH and 0.1 M HCl. Nevertheless, Superdex media release small amounts of dextran under these conditions. However, released dextran can be easily washed away by equilibration with the buffer normally used in the separation procedure.

REFERENCES

1 L. Kågedal, H. Ellegren, B. Engström, A.-K. Lieber, H. Lundström, A. Persson and M. Schenning, *J. Chromatogr.*, 537 (1991) 17.
2 L. Hagel, in J.-C. Janson and L. Ryde'n (Editors), *Protein Purification*, VCH, New York, 1989, pp. 68–69.
3 I. Drevin, L. Larsson, I. Eriksson and B.-L. Johansson, *J. Chromatogr.*, 514 (1990) 137.

4 K. Jones, *Chromatographia*, 25 (1988) 443.
5 B. Law and P. F. Chan, *J. Chromatogr.*, 467 (1989) 267.
6 N. T. Miller and J. M. DiBussolo, *J. Chromatogr.*, 499 (1990) 317.
7 M. J. J. Hetem, J. W. de Haan, H. A. Claessens, L. J. M. van de Ven and C. A. Cramers, *Anal. Chem.*, 62 (1990) 2288.
8 W. Richter and L. Kågedal, *Int. Arch. Allergy Appl. Immunol.*, 42 (1972) 887.
9 T. Scott and E. H. Melvin, *Anal. Chem.*, 25 (1953) 1656.
10 B.-L. Johansson and C. Ellström, *J. Chromatogr.*, 330 (1985) 360.
11 B.-L. Johansson and L. Åhsberg, *J. Chromatogr.*, 351 (1986) 136.
12 K. K. Unger and R. Janzen, *J. Chromatogr.*, 373 (1986) 227.
13 G. K. Sofer and L.-E. Nyström, *Process Chromatography*, Academic Press, London, 1989, pp. 93–105.
14 B.-L. Johansson, U. Hellberg and O. Wennberg, *J. Chromatogr.*, 403 (1987) 85.

Journal of Chromatography, 547 (1991) 31–44
Elsevier Science Publishers B.V., Amsterdam

CHROM. 23 194

Enantiomeric resolution of amino acid derivatives by high-performance liquid chromatography on chiral stationary phases derived from L-proline

C. DABAN HAUROU, G. DECLERCQ* and P. RAMIANDRASOA
École Supérieure de Chimie Organique et Minérale, 12 Rue Cassette, 75006 Paris (France)
and
J. L. MILLET
Prolabo, 12 Rue Pelée, 75011 Paris (France)
(First received February 20th, 1990; revised manuscript received February 8th, 1991)

ABSTRACT

The enantiomeric separation of a series of N-3,5-dinitrobenzoyl amino acid esters was investigated by normal-phase high-performance liquid chromatography on four chiral stationary phases (CSPs) derived from L-proline as chiral selector. The chiral selector was covalently bonded to silica gel by the use of either a spacer with a three (CSP1 and 2) or eleven (CSP3 and 4) carbon chain length. The protective groups were benzyloxycarbonyl or *tert.*-butoxycarbonyl. The natures of the protective group and the spacer were important for chiral recognition. A spacer with eleven carbons allows a better resolution of a large number of N-3,5-dinitrobenzoyl amino acid esters. The mobile phase can induce major changes in the behaviour of solutes, thus leading to better enantioselectivity.

INTRODUCTION

The preparation of chiral stationary phases (CSPs) for high-performance liquid chromatography (HPLC) with a large field of application is of great current interest. Wainer [1] classified CSPs according to the type of interaction, and CSPs derived from amino acids are among the most important, especially the Pirkle-type phases.

The aim of this work was the preparation of new CSPs in which the chiral selector is an amino acid. The structures of these CSPs are shown in Fig. 1. The original feature of these four CSPs is the use of the L-proline, which is generally used in ligand-exchange chromatography (LEC) [2–6]. In general, enantioselective adsorption can be described by the model introduced by Dalgliesh [7], which reduces chiral recognition to the reversible formation of diastereoisomeric complexes between the chiral group of the CSP and the adsorbed derivative. To be resolved, three types of interaction must occur, of which at least one must be stereochemically dependent. Two types of interactions exist (hydrogen bonding and lipophilic interaction), and the third (π–π interaction occurs owing to the protective group, *i.e.*, benzyloxycarbonyl; the *tert.*-butoxycarbonyl group involves steric hindrance. The protected amino acid is

0021-9673/91/$03.50

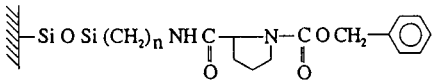

n=3 CBZ L PRO C_3 CSP_1

n=11 CBZ L PRO C_{11} CSP_3

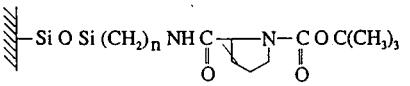

n=3 BOC L PRO C_3 CSP_2

n=11 BOC L PRO C_{11} CSP_4

Fig. 1. Structures of chiral stationary phases CSP1, 2, 3 and 4.

bonded to silica gel by a linear alkyl chain three or eleven carbons long. The latter, not so widely used, should reduce the 'matrix–chiral selector' interactions. The solutes studied were N-3,5-dinitrobenzoyl amino acid esters, which have been used by several workers [8–13].

In this paper, the preparation of these CSPs and solutes is described, then the influence of the amino acid, the spacer and the protective group on the retention and the selectivity is discussed. The study of different mobile phases is also described.

EXPERIMENTAL

Preparation of chiral stationary phases

Before grafting, the silica gel is activated by the method proposed by Engelhardt *et al.* [14]. A 3-g portion of silica gel is hydrated with 1 *M* hydrochloric acid at room temperature for 1.5 h, then dried at 120°C for 12 h.

N-Benzyloxycarbonyl (CBZ) and N-*tert.*-butoxycarbonyl (BOC) amino acids were obtained by the method of Bodansky and Bodansky [15] and Wunsch *et al.* [16]. The activation of the N-benzyloxycarbonyl amino acids was carried out by the method of Lloyd [17].

Benzyloxycarbonyl-L-proline N-hydroxysuccinimide ester (1): yield 100%; m.p. 90°C; ^{1}H NMR (C^2HCl_3), d: 2.0 (m, 4H), 2.7 (s, 4H), 3.5 (t, 2H), 4.5 (t, 1H), 5.2 (s, 2H), 7.5 (s, 5H).

tert.-Butyloxycarbonyl-L-proline N-hydroxysuccinimide ester (2): yield 91%; m.p. 136°C; ^{1}H NMR (C^2HCl_3), d: 1.4 (s, 9H), 2.0 (m, 4H), 3.5 (t, 2H), 4.5 (t, 1H).

Preparation of CSP1 and CSP3

The preparation of the silane was effected by the method of Engelhardt *et al.* [14].

(*S*)-2-({[3-(Trimethoxysilyl)propyl]amino}carbonyl)-1-pyrrolidinecarboxylic

acid benzyl ester (3): yield 40%; ^{1}H NMR (C^2HCl), d: 1.2–1.5 (m, 8H), 3.05–3.45 (m, 4H), 3.52 (m, 9H), 4.2–4.4 (broad, 1H), 5.15 (s, 2H), 6.0–6.7 (m, 1H), 7.3 (s, 5H).

(*S*)-2-({[3-(trimethoxysilyl)propyl]amino}carbonyl)-1-pyrrolidinecarboxylic acid 1,1-dimethylethyl ester (4): yield 87%; ^{1}H NMR(C^2HCl_3), d: 0.5–1.0 (m, 4H), 1.5 (s, 9H), 2.0 (m, 6H), 3.0–3.5 (m, 2H), 3.6 (s, 9H), 4.2 (t, 1H), 7.0 (broad, 1H).

The reaction with the silane and silica gel was performed by suspending the silane in 50 ml of dry toluene, adding the silica (2 g) and refluxing for 16 h with stirring. The stationary phase was subsequently extensively washed with methanol and water.

Hydrolysis of methoxy groups and end-capping were performed by the method proposed by Engelhardt *et al.* [14].

CBZ-L-Pro-C_3 (CSP1): C10.50, H1.50, N1.50%, 0.53 mmol of chiral selector per gram of silica (based on N).

BOC-L-Pro-C_3 (CSP2): N1.65; 0.59 mmol of chiral selector per gram of silica (based on N).

Preparation of CSP2 and CSP4

10-Undecenamide and the 1-amino-10-undecene were obtained by the method of Dobashi and Hara [18].

To prepare the silane, a mixture of 19.5 mmol of 1 or 2 and 200 ml of dry acetonitrile was cooled to 0°C, followed by the addition of a mixture of 1-amino-10-undecene (21.4 mmol), and triethylamine (21.4 mmol) in 50 ml of acetonitrile. The mixture was stirred for 1.5 h at 0°C, then 500 ml of ethyl acetate and 300 ml of water were added. The layers were separated and the organic layer was washed with water, 1.5 *M* HCl and saturated $NaHCO_3$ and dried over Na_2SO_4. The solvent was evaporated and the residue was purified by flash chromatography on silica gel with hexane–acetone (75:25) as eluent.

(*S*)-2-{[(10-undecenyl)amino]carbonyl}-1-pyrrolidinecarboxylic acid benzyl ester (5): yield 99%; m.p. 64°C; ^{1}H NMR(C^2HCl_3), d: 1.35 (s, 14H), 1.8–2.4 (m, 6H), 3.03–3.3 (q, 2H), 3.3–3.6 (t, 2H), 4.2 (s, 2H), 5.5–6.1 (m, 1H), 6.1–6.9 (m, 1H, exchangeable with ^2H_2O), 7.3 (s, 5H).

(*S*)-2-{[(10-undecenyl)amino]carbonyl}-1-pyrrolidinecarboxylic acid 1,1-dimethylethyl ester (6): yield 58%; ^{1}H NMR (C^2HCl_3), d: 1.25 (s, 14H), 1.45 (s, 9H), 2.0 (m, 6H), 3.0–3.55 (m, 4H), 4.0–4.3 (m, 1H), 4.7–7.15 (m, 2H), 5.4–6.1 (m, 1H), 6.2–6.8 (m, 1H, exchangeable).

The chlorosilanes (7 and 8) were obtained by the method of Dobashi [18] and used directly, without purification, for the reaction with silica and end-capping.

CBZ-L-Pro-C_{11} (CSP3): C8.54, H1.45, N0.70%; 0.25 mmol of chiral selector per gram of silica (based on N).

BOC-L-Pro-C_{11} (CSP 4): C8.67, H1.60, N0.90%; 0.32 mmol of chiral selector per gram of silica (based on N).

Preparation of solutes

A mixture of 10 mmol of 3,5-dinitrobenzoyl chloride, 8 mmol of amino acid and 20 ml of 1 *M* NaOH was stirred for 1 h at room temperature, then acidified to pH 2 with 1 *M* HCl. The product was recrystallized from ethanol–water (1:1). Esterification was performed by the method of Boissonas [19]. All compounds showed the expected analytical and spectroscopic data (m.p., ^{1}H NMR).

Chromatographic conditions

Chromatography was carried out with a Jasco Trirotar VI equipped with a Jasco DG 3510 degasser (Prolabo, Paris, France). A Jasco Uvidec 100-VI variable wavelength UV detector (Prolabo) was used. The CSPs were packed into 150 × 4 mm I.D. stainless-steel columns by the classical slurry technique at 450 bar using acetone as the pumping solvent [20].

Solutes were injected at a concentration of 10^{-3} mol/l using a Rheodyne loop injector (20 μl) (Prolabo), at a flow-rate of 0.8 ml/min at room temperature.

The solvents 2,2,4-trimethylpentane (2,2,4-TMP, Rathburn, Walkerburn, U.K.), isopropanol and methylene chloride (Prolabo) were of an analytical-reagent grade.

The elution order of enantiomers was determined by the injection of the racemic mixture with an excess of L-enantiomer.

TABLE I

STRUCTURES OF THE N-3,5-DINITROBENZOYL AMINO ACID DERIVATIVES

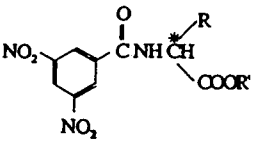

No.	Abbreviation[a]	R	R'
1a	3,5-DNB-Phe-Ala-OMe	$CH_2C_6C_5$	CH_3
1b	3,5-DNB-Phe-Ala-OEt		C_2H_5
1c	3,5-DNB-Phe-Ale-OiPr		$CH(CH_3)_2$
2a	3,5-DNB-Phe-Gly-OMe	C_6H_5	CH_3
2b	3,5-DNB-Phe-Gly-OEt		C_2H_5
2c	3,5-DNB-Phe-Gly-OiPr		$CH(CH_3)_2$
3a	3,5-DNB-Val-OMe	$CH(CH_3)_2$	CH_3
3b	3,5-DNB-Val-OEt		C_2H_5
3c	3,5-DNB-Val-OiPr		$CH(CH_3)_2$
4a	3,5-DNB-Nor-Val-OMe	$(CH_2)_2CH_3$	CH_3
4b	3,5-DNB-Nor-Val-OEt		C_2H_5
4c	3,5-DNB-Nor-Val-OiPr		$CH(CH_3)_2$
5a	3,5-DNB-Leu-OMe	$CH_2CH(CH_3)_2$	CH_3
5b	3,5-DNB-Leu-OEt		C_2H_5
5c	3,5-DNB-Leu-OiPr		$CH(CH_3)_2$
6a	3,5-DNB-Iso-Leu-OMe	$CH(C_2H_5)CH_3$	CH_3
6b	3,5-DNB-Iso-Leu-OEt		C_2H_5
6c	3,5-DNB-Iso-Leu-OiPr		$CH(CH_3)_2$
7a	3,5-DNB-Nor-Leu-OMe	$(CH_2)_3CH_3$	CH_3
7b	3,5-DNB-Nor-Leu-OEt		C_2H_5
7c	3,5-DNB-Nor-Leu-OiPr		$CH(CH_3)_2$
8a	3,5-DNB-Pro-OMe	$(CH_2)_3$	CH_3
8b	3,5-DNB-Pro-OEt		C_2H_5
8c	3,5-DNB-Pro-OiPr		$CH(CH_3)_2$
9a	3,5-DNB-Ala-OMe	CH_3	CH_3
9b	3,5-DNB-Ala-OEt		C_2H_5
9c	3,5-DNB-Ala-OiPr		$CH(CH_3)_2$

[a] Me = methyl; Et = ethyl; iPr = isopropyl.

RESULTS AND DISCUSSION

The structures of the N-3,5-DNB racemates are shown in Table I. All these CSPs permit the separation of a large number of solutes. A comparison of the retentions and selectivities for the solutes obtained on the different CPSs with different mobile phases was made, and the influence of the mobile phase and of the polar modifier was studied.

First, some general statement on the retention and selectivity for all of the solutes can be made regardless of the CSPs and the mobile phase used, namely, an increase in the size of the ester group (methyl, ethyl) or in the branching (isopropyl) leads to a decrease in the capacity factor, k' (Fig. 2). Also, an increase in the linear chain length (Ala, NVal, NLeu) of the amino acid leads to a decrease in k' (Figs. 3 and 4), as expected in normal-phase HPLC. Further, solutes which have the same configuration as the CSPs are more retained.

The 'three-point' attractive interactions model [7] has been widely used as the basis of a chiral recognition model. Several workers have shown that the interactions between the solute and the CSP do not have to be all attractive. A model based on two attractive interactions [21,22] or even one [23] could be sufficient to achieve resolution.

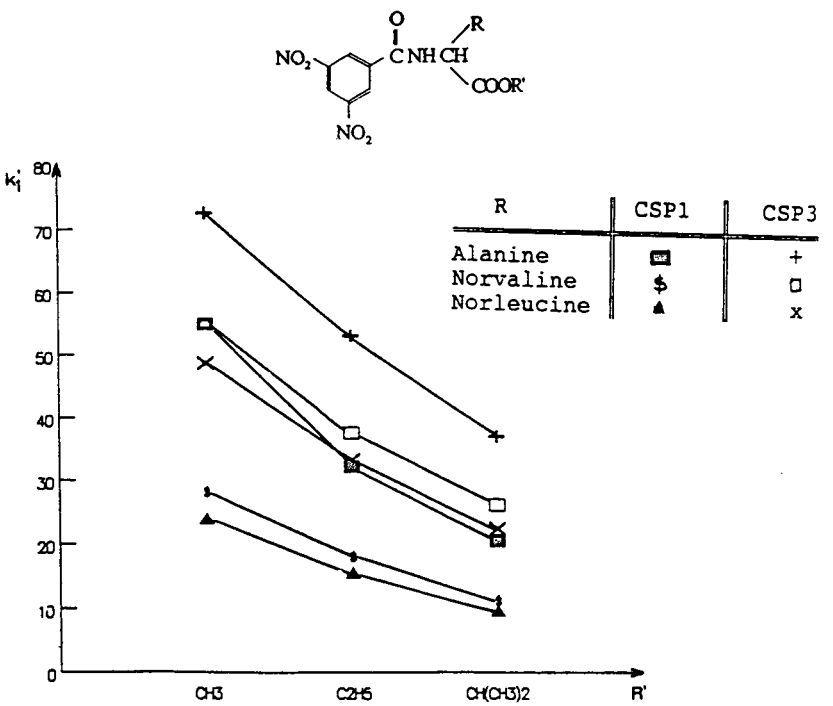

Fig. 2. Influence of the nature of the R' substituent group of N-3,5-DNB-α-amino acid esters on the capacity factor, k'_1, of the first enantiomer eluted, on CSP1 and CSP3. Mobile phase, isooctane–methylene chloride (90:10); flow-rate 0.8 ml/min; UV detection at 254 nm.

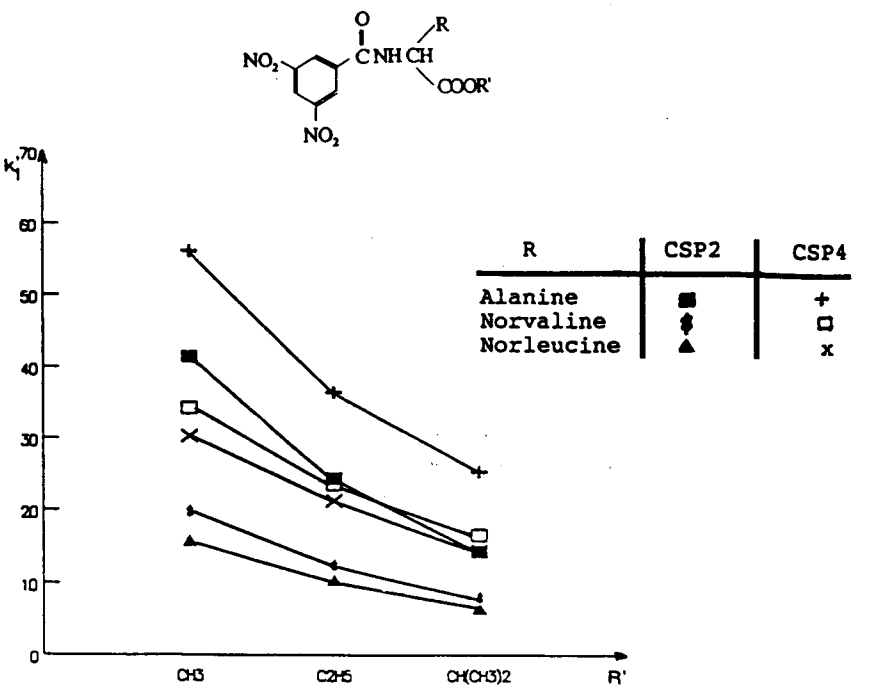

Fig. 3. Influence of the nature of the R′ substituent group of N-3,5-DNB-α-amino acid esters on the capacity factor, k'_1, of the first enantiomer eluted, on CSP2 and CSP4. Conditions as in Fig. 1.

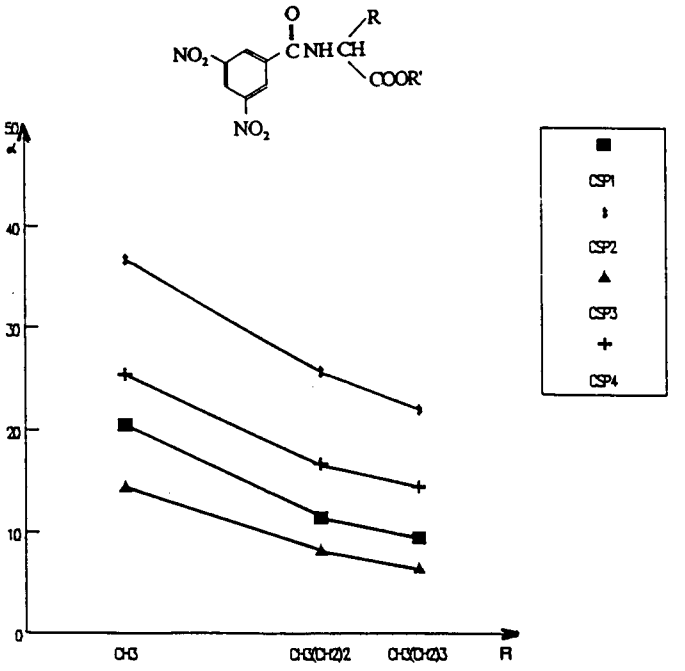

Fig. 4. Influence of the nature of the R substituent group of N-3,5-DNB-α-amino acid esters on the capacity factor, k'_1, of the first enantiomer eluted on the CSPs 1–4. Conditions as in Fig. 1.

TABLE II

ENANTIOMERIC RESOLUTION OF N-3,5-DINITROBENZOYL PHENYLALANINE ESTERS ON CSP3 AND CSP4 USING METHYLENE CHLORIDE AS POLAR MODIFIER

Mobile phase, isooctane–methylene chloride (90:10); flow-rate, 0.8 ml/min; room temperature; UV detection at 254 nm. k'_2 is the capacity factor of the second-eluted enantiomer, $k'_2 = (t_{r_2} - t_0/t_0)$, where t_{r_2} is the retention of the last-eluted enantiomer and t_0 the retention of a non-retained solute. The selectivity, α, between two enantiomers is the ratio of their respective capacity factors (k'_1/k'_2).

Solute	CSP3			CSP4		
	k'_1	k'_2	α	k'_1	k'_2	α
Phe-Ala:						
1a	69.00	77.17	1.12	38.72	40.80	1.05
1b	48.14	54.43	1.13	28.03	29.55	1.05
1c	33.79	38.42	1.14	20.20	21.32	1.05

The results indicate that the chiral recognition mechanism is based on both attractive and steric interactions. The elution order of the enantiomers is not affected by changes in the structure of the CSP or the solute or in the composition of the mobile phase. These results indicate that the chiral recognition mechanism is similar for all four CSPs.

It is not necessary to have interactions to obtain resolution of the racemates but, in general, their presence increases the enantioselectivity by stabilizing the solute–CSP complex (Table II), as stressed by Wainer and Alembik [24]. In the present instance, the blocking agent of the CSP plays only a secondary role in obtaining resolution. Fig. 5 shows the hydrogen bonding, dipole–dipole and steric interactions involved in the chiral recognition mechanism.

Tables IV–IX show that the ester moiety does not play a significant role in the chiral recognition mechanism. The predominant steric interactions seem to occur at the chiral centre of the CSP.

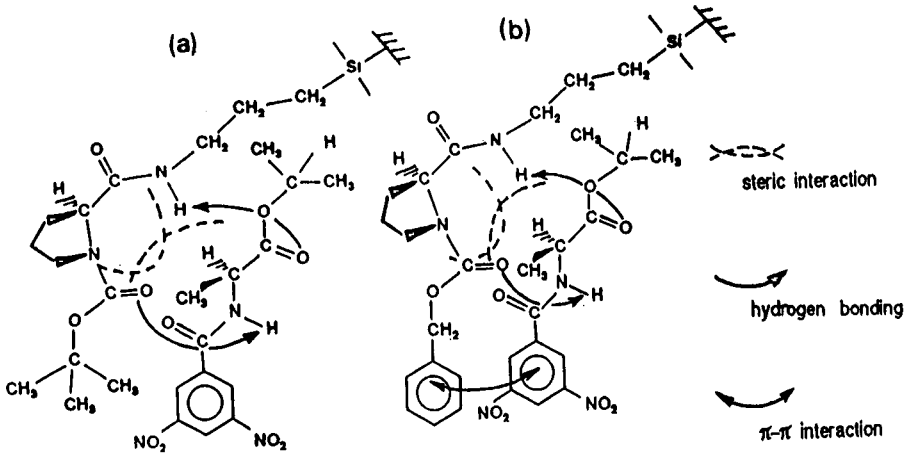

Fig. 5. Proposal chiral recognition model for the isopropyl ester of N-3,5-dinitrobenzoylalanine (**9c**) on (a) CSP2 and (b) CSP1. The most strongly retained enantiomer is represented.

Influence of the mobile phase

The use of methylene chloride or isopropanol, which are defined as a strong dipole and proton acceptor, respectively, (Table III) by Snyder [25] according to the Rohrschneider solubility data (26), leads to different results: the capacity factors are greater when methylene chloride is used although it has a larger polarity ($P'_{2,2,4\text{-TMP/2-PrOH}} = 17.6$, $P'_{2,2,4\text{-TMP/CH}_2\text{Cl}_2} = 40$). This increase in retention generally leads to an increase in the separation factor.

TABLE III

SELECTIVITY PARAMETERS AS DEFINED AND CALCULATED BY SNYDER [25] ACCORDING TO ROHRSCHNEIDER'S DATA [26]

The values in italics indicate the dominant character of the polar modifier; X_e (proton acceptor), X_d (proton donor), X_n (strong dipole), P' (polarity).

Polar modifier	X_e	X_d	X_n	P'
Isopropanol	*0.55*	0.19	0.27	3.90
Methylene chloride	0.29	0.18	*0.53*	3.10

It seems possible to relate the dominant character of each modifier with its ability to favour hydrogen bonding or dipole–dipole interactions. However, solvation or the conformation of both the solute and the CSP are affected by a change in the polar modifier.

The chiral recognition mechanism involves the establishment of dipole–dipole interactions and hydrogen bonding. These interactions do not seem to play an equivalent role in the chiral recognition mechanism.

The use of methylene chloride instead of isopropanol leads to an increase in the separation factor. Isopropanol, because of its proton acceptor character, could interact preferentially with the NH moieties of the CSP and the solute. Hence the solute–CSP interactions are less important, which leads to a decrease in the separation factor.

On the other hand, methylene chloride tends to reduce dipole–dipole interactions between the solute and the CSP but as already mentioned, an increase in the separation factor occurred. This leads to the conclusion that the predominant interaction is hydrogen bonding in the chiral recognition mechanism. Nevertheless, dipole–dipole interactions are fairly important.

It has been demonstrated that the use of 1,2-ethylene chloride [which is a weaker dipole ($X_n = 0.49$) than methylene chloride] instead of methylene chloride leads to an increase in the separation factor [27]. Similar results have been observed by other workers with different CSPs and solutes and an inversion of the elution order of enantiomers has been reported [28].

Influence of the structure of the solutes

The ester group and the alkyl chain of the amino acid are the two main parameters of the structure of the solutes. It is difficult to interpret the variations in the separation factor, α, in terms of the size of the ester group. In general, α is constant or increases slightly when a methyl group is replaced with an ethyl or an isopropyl

TABLE IV

ENANTIOMERIC RESOLUTION OF N-3,5-DINITROBENZOYL AMINO ACID ESTERS ON DIFFERENT CHIRAL STATIONARY PHASES USING ISOPROPANOL AS POLAR MODIFIER

Mobile phase: isooctane–isopropanol (98:2); other conditions as in Table II.

Solute	CSP1			CSP3			CSP2			CSP4		
	k'_1	k'_2	α	k'_1	k'_2	α	k'_1	k'_2	α	k'_1	k'_2	α
Ala:												
9a	36.96	42.49	1.15	27.63	29.95	1.08	14.20	15.54	1.09	21.33	22.17	1.04
9b	20.53	23.25	1.13	20.43	22.40	1.09	8.85	9.55	1.08	14.75	15.25	1.03
9c	16.24	18.28	1.13	17.71	19.57	1.10	6.14	6.50	1.06	11.33	11.83	1.04
Nor-Val:												
4a	20.01	20.68	1.03	19.45	20.84	1.07	7.66	8.15	1.06	16.16	–	1.00
4b	12.33	12.89	1.04	14.33	15.39	1.07	5.17	5.43	1.06	10.37	–	1.00
4c	9.25	9.69	1.05	11.81	12.81	1.08	3.81	–	1.00	7.73	–	1.00
Nor-Leu:												
7a	17.15	–	1.00	19.74	20.90	1.06	6.55	6.99	1.07	14.77	–	1.00
7b	11.62	–	1.00	13.77	14.71	1.07	4.43	4.66	1.05	10.95	–	1.00
7c	7.88	–	1.00	10.47	11.24	1.07	3.33	–	1.00	6.95	–	1.00

group. Isopropyl is a bulkier group than ethyl and is significantly larger than methyl, and exerts a greater degree of conformational control. An exception can be noted on CSP2 (Tables IV and V). The diastereoisomeric complexes are less stable; this difference in stability could be due to the steric hindrance of the protective group.

The esters of N-3,5-DNB-leucine have higher k' values than the esters of N-3,5-DNB-valine, but the valine derivatives are better separated. The k' value measures the overall affinity of a compound for the stationary phase. If the compound has a

TABLE V

ENANTIOMERIC RESOLUTION OF N-3,5-DINITROBENZOYL AMINO ACID ESTERS ON DIFFERENT CHIRAL STATIONARY PHASES USING METHYLENE CHLORIDE AS POLAR MODIFIER

Mobile phase: isooctane–methylene chloride (90:10); other conditions as in Table II.

Solute	CSP1			CSP3			CSP2			CSP4		
	k'_1	k'_2	α	k'_1	k'_2	α	k'_1	k'_2	α	k'_1	k'_2	α
Ala:												
9a	54.94	63.95	1.16	72.54	81.11	1.12	41.25	45.83	1.11	56.03	59.26	1.06
9b	31.96	37.17	1.16	52.89	59.65	1.13	24.43	26.95	1.10	36.50	39.14	1.07
9c	20.43	23.62	1.16	36.91	41.95	1.13	14.42	15.71	1.09	25.39	27.33	1.08
Nor-Val:												
4a	28.48	31.72	1.08	54.90	61.06	1.11	20.15	21.98	1.09	34.19	35.97	1.05
4b	18.33	19.93	1.09	37.30	41.91	1.12	12.79	13.93	1.09	23.68	25.13	1.06
4c	11.45	12.43	1.08	25.93	29.04	1.12	8.29	8.85	1.07	16.72	17.90	1.07
Nor-Leu:												
7a	23.88	24.94	1.04	48.50	53.72	1.11	15.68	17.18	1.09	30.28	31.77	1.05
7b	15.33	16.18	1.05	33.04	36.82	1.11	10.41	11.34	1.09	21.41	22.70	1.06
7c	9.49	10.09	1.06	22.26	24.99	1.12	6.51	6.99	1.07	14.54	15.57	1.07

TABLE VI

ENANTIOMERIC RESOLUTION OF N-3,5-DINITROBENZOYL AMINO ACID ESTERS ON DIFFERENT CHIRAL STATIONARY PHASES USING ISOPROPANOL AS POLAR MODIFIER

Mobile phase: isooctane–isopropanol (98:2); other conditions as in Table II.

Solute	CSP1			CSP3			CSP2			CSP4		
	k'_1	k'_2	α	k'_1	k'_2	α	k'_1	k'_2	α	k'_1	k'_2	α
Val:												
3a	15.37	16.96	1.10	14.59	16.40	1.12	6.50	7.16	1.09	10.78	11.41	1.06
3b	10.32	11.37	1.10	10.54	11.86	1.12	4.29	4.60	1.07	7.55	8.00	1.06
3c	7.55	8.29	1.10	7.86	8.86	1.13	3.19	–	1.00	5.67	6.00	1.06
Leu:												
5a	16.48	–	1.00	18.10	18.98	1.05	6.86	7.08	1.03	14.40	–	1.00
5b	11.25	–	1.00	13.37	14.09	1.05	4.88	–	1.00	10.49	–	1.00
5c	8.47	–	1.00	10.14	10.77	1.06	3.59	–	1.00	7.28	–	1.00
Pro:												
8a	11.62	–	1.00	11.39	–	1.00	5.12	–	1.00	10.32	–	1.00
8b	8.41	–	1.00	8.34	–	1.00	3.23	–	1.00	6.78	–	1.00
8c	6.10	–	1.00	6.21	–	1.00	2.24	–	1.00	4.87	–	1.00

high affinity for the stationary phase, its enantiomers are more likely to be separated [29,30]; an example is given in Tables IV and V with the retention and resolution of linear alkyl chain derivatives. However, this is not always true, as can be seen with the compounds valine and leucine, mentioned at the beginning of this paragraph (Tables VI and VII). A longer retention leads to a better enantiomeric resolution if, and only if, the enantiomeric retention mechanisms are dominant. If, on the other hand, the dominant retention mechanisms are not enantioselective, then an increase in the

TABLE VII

ENANTIOMERIC RESOLUTION OF N-3,5-DINITROBENZOYL AMINO ACID ESTERS ON DIFFERENT CHIRAL STATIONARY PHASES USING ISOPROPANOL AS POLAR MODIFIER

Mobile phase: isooctane–methylene chloride (90:10); other conditions as in Table II.

Solute	CSP1			CSP3			CSP2			CSP4		
	k'_1	k'_2	α	k'_1	k'_2	α	k'_1	k'_2	α	k'_1	k'_2	α
Val:												
3a	16.13	18.37	1.14	29.63	34.57	1.17	10.87	12.23	1.12	18.74	20.30	1.08
3b	10.33	11.79	1.14	18.81	23.20	1.17	6.52	7.22	1.11	12.73	13.86	1.09
3c	6.70	7.60	1.13	14.26	16.65	1.17	4.44	4.81	1.08	9.55	10.66	1.12
Leu:												
5a	30.79	–	1.00	68.14	75.46	1.11	23.35	24.79	1.06	–	–	–
5b	20.71	21.48	1.04	44.92	49.81	1.11	14.65	15.46	1.05	27.89	29.55	1.06
5c	13.36	13.97	1.05	32.27	36.16	1.12	9.92	10.33	1.04	20.33	21.40	1.05
Pro:												
8a	4.90	–	1.00	7.62	–	1.00	4.38	–	1.00	4.82	–	1.00
8b	3.51	–	1.00	5.71	–	1.00	2.58	–	1.00	3.11	–	1.00
8c	2.56	–	1.00	4.05	–	1.00	1.76	–	1.00	2.34	–	1.00

retention will not affect the enantiomeric resolution [31]. In this event, the valine derivative is better resolved.

As has been mentioned previously, the steric hindrance at the chiral centre seems to play an important role in the chiral recognition mechanism. The relative steric hindrance for the α-position of the chiral centre is more pronounced for the valine than for the leucine derivatives, and this could explain the increase in the separation factor. An example of a separation is given in Fig. 6.

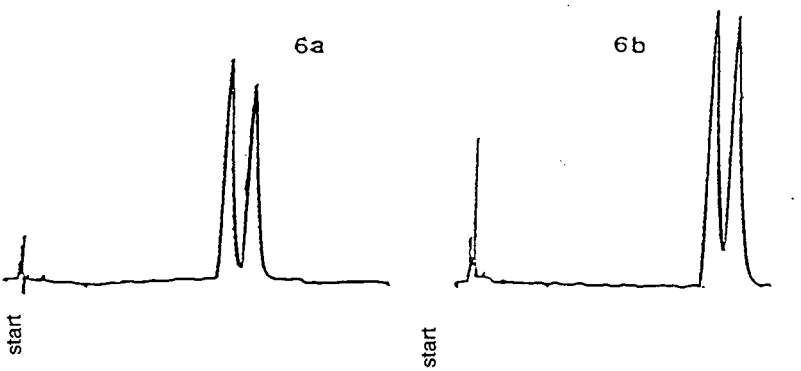

Fig. 6. Examples of separations of (a) the methyl ester of N-3,5-dinitrobenzoylvaline and (b) the isopropyl ester of N-3,5-dinitrobenzoylalanine.

The phenylalanine derivatives are well resolved with either CSP1, 3 or 4 when methylene chloride is used, whereas the phenylglycine derivatives are never resolved (Tables VI and VII). These results are in a good agreement with the literature [9] for the separation of these derivatives on different types of phases. If this difference in the separation factor for phenylalanine and phenylglycine derivatives is due to steric hindrance at the chiral centre, this would indicate that the relative steric bulk at the chiral centre is more important with a benzyl ring than a phenyl ring.

The behaviour of the derivatives of proline is unusual (Tables VIII and IX). It is

TABLE VIII

ENANTIOMERIC RESOLUTION OF N-3,5-DINITROBENZOYL AMINO ACID ESTERS ON DIFFERENT CHIRAL STATIONARY PHASES USING ISOPROPANOL AS POLAR MODIFIER

Mobile phase: isooctane–isopropanol (98:2); other conditions as in Table II.

Solute	CSP1			CSP3			CSP2			CSP4		
	k'_1	k'_2	α	k'_1	k'_2	α	k'_1	k'_2	α	k'_1	k'_2	α
Phe-Ala:												
1a	42.95	43.92	1.01	39.34	42.77	1.09	11.60	–	1.00	24.74	–	1.00
1b	27.26	28.51	1.05	27.41	29.96	1.09	7.43	–	1.00	16.37	–	1.00
1c	18.92	19.92	1.05	19.29	21.21	1.10	5.05	–	1.00	11.68	–	1.00
Phe-Gly:												
2a	34.84	–	1.00	27.72	–	1.00	10.88	–	1.00	20.68	–	1.00
2b	24.32	–	1.00	20.19	–	1.00	7.21	–	1.00	18.00	–	1.00
2c	15.24	–	1.00	17.39	–	1.00	5.05	–	1.00	11.53	–	1.00

TABLE IX

ENANTIOMERIC RESOLUTION OF N-3,5-DINITROBENZOYL AMINO ACID ESTERS ON DIFFERENT CHIRAL STATIONARY PHASES USING METHYLENE CHLORIDE AS POLAR MODIFIER

Mobile phase: isooctane–methylene chloride (90:10); other conditions as in Table II.

Solute	CSP1			CSP3			CSP2			CSP4		
	k'_1	k'_2	α	k'_1	k'_2	α	k'_1	k'_2	α	k'_1	k'_2	α
Phe-Ala:												
1a	39.46	42.21	1.07	69.00	77.17	1.12	19.83	21.08	1.06	38.72	40.81	1.05
1b	24.25	26.22	1.08	48.14	54.43	1.13	12.95	13.65	1.05	28.03	29.55	1.05
1c	17.18	18.61	1.08	33.79	38.72	1.14	9.29	–	1.00	20.20	21.32	1.05
Phe-Gly:												
2a	36.57	–	1.00	60.14	–	1.00	18.42	–	1.00	33.17	–	1.00
2b	23.21	–	1.00	44.71	–	1.00	12.96	–	1.00	23.17	–	1.00
2c	15.41	–	1.00	29.57	–	1.00	8.35	–	1.00	16.84	–	1.00

the only case where the capacity factor decreases when methylene chloride is used instead of isopropanol. The non-resolution of these derivatives (**8a, 8b** and **8c**) could be due to the absence of a hydrogen atom on the nitrogen. Several workers have given the same explanation. Thus, Lloyd [17], who studied a phase derived from (*R*)-phenylglycyl-(*S*)-α-naphthylethylamide, reported the lack of resolution for the methyl ester of N-3,5-dinitrobenzoylproline whatever the mobile phase used [hexane–isopropanol (90:10), hexane–methylene chloride (80:20 or 60:40)].

Hara and Dobashi [32] observed the same phenomena by testing the isopropyl ester of N-4-nitrobenzoylproline in normal-phase HPLC on silica gel with a chiral selector (N-acetyl-L-valine-*tert.*-butylamide) in the mobile phase.

Dobashi *et al.* [33] also reported the lack of resolution of the isopropyl ester of N-4-nitrobenzoylproline on a diamide phase. Berndt and Krüger [34] observed the same results for the isopropyl ester of N-3,5-dinitrobenzoylproline on CBZ-D-phenylglycine and BOC-D-phenylglycine. More recently, Kuropka *et al.* [35] reported the lack of resolution of these derivatives on a phase grafted with acryloyl-D-phenylglycylpropylamide.

The results in Tables II–IX demonstrate that the performance of a given CSP is determined not only by the structure of the resolving agent or the blocking agent, but also by the connecting arm. An example is given by the resolution of the derivatives of isoleucine (**6a, 6b** and **6c**), which are resolved into four diastereoisomers on CSP3, whereas only one peak is observed on CSP1 (Table X). Nevertheless, no calculation of α was made as the four pure diastereoisomers were not available.

The use of the connecting arm has not been elucidated; depending on the blocking group employed, the use of a spacer with a C_{11} alkyl chain usually involves an increase in the separation factor in comparison with its C_3 homologue for phases with a benzyloxycarbonyl group (CSP3 and CSP1), whereas a slight decrease is observed when using CSP4 instead of CSP2. Hence it seems that the spacer interferes with the chiral recognition mechanism by altering the relative importance of phenomena that occur during the process of the separation.

The influence of the connecting arm has been studied by other workers and it is

TABLE X

ENANTIOMERIC RESOLUTION OF N-3,5-DINITROBENZOYL ISOLEUCINE ESTERS ON CSP1 AND CSP3 USING ISOPROPANOL AS POLAR MODIFIER

Mobile phase: isooctane–isopropanol (98:2) other conditions as in Table II.

Solute	CSP1:	CSP3			
	k'_1	k'_1	k'_2	k'_3	k'_4
6a	11.62	12.81	13.81	14.09	14.91
6b	8.41	9.26	9.82	Shoulder	10.66
6c	6.10	6.98	7.37	7.76	7.97

clear that the connecting arm plays a role in the chiral recognition mechanism; the spacer could induce a change in the dominant character of the chiral recognition mechanism, leading eventually to an inversion of the elution order of enantiomers [9].

CONCLUSIONS

CSPs derived from L-proline permit the separation of π-acid dinitrobenzoyl racemates. The use of a spacer with a long alkyl chain allows a better enantioselectivity. The organic modifiers contained in the mobile phase have a great influence on the resolution. NMR studies of bimolecular solute–CSP and solute–solvent complexes would be useful means of elucidating the chiral recognition process, as they would also take into account the contribution of the solvent.

ACKNOWLEDGEMENT

The authors express their thanks to Professor A. M. Siouffi (Marseille) for helpful advice.

REFERENCES

1 I. W. Wainer, *A Practical Guide to Selection and Use of HPLC Chiral Stationary Phases*, J. T. Baker, Phillipsburg, NJ, 1988.
2 G. Gubitz, W. Jellenz, G. Lofler and W. Santi, *J. High. Resolut. Chromatogr. Chromatogr. Commun.*, 2 (1979) 145.
3 P. Roumeliotis, K. K. Unger, A. A. Kurganov and V. A. Davankov, *Angew. Chem.*, 21 (1982) 930.
4 I. A. Yamskov, B. B. Berezin, V. A. Dankov, Y. A. Zolotarev, I. N. Dostevalov and N. F. Myasoedov, *J. Chromatogr.*, 217 (1981) 539.
5 W. Lindner, *Naturwissenschaften*, 67 (1980) 354.
6 A. Foucault, M. Caude and L. Oliveros, *J. Chromatogr.*, 185 (1979) 345.
7 C. E. Dalgliesh, *J. Chem. Soc.*, (1952) 3940.
8 W. H. Pirkle and C. J. Welch, *J. Org. Chem.*, 49 (1984) 138.
9 W. H. Pirkle, M. H. Hyunn and B. Bank, *J. Chromatogr.*, 316 (1984) 585.
10 N. Oi, M. Nagase and T. Doi, *J. Chromatogr.*, 257 (1983) 111.
11 N. Oi, M. Nagase, Y. Inda and T. Doi, *J. Chromatogr.*, 259 (1983) 487.
12 N. Oi, M. Nagase, Y. Inda and T. Doi, *J. Chromatogr.*, 265 (1983) 111.
13 N. Oi and H. Kitahara, *J. Chromatogr.*, 265 (1983) 117.

14 H. Engelhardt, T. Konig and St. Kromidas, *Chromatographia*, 21 (1985) 205.
15 M. Bodansky and A. Bodansky, *The Practice of Peptides Synthesis*, Springer, New York, 1984.
16 E. Wunsch, W. Graf, O. Keller and G. Wersin, *Commun. Synth.*, (1986) 958.
17 M. Lloyd, *J. Chromatogr.*, 351 (1986) 219.
18 Y. Dobashi and S. Hara, *J. Org. Chem.*, 52 (1987) 2490.
19 A. Boissonas, *Helv. Chim. Acta*, 38 (1955) 1491.
20 B. Coq, C. Gonnet and J. L. Rocca, *J. Chromatogr.*, 106 (1975) 249.
21 C. H. Lochmuller and R. R. Ryall, *J. Chromatogr.*, 150 (1978) 511.
22 A. Dobashi and S. Hara, *J. Chromatogr.*, 267 (1983) 11.
23 C. H. Lochmuller, J. M. Harris and R. W. Souter, *J. Chromatogr.*, 71 (1972) 405.
24 I. W. Wainer and M. C. Alembik, *J. Chromatogr.*, 367 (1986) 59.
25 R. Snyder, *J. Chromatogr. Sci.*, 16 (1978) 223.
26 R. Rohrschneider, *Anal. Chem.*, 45 (1973) 1241.
27 C. Daban Haurou, G. Declercq, J. L. Millet and P. Ramiandrasoa, unpublished results.
28 P. Macaudiere, M. Lienne, M. Caude, R. Rosset and A. Tambuté, *J. Chromatogr.*, 467 (1989) 357.
29 W. H. Pirkle, D. W. House and J. M. Finn, *J. Chromatogr.*, 192 (1980) 143.
30 W. H. Pirkle and T. C. Pochapsky, *Chromatographia*, 25 (1988) 652.
31 R. E. Boehm, D. E. Martire and D. W. Armstrong, *Anal. Chem.*, 60 (1988) 522.
32 S. Hara and Y. Dobashi, *Anal. Chem.*, 55 (1983) 2815.
33 A. Dobashi, Y. Dobashi, K. Kinoshita and S. Hara, *Anal. Chem.*, 60 (1988) 1985.
34 H. Berndt and G. Krüger, *J. Chromatogr.*, 348 (1985) 275.
35 R. Kuropka, B. Muller, H. Hocker and H. Berndt, *J. Chromatogr.*, 481 (1989) 380.

Journal of Chromatography, 547 (1991) 45–58
Elsevier Science Publishers B.V., Amsterdam

CHROM. 23 193

Applicability of new chiral stationary phases in the separation of racemic pharmaceutical compounds by high-performance liquid chromatography

F. A. MARIS*, R. J. M. VERVOORT and H. HINDRIKS
AKZO Pharma Division, Organon International BV, Analytical R&D, P.O. Box 20, 5340 BH Oss (Netherlands)
(First received November 5th, 1990; revised manuscript received January 24th, 1991)

ABSTRACT

The potential of contemporary chiral liquid chromatographic columns for the enantioseparation of racemates of pharmaceutical compounds was studied. Sixteen Organon compounds were selected, mostly cardiovascular or CNS-active drugs. Seven chiral stationary phases were used, *viz.*, five different cellulose derivatives, an α_1-acid glycoprotein and a polymethacrylate phase, all coated on silica particles. A good enantioseparation, with a resolution higher than 1.0, was achieved for fifteen of the sixteen racemates. The best results were obtained on a Chiralcel OJ column, on which seven enantiomers were separated. With respect to the chromatographic performance, stability and/or selectivity, the cellulose derivatives (Chiralcel columns) were preferred over the protein and polymethacrylate columns.

INTRODUCTION

A large number of drugs have one or more asymmetric centres. Mostly, these drugs are applied as their racemic mixtures in a pharmaceutical formulation. This procedure is justifiable in cases where both enantiomers have similar activity or where they enhance each other's activity. In some instances, however, one of the enantiomers is inactive and can be considered as being redundant. Moreover, enantiomers can have different biological activities and there are cases in which one of the enantiomers shows a more or less pronounced toxic effect [1,2].

Mostly, liquid chromatography (LC) [1–5] is used for the separation of enantiomers. Experimentally, chiral LC can be divided into two groups [1]: (1) a chiral stationary phase (CSP) with a non-chiral mobile phase and (2) a non-chiral stationary phase with a chiral additive in the mobile phase. In practice, chiral additives are less often used than chiral stationary phases because the equilibration times are longer, there are maintenance problems with the equipment and in preparative applications the chiral additives have to be removed after the isolation.

A few years ago, ten commercially available CSPs were tested in our laboratory on ten Organon compounds. The results obtained at that time could be summarized as follows: (i) CSP columns are expensive and suffer from poor stability; (ii) the low

0021-9673/91/$03.50

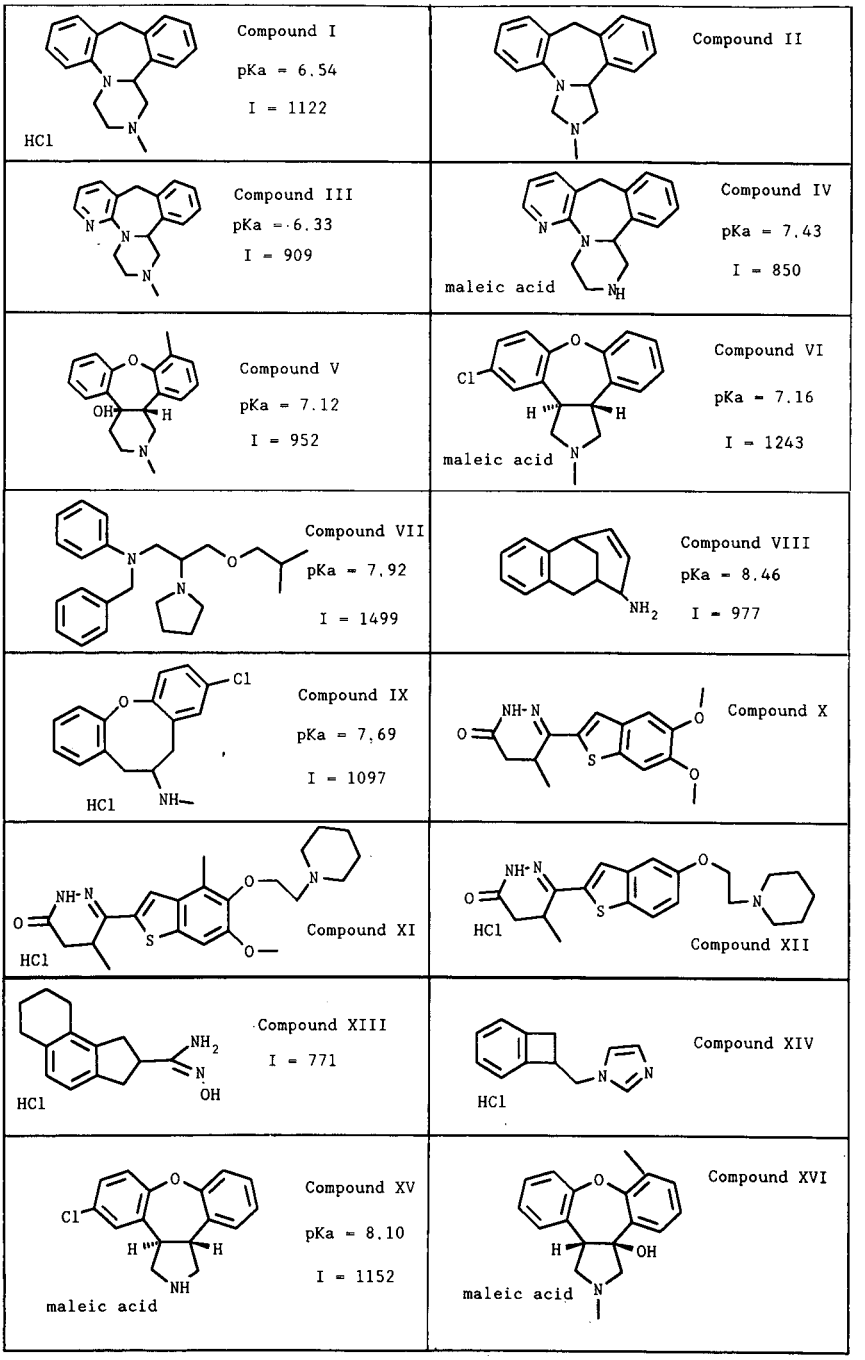

Fig. 1. Structures of the selected Organon compounds and pK_a values and retention indices (I).

efficiency of CSP columns results in broad peaks, which severely affects a reliable determination of the optical purity of an enantiomer; and (iii) owing to the low loadability of CSP columns, chiral chromatography lacks wide applicability on a preparative scale.

Subsequently, many improvements have been made to CSPs, *e.g.*, the coating of cellulose derivatives on 10-μm silica particles (Chiralcel) [6,7] and a new generation of α_1-acid glycoprotein columns (CHIRAL-AGP). Additionally, we tested a recent poly(triphenylmethyl methacrylate) column (Chiralpak OT). In this paper, we report a follow-up study in which sixteen racemic Organon compounds were chromatographed on seven different chiral columns.

EXPERIMENTAL

Chemicals and test compounds

The test compounds (Fig. 1) were synthesized by Organon (Oss, Netherlands). Freshly distilled methanol and Milli-Q purified water were used. Disodium hydrogenphosphate ($Na_2HPO_4 \cdot 12H_2O$) and ethanol were obtained from J. T. Baker (Deventer, Netherlands) and *n*-hexane (extra pure), 2-propanol, diethylamine (for synthesis) and phosphoric acid were obtained from Merck (Darmstadt, Germany).

The pH values of the buffers were measured before dilution with the organic modifiers. The buffers were prepared by dissolving 3.6 g of $Na_2HPO_4 \cdot 12H_2O$ in 1000 ml of water. Concentrated H_3PO_4 was added until the desired pH value was reached.

Apparatus and materials

The chromatographic experiments were carried out on an HP1090M liquid chromatograph, equipped with an HP1040M diode-array detector. Data were collected on an HP7999A HPLC workstation (Hewlett-Packard, Amstelveen, Netherlands).

All CSP materials were obtained as prepacked columns supplied by J. T. Baker. The CSPs used are listed in Table I.

TABLE I

CHIRAL LC COLUMNS USED

Name	Type	Dimensions
Chiralcel OB	Cellulose ester	250 × 4.6 mm I.D.; 10 μm
Chiralcel OC	Cellulose carbamate	250 × 4.6 mm I.D.; 10 μm
Chiralcel OD	Cellulose carbamate	250 × 4.6 mm I.D.; 10 μm
Chiralcel OF	Cellulose carbamate	250 × 4.6 mm I.D.; 10 μm
Chiralcel OJ	Cellulose carbamate	250 × 4.6 mm I.D.; 10 μm
CHIRAL-AGP	α_1-Acid glycoprotein	100 × 4.0 mm I.D.; 5 μm
Chiralpak OT	Poly (triphenylmethyl methacrylate)	250 × 4.6 mm I.D.; 10 μm

TABLE II

RESULTS OF SCREENING EXPERIMENTS

Hex = *n*-hexane; 2-PrOH = 2-propanol; EtOH = ethanol; CH_3OH = methanol; DEA = diethylamine.

Compound No.	Chiralcel																					CHIRAL-AGP: 2-PrOH–0.01 *M* Na_2HPO_4 (1:9) (pH 7.4)			Chiralpak OT					
	OB						OC						OD: Hex–2-PrOH (9:1)			OF: Hex–2-PrOH (9:1)			OJ: Hex–2-PrOH (9:1)						CH_3OH			CH_3OH–0.1% (v/v) DEA		
	Hex–2-PrOH (9:1)			EtOH			Hex–2-PrOH (9:1)			EtOH																				
	k'_1	R	α	k'_1	R	α	k'_1	R	α	k'_1	R	α	k'_1	R	α	k'_1	R	α	k'_1	R	α	k'_1	R	α	k'_1	R	α	k'_1	R	α
I	0.3	0	1	0.2	0	1	0.3	0.57	1.16	0.2	0	1	0.5	0.77	1.10	0.3	0	1	0.3	4.40	2.13	18.9	0.63	1.10	9.2	[c]			–	
II	1.2	0.73	1.56	0.4	2.38	1.73		n.d.			n.d.			n.d.		1.1	4.41	1.57	1.2	0.77	1.09		n.d.		3.2	0.99	1.33	0.9	0.94	1.51
III	0.5	0	1	0.2	0	1	0.9	0.93	1.19	0.3	1.05	1.38	0.8	3.28	1.33	1.2	0.91	1.11	0.4	0	1	8.0	0.53	1.08	5.7	1.18	1.36	0.8	1.24	2.55
IV		–[a]			n.d.[b]			–		1.2	[c]		1.9	0	1	6.0	[c]		1.2	[c]		8.0	1.60	1.18		–		0.8	[c]	
V		–		0.1	0	1	1.5	0	1	0.3	0	1	0.6	1.05	1.13	1.4	1.40	1.18	0.5	1.06	1.19	5.8	0.98	1.11		–			–	
VI	1.0	0	1	0.2	0	1	0.7	0	1	0.5	0	1	0.4	0	1	0.5	1.08	1.18	0.3	1.27	1.28	25.7	0	1		–			–	
VII		–		0.2	0	1		–		0.4	0	1		–			–			–			–			–			–	
VIII				1.4	0	1		–		3.5	0	1	1.2	0	1	1.5	[c]		1.2	6.24	1.72	4.5	0	1	5.2	0	1		–	
IX	0.8	0	1	0.2	0	1	0.6	0	1	0.4	0	1	0.4	0	1	0.5	0	1	0.4	2.22	1.37	12.5	0.66	1.09		–			–	
X		–		1.0	2.12	1.46		–		2.5	2.36	1.30		–			–			–		2.2	1.02	1.20	0.5	0.74	1.20	0.3	1.01	1.31
XI		–		0.4	0	1		–		2.8	2.71	1.66		–			–			–		13.8	[c]			–		0.9	0.88	1.15
XII		–		0.5	[c]			–		3.2	2.03	1.42		–			–			–		10.8	0	1		–		0.6	1.32	1.31
XIII		–		0.1	0	1		–			n.d.			–			–			–		3.1	3.55	2.00	1.7	0	1		–	
XIV		–		0.5	[c]			–			n.d.		2.0	0	1	2.8	1.18	1.18	0.9	1.29	1.24	24.5	0.76	1.09		–			–	
XV		–		0.1	0	1	1.1	0	1		n.d.		0.6	1.47	1.17	0.8	3.59	1.61	0.3	1.56	1.35	10.8	5.11	2.03		–			–	
XVI		–		0.2	0	1		–			n.d.			–			–			n.d.		3.3	0	1	0.9	0	1		–	
$R>1.0$		0			2			0			4			3			5			7			4			1			3	
$R>1.5$		0			2			0			3			1			2			4			3			0			0	

[a] Compounds do not elute within 30 min.

[b] N.d., no data available.

[c] Compounds start to separate.

Standard LC conditions

Chiralpak OT column

A flow-rate of 1.0 ml/min, an injection volume of 10 μl and a column temperature of 15°C were used. Methanol was used as the eluent and UV detection was carried out at 210 nm. Samples of about 1 mg/ml dissolved in methanol were injected.

Chiralcel columns

A flow-rate of 1.0 ml/min, an injection volume of 2–10 μl and a column temperature of 50°C were used. Hexane–2-propanol (9:1), 2-propanol or ethanol was used as the eluent and UV detection was carried out at 210 nm. Samples of about 1 mg/ml dissolved in *n*-hexane or ethanol were injected.

CHIRAL-AGP column

A flow-rate of 1.0 ml/min, an injection volume of 2–10 μl and a column temperature of 30°C were used. 2-Propanol–buffer (pH 7.0 or 3.8) (1:9) was used as the eluent. UV detection was carried out at 210 nm and samples of about 1 mg/ml dissolved in ethanol were injected.

Calculations

The tailing factor (*Tf*), *i.e.*, the peak asymmetry, was calculated at 5% of the peak height using the ratio of the widths of the rear and front sides of a peak.

RESULTS AND DISCUSSION

The aim of this study was to explore the potential of seven chiral LC columns for the separation of the enantiomers of sixteen selected compounds. The strategy for method development was as follows. In first instance a mobile phase composition recommended by the manufacturer was selected. With this mobile phase, all test compounds were screened. Subsequently, for some of the compounds which were not separated or which only started to separate, an optimization of the separation was carried out.

Screening of chiral LC columns

Chiralpak OT

The results of the screening experiments, using methanol as mobile phase, are summarized in Table II. It was found that most compounds were not eluted within 30 min. Of the seven compounds that were eluted, three were well separated, but none with a resolution larger than 1.5. The Chiralpak OT column showed a reasonable selectivity for the three compounds but a poor efficiency. For example, the chromatogram obtained for compound III had a broad first peak and an even broader second peak. The plate numbers were only about 400. Therefore, a reliable determination of the enantiomeric purity was impossible.

Chiralcel

Five of the eight commercially available Chiralcel columns were selected. This selection was based on the similarity of our compounds with compounds already separated and the number of separations shown in manuals and the literature [6–12].

The Chiralcel columns were initially tested using hexane–2-propanol (9:1) as the mobile phase. As an alternative, ethanol is recommended. The screening results are summarized in Table II.

Chiralcel OB and OC gave poor results with hexane–2-propanol. Most of the compounds were not eluted within 30 min, and only for one compound was a slight separation seen. When ethanol was used the retention decreased drastically. This means that the step from hexane–2-propanol (9:1) to ethanol is large with respect to the optimization of the retention.

The third column tested was Chiralcel OD using only hexane–2-propanol as the mobile phase. In this instance 56% of the compounds eluted with k'_1 values less than 2. Compared with Chiralcel OB and OC, this CSP showed better results. Four enantiomers were separated, three of which with a resolution larger than 1.0.

The Chiralcel OF column separated five of the racemates with a resolution larger than 1.0, for two of them larger than 1.5. Using hexane–2-propanol (9:1) six compounds did not elute within 30 min.

The best results were obtained with the Chiralcel OJ column. Seven of the racemates were separated with a resolution larger than 1.0, for four of them larger than 1.5. The best results were obtained for compounds I and VIII with resolutions of 4.4 and 6.2, respectively. As an illustration, the separation of compound VIII is shown in Fig. 2.

Of the sixteen Organon compounds, all the tetracyclic compounds, except compound IV, as well as compounds X, XI and XII were well separated on at least one of the five Chiralcel columns. Most of the compounds which were not separated at all have clearly deviating structures.

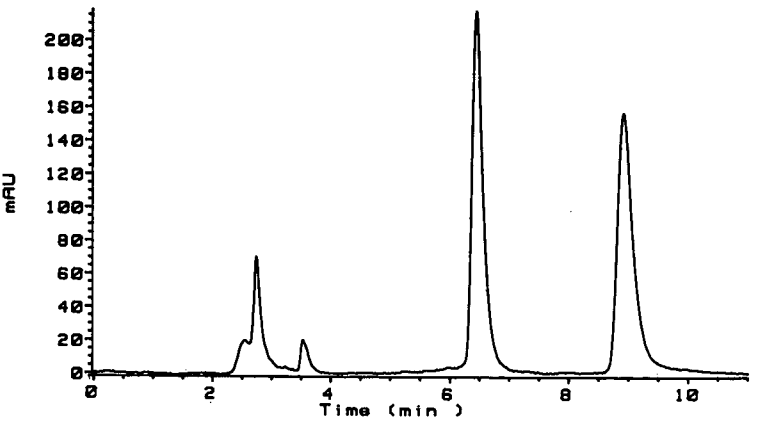

Fig. 2. Chromatogram of the separation of compound VIII on a Chiralcel OJ column. Eluent, hexane–2-propanol (9:1, v/v).

CHIRAL-AGP

The use of an immobilized α_1-acid glycoprotein as CSP is well known. Several applications with this CSP have been published [4,13]. With the CHIRAL-AGP column, we separated four of the compounds with a resolution larger than 1.0 (see Table II).

Although the results are promising, the peak shapes and the tailing factors on the AGP phase were clearly worse than those on the Chiralcel columns. As an example, the separation of compound XIII is shown in Fig. 3.

Optimization studies

When a separation obtained under the screening conditions is not satisfactory or when the compounds have too high retentions, the chromatography can be optimized. One way to do this is by changing the mobile phase composition. Also, diethylamine can be added as a tailing-suppressing agent and finally the column temperature can be varied.

Chiralpak OT

Addition of 0.1% (v/v) of diethylamine to the mobile phase, in order to decrease the silanol activity, resulted in a decrease in the retention for six compounds. This indicates clearly that the Chiralpak OT column has some (residual) silanol activity. However, for four compounds the retention increased. An explanation for this phenomenon has not been found. It was also observed that whenever the retention decreased on adding diethylamine, the separation of the enantiomers improved (Table II).

With compound III, addition of diethylamine did not result in an improvement in the peak shapes but it reduced the retention (see Fig. 4). However, for the separations of compounds X, XI and XII two sharp peaks were obtained using diethylamine. The plate counts were about 2500.

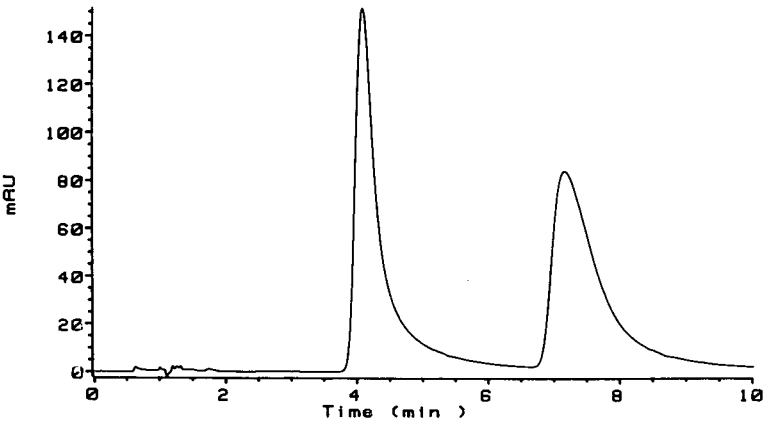

Fig. 3. Chromatogram of the separation of compound XIII on a CHIRAL-AGP column. Eluent, 2-propanol–0.01 *M* Na_2HPO_4 (pH 7.0) (1:9, v/v).

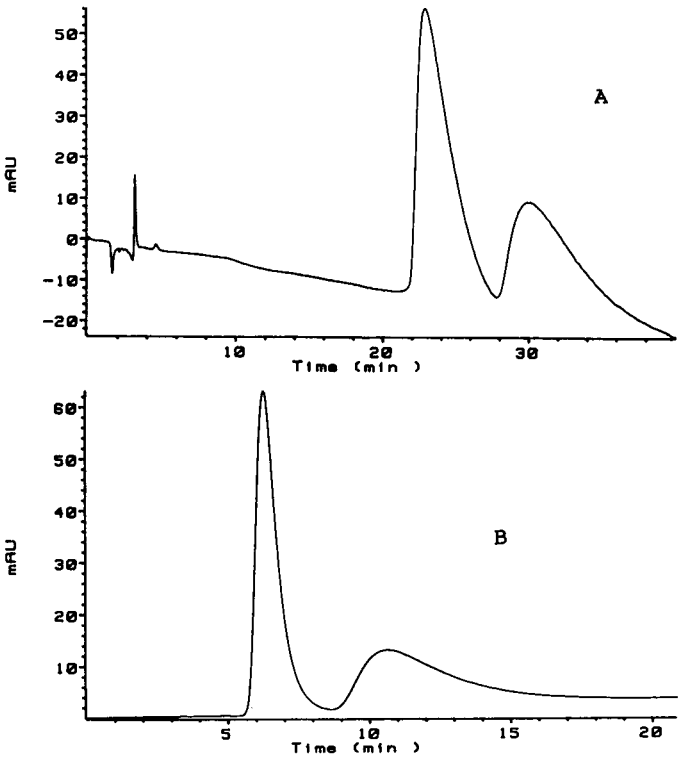

Fig. 4. Chromatogram of the separation of compound III on a Chiralpak OT column (A) without and (B) with the addition of 0.1% (v/v) of diethylamine. Eluent, methanol.

In order to reduce the retention of the test compounds, 4% of dichloromethane was added to the methanol. Although acceptable separations ($R \approx 0.7$) were obtained for the apolar compounds VI and VII, this approach was not used further. It turned out that dichloromethane drastically reduced the column lifetime.

Chiralcel

Influence of column temperature. Contrary to findings in the literature [14–16], we observed on several occasions with ethanol and also hexane–2-propanol mobile

TABLE III

INFLUENCE OF COLUMN TEMPERATURE ON RESOLUTION (R), SELECTIVITY (α), CAPACITY FACTOR (k'_1) OF THE FIRST-ELUTING ENANTIOMER, PLATE NUMBER (N) AND TAILING FACTOR (Tf) FOR THE SEPARATION OF COMPOUND X ON A CHIRALCEL OC COLUMN

Temperature (°C)	R	α	k'_1	N	Tf
30	1.94	1.20	5.1	2540	1.21
40	2.54	1.24	4.2	3380	1.18
50	3.29	1.29	3.3	4439	1.23

phases that the resolution improved when the column temperature was raised. A typical example is given in Table III. A temperature of 50°C was considered optimum, especially as at that point the stationary phase starts to strip off slowly when ethanol is used. Because of the good chromatographic effects 50°C was maintained throughout our screening experiments.

We believe that structural effects can give, at least partly, an explanation of the temperature effect. The rigid part of the molecules studied have 2–4 coupled ring structures which acquire more flexibility at higher temperatures and, therefore, fit better in the cavities. On the other hand, the molecules reported in the literature [14–16] have flexible cyclic groups which are not connected together. It is thought that the fit of these independent groups is optimum at low(er) temperatures.

Varying the content of 2-propanol. In chromatography a capacity factor of 5 is considered to give optimum resolution in a reasonable time. The effect of varying the 2-propanol content in order to obtain better k' values is well illustrated in Fig. 5. With respect to resolution the optimum situation for compound V is attained with hexane–2-propanol (96:4). Further, the peaks of compound V are sharp and show almost no tailing. Surprisingly, with pure hexane as mobile phase the peaks of compound V were clearly broader. A large tailing factor of about 5 and only 500 plates were obtained.

Sometimes hexane–2-propanol (1:1) or even 100% 2-propanol had to be used in order to decrease the retention. This is illustrated in Table IV for compounds XI and XII. A high selectivity was obtained with symmetrical peaks but the use of pure 2-propanol resulted in very broad peaks. For these compounds the results on Chiralcel with ethanol as mobile phase were slightly better (Table II).

Influence of mobile phase additives. As the silica particles are not completely covered during the coating with the stationary phase, residual silanol groups can interact with the solutes. An example is compound IV, where the interaction of the

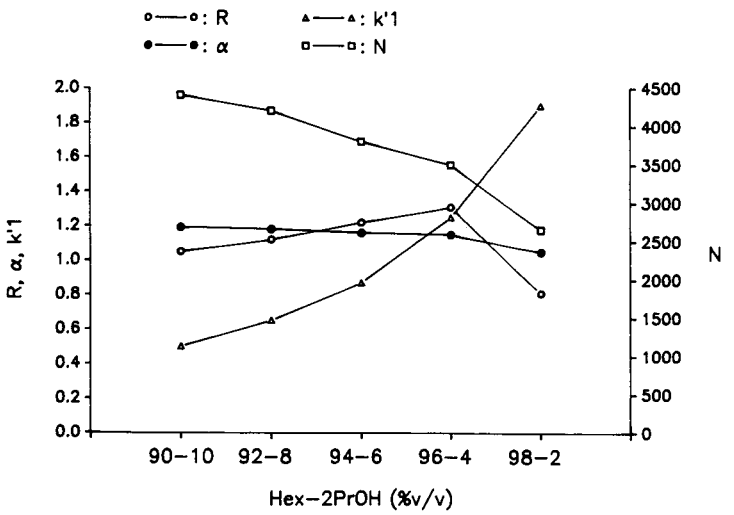

Fig. 5. Influence of the percentage of 2-propanol on (○) resolution (R), (●) selectivity (α), (△) capacity factor (k'_1) and (□) plate numbers (N) for the separation of compound V on a Chiralcel OJ column.

TABLE IV

CHROMATOGRAPHIC DATA FOR COMPOUNDS XI AND XII ON CHIRALCEL OF USING 2-PROPANOL AS MOBILE PHASE

Compound	R	α	k'_1	N	Tf
XI	2.68	1.81	1.6	854	1.18
XII	1.70	1.37	2.1	1006	1.14

secondary N atom in the non-aromatic ring with free silanols results in broad tailing peaks (Fig. 6A). Addition of 0.1% of diethylamine (DEA) as a silanol suppressor leads to sharper, symmetrical peaks and a decrease in the retention time. A further increase in DEA concentration resulted in only marginal improvements.

Viscosity. It was concluded that the plate numbers varied widely with the mobile phase composition. With respect to the plate numbers, we considered that it is desirable to use a viscosity as low as possible. This is also of advantage for the column back-pressure. For these reasons it is preferred to add ethanol instead of 2-propanol to the mobile phase in order to reduce the retention. It is interesting that reducing the content of 2-propanol in hexane–2-propanol mixtures below 2% or using pure etha-

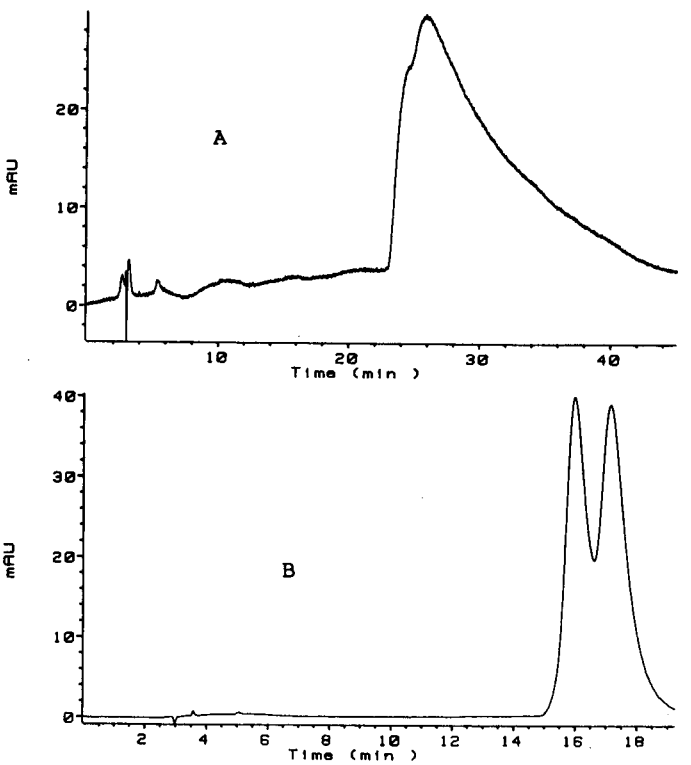

Fig. 6. Chromatograms of compound IV on a Chiralcel OC column (A) without and (B) with the addition of 0.1% (v/v) of diethylamine. Eluent, hexane–2-propanol (9:1, v/v).

nol as the mobile phase results in more tailing. Therefore, it seems advisable always to use between 2 and 10% of 2-propanol.

Stability of the stationary phase. It was found that with ethanol at 50°C the stationary phase is slowly stripped off. This was established from elevation of the background UV signal. The effect is not very serious, but after a few weeks of continuous use a slight increase in silanol activity, measured by an increase in peak tailing, could be observed. However, in comparison with our experiences with other chiral stationary phases, the Chiralcel columns are very stable.

CHIRAL-AGP

Influence of type of modifier and pH of buffer. To determine the influence of the type of modifier at a pH of 7.0, three different modifiers (2-propanol, ethanol and methanol) were selected. The results are summarized in Table V. The mobile phase composition was modifier–0.01 *M* Na_2HPO_4 (pH 7.0) (1:9, v/v). It is obvious that 2-propanol is the strongest eluent and methanol the weakest. The best separations were obtained with 2-propanol.

Under standard conditions compound VII was still retained and did not elute within 30 min. Lowering the pH to 3.8 and thus making the molecule more polar decreased the retention drastically. As is seen in Table VI, this is a general and expected effect. However, it might also result in a complete loss of resolution, as demonstrated for compound V. The effect of the amount of modifier at pH 3.8 is shown in Table VII for 2-propanol. The expected decrease in retention is seen when the amount of modifier is increased. As a result, the resolution is also decreased (almost lost).

Finally, the column temperature can be varied. In Table VIII this is shown for the mobile phase 2-propanol–0.01 *M* Na_2HPO_4 (pH 3.8) (3:97, v/v). The temperature influences the retention and separation in such a way that a low temperature increases the retention and improves the separation. The latter aspect suggests that the separation mechanism for this series of compounds is completely different from that of Chiralcel columns.

Summarizing the results on a CHIRAL-AGP column, we obtained a separation of ten racemates with a resolution larger than 0.5. Two compounds (VII and XIII) were separated on the AGP column and not on the Chiralcel columns. Further, for

TABLE V

EFFECT OF THE TYPE OF MODIFIER ON THE CHROMATOGRAPHIC PERFORMANCE OF A CHIRAL-AGP COLUMN WITH MODIFIER–0.01 *M* Na_2HPO_4 (pH 7.0)/(1:9, v/v) AS ELUENT

Compound	2-Propanol			Ethanol			Methanol		
	k'_1	R	α	k'_1	R	α	k'_1	R	α
V	5.8	0.98	1.11	11.1	0.68	1.08	–		
VII	–[a]			–			–		
XI	13.8	[b]		22.6	0	1	–		
XII	10.8	0	1	16.1	0	1	–		

[a] Compounds do not elute within 30 min.
[b] Compounds start to separate.

TABLE VI

INFLUENCE OF THE TYPE OF MODIFIER AT pH 3.8 USING A CHIRAL-AGP COLUMN WITH MODIFIER–0.01 *M* Na_2HPO_4 (pH 3.8) (1:9, v/v) AS ELUENT

Compound	2-Propanol			Ethanol		
	k'_1	R	α	k'_1	R	α
V	0.8	0	1	0.5	0	1
VII	1.4	[a]		2.9	1.10	1.29
XI	0.9	[a]		1.3	[a]	
XII	0.7	0	1	0.9	[a]	

[a] Compounds start to separate.

compounds IV and XVI a better separation was obtained on the AGP than on a Chiralcel column.

Relationship between structure and performance on Chiralcel columns

Various attempts have been made to elucidate the mechanism of chiral recognition for CSPs [11,17–19]. The aim here is not to develop a recognition model, but to show how sensitive a separation is towards changes in a molecule. As an illustration, we selected four structurally related tetracyclic drugs from the sixteen compounds studied measured under the screening conditions (Table IX). Examination of the table in either a horizontal or a vertical way shows the differences in separation. On the one hand, it implies that the separation of new compounds is still based on trial and error. On the other, it can be concluded, also from Table II, that for almost all the compounds studied a suitable CSP can be found. In our case it was most profitable to start with Chiralcel OJ. This finding is supported by the number of applications published in the literature [6,8]. Also in the application notes from Daicel [9,10] the Chiralcel OJ and OD columns are most often successful. Further, we studied the relationship between pK_a values and peak tailing, and between the retention index,

TABLE VII

INFLUENCE OF THE AMOUNT OF 2-PROPANOL AT pH 3.8 USING A CHIRAL-AGP COLUMN

Compound	Amount of 2-propanol (%)								
	3			6			10		
	k'_1	R	α	k'_1	R	α	k'_1	R	α
V	0.6	0	1	0.4	0	1	0.8	0	1
VII	7.0	1.53	1.40	2.4	1.06	1.27	1.4	[a]	
XI	2.1	0.57	1.18	1.2	0.37	1.18	0.9	[a]	
XII	1.5	0	1	0.9	0	1	0.7	0	1

[a] Compounds start to separate.

TABLE VIII

INFLUENCE OF COLUMN TEMPERATURE USING A CHIRAL-AGP COLUMN WITH 2-PROPANOL–0.01 *M* Na_2HPO_4 (pH 3.8) (3:97, v/v) AS ELUENT

Compound	30°C			40°C			50°C		
	k'_1	R	α	k'_1	R	α	k'_1	R	α
V	0.6	0	1	0.4	0	1	0.5	0	1
VII	7.0	1.53	1.40	5.1	1.53	1.35	3.8	1.36	1.29
XI	2.1	0.57	1.18	1.5	[a]		1.2	0	1
XII	1.5	0	1	1.1	0	1	0.9	0	1

[a] Compounds start to separate.

which is a measure of the polarity [20], and retention on the Chiralcel columns. Also in these cases there are no clear correlations. For example, the pK_a value of compound IV is clearly lower than that of compound VIII (see Fig. 1). However, the tailing of compound IV is much larger. The retention mechanism is also interesting. Increasing the polarity of the mobile phase reduces the retention times, which is comparable to effects in normal-phase chromatography. However, a non-polar compound such as VII does not elute at all. It is clear that more study is needed to clarify the retention and separation mechanism.

TABLE IX

RELATIONSHIP BETWEEN STRUCTURE AND SEPARATION

Basic structure of the compounds selected:

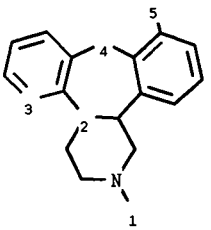

Compound	Structural elements					Chiralcel CSP[a]				
	1	2	3	4	5	OB	OC	OD	OF	OJ
I	CH_3	N	CH	CH_2	H	−	+/−	+/−	−	+
III	CH_3	N	N	CH_2	H	−	+/−	+	+/−	−
IV	H	N	N	CH_2	H	−	+/−	−	+/−	+/−
V	CH_3	C–OH	CH	O	CH_3	−	−	+	+	+

[a] −, resolution is 0; +/−, resolution between 0 and 1; +, resolution larger than 1.

CONCLUSIONS

The enantioselectivity of the Chiralcel columns is excellent for most test compounds, particularly for the tetracyclic compounds. The columns showed good separation efficiency, acceptable plate numbers and symmetrical peaks. The results with these columns were much better than those obtained so far. Although some stripping of the mobile phase was observed, the performance of the columns was not reduced markedly over a long period.

The enantioselectivity of the α_1-acid glycoprotein column is also very good, probably even better than that of a Chiralcel OJ column. The stability of the column is better than that of the first-generation AGP columns. During the experiments we did not observe a decrease in column performance. However, the separation efficiency is still low and tailing peaks are often obtained. This hampers a reliable determination of the optical purity of an enantiomeric compound. The results obtained in this study are also not much better than the results obtained earlier.

The new Chiralpak OT column did not show an improvement in enantioseparation compared with previous columns. Most compounds were not eluted with methanol. For those compounds which were eluted, the separation was not as good as on the Chiralcel columns. The peak shapes were poor and, compared with the Chiralcel columns, the plate numbers were low.

Comparing Chiralcel, CHIRAL-AGP and Chiralpak columns, the Chiralcel columns showed the best results. With respect to selectivity all three types of columns are very suitable. The best results were obtained on a Chiralcel OJ and a CHIRAL-AGP column. Overall it can be concluded that for most compounds, *viz.* fifteen of the sixteen test compounds, a good separation method is available.

REFERENCES

1 S. G. Allenmark, *Chromatographic Enantioseparation: Methods and Applications*, Ellis Horwood, Chichester, 1988.
2 R. W. Stouter, *Chromatographic Separation of Stereoisomers*, CRC Press, Boca Raton, FL, 1985.
3 V. A. Davankov, *Chromatographia*, 27 (1989) 474.
4 A. Metha, *J. Chromatogr.*, 426 (1988) 1.
5 H. Karnes and M. Sarkar, *Pharm. Res.*, 4 (1987) 285.
6 M. Ching, M. Lennard, A. Gregory and G. Tucker, *J. Chromatogr.*, 497 (1989) 313.
7 I. Okamoto, Y. Yuki, H. Namikoshi and Y. Toga, *Chromatographia*, 19 (1984) 280.
8 P. Camilleri, C. Dykes, S. Paknoham and L. Senior, *J. Chromatogr.*, 498 (1990) 414.
9 *Application Guide for Chiral Column Selection*, Daicel Chemical Industries, Tokyo, 1989.
10 *Crownpak, Chiralpak and Chiralcel, Chiral HPLC Columns for Optical Resolution*, Daicel Chemical Industries, Tokyo, 1989.
11 Y. Okamoto, R. Aburatani and K. Hatada, *J. Chromatogr.*, 389 (1987) 95.
12 Y. Okamoto, M. Kawashima and K. Hatada, *J. Chromatogr.*, 363 (1986) 173.
13 J. Hermansson, *J. Chromatogr.*, 298 (1984) 67.
14 H. Y. Aboul-Enein and M. R. Islam, *J. Chromatogr.*, 511 (1990) 109.
15 H. Y. Aboul-Enein and M. R. Islam, *J. Chromatogr. Sci.*, 28 (1990) 307.
16 M. Rudolph, *J. Chromatogr.*, 525 (1990) 161.
17 T. Shibata, I. Okamoto and K. Ishii, *J. Liq. Chromatogr.*, 9 (1986) 313.
18 I. Wainer and M. Alembik, *J. Chromatogr.*, 85 (1986) 385.
19 I. Wainer, R. Stiffin and T. Shibata, *J. Chromatogr.*, 411 (1987) 139.
20 J. K. Baker and C. Y. Ma, *J. Chromatogr.*, 169 (1979) 107.

Journal of Chromatography, 547 (1991) 59–68
Elsevier Science Publishers B.V., Amsterdam

CHROM. 23 225

Chromatographic liquid–liquid ternary phase system with permethylated β-cyclodextrin as chiral additive

MARIA PAWŁOWSKA* and JANUSZ LIPKOWSKI
Institute of Physical Chemistry, Polish Academy of Sciences, Kasprzaka 44, PL 01-224 Warsaw (Poland)
(First received June 26th, 1989; revised manuscript received February 14th, 1991)

ABSTRACT

An enantioselective liquid–liquid high-performance liquid chromatography system based on ternary systems with limited miscibility and chiral additives which are concentrated in the stationary liquid, is proposed, tested and characterized. Enantiomers of different types of compounds were used to probe enantioselectivity of the system. Conditions at which the partition mechanism of the chromatographic separations may be assumed are given and proven experimentally. The water–ethanol–2,2,4-trimethylpentane system at 25°C was used with permethylated β-cyclodextrin as the chiral additive.

INTRODUCTION

The ternary liquid–liquid systems with limited miscibility introduced and developed by Huber and co-workers [1–5] have proved to be of importance in high-performance liquid chromatography (HPLC). In a series of papers [3–6] it has been demonstrated that from the point of view of variation of capacity factor range and selectivity, reproducibility of retention characteristics and long-term stability of chromatographic columns the ternary systems are advantageous over other partition systems.

The principle of the idea may be seen in Fig. 1 representing the phase diagram of the water–ethanol–2,2,4-trimethylpentane system at 25°C. A mixture of a gross composition falling within the range of limited miscibility (L) splits into two liquid phases, one of which is water-rich (and thus "polar") while the other is a hydrocarbon-rich phase ("apolar"). The advantage of using such a system is that by choosing appropriate gross compositions one may modify the "polarity" of the liquid phases being in equilibrium, and in this way one may control the selectivity of the system.

The immiscible ternary phases could be used as liquid phases in partition chromatography. The partition system can be created by one of two methods: by the conventional way [2] or by the "solvent-generated" technique [3–6].

In the conventional method the solid support is coated with the stationary phase before column is packed, or the stationary liquid is injected into the column in the eluent stream.

In the solvent-generated phase technique, one of the liquid phases of the

0021-9673/91/$03.50

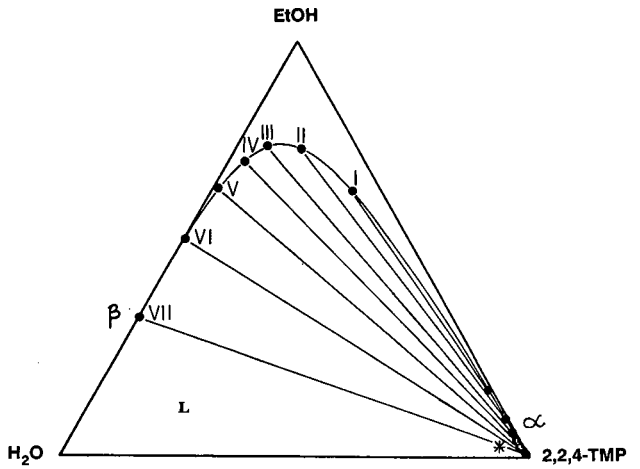

Fig. 1. Triangular phase diagram of the ternary system consisting of water–ethanol–2,2,4-trimethylpentane at 25.0 ± 0.1°C [2]; β = water-rich phase; α = water-poor phase, ✳ = gross composition.

liquid–liquid systems is used as eluent. The corresponding second liquid phase is spontaneously generated on the solid support surface, provided the column used is packed with an appropriate solid support, *i.e.*, the solid support must be better wetted by the stationary liquid phase than by the eluent.

It seemed interesting to extend the use of the ternary HPLC systems to chiral separations. A way to attain this would be to modify the selectivity of the system by means of chiral additives. The main assumption of this approach is that the additives, when present in minute concentrations, do not significantly change miscibility in the ternary system used and that the only important characteristic of the additive is its appropriate enantioselectivity. For this reason cyclodextrins and their derivatives seem to represent a good choice. In a recently reported series of papers, Sybilska and co-workers [7–11] have demonstrated that cyclodextrins may conveniently be used for chiral separations when used as the component of a mobile phase in HPLC.

In this work the ternary partition system water–2,2,4-trimethylpentane–ethanol with chiral additives was used for chiral separation. A hydrophilic solid support was coated with the more polar liquid phase of the ternary phase system containing as a chiral additive different amounts of permethylated β-cyclodextrin, a compound successfully used for enantiomeric resolution in liquid–solid chromatography (LSC) [12,13].

Enantioselectivity of the partition system is shown and column stability and efficiency are discussed.

EXPERIMENTAL

Apparatus

Chromatographic experiments were carried out with a Type 310 high-pressure microbore liquid chromatograph (Institute of Physical Chemistry, Polish Academy of Sciences, Warsaw, Poland) equipped with a UV detector (254 nm) containing a 1-μl

flow cell and a 0.5-μl injector. The column was kept at within ±0.1°C of the desired temperature using a water thermostat (Typ U3, MLW, Germany).

Partition coefficients were determined by a Specord (Carl Zeiss, Jena, Germany) UV–VIS absorption spectrometer equipped with quartz cells with a light path of 30 mm. Magnetically stirred glass vessels kept in the water bath were used for the determination of the static partition coefficients. The water bath (Typ U10, MLW) was used to control the temperature within ±0.1°C.

Reagents

Heptakis (2,3,6-tri-O-methyl)-β-cyclodextrin (TM-β-CD) was supplied by Chinoin (Budapest, Hungary). D-Mandelic and L-mandelic acid enantiomers were supplied by E. Merck and Fluka, respectively. The pure enantiomers of methyl mandelate were prepared in simple esterification reactions from D- and L-mandelic acids in methanol solutions with sulphuric acid as catalyst. 2,2′-Dihydroxy-1,1′-binaphthol was synthesized and purified according to Vogel [14].

All other reagents and solvents were of analytical/reagent grade and were used without purification. The formulae of the investigated compounds are given in Table I.

LiChrosorb Si 60, 5 μm (E. Merck) was used as column packing. The test substances, because of their poor solubility in the eluent, were dissolved in a 2,2,4-trimethylpentane (2,2,4-TMP)–chloroform (2:1, v/v) mixture.

Procedure

The ternary liquid–liquid system consisting of 2,2,4-TMP–ethanol–water was used for static and chromatographic experiments: 95% 2,2,4-TMP, 2% ethanol and 3% water (w/w) (system VII in Fig. 1); the position of the tie line of system VII was constructed according to ref. 15. The less polar phase, α, was used as eluent and the more polar phase, β, as the liquid stationary phase (Fig. 1). The chromatographic column packed with the solid support LiChrosorb Si 60 was loaded with the stationary liquid by pumping the water-rich phase through the column, either without TM-β-CD or containing different amounts of TM-β-CD ($c_{\text{TM-}\beta\text{-CD}}$ = 65 and 130 mg/ml), until the column was filled. The non-stationary part was removed by pumping the corresponding water-poor phase through the column until column bleeding was finished and a steady state had been reached. In further experiments (chiral partition system) the eluent was saturated with TM-β-CD. TM-β-CD is poorly soluble in the water-poor phase used and its concentration in the eluent was about 0.05 mg/ml.

For comparison, chromatographic experiments were carried out in the LSC mode. In this case the composition of the ternary eluent was chosen from the homogeneous region of the phase diagram (above the equilibrium line): 95% 2,2,4-TMP, 3% ethanol and 2% water (w/w).

Liquid–liquid partition coefficients, K_i^{L-L}, for the distribution of test compounds between two coexisting liquid phases of the ternary liquid–liquid system were determined at 25.0 ± 0.1°C by absorption spectrometry as described previously [2]:

$$K_i^{L-L} = \frac{c_i^{\beta}}{c_i^{\alpha}} = K_i^{\beta/\alpha}$$

where c_i^{β} and c_i^{α} are the concentration of component i in the more polar phase (β) and the less polar phase (α), respectively.

TABLE I

STRUCTURES OF INVESTIGATED COMPOUNDS

Compound	Structure
1. Decyl benzene	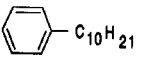
2. 2,2′-Dihydroxy-1,1′-binaphthol	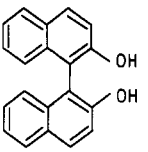
3. Morsuximide	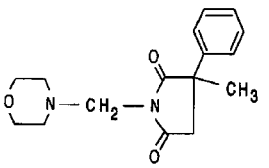
4. Methylphenobarbital	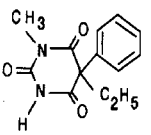
5. Glutethimide	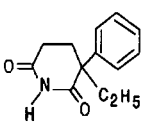
6. Methylmandelate	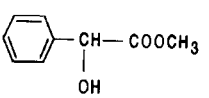
7. Mephenytoin	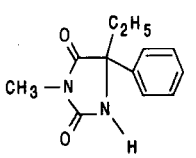

The less polar phase containing appropriate amounts of the dissolved test compounds and the more polar phase with or without chiral additive ($c_{TM\text{-}\beta\text{-}CD}$ = 65 and 130 mg/ml) were used in the static partition experiments.

RESULTS AND DISCUSSION

Verification of retention mechanism

The retention of a substance in a chromatographic system is given by

$$V_{Ri} = V_m + V_s K_i$$

where V_R is the retention volume of solute, V_m is the volume of the mobile phase, V_s is the volume of the stationary phase, and $K_i = c_i^s/c_i^m$, the partition coefficient in the chromatographic system. If the retention of a solute is caused by pure liquid–liquid distribution, the retention volumes, V_{Ri}, of the different substances depend linearly upon their static partition coefficients, K_i^{L-L}. The results of the static partition experiments using two coexisting liquids of the ternary phase system with and without the chiral additive are given in Table II.

The data in Table II show that the values of static partition coefficients depend very strongly on the concentration of TM-β-CD in the water-rich liquid phase. For most of the test compounds the estimated K^{L-L} values increase with increasing concentration of the chiral agent added to the more polar phase indicating that complexation of the investigated solutes by the β-CD derivative takes place. The only exception was found for solute **4**, where the K_i^{L-L} value goes through a maximum point.

Fig. 2 shows the correlation of the static partition coefficients and the chromatographic retention data. The plot in Fig. 2a is for the system without chiral additive and contains data obtained in the LSC mode and the liquid–liquid chromatography (LLC) mode. One can see a shift of the retention data towards the

TABLE II

LIQUID–LIQUID PARTITION COEFFICIENTS OF RACEMIC TEST COMPOUNDS FOR LIQUID–LIQUID SYSTEMS WITHOUT CHIRAL ADDITIVE AND WITH DIFFERENT CONCENTRATIONS OF TM-β-CD IN THE STATIONARY PHASE

Substance	K_i^{L-L}		
	0 mg/ml	65 mg/ml	130 mg/ml
1. Dodecylbenzene	0.001 ± 0.00	0.001 ± 0.00	0.001 ± 0.00
2. 2,2'-Dihydroxy-1,1'-binaphthol[a]	1.10 ± 0.06	3.46 ± 0.06[b]	5.88 ± 0.24[b]
3. Morsuximide	1.42 ± 0.18	1.80 ± 0.03	1.85 ± 0.51
4. Methylphenobarbital[a]	4.34 ± 0.98	8.59 ± 0.36[b]	6.98 ± 0.45[b]
5. Glutethimide[a]	5.21 ± 0.19	6.53 ± 0.28[b]	8.37 ± 0.24[b]
6. Methylmandelate	6.48 ± 0.22	6.98 ± 0.21	10.20 ± 0.28
7. Mephenytoin	7.86 ± 0.36	7.87 ± 0.21	14.49 ± 0.28

[a] Racemic mixtures resolved in chiral LL systems.

[b] K_i^{L-L} represent "average" values for racemic mixtures.

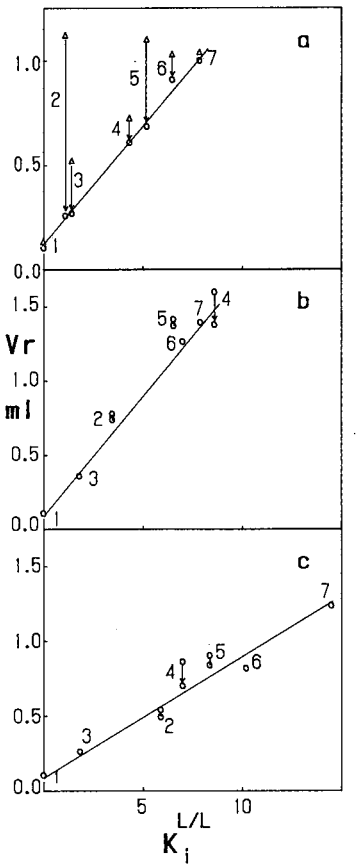

Fig. 2. Correlation of static partition coefficients and chromatographic retention data. Test compounds as in Table I. Column (250 × 1 mm); solid support LiChrosorb Si 60 (5 μm); liquid–liquid phase system VII (Fig. 1). (a) Shift of the retention volume data in the linear regression with the partition coefficients at the transition from LSC to LLC, $c_{TM\text{-}\beta\text{-}CD} = 0$. (b) $c_{TM\text{-}\beta\text{-}CD} = 65$ mg/ml. (c) $c_{TM\text{-}\beta\text{-}CD} = 130$ mg/ml.

linear regression line if the mechanism is changed from LSC to LLC. The plots in Fig. 2b and c give the correlation between retention data and static partition coefficients for liquid–liquid systems with different amounts of TM-β-CD dissolved in the water-rich stationary phase. The investigated liquid–liquid chiral systems show enantioselectivity towards three of the racemic mixtures tested. The retention data of these compounds are presented in the diagrams Fig. 2b and c, but their values are not included in the regression analysis. The parameters of linear regression data for unresolved racemic mixtures are given in Table III. As can be seen from the regression data and the plots in Fig. 2, an excellent linrar correlation has been found for the investigated compounds subsisting a liquid–liquid retention mechanism. The volume of the mobile phase, V_m^{cal}, determined from the intercept of the regression lines and the V_R axis, is the same as that determined by measuring the retention of decylbenzene (*i.e.*, a substance with negligible retention in the liquid–liquid normal-phase systems investigated).

TABLE III

REGRESSION PARAMETERS FOR RETENTION VOLUMES AND PARTITION COEFFICIENTS (OBTAINED FOR UNSEPARATED RACEMATES) ACCORDING TO $V_{Ri} = V_m + K_i^{L-L} V_s$

n, Number of measurements; r, regression coefficient; V_m^{calc}, V_s^{calc}, data calculated by regression; s_V, standard deviation; V_m^{exp}, retention volume for decylbenzene.

$c_{TM-\beta-CD}$ (mg/ml)	Regression parameters				
	n	r	$V_m^{calc} \pm s_V$ (ml)	$V_s^{calc} \pm s_V$ (ml)	V_m^{exp} (ml)
0	7	0.9942	0.113 ± 0.019	0.115 ± 0.004	0.106
65	4	0.9988	0.089 ± 0.021	0.167 ± 0.004	0.110
130	4	0.9971	0.105 ± 0.036	0.075 ± 0.004	0.10

The V_s values which characterize the amount of the stationary liquid phase depend on the phase system used (see Table III). However, no systematic trend is observed when the composition of the liquid is changed. Similar conclusions were reported previously for other systems [3,4].

As the next step in the verification of the distribution mechanism a partition system was used in which only the stationary liquid phase contained TM-β-CD. The eluent in this case was not saturated with the chiral additive. Such systems display exactly the same enantioselectivity as the system with the eluent saturated with TM-β-CD. A loss of enantioselectivity was observed after rather a long time (more then 250 dead volumes, Fig. 3). This stable enantioselectivity may be attributed to the very low solubility of TM-β-CD in the water-poor phase used as eluent.

The results presented above show that the retention mechanism of the chiral system investigated is actually a partition between the two liquid phases; the recognition of enantiomers occurring in the liquid stationary phase.

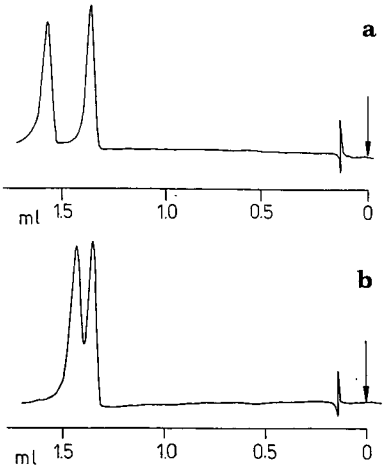

Fig. 3. Enantiomeric resolution of methylphenobarbital in partition system VII with 65 mg/ml TM-β-CD in the stationary phase. Column (250 × 1 mm) packed with LiChrosorb Si 60 (5 μm); flow-rate, 40 μl/min; temperature, 25.0 ± 0.1°C. (a) Eluent saturated with TM-β-CD. (b) Eluent without chiral additive, separation was obtained after more than 250 dead volumes pumped through the column.

TABLE IV

CAPACITY AND SEPARATION FACTORS FOR INVESTIGATED RACEMATES IN LIQUID–LIQUID SYSTEMS WITHOUT CHIRAL ADDITIVE AND WITH DIFFERENT CONCENTRATIONS OF TM-β-CD IN THE STATIONARY PHASE

For the unseparated test racemates $\alpha = 1.0$ and there is only one k' value representing one peak of racemate. For the separated racemates $\alpha > 1.0$ and there are two k' values.

Substance	0 mg/ml	65 mg/ml*		130 mg/ml	
	k'	k'	α	k'	α
2. 2,2'-Dihydroxy-1,1'-binaphthol	1.45	5.91	>1.0	3.71, 4.14	1.12
3. Morsuximide	1.55	2.50	1.0	1.50	1.0
4. Methylphenobarbital	4.83	11.51, 13.51	1.17	5.68, 7.2	1.27
5. Glutethimide	5.46	11.44, 11.85	1.07	7.00, 7.59	1.08
6. Methylmandelate	7.58	10.49	1.0	6.81	1.0
7. Mephenytoin	8.43	11.68	1.0	10.76	1.0

Selectivity and column efficiency

Table IV contains capacity factors (k') and separation factors (α) for the test racemic mixtures in the investigated liquid–liquid system. The partition system containing TM-β-CD exhibits enantioselectivity with compounds **2**, **4**, **5** (Figs. 3–5). The enantiomers of **4** and **5** were also separated in the solvent-generated adsorption system with TM-β-CD in the stationary phase [12,16]. However, the latter one also

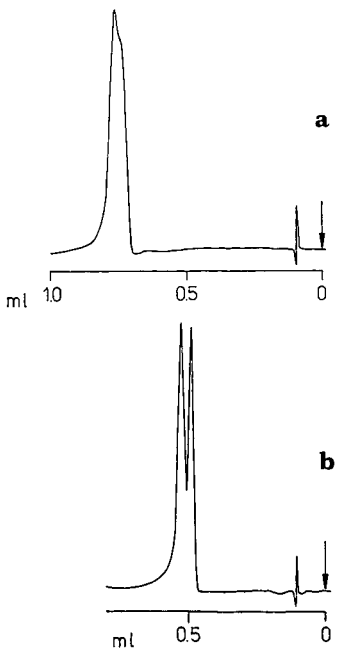

Fig. 4. Change of the enantioseparation of 2,2'-dihydroxy-1,1'-binaphthol with the concentration of chiral agent in the stationary phase. (a) $c_{TM\text{-}\beta\text{-}CD} = 65$ mg/ml. (b) $c_{TM\text{-}\beta\text{-}CD} = 130$ mg/ml. Conditions as in Fig. 3.

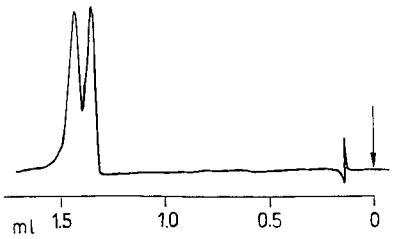

Fig. 5. Enantiomeric resolution of glutethimide in partition system VII with 65 mg/ml TM-β-CD in the stationary phase. Conditions as in Fig. 3.

enables the enantioseparation of the mandelic acid derivatives, which are not separated in the partition system. Conversely, the partition systems separate the enantiomers of binaphthol (**2**), which is not the case with the adsorption-type systems [17]. Thus, changing the retention mechanism from the LSC mode to the LLC mode influences chiral selectivity.

The results in Table IV show that the capacity factors depend on the concentration of the chiral additive in the stationary phase, as reflected by the K_i^{L-L} values listed in Table II. Selectivity of the liquid–liquid system is also dependent on the concentration of chiral agent. For solutes **4** and **5** the enantioselectivity increases only slightly, but for binaphthol the increase in selectivity, and therefore the improvement in resolution, is rather significant (see Fig. 4a and b). The observed dependence of chiral selectivity on the concentration of the chiral additive allows the users to control selectivity, within some limits, by simply modifying the concentration of the chiral agent in the system. This flexibility is not observed in chiral LSC systems.

Table V shows the efficiency of the chromatographic column for an LSC and LLC system without the chiral component and for liquid–liquid systems with different amounts of TM-β-CD in the stationary phase. All chromatographic determinations

TABLE V

COLUMN EFFICIENCY (NO. OF THEORETICAL PLATES) FOR LSC AND LLC SYSTEMS WITH DIFFERENT CONCENTRATIONS OF TM-β-CD IN THE STATIONARY PHASE

Substance	LSC	LLC		
		0 mg/ml	65 mg/ml	130 mg/ml
2. 2,2'-Dihydroxy-1,1'-binaphthol	4600	4600	–	4200 3350
3. Morsuximide	4120	3640	3550	3600
4. Methylphenobarbital	9860	8900	5430 5350	2690 2560
5. Glutethimide	6180	4990	4700 3640	4220 3600
6. Methylmandelate	9300	8410	6240	3300
7. Mephenytoin	8850	7800	4590	1000

were carried out on the same column. The efficiency of the column is about the same for LSC and LLC systems operated without chiral component.

The use of the chiral additive always caused a decrease of column efficiency and peak symmetry. It suggests that the processes of complexation reaction between the enantiomers and TM-β-CD in the stationary liquid phase contributing to the mass-transfer effect are relatively slow. The decrease of efficiency depends very strongly on the solute to be separated and also on the nature of the chiral additive. This question is discussed in more detail elsewhere [13].

It is probable that the drastic decrease in column efficiency, due to the slow kinetics of complexation in the chiral liquid stationary phase for methyl mandelate, makes resolution of its enantiomers impossible. Resolution was successful in an LSC system exhibiting relatively a low decrease in column efficiency [13].

CONCLUSIONS

The results of the present work show convincingly that (1) the ternary liquid–liquid phase systems may be supplemented by chiral modifiers: the systems tested retain the properties of the partition system and show, in addition, chiral properties; (2) the enantioselectivity, which is determined by the type and amount of modifier used, is similar to the enantioselectivity found in previously described solvent-generated adsorption systems [11–13,16,17] but this technique prove to be more flexible in selectivity, *i.e.*, by modifying the amount of the chiral agent used one may exert substantial control over the selectivity of the system.

REFERENCES

1 C. A. Meijers, J. A. R. J. Hulsman and J. F. K. Huber, *Z. Anal. Chem.* 261 (1972) 347.
2 J. F. K. Huber, C. A. M. Meijers and J. A. R. J. Hulsman, *Anal. Chem.* 44 (1972) 111.
3 J. F. K. Huber, M. Pawłowska and P. Markl, *Chromatographia*, 17 (1984) 653.
4 J. F. K. Huber, M. Pawłowska and P. Markl, *Chromatographia*, 19 (1984) 19.
5 J. F. K. Huber, M. Pawłowska and P. Markl, *J. Chromatogr.*, 500 (1990) 257.
6 P. J. Crombeen, S. Heemstra and J. C. Kraak, *J. Liq. Chromatogr.*, 3 (1980) 1151.
7 D. Sybilska, J. Lipkowski and J. Wóycikowski, *J. Chromatogr.*, 253 (1982) 95.
8 J. Dębowski, D. Sybilska and J. Jurczak, *Chromatographia*, 16 (1982) 198.
9 J. Dębowski, D. Sybilska and J. Jurczak, *J. Chromatogr.*, 237 (1982) 303.
10 D. Sybilska, J. Dębowski, J. Jurczak and J. Żukowski, *J. Chromatogr.*, 286 (1984) 163.
11 J. Żukowski, D. Sybilska and J. Bojarski, *J. Chromatogr.*, 364 (1983) 225.
12 J. Żukowski, D. Sybilska, J. Bojarski and J. Szejtli, *J. Chromatogr.*, 436 (1988) 381.
13 J. Żukowski and R. Nowakowski, *J. Liq. Chromatogr.*, 12 (1989) 1545.
14 A. Vogel, *Vogel's Textbook of Practical Organic Chemistry*, Longman, London, 1978.
15 R. E. Treybal, *Liquid Extraction*, McGraw-Hill, New York, 2nd ed., 1963, pp. 13–44.
16 J. Żukowski, *Ph.D. Thesis*, Institute of Physical Chemistry, Polish Academy of Sciences, Warsaw, 1987.
17 M. Pawłowska and J. Żukowski, *Mikrochim. Acta*, III (1990) 55.

Journal of Chromatography, 547 (1991) 69–78
Elsevier Science Publishers B.V., Amsterdam

CHROM. 23 281

Development of a phase system for intermediate polarity compounds in centrifugal partition chromatography

STEVEN J. GLUCK* and MICHAEL P. WINGEIER
Analytical Sciences Department, Building 1897, Dow Chemical, Midland, MI 48667 (USA)
(First received November 15th, 1990; revised manuscript received February 26th, 1991)

ABSTRACT

A new phase system and an approach to developing phase systems relying on composition, physical data and an empirical polarity index have been proposed for general use in centrifugal partition chromatography. The system developed possesses a comparably low viscosity necessary for improved efficiency at a composition where compounds of intermediate polarities have a high solubility in both the upper and lower layers. This system should be useful for traditional isocratic use and in normal-phase ascending gradient separations, because the composition and polarity changes of the lower phase were small relative to the changes in the composition and polarity of the upper phase.

INTRODUCTION

Centrifugal partition chromatography (CPC) is an alternative to preparatory and process-scale liquid chromatography (LC) for the isolation of impurities or purification of a crude material. Compared to LC, CPC has a relatively higher capacity [1,2] attributable to the large volume of stationary phase available to partitioning solutes. Common solvents are used as both the mobile and stationary phases in contrast to LC. Thus, CPC potentially has an economic advantage relative to LC because of a much lower solvent consumption at comparable mass throughputs and the absence of an expensive chromatographic packing. The absence of the silica or otherwise potentially adsorbtive or catalytic surface commonly used in column-packing materials means that sensitive samples have less of a chance to be altered. In contrast to LC, the CPC stationary phase may be switched to become the mobile phase; at the same time the mobile phase becomes the stationary phase (dual-mode operation). Thus, sample recoveries are always 100% and no material is irreversibly sorbed.

Alternatively, LC has the advantage of having a relatively simple method development scheme, because of the limited number of choices for a stationary phase. With a chemically bonded stationary phase or a bare solid surface, LC method development requires little consideration for the effects of the mobile phase on the stationary phase compared to CPC or other counter-current chromatographic techniques. Indeed, the "art" has been reduced to a technology of using expert systems

0021-9673/91/$03.50

for analytical separation development and, more recently, extensive modeling has occurred even in the areas of preparatory separations. In common practice, most LC preparative separations are optimized by investigating the separations on different manufacturers variations of the same sorbent material rapidly on a small scale.

In CPC, phase development is a required and more complex task. Virtually any solvents may be incorporated into a phase system, and most phases developed in the literature have not been chosen out of a systematic optimization scheme. Phase development for CPC seems to have focused along the empirical needs of a crude material to be isolated or purified rather than the development of a phase system which should be applicable to many materials. As an example, the chloroform–methanol–water system has been reported with different mixing ratios by different authors. However, most of these mixing ratios were shown by Foucault and Nakanishi [3] to reside close to the same tie-line of the ternary solvent diagram indicating that all of the authors were using similar upper and lower phase compositions. Another example includes the use of up to five different solvents in the phase system [4]. Perhaps an efficient and well understood ternary system could achieve or at least be a starting place for these types of challenges with less method development time.

Identification of a small set of generally useful phases to fit many applications continues to be a major challenge for optimizing CPC separations. The physical properties of an ideal solvent system for CPC are those which allow the maximum separation efficiency and the highest system throughput. In LC, and usually in CPC, this is a trade-off which must be optimized due to the limiting rate of mass transfer of a solute from the stationary phase to the mobile phase. In CPC, as phase viscosity is lowered, efficiency improves. This phenomenon is dramatic in situations of viscosities of less than about 0.5 cP where an "inverse Van Deemter"-type relationship is observed [5]. In these special cases, separation efficiency reaches a minimum and then increases with flow-rate. This phenomenon is believed to be due from improved mass transfer caused by an increase in mixing and an increase in the interfacial surface area between the two phases. Attempts to increase efficiency with higher flow-rates of the commonly used phase systems usually result in exceeding the apparatus pressure limits of 850 p.s.i.g. before any increase in efficiency is observed. However, over the useful flow-rates, the lower viscosity phase systems appear to have improved efficiencies.

The elution volume of the solute is dependent on the volume of the stationary phase, the volume of the mobile phase and the partition coefficient of the solute between those phases. The phase volumes are experimentally controlled by the flow-rate and angular velocity of the rotor. Experimental control of the partition coefficient is significantly dependent on the polarity of each phase and the polarity and polarizability of the solute. For development and investigative purposes, the use of a solvochromatic parameter may be used to judge the relative phase polarity of mixed solvent systems. This is a rapid, simple and precise parameter to measure compared to actually determining the partition coefficients of a series of solutes for development purposes. Reichart and Dimroth's dye (hereafter referred to as Reichart's dye) number 30 has been documented to relate the relative solvent strengths of aqueous mixtures of acetonitrile–tetrahydrofuran–methanol [6]. Hence, the use of this dye can guide the development of mixed-phase system polarity.

Useful characterization of the solvent system for CPC should include the phase diagram with the densities, viscosities and the polarities of the upper and lower layers

formed by the various mixing ratios of the solvents. The separation of hydrocarbon-type materials is done well on a hexane–methanol–1% water system which has been partially characterized in refs. 3, 7 and 8. Many other phases have been used for different applications of intermediate polarity compounds. One of the more common phase systems is the 1-butanol–water system. It is the goal of this paper to present a scheme for characterization of CPC phases and to present a generally useful phase for separating solutes of intermediate polarity.

EXPERIMENTAL

Viscosity measurement

Kinematic viscosities were measured at 22°C using Cannon-Fenske routine viscometers (Fisher Scientific). Solution densities (22°C) were taken from the mass of 5.00 ml dispensed from a volumetric pipet. Viscosities in centipoise were the density times the kinematic viscosity.

Measurement of solvent polarity

A small amount, 0.01–0.2 mg, of Reichardt's dye, I (Aldrich catalogue number 27,244-2), was dissolved in 5 ml of the test solution (Fig. 1). The solution was placed in a 1-cm-pathlength cuvette and the absorbance was scanned from 800 to 400 nm using a 2-nm slit width and a 0.5-nm sampling interval at the fast slew setting of a Shimadzu UV-3101 PC spectrophotometer. Reichardt's dye has too low of a solubility to be used in non-polar solvents and thus the penta *tert.*-butyl substituted analogue, II (Aldrich catalog number 27,305-8), was used in these cases (Fig. 1). From the absorbance

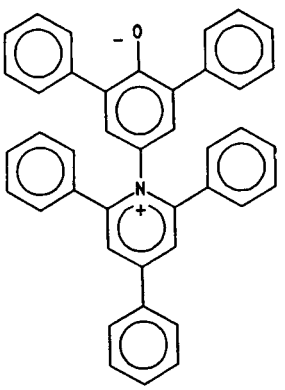

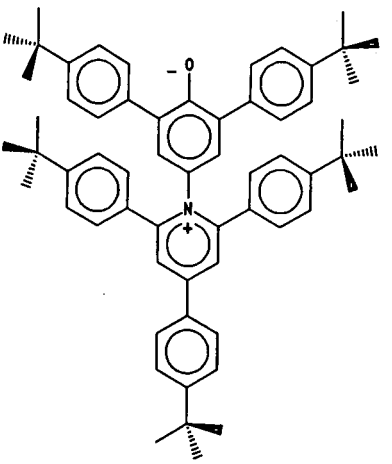

I II

Fig. 1. Structures of Reichardt's dye (I) and the penta *tert.*-butyl substituted analogue (II).

maximum, λ_{max}, in nm of the solvatochromatic dyes, the energy of transition, E_t, was calculated:

$$E_t(\text{kcal/mol}) = 28590/\lambda_{max}$$

The E_t of II, E'_t, can be converted to the E_t of I, commonly known as $E_t(30)$, by a simple linear transformation [9]:

$$E_t(30) = \frac{E'_t - 3.434}{0.9143}$$

To convert the E_t to a dimensionless unit, Reichardt and Harbusch-Gornert [9,10] have recommended the normalized E_tN. The normalized E_tN uses the polarity extremes of water and tetramethylsilane (TMS) as reference solvents:

$$E_tN = \frac{E_t(\text{test solvent}) - E_t(\text{TMS})}{E_t(\text{water}) - E_t(\text{TMS})} = \frac{E_t(\text{test solvent}) - 30.7}{32.4}$$

Therefore, non-polar liquids have an E_tN close to 0 and polar liquids have an E_tN close to 1.

Partition coefficient measurement

Partition coefficients, K, were determined by adding 1 μl of a 50% mixture of ethyl acetate and 1-butanol to 3 ml each of upper and lower phases. The phases were shaken vigourously and allowed to separate twice, thus allowing equilibrium to be established. On-column capillary gas chromatographic (GC) analysis with flame ionization detection was performed for the peak-area determinations of the test solutes. The peak area of the solute in the upper layer divided by the peak area of the solute in the lower layer was taken to be the partition coefficient.

Phase composition determinations

Phase composition was determined by split-injection capillary GC analysis with external standard calibration. The response factors were determined to shift with the composition of the samples and thus the composition of each sample was first estimated and then multiple standards were prepared with a composition similar to that of each sample. Water composition was determined by percentage difference. The tie-lines connecting the upper and lower layers on the methyl *tert.*-butyl ether, acetonitrile and water phase diagram intersected within $\pm 1\%$ of the bulk composition ratio and thus served as an internal check on the determination accuracy.

CPC apparatus

Example separations were performed on a Sanki Model LLN CPC system manufactured by Sanki Engineering. Both twelve-cartridge (4800 50-μl stages) and six-cartridge rotors were used. All separations were at 22°C under the conditions listed.

TABLE I

PHYSICAL AND CHEMICAL DATA REPRESENTATIVE OF SOME PHASES USED IN CPC

The viscosities and densities are at 22°C.

Phase[a]	Volume		Viscosity (cP)		E_tN		Density (g/ml)	
	Upper	Lower	Upper	Lower	Upper	Lower	Upper	Lower
1% Water in MeOH–hexane (1:1)	2	3	0.34	0.37	0.62	0.50	0.665	0.763
Hexane–ACN	1	3	0.35	0.59	0.23	0.45	0.668	0.745
THF–ACN–Hexane (1:2:2)	1	4	0.37	0.39	0.38	0.40	0.709	0.764
EtOAc–EtOH–water (5:2:4)	5	6	0.40	1.59	0.40	0.58	0.759	0.950
Hexane–EtOAc–DMF–water (3:3:4:1)	4	1	0.49	1.48	0.45	0.58	0.816	0.946
CCl_4–MeOH–water (10:9:1)	1	2	0.67	1.22	0.69	0.80	0.814	0.933
Hexane–EtOAc–DMF–water (15:21:18:2)	5	1	1.31	0.58	0.45	0.59	0.814	0.946
CHC_3–MeOH–nPrOH–water (45:60:10:40)	3	1	1.10	0.97	0.69	0.57	1.10	1.51
BuOH–nPrOH–water (4:1:5)	4	3	1.84	0.95	0.70	0.62	0.960	1.19
BuOH–HOAc–water (4:1:5)	1	1	3.02	1.56	—[b]	—[b]	0.848	0.979
BuOH–water (1:1)	1	1	3.06	1.38	0.65	0.89	0.840	0.984
14% Aquaphase PPT–5% PEG 8000 in water	1	1	6.87	42	—[c]	—[c]	1.03	1.05
MtBE–isooctane–MeOH–water (10:2:8:6)	2	5	0.92	1.17	0.61	0.74	0.746	0.872

[a] MeOH = Methanol; ACN = acetonitrile; THF = tetrahydrofuran; EtOAc = ethyl acetate; EtOH = ethanol; DMF = dimethylformamide: CCl_4 = tetrachloromethane; $CHCl_3$ = chloroform; nPrOH = *n*-propanol; BuOH = butanol; HOAc = acetic acid; aqueous PPT from Perstorp Biolytica; MtBE = methyl *tert.*-butyl ether.

[b] Not applicable to acidic solutions.

[c] The absorbance background in these solutions was too high to be able to determine the maximum for Reichardt's dye.

RESULTS AND DISCUSSION

Some fundamental data for a set of CPC phases are presented in Table I for perspective. These data include the relative volumes of the upper and lower layers, the viscosities of each layer, the densities of each layer and the E_tN values for each layer. The hexane–methanol–1% water phase is the most efficient phase ever reported [8]. Typical chromatograms for this phase are shown in Fig. 2a and b which indicate excellent efficiencies. These chromatograms are only presented as a goal for future separation to be obtained in other phases. The low viscosity of this phase system was an important criterion for the high efficiency. The disadvantage of this phase system is the low solubility many materials of moderate polarity exhibit in the hexane phase thus limiting its use for isolation and purification.

In contrast, the butanol–water system has found wide use for isolating intermediate polarity compounds such as peptides and natural products in other liquid–liquid chromatographic apparate and CPC [11]. Compared to this system, a methyl *tert.*-butyl ether–acetonitrile–water (30:30:40) phase system exhibits improved chromatographic efficiency. Fig. 3 shows the relationship between peak width at half height *versus* elution time for a series of test solutes run on both of these systems under similar experimental conditions (5 ml/min ascending flow-rate, 300-rpm, 120-ml six-cartridge rotor). In the butanol–water system, the peak width increased more rapidly than in the methyl *tert.*-butyl ether-acetonitrile–water (30:30:40) phase

TABLE II

PHYSICAL AND CHEMICAL DATA FOR THE METHYL *tert.*-BUTYL ETHER–ACETONITRILE–WATER PHASE SYSTEM

The viscosities and densities are at 22°C. MtBE = methyl *tert.*-butyl ether; ACN = acetonitrile; EtOAc = ethyl acetate; BuOH = butanol.

MtBE–water–ACN composition (v/v/v)	Weight% ACN		Weight% MtBE		E_tN		Density (g/ml)		Viscosity (cP)		K		α
	Upper	Lower	Upper	Lower	Upper	Lower	Upper	Lower	Upper	Lower	EtOAc	BuOH	
25:25:0	0.0	0.0	95.2	4.0	0.284	0.942					8.52	3.95	2.16
25:25:5	8.5	6.8	85.1	4.0	0.487	0.895					8.80	4.66	1.89
25:25:10	18.1	11.5	70.3	4.4	0.569	0.861	0.76	0.97	0.472	1.2	8.00	4.30	1.86
25:25:15	25.7	14.2	58.1	4.7	0.617	0.839					6.92	4.20	1.65
25:25:20	30.7	16.9	47.1	5.2	0.642	0.824	0.79	0.96	0.549	1.18	6.36	4.08	1.56
25:25:25	38.0	18.4	42.2	5.3	0.663	0.817					5.51	3.65	1.51
25:25:30	41.0	20.1	37.4	5.7	0.681	0.807					4.78	3.24	1.48
25:25:35	43.7	22.0	32.1	5.9	0.690	0.800	0.8	0.94	0.612	1.18	4.18	2.86	1.46
25:25:40	45.6	23.2	28.6	6.2	0.702	0.789	0.81	0.94	0.639	1.15	3.58	2.58	1.39
25:25:45	45.2	24.3	24.2	6.6	0.711	0.783	0.84	0.95	0.755	1.14	3.04	2.23	1.36

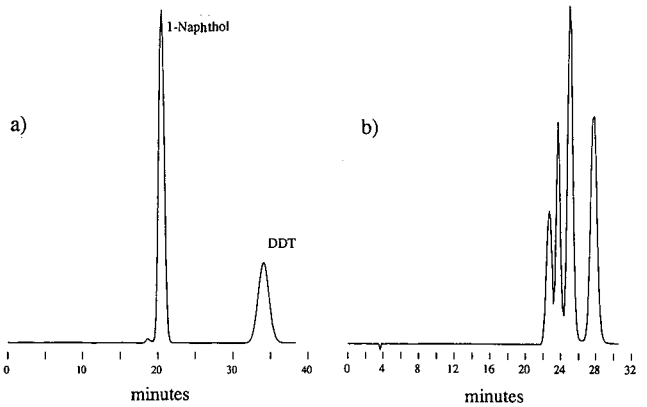

Fig. 2. Example separations of a test mixture using the highest-efficiency CPC phase system known to date. The phases were made from 1% water in methanol equilibrated with an equal volume of hexane. The mobile phase volume (V_m) was 92–94 ml and the total system volume (V_t) was 215 ml (twelve cartridges). (a) 1-Naphthol and DDT. (b) Alltech reversed-phase mixture D consisting of uracil–phenol–benzaldehyde–N,N-diethyl-*m*-toluamide–toluene–ethyl benzene. Component identities have not been determined in this chromatogram.

system. Therefore, the latter phase system would provide better resolution for similarly retained compounds than the butanol–water system. However, neither of these phase systems approach the optimum potential efficiency of the apparatus as shown in Fig. 2a and b.

Phase diagram

The composition of the various mixtures of the methyl *tert.*-butyl ether–acetonitrile–water phase system are given in Table II along with the E_tN polarity values, the densities and the viscosities. The viscosities of this system are lower than others which have been used for moderate-polarity solutes and thus this system should provide superior efficiencies. The volume percent approximation of the weight percent

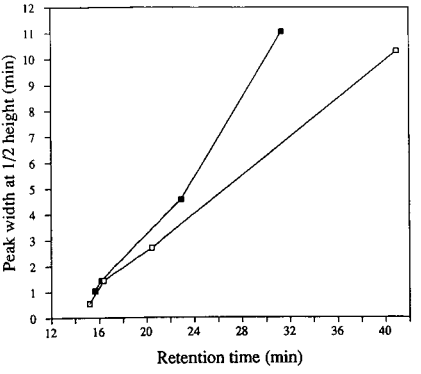

Fig. 3. Relationship between peak width at half height *versus* retention time comparing 1-butanol–water (■) to the methyl *tert.*-butyl ether–acetonitrite–water (30:30:40) phase system, both applicable to the separation of intermediate polarity compounds.

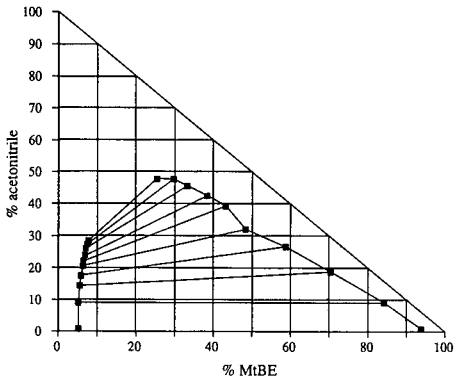

Fig. 4. Approximation of the volume percent phase diagram (calculated from the weight percent phase diagram) of the methyl *tert.*-butyl ether (MtBE)–acetonitrile–water system.

phase diagram is shown in Fig. 4. The composition of the upper and lower layers of ten different solvent mixing ratios were determined by GC. The points on the left represent the composition of the upper layers. The lines between the points are the tie-lines where any solvent mixing ratio will separate into the same upper and lower layer compositions. The binodal is the line representing the boundary between a biphasic and homogeneous phase system. Inspection of the phase diagram indicates that this system could be useful in normal–phase gradient elution. Successful gradient elution in CPC requires one of the phases to have a large change in composition along the binodal of the phase diagram while the other phase has a small change [3].

Phase polarity

The E_tN values show the phases converging in polarity as the tie-lines approach the Plait point (the Plait point is the solvent composition on the binodal where the

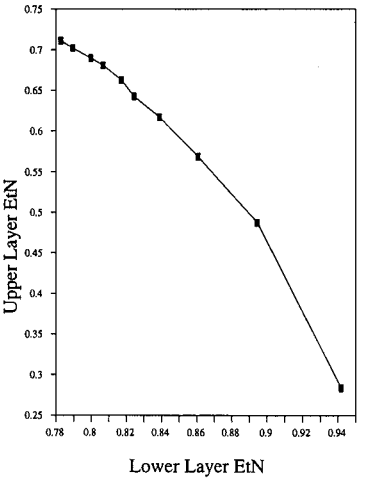

Fig. 5. E_tN polarity index of the upper layer *versus* the lower layer of the methyl *tert.*-butyl ether–acetonitrile–water system.

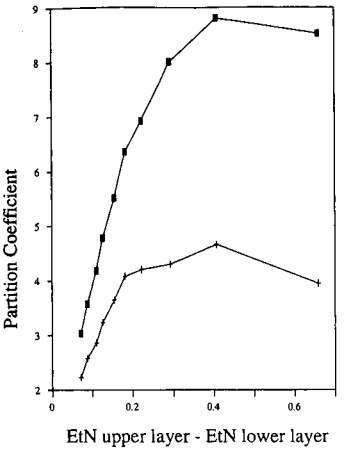

Fig. 6. Partition coefficients of ethyl acetate (■) and 1-butanol (+) *versus* the difference in the polarity index, E_tN, of the upper and lower layers.

tie-lines converge). Therefore, as the polarity of the upper phase increases, the polarity of the lower phase decreases. This relationship is plotted in Fig. 5. The polarity change in the lower phase is small relative to that of the upper phase which is another factor making the use of a normal-phase, ascending-mode gradient attractive.

A pair of solutes exhibiting good solubility in all compositions of this ternary system, ethyl acetate and 1-butanol, was chosen to illustrate the relationship between phase polarity and partitioning. As the differences in the E_tN values of each phase increase, the partition coefficients of both solutes increase (Fig. 6). In addition, the α values (the ratio of the partition coefficients) correlate in a near linear fashion to the differences in the E_tN values (Fig. 7).

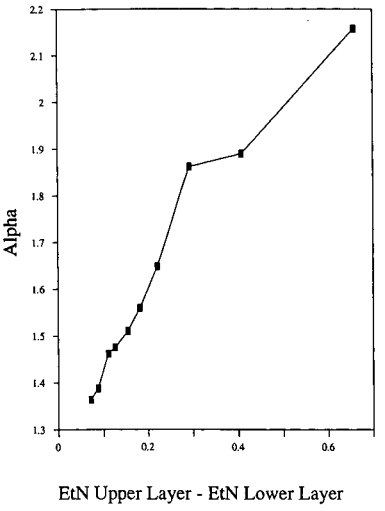

Fig. 7. α values of ethyl acetate and 1-butanol *versus* the difference in the polarity index, E_tN, of the upper and lower layers.

CONCLUSIONS

A new phase system has been developed for general use in CPC. It possesses relatively low viscosities at intermediate ranges of polarities. It should be applicable to the isolation or purification of intermediate-polarity substances. The phase diagram was established for understanding the composition of the phases prepared with different solvent ratios. This phase system should be useful in traditional isocratic separations and also in normal-phase, ascending-gradient separations because the composition and polarity of the lower phase changes little with respect to changes in the composition and polarity of the upper phase.

The relationship between the E_tN, K and α values reveals what may prove to be a rapid means to screen new, potential phases and their usefulness in CPC. The measurement of E_tN is simple, rapid and can be carried out in many laboratories. Classifying CPC phases by their E_tN provides a semi-quantitative measure of phase polarity, a critical selectivity parameter. However, it should be cautiously recognized that E_tN values lack the ability to measure other important selectivity parameters and cannot be determined in acidic media. But even with a recognized quantitative limitation of E_tN values as a means to predict partitioning, we have demonstrated their utility for phase development.

ACKNOWLEDGEMENTS

We are grateful for the helpful discussions from Curt Pfeiffer and Alan Syverud of the Dow Chemical Analytical Sciences Laboratory, Eric Martin of the DowElanco Herbicides Discovery Group, John Dorsey of the University of Cincinnati and Peter Carr of the University of Minnesota.

REFERENCES

1 A. Berthod and D. W. Armstrong, *J. Liq. Chromatogr.*, 11 (1988) 1187.
2 W. Murâyama, Y. Kosuge, N. Nakaya, Y. Nunogaki, K. Nunogaki, J. Cazes and H. Nunogaki, *J. Liq.* Chromatogr., 11 (1988) 283.
3 A. Foucault and K. Nakanishi, *J. Liq. Chromatogr.*, 12 (1990) 2587.
4 R. C. Bruening, E. Oltz, J. Furukawa, K. Nakanishi and K. Kustin, *J. Natl. Prod.*, 49 (1986) 193.
5 P. W. Armstrong, *Anal. Chem.*, 60 (1988) 2513.
6 B. P. Johnson, M. G. Khaledi and J. G. Dorsey, *Anal. Chem.*, 58 (1988) 2354.
7 A. Berthod and D. W. Armstrong, *J. Liq. Chromatogr.*, 11 (1988) 1457.
8 A. Berthod and D. W. Armstrong, *J. Liq. Chromatogr.*, 11 (1988) 567.
9 C. Reichardt and E. Harbusch-Gornert, *Liebigs Ann. Chem.*, 5 (1983) 721.
10 C. Reichardt, *Solvents and Solvent Effects in Organic Chemistry*, VCH, Weinheim, 2nd ed., 1998, pp. 3 and 64.
11 N. B. Mandava and Y. Ito (Editors), *Countercurrent Chromatography*, Marcel Dekker, New York, 1988.

Journal of Chromatography, 547 (1991) 79–87
Elsevier Science Publishers B.V., Amsterdam

CHROM. 23 213

Subfractions of membranes from calf brain synaptosomes obtained and studied by liquid–liquid partitioning

MARIA TERESA MUIÑO BLANCO[a], JOSÉ ALVARO CEBRIAN[a], BJÖRN OLDE and GÖTE JOHANSSON*

Department of Biochemistry, Chemical Center, University of Lund, P.O. Box 124, S-221 00 Lund (Sweden)

(Manuscript received December 12th, 1990)

ABSTRACT

Synaptosomes isolated from calf brain cortex were lysed and fragmented by Yeda press treatment. The obtained membranes have previously been fractionated in a counter-current distribution process using a liquid–liquid two-phase system consisting of water, dextran, Ficoll and poly(ethylene glycol) [*J. Chromatogr.*, 358 (1986) 147]. Using the fact that there are discrete membrane populations, a rapid preparative method for isolation of the two main fractions is presented in the present work, as well as a subfractionation of one of them using liquid–liquid extraction with dextran-bound Procion yellow HE-3G. The content of several membrane constituents, *i.e.* protein, acetylcholinesterase, succinate dehydrogenase and ATPase, as well as opiate binding, were determined for the three fractions. Counter-current distribution of the fractions elucidates their heterogeneity and the effectiveness of the purification.

INTRODUCTION

Biological membranes were fractionated by taking advantage of differences in their partition within (liquid–liquid) aqueous two-phase systems [1]. This was done either by using between one and five extraction steps or by applying a counter-current distribution technique using systems composed of water and the two polymers dextran and poly(ethylene glycol). These techniques have mainly been used for the separation and study of thylakoid membranes [2,3], but membranes of animal origin have also been fractionated in this way. These partitioning studies also include synaptic membranes from *Torpedo californica* [4,5] and *Torpedo marmorata* [6] as well as membranes isolated from brain tissue [7–9]. It has, in a few cases, been shown that membranes with cholinergic [4] or opiate [9] receptors can be effectively extracted into one of the phases by including a suitable receptor ligand, in this phase anchored to the dominating polymer.

While the applications of two-phase partitioning for separation of plant membranes have been without technical problems, work with brain membranes has involved complications [8]. It has been shown that synaptic membranes from calf brain

[a] Present address: Department of Biochemistry, Faculty of Veterinary Science, University of Zaragoza, Zaragoza, Spain.

0021-9673/91/$03.50

change their partition behaviour with time, probably as a result of aggregation or rearrangement of the structural elements of the membranes. This can to some extent be avoided by using systems containing polymers of lower molecular weights and/or addition of stabilizing proteins. In the present work a two-phase system composed of water, dextran, Ficoll and poly(ethylene glycol) was used, which has previously been used for counter-current separation of brain membrane preparations [10]. This system is here shown to separate synaptosome membranes into two classes (without use of affinity ligands). One of these was further fractionated by using a moderate concentration of a dextran-bound dye, Procion yellow HE-3G. The membrane fractions (three in total) were isolated by a simple series of batch extractions.

EXPERIMENTAL

Chemicals

Dextran T-40 (mol. wt. 40 000), dextran 500 (mol. wt . 500 000) and Ficoll 70 (mol. wt. 70 000) were purchased from Pharmacia (Uppsala, Sweden). Poly(ethylene glycol) (PEG, mol. wt. 7000–9000) was obtained from BP Chemicals (Hythe, UK) as Breox 8000. Procion yellow HE-3G was a gift from I.C.I. (Gothenburg, Sweden). Materials for the biochemical assays were obtained from Sigma (St. Louis, MO, USA). All salts and buffer substances were of analytical grade.

Dextran-bound Procion yellow

Procion yellow HE-3G was bound to dextran 500 in basic aqueous solution. This method has been described elsewhere [11–13]. The Procion yellow–dextran (PrY–dextran) contained 7.2 μmol dye per gram of polymer.

Membrane preparation

The preparation of synaptosomes from calf brain cortex was performed by a slightly modified version of the method described by López-Pérez *et al.* [14]. Unless otherwise mentioned, all centrifugation steps were performed in a GSA rotor with a Sorvall RC-2B refrigerated high-speed centrifuge at 3°C. A pair of scissors was used to mince 100 g of cerebral cortex. The minced tissue was suspended in 500 ml of 1 m*M* Tris–HCl buffer, pH 7.4, containing 0.32 *M* sucrose, and homogenized by twenty strokes in a glass Potter–Elvehjem homogenizer with a loose-fitting PTFE pestle at 100 rpm. The homogenate was centrifuged at 1000 g_{max} for 10 min. The pellet was discarded and the supernatant was centrifuged at 20 000 g_{max} for 20 min. The resulting pellet was resuspended in 30 ml of 5 m*M* potassium phosphate buffer, pH 7.8, containing 0.32 *M* sorbitol, and was layered over 200 ml of 6% Ficoll 70, in the same medium as above, in Sorvall GSA centrifuge flasks which were centrifuged at 20 000 g_{max} for 30 min. The white upper part of the pellet was recovered, avoiding the brown mitochondrial fraction, and resuspended in 200 ml of 0.32 *M* sucrose followed by centrifugation at 20 000 g_{max} for 30 min. The resulting pellet was resuspended in 175 ml ice-cold water. The membrane suspension was stored at −30°C. Before use the suspension was thawed (30 min), homogenized with a Potter–Elvehjem homogenizer and passed twice through a Yeda press under 100 atm nitrogen pressure.

Assays

Light scattering was measured at 400 or 500 nm (when dye was present) as the apparent absorbance using a Hitachi 100-60 spectrophotometer. After treating the membranes for 1 h at 50°C in 0.5 *M* phosphoric acid, protein concentrations were determined according to Bradford [15]. Acetylcholinesterase was determined by the method of Ellman *et al.* [16], and succinate dehydrogenase as described by Earl and Korner [17]. ATPase was determined according to Scharschmidt *et al.* [18], and stereospecific opiate binding was determined as described by Medzihradsky [19]. Total phosphate was determined according to Ames and Dubin [20] and 2′,3′-cyclic nucleotide-3′-phosphohydrolase according to Sims and Carnegie [21].

Two-phase systems

The basic composition of the two-phase systems used was 10.3% (w/w) Ficoll 70, 9.3% (w/w) dextran T-40, 2.3% (w/w) PEG and 5 m*M* Tris–orthophosphoric acid buffer, pH 7.8 (concentration based on phosphate). The volume ratio (top/bottom) of the phases was 0.54. All partitionings were carried out at 3°C.

Counter-current distribution (CCD)

A special type of CCD apparatus invented by Åkerlund [22] was used. It allowed rapid separation of the two phases by one centrifugation step. The apparatus contained 60 chambers arranged in a circle which allowed the upper phases to be transferred stepwise to the neighbouring lower phases. The volume of the stationary part of each chamber was 0.96 ml. The membrane samples were included in the systems in chambers number 0 and 1 of the CCD machine, 1.3 ml system per chamber. The same amounts of mixed two-phase system (without membranes) were loaded in chambers 2–59. In some experiments PrY–dextran, used at concentrations of 0.028 or 0.111%, was included in the systems. Mixing time was 4 min, centrifugation time was 12 min, and 58 transfers were performed. After the run, the systems were transformed from two phases to one phase by the addition of 1.3 ml of ice-cold water per chamber. The fractions, after ten- to fifty-fold dilution, were analyzed for light scattering measured as the apparent absorbance at 400 nm or (if Procion yellow was present) 500 nm. The contents of chosen sets of chambers were pooled and concentrated by centrifugation for 120 min at 45 000 g_{max} (after two-fold dilution) and resuspended in 1.2–1.5 ml of distilled water. The fractions were analyzed for cholinergic binding, stereospecific opiate binding, acetylcholinesterase, succinate dehydrogenase and ATPase.

Electrophoresis

Sodium dodecyl sulfate–polyacrylamide gel electrophoresis (SDS-PAGE) according to Laemmli [23] was applied with a gradient of 12–20% polyacrylamide. Membrane samples containing 40–60 mg protein were used. The gels were stained with Coomassie brilliant blue and photometrically scanned with an LKB 2202 Ultrascan laser densitometer.

RESULTS

Preparative extraction

The membranes were separated by partition within a two-phase system (Fig. 1) into two main fractions: class A (with affinity for the upper phase) and class B (with affinity for the interface and partly for the lower phase). To remove traces of contaminating membranes of the other class, the upper phase and lower phase (with interfacial material) were 'washed' twice with pure opposite phase.

The extraction processes were carried out in 50-ml centrifuge tubes with screw caps using systems of 20 g. Concentrated polymer solutions (40% PEG, 40% Ficoll and 32% dextran) were weighed out together with buffer and water to either 20 g (system to give phases for washing) or to 13.5 g (for the first partition step), leaving 6.5 g for the membrane suspension. After equilibration to 3°C the 'washing' systems were mixed and allowed to settle, while Yeda press-treated membranes (corresponding to 29 mg protein) in 6.5 g of suspension were added to the concentrated (13.5 g) system. This was carefully and gently equilibrated by turning the closed tubes upside down twenty times. The system was centrifuged for 15 min at 3000 g_{max} and 3°C. The upper phase was recovered, avoiding material from the interface (by leaving 1 mm height of the upper phase in the tube), and transferred to another tube to which was also added fresh lower phase to the same total volume as the original system. The membrane-containing lower phase (plus interfacial material) was likewise combined

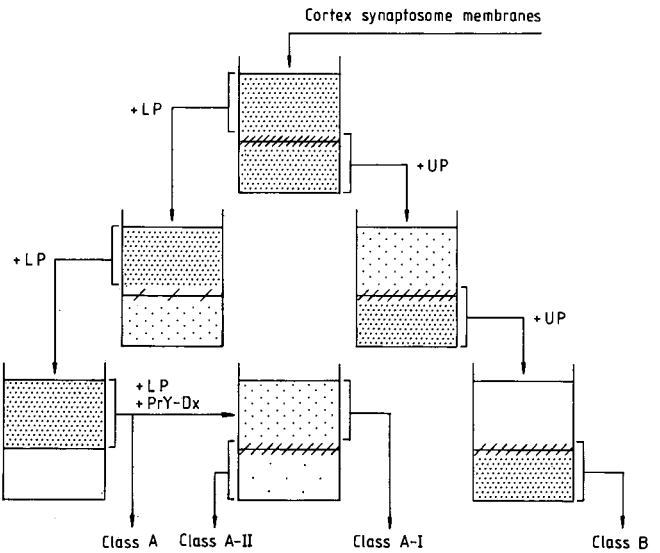

Fig. 1. Flow scheme for the preparative isolation procedure of synaptosomal membrane fractions. UP = pure upper phase; LP = pure lower phase; and PrY–Dx = Procion yellow HE-3G–dextran 500. The two-phase system (20 g) used contained 9.3% (w/w) dextran T-40, 10.3% (w/w) Ficoll 70, 2.3% poly-(ethylene glycol) and 5 m*M* Tris–orthophosphoric acid buffer, pH 7.8 (concentration based on phosphate). The concentration of PrY–dextran in the lower phase was 0.056% (4 μM dye), corresponding to 0.028% (2 μM dye) in the complete system. Membrane concentration in the first system corresponded to 1.5 mg protein per ml. Temperature: 3°C.

with pure upper phase. The two tubes were mixed and centrifuged as above. These washings of the phases were repeated once more. The membranes in the upper phase (fraction A) and the lower phase together with the interface (fraction B) of the other system (see Fig. 1) were recovered and each diluted three times with ice-cold water. The membranes were precipitated by centrifugation (45 000 g_{max} for 2 h) and resuspended in a few milliliters of 5 m*M* Tris–orthophosphoric acid, pH 7.0, for analysis. Alternatively (see below) the upper phase was directly used in a further fractionation with a dextran-bound ligand. The membranes showed good purity when analyzed by counter-current distribution (Fig. 2). The fractions A and B (Fig. 1) differed markedly in contents of enzymes and opiate receptor binding (Table I).

The class A membranes were further fractionated by partitioning in systems containing PrY–dextran. Increasing concentration of the dye, greatly restricted to the bottom phase, lowered successively the percentage of membranes in the upper phase. A preparative separation was done (Fig. 1) using the same protocol as above but including dextran-bound dye (2 μM) at a concentration such that 40% of the class A membranes remained in the upper phase. The two obtained subpopulations, class A-I (in upper phase) and class A-II (at interface plus lower phase), showed different behaviour when analyzed by CCD using a two-phase system containing 2 μM dex-

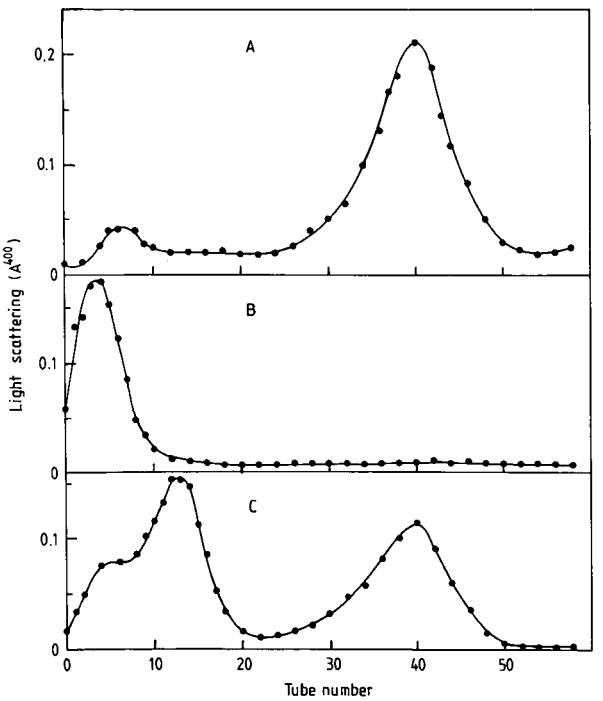

Fig. 2. Counter-current distribution of class A membranes (A), of class B membranes (B), and of original synaptosomal membranes after Yeda press treatment (C), using 58 transfers. The membranes, corresponding to 2–2.5 mg protein, were originally applied in chambers 0 and 1. System as in Fig. 1. For technical details see text. Membrane concentration was measured after dilution as apparent absorbance at 400 nm caused by light scattering. Temperature: 3°C.

TABLE I

ANALYTICAL DATA OF THE ORIGINAL MEMBRANE PREPARATION AND THE FOUR MEMBRANE FRACTIONS A, B, A-I AND A-II SHOWN IN FIG. 1

Specific activities are given relative to protein measured according to Bradford [15].

Fraction	Protein (mg)	Acetyl cholinesterase ($x10^3$) (U/mg)	Succinate dehydrogenase ($x10^3$) (U/mg)	ATPase ($x10^3$) (U/mg)	Specific opiate binding ($x10^5$) (nmol/mg)
Original	29	66	21	225	2.1
A	9.5	81	1.2	271	3.4
B	4.9	3.2	76	312	1.4
A-I	2.8	91	–	397	4.2
A-II	2.8	34	3.7	457	1.7

tran-bound dye (Fig. 3). Analytical data of the subclasses are shown in Table I. The distribution of the various activities within the CCD train in the presence of different concentrations of PrY–dextran (0, 2 and 8 μM dye) (Fig. 4) shows that a moderate concentration of dye in the lower phase gave rise to a further fractionation. With only 2 μM PrY–dextran all the (membrane-bound) succinate dehydrogenase was extracted from the upper phase (recovered in the left peak, Fig. 4B). This shows that membranes of mitochondrial origin are effectively extracted. With 8 μM dye all membranes appear in a single peak to the left in the CCD diagram (Fig. 4C).

Polypeptide pattern

SDS-PAGE of the membrane fractions showed marked differences in the polypeptide pattern (Fig. 5). Some polypeptides dominate in either class A (Fig. 5B) or

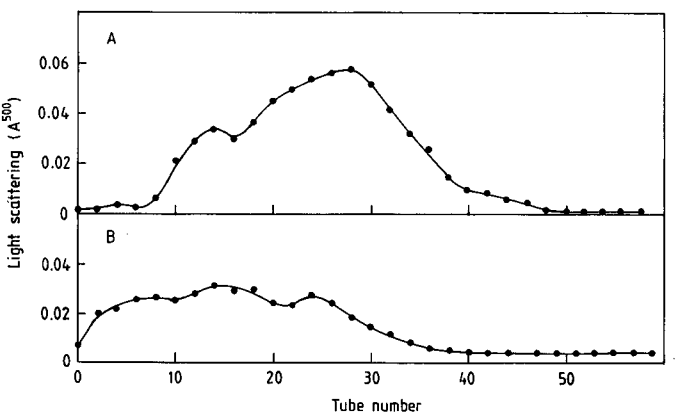

Fig. 3. Counter-current distribution of class A-I membranes (A) and class A-II membranes (B). The membranes (corresponding to 2–2.5 mg protein) were originally included in systems of chambers 0 and 1. The two-phase system contained 2 μM dextran-bound Procion yellow HE-3G. The system composition was otherwise as in Fig. 1. Membrane concentration was measured after dilution as apparent absorbance at 500 nm. Temperature: 3°C.

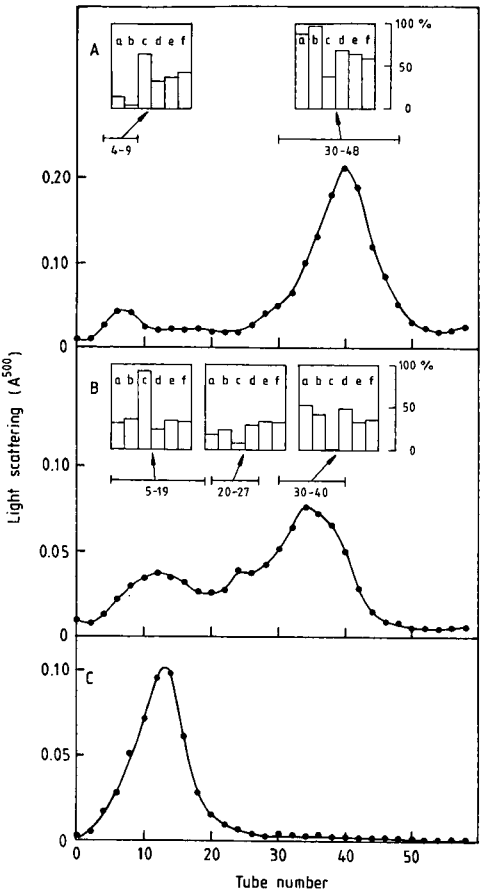

Fig. 4. Effect of dextran-bound Procion yellow HE-3G on the partitioning of class A membranes demonstrated by counter-current distribution. The composition of the two-phase system was the same as in Fig. 1. The system was supplemented by (A) nothing, (B) 0.028% (w/w) PrY–dextran (2 μM dextran-bound dye) and (C) 0.111% (w/w) PrY–dextran (8 μM dextran-bound dye). In (A) and (B) the pooled fractions, indicated by horizontal bars and fraction numbers, were concentrated and washed by centrifugation and analyzed for (a) protein, (b) acetylcholinesterase, (c) succinate dehydrogenase (mitochondrial marker), (d) ATPase, (e) phosphate, and (f) 2′,3′-cyclic nucleotide-3′-phosphohydrolase (myelin marker). The percentage distributions of a–f are shown inset. Temperature: 3°C.

class B (Fig. 5C). Within the subclasses A-I (Fig. 5D) and A-II (Fig. 5E), smaller but significant differences can be seen.

DISCUSSION

The membranes obtained by fragmentation of synaptosomes are of several kinds. Some parts may be non-synaptosomal contaminations, *e.g.* various plasma membranes and membranes originating from extrasynaptosomal mitochondria. The pronounced differences in the membrane fragments in the partition within the two-phase system have been demonstrated by CCD (Fig. 2), with two main fractions.

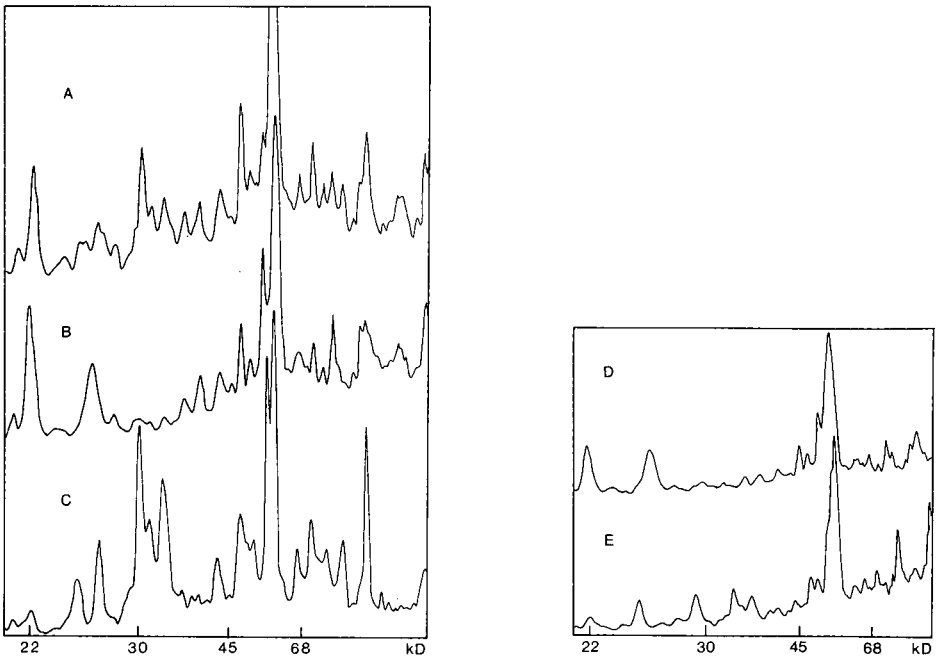

Fig. 5. Scannings of the gels after SDS–PAGE and staining with Coomassie brilliant blue. (A) Original membranes after Yeda press treatment. (B) Class A membranes. (C) Class B membranes. (D) Class A-I membranes. (E) Class A-II membranes. The positions of standard proteins are indicated by their molecular weights in kilodalton (kD).

By using the two-phase system for preparative purposes, larger amounts of purified synaptic membranes (class A), can rapidly be obtained within 30 min. The effectiveness of the extraction (Table I) is shown by the low content of mitochondrial membranes (as measured by succinate dehydrogenase activity) in fraction A (reduced by a factor of 18). On the other hand, acetylcholin esterase and stereospecific opiate binding in this fraction were increased 1.2–1.6 times. Class A membranes contained less myelin, as measured by the activity of 2′,3′-cyclic nucleotide-3′-phosphohydrolase, than the starting material.

The synaptic membranes (class A) are in no way homogeneous, but they contain a variety of membrane fragments differing in composition and properties such as types and concentration of a number of receptors. The synaptosomes from which the membranes are prepared are assumed to consist mainly of presynaptic membranes, but pieces of attached post-synaptic membranes may also occur [14]. By introducing a dextran-bound dye with affinity for membranes, Procion yellow HE-3G, into the lower phase, the class A membranes can be further divided in two subfractions. The nature of the binding sites is unclear, but probably the dye molecule resembles one or more natural ligands, *e.g.* nucleotides. The fact that Procion yellow HE-3G even at very low concentrations (a few micromoles) extracts considerable amounts of membranes points to a strong and probably specific interaction (Fig. 3). The finding that nearly all class A membranes are extracted at high concentration of the dye ligand

indicates that the binding sites are present on most membrane fragments but differ in density or binding strength.

The two fractions class A-I and class A-II are not distinct populations, but the clear differences in polypeptide pattern (Fig. 5D and E) and enzyme activities as well as relative affinity for opiate binding (Table I) show that a simple and quick extraction with a phase containing dye–ligand can also give valuable enrichment of certain types of membranes.

The use of dextran-bound ligands, here illustrated by Procion yellow HE-3G, would allow membranes to be selectively extracted. By using other kinds of ligands (bound to dextran) with specific affinity for various receptors or specific proteins, the membranes enriched in this component could probably selectively be extracted into the lower phase. Affinity partitioning of this kind offers a wide range of possibilities in both choice of ligands and their concentrations. Also, the combination of two ligands in opposite phases and the use of multiple extraction techniques, *e.g.* CCD, would strongly enhance the fractionation power offered by the partition within aqueous two-phase systems. The batch extraction can easily be scaled up to allow the isolation of quantities large enough for detailed characterization of the membranes.

ACKNOWLEDGEMENTS

We thank Mrs. M. Joelsson for valuable technical assistance and preparation of the drawings. This work was supported by grants from the Swedish Natural Science Research Council (G.J.) and C.A.Y.C.I.T. (M.T.M.B. and J.A.C.).

REFERENCES

1 P.-Å. Albertsson, *Partition of Cell Particles and Macromolecules*, Wiley, New York, 3rd ed., 1986.
2 B. Andersson and H.-E. Åkerlund, *Biochim. Biophys. Acta*, 503 (1978) 462.
3 C. Larsson, in J. L. Hall and A. L. Moore (Editors), *Isolation of Membranes and Organelles from Plant Cells*, Academic Press, London, 1983, p. 277.
4 S. D. Flanagan, S. H. Barondes and P. Taylor, *J. Biol. Chem.*, 251 (1976) 858.
5 G. Johansson, R. Gysin and S. D. Flanagan, *J. Biol. Chem.*, 256 (1981) 9126.
6 A. Hartman and E. Heilbronn, *Biochim. Biophys. Acta*, 513 (1978) 382.
7 J. M. Gurd, *J. Neurochem.*, 39 (1982) 1117.
8 G. Johansson, H.-E. Åkerlund and B. Olde, *J. Chromatogr.*, 311 (1984) 277.
9 B. Olde and G. Johansson, *Neuroscience*, 15 (1985) 1247.
10 M. T. Muiño Blanco, J. A. Cebrian Perez, B. Olde and G. Johansson, *J. Chromatogr.*, 358 (1986) 147.
11 P. Gemeiner, D. Mislovicová, J. Zemek and L. Kuniak, *Collect. Czech. Chem. Commun.*, 46 (1981) 419.
12 G. Johansson and M. Andersson, *J. Chromatogr.*, 303 (1984) 39.
13 G. Johansson and M. Joelsson, *J. Chromatogr.*, 393 (1987) 195.
14 M. J. López-Pérez, G. Paris and C. Larsson, *Biochim. Biophys. Acta*, 635 (1981) 359.
15 M. M. Bradford, *Anal. Biochem.*, 72 (1976) 248.
16 G. L. Ellman, K. D. Courtney, V. Andres and R. M. Featherstone, *Biochem. Pharmacol.*, 7 (1961) 88.
17 D. Earl and A. Korner, *Biochem. J.*, 94 (1965) 721.
18 B. F. Scharschmidt, E. B. Keefee, N. M. Blankenship and R. K. Ockner, *J. Lab. Clin. Med.*, 93 (1979) 790.
19 F. Medzihradsky, *Brain Res.*, 108 (1976) 212.
20 B. N. Ames and D. T. Dubin, *J. Biol. Chem.*, 235 (1960) 769.
21 N. R. Sims and P. R. Carnegie, *J. Neurochem.*, 27 (1976) 769.
22 H.-E. Åkerlund, *J. Biochem. Biophys. Methods*, 9 (1984) 133.
23 U. K. Laemmli, *Nature (London)*, 227 (1970) 680.

Journal of Chromatography, 547 (1991) 89–103
Elsevier Science Publishers B.V., Amsterdam

CHROM. 23 203

Analysis and fractionation of natural source diacylglycerols as urethane derivatives by reversed-phase high-performance liquid chromatography

B. G. SEMPORÉ and J. A. BÉZARD*

Laboratoire de Physiologie Animale et Nutrition, Université de Bourgogne, BP 138, 21004 Dijon Cedex (France)

(First received November 8th, 1990; revised manuscript received February 8th, 1991)

ABSTRACT

Reversed-phase high-performance liquid chromatography on a thermostatted octadecylsilyl column was used to separate and fractionate mixtures of diacylglycerols after derivatization with 3,5-dinitrophenyl isocyanate (urethane derivatives). In addition to the separation of commercial diacylglycerol species, the separation of diacylglycerols obtained from peanut oil and cottonseed oil triacylglycerols by chemical hydrolysis is reported. Acetonitrile–acetone mixtures were used for elution of the diacylglycerol urethane derivatives. Unsaturated and saturated derivatives were detected by their refractive indices. They were then collected and their fatty acids analysed as methyl esters by capillary gas chromatography. The elution order of diacylglycerol derivatives in complex mixtures varies as a function of chain length, unsaturation and positional isomerism of the constituent fatty acids. The elution order and resolution vary as a function of temperature. The diacylglycerol composition of mixtures calculated from peak areas is similar to the composition reconstituted from the fatty acid composition of the collected diacylglycerol fractions. The method can be applied to complete compositional analysis but is especially useful for the collection of pure fractions of diacylglycerols during studies of the stereospecific distribution of fatty acids in triacylglycerols.

INTRODUCTION

When studying the stereospecific distribution of fatty acids in triacylglycerol molecules, the fatty acids esterifying the internal *sn*-2 position are those of the *sn*-2-monoacylglycerols issuing from hydrolysis of triacylglycerols by pancreatic lipase [1–3]. The study of the distribution of fatty acids on the external *sn*-1 and *sn*-3 positions, stereospecifically distinct, was more generally performed to date using Brockerhoff's method [4,5]. This method is based on the snake venon phospholipase stereospecificity in the hydrolysis of phospholipid-like molecules synthesized from the mixture of *sn*-1,2- plus *sn*-2,3-diacylglycerols [denoted *sn*-1,2(2,3)-diacylglycerols] issuing from chemical hydrolysis of triacylglycerols [6]. The enzyme distinguishes the two stereoisomers. The present approach consists in separating the *sn*-1,2- and *sn*-2,3-diacylglycerols by high-performance liquid chromatography (HPLC), either as 3,5-dinitrophenyl urethane derivatives on a chiral column [7,8], or as chiral derivatives on a classical silica column [9,10]. However, diacylglycerols issuing from the hydrolysis

0021-9673/91/$03.50

of natural oil triacylglycerols are complex mixtures of molecules differing both in the nature of the component fatty acids and in their positioning. Analysis is difficult. The diacylglycerol mixtures have first to be fractionated into groups according to the positions of the fatty acids, the *sn*-1,3- and the mixture of *sn*-1,2(2,3)-diacylglycerols. The *sn*-1,2(2,3)-diacylglycerol group then has to be fractionated according to the nature of the fatty acids. For further accurate analysis the diacylglycerol fractions must be collected as pure as possible; they therefore have to be well separated to avoid minor contamination between fractions. The proportions of the different fractions in the mixture have additionally to be evaluated with high precision for further accurate calculations.

The diacylglycerol separation method chosen in this work was reversed-phase HPLC. Although widely used in the separation and fractionation of triacylglycerols [11], HPLC has to date rarely been applied to diacylglycerol mixtures. Krüger *et al.* [12] and Ryan and Honeyman [13] developed HPLC methods for the separation and determination of diacylglycerols after derivatization with α-naphthyl isocyanate and a fluorescent marker, N-dansyl (DNS) ethanolaminophosphate, respectively. However, these methods were not entirely convenient for the simultaneous determination of the homologous distribution and the ratio of positional isomers of diacylglycerols.

Kondoh and Takano [14] devised an original detection method for acylglycerols (acylglycerol selective post-column reaction detector), which they applied to the simultaneous determination of mono-, di- and triacylglycerols. However, the detection method involves destroying the partial acylglycerols and does not allow their collection for further analysis.

For our purpose of the stereospecific analysis of triacylglycerols, in this work we studied the HPLC separation of complex mixtures of diacylglycerols according to the nature of the constituent fatty acids (chain length and unsaturation) and their positioning (*sn*-1,3- and *sn*-1,2(2,3)-diacylglycerols). Analyses were carried out in part on underivatized diacylglycerols but particularly on the 3,5-dinitrophenyl isocyanate derivatives, which we expect to use in the separation of the *sn*-1,2- and *sn*-2,3-isomers on a chiral column.

EXPERIMENTAL

Samples

Synthetic *rac*-1,2 and *sn*-1,3-dioleoylglycerols (*rac*-1,2-18:1 18:1 and *sn*-1,3-18:1 18:1, respectively) were obtained from Serdary Research Labs.(London, Ontario, Canada). Synthetic optically active *sn*-,1,2-dioleoylglycerol (*sn*-1,2-18:1 18:1) and *sn*-1,2-dipalmitoylglycerol (*sn*-1,2-16:0 16:0) were purchased from Sigma (St. Louis, MO, USA). Prior to use the *rac*-1,2-18:1 18:1 from Serdary was purified and resolved into *rac*-1,2-18:1 18:1 and *sn*-1,3-18:1 18:1 (impurity), separately recovered by thin-layer chromatography (TLC) on borate-impregnated silica gel (5%, w/w) using light petroleum–diethyl ether (50:50, v/v) as the developing solvent [15].

Natural source diacylglycerols (DGs) were prepared by Grignard degradation with ethylmagnesium bromide [16] or pancreatic lipase hydrolysis [17] of triacylglycerols (TGs) from peanut oil and cottonseed oil. The oil TGs were first fractionated by argentation TLC according to their unsaturation and then fractionated by reversed-phase HPLC [18]. The DGs were separated from the hydrolysis mixture by

TLC on borate-impregnated silica gel into *sn*-1,3- and *sn*-1,2(2,3)-diacylglycerols according to decreasing R_F values. The TGs fractionated by combined TLC-HPLC were palmitoyldioleoylglycerol (16:0 18:1 18:1), a complex mixture of stearoyldioleoylglycerol plus palmitoyloleoyleicosenoylglycerol (18:0 18:1 18:1 + 16:0 18:1 20:1), trioleoylglycerol (18:1 18:1 18:1), palmitoyloleoyllinoleoylglycerol (16:0 18:1 18:2), dioleoyllinoleoylglycerol (18:1 18:1 18:2) and oleoyldilinoleoylglycerol (18:1 18:2 18:2) from peanut oil. Palmitoyloleoyllinoleoylglycerol (16:0 18:1 18:2) was also isolated from cottonseed oil in order to compare it with peanut oil and with previous results obtained by a different method [19].

The diacylglycerols prepared after hydrolysis of these natural triacylglycerols were the two series of *sn*-1,3- and *sn*-1,2(2,3)-isomers of dilinoleoylglycerol (18:2 18:2), oleoyllinoleoylglycerol (18:1 18:2), palmitoyllinoleoylglycerol (16:0 18:2), dioleoylglycerol (18:1 18:1), palmitoyloleoylglycerol (16:0 18:1), oleoyleicosenoylglycerol (18:1 20:1) and stearoyloleoylglycerol (18:0 18:1).

They were identified during HPLC analysis by comparison with the above commercial diacylglycerols and with the series of natural *sn*-1,2(2,3)-diacylglycerols identified after fractionation by gas chromatographic (GC) analysis of their constituent fatty acids and by HPLC on a chiral stationary phase to confirm the type of isomerism.

Preparation of 3,5-dinitrophenyl isocyanate derivatives of diacylglycerols

The procedures used to prepare the 3,5-dinitrophenyl isocyanate derivatives of DGs was derived from that employed by Ôi and Kitahara [20] for chiral alcohols and adapted to DGs by Itabashi and Takagi [7,8].

Amounts of 1–5 μmol (0.6–3 mg) of DGs were dissolved in 4 ml of dry toluene in an 8-ml glass tube with a PTFE-lined screw-cap; 10–50 μmol (2–10 mg) of 3,5-dinitrophenyl isocyanate (Sumitomo, Osaka, Japan) and 40 μl of dry pyridine were added to the solution and the mixture was left for 1 h at ambient temperature with occasional shaking. At the end of the reaction the solvent was removed under nitrogen and the residue was dissolved in 0.2 ml of chloroform. The DG derivatives were isolated by TLC on silica gel $60F_{254}$-precoated plates (Merck, Darmstadt, Germany). The plates containing a fluorescence indicator were previously activated at 110–120°C for 1 h in an oven. The developing solvent was hexane–ethylene dichloride–ethanol (40:10:3, v/v/v). After drying under nitrogen the diacylglycerol derivative bands were delineated under UV light (254 nm),the corresponding silica gel was scraped off the plate and the urethane derivatives were extracted with diethyl ether.

Alternatively, the crude diacylglycerol urethane derivatives were purified by reversed-phase HPLC instead of TLC. In this instance, at the end of the derivatization reaction the mixture was decanted. The limpid upper phase was filtered through hyperfine glass-wool into another vial. The solvent was evaporated under nitrogen and the urethane derivatives were dissolved in chloroform for storage, in acetonitrile or in the solvent used for reversed-phase HPLC for fractionation.

Purification of crude diacylglycerol derivatives was coupled with fractionation according to carbon number, degree of unsaturation and positional isomerism (*sn*-1,3-diacylglycerol derivatives were separated from *sn*-1,2(2,3)-isomers). Isocratic operation was applied with the solvent system acetonitrile–acetone (55:45 and 60:40, v/v) at different temperatures. The temperature was ambient (16–18°C) for the three

diacylglycerol mixtures: *sn*-1,2(2,3) 18:1 18:1 and 16:0 18:1, *sn*-1,2(2,3) 18:1 18:2 and 18:1 18:1 and *sn*-1,2(2,3) 18:2 18:2 and 18:1 18:2. They were isolated after hydrolysis of the natural triacylglycerols 16:0 18:1 18:1, 18:1 18:1 18:2 and 18:1 18:2 18:2, respectively. A constant subambient thermostatically controlled temperature [21] of 10–12°C was used to improve separation of the critical pairs (18:1 18:2 and 16:0 18:2) in the mixture *sn*-1,2(2,3)-18:1 18:2, −16:0 18:2 and −16:0 18:1 issuing from hydrolysis of the peanut oil or cottonseed oil 16:0 18:1 18:2 triacylglycerol. An ambient temperature of *ca.* 20°C was used for the mixture of all these diacylglycerols and their *sn*-1,3-isomers.

Column liquid chromatography

HPLC was carried out using a Model 6000 A solvent-delivery system connected either to a Model R 401 differential refractometer or to a Model 450 variable-wavelength UV detector (Waters Assoc., Milford, MA, USA). Separations were achieved on two stainless-steel columns: a Superspher RP-18 and a chiral column. A prepacked 250 mm × 4 mm I.D. Hibar LiChroCART HPLC cartridge, LiChrospher 100 CH-18/II SUPER (4 μm particles) column was obtained from Merck. The 250 mm × 4 mm I.D. chiral column used in several controls, packed with 5-μm particles of N-(*R*)-1-(α-naphthyl)ethylaminocarbonyl-(*S*)-valine chemically bonded to δ-aminopropylsilanized silica (Sumipax OA-4100) was purchased from Sumitomo. A Guard-Pac precolumn module was attached to the inlet of each column: a LiChroCART 4-4 filled with LiChrosorb 100 RP-18 (Merck) for the RP-18 column and a LiChroCART 4-4 filled with LiChrosorb Si 60 (Merck) for the chiral column.

The analyses were carried out isocratically at a constant flow-rate of 0.9, 1 or 1.2 ml min^{-1} at ambient temperature (chiral OA-4100 column and LiChrospher RP-18) or at a constant controlled temperature [21] below or above ambient temperature (LiChrospher RP-18).

Several solvent systems were used as mobile phase, depending on the separation desired: acetone–acetonitrile (45:55 or 40:60, v/v) for underivatized or 3,5-dinitrophenyl isocyanate-derivatized diacylglycerols on the RP-18 column; hexane–ethylene dichloride (or methylene chloride)–ethanol (80:20:1, v/v/v) for diacylglycerol enantiomer resolution on the chiral column OA-4100, as 3,5-dinitrophenyl urethane derivatives. Acetonitrile (Far UV HiperSolv) was from BDH. Acetone, hexane (SDS, Peypin, France) were of analytical-reagent grade. Ethylene dichloride (HPLC grade) was purchased from Fluka (Buchs, Switzerland). Dichloromethane of analytical-reagent grade was obtained from Prolabo (Paris, France) and ethanol of the same grade from Carlo Erba (Milan, Italy). Water was doubly distilled. Solvents were filtered through a Millipore membrane (pore size 0.5 μm) and the mobile phase mixtures were vacuum degassed for 2 min before use.

Samples for HPLC separations initially in chloroform were generally dissolved in pure acetonitrile or in the solvent used as the mobile phase for injection onto the HPLC column.

For quantitative determinations, peak areas were measured by means of an Enica 21 integrator–calculator (Delsi Instruments, Suresnes, France).

Gas chromatography

The fatty acid composition of underivatized diacylglycerols recovered after hy-

drolysis and the fatty acid composition of the 3,5-dinitrophenyl isocyanate derivatives of the HPLC-collected diacylglycerols (RP-18 column) were determined by GC of the methyl esters prepared from methanol–boron trifluoride [22]. The analyses were carried out on a Becker-Packard Model 417 gas chromatograph, equipped with a laboratory-made 30 m × 0.4 mm I.D. glass capillary column coated with Carbowax 20M (Applied Science Labs., State College, PA, USA) at a constant temperature of 195°C and a nitrogen flow-rate of 3 ml min^{-1}. The apparatus was equipped with an ROS injector [23] (Spiral, Dijon, France) and a flame ionization detector. Peak areas were measured with an Enica 21 integrator–calculator. Calibration factors for quantitative determinations were calculated using standard mixtures of fatty acids (Nu Chek Prep, Elysian, MN, USA).

Definitions

Different parameters were determined to characterize the chromatographic diacylglycerol separations. The equivalent carbon number (*ECN*) [11] of the diacylglycerol fractions, equivalent to the partition number (*PN*) [3], was calculated from the total acyl carbon number (*CN*) and total number of double bonds (*DB*) of the two constituent fatty acids, according to [11]

$$ECN = CN - 2DB$$

Peak elution was characterized by the retention time, t_R (min), corrected for the column void volume.

Separation between two peaks 1 and 2 (in order of elution) was characterized by the separation factor α, that is, the ratio of their corrected retention times, t_{R2}/t_{R1}. Separation was considered to be complete from $\alpha = 1.10$.

Resolution between two peaks 1 and 2 was characterized by the resolution factor R_s calculated from the retention times and the peak widths at the baseline (w) according to [24]

$$R_s = 2(t_{R2} - t_{R1})/(w_2 + w_1)$$

From $R_s = 1$ two peaks are reasonably well separated.

RESULTS AND DISCUSSION

Separation of underivatized diacylglycerols

Mixtures of underivatized dipalmitoyl- and dioleoylglycerol stereoisomers were separated by reversed-phase HPLC using different acetonitrile–acetone mixtures as mobile phase: 50:50, 55:45 or 60:40 (v/v). Dioleoylglycerols were easily eluted as two well separated peaks corresponding to the first-eluted single *sn*-1,3-isomer followed by the mixture of the two *sn*-1,2- and *sn*-2,3-isomers eluted as a single unshouldered peak (Fig. 1B). The retention times under the conditions used [19°C with acetonitrile–acetone (60:40, v/v) at 1 ml min^{-1}] were 14.7 and 16.2 min from the injection point, respectively. In contrast, dipalmitoylglycerol isomers were incompletely separated whatever the chromatographic conditions, probably because of poor dissolution of the saturated acylglycerols in the mobile phase and in the injection solvent. It was

nevertheless possible to determine the elution order of the different isomers. The *sn*-1,3-isomers were eluted first, followed by the *sn*-1,2(2,3)-isomer mixture, and the unsaturated dioleoylglycerols preceded the saturated dipalmitoylglycerols. This corresponds to what was previously observed by Kondoh and Takano [14], although using other analytical conditions.

Because of the difficulties encountered in the separation of the saturated diacylglycerols and as the objective was to collect pure mixtures of *sn*-1,2(2,3)-isomers to be separated further into optical isomers on a chiral column as 3,5-dinitrophenyl isocyanate derivatives, these derivatives were henceforth used with several additional advantages. First, derivatization improves the solubility of the more saturated diacylglycerols in the solvents used in HPLC with refractometric detection, *i.e.*, acetonitrile and acetone. Second, with derivatized diacylglycerols, fractionation according to the nature and the positions of fatty acids in the glycerol moiety can be easily combined. Third, the previous purification step by TLC of the DG derivatives before analysis on a chiral column with UV detection, as recommended by Itabashi and Takagi [7,8], is avoided. Last, derivatization of diacylglycerols can be carried out more rapidly after hydrolysis of triacylglycerols and just after their isolation on borate-impregnated silica gel TLC plates, decreasing the extent of possible isomerization due to the free hydroxyl group of glycerol. Fig. 1A illustrates the good separation

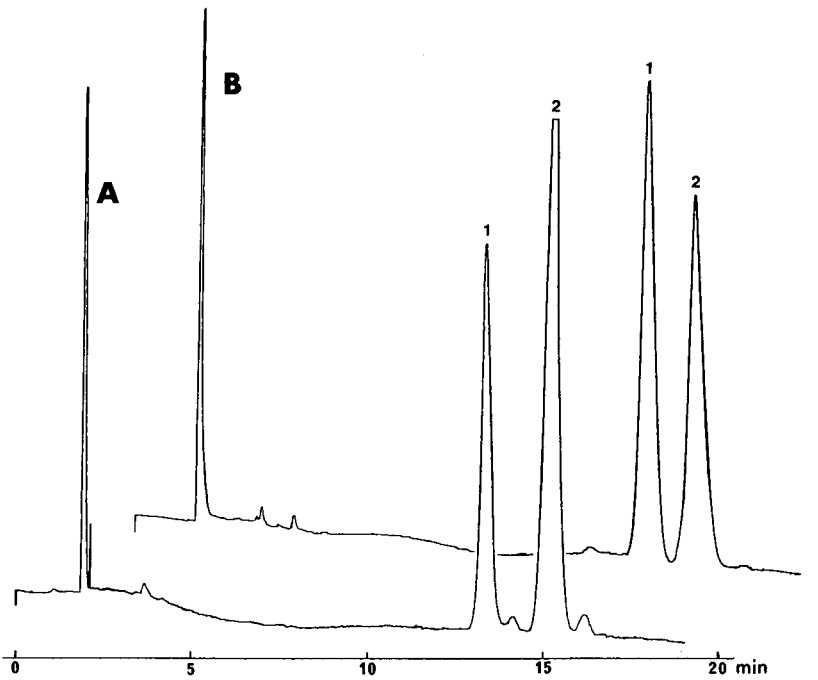

Fig. 1. HPLC separation of dioleoylglycerol isomers (A) as 3,5-dinitrophenyl isocyanate derivatives and (B) underivatized on an RP-18 column. 1 = *sn*-1,3-Dioleoylglycerol (*sn*-1,3-18:1 18:1); 2 = *sn*-1,2(2,3)-dioleoylglycerol [*sn*-1,2(2,3)-18:1 18:1]. The minor satellite peaks emerging after the major peaks in A were not identified. Analytical conditions: stainless-steel column (250 mm × 4 mm I.D.) packed with 4-μm octadecylsilyl (C_{18}) reversed-phase material; eluent, acetonitrile–acetone (60:40, v/v) at 1 ml min^{-1}; temperature thermostatically controlled at 19°C; refractive index detection; isocratic analysis.

of the two pairs of derivatized *sn*-1,3- and *sn*-1,2(2,3)-dioleoylglycerols in 13.2 and 15.0 min, respectively. The retention times were slightly shorter than those for the underivatized diacylglycerols and the separation was better with narrower peaks. The separation and the resolution factors were 1.13 and 2.77, respectively, with the derivatives and only 1.10 and 1.83, respectively, with underivatized dioleoylglycerols.

Properties of diacylglycerol derivatives

Several problems were encountered in the preparation, purification and conservation of the DG derivatives. The first problem was the poor solubility of the more saturated diacylglycerols in toluene. In several instances it was necessary to heat the reaction mixture slightly. The second problem was the fractionation of pure DG derivatives from the reaction mixture on a TLC plate as proposed by Itabashi and Takagi [7,8]. In the purification of *rac*-1,2-dipalmitoylglycerol, they observed two bands. The lower yellow band corresponded to the excess of 3,5-dinitrophenyl isocyanate reagent and the upper band to the DG derivatives. On the plates we used the reaction mixture products were separated into more than two bands. The analysis by reversed-phase HPLC of the compounds adsorbed in each band showed that only the main band, located just above that of the remaining reagent, contained DG derivatives. This was confirmed by HPLC on the chiral column. Because of this difficulty of identification of the proper band, the previous purification step by TLC was abandoned and the mixture was directly fractionated by reversed-phase HPLC. The remaining reagent eluted with the injection solvent and, as indicated above, the DG derivatives were separated according to the nature and the positions of the constituent fatty acids.

The last problem encountered was the lack of stability of the unsaturated diacylglycerol urethane derivatives during storage when compared with the underivatized molecules. In an experiment with twelve mixtures of mixed diacylglycerols, the relative decrease in the proportion of linoleic acid was 10–30% and that of oleic acid 4–5% after 1 month of storage. This decrease was only partly due to oxidation; another additional type of degradation occurred that remains to be elucidated. It is thus recommended to proceed rapidly to stereospecific analysis of the diacylglycerol urethane derivatives after fractionation by reversed-phase HPLC in order to obtain accurate results.

Separation of diacylglycerol derivatives

A wide range of diacylglycerols were prepared by deacylation of natural triacylglycerols from peanut and cottonseed oils (see Experimental). They were separated as urethane derivatives by reversed-phase HPLC.

Figs. 2 and 3 illustrate the separation of diacylglycerol mixtures, separately (Fig. 2) or mixed (Fig. 3). Tables I and II give some observed chromatographic parameters calculated for the two series of *sn*-1,3- and *sn*-1,2(2,3)-diacylglycerols. Fig. 3 shows that all the *sn*-1,2(2,3)-diacylglycerols studied were clearly separated, even the critical pairs, *i.e.*, those presenting the same equivalent carbon number (*ECN*) in a given series of isomers (Table I), *e.g.*, *sn*-1,2(2,3)-18:1 18:1 and −16:0 18:1, peaks 9 and 10 on the chromatogram in Fig. 3B. In both series of isomers (Table I) the diacylglycerols were eluted according to increasing *ECN*, and when the *ECN* was the same the more unsaturated of the pair eluted earlier (*e.g.*, in the above example). For

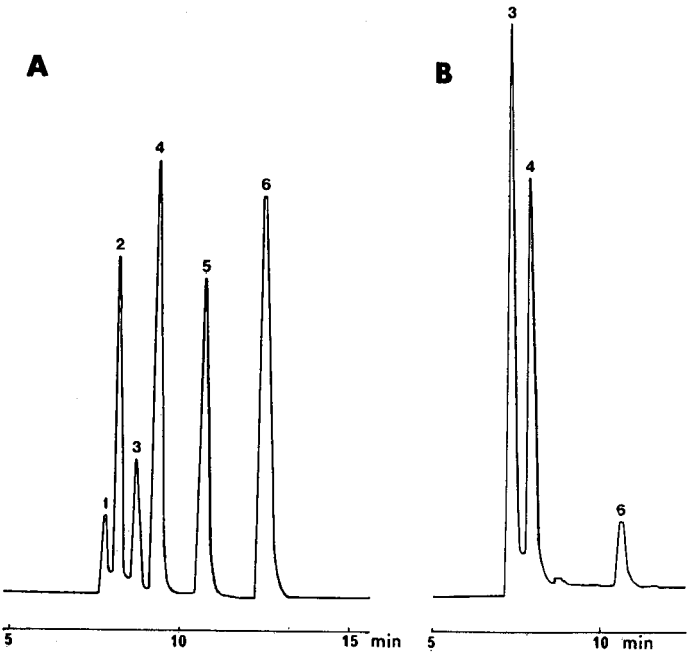

Fig. 2. RP-18 HPLC analysis of 3,5-dinitrophenyl isocyanate derivatives of natural source *sn*-1,3- and *sn*-1,2(2,3)-diacylglycerols formed by deacylation of one peanut oil triacylglycerol (16:0 18:1 18:2). 1 = *sn*-1,3-18:1 18:2; 2 = *sn*-1,3-16:0 18:2; 3 = *sn*-1,2(2,3)-18:1 18:2; 4 = *sn*-1,2(2,3)-16:0 18:2; 5 = *sn*-1,3-16:0 18:1; 6 = *sn*-1,2(2,3)-16:0 18:1. (A) Mixture of *sn*-1,3- and *sn*-1,2(2,3)-isomers; (B) only *sn*-1,2(2,3)-isomers. Analytical conditions: eluent, acetonitrile–acetone (A, 60:40, v/v; B, 55:45, v/v) at 1.2 ml min^{-1}; ambient temperature (19°C); other conditions as in Fig. 1.

diacylglycerols with the same two-component fatty acids or the same *ECN*, the *sn*-1,3-isomers eluted earlier than the corresponding *sn*-1,2(2,3)-isomers. The data reported in Table I quantify the separation observed between peaks of each series and those in Table II between adjacent peaks. The resolution factor, R_s, between two adjacent peaks was found in each instance to be at least equal to 1, confirming their good separation. In each series of isomers (Table I), the *sn*-1,2(2,3)-diacylglycerols were better separated than the corresponding *sn*-1,3-isomers, exhibiting higher separation and resolution factors between two successive peaks. This property is important, because in the stereospecific analysis of triacylglycerols the *sn*-1,2(2,3)-diacylglycerols have to be separated from the *sn*-1,3-isomers after deacylation and fractionated by reversed-phase HPLC, as derivatives, before further separation on a chiral column. The good separation observed here leads to good purity of the fractionated diacylglycerols.

If one compares the separation parameters (last two columns in Table I) for *sn*-1,3- and *sn*-1,2(2,3)-isomers of a given diacylglycerol, it can be seen that generally they increased with increasing retention times. This means that if necessary, the separation could be improved between isomers by choosing chromatographic conditions that increase the retention time, such as a lower column temperature. For a given

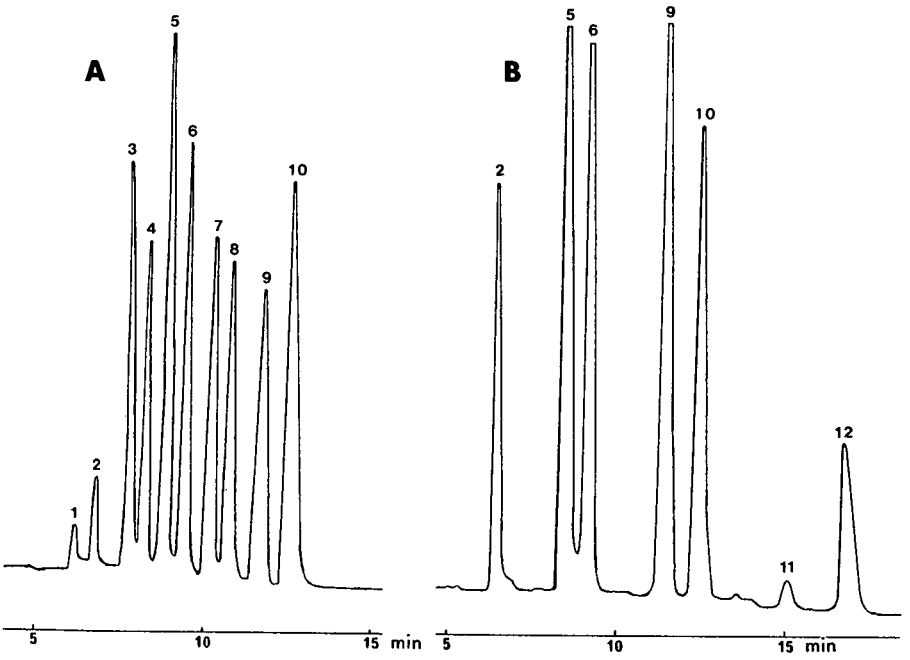

Fig. 3. RP-18 HPLC analysis of 3,5-dinitrophenyl isocyanate derivatives of natural source *sn*-1,3 and *sn*-1,2(2,3)-diacylglycerols formed by deacylation of several peanut oil triacylglycerols. 1 = *sn*-1,3-18:2 18:2; 2 = *sn*-1,2(2,3)-18:2 18:2; 3 = *sn*-1,3-18:1 18:2; 4 = *sn*-1,3-16:0 18:2; 5 = *sn*-1,2(2,3)-18:1 18:2; 6 = *sn*-1,2(2,3)-16:0 18:2; 7 = *sn*-1,3-18:1 18:1; 8 = *sn*-1,3-16:0 18:1; 9 = *sn*-1,2(2,3)-18:1 18:1; 10 = *sn*-1,2(2,3)-16:0 18:1; 11 = *sn*-1,2(2,3)-18:1 20:1; 12 = *sn*-1,2(2,3)-18:0 18:1. (A) Mixture of *sn*-1,3- and *sn*-1,2(2,3)-isomers; (B) only *sn*-1,2(2,3)-isomers. Analytical conditions: eluent, acetonitrile–acetone (60:40, v/v) at 1.2 ml min^{-1}; temperature, (A) 20°C and (B) 19°C; other conditions as in Fig. 1.

series of isomers, a decrease in the analysis temperature considerably improves the separation of the different diacylglycerols. This is illustrated in Fig. 4A and B, which show chromatograms registered in the separation of two mixtures of *sn*-1,2(2,3)-isomers of oleoyllinoleoylglycerol (18:1 18:2), palmitoyllinoleoylglycerol (16:0 18:2) and palmitoyloleoylglycerol (16:0 18:1) at 19 and 10°C, respectively. Both mixtures resulted from hydrolysis of the triacylglycerol 16:0 18:1 18:2, but isolated from two different oils: peanut oil for the first mixture and cottonseed oil for the second. Table III gives some chromatographic parameters for these analyses. As can clearly be seen in Fig. 4 and Table III, when the analysis temperature was decreased from 19 to 10°C, with the other conditions remaining unchanged, the corrected retention times were increased by 37% for the more unsaturated and by 53% for the more saturated diacylglycerols. The separation factor was increased by *ca.* 6% for the two pairs of adjacent peaks. The better separation of the first two peaks at 10°C leads to less contamination of the second fraction by the first, after collection of the three fractions for further stereoisomerism HPLC analysis on a chiral column. The resolution factor for the first two adjacent peaks increased by 34% from 19 to 10°C whereas it did not increase or even decreased for the second pair of adjacent peaks (2 and 3) because of

TABLE I

SOME CHEMICAL AND CHROMATOGRAPHIC PARAMETERS OF DIFFERENT *sn*-1,3- AND *sn*-1,2(2,3)-DIACYLGLYCEROLS SEPARATED BY REVERSED-PHASE HPLC AS URETHANE DERIVATIVES

Isomers	Peak No.	Diacylglycerols	*CN*[a]	*DB*[b]	*ECN*[c]	t_R (min)[d]	A[e]		B[f]	
							α[g]	R_s[h]	α[g]	R_s[h]
sn-1,3-	1	18:2 18:2	36	4	28	4.3				
	2	18:1 18:2	36	3	30	5.9	1.37	5.88		
	3	16:0 18:2	34	2	30	6.3	1.07	1.19		
	4	18:1 18:1	36	2	32	8.3	1.31	5.16		
	5	16:0 18:1	34	1	32	8.8	1.06	1.00		
sn-1,2(2,3)-	6	18:2 18:2	36	4	28	4.9			1.14	2.42
	7	18:1 18:2	36	3	30	6.8	1.40	6.62	1.15	2.78
	8	16:0 18:2	34	2	30	7.5	1.10	1.60	1.19	3.29
	9	18:1 18:1	36	2	32	9.7	1.30	5.30	1.17	3.10
	10	16:0 18:1	34	1	32	10.5	1.08	1.43	1.19	3.61

[a] *CN* = carbon number = total acyl carbon number of the two component fatty acids.
[b] *DB* = total double-bond number.
[c] Equivalent carbon number $ECN = CN - 2DB$.
[d] Retention time corrected for the column void volume.
[e] Between two successive diacylglycerols as listed in column 2.
[f] Between *sn*-1,3- and *sn*-1,2(2,3)-isomers of diacylglycerols with the same two component fatty acids.
[g] Separation factor between two peaks or ratio of the corrected retention times.
[h] Resolution factor between two peaks 1 and 2 calculated from the retention times (t_R) and the peak widths (w) according to the equation $R_s = 2(t_{R2} - t_{R1})/(w_2 + w_1)$.

TABLE II

SOME CHROMATOGRAPHIC PARAMETERS OF DIACYLGLYCEROL ISOMERS SEPARATED BY REVERSED-PHASE HPLC AS URETHANE DERIVATIVES AND LISTED ACCORDING TO ELUTION ORDER

Parameter	Diacylglycerol isomers[a]				
	sn-1,3- (18:2 18:2)	*sn*-1,2(2,3)- (18:2 18:2)	*sn*-1,3- (18:1 18:2)	*sn*-1,3- (16:0 18:2)	*sn*-1,2(2,3)- (18:1 18:2)
Equivalent carbon number, *ECN*[b]	36	36	36	34	36
Separation factor, α[c]		1.14	1.20	1.07	1.08
Resolution factor, R_s[d]		2.42	3.92	1.19	1.61
	sn-1,2(2,3)- (16:0 18:2)	*sn*-1,3- (18:1 18:1)	*sn*-1,3- (16:0 18:1)	*sn*-1,2(2,3)- (18:1 18:1)	*sn*-1,2(2,3)- (16:0 18:1)
Equivalent carbon number, *ECN*[b]	34	36	34	36	34
Separation factor, α[c]	1.10	1.11	1.06	1.10	1.08
Resolution factor, R_s[d]	1.60	2.06	1.00	2.15	1.43

[a] *sn*-1,3- and *sn*-1,2(2,3)-diacylglycerol isomers are listed according to their elution order (see Fig. 4).
[b–d] Definitions as in Table I.

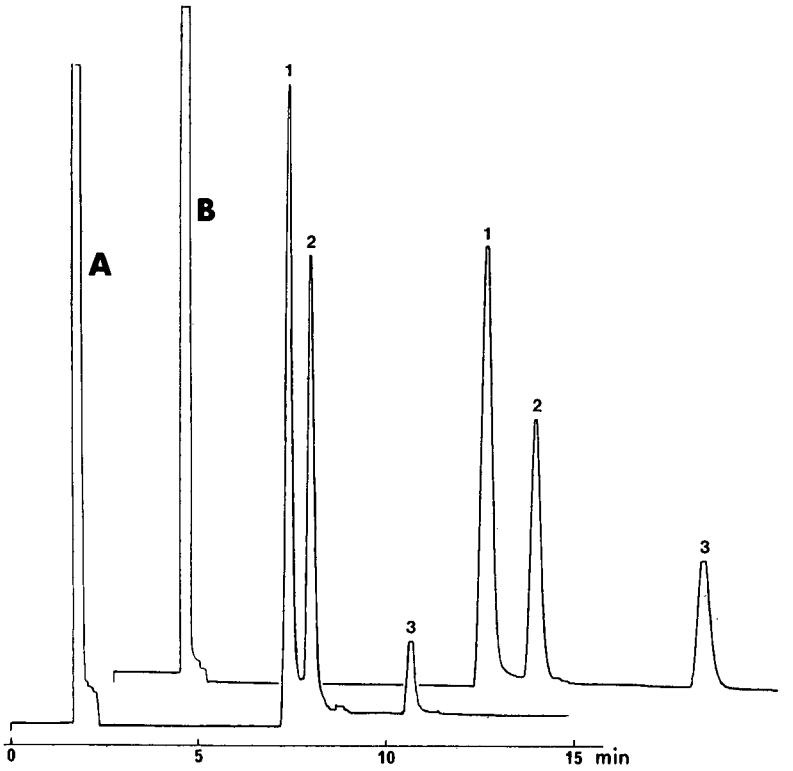

Fig. 4. RP-HPLC separations of 3,5-dinitrophenyl isocyanate derivatives of 1,2(2,3)-diacylglycerols originating from Grignard degradation of (A) peanut oil palmitoyloleoyllinoleoylglycerol (16:0 18:1 18:2) and (B) the same triacylglycerol of cottonseed oil at (A) 19°C and (B) 10°C. Other conditions as in Fig. 2B. Peaks: 1 = *sn*-1,2(2,3)-18:1 18:2; 2 = *sn*-1,2(2,3)-16:0 18:2; 3 = *sn*-1,2(2,3)-16:0 18:1.

TABLE III

SOME CHEMICAL AND CHROMATOGRAPHIC PARAMETERS OF *sn*-1,2(2,3)-DIACYLGLYCEROL URETHANE DERIVATIVES ANALYZED BY HPLC AT TWO DIFFERENT TEMPERATURES

sn-1,2(2,3)-Diacylglycerol	*ECN*[a]	19°C			10°C			t_R(10°C)/t_R(19°C)
		t_R[b]	α[c]	R_s[d]	t_R[b]	α[c]	R_s[d]	
18:1 18:2	30	6.0			8.2			1.37
16:0 18:2	30	6.6	1.10	0.92	9.6	1.17	1.23	1.45
16:0 18:1	32	9.2	1.39	4.08	14.1	1.47	3.91	1.53

[a–d] Definitions as in Table I.

rapid peak broadening with decreasing temperature. However, when lowering the analysis temperature to improve the resolution, the solubility in the eluting solvent of certain saturated diacylglycerols of long chain length can become a problem, in spite of the higher solubility of derivatized acylglycerols when compared with the underivatized compounds. In this instance, the use of longer columns at ordinary temperature would possibly represent a better alternative.

Quantitative analysis of diacylglycerol derivatives

In the stereospecific analysis of triacylglycerols, several quantitative aspects should be considered. First, deacylation with a Grignard reagent must generate representative diacylglycerols, *i.e.*, without any selective hydrolysis according to the nature or the positioning of fatty acids in the glycerol moiety. Second, the derivatization procedure must not modify the proportion and the fatty acid composition of the original diacylglycerols. Third, the derivatized diacylglycerols must be quantitatively detected by HPLC so that their proportion in a mixture can be easily calculated from the peak areas. These different aspects were examined in the following three series of experiments.

To check the absence of selectivity or of side-reactions in the derivatization procedure, twelve mixtures of natural source diacylglycerols derived from five oil triacylglycerols (Tables IV and V) were analysed in two ways. After isolation and before derivatization, an aliquot of the *sn*-1,2(2,3)-diacylglycerol mixtures was analysed by GC for fatty acid composition. The remainder was derivatized with 3,5-dinitrophenyl isocyanate and the derivatives were fractionated by HPLC. The collected HPLC fractions were analysed by GC in the presence of a known amount of heptadecanoic acid for determination of the fatty acid composition and fraction proportion. The overall fatty acid composition of the cumulated HPLC fractions was calculated from these data.

The results are reported in Table IV. The fatty acid composition of the fractionated diacylglycerol fractions easily allows their identification. Some contamination occurred between adjacent fractions, which explains some unexpected figures. For example, in the first sample, 16:0 18:1 was eluted immediately after 18:1 18:1 (they form a critical pair) and was contaminated by peak tailing. This explains the too high percentage of 18:1 as compared with 16:0 in this diacylglycerol. This type of contamination was taken into account in the calculation of the reconstituted total diacylglycerol fatty acid composition. This recalculated fatty acid composition can be compared in Table IV with the experimental values initially determined on the aliquot. There is great similarity between the two series of data, the average difference being only 2% with a maximum of 5.5%. We can therefore conclude that probably the derivatization procedure and HPLC separation did not induce any modification of the initial diacylglycerols (composition and proportion).

To check the quantitative detection of the diacylglycerol derivatives by differential refractometry in HPLC analysis, the proportions, as percentages, of the different fractions were calculated from the peak areas and from the fatty acid compositions of the collected fractions as above. The two series of data reported in Table V (third and fourth columns) can be compared and are found to be similar, the average difference not exceeding 3.8%. The greatest differences were observed for diacylglycerols 16:0 18:1 formed from the 2nd and 5th triacylglycerols (16:0 18:1 18:2) as

TABLE IV

PERCENTAGES AND FATTY ACID COMPOSITIONS OF THE *sn*-1,2(2,3)-DIACYLGLYCEROLS FORMED BY DEACYLATION OF NATURAL TRIACYLGLYCEROLS

	Peanut oil								
Triacylglycerols[a]	16:0	18:1	18:1		16:0	18:1	18:2		
Diacylglycerols[b]	18:1	18:1	16:0 18:1	Total	18:1	18:2	16:0 18:2	16:0 18:1	Total
(mol%)[c]	(41.7)	(58.3)	Calc.[d]	Exp.[e]	(46.4)	(42.4)	(11.2)	Calc.[d]	Exp.[e]
Fatty acids (mol%)									
16:0	1.5	45.7	27.3	27.2	1.1	41.6	47.1	23.2	22.2
18:1	98.4	53.9	72.3	72.1	49.3	4.0	48.1	29.9	29.5
18:2					48.9	53.7	1.8	45.6	44.6
	Peanut oil								
Triacylglycerols[a]	18:1	18:1	18:2		18:1	18:2	18:2		
Diacylglycerols[b]	18:1	18:2	18:1 18:1	Total	18:2	18:2	18:1 18:2	Total	
(mol%)[c]	(77.3)	(22.7)	Calc.[d]	Exp.[e]	(43.8)	(56.2)	Calc.[d]	Exp.[e]	
Fatty acids[f] (mol%)									
16:0									
18:1	49.6	97.2	60.4	60.0	2.2	50.4	29.3	28.1	
18:2	49.6	0.8	38.5	39.2	96.5	48.2	69.4	71.1	
	Cottonseed oil								
Triacylglycerols[a]	16:0	18:1	18:2						
Diacylglycerols[b]	18:1	18:2	16:0 18:2	16:0 18:1	Total				
(mol%)[c]	(48.1)	(30.3)	(21.6)	Calc.[d]	Exp.[e]				
Fatty acids[f] (mol%)									
16:0	1.1	47.7	50.0	25.8	25.9				
18:1	49.4	2.8	49.2	35.2	34.0				
18:2	49.3	48.9		38.5	39.6				

[a] Triacylglycerols isolated from peanut (the first four) and cottonseed (the last one) oils by combined argentation TLC and reversed-phase HPLC and deacylated by Grignard reaction.

[b] *sn*-1,2(2,3)-Diacylglycerols formed by deacylation of natural triacylglycerols, isolated on borate-impregnated silica TLC plates, derivatized with 3,5-dinitrophenyl isocyanate and fractionated by reversed-phase HPLC.

[c] Percentages of the diacylglycerol derivative fractions calculated from the fatty acid composition of the collected fractions after addition of a known amount of heptadecanoic acid. Contamination between peaks was not corrected for.

[d] Fatty acid composition of total diacylglycerol derivatives calculated from the percentages and the fatty acid compositions of the fractions isolated by HPLC.

[e] Fatty acid composition of the total diacylglycerols before derivatization.

[f] Traces ($< 1.5\%$) of 18:0 and 16:1 are not reported but were taken into account in the percentage calculations.

TABLE V

PERCENTAGES OF THE *sn*-1,2(2,3)-DIACYLGLYCEROLS FORMED BY DEACYLATION OF TRIACYLGLYCEROLS AND FRACTIONATED AS URETHANE DERIVATIVES BY REVERSED-PHASE HPLC

Triacylglycerols[a]	Diacylglycerols[b]	Concentration (mol%)		
		Peak areas[c]	Fatty acids[d]	*sn*-2-MG[e]
16:0 18:1 18:1	18:1 18:1	46.9	46.1	47.9
	16:0 18:1	53.1	53.9	52.0
16:0 18:1 18:2	18:1 18:2	49.2	48.1	49.1
	16:0 18:2	42.2	41.4	40.1
	16:0 18:1	8.6	10.5	10.8
18:1 18:1 18:2	18:1 18:2	77.9	77.6	78.1
	18:1 18:1	22.1	22.4	21.9
18:1 18:2 18:2	18:2 18:2	44.8	43.3	44.0
	18:1 18:2	55.2	56.7	56.0
16:0 18:1 18:2	18:1 18:2	50.5	48.4	48.5
	16:0 18:2	29.4	29.8	30.4
	16:0 18:1	20.1	21.8	21.1

[a] Triacylglycerols isolated from peanut oil (the first four) and cottonseed oil (the last) by combined argentation TLC and reversed-phase HPLC.

[b] *sn*-1,2(2,3)-Diacylglycerol fractions separated as derivatives and collected by reversed-phase HPLC.

[c] Percentages calculated from peak areas registered in HPLC analysis of the mixture of diacylglycerol derivatives with refractometric detection (without any area correction according to fatty acids). Results are means of 3–5 different analyses.

[d] Percentages calculated from the fatty acid composition of the collected fractions after addition of a known amount of heptadecanoic acid.

[e] Percentages calculated from the percentages of *sn*-2-monoacylglycerols, as reported in the text.

listed in the table (18% and 8%, respectively). For better separation of the first two fractions, the HPLC analysis was carried out at 12°C. The last fraction, 16:0 18:1, was eluted late and the peak area was probably underestimated. However, under identical analytical conditions and with the range of fatty acids used in this work, we can conclude that the proportion of the different fractions of diacylglycerols separated by HPLC as urethane derivatives and detected by their refractive indices can be calculated from peak areas. Application of correction factors to peak areas according to the constituent fatty acids did not appear to be necessary for the samples analysed.

To check whether the *sn*-1,2(2,3)-diacylglycerols formed by hydrolysis were representative of the original triacylglycerols, their theoretical percentages were calculated from the *sn*-2-monoacylglycerol composition after enzymatic (pancreatic lipase) hydrolysis, assumed to generate representative *sn*-2-monoacylglycerols. An example is as follows: after hydrolysis of the triacylglycerol 16:0 18:1 18:1 by rat pancreatic lipase, the composition of the *sn*-2-monoacylglycerol was 16:0 4.1% and 18:1 95:9%. The two *sn*-1,2(2,3)-diacylglycerols theoretically formed in equal proportions from the *sn*-2-triacylglycerol 16:0 18:1 18:1 (18:1 at internal position) would be 16:0 18:1 47.95% and 18:1 18:1 (47.95%). The unique diacylglycerol formed from 18:1 16:0 18:1 would be 16:0 18:1 4.1%. The theoretical proportions of *sn*-1,2(2,3)-diacylglycerols would be 16:0 18:1 52.05% and 18:1 18:1 47.95%.

The results obtained are reported in Table V (last column). They can be compared with the results given in the fourth column. Both series of figures are very similar, the average difference being only 2.1% with a maximum of 3.7%. If it is considered that pancreatic lipase forms representative *sn*-2-monoacylglycerols, the *sn*-1,2(2,3)-diacylglycerols formed by deacylation also appear to be representative of the hydrolysed triacylglycerols.

In conclusion, the results reported in this section clearly show that representative *sn*-1,2(2,3)-diacylglycerols are generated by deacylation of triacylglycerols, that they can be accurately analysed by reversed-phase HPLC using differential refractometric detection and that they can be fractionated by HPLC for further stereospecific analysis on a chiral column.

ACKNOWLEDGEMENT

We are grateful to J. Gresti for skillful assistance in the GC and HPLC analyses and in the reproduction of the chromatograms.

REFERENCES

1 F. H. Mattson and L. W. Beck, *J. Biol. Chem.*, 214 (1955) 115.
2 P. Savary, J. Flanzy and P. Desnuelle, *Biochim. Biophys. Acta*, 24 (1957) 414.
3 C. Litchfield, *Analysis of Triglycerides*, Academic Press, New York, London, 1972.
4 H. Brockerhoff, *J. Lipid Res.*, 6 (1965) 10.
5 H. Brockerhoff, *J. Lipid Res.*, 8 (1967) 167.
6 H. Brockerhoff, *Lipids*, 6 (1971) 942.
7 Y. Itabashi and T. Takagi, *J. Chromatogr.*, 402 (1987) 257.
8 T. Takagi and Y. Itabashi, *Lipids*, 22 (1987) 596.
9 P. Michelsen, E. Aronsson, G. Odham and B. Akesson, *J. Chromatogr.*, 350 (1985) 417.
10 P. Laakso and W. W. Christie, *Lipids*, 25 (1990) 349.
11 V. K. S. Shukla, *Prog. Lipid Res.*, 27 (1988) 5.
12 J. Krüger, H. Rabe, G. Reichmann and B. Rüstow, *J. Chromatogr.*, 307 (1984) 387.
13 P. J. Ryan and T. W. Honeyman, *J. Chromatogr.*, 331 (1985) 177.
14 Y. Kondoh and S. Takano, *J. Chromatogr.*, 393 (1987) 427.
15 M. Yurkowski and H. Brockerhoff, *Biochim. Biophys. Acta*, 125 (1966) 55.
16 W. W. Christie and J. H. Moore, *Biochim. Biophys. Acta*, 176 (1969) 445.
17 F. E. Luddy, R. A. Barford, S. F. Herb, P. Magidman and R. W. Riemenschneider, *J. Am. Oil Chem. Soc.*, 41 (1964) 693.
18 J. A. Bézard and M. A. Ouedraogo, *J. Chromatogr.*, 196 (1980) 279.
19 J. A. Bézard, M. A. Ouedraogo and G. Semporé, *Rev. Fr. Corps Gras*, 37 (1990) 171.
20 N. Ôi and H. Kitahara, *J. Chromatogr.*, 265 (1983) 117.
21 M. Narce, J. Gresti and J. A. Bézard, *J. Chromatogr.*, 448 (1988) 249.
22 H. T. Slover and E. Lanza, *J. Am. Oil Chem. Soc.*, 58 (1979) 933.
23 A. Ros, *J. Gas Chromatogr.*, 3 (1965) 252.
24 L. R. Snyder and J. J. Kirkland, *Introduction to Modern Liquid Chromatography*, Wiley, New York, 2nd ed., 1979.

Journal of Chromatography, 547 (1991) 105–112
Elsevier Science Publishers B.V., Amsterdam

CHROM. 23 302

Determination of a cholesterol oxide mixture by a single-run high-performance liquid chromatographic analysis using benzoylation

LUCIE FILLION and JOHN A. ZEE*

Département de Nutrition Humaine et de Consommation, Faculté des Sciences de l'Agriculture et de l'Alimentation, Université Laval, Sainte-Foy, Québec G1K 7P4 (Canada)

and

CLAUDE GOSSELIN

Département de Sciences et Technologie des Aliments, Faculté des Sciences de l'Agriculture et de l'Alimentation, Université Laval, Sainte-Foy, Québec G1K 7P4 (Canada)

(First received February 13th, 1990; revised manuscript received February 26th, 1991)

ABSTRACT

A rapid, single-run high-performance liquid chromatographic method has been developed to separate and quantify benzoate esters of cholesterol oxides, providing high sensitivity via ultraviolet detection. The mobile phase was 85% isopropanol–water (v/v). Analyses of 7-ketocholesterol, cholestane-triol, epoxycholesterol, 7-hydroxycholesterol and 25-hydroxycholesterol were done using a 30 cm × 3.9 mm I.D. Novapak C_{18} column and a variable-wavelength ultraviolet detector (set at 230 nm). Linearity was excellent since a good correlation was observed. As low as 500 ng of cholesterol benzoate per 20 μl of solution can be detected by this method.

INTRODUCTION

Adverse physiological responses are reportedly associated with several cholesterol oxidation products (COPS) [1–5]. Of particular concern is evidence that cholesterol oxides of dietary origin can be assimilated [6,7] and carried by lipoproteins to arterial tissue where they may initiate the development of atherosclerosis [8–10].

In spite of significant advances in recent years, high-performance liquid chromatographic (HPLC) techniques using UV detectors are not sensitive enough to separate and quantify complex mixtures of cholesterol oxides. It is difficult to analyze most common cholesterol of toxicological interest in a single HPLC run. Using UV detection, a limited number of underivatized cholesterol oxides may be analyzed simultaneously [11–16]. Significant improvements, however, are realized by increasing the UV absorption of cholesterol oxides through derivatization. Attaching a chromophore to the functional groups of cholesterol facilitates the UV detection of very low levels. Although *p*-nitrobenzoylation [17] and picration [18] have been used with UV detection for the analysis of epoxycholesterol epimers, to date no HPLC method

0021-9673/91/$03.50

for the analysis of cholesterol oxide mixtures based on UV-absorbing derivatives has been published in detail.

The present investigation was undertaken to develop an HPLC method based on UV detection of 3,5-dinitrobenzoyl chloride (DNBC) or benzoyl chloride (BC) derivatives of cholesterol oxides for accurate COP analyses.

EXPERIMENTAL

Reagents

The compounds studied, 7-hydroxycholesterol (cholestan-5-ene-3β,7α-diol), α-epoxycholesterol (5,6α-epoxy-5α-cholestane-3-β-ol), 25-hydroxycholesterol (cholest-5-ene-3β,25-diol); 7-ketocholesterol (3β-hydroxycholest-5-ene-7-one) and cholestane-triol (cholestane-3β,5α,6β-triol) were purchased from Sigma (St. Louis, MO, USA), Steraloids (Wilton, NH, USA) or Research Plus (Bayonne, NJ, USA), stored under desiccated nitrogen and used without further preparation. All solvents used were of HPLC grade (Caledon Labs, Georgetown, Canada) degassed by vacuum filtration through 0.45-μm filters (Millipore, Bedford, MA, USA) immediately prior to use. Pyridine (silylation reagent grade, Pierce, Morton Grove, IL, USA) was used as the solvent for the derivatization procedure.

Derivatization procedures

3,5-Dinitrobenzoyl chloride. Derivatization of cholesterol oxides by DNBC (Regis, Morton Grove, IL, USA) was done according to the method of Carey and Persinger [19]. Briefly, 4 ml of tetrahydrofuran, 40 mg of DNBC and 3 drops of pyridine were added to 1 mg of an oxide in a 5-ml of an oxide in a 5-ml Reacti-vial (Pierce), sealed with a Teflon cap and heated to 60°C for 1 h in a Reacti-block (Pierce). The solvent was evaporated under nitrogen with warming (30°C). The residue was dissolved in 3 ml of diethyl ether and washed with 3 volumes of dilute aqueous sodium bicarbonate (0.01 *M*) and once with distilled water.

Benzoyl chloride. Derivatization of cholesterol oxides by BC was done according to the method of Fitzpatrick and Siggia [20]. Each cholesterol oxide (0.10 mg) was dissolved in 4 ml of pyridine in a 5-ml Reacti-vial (Pierce) to which 0.2 ml of BC (Sigma) was added. The mixture was shaken ten times, heated at 80°C for 20 min and extracted in a separatory funnel containing 50 ml of 0.1 *M* HCl and 50 ml of diethyl ether. The ether phase was washed three times with 50 ml 0.1 *M* HCl to remove pyridine.

Trials using different volumes of pyridine (1–4 ml) and BC (0.01–0.2 ml) or omitting the washing procedure were also performed for comparison.

HPLC procedure

The following COPs were analyzed by HPLC: 7-hydroxycholesterol, α-epoxycholesterol, 25-hydroxycholesterol, 7-ketocholesterol and cholestane-triol. HPLC was performed using a delivery pump (Model 2150, LKB, Bromma, Sweden) equipped with a Rheodyne 20-μl injection loop. Reversed-phase separation was performed with a RCM-100 radial compression unit equipped with a 4-μm Novapak C_{18} column (30 cm × 3.9 mm I.D., Waters Assoc. Milford, MA, USA). Elution of dinitrobenzoates was monitored at 254 nm and benzoates at 230 nm by a variable-

wavelength UV detector (Model 2151, LKB). Chromatograms were processed on an integrator (Model HP 3393A, Hewlett-Packard, Avondale, PA, USA). Spectra were recorded from 200 to 400 nm by means of a photodiode array detector (Model 1040, Hewlett-Packard) connected to a computer (Model 9000, Series 300, Hewlett-Packard). The upslope, apex and downslope were recorded for confirmation of peak purity. Combinations of mobile phase systems were used, *i.e.* isopropanol–water (65:35 to 90:10, v/v) and acetonitrile–water (65:35 to 90:10, v/v). The limit of detection of the COP derivatives was determined by analyzing standard COP solutions of decreasing concentrations (5 μg per 20 μl).

Linear response of COPs as benzoate derivatives

To determine the response linearity for COPs studied, approximately 200 μg of each oxide were dissolved in 5 ml of pyridine, from which appropriate dilutions were made to give concentrations corresponding to 0.8–10 μg of each oxide per 20-μl injection. Plots of area *versus* quantity were made for regression analysis using Stat View 512+ software for Macintosh, version 1986 (Brain Power, Calabasas, CA, USA).

RESULTS AND DISCUSSION

No increase in sensitivity could be obtained using the DNBC method described by Carey and Persinger [19] since it was not possible to derivatize the oxides due to the failure of DNBC to react with certain molecules of high molecular weight. According to these authors, the yield of DNBC derivatives could depend on the solvent employed to extract them. Fitzpatrick and Siggia [20] reported the derivatization of cholesterol using DNBC, but cautioned that rapid hydrolysis occurred spontaneously, returning the derivatives to their original form, probably due to the presence of polar groups. For these reasons, DNBC was not retained for the derivatization of COPs.

For the Fitzpatrick and Siggia [20] procedure, it was necessary to increase the heating time to ensure total derivatization of the cholesterol oxides. The reaction with all COPs was complete after 1 h at 80°C after which no further increase in UV absorption was observed. This is well illustrated with cholestane-triol in Fig. 1.

Derivatization with 0.05 ml of BC in 1 ml of pyridine appeared to provide the best conditions. The molar ratio of BC to cholesterol oxide should be at least 500 to ensure a complete reaction. Beyond this point, no increase in the formation of the cholesterol derivatives was observed. Greater than 0.05 ml of BC per ml of pyridine resulted in supersaturation of the solution and rapid crystal formation.

It was also observed that washing the organic extract caused losses of oxide derivatives of up to 74% (Table I), undoubtedly due to hydrolysis. The washed derivatives were unstable after 2 h, HPLC analysis showing decreased peak area, whereas unwashed benzoyl derivatives remained stable for 2 days when kept in a tightly capped vial at room temperature.

The best resolution of benzoylated COPs was obtained using a mixture of isopropanol–water (85:15) (Fig. 2, Table II). At this ratio, the relative retention time (k') of all COPs was ≤ 7.32. Other solvent combinations failed to elute all cholesterol oxides or gave poor resolution of some. However, even with this mobile phase, the isomeric oxides were not resolved (*e.g.* 7α- and 7β-hydroxy; α- and β-epoxide); the

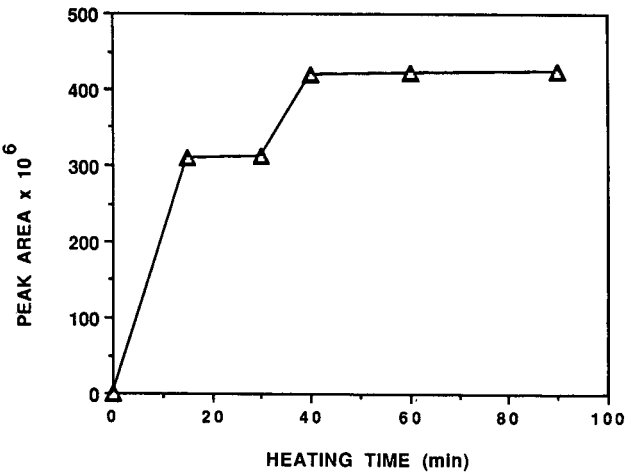

Fig. 1. Response of cholestane-triol absorption peak at 230 nm to heating time during derivatization with benzoyl chloride.

isomers were eluted at the same retention time. Also, triol retention time reported by Tsai *et al.* [15] is greater than 55 min, too long for the simultaneous determination of this compound in a COP mixture. With the present method, however, the retention time for triol is only 12.5 min. This may be attributable to decreased hydrophobicity as a result of benzoylation of the hydroxyl groups of cholestane-triol.

Confirmation of peak purity of each oxide was obtained by concordance of spectra taken at upslope, apex and downslope of the peak. Small differences may be attributable to the background effect of solvent (Fig. 3).

Spectral analysis of COPs also confirmed that all derivatized compounds showed high absorbance at 230 nm. This is well illustrated by the 25-hydroxy compound which is normally detected at 205 nm [13] or at 210 nm [12]. When detected as the benzoate derivative, the maximum sensitivity for 25-hydroxycholesterol was observed at 230 nm (Fig. 4). Absorbance at 230 nm for 7-hydroxycholesterol, 23-hy-

TABLE I

INFLUENCE OF WASHING PROCEDURE ON DERIVATIZED COPs RECOVERIES

Analyses were performed in triplicate.

COP	Unwashed (mg)	Washed (mg)	Losses[a] (%)
7-Ketocholesterol	3.2	0.82	74.4
Cholestane-triol	3.5	2.04	41.6
Epoxycholesterol	6.9	3.66	46.9
7-Hydroxycholesterol	2.9	0.99	65.5
25-Hydroxycholesterol	3.4	1.45	57.3

[a] Losses due to washing with respect to the unwashed procedure.

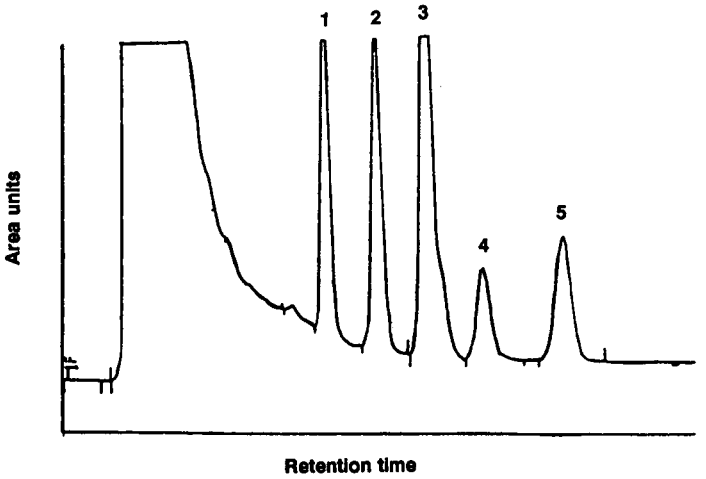

Fig. 2. Typical chromatogram of a mixture of derivatized COPs at 230 nm. Individual oxide concentration, 3 μg per 20 μl approximately; mobile phase, isopropanol–water 85:15 (v/v) at 1 ml/min and recorder chart speed 0.5 cm/min. Peaks: 1 = 7-ketocholesterol; 2 = cholestane-triol; 3 = epoxycholesterol; 4 = 7-hydroxycholesterol; 5 = 25-hydroxycholesterol. For retention times see Table II.

droxycholesterol, epoxycholesterol or cholestane-triol was increased by a factor of at least 10^6 by derivatization. Fitzpatrick and Siggia [20] reported a similar multiple for the amount of underivatized sterol to give an absorbance equivalent to that of the derivatives.

A minor improvement was observed for 7-ketocholesterol, of which the benzoyl derivative gave an absorbance increased by a factor of 3. This compound, however, gave an excellent response at 233 nm without derivatization.

In the present study, the minimum detectable amount of derivatized cholesterol oxides varied among the different compounds, averaging 500 ng, the detection limit being established at concentrations where integration was no longer possible. Also, omission of the washing procedure resulted in the presence of a large solvent peak which could interfere with the integration of small COP peaks.

This improvement in UV sensitivity offers a significant advantage over previous HPLC methods which allow analysis of only a limited number of oxides (such as

TABLE II

RELATIVE RETENTION TIMES OF COPs

Peak No.	COP	Retention time (min)	Relative retention time (k')
1	7-Ketocholesterol	10.40	3.36
2	Cholestane-triol	12.50	4.25
3	Epoxycholesterol	14.30	5.00
4	7-Hydroxycholesterol	16.70	6.01
5	25-Hydroxycholesterol	19.82	7.32

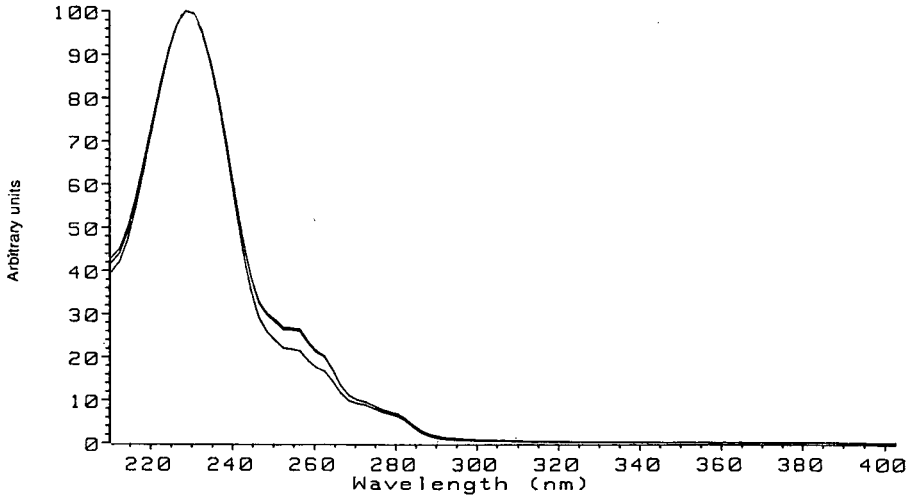

Fig. 3. Comparison between spectra of upslope, apex and downslope of cholestane-triol.

7-ketocholesterol and 7-hydroxycholesterol or epoxycholesterols) as underivatized compounds [14–16]. Oxides such as 25-hydroxycholesterol are detectable only at shorter UV wavelengths [12,13] while others such as 7-ketocholesterol require longer wavelengths. In the present study, 25-hydroxycholesterol could be simultaneously analyzed with the others since all were detectable at one single wavelength. Also, a good baseline was observed in comparison to those obtained at the short UV wavelength in the Csiky study [12].

Linearity of response was good for benzoyl derivatives throughout the range of concentrations studied (0.8–10 μg pr 20 μl). Regression analysis of plots of weight

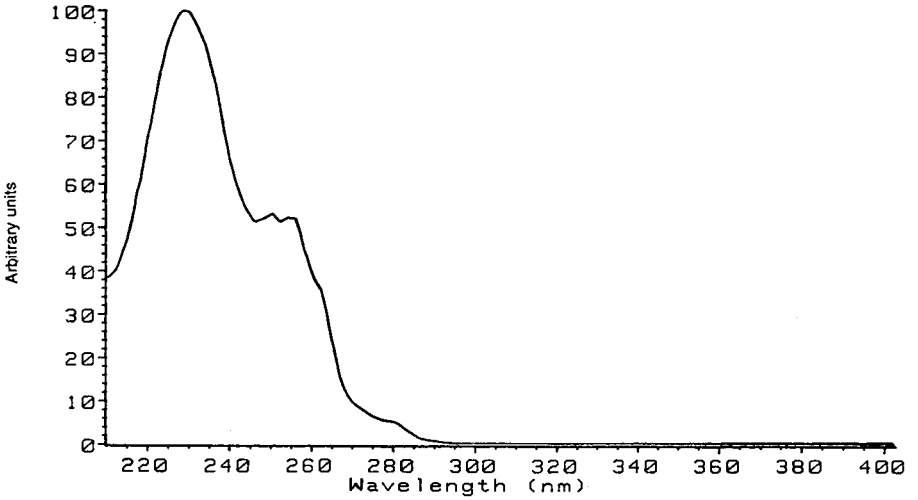

Fig. 4. UV spectrum of 25-hydroxycholesterol.

TABLE III

LINEARITY OF RESPONSE OF COPs AS BENZOATE DERIVATES

COPs	r^2	Slope[a]	y-Intercept[b]	Standard error
7-Ketocholesterol	0.997	1.002	0.155	0.22
Cholestane-triol	0.987	2.095	−1.012	0.76
Epoxycholesterol	0.980	0.432	−0.084	0.05
7-Hydroxycholesterol	0.944	0.644	−0.025	0.41
25-Hydroxycholesterol	0.999	0.008	0.000	0.00

[a] Based on six values, except for 25-hydroxycholesterol (five values).
[b] Area values were divided by a factor of 10^9.

versus area for each benzoyl derivative gave high r^2 values ($r^2 \geq 0.944$), suggesting that quantitation of the major oxidation products by the HPLC technique reported herein is reliable and reproducible (Table III).

For further application of this method to food samples, COPs may be separated from cholesterol and concentrated by filtration through a silica gel column prior to HPLC [14]. This clean-up procedure not only allows the detection of low levels of COPs usually found in foods, but also permits the suppression of autoxidation of cholesterol during extraction and quantification of COPs [21].

CONCLUSION

Results indicate that derivatization of COPs by BC using isocratic reversed-phase HPLC with UV detection is an efficient method for the separation and quantitation of cholesterol oxides when analyzed as their benzoate derivatives. This HPLC method is particularly useful for separating mixtures of autoxidation products of cholesterol having a wide range of UV absorbance maxima in the underivatized form. Moreover, the method is rapid, reproducible and suitable for routine quantitation of oxidized cholesterol products in foods. Application of this technique to meat products will be reported in another paper.

ACKNOWLEDGEMENT

The authors wish to express their gratitude to Health and Welfare Canada for funding this study (No. 10-MIN. SANTE NAT-6605-27).

REFERENCES

1 N. A. Highley, S. L. Taylor, A. M. Herian and K. Lee, *Meat Sci.*, 16 (1986) 175.
2 A. A. Kandutsch and H. W. Chen, *Lipids*, 13 (1978) 704.
3 A. Sevanian and A. R. Peterson, *Food Chem. Toxicol.*, 24 (1986) 1103.
4 L. L. Smith, *Cholesterol Autoxidation*, Plenum Press, New York, 1981.
5 C. B. Taylor, S. K. Peng, N. T. Werthessen, P. Tham, and K. T. Lee, *Am. J. Clin. Nutr.*, 32 (1979) 40.
6 S. Kikuchi, Y. Imai, S. Ziro, T. Matsuo and S. Noguchi, *J. Pharmacol. Exp. Ther.*, 159 (1968) 399.
7 G. Maerker, E. H. Nungesser and F. J. Bunick, *Lipids*, 23 (1988) 761.
8 S. M. Jacobson, M. G. Price, A. E. Shamoo and F. P. Heald, *Atherosclerosis*, 57 (1985) 209.
9 S. K. Peng, C. B. Taylor, E. H. Mosbach, W. Y. Huang, J. C. Hill and B. Mikkelson, *Atherosclerosis*, 41 (1982) 395.

10 S. K. Peng, G. A. Phillips, X. Guang-Zhi and R. J. Morin, *Atherosclerosis*, 64 (1987) 1.
11 G. A. S. Ansari and L. L. Smith, *J. Chromatogr.*, 175 (1979) 307.
12 I. Csiky, *J. Chromatogr.*, 241 (1982) 381.
13 I. Kou and R. P. Holmes, *J. Chromatogr.*, 330 (1985) 339.
14 S. W. Park and P. B. Addis, *J. Food Sci.*, 50 (1985) 1437.
15 L. S. Tsai, K. IJichi and C. A. Hudson, *J. Am. Oil. Chem. Soc.*, 58 (1981) 931.
16 L. S. Tsai and C. A. Hudson, *J. Food Sci.*, 50 (1985) 229.
17 K. Sugino, J. Terao, H. Murakami and S. J. Matsushita, *Agric. Food Chem.*, 34 (1986) 36.
18 K. Lee, A. M. Herian and T. J. Richardson, *Food Protect.*, 47 (1984) 340.
19 M. A. Carey and H. E. Persinger, *J. Chromatogr. Sci.*, 10 (1972) 537.
20 F. A. Fitzpatrick and S. Siggia, *Anal. Chem.*, 45 (1973) 2310.
21 K. Kudo, G. Emmons, E. W. Casserly, D. P. Via, L. C. Smith, J. St. Pyrek and G. J. Schroepfer Jr., *J. Lipid Res.*, 30 (1989) 1097.

Journal of Chromatography, 547 (1991) 113–120
Elsevier Science Publishers B.V., Amsterdam

CHROM. 23 230

Two-parameter mobile phase optimization for the simultaneous high-performance liquid chromatographic determination of dopamine, serotonin and related compounds in microdissected rat brain nuclei

MARÍA LEMA, JORGE OTERO* and JAVIER MARCÓ
Department of Physiology, Faculty of Biology, University of Santiago, 15706 Santiago de Compostela, Galicia (Spain)
(Received December 27th, 1990)

ABSTRACT

A new high-pressure liquid chromatography method with electrochemical detection is described that allows the simultaneous determination of dopamine, serotonin, 3,4-dihydroxyphenylacetic acid, 3-methoxy-4-hydroxyphenylacetic acid, 5-hydroxytryptophan and 5-hydroxyindoleacetic acid in microdissected nuclei from individual rat brains. No sample pre-treatment steps are required. Resolution and analysis time were optimized by a simple limited optimization procedure, involving two-parameter factorial design.

INTRODUCTION

A great number of methods based on high-performance liquid chromatography with electrochemical detection (HPLC–ED), especially in the ion-pair mode (IP), have been developed, successfully dealing with the quantitative analysis of endogenous catecholaminergic and indolaminergic compounds [1–11]. However, laborious sample preparation or large analysis times are often required that could lead to a loss of sensitivity for later-eluted substances. In addition, differences in instrumentation and experimental conditions can make it difficult to reproduce a reported separation, and so the need for formal optimization strategies arises. In this way, two-parameter optimization has proved to be a practical approach in the improvement of chromatographic separations [12,13].

The aim of this work is to develop a selective chromatographic method for simultaneous measurement in microdissected rat brain nuclei of the aminergic neurotransmitters dopamine (DA) and serotonin (5HT), their major metabolites, 3,4-dihydroxyphenylacetic acid (DOPAC), 3-methoxy-4-hydroxyphenylacetic acid (HVA), 5-hydroxyindoleacetic acid (5HIAA), and the serotonin precursor 5-hydroxytryptophan (5HTP). For this purpose, an optimization strategy was followed that involved the use of factorial design coupled with computer-aided chromatogram prediction and evaluation. From the mobile phase parameters that can be

0021-9673/91/$03.50

used for controlling selectivity for ionized solutes [14–16], pH and organic modifier content were selected, in order to optimize both resolution and analysis time. An evaluation procedure that allowed us to relate variations in separation performance to variations in mobile phase composition was used, based on the multi-criteria decision making method [17]. Compounds expected to be present in biological samples as major interfering peaks, norepinephrine (NE) and its metabolite 3-methoxy-4-hydroxyphenylethyleneglycol (MHPG), have been also considered. Thus, a limited optimization approach [18] was undertaken, resolution between NE and MHPG not being taken into account.

EXPERIMENTAL

Reagents

Citric acid monohydrate, sodium octyl sulphate (SOS), EDTA disodium salt and glacial acetic acid were from Scharlau (Barcelona, Spain). Anhydrous sodium acetate, sodium metabisulphite, perchloric acid (PCA) and methanol (HPLC grade) were from Merck (Darmstadt, Germany). All standards were obtained from Sigma (St. Louis, MO, USA). Water was purified using a Milli-Q system (Millipore).

Chromatographic system

The HPLC system consisted on a solvent delivery pump (Model 420, Kontron, Zürich, Zwitzerland) equipped with a pulse damper, a six-port rotary valve (Model 7125, Rheodyne, Berkeley, CA, USA) and a 20-μl sample loop. The amperometric detector was a BAS LC-4B (West Lafayette, IN, USA) coupled with a TL-5A glassy carbon electrode, and the recorder was a Hewlett-Packard HP-3390 A integrator. The detector potential was set at +0.7 V *vs.* Ag/AgCl. A LiChrospher RP-18 125 mm × 4 mm 5 μm (Merck, Darmstadt, Germany) analytical column operated at a flow-rate of 0.9 ml/min was used. All separations were performed at room temperature (20–22°C).

Mobile phases and standards

The mobile phases consisted of a 0.1 *M* sodium acetate–0.02 *M* citric acid buffer containing 0.1 m*M* Na_2EDTA and 0.69 m*M* SOS, mixed with methanol to the desired volume ratio. The pH was adjusted by adding glacial acetic acid to the methanol–buffer mixture. After pH adjustment, mobile phases were filtered through 0.2-μm nylon filters (Alltech Assoc.) and degassed under vacuum. Stock solutions of standards (100 μg/ml) were prepared in 0.1 *M* PCA containing 0.1 m*M* EDTA and 0.2 m*M* sodium metabisulphite, and stored at −80°C. Working standards (10 ng/ml) were prepared daily making appropriate dilutions of the stock solution with mobile phase.

Experimental design and calculations

A two parameters–two levels (2 × 2) factorial design was used to measure the effects of mobile phase pH and methanol content over the capacity factors (k') of the compounds to be separated, following the methods decribed by Box *et al.* [19]. Upper and lower levels have to be established for both variables, defining a bidimensional, rectangle-shaped, factor space. Chromatograms of standards must be obtained at the four mobile phase compositions corresponding to the rectangle vertices. These were

assayed in a random order during four consecutive days, allowing the system to be stabilized between successive trials. Chromatographic data were recorded at the same hour every day, in order to avoid daily variations in experimental conditions.

A model equation [20] was fitted for each compound from the factorial design retention data:

$$\ln k' = \beta_0 + \beta_1 X_1 + \beta_2 X_2 + \beta_{12} X_1 X_2 \quad (1)$$

where the variables X_1 (pH) and X_2 (methanol) were transformed ranging from -1 to $+1$; β_1 and β_2 are the main effects of each variable on the ln k' of compounds, β_{12} the term reflecting interaction between both variables, and β_0 the independent term. The β coefficients were obtained through Yate's algorithm (see ref. 19).

Chromatographic resolution (R_s) was calculated by the expression:

$$R_s = \tfrac{1}{4} N^{0.5} (\alpha - 1/\alpha) (k'_2/k'_2 + 1) \quad (2)$$

where $\alpha = k'_2/k'_1$ and the indices for k' indicate elution order of two adjacent peaks. The column plate number (N) was thus assumed to remain constant, and a very conservative value ($N = 1500$) was used.

Software. All calculations were performed using a standard spreadsheet program (Symphony, Lotus Development). The program has built-in simulation facilities which allowed easy implementation of all required formulae and data structure definition (for details, contact the authors). In all, the time required for the design and implementation of mathematic and logic statements, enter basic data and obtain the desired output was about 4 h of interactive work.

Preparation of tissue samples

Male Sprague–Dawley rats weighing 250–300 g. were used. After decapitation, brains were quickly removed, frozen and stored at -80°C until analysis (less than 1 week). The brain was sliced into 300-μm thick coronal sections using a cryo-cut (American Optical) with a chamber temperature of -10°C. A micropunch technique [21] was used to dissect out from the unfixed, frozen brain sections the following nuclei: accumbens (A), caudate putamen (CP), olfactory tubercle (TUL) and suprachiasmatic (SQ). From consecutive brain slices, the nuclei were bilaterally (CP, TUL, A) or unilaterally (SQ) micropunched, using 800- or 900-μm stainless-steel needles. A total of two (SQ), four (A, TUL) or six (CP) punches/brain were taken using the atlas of König and Klippel [22] as a guide. The frozen samples were pushed into 500-μl polypropylene microcentrifuge tubes and homogenized by ultrasonic disruption in 35 μl (SQ), 100 μl (A), 150 μl (TUL) or 200 μl (CP) of chilled mobile phase. Following centrifugation (12 000 g for 10 min at 4°C), 20 μl of the supernatant were injected into the chromatographic system.

RESULTS AND DISCUSSION

In order to find the methanol content interval giving a suitable k' range for the considered compounds, values of 5, 10 and 15% (v/v) were first tested (data not shown). The pH interval was set on the basis of previous experience with the buffer

TABLE I

FACTORIAL DESIGN. EXPERIMENTAL DESIGN: pH AND METHANOL LEVELS, TESTED MOBILE PHASE COMPOSITIONS, TRIAL ORDER AND RESULTING CAPACITY FACTORS

Fitted model for each compound: β_1 (pH main effect), β_2 (methanol main effect), β_{12} (interaction of pH and methanol) and β_0 (independent term).

Trial order	pH	Methanol content (%, v/v)	NE	MHPG	DA	DOPAC	HVA	5HTP	5HT	5HIAA
			Capacity factors (k')							
1	3.90	12.0	0.67	0.81	2.19	1.69	4.77	1.08	6.08	3.30
2	4.90	10.0	1.26	1.55	5.25	1.08	5.55	1.59	16.82	3.06
3	4.90	12.0	1.04	1.22	3.96	0.90	3.94	1.24	11.85	2.45
4	3.90	10.0	0.82	1.00	2.92	2.04	6.71	1.39	8.62	4.28
			β coefficients							
		β_1	0.438	0.422	0.588	−0.632	−0.191	0.137	0.669	−0.315
		β_2	−0.196	−0.227	−0.284	−0.185	−0.342	−0.254	−0.350	−0.240
		β_{12}	0.001	−0.014	0.003	0.006	−0.001	0.003	−0.001	0.019
		β_0	−0.084	0.104	1.223	0.301	1.637	0.271	2.313	1.166

used. Levels for the factorial design are shown in Table I, together with the k' found for each compound with the four tested mobile phase compositions and the estimated β coefficients. Methanol content exerts greater effects over later eluting compounds. The major factor affecting both retention and selectivity appeared to be pH, which had opposite effects on retention of basic and acidic compounds. This result agrees well with current theory, weak bases being expected to be more ionized and then less retained as pH decreased, and the opposite occurring for weak acids [23]. The mobile phase pH had a positive and small effect on retention of 5HTP, a zwitterionic species. All interaction terms were negligible with respect to main effects.

Although additional experiments could be made at this point to further improve the fitted model, it was decided to proceed with the optimization procedure by making use of the available data. A grid of 0.05 pH units and 0.1 methanol content units was used for systematic chromatogram prediction within the factor space; further diminishing interval size was thought to reflect only minor changes in separation performance. A matrix containing predicted k' and resolutions (eqns. 1 and 2) for the resulting 441 mobile phase compositions was obtained. Resolution between NE and MHPG was never computed.

Resolution for the critical pair (minimum resolution, or $R_{s\min}$) and analysis time were chosen as the major optimization criteria. The retention time of the last eluted substance ($t_{\max}$) was taken as a measure of analysis time. In order to avoid interferences with the sample front an additional, exclusive criterion was introduced. So, chromatograms showing peaks, other than NE or MHPG, with a predicted retention time lower than 2.5 min were discarded. To optimize simultaneously both resolution and analysis time, the multi-criteria decision making (MCDM) method suggested by Smilde *et al.* [17] was applied. Briefly, a two-dimensional graph is made, plotting the predicted $R_{s\min}$ values against the corresponding $t_{\max}$ values. The points constituting

the edge of the obtained scatter plot are named as the pareto-optimal (PO) points, which represent the best possible combinations of both criteria.

Criticisms made to the MCDM approach lie, mostly, on the fact that MCDM plots do not illustrate the relation between the behaviour of the optimization criteria and the variations in mobile phase composition [18]. Attempts to circumvent this problem have been made by mapping the PO points over a diagrammatic representation of the factor space [17,24]. In the present report the MCDM plot shows not only the PO points, but all those having a predicted $R_{s_{min}}$ value of 1.0 or higher (Fig. 1). The employed software allowed rapid identification of these points, which defined a discrete region of the factor space (pH from 3.90 to 4.15 and methanol content from 10 to 12%). Points corresponding either to the same eluent pH or to the same methanol content were linked by continuous and discontinuous lines, respectively. All points with the same pH value fell in a smooth line, and adjacent points on this line differed by 0.1% methanol content. At least for this region, it is clear from Fig. 1 that the pay-off between $R_{s_{min}}$ and t_{max} was closely related to variations in eluent composition. As was seen later, the analysis time was predicted to be determined by a same peak (5HT) for all points in the plot. An inflexion appeared when plotting $R_{s_{min}}$ versus t_{max} for pH values of 4.10 and 4.15, showing that a variation in methanol content could change the pair of peaks determining $R_{s_{min}}$. However, for pH values from 3.90 to 4.05, a same pair of peaks (MHPG and 5HTP) showed the minimal predicted resolution over the entire methanol range.

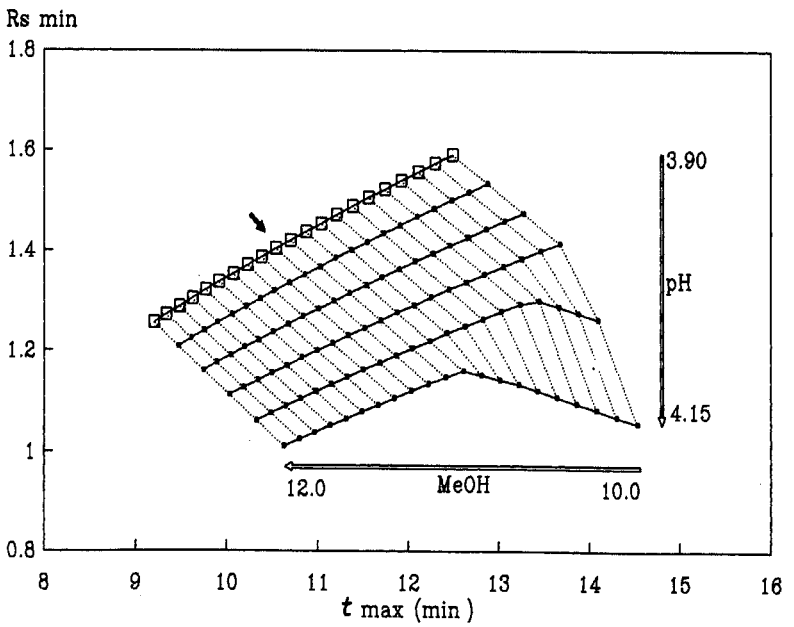

Fig. 1. Multi-criteria decision making plot. Points corresponding to the same eluent pH are linked by solid lines, contiguous lines differing by 0.05 pH units. Points for a same methanol (MeOH) content are linked by dotted lines, contiguous lines differing by 0.1% methanol content. The pareto-optimal points (squares) correspond to the eluents of pH 3.90. The small arrow points to the selected pareto-optimal mobile phase composition: pH 3.90, 11.1% (v/v) methanol content.

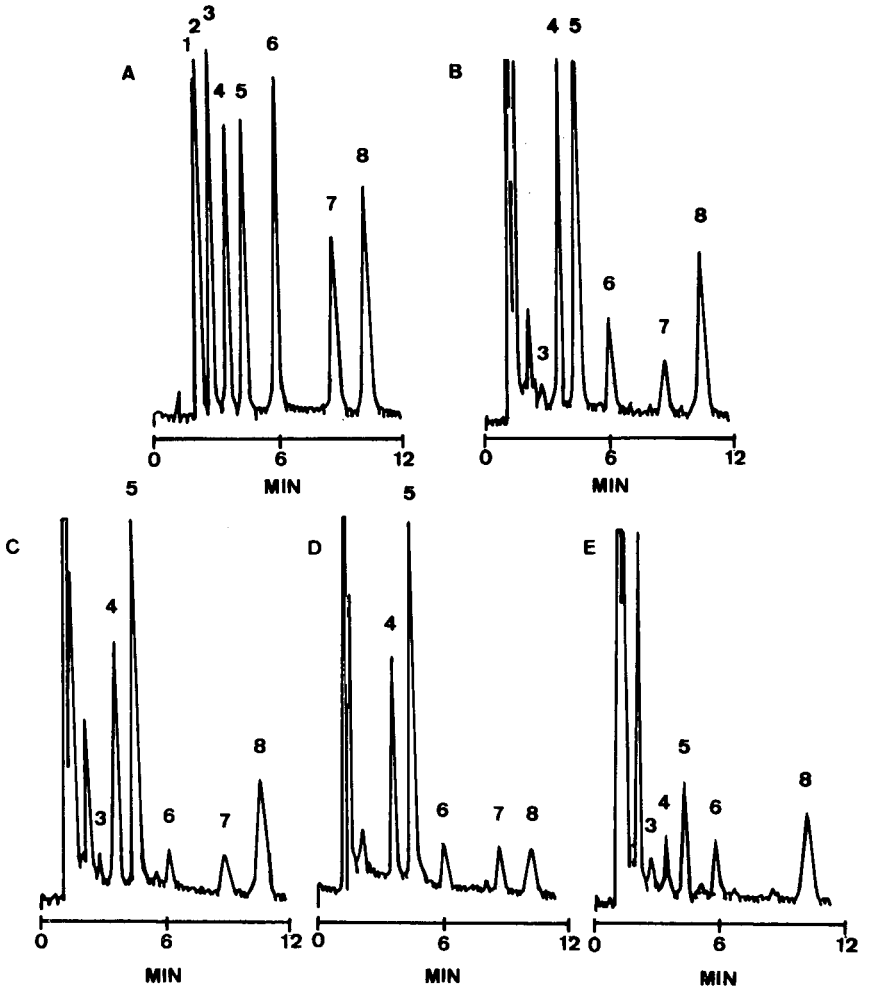

Fig. 2. Chromatograms recorded at the selected pareto-optimal mobile phase composition (pH 3.90, 11.1% (v/v) methanol content). (A) Chromatogram of a standard mixture containing 200 pg/20 μl injection of each compound. Chromatograms of microdissected nuclei from a single rat brain: (B) olfactory tubercle; (C) accumbens; (D) caudate putamen; (E) suprachiasmatic. Peaks: 1 = NE; 2 = MPHG; 3 = 5HTP; 4 = DOPAC; 5 = DA; 6 = 5HIAA; 7 = HVA; 8 = 5HT. Sensitivity 0.5 nA full scale. See text for other chromatographic conditions.

The PO points corresponded to the eluents with a pH value of 3.90. The PO point for 11.1% methanol content was selected for checking in the HPLC system. These conditions gave a predicted $R_{s_{min}}$ value higher than 1.4, which we considered appropriate for quantitative analysis. The predicted analysis time was less than 10.5 min. The chromatogram obtained is presented (Fig. 2A) and was considered entirely satisfactory for the initial purposes. The predicted and actual retention times were found to be in good agreement, with a difference of 0.27% to 5.43% (Table II). Although separation quality is increased towards the lower pH limit, it was discarded

TABLE II

PREDICTED AND ACTUAL RETENTION TIMES FOR THE SELECTED PARETO-OPTIMAL MOBILE PHASE COMPOSITION (pH 3.90, 11.1% (V/V) METHANOL CONTENT)

	Compound							
	NE	MHPG	DA	DOPAC	HVA	5HTP	5HT	5HIAA
Retention time (min)								
Predicted	2.25	2.46	4.55	3.69	8.53	2.87	10.54	6.12
Actual	2.23	2.33	4.50	3.70	8.94	2.88	10.50	6.10
Difference (%)	0.89	5.43	1.10	0.27	4.69	0.35	0.38	0.33

to explore more acidic pH values because too low capacity factors were expected for 5HTP. The optimization procedure was consequently stopped at this point.

The validity of the method was tested with microdissected rat brain nuclei. Chromatograms from TUL, A, CP and SQ obtained from a single rat brain are presented (Fig. 2B–E). No interference with unknown peaks was seen for the determination of the compounds of interest. The mean within-assay coefficient of variation, calculated by making 15 consecutive injections of the same working standard solution, was about 5%. The limit of detection, calculated at a signal-to-noise ratio of 2:1, ranged from 6 pg for 5HTP to 14 pg for HVA.

In summary, an HPLC method has been described that is ideally suited to the simultaneous determination of compounds of the dopaminergic and serotoninergic pathways in micropunches from individual rat brains. The employed optimization procedure is simple and could be reliable in solving similar separation problems. Furthermore, knowledge of the followed methodology can aid in fitting this HPLC method to different experimental conditions and/or analytical purposes.

ACKNOWLEDGEMENTS

The authors thank R. Vieira, J. Míguez and G. Rozas for help with the manuscript. This work was supported by CICYT grant (PB 86-0381) and Xunta de Galicia grant (XUGA 803C0588).

REFERENCES

1 I. N. Mefford and J. D. Barchas, *J. Chromatogr.*, 181 (1980) 187.
2 I. N. Mefford, M. Gilberg and J. D. Barchas, *Anal. Biochem.*, 104 (1980) 469.
3 P. T. Kissinger, C. S. Bruntlett and R. E. Shoup, *Life Sci.*, 28 (1981) 455.
4 I. N. Mefford, *J. Neurosci. Meth.*, 3 (1981) 207.
5 A. M. Krstulovic, *J. Chromatogr.*, 229 (1982) 1.
6 E. Shohami, M. Segal and D. M. Jacobowitz, *J. Neurosci. Meth.*, 8 (1983) 275.
7 P. Kontur, R. Dawson and A. Monjan, *J. Neurosci. Meth.*, 11 (1984) 5.
8 S. M. Lasley, I. A. Michaelson, R. D. Greenland and E. M. Mcginnis, *J. Chromatogr.*, 305 (1984) 27.
9 K. J. Renner and V. N. Luine, *Life Sci.*, 34 (1984) 2193.
10 C. D. Kilts and C. M. Anderson, *Neurochem. Int.*, 9 (1986) 437.
11 A. Jakubovic, D. Fu and H. C. Fibiger, *J. Pharmacol. Meth.*, 17 (1987) 1.
12 H. A. H. Billier, J. Vuik, J. K. Strasters and L. de Galan, *J. Chromatogr.*, 384 (1987) 153.

13 F. Szokoli, Zs. Németh and J. Inczédy, *Chromatographia*, 29 (1990) 265.
14 I. Molnár and Cs. Horváth, *Clin. Chem.*, 22 (1976) 1497.
15 Cs. Horváth, W. Melander, I. Molnár and P. Molnár, *Anal. Chem.*, 49 (1977) 2295.
16 H. A. H. Billiet and L. de Galan, *J. Chromatogr.*, 485 (1989) 27.
17 A. K. Smilde, A. Knevelman and P. M. J. Coenegracht, *J. Chromatogr.*, 369 (1986) 1.
18 A. Bartha, H. A. H. Billiet and L. de Galan, *J. Liq. Chromatogr.*, 12 (1989) 173.
19 G. E. P. Box, W. G. Hunter and J. S. Hunter, *Statistics for experimenters. An Introduction to Design, Data Analysis and Model Building*, Wiley, New York, 1978.
20 P. Wester, J. Gottfries, K. Johansson, F. Klintebäck and B. Winblad, *J. Chromatogr.*, 415 (1987) 261.
21 M. Palkovits and M. J. Brownstein, in A. C. Cuello (Editor), *Brain Microdissection techniques*, Wiley, New York, 1983, p. 1.
22 J. K. König and R. A. Klippel, *The Rat Brain: a Stereotaxic Atlas of the Forebrain and Lower Parts of the Brain Stem*, R. E. Krieger, New York, 1967.
23 I. Molnár and Cs. Horváth, *J. Chromatogr.*, 145 (1978) 371.
24 A. K. Smilde, C. H. P. Bruins and D. A. Doornbos, *J. Chromatogr.*, 410 (1987) 1.

Journal of Chromatography, 547 (1991) 121–129
Elsevier Science Publishers B.V., Amsterdam

CHROM. 23 214

Investigation of the chemical stability of (D-Phe^6, Gln^8) GnRH (1–9)-ethylamide (Folligen) by high-performance liquid chromatography

B. SZÖKE, Gy. KÉRI, M. IDEI*, A. HORVÁTH, Gy. BÖKÖNYI and I. TEPLÁN
First Institute of Biochemistry of Semmelweis Medical School and Hungarian Academy of Sciences, Puskin u 9, H-1088 Budapest (Hungary)
(First received July 17th, 1990; revised manuscript received February 13th, 1991)

ABSTRACT

The stability of a new, superactive gonadotropin hormone-releasing hormone (GnRH) analogue (D-Phe^6, Gln^8) GnRH (1–9)-ethylamide [Folligen], which may be a new drug in the "GnRH family" was investigated during storage at different temperatures, both in solid (lyophilized) form and in aqueous solution. Samples stored for various periods of time were analysed for Folligen content and for degradation products using two validated reversed-phase high-performance liquid chromatographic (HPLC) methods. The HPLC technique and the calculation method applied were found to be applicable to monitoring the chemical stability and the possible degradation products of Folligen. It is concluded that under the given experimental conditions Folligen is stable (1) in lyophilized form kept at ambient temperature at least for 1 year, (2) in frozen aqueous solution kept at −20°C for at least 11 months, (3) in sterile aqueous solution kept in a refrigerator (5–8°C) for 5 months, (4) in sterile aqueous solution kept at ambient temperature (20–25°C) for 5 weeks and (5) in sterile aqueous solution kept at 37°C for 6 days.

INTRODUCTION

On the basis of previous studies on different species-specific gonadotropin hormone-releasing hormones (GnRHs), a novel GnRH analogue has been developed in our laboratory. It was synthesized by a classical large-scale liquid-phase method and has been patented as Folligen [1–4].

Folligen stimulates reproductive functions, induces follicular maturation and ovulation in various kinds of fish and mammals [1,5,6] and stimulates luteinizing hormone (LH) and follicle stimulating hormone (FSH) release in rat pituitary cells [1,2,6]. It is effective in accomplishing the artificial propagation of fish both during and out of the spawning season [1,7,8] and in treating cows with various sexual disorders (anestrous, inactive ovaries, acycling, discycling etc.) [2,3,5,6,9,10]. It has a unique anti-tumour activity in dimethylbenzanthracene-induced mammary carcinomas in rats, it causes almost 100% tumour remission without blocking ovarian functions and it has a direct inhibitory effect on MDAMB 230 human breast cancer cells [11,12].

All these results are very promising for the development of a new drug in the

0021-9673/91/$03.50

"GnRH family" which may have the above-mentioned advantages compared with known peptides. In the very complex process of developing a new pharmaceutical, a step of paramount importance is to study the stability of the given compound.

The objective of this study was to establish stability data for (D-Phe^6, Gln^8) GnRH (1–9)-ethylamide (Folligen) under different storage conditions using a high-performance liquid chromatographic (HPLC) technique for monitoring possible degradation products.

EXPERIMENTAL

Folligen

The structure is (D-Phe^6,Gln^8) GnRH (1–9)-ethylamide · CH_3COOH, pyro-Glu–His–Trp–Ser–Tyr–D-Phe–Leu-Gln–Pro–NHC_2H_5 · CH_3COOH, molecular weight 1274.38 and purity 99.1% (calculated on the basis of the peak area of HPLC traces recorded at 215 nm). Folligen was synthesized in our laboratory.

For solid samples, a solution of 0.5 mg/ml Folligen in distilled water was prepared and dispensed into amber-glass vials (1 ml each). The vials were lyophilized, stored as described below and reconstituted in 1 ml of distilled water just before analysis.

For solution samples, a solution of 0.5 mg/ml Folligen in distilled water was prepared and sterilized by passing it through a 0.2-μm Millipore filter unit. This solution was dispensed into sterile glass microtubes (150 μl each) and sealed first by PTFE tape and then Parafilm under sterile conditions.

Storage

Solid samples were stored in amber-glass vials in a desiccator containing potassium hydroxide pellets. The desiccator was evacuated by a vacuum pump and kept at ambient temperature.

Solution samples were kept in clear-glass microtubes, either at 37°C, at ambient temperature (20–25°C), in a refrigerator (5–8°C) or in a freezer (−20–25°C).

Chemicals

Acetic acid and trifluoroacetic acid were purchased from Fluka (Buchs, Switzerland), ammonia solution from of Reanal (Budapest, Hungary) and acetonitrile from Pierce (Rockford, IL, USA).

Analysis

The Folligen content of the samples and the formation of degradation products were followed by HPLC. A pair of injections using the full-loop filling method were made from duplicate samples and analyzed by two different validated HPLC methods. This resulted in eight data points per incubation time at each incubation temperature.

HPLC conditions

The flow-rate was 1 ml/min [ISCO (Lincoln, NE, USA) Model 2350 pumps]; detection, UV absorbance at 215 nm; sensitivity, 0.5 a.u.f.s. (channel 1) and 0.1 a.u.f.s. (channel 2); ISCO V4 UV detector; injection, 25 μl of sample into a 10-μl loop

(= 5 μg of Folligen). Two methods were used, as follows. Method A: column, Vydac 218TP5 ODS, 5 μm (250 × 4.6 mm I.D.) [Separations Group (Vydac), Hesperia, CA, USA]; eluent, 0.1% trifluoroacetic acid in acetonitrile–water (28:72, v/v). Method B: column, Shandon (Astmoor, Cheshire, UK) ODS-Hypersil, 5 μm (250 × 4 mm I.D.); eluent: acetonitrile–0.02 *M* ammonium acetate (pH 5.0) (33:67, v/v).

Calculation method

Digital data collected from HPCL runs were analysed by ISCO's ChemResearch chromatography software using an IBM XT compatible computer (data collection sampling rate 4 s^{-1}). Integrated peak areas of Folligen and those of impurities derived from four chromatograms per time point were averaged and standard deviations were calculated. The amount of degradation products was calculated by subtracting the average total area of non-Folligen peaks in control runs from that in chromatograms of stored samples.

RESULTS

The average peak areas and standard deviations for Folligen and the degradation products calculated from four chromatograms per time point are shown as a function of storage time in Tables I–V. "Not detectable" or "0" is given for the amount of degradation products in these tables whenever one of the folowing two criteria was fulfilled, respectively: (1) no extra peaks or increase in the amount of existing impurities compared with control (0 day) runs could be visually observed on the more sensitive recorder trace; or (2) the amount of degradation products calculated as described under Experimental was less than 0.1% of the intact Folligen peak area.

Fig. 1 shows the chromatograms of Folligen and its degradation products obtained by the chromatographic methods A and B (see *HPLC conditions*).

TABLE I

STABILITY OF FOLLIGEN IN SOLID (LYOPHILIZED) FORM

Storage time (months)	Peak area			
	Folligen		Degradation products	
	Mean S.D.[a]	%	Mean S.D.[a]	%
Method A				
0	38833 ± 999	100.0	0.0	0.0
4	40001 ± 806	103.0	Not detectable	
8	37893 ± 847	97.6	Not detectable	
12	38487 ± 1287	99.1	Not detectable	
Method B				
0	37864 ± 733	100.0	0.0	0.0
4	38944 ± 122	100.3	Not detectable	
8	37790 ± 662	97.3	Not detectable	
12	37551 ± 813	96.7	Not detectable	

[a] $n = 4$.

TABLE II

STABILITY OF FOLLIGEN IN AQUEOUS SOLUTION AT 37°C

Storage time (days)	Peak area			
	Folligen		Degradation products	
	Mean S.D.[a]	%	Mean S.D.[a]	%
Method A				
0	35812 ± 436	100.0	0.0	0.0
3	35999 ± 793	100.5	Not detectable	
6	36001 ± 474	100.5	Not detectable	
10	35203 ± 676	98.3	5 ± 160	0.0
14[b]	34976 ± 676	97.7	38 ± 75	0.1
21[b]	37052 ± 72	103.5	193 ± 203	0.5
28[b]	34000 ± 209	94.9	310 ± 196	0.9
Method B				
0	35159 ± 611	100.0	0.0	0.0
3	36677 ± 495	104.3	Not detectable	
6	36294 ± 1101	103.2	Not detectable	
10	35593 ± 1210	101.2	83 ± 110	0.2
14[b]	35530 ± 125	101.1	65 ± 102	0.2
21[b]	37674 ± 79	107.2	146 ± 54	0.4
28[b]	34203 ± 362	97.3	157 ± 71	0.4

[a] $n = 4$.
[b] $n = 2$.

Solid (lyophilized) samples

As can be seen from Table I, no degradation of Folligen could be detected by either method during the investigated period of 1 year.

Aqueous solutions kept at 37°C

The first signs of degradation were observed on the tenth day of incubation (see Table II). Since the last preceding analysis was carried out on the sixth day, we can claim that Folligen is stable in sterile aqueous solution at 37°C for 6 days. On days 14, 21 and 28, the number of analysable samples was reduced because of evaporation.

Aqueous solutions kept at ambient temperature (20–25°C)

No breakdown of Folligen was observed for 35 days of storage in solutions kept on a laboratory bench (Table III). During this period, room temperature fluctuated between 20 and 25°C. Unfortunately, digitized data for 260-day runs by Method B were lost owing to disk failure, although analogue chromatograms showed a similar extent of degradation to that found by Method A.

Aqueous solutions kept in a refrigerator (5–8°C)

The first appearance of degradation products was visually observed on the 260-day chromatograms. This was supported by integration results of runs with Method A (see Table IV). As the last preceding analyses were performed on the 150th day of storage, Folligen is considered to be stable in sterile aqueous solution at 5–8°C for 150 days.

TABLE III

STABILITY OF FOLLIGEN IN AQUEOUS SOLUTION AT AMBIENT TEMPERATURE

Storage time (days)	Peak area			
	Folligen		Degradation products	
	Mean S.D.[a]	%	Mean S.D.[a]	%
Method A				
0	35812 ± 436	100.0	0.0	0.0
3	35109 ± 113	98.0	Not detectable	
7	34791 ± 191	97.1	Not detectable	
14	34839 ± 316	97.3	Not detectable	
21	35988 ± 178	100.5	Not detectable	
28	35643 ± 459	99.5	Not detectable	
35	35145 ± 452	98.1	Not detectable	
50	36456 ± 498	101.8	243 ± 139	0.7
260	34978 ± 78	97.7	540 ± 162	1.5
306[b]	33543 ± 238	93.7	723 ± 133	2.0
Method B				
0	35159 ± 611	100.0	0.0	0.0
3	35006 ± 627	99.6	Not detectable	
7	34698 ± 464	98.7	Not detectable	
14	34756 ± 367	98.9	Not detectable	
21	36601 ± 390	104.1	Not detectable	
28	34780 ± 203	98.9	Not detectable	
35	35490 ± 463	100.9	Not detectable	
50	36228 ± 759	103.0	73 ± 117	0.2
260	Digital data lost because of disk failure			
306[b]	34057 ± 888	96.9	718 ± 140	2.0

[a] $n = 4$.
[b] $n = 2$.

Frozen aqueous solutions kept at −20°C

In frozen aqueous solutions kept at −20°C, Folligen remained intact during the whole of the investigated period of 326 days (see Table V). It should be noted that we have no data regarding how repeated thawing and freezing would affect the stability of the peptide.

Summary of results

Folligen in sterile aqueous solution (pH 5.5–6.0) was found to be stable for 6 days at 37°C, for 35 days at ambient temperature, for 5 months when kept in a refrigerator and for at least 11 months when fozen at −20°C.

It is not very suprising that no degradation was found with solid samples during the investigated period of 1 year, as peptides are usually stable for years in lyophilized form. It should not be disregarded, however, that this result was obtained with the exclusion of humidity (in a vacuum desiccator) and light (in amber-glass vials), and we have no data about the influence of these factors on the stability of Folligen.

TABLE IV

STABILITY OF FOLLIGEN IN AQUEOUS SOLUTION KEPT IN A REFRIGERATOR (5–8°C)

Storage time (days)	Peak area			
	Folligen		Degradation products	
	Mean S.D.[a]	%	Mean S.D.[a]	%
Method A				
0	35812 ± 436	100.0	0.0	0.0
10	34884 ± 212	97.4	Not detectable	
20	35567 ± 217	99.3	Not detectable	
30	34655 ± 192	96.8	Not detectable	
42	35425 ± 395	98.9	Not detectable	
60	35392 ± 417	98.8	Not detectable	
150	35178 ± 123	98.2	Not detectable	
260	35492 ± 376	99.1	55 ± 132	0.2
326	34678 ± 627	96.8	0 ± 128	0.0
Method B				
0	35159 ± 611	100.0	0.0	0.0
10	35180 ± 399	100.1	Not detectable	
20	34921 ± 278	99.3	Not detectable	
30	34765 ± 438	98.9	Not detectable	
42	35210 ± 151	100.1	Not detectable	
60	35499 ± 369	101.0	Not detectable	
150	34761 ± 430	98.9	Not detectable	
260	35004 ± 382	99.6	0 ± 24	0.0
326	34759 ± 651	98.9	88 ± 70	0.3

[a] $n = 4$.

DISCUSSION

The stability of a nonapeptide GnRH analog, Folligen, was investigated both in solid (lyophilized) form and in aqueous solution during storage at different temperatures. Samples stored for various time periods were analysed for Folligen content and for degradation products by HPLC.

There are two possibilities for investigating the stability of a compound: (1) to determine the decrease in the peak area of the investigated parent compound (parent peak area method); or (2) to determine the sum of the peak areas of the degradation products (degradation products peak area method). In our opinion, the most accurate and most reliable information can be obtained by using the two methods simultaneously.

In our experiments, the sample-to-sample reproducibility was not better than 5% (evaporation of the sample and losses during the lyophilization are among the reasons). As a consequence, the peak area of the undegraded parent compound (Folligen) is not a sensitive indicator of its degradation, because low levels of degradation (lower in percentage than the reproducibility) could not be statistically verified.

With a compound of low degradability, this parent peak area method (method

TABLE V

STABILITY OF FOLLIGEN IN FROZEN AQUEOUS SOLUTION AT −20°C

Storage time (days)	Peak area			
	Folligen		Degradation products	
	Mean S.D.[a]	%	Mean S.D.[a]	%
Method A				
0	35812 ± 436	100.0	0.0	0.0
20	35530 ± 359	99.2	Not detectable	
42	35448 ± 1065	99.0	Not detectable	
60	34997 ± 524	97.7	Not detectable	
161	34629 ± 857	96.7	Not detectable	
260	36278 ± 1155	101.3	Not detectable	
326	35363 ± 305	98.7	Not detectable	
Method B				
0	35159 ± 611	100.0	0.0	0.0
20	35533 ± 330	101.1	Not detectable	
42	35702 ± 128	101.5	Not detectable	
60	34658 ± 154	98.6	Not detectable	
161	36177 ± 1871	102.9	Not detectable	
260	35950 ± 208	102.3	Not detectable	
326	36098 ± 300	102.7	Not detectable	

[a] $n = 4$.

1) is ineffective. Although these difficulties could have been overcome by using an internal standard, an added compound might have influenced the stability of the investigated compound and this method was therefore avoided. In this instance it is more favourable to characterize the degradability by the sum of the peak areas of the degradation products (method 2), in spite of the fact that the relative responses are

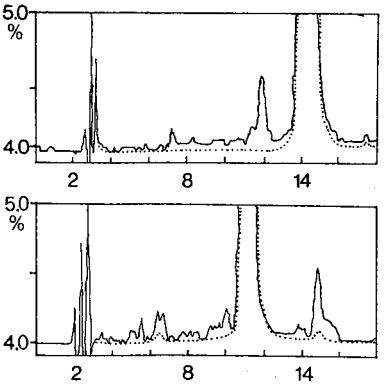

Fig. 1. Chromatograms of Folligen (mean peak on both chromatograms) and its degradation products obtained by chromatographic methods A (top) and B (bottom). For chromatographic parameters, see Experimental. Abscissa: time in minutes; ordinate: relative detector response as a percentage. Dotted lines show the chromatograms of pure (undegraded) Folligen.

not known. In product qualification and in stability investigations (where the degradation products generated by UV irradiation, heating, freezing, etc., are not identified and as a consequence their molar responses relative to the parent compound are not known), characterization of the product by the chromatographic purity is generally accepted. In these instances the concentrations of the parent compound and those of the degradation products or contaminants are given as percentages of the sum of the peak areas. The concentrations specified in this way may differ from the absolute concentrations of the components. This is why the term "chromatographic purity" always must be applied.

This method of calculation implicitly involves the assumption that the value of all the relative molar responses of the individual peaks is 1, which may not be taken for granted, of course. However, considering an even worse case (when the relative responses of the degradation products are not 1 but, *e.g.*, 3) the highest degree of degradation is not 2% but 6% (Table III, day 306), which hardly exceeds the reproducibility mentioned before. This low degree of degradation would be undetectable or hardly detectable by the parent peak area method.

In our opinion, the most reliable method is to characterize the degree of degradation by both methods and to use the worst value (the higher degree of degradation) in each instance. In Table I–V we give the results of both methods for comparison.

In the stability investigation, two HPLC methods with different selectivities were used to minimize the possibility that a degradation product is not detected because of its coelution with the Folligen peak. Both methods were previously examined according to pharmaceutical industry standards and proved to be suitable for separating impurities and degradation products from Folligen.

For sample introduction, the full-loop-filling method was used in order to increase the precision and reproducibility. Two injections of duplicate samples were analysed by the two different methods, yielding eight data points for each incubation time. UV absorption detection was used at 215 nm, a wavelength at which any peptide fragment formed by degradation could be detected. Detector signals were recorded at two different sensitivities by an analogue recorder. One setting was chosen to give *ca.* 50% deflection of full-scale for the Folligen peak, and the other setting was five times more sensitive in order to enable us to detect by visual inspection peaks as small as 0.1% of the peak height of Folligen. In addition to analogue recording, detector signals were also digitized and data were stored on floppy disk for later quantitative analysis by computer. In this way, even peaks of 0.1% of the total peak area could be integrated.

Folligen was considered not to be degraded as long as no signs of degradation could be visually observed on the more sensitive recorder trace or the combined area of non-Folligen peaks did not exceed that in control runs (0 day) by more than 0.1% of the Folligen peak area. Therefore, the stability data obtained should be interpreted such that during these periods less than 0.1% degradation product is formed from Folligen under the indicated conditions.

REFERENCES

1 Gy. Kéri, T. Gulyás, A. Horváth, B. Szöke, Gy. Bökönyi and I. Teplán, *Pept. Res.*, 3 (1990) 142.
2 A. Horváth, Gy. Kéri, T. Gulyás, S. Vigh and I. Teplán, *Biochem. Biophys. Res. Commun.*, 138 (1986) 419.

3 Gy. Kéri, T. Gulyás, A. Horváth, Gy. Bökönyi, B. Szöke, Zs. Vadász and I. Teplán, in D. Theodoropoulos (Editor), *Peptides 1988*, Walter de Gruyter, Berlin, New York, 1989, p. 655i.
4 A. Horváth, Gy. Kéri, T. Gulyás, I. Teplán, Gy. Bökönyi and S. Vigh, *US Pat.*, 4 758 552 (1986).
5 A. Horváth, Gy. Kéri, T. Gulyás, J. Molnár and I. Teplán, in M. Gruber (Editor), *Proceedings of the 13th International Congress of Biochemistry, Amsterdam, The Netherlands, 1985*, Elsevier, Amsterdam, 1985, p. 774.
6 Gy. Kéri, T. Gulyás, A. Horváth, Gy. Bökönyi, B. Szöke, J. Horváth, A. Balogh and I. Teplán, in *Abstracts of the 11th American Peptide Symposium, San Diego, La Jolla, 1989*, p.58.
7 Gy. Kéri, A. Horváth, T. Gulyás and I. Teplán, in D. Theodoropoulos (Editor), *Peptides 1986*, Walter de Gruyter, Berlin, New York, 1987, p. 513.
8 T. Gulyás, A. Horváth, Gy. Kéri, K. Nikolics, B. Szöke and I. Teplán, *US Pat.*, 4 647 552 (1983).
9 T. Nakao, K. Narita, H. Tanaka, J. Hara, H. Shirakava, N. Noshiro, N. Saga and K. Kawata, *Theriogenology*, 20 (1990) 111.
10 T. Nakao, N. Sugihashi, N. Saga and K. Kawata, *Jpn. J. Vet. Sci.*, 45 (1990) 269.
11 Gy. Kéri, O. Csuka, A. Balogh, B. Szöke and I. Teplán, *Tumor Biol.*, in press.
12 Gy. Kéri, R. I. Nicholson, I. Teplán, T. Gulyás, A. Horváth, Gy. Bökönyi, B. Szöke, O. Csuka and A. Balogh, *Hung. Pat. Appl.*, 2347/88, 1988.

Journal of Chromatography, 547 (1991) 131–144
Elsevier Science Publishers B.V., Amsterdam

CHROM. 23 260

Characterization of recombinant eel growth hormone

SEIJI SUGIMOTO*, KAZUO YAMAGUCHI and YOSHIHARU YOKOO
Tokyo Research Laboratories, Kyowa Hakko Kogyo Co., Ltd., 3–6–6 Asahimachi, Machida, Tokyo 194 (Japan)
(Received February 1st, 1991)

ABSTRACT

The characterization of purified recombinant eel growth hormone (rEGH) is described. N-Terminal sequence analysis, amino acid composition analysis, and tryptic mapping confirmed that the primary structure of rEGH was identical with that of its natural counterpart except for an additional Met at the N-terminus. Peptide mapping also revealed that rEGH had two disulphide bonds, Cys49–Cys160 and Cys177–Cys185, as in mammalian growth hormones (GHs). Recombinant EGH was classified as an α-helix-rich protein, similar to mammalian GHs, from the circular dichroism spectrum. Recombinant EGH was immunochemically identical with pituitary-derived EGH. Gel filtration chromatography and light-scattering analysis indicated that rEGH exists as the monomer, as does pituitary-derived EGH.

INTRODUCTION

Several vertebrate growth hormones (GHs) have been isolated [1–6]. Some of these GHs have been expressed by recombinant techniques in *Escherichia coli* (*E. coli*) [1,3,4,7–9]. Human GH has been applied in dwarfism and bovine GH is being developed to stimulate lactation in dairy cows [10–12]. These applications followed from the identification of the three-dimensional structure and biological activity of recombinant GHs with those of pituitary-derived GHs [13]. Teleost GHs are also expected to be useful in promoting growth in aquaculture. We have produced purified recombinant salmon GH (unpublished results) and recombinant eel GH (rEGH) [14–15]. However, the characterization of recombinant teleost GHs has not been reported.

Two forms of eel GH (EGH I and II) were isolated from eel pituitaries and their primary structures were determined by Kishida *et al.* [16] and Yamaguchi *et al.* [17]; EGH II lacks three amino acids present at the N-terminus in EGH I. Molecular cloning of EGH cDNA and its expression in *E. coli* were performed by Saito *et al.* [4].

We have reported a preparation of rEGH, in which expressed in *E. coli* as inclusion bodies was refolded and purified [14]. However, we found minor analogues (deamidated, oxidated and/or formylated rEGH) in the purified rEGH by polyacrylamide gel electrophoresis and reversed-phase high performance liquid chromatography (RP-HPLC) [18]. Subsequently we investigated the causes of these modifications. Recently we established a procedure for the large-scale preparation of rEGH free

0021-9673/91/$03.50

from these analogues [15]. This was the first report of the purification of recombinant teleost GH.

In this paper, we describe the biochemical and biophysical characterization of rEGH.

Natural human, bovine and ovine GHs have already been characterized by several methods. These investigations showed that these GHs have close similarity not only in their primary structure but also in the location of disulphide bonds, in their secondary structure, etc. Disulphide bonds in these GHs were located at the same position. These GHs were classified as α-helix-rich protein by circular dichroism spectrometry [8,13,19–25].

Molecular weight was also investigated. However, it is not yet clarified whether dimerization of these GHs takes place. Ten years ago, molecular weight measurements of pituitary-derived GHs in neutral pH solution by gel filtration chromatography (GFC), osmotic pressure and sedimentation equilibrium methods revealed that human GH exists as a monomer [20,22] and other mammalian GHs as a dimer [21]. Fernandez and Delfino [24], however, reported that pituitary-derived bovine GH showed the characteristics of a rapid monomer–dimer equilibrium whose dissociation constant was determined as $6.6 \cdot 10^{-6}$ *M* by frontal analysis. This means that the molecular weight of bovine GH in neutral pH solution depends on the concentration of bovine GH. Recently, several investigators purified recombinant bovine GH expressed in *E. coli* and showed that the molecular weight of recombinant bovine GH was identical with that of pituitary-derived bovine GH by GFC [8,13,25]. Langley *et al.* [13] showed that pituitary-derived bovine GH and recombinant bovine GH, whose tertiary structure was identical with those of the natural counterparts by several characterization methods, existed as a monomer (18 kilodalton). However, Wingfield *et al.* [8] showed that both the pituitary-derived and recombinant bovine GHs existed as a dimer (35 kilodalton). Brems *et al.* [25] reported that recombinant bovine GH was not eluted from a TSK-2000 column when the mobile phase contained less than 1.0 *M* guanidine hydrochloride (GuHCl). The GFC results could be baised by the chromatographic process, *e.g.*, by sample dilution or binding of protein to the resin.

In this work, to characterize the quaternary structure of rEGH, we particularly measured the molecular weight of rEGH by several methods and found that it exists as a monomer in neutral pH solution.

EXPERIMENTAL

N-Terminal sequence analysis

N-Terminal sequence analysis was carried out with a Model 470A gasphase sequencer (Applied Biosystems). Recombinant EGH preparation (2300 pmol) was dialysed against 0.1% SDS and the dialysate was applied to the sequencer.

Amino acid composition analysis

Protein and peptides were hydrolysed in 6 *M* hydrochloric acid at 110°C for 22 h. Amino acid analysis was carried out by the Waters Pico Tag method of Bidlingmeyer *et al.* [26]. Amino acid standard solution was purchased from Wako.

Tryptic mapping of rEGH

A 196-μg amount of rEGH in 200 μl of 10 m*M* Tris–HCl (pH 8.0) was digested with trypsin–TPCK (Worthington) for 4 h at 37°C using 1% (w/w) enzyme. The digestion was stopped by acidification with 1 *M* hydrochloric acid to pH 2–3. RP-HPLC was carried out on a TSK gel ODS-120T column (30 × 0.46 cm I.D.) with a Tri-Rotar SR2 HPLC system. Linear gradient elution from 0 to 70% acetonitrile in 0.1% trifluoroacetic acid was performed in 60 min. The column oven temperature was kept at 35°C. The flow-rate was 0.7 ml/min. UV detection was carried out at 220 nm.

S-Carboxymethylation

Each of the peaks of T15 and T39 was dried, reduced in 0.5 ml of 6 *M* GuHCl–1 m*M* EDTA–2 m*M* dithiothreitol–100 m*M* Tris–HCl (pH 8.3) at 37°C for 1 h, and subsequently S-carboxymethylated by adding 5 μl of 700 m*M* iodoacetic acid. RP-HPLC was carried out as described above, except with a linear gradient from 0 to 43.2% acetonitrile in 0.1% trifluoroacetic acid in 80 min.

Circular dichroism (CD)

CD measurements were made at room temperature with a J-500 A spectropolarimeter, (JASCO). The protein concentration in solution was 0.4–0.5 mg/ml. The buffer was 10 m*M* Tris–HCl (pH 8.0).

A cell of path length 0.14 mm was used. The full-scale range was 50 millidegree, the time constant was 1 s and the scan speed was 10 nm/min. The mean residue ellipticities [θ], in degrees cm^2/dmol, were calculated using a mean residue mass of 113.4 dalton for rEGH and 115.9 dalton for pituitary-derived human GH. The secondary structure content was calculated from the mean residue ellipticity at 208 nm by the method of Greenfield and Fasman [27].

Protein concentration determination

Protein concentration was determined using a Bio-Rad Labs. protein assay kit [28] using bovine serum albumin as a standard.

Radioimmunoassay (RIA)

The procedures demployed for the purification of pituitary-derived EGH and the preparation of antisera against the pituitary-derived EGH have been described previously [16]. Iodination of pituitary-derived EGH and RIA using a double antibody method were performed as described by Kishida and Hirano [29].

Sodium dodecyl sulphate polyacrylamide gel electrophoresis (SDS-PAGE)

SDS-PAGE and staining with Coomassie Brilliant Blue were carried out essentially as described by Laemmli [30]. Stacking gels contained 4% (w/v) acrylamide and separation gels contained 14% (w/v) acrylamide. The sample buffer contained 2-mercaptoethanol (5%), except for samples referred to as unreduced.

Gel filtration chromatography (GFC)

GFC was carried out on a YMC-Pack Diol-120 column (30 × 0.8 cm I.D.) (YMC) with a Model 302 HPLC system (Gilson). Isocratic elution with 100 m*M*

phosphate buffer–200 m*M* NaCl (pH 7.2) including GuHCl at various concentrations, were performed in 60 min at ambient temperature. The flow-rate was 0.7 ml/min and the injection volume was 100 μl. UV detection was carried out at 280 nm. A molecular weight standard was obtained from Pharmacia. Samples were prepared by appropriate dilutions from stock solutions of 200 m*M* sodium chloride–100 m*M* phosphate buffer (pH 7.2), 8 *M* GuHCl–200 m*M* sodium chloride–100 m*M* phosphate buffer (pH 7.2) and 1 mg/ml rEGH–100 m*M* ammonium sulphate–10 m*M* Tris–HCl buffer (pH 8.0). The final protein concentration was 0.2 mg/ml.

Light scattering

Light-scattering analysis was carried out with a DLS-700 dynamic light-scattering spectrophotometer equpped with helium–neon laser at 632.8 nm (Otsuka Electronics). Recombinant EGH in 100 m*M* ammonium sulphate–10 m*M* Tris–HCl buffer (pH 8.0) was concentrated to 6.5 mg/ml using a YM-10 ultrafiltration membrane (Amicon) and diluted to 1.3, 2.6, and 3.9 mg/ml with the same buffer. Dust-free samples were prepared by filtering each solution through a Millex-GV 0.22-μm filter (Millipore), before analysis. All data were collected at 25°C and a 90° scattering angle. Refractive indeces were measured with an RM-102 refractometer (Otsuka electronics). The molecular weight of rEGH was calculated utilizing Debye's light-scattering equation [31], $KC/R_{90} = 1/M + 2A_2\ C + 3A_3C^2 + \ldots$, where $K = 2\pi^2 n_0^2 (\mathrm{d}n/\mathrm{d}C)^2 / N_A\lambda^4$, R_{90} is the Rayleigh ratio when the angle formed between the directions of the incident and scattered rays is 90°, C is the concentration of protein, M is the molecular weight of the protein, n and n_0 are the refractive indeces of the protein solution and the solvent, respectively, $\mathrm{d}n/\mathrm{d}C$ is the refractive index increment of the protein, N_A is Avogadro's number, λ is wavelength of laser and A_2, A_3, etc., are the second, third and higher virial coefficients, using the software with the DLS-700 dynamic light-scattering spectrophotometer.

RESULTS AND DISCUSSION

N-Terminal sequence analysis

The results of automated N-terminal sequence analysis of the rEGH are shown in Table I. Analysis was carried out up to the tenth residue. The sequencing result matched exactly the known sequence of pituitary-derived EGH II [16], but with an additional Met at the N-terminus. A sequence without the additional Met was not detected.

The design of the rEGH expression plasmid [4] was such that the coding sequence begins with an initiation codon for formyl-Met. Recombinant EGH, expressed in *E. coli* cells as inclusion bodies, consisted of 90% of rEGH with Met at the N-terminus and 10% of rEGH beginning with formyl-Met, which as detected by RP-HPLC [18] and removed in the purification process [15]. The sequencing result indicated that rEGH was unprocessed in terms of removal of the N-terminal Met residue. This observation supports the recent suggestion of Hirel *et al.* [32] that initiating Mets followed by amino acid residues with a side-chain of large radius are not removed in prokaryotes.

The presence of an N-terminal Met did not seem to affect the biological potency in a receptor binding assay [33] of the bacterially synthesized EGH, which is not

TABLE I

N-TERMINAL AMINO ACID SEQUENCE OF RECOMBINANT EGH

Cycle	Residue	Yield (pmol)
1	Met	340
2	Ile	570
3	Ser	40
4	Leu	320
5	Tyr	560
6	Asn	270
7	Leu	310
8	Phe	450
9	Thr	40
10	Ser	20

surprising because a human GH variant present in pituitary human GH preparations at about 5% (fast-human GH) has a blocked N-terminal end, owing to the presence of an acetyl group [34].

TABLE II

AMINO ACID COMPOSITION OF RECOMBINANT EGH

Residue	Theoretical number of residues[a]	Calculated number of residues[b]
Asx	22	20.7
Glx	16	17.1
Ser	16	15.0
Gly	11	11.6
His	5	4.5
Arg	9	8.6
Thr	11	10.8
Ala	10	10.7
Pro	6	5.3
Tyr	9	8.4
Val	9	8.9
Met	5[c]	4.9
Ile	10	11.4
Leu	22	22.2
Phe	8	8.4
Lys	14	13.7
Cys	4	ND[d]
Trp	1	ND

[a] The theoretical number of residues is based on the sequence of Saito *et al.* [4].

[b] The calculated number of residues represents the average of values obtained from three separate hydrolyses.

[c] The theoretical value of Met includes an additional Met at the N-terminus.

[d] ND, not determined.

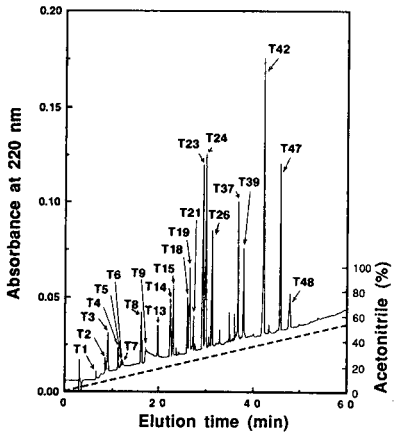

Fig. 1. Tryptic mapping of rEGH by RP-HPLC. A 20-μl volume of the digest was injected.

```
 1       5       10      15      20      25      30
M I S L Y N L F T S A V N R A Q H·L H T L A A E I Y K E F E R
←————————T48————————→ ←————————T24————————→ ←T8→
          ←——T5——→ ←T7→

        35      40      45      50      55      60
S I P P E A H R Q L S K T S P L A G C Y S D S I P T P T G K
←——T9——→ ←T4→ ←————————————————T39————————
                ←————————T37————————→

        65      70      75      80      85      90
D E T Q E K S D G Y L L R I S S A L I Q S W V Y P L K T L S
————→ ←——T19——→ ←————————T42————————→ ←——
←——T2——→

        95      100     105     110     115     120
D A F S N S L M F G T S D G I F D K L E D L N K G I N E L M
————————————T47————————————→ ←——T21——

        125     130     135     140     145     150
K V V G D G G I Y I E D V R N L R Y E N F D V H L R N D A G
→ ←————————T26————————→ ←T6→ ←————T23————→ ←——T13

        155     160     165     170     175     180
L M K N Y G L L A C F K K D M H K V E T Y L K V T K C R R F
————→ ←——T37/T39——→  ←————T18————→ ←T1→ ←——
                      ←T3→ ←——T14——→

        185 187
V E S N C T L
T15————→
```

Fig. 2. The deduced amino acid sequence of EGH II cDNA and the alignment of peptides from rEGH. Tryptic peptides derived from rEGH (see Fig. 1 and Table III) are shown with numbered arrows.

Amino acid composition analysis

Results of the amino acid composition analysis of rEGH (Table II) were in good agreement with the theoretical values.

Tryptic mapping of rEGH

A tryptic digest of rEGH was analysed by RP-HPLC (Fig. 1). Correspondence between peaks and fragments and the results of amino acid composition analysis of each peak are summarized in Fig. 2 and Table III, respectively. All fragments of rEGH were detected except Lys163. The results indicated that the primary structure of rEGH was identical with that of pituitary-derived EGH.

Lys163 seemed not to be retained by its hydrophilicity. Peaks T5 and T7 seemed to be produced by contaminated chymotryptic activity in the trypsin preparation. The C-terminal peptide bond of Lys108 was not cleaved. This observation supports the suggestion of Schroeder *et al.* [35] and others [36,37] that an acidic amino acid residue just before and/or after Arg or Lys interrupts cleavage of peptide bonds after these basic residues in trypsin digestions. The C-terminal peptide bond of Arg178 also was not cleaved. This interruption seemed to be caused by the steric hindrance of the disulphide bond between Cys177 and Cys185 (see below). A broad peak, T9, was fractionated into four fractions. The amino acid compositions of each of them were very similar and corresponded to a Ser31–Arg38 fragment (data not shown). This result indicated that a single fragment eluted as a broad peak. This observation supports the suggestion of Gesquiere and Diesis [38] that the peak of a peptide including a Pro–Pro sequence in RP-HPLC is broad or split because of slow *cis–trans* isomerization of Pro–Pro bonds.

The results of N-terminal amino acid sequence analysis, amino acid composition analysis and tryptic mapping revealed that rEGH had the natural primary structure with an additional Met at the N-terminus.

Location of disulphide bonds

Amino acid composition analysis (cysteine and cystine were not detected) of peaks T15 and T39 of tryptic mapping (Fig. 1) revealed that these peaks correspond to a mixture of equal amounts of fragments Thr43–Lys60 and Asn154–Lys162 and to that of fragments Cys177–Arg179 and Phe180–Leu187, respectively. No other peak of which the amino acid composition corresponded to fragments including a cysteine residue was detected.

The rechromatograms of the reduced and carboxymethylated peptides from peaks T15 and T39 are shown in Figs. 3 and 4, respectively. A single peak T15-1 was detected on the rechromatogram of carboxymethylated peak T15. The amino acid composition of peak T15-1 and the difference in the amino acid composition between peaks T15 and T15-1 corresponded to Phe1180–Leu187 and Cys177–Arg179, respectively. Therefore, a disulphide bond between Cys177 and Cys185 is suggested. Fragment Cys177–Arg179 seemed not to be retained by its hydrophilicity. Two peaks, T39-1 and T39-2, were observed for peak T39. The amino acid compositions of the peptides corresponded to those of the fragments Thr43–Lys60 and Asn154–Lys162, respectively. These results indicated that another disulphide bond was formed between Cys149 and Cys160.

Unfortunately, the positions of the disulphide bonds in pituitary-derived EGH

were not confirmed, whereas those of pituitary-derived human and bovine GHs were confirmed at Cys49–Cys160 and Cys177–Cys185 [22,23]. It is assumed, however, that the locations of disulphide bonds are conserved among vertebrate GHs, because the primary structure of vertebrate GHs is conserved well from human to teleost, and especially the position of Cys is conserved at all four sites [17,39]. It is concluded, therefore, that the location of the disulphide bonds in rEGH is the same as that in pituitary-derived EGH.

CD

Fig. 5 shows the far-UV CD spectra of rEGH and pituitary-derived human GH (Sigma). The far-UV CD spectrum of rEGH was very similar to that of pituitary-derived human GH. Both spectra had negative bands at 208 and 219 nm. The far-UV CD spectrum reflects the secondary structure of a protein [40,41]. The spectra classified these GHs as α-helix-rich protein [40,41]. α-Helix contents of rEGH and pituitary-derived human GH were calculated as 45% and 56%, respectively, using Greenfield and Fasman's method [27]. Pituitary-derived vertebrate GHs were classified as

TABLE III

AMINO ACID ANALYSIS OF TRYPTIC PEPTIDE FROM RECOMBINANT EGH

Values represent the average number of residues per molecule obtained from three separate hydrolyses. Numbers in parentheses represent the number of residues determined by the sequence deduced from EGH cDNA [4]. Conditions for trypsin digestion, chromatography and amino acid composition analysis as described under Experimental.

Residue	Fragment no.										
	T1	T2	T3	T4	T5	T6	T7	T8	T9	T13	T14
Asx[a]		1.0(1)	0.8(1)		1.1(1)	1.0(1)				2.0(2)	
Glx[a]		3.0(3)		0.9(1)			1.0(1)	2.1(2)	1.2(1)		1.0(1)
Ser				0.9(1)	1.0(1)				0.9(1)		
Gly										1.0(1)	
His			1.0(1)				1.7(2)		0.8(1)		
Arg					1.0(1)	0.9(1)		1.0(1)	0.9(1)		
Thr	0.9(1)	1.0(1)			1.0(1)						0.8(1)
Ala					1.1(1)		1.0(1)		1.1(1)	1.0(1)	
Pro									1.9(2)		
Tyr											1.0(1)
Val	1.0(1)				1.0(1)						1.0(1)
Met			0.2(1)							0.4(1)	
Ile									1.2(1)	0.9(1)	
Leu				1.1(1)		1.0(1)	1.3(1)				1.1(1)
Phe								1.0(1)			
Lys	1.0(1)	1.0(1)	1.2(1)	1.1(1)						1.0(1)	1.2(1)
Cys											
Trp											
Total	3	6	4	4	6	3	5	4	8	7	6
Position	174–176	61–66	164–167	39–42	8–13	135–137	14–18	27–30	31–38	147–153	168–173

[a] Glx, Asx, acid + amide.
[b] ND, not detected.

α-helix-rich protein. The α-helix contents of human, bovine, ovine, and salmon GHs were reported to be 50–60%, 50%, 40–45% [20,21] and 48% (unpublished data), respectively. The content for human GH (56%) was in good agreement with the previously reported value of 50–60%. Recombinant EGH was also classified as α-helix-rich protein as well as other vertebrate GHs, and the content was similar to those of bovine, ovine or salmon GH rather than human GH.

RIA

The RIA results showed equivalence between rEGH and pituitary-derived EGH, in terms of recognition by the polyclonal antibody used (data not shown). As antibody–ligand binding is known to be conformation specific rather than sequence specific, correct conformation of rEGH was confirmed by the RIA results. Recently, Hirano [33] has shown that hepatic GH receptor of the eel does not distinguish rEGH from pituitary-derived EGH.

The RIA and receptor assay results further suggested that the three-dimensional structure of rEGH was virtually identical with that of its natural counterpart.

T15	T18	T19	T21	T23	T24	T26	T37	T39	T42	T47	T48
1.0(1)	0.9(1)	1.0(1)	1.0(1)	1.8(2)		2.1(2)	2.9(3)	2.3(2)		5.9(6)	2.2(2)
1.1(1)	1.2(1)		1.2(1)	1.3(1)	2.0(2)	1.4(1)	2.9(3)		1.0(1)	1.3(1)	
1.0(1)		1.1(1)					2.6(3)	2.8(3)	2.5(3)	3.6(4)	1.7(2)
		1.1(1)	0.9(1)			3.0(3)	2.6(3)	3.1(3)		2.0(2)	
	1.0(1)			0.7(1)	1.8(2)						
1.9(2)		1.0(1)		0.8(1)		0.8(1)					0.7(1)
1.0(1)	1.3(1)				1.1(1)		3.9(4)	2.8(3)		2.0(2)	0.7(1)
					3.1(3)		2.1(2)	1.8(2)	0.9(1)	1.1(1)	0.7(1)
							3.2(3)	2.7(3)	0.9(1)		
	0.9(1)	0.9(1)		1.1(1)	1.0(1)	1.0(1)	2.1(2)	2.0(2)	1.0(1)		1.1(1)
1.0(1)	0.9(1)			1.2(1)		2.5(3)			1.2(1)		0.9(1)
			0.8(1)							0.9(1)	1.0(1)
			1.2(1)		1.1(1)	2.3(2)	1.3(1)	1.4(1)	2.4(2)	1.1(1)	1.4(1)
1.1(1)	1.1(1)	1.9(2)	1.0(1)	1.1(1)	2.2(2)		3.4(3)	3.3(3)	2.2(2)	4.2(4)	2.3(2)
1.0(1)				1.1(1)			1.3(1)	1.2(1)		3.2(3)	1.4(1)
	1.9(2)		0.9(1)		0.9(1)		2.6(3)	1.7(2)	0.9(1)	1.7(2)	
ND[b](2)							ND (2)	ND (2)			
									ND (1)		
11	19	7	7	9	13	13	33	27	14	27	14
177–187	164–173	67–73	115–121	138–146	14–26	122–134	43–66	43–60	74–87	88–114	0–13
							154–162	154–162			

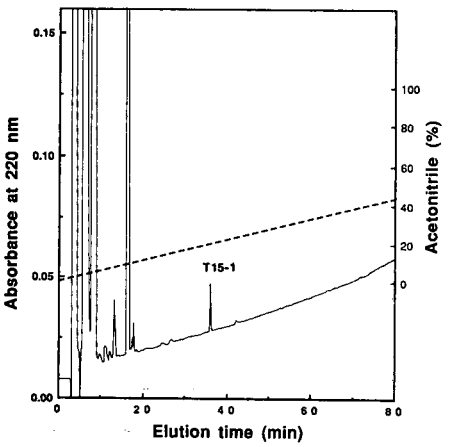

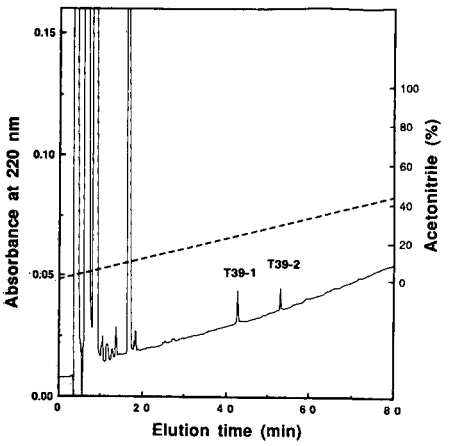

Fig. 3. HPLC separation of carboxymethylated peptides derived from peak T15, tryptic peptide of rEGH. A 450-μl volume of carboxymethylated peptide solution was injected.

Fig. 4. HPLC separation of carboxymethylated peptides derived from peak T39, tryptic peptide of rEGH. A 450-μl volume of carboxymethylated peptide solution was injected.

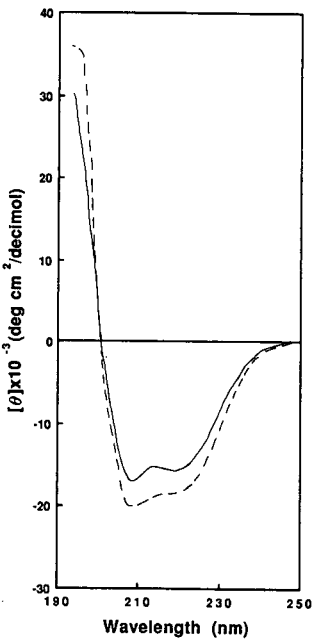

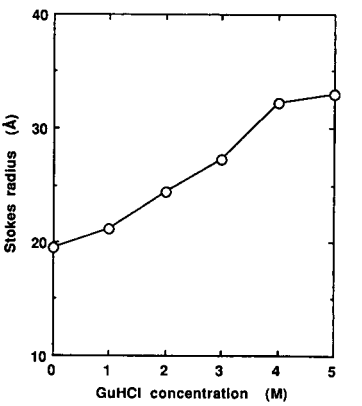

Fig. 5. CD spectra of (solid line) rEGH and (dashed line) pituitary-derived human GH.

Fig. 6. Stokes radius of rEGH at various concentrations of GuHCl. A calibration graph was obtained in the absence of GuHCl by utilizing molecular weight standards of bovine serum albumin (35.5 Å), ovalbumin (30.5 Å), chymotrypsinogen A (20.9 Å) and ribunuclease A (16.4 Å) at a concentration of 0.2 mg/ml.

TABLE IV

MOLECULAR WEIGHT OF EGHs

Methods	Molecular weight (kilodalton)	
	Recombinant EGH	Pituitary-derived EGH
SDS-PAGE (reduced)	25	25
SDS-PAGE (unreduced)	21	21
GFC	23	Monomer[a]
Light scattering	21	ND[b]
Theoretical value	21.327	21.196

[a] From Ref. 16.
[b] ND, not determined.

SDS-PAGE

The apparent masses of rEGH and pituitary-derived EGH given by SDS-PAGE are given in Table IV. The apparent mass of the reduced rEGH was 25 kilodalton, whereas the unreduced rEGH migrated faster (21 kilodalton). This is in agreement with observations on other disulphide-containing proteins [42], and may reflect a more compact SDS–protein complex when disulphide bonds are formed. The co-migration of rEGH with pituitary EGH, under both reduced and unreduced conditions, suggested that rEGH was correctly oxidized with regard to disulphides.

GFC

Recombinant EGH behaved as a monomer (23 kilodalton) in GFC. The result showed good agreement with the previous result for pituitary-derived EGH [16] (Table IV).

As mentioned in the introduction, however, the GFC results could be biased by the chromatographic process. Therefore, to study the dimerization of rEGH and the interaction between rEGH and the GFC support, the apparent Stokes radius of rEGH in GuHCl of various concentrations was determined (Fig. 6). Recombinant EGH was eluted as a single peak in each instance. The Stokes radius of rEGH in the absence of GuHCl was 19.5 Å. The radius increased gradually with increase of GuHCl concentration, with the largest increase at 3–4 *M* GuHCl. At 5 *M* GuHCl, the radius reached 32.9 Å. The shape of this sigmoidal curve for rEGH was similar to that for other proteins [25,43]. The largest increase, at 3–4 *M* GuHCl, corresponds to unfolding of the tertiary structure of rEGH protein, which was detected by fluorescence analysis. Unfolding of the tertiary structure of protein causes a change in the microenvironment of the Trp residue, and this change was detected as a change in the intensity of fluorescence emission and/or a shift of the emission wavelength. A single Trp residue is present in EGH protein (Fig. 2). The emission wavelength was scanned from 300 to 400 nm at an excitation wavelength of 280 nm. The wavelength of maximum emission shifted from 340 to 350 nm between 3 and 4 *M* GuCHl, whereas a significant shift was not observed at other GuHCl concentrations (data not shown).

Dissociation of rEGH dimer and disappearance of the interaction between

rEGH and the GFC support should cause an abnormal decrease and increase in the apparent Stokes radius at certain concentrations of GuHCl, respectively. In Fig. 6, no such decrease or increase is observed. Hence rEGH existed as a monomer and the observed Stokes radius and molecular weight of rEGH in the absence of GuHCl in GFC were not biased by the interaction between rEGH and the GFC support, unless dissociation of rEGH dimer or disappearance of the interaction occurred with unfolding of rEGH protein.

Light scattering

The molecular weight of rEGH was measured by light scattering (Fig. 7). The calculated molecular weight (21 kilodalton) was virtually identical with the theoretical value from the amino acid sequence (Table IV). Oligomerization of protein results in a non-linear line in a Debye plot. A linear relationship, as in this instance, showed the absence of protein oligomerization within the range of protein concentration applied [44,45]. Therefore, the light-scattering results indicated that rEGH exists as a monomer at protein concentrations at least lower than 6.5 mg/ml.

The results of GFC at various concentrations of GuHCl supported the conclusion from GFC without GuHCl that rEGH exists as a monomer. However, we cannot deny the possibility that dissociation of rEGH dimer or disappearance of the interaction between rEGH and the GFC support occured with unfolding of rEGH protein. Also, it is difficult to discuss the effect of rEGH concentration on dimerization because of sample dilution during GFC. Hence it is important to confirm the molecular weight by other methods, such as light scattering or sedimentation equilibrium, although these methods require higher concentrations of protein than in GFC.

Together with the results of the receptor assay by Hirano [33], it is concluded that pituitary-derived EGH also exists as a monomer, because the binding ability of natural EGH would be lower than that of rEGH if oligomerization occurred in natural EGH.

In conclusion, biochemical, biophysical, and immunochemical properties of rEGH were characterized in comparison with pituitary-derived eel, human, bovine,

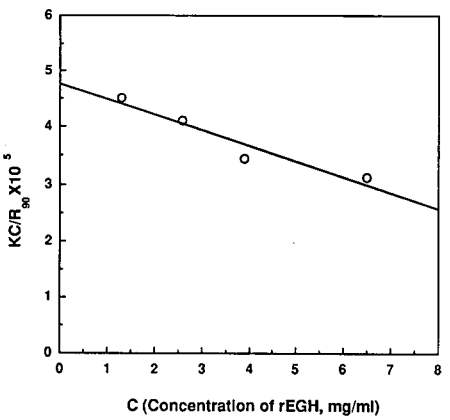

Fig. 7. Debye plots for rEGH. The refractive index of the buffer was 1.3317 and the refractive index increment of the rEGH was 0.1861.

and ovine GHs. The results of N-terminal amino acids sequence analysis, amino acid composition analysis and tryptic mapping revelaed that rEGH had the natural primary structure with an additional Met at the N-terminus. Together with the results of the receptor assay by Hirano [33], the RIA, GFC and light-scattering results suggested that the rEGH was folded into native three-dimensional structure and existed as a monomer, as does pituitary-derived EGH. Other results also supported this conclusion. These data also indicated the usefulness of the large-scale preparation procedure described previously [15].

The large-scale production of *E.coli*-derived rEGH, whose properties are identical with those of the pituitary-derived EGH, will aid future applications of recombinant GH in aquaculture and basic studies on the mode of action of the hormone.

ACKNOWLEDGEMENTS

We are grateful to Professor T. Hirano of the University of Tokyo for performing RIA and for valuable discussions. We thank Dr. S. Nakamura (Otsuka Electronics) for the light-scattering analyses. We also thank Miss Katsuko Shimokawa for skilful assistance.

REFERENCES

1 D. V. Goeddel, H. L. Heyneker, T. Hozumi, R. Arentzen, K. Itakura, D. G. Yansura, M. J. Ross, G. Miozzari, R. Crea and P. H. Seeburg, *Nature (London)*, 281 (1979) 544.
2 W. L. Miller, J. A. Martial and J. D. Baxter, *J. Biol. Chem.*, 255 (1980) 7521.
3 S. Sekine, T. Mizukami, T. Nishi, Y. Kuwana, A. Saito, M. Sato, S. Itoh and H. Kawauchi, *Proc. Natl. Acad. Sci. USA*, 82 (1985) 4306.
4 A. Saito, S. Sekine, Y. Komatsu, M. Sato, T. Hirano and S. Itoh, *Gene*, 73 (1988) 545.
5 N. Sato, K. Watanabe, K. Murata, M. Sakaguchi, Y. Kariya, S. Kimura, M. Nonaka and A. Kimura, *Biochim. Biophys. Acta*, 949 (1988) 35.
6 M. Watahiki, M. Yamamoto, M. Yamakawa, M. Tanaka and K. Nakashima, *J. Biol. Chem.*, 264 (1989) 312.
7 K. C. Olson, J. Fenno, N. Lin, R. N. Harkins, C. Sinder, W. H. Kohr, M. J. Ross, D. Fodge, G. Prender and N. Stebbing, *Nature (London)*, 293 (1981) 408.
8 P. T. Wingfield, P. Graber, G. Buell, K. Rose, M. G. Simona and B. D. Burleigh, *Biochem. J.*, 243 (1987) 829.
9 K. E. Langley, T. F. Berg, T. W. Strickland, D. M. Fenton, T. C. Boone and J. Wypych, *Eur. J. Biochem.*, 163 (187) 313.
10 P. J. Brumby, and J. Hancock, *N.Z. J. Sci. Technol., Sect. A*, 36 (1955) 417.
11 L. J. Machlin, *J. Diary Sci.*, 56 (1973) 575.
12 C. J. Peel, D. E. Bauman, R. C. Gorewit and C. J. Sniffen, *J. Nutr.*, 111 (1981) 1662.
13 K. E. Langley, P.-H. Lai, J. Wypych, R. R. Everett, T. F. Berg, L. F. Krabill, J. M. Davis and L. M. Souza, *Eur. J. Biochem.*, 163 (1987) 323.
14 S. Sugimoto, Y. Yokoo, Y. Inui and T. Hirano, *Agric. Biol. Chem.*, 55 (1991) 1635.
15 S. Sugimoto and Y. Yokoo, *Kagaku Kogaku Ronbunshu*, 17 (1991) 620.
16 M. Kishida, T. Hirano, J. Kubota, S. Hasegawa, H. Kawauchi, K. Yamaguchi and K. Shirahata, *Gen. Comp. Endocrinol.*, 65 (1987) 478.
17 K. Yamaguchi, A. Yasuda, M. Kishida, T. Hirano, H. Sano and H. Kawauchi, *Gen. Comp. Endocrinol.*, 66 (1987) 447.
18 S. Sugimoto, K. Yamaguchi and Y. Yokoo, *J. Chromatogr.*, 515 (1990) 483.
19 H. Edelhoch, P. G. Condliffe, R. E. Lippoldt and H. G. Burger, *J. Biol. Chem.*, 241 (1966) 5205.
20 T. A. Bewley and C. H. Li, *Biochemistry*, 11 (1972) 884.
21 T. A. Bewley and C. H. Li, *Biochemistry*, 11 (1972) 927.
22 C. H. Li, *Mol. Cell. Biochem.*, 46 (1982) 31.

23 M. Wallis, *FEBS Lett.*, 35 (1973) 11.
24 H. N. Fernandez and J. M. Delfino, *Biochem. J.*, 209 (1983) 107.
25 D. N. Brems, S. M. Plaisted, H. A. Havel, E. W. Kauffman, J. D. Stodola, L. C. Eaton and R. D. White, *Biochemistry*, 24 (1985) 7662.
26 B. A. Bidlingmeyer, S. A. Cohen and T. L. Tarvin, *J. Chromatogr.*, 336 (1984) 93.
27 N. Greenfield and G. D. Fasman, *Biochemistry*, 10 (1969) 4108.
28 M. Bradford, *Anal. Biochem.*, 72 (1976) 248.
29 K. Kishida and T. Hirano, *Nippon Suisan Gakkaishi*, 54 (1988) 1321.
30 U. K. Laemmli, *Nature (London)*, 227 (1970) 680.
31 P. Debye, *J. Phys. Colloid. Chem.*, 51 (1947) 18.
32 P.-H. Hirel, J.-M. Schmitter, P. Dessen, G. Fayat and S. Blanquet, *Proc. Natl. Acad. Sci. USA*, 86 (1989) 8247.
33 T. Hirano, *Gen. Comp. Endocrinol.*, 81 (1991) 383.
34 U. J. Lewis, R. N. P. Singh, G. F. Tutwiler, M. B. Sigel, E. F. VanderLaan and W. P. VanderLaan, *Recent Prog. Horm. Res.*, 36 (1980) 447.
35 W. A. Schroeder, J. R. Shelton, J. B. Shelton, J. Cormick and R. T. Jones, *Biochemistry*, 2 (1963) 992.
36 T. Koide and T. Ikenaka, *Eur. J. Biochem.*, 32 (1973) 417.
37 C. H. W. Hirs, S. Moore and W. H. Stein, *J. Biol. Chem.*, 219 (156) 623.
38 J. C. Gesquiere and E. Diesis, *J. Chromatogr.*, 478 (1989) 121.
39 K. Yamaguchi, J. L. Specker, D. S. King, Y. Yokoo, R. S. Nishioka, T. Hirano and H. A. Bern, *J. Biol. Chem.*, 263 (1988) 9113.
40 J. P. Hennessey, Jr., and W.C. Johnson, Jr., *Biochemistry*, 20 (1981) 1085.
41 P. Manavalan and W. C. Johnson, Jr., *Nature (London)*, 305 (1983) 831.
42 J. M. Schoemaker, A. H. Brasnett and F. A. O. Marston, *EMBO J.*, 4 (1985) 775.
43 S. Endo, Y. Saito and A. Wada, *Anal. Biochem.*, 131 (1983) 108.
44 E. P. Pittz, J. C. Lee, B. Bablouzian, R. Townend and S. N. Timasheff, *Methods Enzymol.*, 27 (1973) 209.
45 K. Hayashi, in Y. Uritani, N. Shimura, M. Nakamura and M. Funadzu (Editors), *Seibutsu Kaguku Jikken-ho C-2 Tampakushitsu no Bunshiryo Bunshikei*, Tokyo Daigaku Shuppan-kai, Tokyo, 1973, pp. 59–77.

Journal of Chromatography, 547 (1991) 145–153
Elsevier Science Publishers B.V., Amsterdam

CHROM. 23 247

Evaluation of displacement chromatography for the recovery of lactate dehydrogenase from beef heart under scale-up conditions

SIDDHARTHA GHOSE and BO MATTIASSON*
Department of Biotechnology, Box 124, Chemical Center, University of Lund, 221 00 Lund (Sweden)
(First received October 4th, 1990; revised manuscript received February 21st, 1991)

ABSTRACT

A complex mixture of proteins was subjected to displacement development from a Tris Acryl DEAE anion-exchange column. Lactate dehydrogenase was used as the target protein in the evaluation of the resolution and separation under scale-up conditions. The conditions of operation were scaled up in terms of column size and protein load. Column length was found to play an important role in resolving the mixture. The performance of the displacement mode run was compared with a conventional ion-exchange elution run in terms of fraction purity and specific activities. In general, displacement chromatography of the complex mixture yielded better results.

INTRODUCTION

The recovery and purification of proteins from crude mixtures is a multi-stage process in which a number of different unit operations in downstream processing can be involved. Chromatography is one such separation method and is a powerful tool for separation towards the end stages. Chromatographic separation can be based on ionic charge, hydrophobicity, molecular size and biospecific affinity, among others. The majority of operations have been conducted in the elution mode.

The use of displacement development in preparative-scale chromatography has been carried out by a number of researchers in recent years for the purification of peptides [1–4], amino acids [2,5–10] and antibiotics [3,11,12]. These applications have involved the use of both reversed-phase (C_8 and C_{18}) and ion-exchange high-performance liquid chromatographic (HPLC) columns. Good resolutions have been obtained with loadings higher than those applied on analytical scale. The systems consisted mainly of binary and ternary mixtures. The small particle sizes, in the range of 5–10 μm, presumably played an important role in the separations.

Protein purifications by displacement chromatography have also been tried and the capacity and power of such a process were demonstrated through the separation of A and B forms of β-lactoglobulin by Torres *et al.* [13] and later by Liao *et al.* [14] using two different types of displacers. Preparative amounts of these two protein forms, differing in p*I* by only 0.1 unit, were separated on HPLC anion exchangers.

0021-9673/91/$03.50

However, the application of displacement chromatography to protein purification from complex mixtures has been limited, although the potential has been shown by the work done on alkaline phosphatase purification from *Escherichia coli* periplasmic space protein [15], GC-2 globulin from human serum [16] and monoclonal antibody purification by complex displacement chromatography [17].

Although the above approaches have yielded promising results, the general practice has been to use relatively simple protein mixtures on small-scale HPLC columns operating at relatively low flow-rates. Through the work outlined in this paper, it was attempted to show the possibility of running displacement chromatography using a conventional low-pressure column with a complex protein mixture and comparing the performance *vis-à-vis* conventional elution. Purification of lactate dehydrogenase (LDH) from beef heart proteins was attempted. The problems encountered with such complex systems have been addressed by Peterson [18] using serum proteins and the importance of these non-ideal considerations were apparent in this work.

EXPERIMENTAL

The displacer carboxymethylstarch (CMS) was obtained as a gift from Reppe Glykos (Räppe, Sweden) and was used as a 20 g/l solution in 0.01 *M* Tris–HCl (pH 8.5). β-NADH and sodium pyruvate used in the LDH activity assay were purchased from Sigma (St. Louis, MO, USA). The column gel Tris Acryl DEAE M was supplied by IBF France.

Preparation of beef heart homogenate

The homogenate was prepared by first blending in a kitchen mixer 100 g of beef heart with 100 g of ice and 100 ml of 0.05 *M* sodiumphosphate buffer containing 1 m*M* β-mercaptoethanol (pH 7.0). The homogenized mass was mixed well with an additional 50 ml of the buffer and then centrifuged at 20 000 *g* for 10 min. The supernatant was filtered over glass-wool to remove any fat, then ammonium sulphate was added to 30% saturation. This was followed by a second centrifugation at 20 000 *g* for 5 min, the supernatant from which was made up to 65% saturation. A final centrifugation was then carried out at 20 000 *g* for 10 min. The pellet obtained from the last step was dissolved in water and dialysed against the column equilibrating buffer to obtain the homogenate in its ready to use form.

Column chromatography

Tris Acryl DEAE M, a weak anion exchanger, was used as the column gel material. Prior to packing, it was washed several times with the column equilibrating buffer (0.01 *M* Tris–HCl, pH 8.5) and degassed gently with constant stirring. The gel was slurry packed into a Bio-Rad Labs. column under a hydrostatic pressure head of about 85–100 cm. Solutions were pumped through an LKB 2132 Microperpex peristaltic pump via a manually operated valve system. UV detection at 280 nm was carried out with an LKB 2138 Uvicord-S detector and the column effluent was sampled using an LKB 2112 Redirac fraction collector. The detector output was recorded on an LKB 2210 single-channel chart recorder.

LDH activity measurement

Lactate dehydrogenase (E.C. 1.1.1.27) activity was measured as proportional to the initial rate of decrease of absorbance at 340 nm of NADH due to its oxidation to NAD^+ in the reaction converting pyruvate to lactate. A 10-μl volume of the sample was added to a reaction mixture containing 2.8 ml of 0.01 *M* Tris–HCl (pH 7.3), 0.1 ml of 6.6 m*M* NADH in buffer and 0.1 ml of 30 m*M* sodium pyruvate in buffer. Absorbance changes were measured with a Shimadzu UV-260 spectrophotometer.

Sodium dodecyl sulphate–polyacrylamide gel electrophoresis (SDS-PAGE)

Some of the output fractions were subjected to SDS-PAGE using a Bio-Rad Labs. mini gel slab. A 3% stacking and 12.5% running gel were used. The best running times were found to be 30 min at 50 V followed by 45 min at 200 V. The gels were fixed in 40% methanol–10% acetic acid and stained using a 0.1% Kenacid Blue R solution in the fixative base. The gels were finally destained in 40% methanol–10% acetic acid solution. The gels were then soaked in 25% acetic acid containing 4% of glycerol to prevent them from cracking on drying.

RESULTS AND DISCUSSION

The work done on the displacement chromatography of peptide mixtures [1–4] and simple protein samples [3,13,14,19–21] using HPLC columns has yielded very positive results regarding the preparative-scale capacity of this operating mode. Its application to systems of a more complex nature has been limited, although the work done so far [15–17] has demonstrated its feasibility. We chose a system consisting of proteins from beef heart and investigated the separation and recovery of LDH by displacement from an anion exchanger.

An important aspect of the work was the displacer itself. The choice of carboxymethylstarch (CMS) was based on the use of similar substituted polymers [carboxymethyldextrans (CMDs) and carboxymethylcellulose] by other workers [13,15–17]. From titration analysis, its pK_a value was observed to be *ca.* 5.8 and it had a hydroxyl group equivalent of $4.7 \cdot 10^{-4}$ mequiv. NaOH/mg polymer. Carboxymethyl-substituted dextrans synthesized using the method of Peterson [18] were observed to have values higher than this, even the relatively weak affinity ones. However, the displacement worked well with the CMS, indicating that the dextran-based displacers would have been over-effective. The use of CMDs has been extensively studied by other workers [13,15–17]. The CMDs have different degrees of substitution and have been used both as spacers and as a final displacer.

Effect of column length

A displacement run was made on a 9.1 × 1.0 cm I.D. column (run I). The profile for the absorbance at 280 nm and LDH activity at the column outlet are shown in Figure 1. LDH activity higher than 1.0 ($\Delta A/\Delta t$) appears over one column volume of eluent, which can be considered reasonable given the size of the column and the load. However, the resolution was poor in that no recognizable plateaux typical of displacement chromatography were observed. In order to improve upon this, a run was carried out under identical conditions except that a 25.0 × 1.0 cm I.D. column was used (run II). The corresponding absorbance and activity profiles are

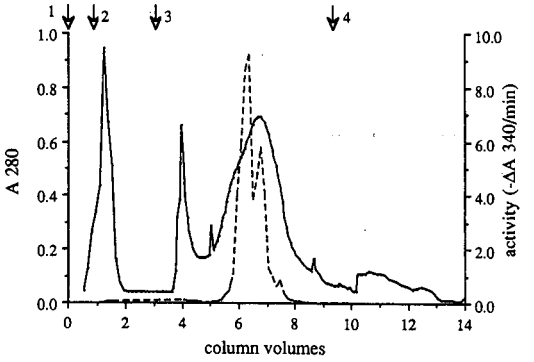

Fig. 1. Column outlet profile for displacement run on a 9.0 × 1.0 cm I.D. column of Tris Acryl DEAE M. The equilibrating buffer was 0.01 *M* Tris–HCl (pH 8.5) and all solutions were prepared using this. Displacer, 20 g/l CMS; protein load, 6 ml of homogenate. Arrows: (1) start protein load; (2) stop protein load, start buffer wash; (3) stop buffer wash, start displacer flow; (4) stop displacer flow, start column wash. Solid line, absorbance at 280 nm; dashed line, activity.

shown in Fig. 2. The one large peak in the previous run containing the LDH is resolved into four smaller peaks with the LDH being maintained within about one column volume of the eluent.

The LDH activity profile undergoes some kind of transition between the two column runs and also shows a drop in the maximum observed value. It is difficult to give any conclusive reason for the differences. It is plausible that some type of interactions between the two predominant isoenzyme forms in the heart, H_4 and H_3M, could be of importance.

The purities of the fractions can be compared from the SDS-PAGE of the active fractions from runs I and II. These are shown in Figs. 3 and 4, respectively, and a marked improvement can be observed. A high-molecular-weight contaminant from the smaller column is removed to a large extent in the second run. LDH forms the major component.

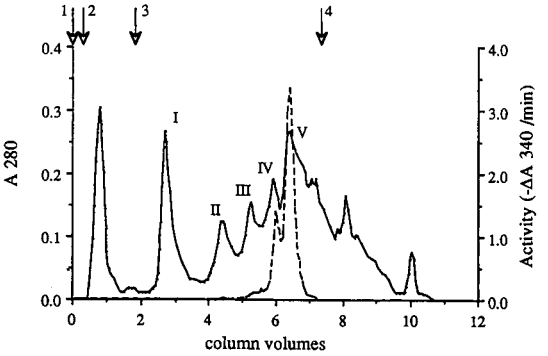

Fig. 2. Column outlet profile for displacement run on a 25.0 × 1.0 cm I.D. column of Tris Acryl DEAE M. Conditions, arrows and lines as in Fig. 1.

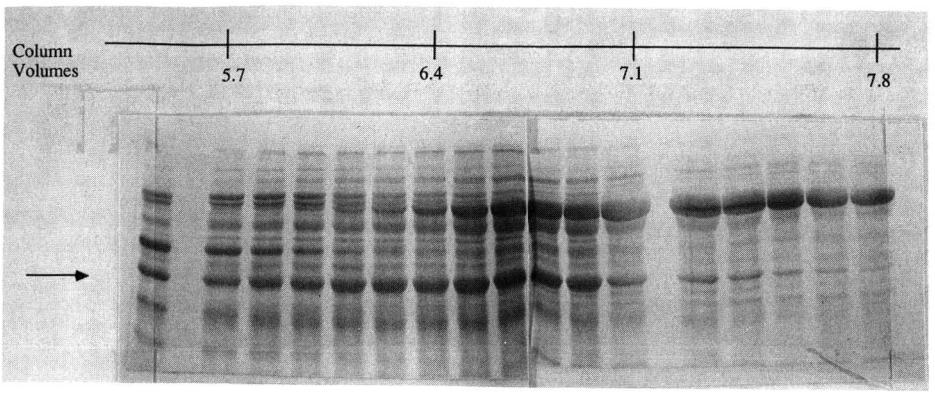

Fig. 3. SDS-PAGE of some of the LDH-active fractions between column volumes 5.5 and 8.0 from the displacement run in Fig. 1. Position of LDH isoenzyme H4 is depicted by the arrow.

The absorbance profile in Fig. 2 under displacement (between arrows 3 and 4) shows the formation of peaks of increasing height (peaks II–V), although there are no sharp step profiles as dictated by the theory [22,23]. This non-ideality can be attributed mainly to the relatively larger particle sizes (40–80 μm) of the column gel and to non-homogeneity in size. This compares poorly with HPLC-based material used by other workers, which yielded better resolutions. However, in spite of the drawbacks, the system presented here has great operational simplicity and is capable of reasonable fractionation of a relatively large protein load.

Effect of displacer solution pH

An important point addressed was that of the pH of the displacer solution. The column equilibrating buffer used in the runs was 0.01 *M* Tris–HCl (pH 8.5). A 20 g/l solution of the displacer in this buffer decreased the pH to 3.8. Under these conditions any number of ionic effects could have an influence and the observed behaviour results from a combination of displacement and pH changes as in conventional elu-

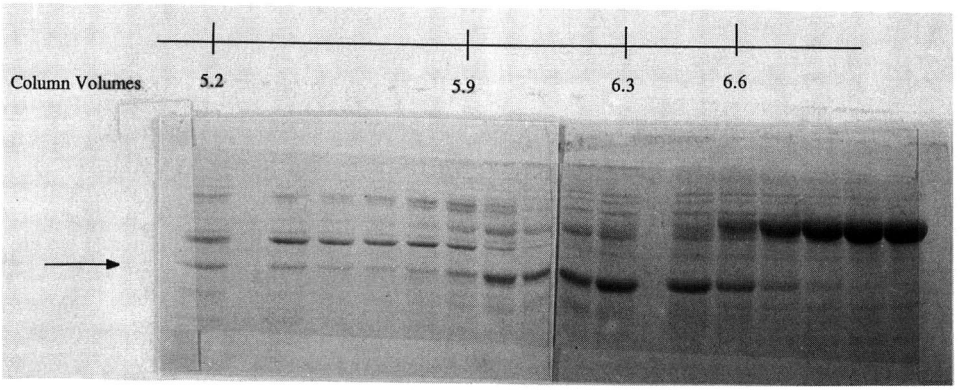

Fig. 4. SDS-PAGE of some of the LDH-active fractions between column volumes 5.5 and 7.0 from the displacement run in Fig. 2. Position of LDH isoenzyme H4 is depicted by the arrow.

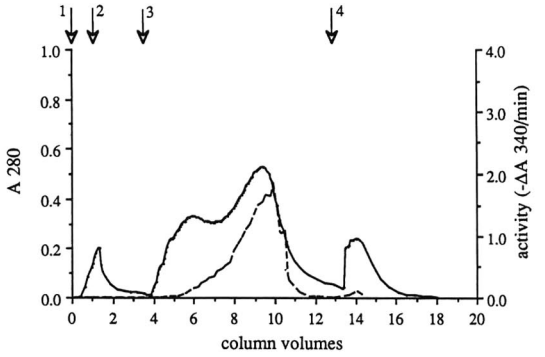

Fig. 5. Column outlet profile for a displacement run on an 8.0 × 1.0 cm I.D. column of Tris Acryl DEAE M under conditions in which the pH of the displacer solution in the buffer base was not adjusted. Conditions, arrows and lines as in Fig. 1, except displacer solution, 20 g/l in buffer.

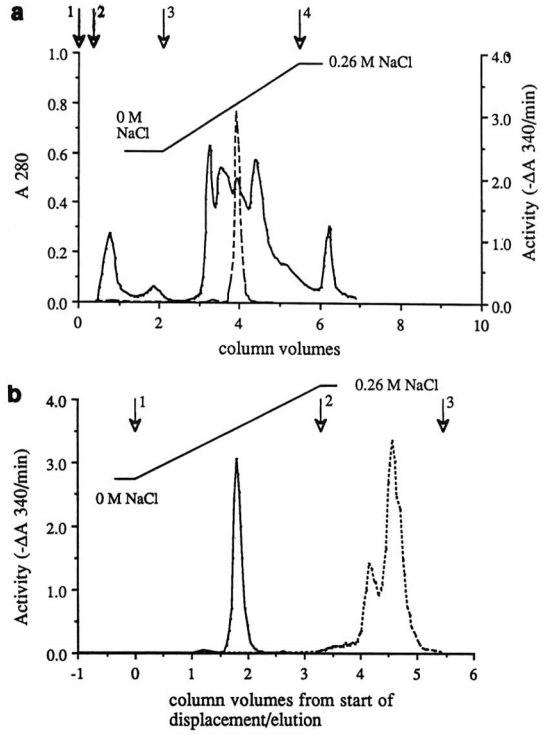

Fig. 6. (a) Column outlet profile for ion-exchange run with salt elution on a 24.0 × 1.0 cm I.D. column of Tris Acryl DEAE M. Equilibrating buffer, protein load and lines as in Fig. 1. Arrows: (1) start protein load; (2) stop protein load, start buffer wash; (3) stop buffer wash, start salt elution; (4) stop salt elution, start column wash. (b) Comparison of the appearance of the LDH-active peaks from the start of displacement/elution. Arrows: (1) start of displacement/elution; (2) end of gradient elution; (3) end of displacement.

tion. Hence, adjustment of the pH was always carried out prior to the runs. However, a displacement run was conducted on an 8.0 × 1.0 I.D. column without pH adjustment and the absorbance and activity profiles are shown in Fig. 5. It can be said that at a lower pH the CMS would possess less negative charge but its effectiveness as a displacer need not necessarily be affected drastically, as the solute system would also undergo some kind of a charge distribution, correspondingly reducing its affinity for the column. The overall profile and activity profiles are, however, much poorer, suggesting the importance and need for proper pH control.

Comparison with conventional ion exchange

A comparative evaluation of the performance under displacement was made with a conventional elution run on a 24 × 1.0 cm I.D. column (Fig. 6a). Elution was carried out using a salt gradient from 0 to 0.5 *M* sodium chloride in buffer in 120 min. The gradient was operated for 62 min. The activity profile obtained, shown in Fig. 6b from the start of elution, was much sharper than that from the displacement run and appears over a smaller eluent volume. However, analysis of the active fractions by SDS-PAGE (Fig. 7) indicates a much lower degree of purification. This is also evident from the specific activity plots in Fig. 8. The separation could be improved through the use of a shallower gradient, but then a higher dilution effect would result.

The recovery of LDH from beef heart proteins can be compared in terms of complexity of the protein system with the purification of alkaline phosphatase from periplasmic space protein [15], Gc-2 globulin from human serum [16] and monoclonal antibody purification by complex displacement chromatography [17]. CMDs were used as spacers and the final displacers in the first two separations. The protein loads were comparatively large although two displacement steps were incorporated for recovery of the target proteins. HPLC was used in the separations. In the mAb purification, a slightly different methodology was used. The displacer (carboxymethylcellulose) bound to the protein of interest while actually displacing the impurities. Final removal was carried out with saline solution.

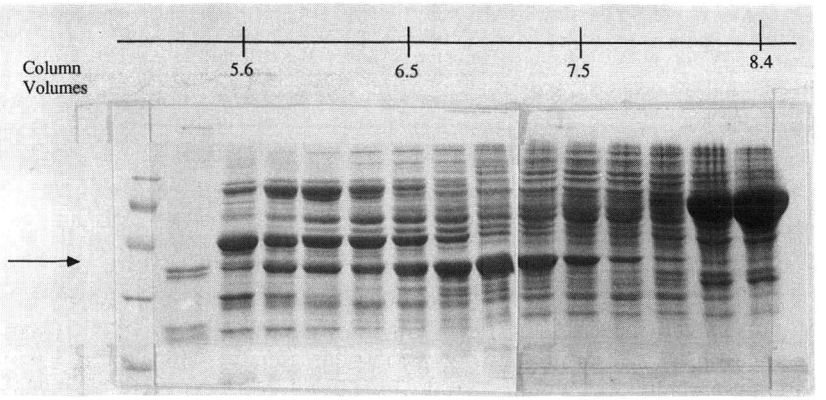

Fig. 7. SDS-PAGE of some of the LDH-active fractions between column volumes 3.5 and 4.5 from the elution run in Fig. 6a. Position of LDH isoenzyme H4 is depicted by the arrow.

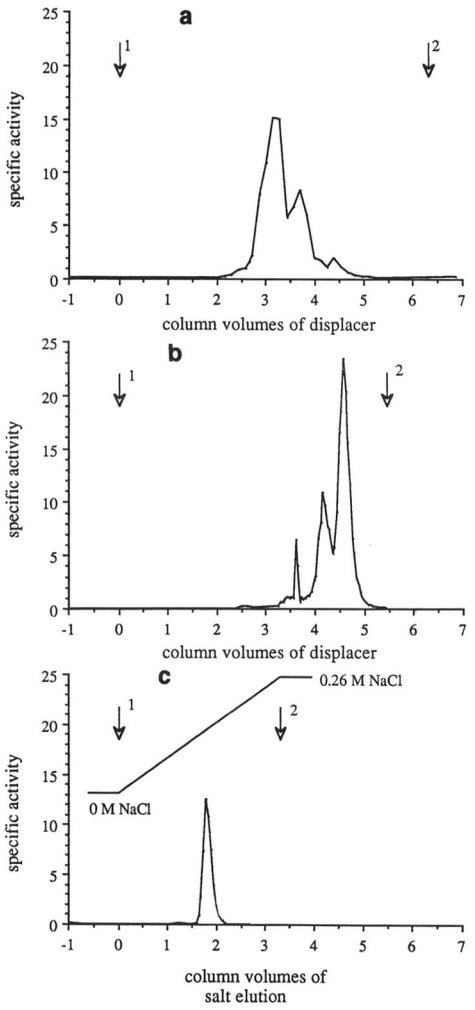

Fig. 8. Specific activity profiles for the following cases: (a) displacement on a 9.0 × 1.0 cm I.D. column; (b) displacement on a 25.0 × 1.0 cm I.D. column; (c) salt elution on a 24.0 × 1.0 cm I.D. column. Arrows 1 and 2 depict the part of the chromatogram where displacement/salt elution was carried out.

CONCLUSIONS

Adsorption chromatography is a widely used and powerful tool for the separation and recovery of proteins and other biomolecules. The mode of recovery has been mostly elution with salt and/or pH gradients in ion-exchange systems and changes in mobile phase composition for reversed-phase separations. Operation in the displacement mode has shown considerable advantages for preparative-scale purification. When applied to complex protein mixtures as presented in this work, there are distinct advantages over conventional ion exchange in terms of purity of product

and overall yields. It is not justified at this stage to generalize for all systems, especially where non-idealities and more fundamental molecular interactions could play an important role, as in most biological systems. The results do, however, agree well with the expectations already established.

ACKNOWLEDGEMENTS

We thank the Swedish National Board for Technical Development (STU) and the Swedish Council for Forestry and Agricultural Research (SJFR) for financial assistance during the course of this work.

REFERENCES

1 G. Viscomi, S. Lande and C. Horváth, *J. Chromatogr.*, 440 (1988) 157.
2 C. Horváth, J. Frenz and Z. El Rassi, *J. Chromatogr.*, 255 (1983) 273.
3 G. Subramanium, M. Phillips and S. W. Cramer, *J. Chromatogr.*, 439 (1988) 341.
4 S. Cramer and C. Horváth, *Prep. Chromatogr.*, 1, No. 1 (1988) 29.
5 S. M. Partridge and R. G. Westfall, *Biochem. J.*, 44 (1949) 418.
6 S. M. Partridge, *Biochem. J.*, 45 (1950) 459.
7 S. M. Partridge, R. C. Brimley and K. W. Pepper, *Biochem. J.*, 46 (1950) 334.
8 S. M. Partridge and R. C. Brimley, *Biochem. J.*, 48 (1951) 338.
9 S. M. Partridge and R. C. Brimley, *Biochem. J.*, 51 (1952) 628.
10 F. Cardinalli, A. Ziggiotti and G. C. Viscomi, *J. Chromatogr.*, 499 (1990) 37.
11 H. Kalasz and C. Horváth, *J. Chromatogr.*, 215 (1981) 295.
12 K. Valko, P. Slégel and J. Bati, *J. Chromatogr.*, 386 (1987) 345.
13 A. R. Torres, B. E. Dunn, S. C. Edberg and E. A. Peterson, *J. Chromatogr.*, 316 (1984) 125.
14 A. W. Liao, Z. El Rassi, D. M. LeMaster and C. Horváth, *Chromatographia*, 24 (1987) 881.
15 B. E. Dunn, S. C. Edberg and A. R. Torres, *Anal. Biochem.*, 168 (1988) 25.
16 A. R. Torres, G.d. G. Krueger and E. A. Peterson, *Anal. Biochem.*, 144 (1985) 469.
17 A. R. Torres and E. A. Peterson, *J. Chromatogr.*, 499 (1990) 47.
18 E. A. Peterson, *Anal. Biochem.*, 90 (1978) 767.
19 A. R. Torres, S. C. Edberg and E. A. Peterson, *J. Chromatogr.*, 389 (1987) 177.
21 A. R. Torres and E. A. Peterson, *J. Biochem. Biophys. Methods*, 1 (1979) 349.
22 M. W. Phillips, G. Subramanium and S. M. Cramer, *J. Chromatogr.*, 454 (1988) 1.
23 C. Horváth, A. Nahum and J. H. Frenz, *J. Chromatogr.*, 218 (1981) 365.

Journal of Chromatography, 547 (1991) 155–160
Elsevier Science Publishers B.V., Amsterdam

CHROM. 23 196

High-performance liquid chromatographic assay of anthranilate synthase from plant cell cultures

CHARLOTTE POULSEN*

*Danisco A/S, Langebrogade 1, 1001 Copenhagen K (Denmark) and *Biotechnology Delft Leiden, Plant Cell Biotechnology Group, Center for Bio-Pharmaceutical Sciences, Division of Pharmacognosy, Leiden University, P.O. Box 9502, 2300 RA Leiden (Netherlands)*

and

Ed. J. M. PENNINGS and ROBERT VERPOORTE

Biotechnology Delft Leiden, Plant Cell Biotechnology Group, Center for Bio-Pharmaceutical Sciences, Division of Pharmacognosy, Leiden University, P.O. Box 9502, 2300 RA Leiden (Netherlands)

(First received November 26th, 1990; revised manuscript received February 8th, 1991)

ABSTRACT

An assay is described for the enzyme anthranilate synthase (E.C. 4.1.3.27) from plant cell cultures, based on the fluorimetric detection of anthranilate after high-performance liquid chromatography on a LiChrosorb RP-8 Select B column. Depletion of the substrate chorismate and the presence of interfering enzymes can be followed by UV measurement. The rate of anthranilate formation was linear for at least 3 h at 30°C. The calibration graph was linear for at least 20 n*M* to 95 μM. Anthranilate synthase was measured in *Catharanthus roseus, Tabernaemontana divaricata, Cinchona robusta, Rubia tinctorum* and *Euonymus europaeus*. The highest specific activity was found in *C. roseus* after induction for indole alkaloid production.

INTRODUCTION

Anthranilate synthase (E.C. 4.1.3.27) catalyses the conversion of chorismate to anthranilate utilizing either glutamine or ammonium as amide donor and Mg^{2+} as cofactor (see Fig. 1). This is the first step in the branching of the shikimate pathway to tryptophan biosynthesis. Tryptophan is a key precursor for the indole alkaloids in plants, among which there are several pharmacologically important compounds [1]. Several studies have indicated that loss of control at the anthranilate synthase step

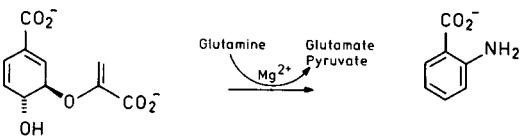

Chorismate Anthranilate

Fig. 1. Reaction scheme of anthranilate synthase.

0021-9673/91/$03.50

can lead to largely unregulated accumulation of tryptophan [2–4]. As part of a programme to study the regulation of the biosynthesis of indole alkaloids, we were interested in a rapid and specific assay for anthranilate synthase. Existing methods measure anthranilate synthase activity fluorimetrically either by following the anthranilate formation directly [5] or after extraction of anthranilate into ethyl acetate from an acidified incubation mixture [5]. These two assays were developed for the bacterial enzyme, but have also been applied to plant enzymes [6–8]. With these assays possible chorismate (substrate) depletion, due to other chorismate–utilizing enzymes, cannot be detected. In crude plant extracts several chorismate–utilizing enzymes are present. We also found that even desalted cell-free plant extracts can cause a considerable background fluorescence in these assays. We therefore developed a high-performance liquid chromatographic (HPLC) assay for anthranilate synthase in which the anthranilate formed is detected by fluorescence and the chorismate decrease can be followed by UV measurement. The product is separated from other fluorescent compounds in the crude extract by reversed-phase chromatography on a column especially selected for basic compounds [9].

EXPERIMENTAL

Chemicals

The inorganic chemicals used were of analytical-reagent grade. Anthranilate and L-glutamine were obtained from Merck (Darmstadt, Germany), leupeptin, phenylmethyl sulphonyl fluoride (PMSF) and pepstatin from Boehringer (Mannheim, Germany) and chorismate (80% pure, barium salt, C1259) and polyvinylpyrrolidone (insoluble form) from Sigma (St. Louis, MO, USA). PD-10 columns were purchased from Pharmacia (Uppsala, Sweden).

High-performance liquid chromatography

The HPLC system consisted of a Model 2248 HPLC pump from LKB (Bromma, Sweden), a Rheodyne Model 7125 injector with a 20-μl loop, a Model 2158 Uvicord SD detector from LKB equipped with an 8-μl flow cell and operating at 280 nm and a Shimadzu (Kyoto, Japan) RF 530 fluorescence detector with a 12-μl flow cell. The excitation wavelength was 340 nm and the emission wavelength 400 nm. All analyses were carried out at room temperature on a 250 mm × 4.0 mm I.D. LiChrosorb RP-8 Select B column (Merck) with a particle size of 7 μm at a flow-rate of 1 ml/min. A guard column (Merck) was always used in combination with the analytical column. The eluent consisted of 50 m*M* H_3PO_4 (final concentration) in water–methanol (65:35, v/v); the pH of the buffer was adjusted to 2.5 with 6 *M* NaOH before addition of methanol. The eluent was filtered through a 0.45-μm nylon (RC 55) filter (Schleicher & Schüll, Dassel, Germany) and finally degassed under vacuum.

Cell cultures

Cell suspension cultures were routinely grown at 25°C on a type G10 gyrotary shaker (New Brunswick Scientific, Edison, NJ, USA) at 120 rpm. Subculturing of *Catharanthus roseus* cells was done every 7 days and of the other cell cultures every 14 days using a five-fold dilution of cells. *C. roseus* cells were grown in LS medium [10] containing 3% sucrose, 2 mg/l 1-napthaleneacetic acid and 0.2 mg/l kinetine. The

induction medium was according to Berlin *et al.* [11]. *Cinchona robusta* cells were grown in B5 medium [12] with 2% sucrose, 2 mg/l (2,4-dichlorophenoxy)acetic acid and 0.2 mg/l kinetine. *Rubia tinctorum* cells were grown in B5 medium [12] with 2% sucrose, 2 mg/ml (2,4-dichlorophenoxy)acetic acid, 0.5 mg/l l-naphthaleneacetic acid, 0.5 mg/l indoleacetic acid and 0.2 mg/l kinetine. *Tabernaemontana divaricata* cells were grown in MS medium [13] with 3% sucrose, 1 mg/l (2,4-dichlorophenoxy)acetic acid and 1 mg/l kinetine. *Euonymus europaeus* cells were grown in MS medium [13] with 3% sucrose, 1 mg/l (2,4-dichlorophenoxy)acetic acid and 0.2 mg/l kinetine.

Enzyme extraction

Cells were harvested by suction, washed once with water and immediately frozen in liquid nitrogen. Cells were stored at −80°C. Liquid nitrogen-frozen cells were homogenized for 1 min at maximum speed in a Waring blender equipped with a stainless-steel bucket. All procedures were carried out at 4°C. To the cell powder, 0.05 g of polyvinylpyrrolidone and 1 ml of extraction buffer [0.1 *M* Tris–HCl (pH 7.5)–10% glycerol–1 m*M* EDTA–1 m*M* dithiothreitol–10 μM leupeptin] were added per gram fresh weight of tissue. After thawing, the homogenate was centrifuged at 10 000 *g* for 30 min. The supernatant was always desalted on Sephadex G-25 (Pharmacia PD-10 columns) equilibrated with 0.1 *M* Tris–HCl (pH 7.5). The non-desalted homogenate could be stored at −80°C without loss of enzyme activity for at least 3 months. Protein was determined according to Peterson [14].

Assay of anthranilate synthase

The incubation mixture (total volume 0.5 ml) contained 0.1 *M* Tris–HCl (pH 7.5), 1 m*M* barium chorismate, 20 m*M* L-glutamine, 10 m*M* $MgCl_2$ and 250 μl of desalted enzyme preparation. The incubation was started by addition of chorismate. After incubation for 1 h at 30°C, the reaction was stopped by the addition of 125 μl of 1 *M* H_3PO_4. Blanks were made by adding H_3PO_4 before the incubation. After centrifugation, the samples were analysed by HPLC as described above. The injection volume was 20 μl. The detector attenuation on the fluorescence detector was set according to the amount of enzyme activity in the incubation mixture.

RESULTS AND DISCUSSION

A representative chromatogram obtained with enzyme from *C. roseus* is shown in Fig. 2. The minimum detectable amount of anthranilate, defined as three times the value of the baseline noise, was 0.05 ng. The separation shown in Fig. 2 was achieved on a 3-year-old column, which had been used for multiple purposes, but the requirements on the column are very small with this assay. We always use a guard column in combination with the analytical column, and this guard column has to be replaced regularly when the HPLC system is used to determine anthranilate synthase in crude plants extracts. In the system described here, chorismate and isochorismate are well separated with retention times of 4.8 and 3.5 min, respectively (UV detection, chromatogram not shown). We have therefore also applied this HPLC system to determinations of isochorismate synthase (E.C. 5.4.99.6) [15]. A methanol concentration of 35% is the optimum, owing to strongly adsorbed compounds which elute at higher methanol concentrations.

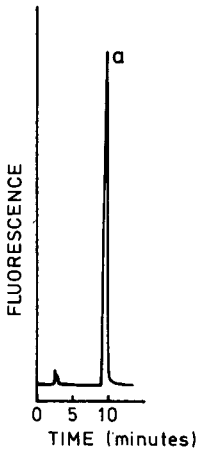

Fig. 2. Determination of anthranilate synthase activity by HPLC. Anthranilate (a) was separated on a LiChrosorb RP-8 Select B column, as described under Experimental. The fluorescence detector was set at high sensitivity, the attenuation was 32 and the injection volume was 20 μl.

The retention of anthranilate on a LiChrosorb RP-Select B column was found to be independent of salt concentration. However, the pH of the eluent has a very strong effect on the retention time of both anthranilate and chorismate. The retention time of anthranilate increased with increasing pH, whereas the retention time of chorismate decreased. For the assay pH 2.5 was found to be optimum. Blanks contain small amounts of anthranilate, which originates solely from the substrate barium chorismate. It is possible to eliminate this blank by using the purer, free acid of chorismate (Sigma, C1761). It is no problem, however, to correct for the blank.

An advantage of the HPLC assay described here is that it is linear over a much larger product concentration than the spectrofluorimetric assay in which anthranilate is extracted into ethyl acetate. The calibration graph is linear at least from 0.4 pmol to 1.9 nmol of anthranilate per 20-μl injection volume which corresponds to linearity from 20 nM to 95 μM.

In all the plant cell cultures it was impossible to measure anthranilate synthase in a non-desalted cell-free extract. Desalting is not a prerequisite for the HPLC method as such; anthranilate synthase is simply not active in our non-desalted crude extracts. This is probably due to the presence of tryptophan [7], a potent inhibitor of anthranilate synthase.

A major advantage of the present HPLC method is that both the formation of the product anthranilate and the disappearance of the substrate chorismate can be followed. In assays of partially purified anthranilate synthase preparations, the amount of anthranilate formed can be directly correlated with the amount of chorismate reacted. However, in crude enzyme preparations several chorismate-utilizing enzymes are present. We were unable, for instance, to measure anthranilate synthase in *C. robusta* suspension cells elicited for anthraquinone production (elicited with autoclaved and freeze-dried *Phytophthora cinnamomi*, 0.5 mg/ml, the cells being harvested after overnight culture). By injection into the HPLC system from an incuba-

tion mixture it was obvious that the chorismate was used up within the first 5 min; this proved to be caused by a very high chorismate mutase (E.C. 5.4.99.5) activity, making it impossible to measure anthranilate synthase in elicited *C. robusta*. Chorismate mutase has only chorismate as substrate and has no cofactor requirements.

The crude anthranilate synthase enzyme was very unstable; the enzyme lost 25% of its activity in 3.5 h when kept on ice in Tris–HCl buffer without additives. The stability was increased substantially when protease inhibitors and glycerol were added. The rate of anthranilate formation was linear for at least 3 h as measured with the *C. roseus* enzyme, when using enzyme that had been desalted on a PD-10 column equilibrated with extraction buffer plus 0.2 m*M* PMSF and 1 μM pepstatin.

In Table I the specific activity of anthranilate synthase is shown in different cell cultures harvested in the exponential and stationary phase, respectively. It is remarkable that the anthranilate synthase activity in desalted *T. divaricata* preparations was so low, as this is an indole alkaloid-producing cell line. In order to determine if the *T. divaricata* cell-free extracts contained an inhibitor of anthranilate synthase, we tried to mix *C. roseus* and *T. divaricata* cell-free extracts. This experiment showed that the desalted *T. divaricata* cell-free extracts were not inhibitory for the *C. roseus* enzyme. It was possible to increase the specific activity of anthranilate synthase in *T. divaricata* by further adding pepstatin and PMSF as protease inhibitors. Probably the *in vivo* activity of anthranilate synthase in *T. divaricata* is higher. Work to elucidate this is in progress. Interestingly, a slight induction of anthranilate synthase in *C. roseus* was found (Table I) after induction for production of indole alkaloids. It is well known that tryptophan decarboxylase (E. C. 4.1.1.28) is induced upon induction of *C. roseus* for indole alkaloid production [16]. However this is, as far as we know, the first time that plant anthranilate synthase has been reported to be induced after transfer to production medium for indole alkaloids. The enzyme level found in *R. tinctorum* and

TABLE I

SPECIFIC ACTIVITY OF ANTHRANILATE SYNTHASE IN DIFFERENT CELL CULTURES

Cell culture	Age of culture (days)	Anthranilate synthase (pkatal/mg protein)[b]
Catharanthus roseus	2	5.3
	4	5.3
	7	5.0
	3[a]	5.4
	6[a]	7.1
Tabernaemontana divaricata	6	0.1
	14	0.1
Cinchona robusta	5	1.1
	12	1.3
Rubia tinctorum	5	1.7
	12	0.7
Euonymus europaeus	7	1.5
	14	3.0

[a] The cells were induced by subculture to induction media.

[b] Values are averages for duplicate samples; pkatal = pmol anthranilate formed per second.

E. europaeus, two non-indole alkaloid-producing cell lines, probably represents the enzyme level necessary for sustaining the cell culture with tryptophan for protein synthesis.

In conclusion, a reliable HPLC assay has been developed for anthranilate synthase from both crude and purified enzyme preparations. No extraction into organic solvents is needed and the assay is linear over a wide range. A major advantage is that substrate depletion and the presence of interfering enzymes using chorismate as substrate can easily be detected when both fluorescence and UV detection are used.

ACKNOWLEDGEMENTS

We thank Mr. A. G. M. Goosen and K. W. Weisz for expert assistance with the cell cultures. We are also grateful to Professor M. H. Zenk (Münich) for donating the *Rubia* cell culture.

REFERENCES

1 R. B. Herbert, *The Biosynthesis of Secondary Metabolites*, Chapman and Hall, London, 1989.
2 J. M. Widholm, *Biochim. Biophys. Acta*, 279 (1972) 48.
3 J. M. Widholm, *Biochim. Biophys. Acta*, 261 (1972) 52.
4 J. M. Widholm, *Physiol. Plant.*, 30 (1974) 13.
5 M. I. Gibson and F. Gibson, *Biochem. J.*, 90 (1964) 248.
6 W. L. Belser, J. Baron Murphy, D. P. Delmer and S. E. Mills, *Biochim. Biophys. Acta*, 237 (1971) 1.
7 J. M. Widholm, *Physiol. Plant.*, 25 (1971) 75.
8 C. N. Hankins, M. T. Largen and S. E. Mills, *Plant Physiol.*, 57 (1976) 101.
9 *RP-Select B, Data Sheet*, E. Merck, Darmstadt, 1985.
10 E. M. Linsmaier and F. Skoog, *Physiol. Plant.*, 18 (1965) 100.
11 J. Berlin, E. Forche, V. Wray, J. Hammer and W. Hösel, *Z. Naturforsch. C* , 38 (1983) 346.
12 O. L. Gamborg, R. A. Miller and K. Ojima, *Exp. Cell Res.*, 50 (1968) 151.
13 T. Murashige and F. Skoog, *Physiol. Plant.*, 15 (1962) 473.
14 G. L. Peterson, *Anal. Biochem.* 83 (1977) 346.
15 C. Poulsen, R. van der Heijden and R. Verpoorte, *Phytochemistry*, in press.
16 K.-H. Knobloch, B. Hansen and J. Berlin, *Z. Naturforsch. C*, 36 (1981) 40.

Journal of Chromatography, 547 (1991) 161–166
Elsevier Science Publishers B.V., Amsterdam

CHROM. 23 249

Relationship between retention parameters in reversed-phase high-performance liquid chromatography and antitumour activity of some pyrimidine bases and nucleosides

S. V. GALUSHKO* and I. P. SHISHKINA
Institute of Bioorganic Chemistry, Academy of Sciences of the Ukrainian SSR, 252660 Kiev 94 (USSR)
and
I. V. ALEKSEEVA
Institute of Molecular Biology and Genetics, Academy of Sciences of the Ukrainian SSR, Kiev (USSR)
(First received September 7th, 1989; revised manuscript received February 27th, 1991)

ABSTRACT

The relationship between retention parameters on octadecyl stationary phases of some pyrimidine bases and nucleosides and their antitumour activity was studied. The differences between the free energy of sorption and hydrophobic contact area of the natural compounds and their synthetic analogues can be used as sensitive parameters correlated with the potential activity of the compounds.

INTRODUCTION

The relationship between the hydrophobic properties of a substance and its biological activity has long been established. The correlations between the activity and the distribution coefficients of a substance in an octanol–water system are widely used [1–4]. An octanol–water system can be regarded as a model of a biomembrane–water system. However, this model is only a coarse approximation. The isotropic liquid octanol differs appreciable from an anisotropic biomembrane. The stationary phase in reversed-phase high-performance liquid chromatography (RP-HPLC) also has a strongly anisotropic character and there is a great similarity between the mobile phase–stationary phase surface and the membrane–water surface [2]. Hence a chromatographic system consisting of water and a hydrocarbon layer bonded to a hydrophilic matrix may serve as a more suitable model of a membrane than an octanol–water system. Moreover, the parameters of interaction with the surface of an RP sorbent can produce additional information on the physico-chemical properties of substances that are difficult to study in an octanol–water system. These include many pyrimidine bases and nucleosides, which are highly polar compounds containing ionogenic groups of acidic and basic character. The aim of this work was to compare the parameters of the interactions of some compounds with an octadecyl sorbent surface and their antitumour activity.

0021-9673/91/$03.50

EXPERIMENTAL

Chromatographic conditions

The experiments were performed on an LKB (Bromma, Sweden) liquid chromatographic system consisting of a Model 2151 variable-wavelength monitor, two Model 2150 HPLC pumps, a Model 2152 LC controller, a Model 2154 injector and a Model 2220 recording integrator. The columns used were a Separon SIX C_{18} (5 μm) glass column (150 × 3.3 mm I.D.) (Laboratorní Přistroje, Prague, Czechoslovakia), a Silasorb C_{18} (10 μm) column (100 × 1.0 mm I.D.) (LaChema, Brno, Czechoslovakia) (these sorbents with a silica gel matrix) and an octadecyl polyol Si 100 (5 μm) stainless-steel column (250 × 4.6 mm I.D.) (Serva, Heidelberg, Germany) with a propylglycerol matrix. The mobile phases were 0–60% water–methanol mixtures for compounds **II–IX** (Fig. 1) or 0.1 *M* phosphate buffer–0.1–1.0 *M* ammonium sulphate for the other compounds at a flow-rate 0.01 ml/min (column of 1 mm I.D.) or 0.5 ml/min (other columns).

Materials

Compound names are abbreviated as in Fig. 1. 6-AzaCyd and its derivatives were obtained from the Institute of Molecular Biology and Genetics of the Ukrainian SSR Academy of Sciences, 5-AzaCyd, Ara-C and Ara-U from Chemical Dynamic (Sourth Plainfield, NY, USA) and other bases and nucleosides from Reakhim, (Moscow, USSR). Orthophosphoric acid, methanol and ammonium sulphate were obtained commercially (analytical-reagent grade) and were used without further purification. Water was doubly distilled and filtered for HPLC use.

RESULTS AND DISCUSSION

We studied 16 synthesized analogues of pyrimidine bases and nucleosides: N-4- and O′-substituted 6-azacytidine (Fig. 1), 6-azauridine (6-AzaUrd), 6-azauracil (6-AzaUra), 6-azathymine (6-AzaThy), 6-azacytosine (6-AzaCyt), 5-azacytidine (5-

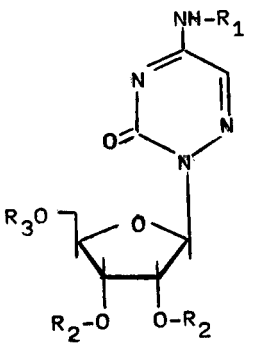

Fig. 1. 6-AzaCyd and its derivatives. **I**, $R_1 = R_2 = R_3 = H$(6-AzaCyd); **II**, $R_1 = C_6H_5COOH$, $R_2 = R_3 = H$; **III**, $R_1 = C_6H_5COOCH_3$, $R_2 = R_3 = H$; **IV**, $R_1 = C_6H_5$, $R_2 = R_3 = H$; **V**, $R_1 = CH_2C_6H_5$, $R_2 = R_3 = H$; **VI**, $R_1 = R_2 = H$, $R_3 = COC_6H_5$; **VII**, $R_1 = H$, $R_2 = R_3 = COC_6H_5$; **VIII**, $R_1 = CH_2CONH_2$, $R_2 = H$, $R_3 = COC_6H_5$; **IX**, $R_1 = (CH_2)OH$, $R_2 = R_3 = COC_6H_5$; **X**, $R_1 = CH_2CONH_2$, $R_2 = R_3 = H$ (Gl).

AzaCyd), 5-fluorouracil (F-Ura), cytosine arabinoside (Ara-C) and uracil arabinoside (Ara-U).

The synthetic analogues studied can be classified in terms of their antitumour activity in three groups: a highly active group (Ara-C, F-Ura and 5-AzaCyd [5–8]), a moderately active group (6-AzaCyd, 6-AzaUrd, Ara-U [9–11] and Gl) and an inactive group (**II–IX**). The following parameters were used: the hydrophobic contact area, the change in free sorption energy and ionization constants. Previously we studied the parameters of some compounds on a Silasorb C_{18} [12,13] and on octadecyl polyol Si 100 [14] sorbents.

All the compounds used are ampholytes. The values of the constants that characterize their acid–base properties are given in Table I (taken from ref. 12).

The changes in the acid–base properties of the compounds considerably affect their retention by a hydrophobic sorbent. The sharp decrease in the capacity factor on transition of the compounds from a molecular to an ionized form is observed for 5- and 6-aza derivatives at a much lower pH than for the unmodified compounds (Fig. 1 in ref. 12).

To compare the interactions of bases and nucleosides with a hydrophobic surface, we determined the values of the change in the area of contact with a hydrophobic surface $\Delta(\Delta\Phi)$ and the change in the free energy of sorption on this surface $\Delta(\Delta G)$ on going from synthetic analogues to natural bases and nucleosides.

The values of $\Delta(\Delta G)$ were determined as $-RT \ln \alpha$ [separation factor $\alpha = k'_1/k'_2$, where k'_1 and k'_2 are the capacity factors for compounds 1 and 2, respectively (Table I), R is the molar gas constant and T is the temperature] in an eluent containing no methanol.

It is useful to introduce two values of $\Delta(\Delta G)$: $\Delta(\Delta G)_1$ for molecular forms and $\Delta(\Delta G)_2$ for physiological pH (7.0–7.5). To determine $\Delta(\Delta G)_1$, we measured k' for pH values of MP that correspond to deriving compounds in the molecular form (pH 7 for

TABLE I

PARAMETERS OF THE COMPOUND–SORBENT SURFACE CONTACT

Compound		$\Delta(\Delta\Phi)$		$-\Delta(\Delta G)_1$ (kJ/mol)	$-\Delta(\Delta G)_2$ (kJ/mol)
1	2	Å^2	%		
Ura	6-AzaUra	13	40	0.1	3.3
Cyt	6-AzaCyt	12	52	0.5	
Thy	6-AzaThy	6	8	1.1	2.3
Ura	F-Ura	− 6	8	−0.35	
Cyd	6-AzaCyd	16	21	2.1	
Urd	6-AzaUrd	23	27	2.2	4.2
Cyd	5-AzaCyd	8	10	0.7	
Cyd	Ara-C	− 5	7	−0.9	
Urd	Ara-U	− 10	12	−1.5	
Cyd	Gl	− 15	19	−1.2	
Cyd	**II**	− 80	103	−3.4	
Cyd	**III–IX**[a]	>100	>130[a]	−4 to −15[a]	

[a] The compounds having the $\Delta(\Delta\Phi)a$ values exceeding 100% compared with Cyd (**III–IX**) are combined in one group.

Cyt, Cyd and their derivatives; pH 3 for Ura, Urd and their derivatives). The value of $\Delta(\Delta\Phi) = \Delta\Phi_1 - \Delta\Phi_2$ for compounds 1 and 2 can easily be calculated by using the dependence of ln α on the surface tension of MP. For uncharged compounds in eluents that contain no organic solvents, solvophobic theory gives the following relationship [15,16]:

$$\ln \alpha = \frac{N\Delta(\Delta\Phi)\gamma}{RT} + \text{constant} \tag{1}$$

where N is Avogadro's number and γ is the surface tension. The surface tension of an inorganic salt solution in water is, to a good approximation, a linear function of the salt concentration and can be expressed by $\gamma = \gamma_0 + rm$, where m is the molal salt concentration, r is a coefficient that depends of the nature of the salt [$r = 2.17$ for $(NH_4)_2SO_4$] and γ_0 is the surface tension of pure water ($\gamma_0 = 72.0$ dyn/cm). By finding the dependence ln α = f(m) we obtained the values of $\Delta(\Delta\Phi)$ for pairs of natural compounds, their unsubstituted derivatives and Gl (**X**) (Table I).

A different situation is observed for compounds **II–IX**. To elute these substances, it is necessary to use methanol-containing eluents. Then, according to [15,16], we have

$$\ln \alpha = \frac{N\Delta(\Delta\Phi)\gamma}{RT} + \Delta(\Delta G)_{\text{e.s.}} + \Delta(\Delta G)_{\text{vdW}} + \text{constant} \tag{2}$$

where $\Delta(\Delta G)_{\text{e.s.}}$ and $\Delta(\Delta G)_{\text{vdW}}$ are the changes in the free energy of electrostatic and Van der Waals interaction with MP, respectively. As shown by Horváth *et al.* [15,16], the electrostatic interactions of uncharged molecules with MP, with the methanol content in MP changing slightly, are virtually constant. For the compounds studied (**II–IX**), a linear ln k' = f(γ) dependence is observed [14]. This enables us to conclude that for the compounds studied the term $\Delta(\Delta G)_{\text{vdW}}$ either changes slightly with changing methanol content in the mobile phase, or varies linearly with the surface tension of the mobile phase. In the latter instance we have

$$\ln \alpha = \frac{N\Delta(\Delta\Phi)\gamma a}{RT} + \text{constant} \tag{3}$$

where a is a factor allowing for the change in the term $\Delta(\Delta G)_{\text{vdW}}$. Thus, in this instance also, the value of $\Delta(\Delta\Phi)a$ can be used to find correlations. The values of $\Delta(\Delta\Phi)$ and $\Delta(\Delta G)$ are given in Table I. It can be seen that for the compounds studied there is some correlation between the values of $\Delta(\Delta\Phi)$ and $\Delta(\Delta G)$, indicating a considerable contribution from the cavity term to the selectivity of separation of the compounds studied.

From the results, the compounds can be divided into three groups. The first group includes F-Ura, 5-AzaCyd, Ara-C, Ara-U and 6-AzaThy, for which the differences in the area of hydrophobic contact of their molecules with a surface are minimal in comparison with the natural analogues. The differences for these compounds are not more than 10% compared with the natural analogues.

The second group is characterized by moderate deviation (20–25%). The third group, which is the largest, includes compounds that exhibit a 40–50% higher deviation from the value of hydrophobic contact area for the natural analogues. It should be noted that the compounds displaying a large deviation in the values of $\Delta(\Delta\Phi)$ do not show antitumour activity. On the other hand, all compounds showing high antitumuour activity belong to the first group, characterized by low values of $\Delta(\Delta\Phi)$. Moderately active compounds belong to the second group. If we consider the relative changes in the free energy of sorption, $\Delta(\Delta G)$, we can see that this value as a rule does not exceed ± 1.0 kJ/mol for highly active nucleosides; it is $\pm(1.5–2.2)$ kJ/mol for moderately active compounds and more than ± 3.0 kJ/mol for inactive compounds.

For bases, the values of $\Delta(\Delta G)_1$ are small for the molecular forms of 6-AzaThy and 6-AzaUra (pH 2–5) and they rise sharply as a result of their ionization at pH 6.5–7.5, reaching values of 2.1–3.3 kJ/mol. Thus, as distinct from their natural analogues, 6-AzaThy, 6-AzaUra and 6-AzaUrd are characterized by a high degree ionization under physiological pH, so that it is energetically disadvantageous for them to penetrate into a weakly polar medium. Highly active F-Ura has minimal values for both $\Delta(\Delta G)$ and $\Delta(\Delta\Phi)$.

We can therefore conclude that the differences between the hydrophobic contact areas of a natural pyrimidine compound and its synthetic analogues $\Delta(\Delta\Phi)$ is a sensitive parameter correlated with the potential activity of the compounds. A useful parameter for this purpose is also $\Delta(\Delta G)$. We consider it most promising to search for active compounds among analogues of natural substances that have simultaneously the following characteristics; (1) the difference in the areas of contact with a hydrophobic surface do not exceed 20%; (2) the change in the free energy of sorption on transition from the natural compound to a potential inhibitor or an antagonist does not exceed $\pm 1.5–2.5$ kJ/mol in water at pH 7.0–7.5; and (3) the pK is such that under physiological pH the ionization state of the synthetic analogues is not different from that of the natural compound.

It should be noted that parameters such as $\Delta(\Delta\Phi)$, $\Delta(\Delta G)$ and pK are relatively easy to determine.

REFERENCES

1 H. Fruhbeis, R. Klein and H. Wallmeier, *Angew. Chem.*, 99 (1987) 417.
2 T. Braunmann, *J. Chromatogr.*, 373 (1986) 191.
3 C. Hansch and F. Lee, *Substituent Constants for Correlation Analysis in Chemistry and Biology*, Wiley, New York, 1979.
4 J. Balsani, M. Cools and E. De Clercq, *Biochem. Biophys. Res. Commun.*, 158 (1989) 413.
5 J. Burchenal, in J. Burchenal and H. Oettgen (Editors), *Cancer Achievements, Challenges, and Prospects for the 1980s*, Grune and Stratton, New York, 1981, p. 249.
6 J. Burchenal, *et al.*, in J. Rideont, D. Henry and L. Beacham, III (Editors), *Nucleoside Analogues, Chemistry, Biology and Medical Application, Proceedings of the 5th International Round Table*, Academic Press, New York, 1983, p. 48.
7 J. Beranek and E. Acton, *Collect. Czech. Chem. Commun.*, 49 (1984) 2551.
8 A. Cihak, *Eur. J. Cancer*, 14 (1978) 117.
9 W. Prusoff and P. Fisher, in P. Walker *et al.* (Editors), *Nucleoside Analogues, Chemistry, Biology and Medical Application*, Plenum Press, New York, 1979, p. 281.
10 N. Petrusha, *Farmakol. Toxikol.*, 2 (1987) 75.
11 W. Muller and P. Zahn, *Cancer Res.*, 39 (1979) 1102.
12 S. V. Galushko, I. P. Shishkina and A. T. Pilipenko, *J. Chromatogr.*, 445 (1988) 59.

13 S. V. Galushko, I. P. Shishkina and A. T. Pilipenko, *Zh. Anal. Khim.*, 43 (1987) 1684.
14 S. V. Galushko, I. P. Shishkina and I. V. Alekseeva, *Zh. Anal. Khim.*, 45 (1990) 1684.
15 Cs. Horváth, W. Melander and I. Molnár, *J. Chromatogr.*, 125 (1976) 129.
16 Cs. Horváth, W. Melander and I. Molnár, *Anal. Chem.*, 49 (1977) 142.

Journal of Chromatography, 547 (1991) 167–173
Elsevier Science Publishers B.V., Amsterdam

CHROM. 23 181

Reversed-phase high-performance liquid chromatographic study of the lipophilicity of a series of analogues of the antibiotic "calvatic acid"

ROSELLA CALVINO, ROBERTA FRUTTERO and ALBERTO GASCO*
Dipartimento di Scienza e Tecnologia del Farmaco, Corso Raffaello 31, 10125 Turin (Italy)
(First received October 18th, 1990; revised manuscript received February 6th, 1991)

ABSTRACT

The lipophilicity of a series of *para*- and *meta*-substituted phenyl-ONN-azoxycyanides, analogues of the antibiotic 'calvatic acid', was studied by reversed-phase high-performance liquid chromatography using methanol–water or acetonitrile–water as the mobile phase and a LiChrospher 100 RP-18 column. An excellent linear relationship between the logarithm of the capacity factors ($\log k'$) for each compound and the volume fraction of the organic modifier (φ) was found. The extrapolation of $\log k'$ to $\varphi = 0$ gives $\log k_w$ for every compound. From these values τ_w constants were calculated for each substituent. Good correlations were found between $\log k_w$ and $\log P_{oct/H_2O}$ and between τ_w and Hansch's π hydrophobic parameter.

INTRODUCTION

The cyano-NNO-azoxy group (ONN-azoxycyanide group) is an interesting function present in "calvatic acid" (**1**), an antibiotic produced by some Basidiomycetes [1,2]. This moiety is responsible for the antimicrobial properties of the antibiotic [3,4].

The ability of **1** to inhibit [^{3}H]colchicine binding to rat liver soluble tubulin [2] prompted us to prepare and test for their potential antitumour properties several new derivatives bearing the cyano-NNO-azoxy group linked to different vectors [5].

In recent work we showed that the electronic and hydrophobic constants of this function are similar to those of the nitro group [6]. In this paper, in order to complete the physico-chemical characterization of the –N(O)=NCN group, we report the results of an investigation in which the aryl-ONN-azoxycyanides **2–19** and **24** and the heteroaryl-ONN-azoxycyanides **20–23**, **25** and **26** were studied by reversed-phase high-performance liquid chromatography (RP-HPLC).

EXPERIMENTAL

Azoxycyanide derivatives **2–26** (Fig. 1) were synthesized and purified according to methods reported previously [5,6]. Methanol and acetonitrile were of analytical-reagent grade. The partition coefficients of the derivatives **20–26** were obtained using the shake-flask method at room temperature using octanol as lipid phase and water as

0021-9673/91/$03.50

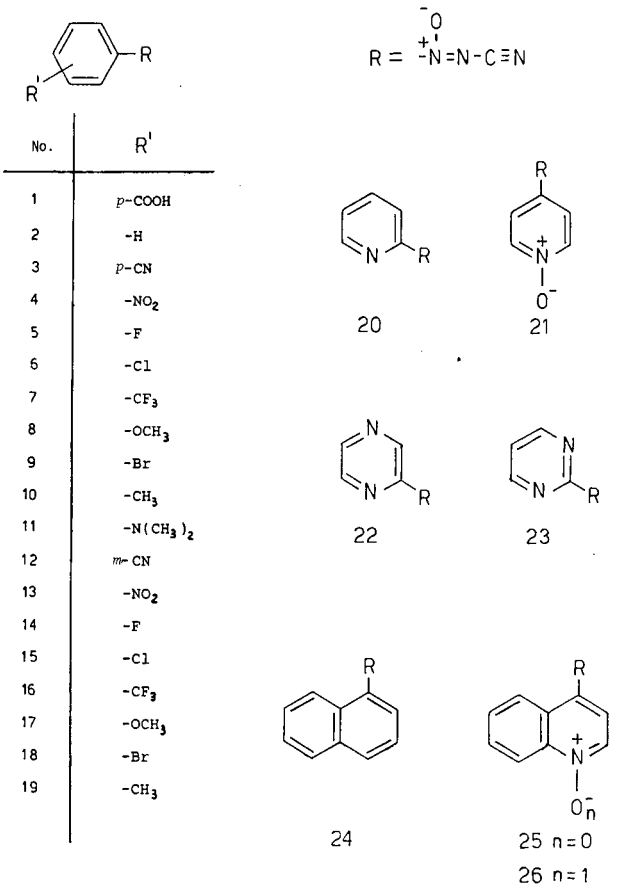

Fig. 1. Formulae of compounds **1–26**.

hydrophilic phase. Each tabulated log P value is the average of four determinations made with different concentrations of solute (10^{-3}–10^{-4} M) (Tables I and II). No concentration dependence of the partition coefficients was observed. Owing to the low pK_a of compound **11**, no correction for partial ionization was taken into account.

Linear regression analyses were performed by the usual procedure on a IBM AT personal computer. Standard errors of the slope and intercept are reported in parentheses.

Chromatographic procedure

RP-HPLC experiments were performed on a Perkin-Elmer Series 2B liquid chromatograph equipped with a Perkin-Elmer LC75 variable-wavelength detector and a Rheodyne Model 7105 injection valve. A Perkin-Elmer LCI 100 integrator was used. A LiChrospher 100 RP-18 (10 μm) column (250 × 4.0 mm I.D.) (Merck) was employed.

Methanol–water or acetonitrile–water mixtures at various compositions (φ) were used as mobile phases.

The samples were dissolved in acetonitrile at concentrations suitable for UV detection and 1–5 μl of solution were injected into the chromatographic column. Each chromatographic run was repeated at least three times. Measurements of the retention times (t_R) were taken at room temperature.

The flow-rate was 1.5 ml/min and the column dead time (t_0) was determined according to the Knox and Kaliszan method [7]. From the solute retention time t_R, the logarithm of the capacity factor, log k', was calculated by the equation

$$\log k' = \log\left(\frac{t_R - t_0}{t_0}\right) \tag{1}$$

RESULTS AND DISCUSSION

Retention parameters

Generally, the dependence of log k' on mobile phase composition is complex [8]. By using methanol–water mixtures as mobile phases and working with non-ionized solutes, the linear relationship between log k' and the volume fraction of organic modifier

$$\log k' = \log k_w - a\varphi \tag{2}$$

where k_w is the capacity factor for pure water as a mobile phase and a is a constant, holds over the range $10 \leqslant \varphi \leqslant 80$ [9].

Log k' values for *meta*- and *para*-substituted phenyl-ONN-azoxycyanide and heteroaryl-ONN-azoxycyanide derivatives **2–26** measured at various methanol–water ratios (φ_M) are reported in Table I. The values in Table I show for each compound an excellent linear relationship with the φ_M values (see Table III) over the whole volume fraction range considered according to eqn. 2. From these correlations it was possible to extrapolate for each derivative the corresponding log $k_{w(M)}$ value.

Similar results were obtained using acetonitrile–water mixtures ($20 \leqslant \varphi \leqslant 80$) as the mobile phase (see Tables II and III). As an example, Fig. 2 shows the plot of log k' *vs.* volume fraction for both methanol and acetonitrile for compound **5**. For this series of derivatives, the log $k_{w(M)}$ values are always greater than the corresponding log $k_{w(A)}$ values. Log $k_{w(M)}$ is correlated with log $k_{w(A)}$ according to the equation

$$\log k_{w(M)} = -0.16(\pm 0.11) + 1.28(\pm 0.05)\log k_{w(A)} \tag{3}$$

$$n = 25;\ s = 0.160;\ r = 0.980$$

Relationship between capacity factors and partition coefficients

Log k' values at various methanol–water and acetonitrile–water compositions correlate very well with log P values measured in the reference system *n*-octanol–water. The correlation coefficient r and the standard deviation s were spread over the ranges $r = 0.969$–0.996, $s = 0.234$–0.080 for the methanol–water system and $r = 0.962$–0.988, $s = 0.227$–0.112 for the acetonitrile–water system.

Log $k_{w(M)}$ and log $k_{w(A)}$ are strongly correlated to log P by means of the

TABLE I

LOG k' VALUES WITH METHANOL–WATER MOBILE PHASES

Compound	Volume fraction of organic modifier, $\varphi_{(M)}$							
	0.10	0.20	0.30	0.40	0.50	0.60	0.70	0.80
2		1.74	1.44	1.13	0.75	0.42	0.13	−0.22
3	1.78	1.33	0.98	0.65	0.29	−0.04	−0.32	−0.71
4		1.44	1.11	0.82	0.46	0.13	−0.15	−0.52
5		1.66	1.35	1.05	0.69	0.34	0.05	−0.33
6			1.74	1.40	0.97	0.60	0.29	−0.10
7			1.86	1.49	1.06	0.68	0.24	−0.18
8			1.74	1.40	0.97	0.57	0.26	−0.11
9			1.86	1.50	1.08	0.67	0.35	−0.06
10			1.87	1.52	1.08	0.68	0.36	−0.04
11				1.68	1.11	0.69	0.37	−0.02
12	1.86	1.36	1.00	0.65	0.33	0.01	−0.27	−0.62
13		1.52	1.19	0.91	0.56	0.23	−0.07	−0.42
14		1.74	1.42	1.14	0.78	0.43	0.13	−0.23
15			1.79	1.48	1.06	0.69	0.35	−0.02
16			1.89	1.54	1.10	0.67	0.30	−0.13
17			1.75	1.43	1.00	0.61	0.28	−0.07
18			1.92	1.58	1.15	0.75	0.40	0.02
19			1.87	1.53	1.09	0.69	0.36	−0.02
20	1.30	0.89	0.57	0.29	0.02	−0.22	−0.44	−0.70
21	0.58	0.19	−0.11	−0.36	−0.66	−0.77	−1.01	−1.44
22	0.76	0.42	0.16	−0.06	−0.27	−0.44	−0.66	−0.94
23	0.63	0.31	0.06	−0.16	−0.35	−0.52	−0.71	−0.98
24				1.83	1.33	0.86	0.48	0.06
25			1.66	1.31	0.82	0.43	0.11	−0.24
26		1.52	1.08	0.77	0.34	0.02	−0.24	−0.55

Collander-type equations

$$\log P = -1.07(\pm 0.10) + 1.16(\pm 0.04)\log k_{w(M)} \quad (4)$$

$$n = 25;\ s = 0.146;\ r = 0.988$$

and

$$\log P = -2.06(\pm 0.33) + 1.82(\pm 0.14)\log k_{w(A)} \quad (5)$$

$$n = 25;\ s = 0.150;\ r = 0.952$$

Group contribution to hydrophobicity

From the log k_w values reported in Table III, it is possible to calculate the hydrophobic constants τ_w [10] (see Table IV) according to the equation

$$\tau_w = \log(k_{wj}/k_w) \quad (6)$$

TABLE II

LOG k' VALUES WITH ACETONITRILE–WATER MOBILE PHASES

Compound	Volume fraction of organic modifier, $\varphi_{(A)}$							
	0.10	0.20	0.30	0.40	0.50	0.60	0.70	0.80
2		1.47	1.07	0.72	0.39	0.10	−0.16	−0.42
3	1.63	1.23	0.88	0.56	0.24	−0.07	−0.34	−0.67
4		1.40	1.03	0.69	0.35	0.03	−0.26	−0.59
5		1.45	1.08	0.73	0.40	0.10	−0.17	−0.46
6		1.83	1.39	0.97	0.61	0.28	0.01	−0.28
7			1.58	1.11	0.68	0.32	0.01	−0.31
8		1.75	1.25	0.83	0.47	0.16	−0.10	−0.38
9			1.48	1.06	0.66	0.33	0.05	−0.23
10		1.89	1.39	0.98	0.59	0.28	0.01	−0.26
11		1.91	1.34	0.87	0.50	0.20	−0.06	−0.32
12	1.59	1.23	0.85	0.52	0.22	−0.09	−0.37	−0.66
13		1.44	1.02	0.66	0.34	0.02	−0.27	−0.57
14		1.54	1.12	0.75	0.43	0.12	−0.15	−0.42
15		1.90	1.41	0.98	0.62	0.29	0.02	−0.24
16			1.55	1.07	0.67	0.31		−0.30
17		1.80	1.28	0.87	0.52	0.20	−0.07	−0.34
18			1.50	1.04	0.67	0.34	0.06	−0.20
19		1.90	1.40	0.97	0.61	0.29	0.02	−0.24
20	0.95	0.61	0.33	0.10	−0.13	−0.36	−0.59	−0.81
21	0.41	0.06	−0.24	−0.48	−0.72	−0.98	−1.26	−1.43
22	0.62	0.37	0.15	−0.05	−0.26	−0.47	−0.71	−0.96
23	0.49	0.24	0.02	−0.17	−0.37	−0.58	−0.83	−1.07
24			1.72	1.19	0.76	0.41	0.11	−0.16
25		1.61	1.09	0.68	0.35	0.08	−0.17	−0.39
26	1.64	1.07	0.63	0.27	−0.01	−0.25	−0.50	−0.69

where k_w is the capacity factor for 100% water eluent of the parent azoxycyanide **2** and k_{wj} is that of substituted compound j.

As the methanol–water mobile phase is the best HPLC reference system for determining hydrophobic parameters [11], we investigated correlations between $\tau_{w(M)}$ and $\pi_{N(O)=NCN}$ derived from the phenylazoxycyanide system [6] according to the equation

$$\tau_{w(M)} = 0.13(\pm 0.03) + 0.85(\pm 0.06)\pi \qquad (7)$$

$$n = 18;\ s = 0.124;\ r = 0.958$$

No improvement was obtained by treating *meta*- and *para*-substituted derivatives as separate series. Similar results ($r = 0.950, s = 0.079$) were obtained for the correlation between $\tau_{w(A)}$ and π values.

In a previous study [6] we found that the $\pi_{RC_6H_5-N(O)=NCN}$ scale derived from

TABLE III

SLOPES AND LOG k_w VALVES IN EQN. 2 FOR AZOXYCYANIDES AND LOG P VALUES

Compound	Log P	Methanol			Acetonitrile		
		Log k_w	Slope	r	Log k_w	Slope	r
2	1.87	2.41 (±0.02)	−3.29 (±0.05)	0.999	2.01 (±0.06)	−3.12 (±0.11)	0.997
3	1.18	2.05 (±0.03)	−3.47 (±0.07)	0.999	1.88 (±0.03)	−3.22 (±0.06)	0.999
4	1.51	2.10 (±0.02)	−3.26 (±0.04)	0.999	2.03 (±0.03)	−3.30 (±0.05)	0.999
5	1.80	2.34 (±0.02)	−3.30 (±0.04)	0.999	2.03 (±0.04)	−3.17 (±0.08)	0.998
6	2.33	2.85 (±0.04)	−3.70 (±0.07)	0.999	2.44 (±0.08)	−3.50 (±0.15)	0.996
7	2.47	3.10 (±0.03)	−4.10 (±0.05)	0.999	2.62 (±0.09)	−3.75 (±0.16)	0.996
8	2.15	2.86 (±0.04)	−3.74 (±0.08)	0.999	2.31 (±0.10)	−3.48 (±0.19)	0.993
9	2.50	3.02 (±0.04)	−3.86 (±0.06)	0.999	2.42 (±0.09)	−3.40 (±0.16)	0.999
10	2.39	3.03 (±0.04)	−3.85 (±0.07)	0.999	2.47 (±0.10)	−3.56 (±0.18)	0.993
11	2.30	3.24 (±0.16)	−4.14 (±0.26)	0.994	2.45 (±0.14)	−3.63 (±0.26)	0.987
12	1.15	2.08 (±0.05)	−3.43 (±0.11)	0.997	1.85 (±0.04)	−3.19 (±0.07)	0.998
13	1.45	2.15 (±0.02)	−3.21 (±0.03)	0.999	2.03 (±0.05)	−3.30 (±0.09)	0.998
14	1.85	2.42 (±0.03)	−3.28 (±0.05)	0.999	2.10 (±0.06)	−3.23 (±0.12)	0.997
15	2.40	2.91 (±0.04)	−3.67 (±0.06)	0.999	2.48 (±0.10)	−3.53 (±0.18)	0.993
16	2.52	3.14 (±0.04)	−4.07 (±0.07)	0.999	2.57 (±0.10)	−3.68 (±0.17)	0.996
17	2.24	2.86 (±0.04)	−3.69 (±0.07)	0.999	2.36 (±0.10)	−3.49 (±0.19)	0.992
18	2.56	3.08 (±0.03)	−3.83 (±0.06)	0.999	2.42 (±0.10)	−3.37 (±0.18)	0.995
19	2.49	3.02 (±0.04)	−3.81 (±0.07)	0.999	2.47 (±0.10)	−3.54 (±0.20)	0.992
20	0.53	1.45 (±0.06)	−2.77 (±0.11)	0.995	1.12 (±0.04)	−2.46 (±0.07)	0.997
21	−0.41	0.75 (±0.06)	−2.66 (±0.13)	0.993	0.60 (±0.04)	−2.62 (±0.07)	0.997
22	0.10	0.90 (±0.04)	−2.30 (±0.08)	0.996	0.83 (±0.01)	−2.20 (±0.03)	0.999
23	−0.13	0.77 (±0.04)	−2.18 (±0.08)	0.996	0.70 (±0.02)	−2.18 (±0.04)	0.998
24	3.17	3.54 (±0.08)	−4.38 (±0.13)	0.999	2.71 (±0.14)	−3.71 (±0.24)	0.992
25	2.07	2.80 (±0.08)	−3.86 (±0.13)	0.998	2.10 (±0.12)	−3.26 (±0.23)	0.988
26	1.12	2.14 (±0.06)	−3.44 (±0.12)	0.997	1.72 (±0.12)	−3.23 (±0.24)	0.984

substituted phenyl-ONN-azoxycyanides and the $\pi_{RC_6H_5NO_2}$ scale derived from substituted nitrobenzenes [12] are strongly correlated by the equation

$$\pi_{RC_6H_5N(O)=NCN} = -0.02(\pm 0.02) + 0.96(\pm 0.03)\pi_{RC_6H_5NO_2} \quad (8)$$

$$n = 18;\ s = 0.06;\ r = 0.991$$

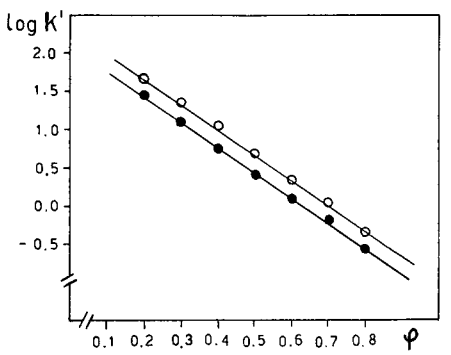

Fig. 2. Log k' *versus* volume fraction (○ = φ_M; ● = φ_A) for compound **5**.

TABLE IV

HYDROPHOBIC SUBSTITUENT CONSTANTS, τ_w, DERIVED FROM TABLE III

Compound	Methanol–water: $\tau_{w(M)}$	Acetonitrile–water: $\tau_{w(A)}$	π
2	0	0	0
3	−0.36	−0.13	−0.69
4	−0.31	0.02	−0.36
5	−0.07	0.02	−0.07
6	0.44	0.43	0.46
7	0.69	0.61	0.60
8	0.45	0.30	0.28
9	0.61	0.41	0.63
10	0.62	0.46	0.52
11	0.83	0.44	0.43
12	−0.33	−0.16	−0.72
13	−0.26	0.02	−0.42
14	−0.01	0.09	−0.02
15	0.50	0.47	0.52
16	0.73	0.56	0.65
17	0.45	0.35	0.37
18	0.67	0.41	0.69
19	0.61	0.46	0.62

This means that it is possible to derive, from the equations discussed above, retention parameters for azoxycyanide derivatives from lipophilicity parameters for the corresponding nitrobenzenes.

REFERENCES

1 A. Gasco, A. Serafino, V. Mortarini, E. Menziani, M. A. Bianco and J. C. Scurti, *Tetrahedron Lett.*, (1974) 3431.
2 R. Calvino, R. Fruttero, A. Gasco, A. Miglietta and L. Gabriel, *J. Antibiot.*, 39 (1986) 864, and references cited therein.
3 V. Mortarini, G. Ruà, A. Gasco, M. A. Bianco and A. Sanfilippo, *Eur. J. Med. Chem.*, 12 (1977) 59.
4 R. Fruttero, C. Tironi and R. Calvino, *Pharmazie*, 43 (1988) 551.
5 R. Fruttero, R. Calvino, A. Di Stilo, A. Gasco, I. Galatulas and R. Bossa, *Pharmazie*, 43 (1988) 499 (this paper contains omissions; the compounds reported in Table I have progressive numbers from 8 to 13).
6 R. Calvino, R. Fruttero, A. Garrone and A. Gasco, *Quant. Struct.–Act. Relat.*, 7 (1988) 26, and references cited therein.
7 J. H. Knox and R. Kaliszan, *J. Chromatogr.*, 349 (1985) 211.
8 R. Kaliszan, *Quantitative Structure–Chromatographic Retention Relationships*, Wiley, New York, 1987.
9 N. El Tayar, H. van de Waterbeemd and B. Testa, *J. Chromatogr.*, 320 (1985) 293.
10 C. M. Riley, E. Tomlinson and T. M. Jefferies, *J. Chromatogr.*, 185 (1979) 197.
11 Th. Braumann, *J. Chromatogr.*, 373 (1986) 191.
12 T. Fujita, J. Iawasa and C. Hansch, *J. Am. Chem. Soc.*, 86 (1964) 5175.

Journal of Chromatography, 547 (1991) 175–183
Elsevier Science Publishers B.V., Amsterdam

CHROM. 23 209

Combination of ion-pair and column switching in high-performance liquid chromatography of tropane alkaloids

TOSHIYUKI OSHIMA*, KAZUHIKO SAGARA, FUSAYOSHI HIRAYAMA and TAKU MIZUTANI

Research Centre, Taisho Pharmaceutical Co., Ltd., 1–403, Yoshino-cho, Ohmiya-shi, Saitama 330 (Japan)

LI-YI HE, YU-YI TONG and YU-HENG CHEN

Institute of Materia Medica, Chinese Academy of Medical Sciences, 1 Xing Nong Tan Street, Beijing (China)

and

HIDEJI ITOKAWA

Tokyo College of Pharmacy, 1432–1, Horinouchi, Hachioji-shi, Tokyo 192-03 (Japan)

(First received November 5th, 1990; revised manuscript received February 5th, 1991)

ABSTRACT

Ion-pair high-performance liquid chromatography was combined with column switching to determine tropane alkaloids, mainly hyoscyamine, in complex preparations of gastrointestinal drugs using a three-pump system. The mobile phases were all the same except for the concentration of the counter ion, sodium dodecyl sulphate (SDS). The tropane alkaloid fraction immediately eluted by the primary mobile phase without SDS from a pretreatment column was transferred to an analytical column and separated by the ion-pair mobile phase. A tertiary pump was used to supply SDS to the trapped fraction in the loop after elution through the pretreatment column. Linear calibration graphs were obtained in the range 0.3–30 μg/ml for anisodine, anisodamine and scopolamine and 0.3–300 μg/ml for hyoscyamine (atropine). Hyoscyamine levels in model preparations of gastrointestinal drugs were determined by this column switching system with a recovery of about 97%.

INTRODUCTION

Crude drugs derived from solanaceous plants containing tropane alkaloids and their extracts, such as scopolia and belladonna extracts, are used in antidiarrhoeal and gastrointestinal drug preparations as anodynes and anticonvulsants. Scopolia extract is an important ingredient of gastrointestinal drugs and other crude drugs are often prepared with scopolia extract. The determination of tropane alkaloids, mainly hyoscyamine and scopolamine, has been attemped by chromatographic techniques such as thin-layer chromatography [1], gas chromatography [2,3] and high-performance liquid chromatography (HPLC) [4–14]. HPLC is a useful technique for the determination of tropane alkaloids from the viewpoint of resolution and sensitivity. Although several HPLC methods have been applied to solanaceous crude drugs and their extracts and preparations, time-consuming pretreatment, such as partitioning

0021-9673/91/$03.50

between alkaline ammonia and chloroform or diethyl ether, is required, particularly for preparations. This is because the common combination dosage of scopolia extract is low and impurities from large doses of other crude drugs or ingredients interfere chromatographically.

Recently we developed two ion-pair HPLC systems. One is for the determination of four tropane alkaloids [13], anisodamine, anisodine, hyoscyamine and scopolamine, but it requires alkaline ammonia–chloroform extraction. The other is a simple and rapid method [14] with no complicated pretrearments required. The advantage of ion-pair chromatography is that the retention time of an ionic compound can be controlled by changing the type and concentration of the counter ions and the pH of the mobile phase. However, even these ion-pair chromatographic methods are not applicable to preparations containing some crude drugs without complicated pretreatment.

The column switching system [15] can be used for on-line sample clean-up and the analysis of complex preparations and trace amounts of urine or blood analytes, etc. Highly selective separations can be achieved by changing transfer techniques and/or switching functions or by altering the chromatographic modes of separation during the overall process. One simple approach is to transfer selectively a desired fraction eluted from a primary to a secondary column for further separation.

Coupling these two techniques permits the on-line determination of tropane alkaloids in complex preparations with no complicated pretreatment. In this study, application of combined ion-pair and column switching to the determination of tropane alkaloids, mainly hyoscyamine, in complex preparations is described.

EXPERIMENTAL

Materials

Scopolia acutangulus was collected in Yunnan. *Scopolia japonica, Duboisia leichhardtis*, fennel, plectranthi herb, scutellaria root, glycyrrhiza, cinnamon bark, gentian, geranium herb, amomum seed, ginger, swertia herb, rhubarb, ginseng, alpinia rhizome, evodia fruit, corydalis tuber, phellodendron bark, sophora root and magnolia bark were available from markets. Scopolia extract was according to the Pharmacopoeia of Japan.

Chemicals and reagents

Atropine hydrosulphate (as hyoscyamine) and scopolamine hydrobromide standards were purchased from Wako (Osaka, Japan). Anisodine and anisodamine were isolated and purified at the Bejing Institute of Materia Medica. Methanol for chromatography, phosphoric acid, sodium phosphate dihydrate and sodium dodecyl sulphate (SDS) of biological grade were obtained from Wako.

Apparatus

The Shimadzu LC-6AD system consisted of a SIC chromatocoder 12 computing integrator, three pumps (two Shimadzu LC-6ADs for the primary and secondary pumps and a Waters M-45 for the tertiary pump), a Shimadzu SIL-6A system controller, a Rheodyne 7001 pneumatic switching valve and a Shimadzu SPD-6A UV detector. The pretreatment column (50 mm × 4 mm I.D.) and analytical column (250

mm × 4 mm I.D.) were packed with TSK Gel 120A, 5 μm (TOSOH, Tokyo, Japan) by slurry packing. The loop volume was 1 ml.

HPLC conditions

The primary mobile phase for the pretreatment column was a mixture of 1/15 *M* sodium phosphate solution (adjusted to pH 3.5 with 1/15 *M* phosphoric acid) and methanol (48:52). The secondary mobile phase for the analytical column was the primary mobile phase containing 17.5 m*M* SDS. The tertiary mobile phase was the primary mobile phase containing 175 m*M* SDS. The column temperature was maintained at 35°C and the flow-rates of the primary, secondary and tertiary mobile phases were 0.9, 1.0 and 0.1 ml/min, respectively. The eluted substances were detected by a UV detector at 210 nm.

Sample preparation and assay procedure

Solanaceous plants. Dry powders of each crude drug (0.5 g) were refluxed for 30 min in 25 ml of the primary mobile phase, cooled, centrifuged at 1600 *g* and decanted. The residue was washed twice with 10-ml of the primary mobile phase. The extract and washings were diluted to 50 ml with the primary mobile phase. A 20-μl portion of this solution was injected into the pretreatment column of the HPLC system. The eluate fraction from 0.25 to 1.25 min was trapped in the loop and transferred to the analytical column. The hyoscyamine, scopolamine, anisodine and anisodamine concentrations were calculated from the relevant peak areas.

Other crude drugs. Using appropriate amounts of the crude drugs listed in Table I and water–methanol (48:52) as the extraction solvent instead of the primary mobile phase, the sample solutions were prepared as described for the solanaceous plants.

Model preparations. The corresponding amounts listed in Table II of each crude drug sample solution were mixed, evaporated and dissolved in 50 ml of the primary mobile phase to result in model preparations I and II. Each blank model preparation was prepared in the same manner but without scopolia extract. A 20-μl aliquot of each sample solution was analysed with the column switching system and also with the analytical column alone with the secondary mobile phase.

TABLE I

CRUDE INGREDIENTS OF GASTROINTESTINAL DRUG PREPARATIONS

Crude drug	Sample amount (g)	Crude drug	Sample amount (g)
Ginger	1.0	Cinnamon bark	1.0
Glycyrrhiza	1.5	Fennel	1.0
Alpinia rhizome	1.0	Plectranthi herb	0.5
Ginseng	1.5	Scutellaria root	3.0
Amomum seed	0.1	Swertia herb	1.0
Gentian	0.2	Geranium herb	1.5
Corydalis tuber[a]	0.8	Rhubarb	0.2
Evodia fruit[a]	1.0	Phellodendron bark[a]	3.0
Magnolia bark[a]	1.5	Sophora root[a]	1.5

[a] Crude drug contains alkaloids.

TABLE II

PRESCRIPTION OF MODEL GASTROINTESTINAL DRUGS

Model preparation I		Model preparation II	
Component	Amount (g)	Component	Amount (g)
Ginger	0.1	Swertia herb	0.05
Cinnamon bark	0.3	Gentian	0.2
Fennel	0.2	Geranium herb	0.5
Amomum seed	0.1	Phellodendron bark	0.5
Ginseng	0.3	Plectranthi herb	0.5
Glycyrrhiza	0.15	Scopolia extract	0.03
Scopolia extract	0.03		
Recovery of hyoscyamine (%)	96.6		97.0
R.S.D. (%, $n = 5$)	1.2		1.7

Calibration graphs

Calibration graphs for hyoscyamine, scopolamine, anisodine and anisodamine obtained by the column switching system were obtained over the ranges 0.6–322.0, 0.3–31.0, 0.3–30.0 and 0.3–33.0 μg/ml, respectively, and the corresponding regression equations were $y = 17700x - 550$ ($r = 0.999$), $y = 16020x + 570$ ($r = 0.999$), $y = 15280x + 440$ ($r = 0.999$) and $y = 14680x - 680$ ($r = 0.999$).

RESULTS AND DISCUSSION

HPLC conditions

A column switching system using two columns for pretreatment and analysis generally includes the fractional transfer of the effluent from the pretreatment column. As the fraction to be transferred is a front, middle or end eluting zone, a large volume, sometimes up to 1 ml, of the effluent is transferred. Although the chromatographic modes in the column switching system can be controlled by changing the composition of the mobile and/or the stationary phases, when the same stationary phase is used for both the pretreatment and analytical columns, considerably different mobile phases are required. In this instance, the composition of the effluent must be very similar to that of de secondary mobile phase for subsequent analysis, because a large volume of the effluent from the pretreatment column, which has a different solvent system, strongly affects the separation efficiency of the analytical column. Adjusting the composition of the effluent to be transferred by adding water or organic solvent after elution from the pretreatment column causes an increase in volume. The retention of ionic compounds such as tropane alkaloids can be controlled by adding a counter ion to the mobile phase. Therefore, the addition of a small volume of solvent containing a high concentration of counter ions to adjust the final counter ion concentration can minimize this disadvantage. Our separation strategy was as follows: tropane alkaloids were eluted immediately from the ODS pretreatment column by the primary mobile phase without the counter ion, and the separated on the ODS analytical column under ion-pair conditions.

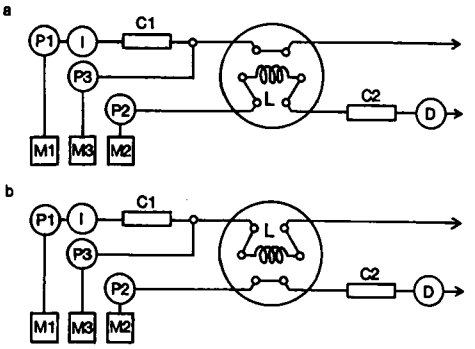

Fig. 1. Schematic diagram of the column switching system. (a) Waiting and analysis mode; (b) trapping mode. P1, P2, P3 = pumps; C1 = pretreatment column; C2 = analytical column; D = detector; L = loop; M1 = primary mobile phase; M2 = secondary mobile phase; M3 = tertiary mobile phase.

There are several transfer techniques for introducing a desired fraction into a secondary column, namely direct, indirect, reversed, loop and backflush. Direct or loop transfer techniques were suitable for this system. Loop transfer was examined to avoid an increase in column pressure when the pretreatment and analytical columns were connected. This system is shown in Fig. 1. The ion-pair chromatographic conditions for the secondary column were similar to those in our previous study [13]. A 5-cm long pretreatment column was used to minimize the transfer fraction volume. Four tropane alkaloids were eluted from 0.4 to 1.1 min (Fig. 2a). A 25-cm long column was used for analysis. The loop volume was 1.0 ml for complete alkaloid transfer. First, 1.0 ml of the eluate from the pretreatment column without SDS was directly transferred to the analytical column, but split peaks of tropane alkaloids appeared, as shown in Fig. 2b. It seems that this phenomena was due to an insufficient counter ion effect. A tertiary pump as used to supply SDS before the analytical column. The tertiary pump solution contained ten times more SDS. After trapping the sample, the final SDS concentration in the loop mobile phase was maintained at 17.5 m*M*, the same as in the secondary mobile phase, by keeping the flow-rate constant at 10% of the total. The flow-rates were set at 0.9, 1.0 and 0.1 ml/min for the primary, secondary and tertiary mobile phases, respectively. The ratio of the buffer to methanol was the same in all mobile phases. As shown in Fig. 2c, a clearly separated peak was obtained. When the eluted fraction from 0.25 to 1.25 min after the injection was transferred to the analytical column, the recoveries of hyoscyamine, scopolamine, anisodine and anisodamine from the pretreatment column were 99.5% [relative standard deviation (R.S.D.) = 0.5%], 97.7% (R.S.D. 0.6%), 100.0% (R.S.D. 0.6%) and 98.8% (R.S.D. 0.5%), respectively, with $n = 5$.

Analysis of solanaceous plants

Tropane alkaloids in *Scopolia japonica, Scopolia acutangulus* and *Duboisia leichhardtis*, which had been analysed by ion-pair HPLC after ammonia–alkaline chloroform extraction, were separated clearly by this column switching system (Fig. 3). The analytical results showed good agreement with our previous data [13].

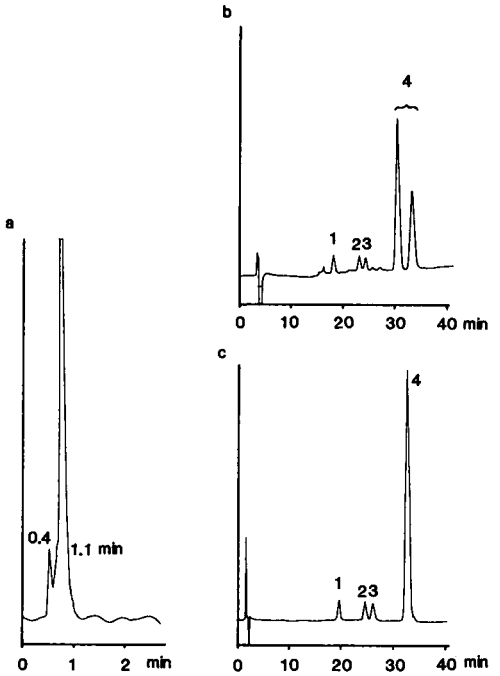

Fig. 2. (a) Chromatogram of the mixture of the four tropane alkaloids from the pretreatment column. (b) Chromatogram of the four tropane alkaloids by column switching without tertiary mobile phase. (c) Chromatogram of the four tropane alkaloids by column switching. Peaks: 1 = anisodine; 2 = anisodamine; 3 = scopolamine; 4 = hyoscyamine. Injection volume, 20 μl. Standard solution contains anisodine, anisodamine and scopolamine at concentrations of 10 μg/ml each and hyoscyamine at 160 μg/ml.

Analysis of model preparations

Scopolia extract is an important ingredient of gastrointestinal drug mixtures, and contains hyoscyamine and scopolamine. Many kinds of crude drugs are often combined with scopolia extract in gastrointestinal preparations. Representative crude

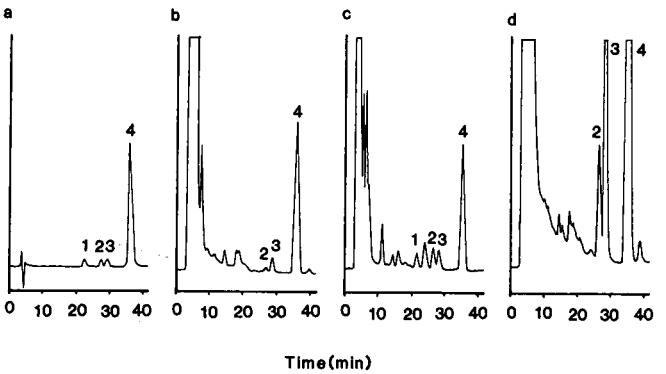

Fig. 3. Chromatograms of solanaceous crude drugs. (a) Standards; (b) *Scopolia japonica*; (c) *Scopolia acutangulus*; (d) *Duboisia leichhardtis*. Peaks as in Fig. 2.

drugs are given in Table I. The dosage form of scopolia extract is lower than that of other crude drugs. The determination of the tropane alkaloids in these gastrointestinal drugs is difficult without complicated pretreatment. Therefore, the present column switching system was applied to the analysis of a complex gastrointestinal drug preparation using two model mixtures. Table II lists the prescription of the model gastrointestinal drugs. The model preparation II has an alkaloid crude drug, phellodendron bark, and the other does not. Corresponding blank model preparations that contained no scopolia extract were prepared to check the interferences at the position of tropane alkaloids on the chromatograms.

Figs. 4 and 5 show the chromatogram of these two model preparations. In the model preparation I and the corresponding blank, there were many interfering peaks from other crude drugs from the analytical column without a clean-up procedure. Therefore, no tropane alkaloids were directly determined (Fig. 4a and a'). However, most interferences from other crude drugs were removed by the column switching procedure in the full model preparation I (Fig. 4b). No peak appeared at the position of hyoscyamine on the chromatogram of the blank model preparation I (Fig. 4b'). It was difficult to determine scopolamine because of the low concentraions. Regarding the analysis of the model preparation II, phellodendron bark seemed to interfere with the hyoscyamine and scopolamine peaks, as berberine-type alkaloids in phellodendron bark would show a similar behaviour to tropane alkaloids and would not be removed by the pretreatment column. However, most berberine-type alkaloids were

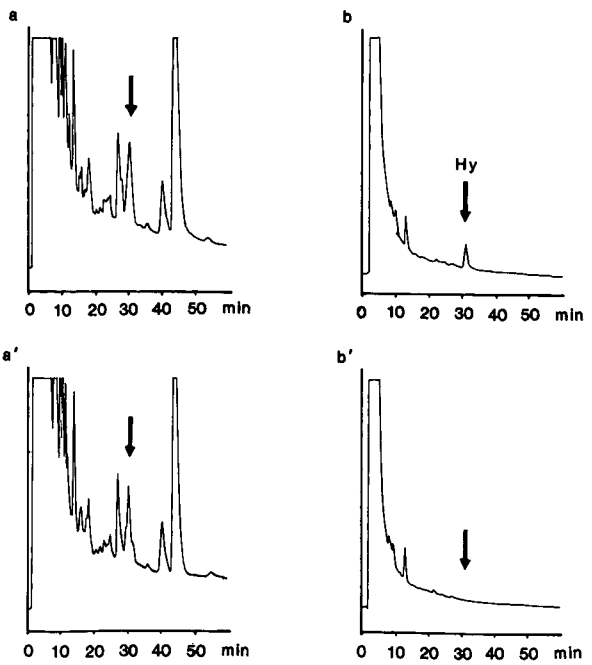

Fig. 4. Chromatograms of (a) model preparation I without clean-up procedure, (a') blank model preparation I without clean-up procedure, (b) model preparation I by column switching, (b') blank model preparation I by column switching. Peak: Hy = hyoscyamine.

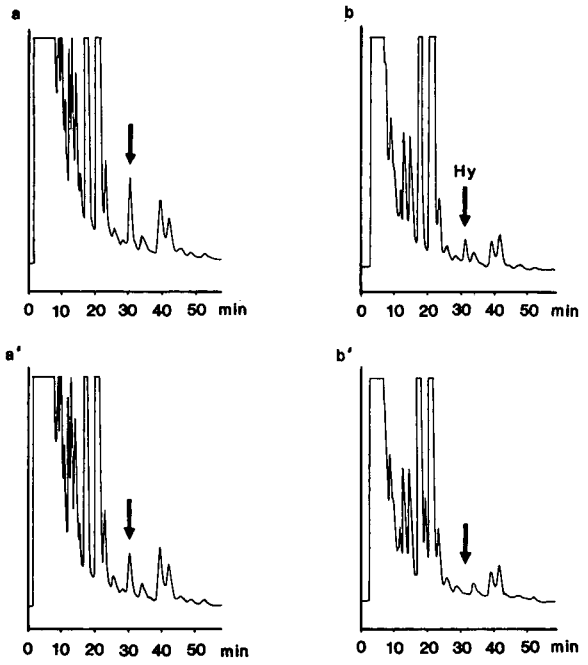

Fig. 5. Chromatograms of (a) model preparation II without clean-up procedure, (a′) blank model preparation II without clean-up procedure, (b) model preparation II by column switching; (b′) blank model preparation II by column switching. Peak: Hy = hyoscyamine.

separated from hyoscyamine on the analytical column. As shown in Fig. 5a and a′, hyoscyamine interfered with the blank model preparation II without clean-up, but this peak was removed by the column switching system. (Fig. 5b and b′). Glycyrrhiza and amomum seed were the interferences in the model preparation I and gentian in the model preparation II. The recoveries of hyoscyamine from scopolia extract in the model preparations I and II were 96.6 and 97.0%, respectively. In addition to the model preparations, several crude drugs that could be combined with scopolia extract in gastrointestinal drug preparations were checked and no significant interference of hyoscyamine was found.

CONCLUSIONS

The determination of tropane alkaloids, especially hyoscyamine, in complex preparations was achieved by combining ion-pair chromatography and column switching using the third pump to supply SDS before transfer to the analytical column. This system seems to be applicable to the on-line determination of other ionic components in complex preparations.

REFERENCES

1 A. Baerheim Svendsen and R. Verpoorte, *Chromatography of Alkaloids*, Elsevier, Amsterdam, 1983.
2 H. Mechler and H. W. Kohlenbach, *Planta Med.*, 33 (1978) 350.
3 M. Ylinder, T. Naaranlahti, S. Lapinjoki, A. Hugtikangas, M.-L. Salonen, L. K. Simola and M. Lounnasman, *Planta Med.*, 52 (1986) 85.
4 L. J. Pennington and W. F. Schmidt, *J. Pharm. Sci.*, 71 (1982) 951.
5 E. Stahl and H. Jork, *Dtsch. Apoth.-Ztg.*, 124 (1984) 1706.
6 P. Duez, S. Chamart, M. Hanocq and L. Molle, *J. Chromatogr.*, 392 (1985) 422.
7 S. Paphassarang and J. Raynand, *J. Chromatogr.*, 319 (1985) 412.
8 B. Pekic, B. Slavica, Z. Lepojevic and M. Gorunovic, *Pharmazie*, 40 (1985) 415.
9 M. Anetai and T. Yamagishi, *Hokkaidoritsu Eisei Kenkyushoho*, 35 (1985) 52.
10 M. Anetai and T. Yamagishi, *Hokkaidoritsu Eisei Kenkyushoho*, 36 (1986) 66.
11 T. Fujita, *Shimadzu Hyoron*, 43 (1986) 89.
12 K.-H. Plank and K. G. Wagner, *Z. Naturforsch. C.*, 41 (1986) 391.
13 L. Y. He, G. D. Zhang, Y. Y. Tong, K. Sagara, T. Oshima and T. Yoshida, *J. Chromatogr.*, 481 (1989) 428.
14 T. Oshima, K. Sagara, Y. Y. Tong, G. D. Zhang and Y. H. Chen, *Chem. Pharm. Bull.*, 37 (1989) 2456.
15 K. A. Ramsteiner, *J. Chromatogr.*, 456 (1988) 3.

Journal of Chromatography, 547 (1991) 185–193
Elsevier Science Publishers B.V., Amsterdam

CHROM. 23 257

Separation and identification of phytoalexins from leaves of groundnut (*Arachis hypogaea*) and development of a method for their determination by reversed-phase high-performance liquid chromatography

CHRISTINE EDWARDS[a] and RICHARD N. STRANGE*

Department of Biology, Darwin Building, University College London, Gower Street, London WC1E 6BT (UK)

(First received November 20th, 1990; revised manuscript received March 1st, 1991)

ABSTRACT

Leaves of groundnut, *Arachis hypogaea*, infected with the early leaf spot fungus, *Cercospora arachidicola*, were extracted in aqueous ethanol and the phytoalexins partitioned into ethyl acetate. Flash chromatography of the ethyl acetate extract on silica gel yielded fractions with one to five compounds from which the phytoalexins could be isolated by semipreparative reversed-phase high-performance liquid chromatography (HPLC). The major phytoalexins were demethylmedicarpin, formononetin, 7,4′-dimethoxy-2′-hydroxyisoflavanone and medicarpin. Minor components were 7,2′-dihydroxy-4′-methoxyisoflavanone and daidzein. Compounds were identified by cochromatography and comparison of their ultraviolet and mass spectra with authentic samples using an HPLC system equipped with a diode-array detector, HPLC mass spectrometry and gas chromatography–mass spectrometry of their trimethylsilyl derivatives. A solid-phase extraction method was developed for processing large numbers of samples. Acetonitrile eluates from C_{18} cartridges were separated by reversed-phase HPLC and the phytoalexins quantified by reference to external standards of the authentic compounds.

INTRODUCTION

Phytoalexins are antimicrobial compounds which accumulate in plants in response to challenge by parasites and other traumas. In some interactions of plants and microbes there is good evidence that they are determinants of resistance [1,2]. We previously reported that the pterocarpan, medicarpin, was the predominant phytoalexin present in groundnut leaves infected by the fungus, *Cercospora arachidicola* [3]. However, further experiments showed that other antifungal compounds were also present. Before the role of medicarpin and these other phytoalexins in resistance to fungal leaf spot diseases could be assessed, it was necessary to identify them and devise means for their accurate determination.

In this paper, we report methods for phytoalexin isolation in quantities suffi-

[a] Present address: Department of Biology, University of Dundee, Dundee, Scotland, UK.

0021-9673/91/$03.50

cient for structural determination and a technique for their quantitative analyis in small samples involving solid-phase extraction and reversed-phase high-performance liquid chromatography (HPLC). Since low concentrations of phytoalexins were elicited by abiotic agents such as UV light or the salts of heavy metals, leaves infected with *C. arachidicola* were used as a source of the antifungal compounds.

EXPERIMENTAL

Chemicals

HPLC-grade acetonitrile and methanol were obtained from Fisons (Loughborourgh, UK). Ethyl acetate, methanol and cyclohexane (GPR) were purchased from BDH (Poole, UK). Chloroform and acetic acid (AR) were bought from May and Baker (Ongar, UK). Pure water was obtained from an Elga (High Wycombe, UK) pure-water system.

All other chemicals were of analytical grade and were purchased from BDH or Sigma (Poole, UK). Spherisorb ODS 1 (10 μm) was obtained from Phase Separations (Deeside, UK). Silica gel 60 and thin-layer chromatography (TLC) plates were obtained from BDH.

The phytoalexin standards demethylmedicarpin, medicarpin and 7,2′-dihydroxy-4′-methoxyisoflavanone were gifts from Professor P. M. Dewick (Department of Pharmacology, University of Nottingham, Nottingham, UK). Medicarpin, formononetin and daidzein were gifts from Professor W. Barz (Lehrstuhl für Biochemie der Pflanzen, Universität Münster, Münster, Germany).

Extraction of phytoalexins

Method 1. Groundnut leaves from the cultivars Flamingo and Egret (1 or 125 g fresh weight), infected with *C. arachidicola*, were collected from experimental plots near Harare, Zimbabwe and air-dried. They were vacuum-infiltrated with 60% ethanol and agitated at intervals for 24 h. After removal of the ethanol *in vacuo* at 40°C, the remaining aqueous solution was partitioned three times against ethyl acetate. The ethyl acetate fractions were combined and dried over anhydrous sodium sulphate.

Method 2. For analytical samples, leaves infected with *C. arachidicola* (1 g fresh weight) were extracted by facilitated diffusion[4] in 60% ethanol. The ethanol was decanted and diluted to 25% before being applied to a solid-phase cartridge. This consisted of 500 mg Techoprep C_{18} (25–40 μm: HPLC Technology, Macclesfield, UK), conditioned with methanol and washed with water. After application of the sample, the cartridge was washed with 5 ml of 25% ethanol, and the phytoalexins were eluted with 1 ml of acetonitrile.

The efficiency of these methods was examined by applying them to samples treated with silver nitrate, a poor elecitor of phytoalexins in groundnut leaves. Ten 5-μl droplets of silver nitrate solution ($10^{-3}M$) were applied to fully expanded, detached leaves and incubated for 48 h. Samples (1 g each), spiked with medicarpin (100 μg per sample) or not, were extracted by method 1 or method 2. In method 2, the cartridges were additionally eluted with a second millilitre of acetonitrile which was analysed separately. Material not retained on the cartridges was concentrated *in vacuo* and also analysed for the presence of medicarpin.

Isolation and purification of phytoalexins

Phytoalexins extracted by method 1 from large samples (125 g) were separated by a two-stage process consisting of flash chromatography [5] and semipreparative HPLC.

The ethyl acetate solution was evaporated to dryness *in vacuo*, the residue dissolved in 10 ml of chloroform and the chloroform solution separated on a column of silica gel 60 (Merck, 40–60 μm, 230–400 mesh, obtained from BDH; 150 mm × 20 mm). After conditioning the column with cyclohexane, the chloroform sample (5 ml) was applied and the phytoalexins eluted with a stepwise gradient of ethyl acetate in cyclohexane starting with 100% cyclohexane. At each step of the gradient (100 ml) the ethyl acetate content was increased by 10% (v/v), and two 50-ml fractions were cut. After the ethyl acetate concentration of the eluent had reached 50%, a final fraction consisting of 100 ml of 100% ethyl acetate was collected. All fractions were examined by analytical HPLC or TLC.

Phytoalexins in fractions from the silica column were isolated by semipreparative HPLC. The apparatus consisted of an Altex pump (Beckman Instruments, Berkeley, CA, USA), a column of Spherisorb ODS 1 (Phase Separations, 250 mm × 10 mm I.D.; 10 μm particle size), a Pye-Unicam UV detector (Philips Analytical, Cambridge, UK) set at 290 nm and a Tekman chart recorder (Tekman Electronics, Bicester, UK). Samples (250–500 μl) were introduced to the column via a 2-ml loop attached to an Altex valve and eluted in acetonitrile–water (1:1, v/v). Fractions corresponding to absorption peaks were collected manually. Purity of the compounds was checked by TLC using iodine vapour to visualize the spots and by HPLC using a system equipped with a diode-array detector (see below).

Thin-layer chromatography

Samples were run on TLC plates (silica gel 60 on an aluminium support; Merck No. 3554) in a tank saturated with a solvent system consisting of ethyl acetate–cyclohexane (1:1, v/v). Spots were detected by exposure to iodine vapour or spraying with diazotized *p*-nitroaniline [16], and those that were antifungal by spraying with a spore suspension of *Cladosporium cucumerinum* made up in half strength Czapek-Dox medium at a density of 0.8 absorbance units at 620 nm. After spraying, the plates were incubated at high humidity in the dark for 48 h [7].

Analytical HPLC

A Philips apparatus was used, consisting of two pumps (PU 4100), an automatic sampler (PU 4700) and a diode-array detector (PU 4021) interfaced to a trivector data system (Philips Analytical). Compounds were separated on a column of Spherisorb ODS 1 (250 mm × 4.6 mm I.D.; 10 μm particle size) protected by an Upchurch low-volume guard column (20 mm × 2 mm I.D., Anachem, Luton, UK) packed with Techoprep C_{18} (25–40 μm; HPLC Technology). The mobile phase was a gradient of acetonitrile in 1% acetic acid in which the acetonitrile concentration was increased from 35% to 40% over the first 12 min and then to 75% over the next 23 min. A reequilibration time of 5 min was allowed to elapse before the next sample was injected. The flow-rate was 1.5 ml/min and the eluent was monitored at 290 nm at an absorbance range of 0.04 a.u.f.s. Compounds were identified on the basis of retention time and comparison of their UV spectra with those of authentic samples. They were

quantified by comparison of peak areas with those of external standards. Purity of isolated compounds was tested by determining the similarity of several spectra cut during the elution of a peak.

Identification of phytoalexins

Ultraviolet spectroscopy. The UV spectra of purified compounds were obtained on a Varian-Cary spectrophotometer (Varian Assoc., Palo Alto, Ca, USA). Methanolic solutions were scanned from 220 to 340 nm.

Purified compounds were quantified by their absorbance using previously calculated molar extinction coefficients: medicarpin (287 nm), 2 log $\varepsilon = 3.90$ [8]; isoflavanones (277 nm), log $\varepsilon = 4.00$; formononetin (250 nm), log $\varepsilon = 4.35$ and demethylmedicarpin (287 nm), log $\varepsilon = 3.93$ [9].

Gas Chromatography–mass spectrometry (GC–MS). A Carlo Erba Strumentazione HPGC 5160 (Fisons Instruments, Crawley, UK) was fitted with a BP1 fused-silica/quartz capillary column (50 m × 0.32 mm I.D. with 0.5 μm film: SGE). The carrier gas, helium, was introduced into the system with a column head pressure of 130 KPa. Dried samples were derivatised in a mixture of trimethylchlorosilane (Sigma) and pyridine (1:1) and introduced into the instrument with a splitless on-column injector. The components were separated using the following GC programme: 50°C increasing to 250°C at 40°C/min with a further increase to 300°C at 5°C/min where it was maintained for 15 min. Ions were detected by a Hewlett-Packard 5970 series mass-selective detector (Hewlett Packard, Wokingham, UK) using an electron energy of 70 eV.

LC–MS. Samples were separated by gradient elution with a flow-rate of 1 ml/min on a Hichrom ODS 2 column (3 μm particle size; 150 mm × 4.9 mm I.D.). Solvent A was 20% acetonitrile in 0.1 *M* ammonium acetate and solvent B was 80% acetonitrile in 0.1 *M* ammonium acetate. Solvent B was maintained at 15% for 1 min, increased to 25% over the next 12 min and to 90% over the following 18 min. The column was reequilibrated by decreasing solvent B to 15% over 4 min and maintaining it at this percentage for the next 3 min. Analytes were monitored at 254 nm, and the mass spectra of the compounds giving rise to the peaks were determined by means of a Vestec 201 thermospray mass spectrometer with positive-ion discharge (1000 V: Vestec, Houston, TX, USA). Start conditions were: control, 144°C; tip heater, 288°C; source block, 326°C and vapour, 343°C.

HPLC–UV spectrophotometry. Samples were run on the analytical HPLC system and the retention times and spectra obtained from the diode-array detector compared with those of authentic compounds.

RESULTS

At least six antifungal zones that corresponded with areas of UV absorption were visible on TLC plates which had been spotted with extracts from diseased groundnut leaves and sprayed with spore suspension of *C. cucumerinum.* Flash chromatography of extracts resulted in fractions containing one to five major components which could be separated by semipreparative HPLC (Fig. 1).

Medicarpin had an R_F of 0.71 on TLC and gave a pale orange spot when

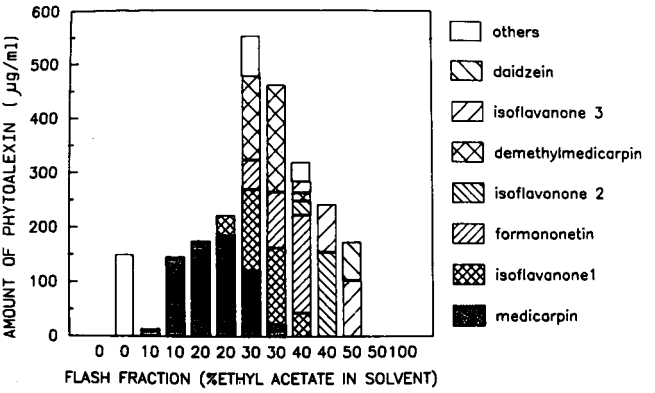

Fig. 1. Distribution of phytoalexins in fractions from flash chromatography on silica gel. Two 50-ml fractions were collected for each concentration of ethyl acetate in the mobile phase apart from the final fraction which was 100 ml and was eluted with 100% ethyl acetate. 'Others' were unidentified compounds. Isoflavanone 3 was a compound with a UV spectrum and mass fragmentation pattern corresponding to an isoflavanone but was not characterized further. Isoflavanone 2 was identified as 7,2′-dihydroxy-4′-methoxyisoflavanone by GC–MS of the TMSi derivative, cochromatography by HPLC and matching of the UV spectrum with that of an authentic sample of the compound. Isoflavanone 1 was identified as 7,4′-dimethoxy-2′-hydroxyisoflavanone by GC–MS and LC–MS.

sprayed with diazotized *p*-nitroaniline. The absorption maxima in methanol were at 282 nm and 286.5 nm. GC–MS of the trimethylsilyl (TMSi) derivative gave m/z – 342 (M^+) and prominent peaks at 327 ($M^+ - 15$), 219 ($M^+ - 123$), 206 ($M^+ - 136$), 164 ($M^+ - 178$), 148 ($M^+ - 194$) and 73 (TMSi). On LC–MS the compound had a retention time of 24.72 min and gave an MH^+ of 271. The retention time on the analytical HPLC system was 21.12 min compared with 21.10 min for an authentic sample, and good agreement of UV spectra was obtained.

Formononetin had an R_F of 0.42 on TLC and gave a very pale orange–yellow derivative when sprayed with diazotized *p*-nitroaniline. The absorption maxima in methanol were at 249 and 299 nm. GC–MS of the TMSi derivative gave m/z – 340 (M^+) with prominent peaks at 325 ($M^+ - 15$), 208 ($M^+ - 132$), 163 ($M^+ - 177$), 132 ($M^+ - 208$) and 73 (TMSi). An MH^+ of 269 was obtained at a retention time of 21.72 min on LC–MS. On analytical HPLC an authentic sample eluted at 19.02 min and a compound with a similar spectrum from infected leaf samples at 19.10 min.

Demethylmedicarpin had an R_F value of 0.54 on TLC and gave a bright orange derivative on reaction with diazotized *p*-nitroaniline. The absorption spectra in methanol was similar to that of medicarpin with λ_{max} at 282 and 286.5 nm. GC–MS of the TMSi derivative gave m/z 400 (M^+) with prominent peaks at 385 ($M^+ - 15$), 219 ($M^+ - 181$), 206 ($M^+ - 194$), 185 ($M^+ - 215$) and 73 (TMSi). LC–MS gave a peak at retention time 12.60 min with MH^+ of 257. The authentic compound eluted at 11.20 min and a compound with a similar spectrum obtained from infected leaves at 11.10 min on the analytical HPLC.

An isoflavanone, referred to as isoflavanone 1, was identified as 7,4′-dimethoxy-2′-hydroxyisoflavanone, had an R_F value of 0.46 on TLC and produced a yellow–orange derivative when sprayed with diazotised *p*-nitroaniline. The absorption maxi-

ma in methanol were at 277 and 311 nm. GC–MS of the TMS derivative gave *m/z* 372 (M^+) with prominent peaks at 357 ($M^+ - 15$), 209 ($M^+ - 163$), 193 ($M^+ - 179$), 164 ($M^+ - 208$), 149 ($M^+ - 223$) and 121 ($M^+ - 251$). LC–MS gave a peak at retention time 23.34 min with an MH^+ of 301. No authentic material was available for chromatographic and spectral comparison.

A second isoflavanone, referred to as isoflavanone 2, was identified as 7,2′-dihydroxy-4′-methoxyisoflavanone by co-chromatography and matching of the UV spectrum with that of authentic material. GC–MS of the TMS derivative gave *m/z* 430 (M^+) with prominent peaks at 415 ($M^+ - 15$), 281 ($M^+ - 149$), 222 ($M^+ - 208$) and 207 ($M^+ - 223$). LC–MS gave a peak at a retention time of 15.14 min with MH^+ 287. The retention times of the authentic compound and samples from infected leaves on analytical HPLC were 13.38 and 13.42 min, respectively, and their spectra corresponded with absorption maxima at 275 and 311 nm.

An isoflavone was identified as daidzein. GC–MS of the TMS derivative gave *m/z* 398 (M^+) with prominent peaks at 383 ($M^+ - 15$), 281 ($M^+ - 117$) and 207 ($M^+ - 191$). LC–MS gave a peak at a retention time of 9.39 min with an MH^+ of 255. The authentic compound eluted at 9.10 min on the analytical HPLC system and a compound with a similar spectrum (λ_{max} 245 and 2989 nm) obtained from infected leaves eluted at 9.13 min.

Structures of the six compounds are presented in Fig. 2.

Analytical reversed-phase HPLC with a gradient of acetonitrile in 1% acetic acid on a column of Spherisorb ODS 1 (10 μm; 250 mm × 4.6 mm I.D.) gave good separation of the principal phytoalexins (Fig. 3). Demethylmedicarpin, formonone-

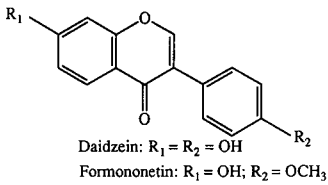

Daidzein: $R_1 = R_2 = OH$
Formononetin: $R_1 = OH$; $R_2 = OCH_3$

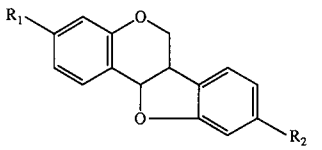

Medicarpin: $R_1 = OH$; $R_2 = OCH_3$
Demethylmedicarpin: $R_1 = R_2 = OH$

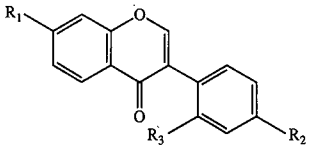

Isoflavone 1: $R_1 = R_2 = OCH_3$; $R_3 = OH$
Isoflavone 2: $R_1 = R_3 = OH$; $R_2 = OCH_3$

Fig. 2. Structures of the phytoalexins identified in leaves of groundnuts infected by the fungal parasite *C. arachidicola*.

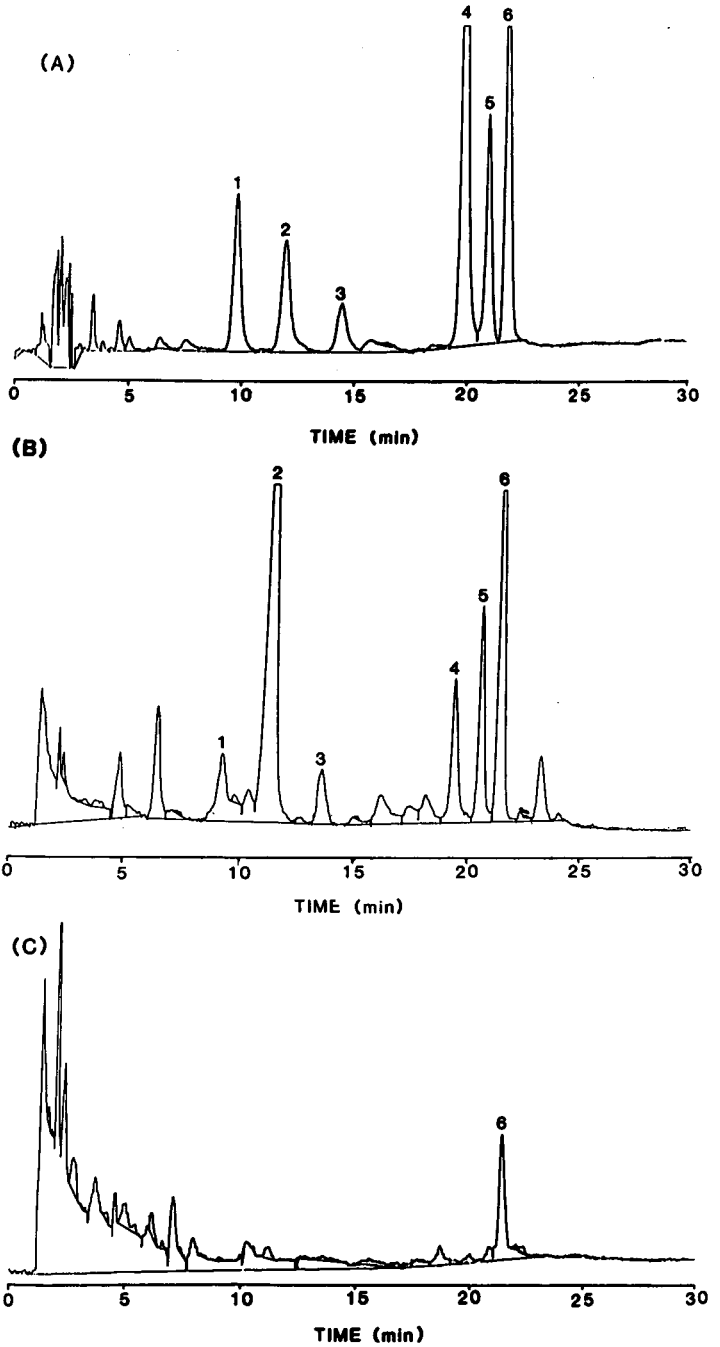

Fig. 3. HPLC of phytoalexins found in leaves of groundnuts infected by the fungal parasite *C. arachidicola*. (A) Chromatogram of six phytoalexin standards; a 10-μl sample containing the following concentrations of phytoalexins was injected: 1, daidzein, 50 μg/ml; 2, demethylmedicarpin, 25 μg/ml; 3, isoflavanone 2 (7,2′-dihydroxy-4′-methoxyisoflavanone), 10 μg/ml; 4, formononetin, 150 μg/ml; 5, isoflavanone 1 (7,4′dimethoxy-2′-hydroxyisoflavanone), 65 μg/ml; 6, medicarpin 100 μg/ml. (B) Typical chromatogram of an extract from infected groundnut leaves with peaks labelled as in (A). (C) Typical chromatogram of an extract from uninfected groundnut leaves showing traces of medicarpin only.

TABLE I

CONCENTRATIONS OF PHYTOALEXINS ACCUMULATED IN UNINFECTED AND INFECTED GROUNDNUT LEAVES (CV. EGRET) 18 DAYS AFTER INOCULATION WITH *CERCOSPORA ARACHIDICOLA*

Compound	Concentration (mean ± S.D., $n=5$) (μg/g fresh weight)	
	Infected	Uninfected
Daidzein	8.45 ± 3.98	5.48 ± 2.24
Demethylmedicarpin	57.50 ± 26.25	2.69 ± 2.48
Isoflavanone 2[a]	3.70 ± 1.84	0.37 ± 0.52
Formononetin	127.29 ± 7.79	4.79 ± 1.56
Isoflavanone 1[b]	53.82 ± 14.62	1.63 ± 1.32
Medicarpin	122.10 ± 25.75	14.32 ± 9.87

[a] Isoflavanone 2 was identified as 7,2′-dihydroxy-4′-methoxyisoflavanone by GC–MS of the TMSi derivative, co-chromatography by HPLC and matching of the UV spectrum with that of an authentic sample of the compound.
[b] Isoflavanone 1 was identified as 7,4′-dimethoxy-2′-hydroxyisoflavanone by GC–MS and LC–MS.

tin, 7,4′-dimethoxy-2′-hydroxyisoflavanone and medicarpin were prominent compounds in extracts of groundnut leaves (cv. Egret) infected with *C. arachidicola* and harvested 18 days later. Daidzein and 7,2′-dihydroxy-4′-methoxyisoflavanone were minor components. The phytoalexins were essentially absent from uninfected leaves apart from low concentrations of medicarpin (Fig. 3 and Table I).

Method 2, using solid-phase extraction, was as efficient as method 1 for the extraction of phytoalexins and more appropriate for the analysis of large numbers of samples (Table II). In tests of samples spiked with medicarpin, most of the compound

TABLE II

COMPARISON OF RECOVERY OF MEDICARPIN FROM LEAF EXTRACTS BY LIQUID–LIQUID AND SOLID-PHASE EXTRACTION

Treatment	Medicarpin (mean ± S.D., $n=3$) (μg/ml)
Liquid–liquid extraction (method 1)	
Unspiked sample [a]	12.55 ± 4.79
Spiked sample[b]	114.71 ± 4.68
Solid-phase extraction (method 2)	
Unretained eluate (unspiked)	0.00
Unretained eluate (spiked)	0.00
First ml of acetonitrile eluate (unspiked)	22.74 ± 5.57
First ml of acetonitrile eluate (spiked)	120.98 ± 5.65
Second ml of acetonitrile eluate (unspiked)	0.00
Second ml of acetonitrile eluate (spiked)	3.99 ± 3.92

[a] Unspiked samples were extracts of leaves which had been treated with silver nitrate (see text for details).
[b] Spiked samples were extracts of leaves which had been treated with silver nitrate and spiked with 100 μg of medicarpin (see text for details).

was eluted in the first millilitre of acetonitrile from the solid-phase cartridge and <4% in the second millilitre. In view of this result and the good recovery in the first millilitre of eluate a single millilitre would seem appropriate for routine work.

DISCUSSION

Accumulation of isoflavone and isoflavanone phytoalexins is a common response of legumes to challenge with phytopathogenic fungi [10,11]. The identification of the compounds reported in this paper (Fig. 2) was therefore not surprising although they contrast with the stilbenes elicited in groundnut cotyledons [12,13]. Formononetin, daidzein and 7,2′-dihydroxy-4′-methoxyisoflavanone are precursors of medicarpin [14,15], 4′-methylation of daidzein results in the formation of formononetin which is 2′-hydroxylated and reduced to the isoflavanone. Cyclisation of this compound leads to the formation of medicarpin. In contrast, demethylmedicarpin by analogy with the demethylation of pisatin [2] and comparison with the modification of medicarpin by the fungus, *Ascochyta rabiei* [16], is probably a degradation product.

With regard to the techniques described in this paper, the use of flash chromatography was a helpful first stage in the purification of phytoalexins and resulted in fractions containing one to five compounds. These were easily separated on semipreparative HPLC with an isocratic mobile phase. For the routine analysis of phytoalexins in small samples from infected groundnut leaves, solid-phase extraction proved to be a practical and reliable alternative to liquid–liquid extraction. Although reasonable separation was achieved on Sherisorb ODS 1 (10 μm) there is no doubt that the use of a smaller size of particle in the stationary phase would enhance resolution.

ACKNOWLEDGEMENTS

We would like to thank Annette Slade and Graham Wallace for their assistance with GC–MS and Dr. Ivor Lewis for LC–MS. This work was supported by the Commission of the European Communities under Contract No. TSD. A. 201 UK(H).

REFERENCES

1 J. W. Mansfield, in J. A. Bailey and J. W. Mansfield (Editors), *Phytoalexins*, Blackie, Glasgow, 1982, pp. 253–282.
2 H. D. VanEtten, D. E. Matthews and P. S. Matthews, *Ann. Rev. Phytopathol.*, 27 (1989) 143.
3 R. N. Strange, J. L. Ingham, D. L. Cole, M. E. Cavill, C. Edwards, J. C. Cooksey and P. J. Garratt, *Z. Naturforsch. C*, 40 (1985) 313.
4 N. T. Keen, *Phytopathology*, 68 (1978) 1237.
5 W. C. Still, M. Khan and A. Mitra, *J. Org. Chem.*, 43 (1978) 2923.
6 I. Smith (Editor), *Chromatographic Techniques*, Heinemann, London, 1958, p. 189.
7 A. L. Homans and A. Fuchs, *J. Chromatogr.*, 51 (1970) 327.
8 D. A. Smith and S. W. Banks, *Physiol. Pl. Pathol.*, 1 (1971) 41.
9 P. M. Dewick and M. J. Steele, *Phytochemistry*, 21 (1982) 1599.
10 U. Jaques, H. Klebman and W. Barz, *Z. Naturforsch. C.*, 42 (1987) 1171.
11 P. M. Dewick and M. Martin, *Phytochemistry*, 18 (1979) 591.
12 G. E. Aguamah, P. Langcake, D. P. Leworthy, J. A. Page, R. J. Pryce and R. N. Strange, *Phytochemistry*, 20 (1981) 1381.
13 C. J. Cooksey, P. J. Garratt, S. E. Richards and R. N. Strange, *Phytochemistry*, 27 (1988) 1015.
14 P. M. Dewick, *Phytochemistry*, 14 (1975) 979.
15 D. A. Smith and S. W. Blanks, *Phytochemistry*, 25 (1986) 979.
16 B. Kraft, L. Schwenen, D. Stockl and W. Barz, *Arch. Microbiol.*, 147 (1987) 201.

Journal of Chromatography, 547 (1991) 195–201
Elsevier Science Publishers B.V., Amsterdam

CHROM. 23 265

Liquid chromatographic analysis of cationic polymerized phenyl glycidyl ether

Š. PODZIMEK* and J. EICHLER
Research Institute for Synthetic Resins and Lacquers, CS-532 07 Pardubice (Czechoslovakia)
and
M. TKACZYK
Institute of Macromolecular Chemistry, Czechoslovak Academy of Sciences, CS-162 06 Prague (Czechoslovakia)
(First received August 7th, 1990; revised manuscript received March 6th, 1991)

ABSTRACT

Products of cationic polymerization of phenyl glycidyl ether were analysed by gel permeation chromatography and high-performance liquid chromatography. Individual oligomers were isolated by semipreparative high-performance liquid chromatography for the purposes of identification by mass spectrometry and gel permeation chromatography calibration. An equation for the conversion of the molecular weight of oligostyrene to that of oligophenyl glycidyl ether was derived. This equation was used for the determination of oligophenyl glycidyl ether molecular weight distribution by gel permeation chromatography. Molecular weight distribution curves of oligophenyl glycidyl ether samples were determined by high-performance liquid chromatography and gel permeation chromatography and compared.

INTRODUCTION

Cationic polymerization of the glycidyl (2,3-epoxypropyl) group represents an important curing reaction of epoxy resins. The term curing is used to describe the process by which one or more reactants, *i.e.*, an epoxide and a curing agent, are transformed from low-molecular-weight materials to a highly cross-linked network. The curing of the epoxy resins is based on the reaction between the epoxide molecules themselves, or the reaction between the epoxy group and other types of reactive molecules. The former is polymerization, and the latter is an addition reaction, but both result in coupling as well as cross-linking. A typical example of cationic polymerization of epoxy resins is the reaction with Lewis acids. Boron trifluoride can be used as a Lewis acid and is normally complexed with a Lewis base, *e.g.*, hydroxyl,

0021-9673/91/$03.50

thiol or amine. The polymerization of an epoxide in the presence of boron trifluoride hydrate can be expressed in a simplified form by the following scheme:

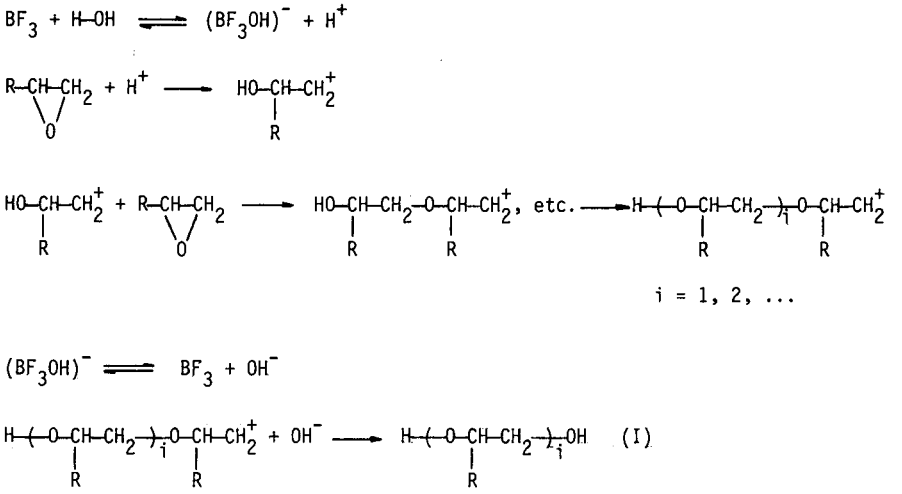

In the case of phenyl glycidyl ether (PGE), R = $-CH_2-O-C_6H_5$ and molecular weight is given by the equation:

$$M = 18 + 150i \tag{1}$$

PGE is a suitable model compound for diglycidyl ether of bisphenol A (DGEBA), as it is evident from their formulae:

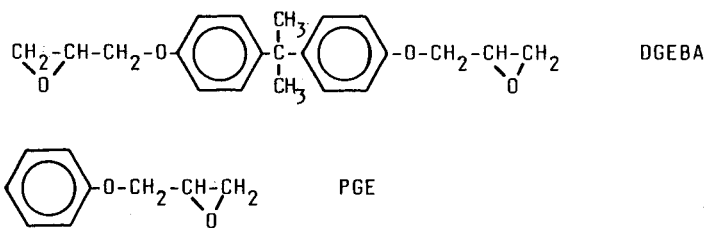

DGEBA-based epoxy resins are the most commonly used. PGE contains only one epoxy group in its molecule, and consequently the linear soluble products arise by its polymerization. Owing to their solubility, they can easily be analysed by liquid chromatography. Gel permeation chromatography (GPC) and high-performance liquid chromatography (HPLC) have been used many times for the characterization of DGEBA-based epoxies [1–4]. The reaction of commercial epoxy resin (Epon 815) or PGE with boron trifluoride isobutanol or triol (Voranol 2070) complex has been recently investigated by GPC, differential scanning calorimetry (DSC) and gas chromatography–mass spectrometry (GC–MS) [5]. It was found that the molecular weight of polymerized PGE decreased marginally with the decreasing amount of BF_3.

GC–MS study proved the presence of the cyclic dimer with a molecular weight of 300. DSC analysis of cross-linked epoxy resin showed that the degree of cross-linking increased with increasing BF_3, which was evident from the increasing glass transition temperature.

The aims of this work are (1) the finding of separation conditions for HPLC analysis of oligophenyl glycidyl ether (OPGE), (2) the calibration of GPC columns for this material and (3) the identification of major products arising during the reaction of PGE with boron trifluoride hydrate.

EXPERIMENTAL

Gel permeation chromatography and high-performance liquid chromatography

The Spectra-Physics SP 8100 liquid chromatograph was used for GPC and HPLC analyses. The eluents were monitored with an SP 8440 UV–VIS variable-wavelength detector at 270 nm (maximum of UV spectrum of 2,3-dihydroxypropyl phenyl ether). The SP 4200 computing integrator served for data handling. This system provides for automatic reporting and plotting of background-corrected UV spectra and absorbance ratios during the course of a chromatographic run.

A set of four Microgel (Chrompack) columns, 250 × 7.7 mm (50, 100, 500, 10^3 Å), was used for GPC analyses with tetrahydrofuran (THF) as the mobile phase. Polystyrene standards purchased from Polymer Labs. (nominal molecular weights 162, 580, 1250, 1800, 3600, 7600 and 9200) were used for the calibration of GPC columns. The columns were thermostated at 40°C.

The reversed-phase HPLC with gradient elution on THF–methanol–water was carried out using Separon SGX C_{18} stainless-steel columns packed with spherical octadecylsilica gel, particle size 7 μm (Tessek, Czechoslovakia).

The simplest method of evaluation of GPC data, assuming no dispersion, was used. A chromatographic curve was divided by drawing n vertical lines from the baseline to points on the curve. The areas of these slices were used for the computation of cumulative weight distribution:

$$I_w(M_j) = \sum_{i=1}^{j} A_i \Big/ \sum_{i=1}^{n+1} A_i \qquad (2)$$

where $I_w(M_j)$ is the value of cumulative weight distribution function at the point j. The molecular weight M_j corresponding to elution time at the point j was calculated from the calibration dependence of OPGE, which was derived from the calibration dependence of oligostyrene (OS) by means of eqn. 3.

To construct the distribution curves from HPLC chromatograms, the areas of peaks of byproducts eluting between oligomers i and $i + 1$ were added to the area of oligomer i. The resulting areas were introduced into eqn. 2. Molecular weights of individual oligomers were calculated from eqn. 1.

Mass spectrometry

All mass spectra were determined using an AEI double-focusing mass spectrometer operated through an MSS electronic console. Samples were emitted into the ion source by direct inlet. The source temperature was 180°C, ionization energy 70 eV, emission 100 μA, accelerating voltage 6 kV and scan-rate 8 s/decade.

Polymerization of PGE

Polymerization of PGE was induced by 2–4% curing agent containing 10% BF_3, 21.6% water and 68.4% polyethylene glycol (PEG) 300. The polymerization was performed in bulk at the room temperature.

RESULTS AND DISCUSSION

Representative GPC and HPLC patterns of the same product of cationic polymerization of PGE are shown in Figs. 1 and 2. The gradient profile used for the analysis ensures at least partial separation of approximately twenty oligomers, which usually represents *ca.* 95% of molecules in the analyzed samples. With increasing polymerization degree, the resolution between the neighbouring oligomers decreases, as is usual in HPLC separations of oligomeric series, where restricted diffusion within the pores of the column packing and possible effects of molecular conformation contribute to band broadening of the large molecules of higher oligomers [6].

The compounds belonging to the peaks 1–13 were isolated by semipreparative HPLC (Fig. 3), and the purity of the fractions was verified by analytical HPLC (Fig. 4) under the same conditions as those used in Fig. 2. The overlap of the chromatograms in Fig. 4 with that in Fig. 2 shows that fractions obtained by semipreparative HPLC do not contain perceptible amounts of neighbouring oligomers and are suitable for GPC calibration. Compounds 1–4 were analyzed by mass spectrometry. The molecular weights of these compounds were 168, 318, 468 and 618, which correspond to the products according to formula I. Eight of the most intensive fragment ions that were

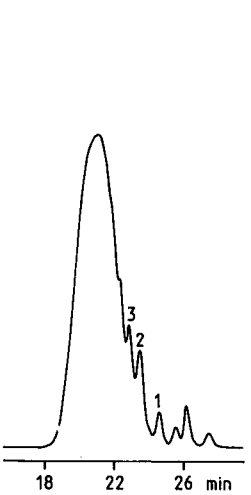

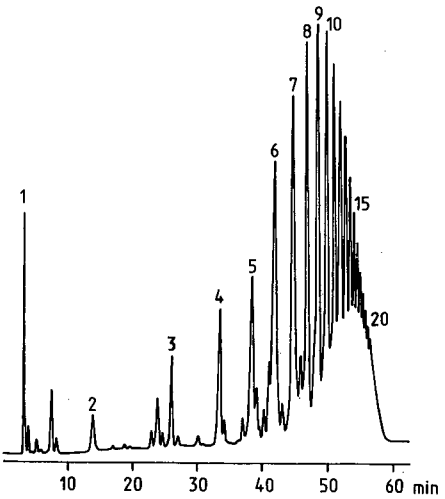

Fig. 1. GPC trace of the product of cationic polymerization of PGE. Columns, Microgel 50, 100, 500 and 10^3 Å (250 × 7.7 mm); mobile phase, THF; flow-rate, 1 ml/min; detection, UV at 270 nm; sample size, 10 μl (0.35% in THF). Peaks 1, 2, 3 = oligomers according to formula I.

Fig. 2. HPLC trace of the product of cationic polymerization of PGE. Column, Separon SGX C_{18} (250 × 4 mm); solvent gradient, THF–methanol–water (55% methanol in water from 0 to 5 min, then linear gradient to 30% THF in methanol for 50 min, 30% THF in methanol from 55 to 65 min); detection, UV at 270 nm; sample size, 10 μl (1.4% in THF). Peaks 1, 2, ... = oligomers according to formula I.

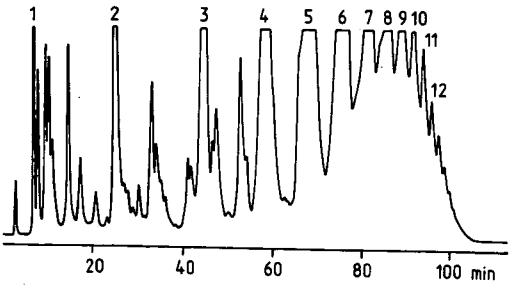

Fig. 3. Semipreparative HPLC trace of OPGE. Column, Separon SGX C_{18} (250 × 8 mm); solvent gradient, THF–methanol–water (55% methanol in water from 0 to 10 min, then linear gradient to 30% THF in methanol for 100 min); flow-rate, 2 ml/min; detection, UV at 254 nm; sample size, 100 μl (70% in THF). Peaks 1, 2, ... = oligomers according to formula I.

detected in the mass spectra of compounds 1–4 are summarized in Table I. Identity of the compound 1 was also confirmed by the same retention times and UV spectra of this substance and pure 2,3-dihydroxypropyl phenyl ether, which was prepared according to the procedure described in ref. 7. Similarly, the next major peaks (5, 6, 7, ...) may be assigned to the oligomers according to formula I.

Peaks of other substances which were not identified occur in the chromatograms, but their concentrations are small. It is possible that these peaks represent another oligomer range, *e.g.*, oligomers with PEG incorporated in the chain or cyclic oligomers formed by backbiting, etc. The identification of these products is not the aim of this work.

The GPC calibration curve of the oligomers of PGE is shown in Fig. 5 together with the calibration curve of OS. The OPGE calibration curve was obtained by relating the logarithms of molecular weight to the elution times of oligomers 1–13 which were isolated by semipreparative HPLC. A very good correlation of this dependence supports the proposed oligomer structure. The relationship

$$M_{\mathrm{OPGE}} = 0.312104 M_{\mathrm{OS}}^{1.153284} \tag{3}$$

was derived by comparing the calibration dependences of OPGE and OS. The

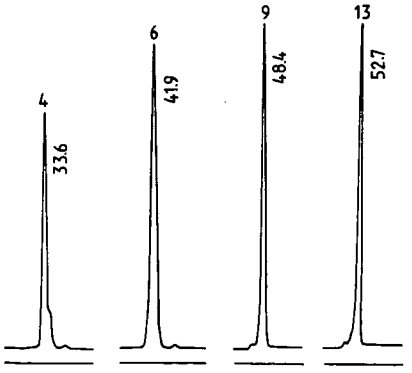

Fig. 4. HPLC traces of fractions isolated by semipreparative HPLC. Conditions as in Fig. 2.

TABLE I

EIGHT OF THE MOST INTENSIVE FRAGMENT IONS IN MASS SPECTRA OF COMPONENTS 1–4

Component	*m/z* (relative abundance)							
1	65 (6)	77 (19)	78 (6)	94 (100)	95 (13)	107 (7)	108 (8)	168 (26)
2	57 (28)	77 (65)	94 (100)	95 (23)	107 (64)	121 (26)	133 (66)	318 (39)
3	57 (14)	77 (33)	94 (32)	107 (44)	119 (29)	121 (20)	133 (100)	134 (14)
4	77 (26)	107 (38)	119 (23)	133 (100)	169 (33)	193 (40)	207 (26)	319 (37)

relationship (eqn. 3) is valid for THF, 40°C and the molecular weight range 168–1968. The extrapolation of eqn. 3 to higher molecular weights, where only OS standards are available, may be permitted to determine the molecular weight distribution of OPGE by GPC.

The cumulative weight distribution curves of the OPGE sample (the chromatograms in Figs. 1 and 2) determined by GPC and HPLC are shown in Fig. 6. The agreement of both distribution curves is evident. If the chromophoric properties of some compounds were significantly different from the others then the distribution curves would be incorrect. As the detections at other wavelengths (254, 280 nm) give practically the same relative areas of oligomer peaks in HPLC profiles as that at 270 nm, we do not suppose the presence of a significant amount of compounds with considerable different chromophoric characters, and therefore any gross errors in the obtained distribution curves are improbable.

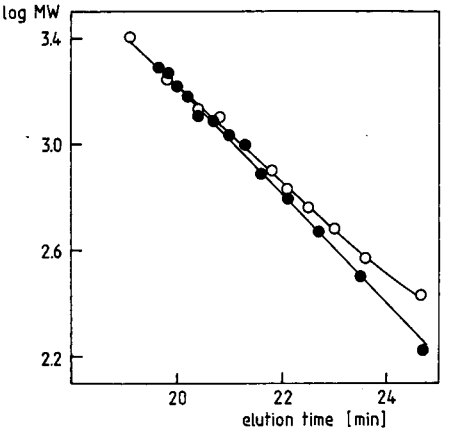

Fig. 5. GPC calibration curves of the oligomers of PGE (●) and OS (○) for Microgel columns 50, 100, 500 and 10^3 Å (250 × 7.7 mm) in THF at 40°C. Flow-rate, 1 ml/min. MW = Molecular weight.

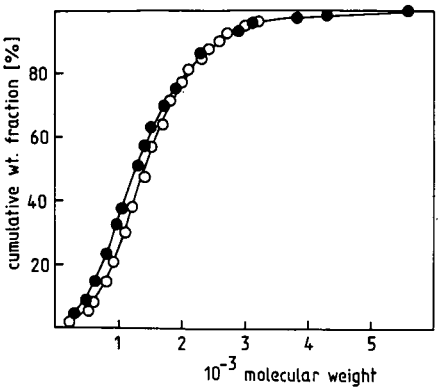

Fig. 6. Cumulative weight distribution curves of the OPGE sample determined by GPC (●) and HPLC (○).

CONCLUSIONS

GPC and HPLC enable detailed characterization of the products of cationic polymerization of PGE and can be used as suitable methods to study the influence of reaction conditions on the composition of the resulting products. OS can be used as a calibration standard for GPC and an OS calibration curve can be converted to the calibration curve of oligomers based on PGE by means of eqn. 3. The molecular weight distribution curves determined by GPC and HPLC are in very good agreement. The described calibration procedure, *i.e.*, the isolation of individual oligomers by semipreparative HPLC and finding the conversion equation based on OS, can be used as a general calibration method for oligomers.

REFERENCES

1 H. Batzer and S. A. Zahir, *J. Appl. Polym. Sci.*, 19 (1975) 585.
2 G. L. Hagnauer, *Ind. Res. Dev.*, 23 (1981) 128.
3 D. R. Scheuing, *J. Coat. Technol.*, 57 (1985) 47.
4 G. Eppert, G. Liebscher and C. Stief, *J. Chromatogr.*, 238 (1982) 385.
5 A. J. Ryan, U. R. Vaidya, W. Mormann and C. W. Macosko, *Polym. Bull.*, 24 (1990) 521.
6 L. R. Snyder and M. A. Stadalius, in Cs. Horváth (Editor), *High-Performance Liquid Chromatography —Advances and Perspectives*, Vol. 4, Academic Press, Orlando, FL, 1986, p. 195.
7 V. Ulbrich, J. Makeš and M. Jureček, *Collect. Czechoslov. Chem. Commun.*, 29 (1964) 1466.

Journal of Chromatography, 547 (1991) 203–210
Elsevier Science Publishers B.V., Amsterdam

CHROM. 23 304

Analysis of fulvic acids by ion-pair chromatography

B. SMITH
The British Geological Survey, Keyworth, Nottingham (UK)
and
P. WARWICK*
Department of Chemistry, Loughborough University of Technology, Loughborough, Leicestershire LE11 3TU (UK)
(First received November 19th, 1990; revised manuscript received March 5th, 1991)

ABSTRACT

Ion-pair chromatography, using tetrabutyl ammonium hydroxide and a reversed-phase column, has been applied to the analysis of groundwater in order to demonstrate the usefulness of the technique in the investigation of dissolved organic matter. Results show that fulvic acid, present in groundwater, can be separated into a number of naturally occurring organic constituents. Chromatograms obtained from fulvic acid that was extracted from the groundwater using DEAE cellulose were very similar to those obtained from the groundwater. Ion-pair chromatography is therefore useful for investigating the components that constitute fulvic acid which may be present in groundwater or extracted from the groundwater. Metal complexation studies can also be investigated by ion-pair chromatography.

INTRODUCTION

Fulvic acids are a heterogeneous class of naturally occurring compounds which constitute a large proportion of dissolved organic matter in groundwater. They are important because of their ability to bind with and mobilise metal species and anthropogenic organic species [1,2]. The heterogeneous nature of these compounds means that, even within a sample of fulvic acid, there is a distribution of molecular size and charge [3,4]. Studies on these distributions, and their importance to (say) metal binding have been hindered by a lack of suitable analytical techniques. Chromatographic separations of components within a fulvic acid sample have been attempted and these have given some insight into the importance of the components that make up fulvic acid. Size-exclusion chromatography has been extensively used to investigate the size distribution of the molecules [5–7] but, this technique gives little information on the components within a fulvic acid sample. High-performance ion chromatography has been used to separate many naturally occurring organic molecules, but its application to fulvic acid analysis is severely limited due to the high affinity of the resin for acidic groups present in the fulvic molecule. Reversed-phase chromatography has been used to analyse fulvic acids using conventional bonded reversed-phase packings and UV and fluorescence detection [8–10]. Reversed-phase chromatography has also been

0021-9673/91/$03.50

used to fractionate a sample of fulvic acid into five molecular weight ranges and to investigate the effect of molecular weight on the hydrophilicity of the fulvic acid [11]. This chromatographic technique has also been attempted using a microcolumn [12]. Combinations of ion-suppression and reversed-phase chromatography using 1% acetic acid in a water–methanol–acetonitrile mixture have been used to fractionate fulvic acids into hydrophobic and hydrophilic fractions. These studies have generally provided chromatograms of poor resolution because, within the pH range of the suppression for silica bonded columns, fulvic acids are highly charged and would also be excluded from the column packing material by steric effects. Recent work on ion-suppression chromatography [8] has shown that better resolution was obtained when using ion-suppression (pH 4.0) and a Novapak column.

This work describes the application of ion-pair chromatography together with a wide pore polymeric reversed-phase column packing and diode array detection for the analysis of naturally occurring high-molecular-weight organics. As far as the authors are aware this is the first reported application of this technique to the analysis of this type of material.

In ion-pair/reversed-phase chromatography a hydrophobic counterion is added to the mobile phase. This counterion dynamically interacts with the solvated acid and stationary phase to produce an ion pair that has significantly more hydrophobic character than that of the original acid. Such reagents have been routinely used in the analysis of low-molecular-weight organic acids [13]. However, a literature search has not revealed their use for the separation and characterisation of humic and fulvic acids. The major advantage of ion-pair chromatography over ion-suppression chromatography is that near neutral pH conditions may be maintained thus limiting the effect of pH changes on both the stationary phase and solvated molecule.

EXPERIMENTAL

Instrumentation

A Waters Model 600E low pressure mixing quaternary solvent delivery system equipped with semi-preparative pump heads was used. All experiments were performed using a 25 cm × 4.6 mm I.D. Polymer Labs. PLRP-S (300 Å) fitted with a PLRP-S reversed-phase guard column. Samples were introduced into the column by a Waters Wisp 712 autoinjector. The eluate was monitored for UV absorbance using a Waters 990 photodiode array detector. This enabled the UV absorbance of the mobile phase to be determined over the wavelength range 200 to 400 nm.

Materials

Mobile phases of water–acetonitrile mixtures were purchased from Romil Chemicals and were far UV HPLC grade. Tetrabutyl ammonium hydroxide in phosphate buffer was purchased from Fison Scientific and was used as the ion-pair reagent in the separations described below. The concentration of the ion pair reagent in HPLC water was 0.005 *M*. All mobile phases were prefiltered (0.45 μm Nylopore) and degassed with helium before use.

Groundwater taken from a shallow sand aquifer at Drigg in Cumbria was filtered through 0.45 μm Nylopore filter before use. The chemical analysis of the groundwater has been reported [14]. The effects of fulvic acid concentration, and

ionic strength of the groundwater, on the separation were investigated by rotary evaporating a sample of the groundwater to ten times concentration at 35°C (× 10 groundwater).

In order to examine the effects of extracting fulvic acids from the groundwater on chromatographic separation, DEAE cellulose was used to extract fulvic acid from the groundwater [15].

METHOD DEVELOPMENT

Isocratic elution

To investigate the usefulness of isocratic elution and to optimize chromatographic conditions for subsequent gradient elution, chromatograms were run with binary mobile phases consisting of 80:20, 60:40, 40:60 and 20:80, acetonitrile–ion pair solution. The mobile phase flow-rate used in these separations was 1 ml/min. A volume of 20 μl of × 10 Drigg groundwater was injected into the column and the eluate monitored by the photodiode array detector. In order to determine the elution time of non-retained material, HPLC water was injected into the column and detected by the resulting refractive index change in the eluate.

The results of these experiments are summarised in Table I which shows that the retention time of the injected material increases as the concentration of acetonitrile in the mobile phase is lowered. This is consistent with a hydrophobic interaction between the stationary phase and the injected material. With a mobile phase consisting of acetonitrile–ion pair reagent (80:20) retention is strong enough to prevent elution of the more non-polar components. The best mobile phase composition to allow isocratic separation of the components of Drigg groundwater appears to lie between acetonitrile–ion pair reagent (40:60) and acetonitrile–ion pair reagent (20:80).

TABLE I

RESULTS OF CHANGES IN MOBILE PHASE COMPOSITION

Mobile phase composition acetonitrile–ion pair (%)	t_R solvent front (min)	t_R sample peaks (min)
80:20	3.2	3.0
60:40	3.2	3.0, 3.4
40:60	3.2	4.4, 6.6, 8.4, 17
20:80	3.2	6.0

Gradient elution

To obtain greater resolution near the solvent front and to elute strongly retained material, gradient elution was used. Best separation of the components in × 10 groundwater was achieved using the mobile phases and the gradient solvent profiles shown in Fig. 1. The chromatogram contains six UV absorbing maxima with retention times of 3.2, 4.58, 5.52, 10.18, 13.36 and 17.62 min, labelled A to F in the figure. Complete resolution of fulvic acids are unlikely because of the intrinsic heterogeneity of such materials [3,4]. The UV absorption spectra of each eluted peak showed that

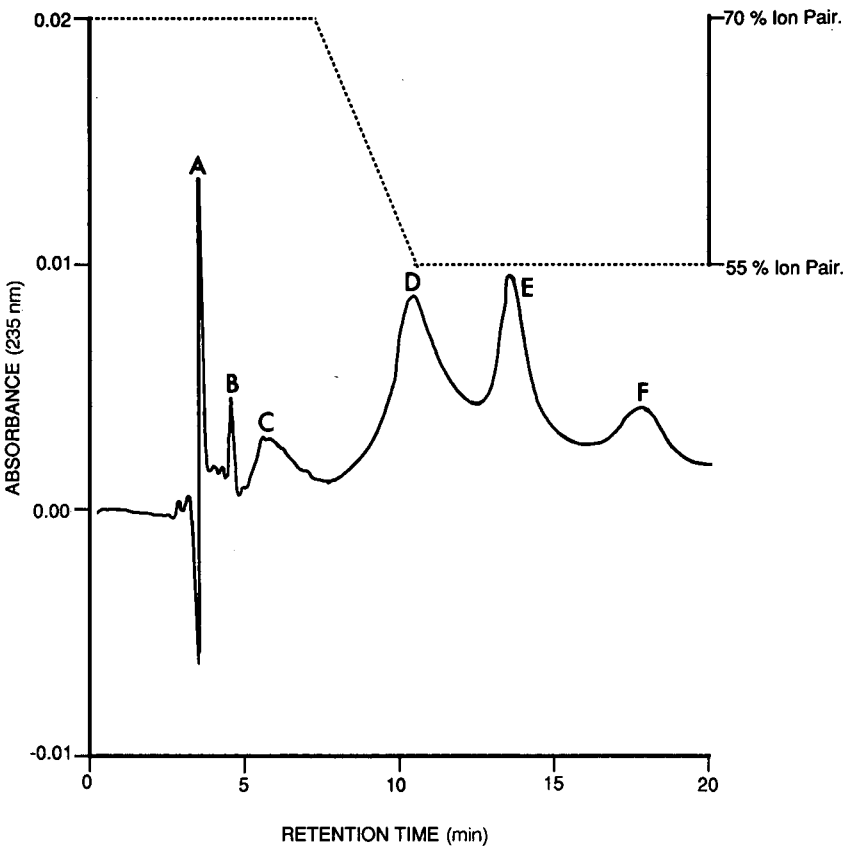

Fig. 1. Chromatogram obtained by the binary separation of × 10 groundwater at a monitoring wavelength of 235 nm.

peaks C, D, E and F were typical of fulvic materials [16] whereas the spectrum observed from peak B was clearly not. To check the reproducibility of the separation, aliquots of the same sample were injected onto the column. The resulting chromatograms were identical.

A volume of 20 μl of HPLC-grade distilled water was injected in to the column in order to observe the UV absorption of the mobile phase as its composition changes with time. The resulting chromatogram showed a peak with a similar retention time to peak A in Fig. 1. This absorption peak is probably due to a refractive index change of the eluate as suggested by its absorption spectrum.

Fig. 2 and 3 are chromatograms obtained by injecting 200 μl of unconcentrated groundwater and 20 μl of extracted fulvic acid in HPLC water (100 μg ml^{-1}). The chromatograms observed from the separations of the groundwater and the extracted material are almost identical to the chromatogram observed from the × 10 groundwater except for the peak (B) at an elution time of 4.58 min. In Fig. 3 this peak is absent. The UV absorption spectrum of this peak indicates that this component is not

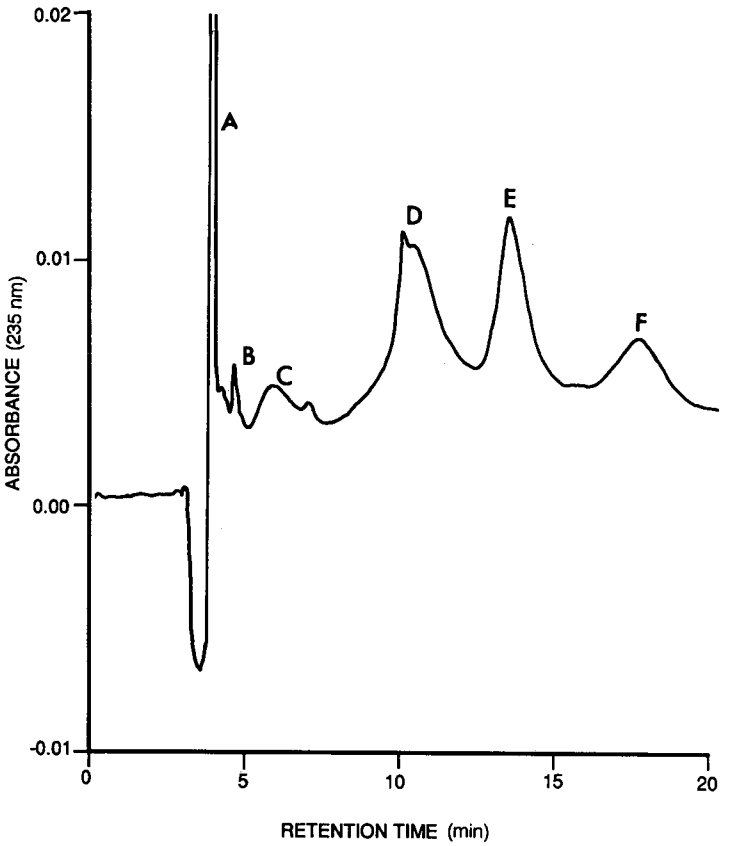

Fig. 2. Chromatogram obtained by the binary gradient separation of 200 μl of unconcentrated groundwater at a monitoring wavelength of 235 nm.

fulvic material and is probably due to the presence of inorganic species in the samples. Further evidence for peak identification was gained from treating × 10 groundwater with DEAE-cellulose and filtering (0.45 μm filter) the treated groundwater before separation on the column. Fig. 4 shows the chromatogram of DEAE treated × 10 groundwater. The separation shows clearly that the fulvic material (peaks C, D, E and F) is extracted from the groundwater, whereas the component which produces peak B is not removed from the water by this treatment. Groundwater was filtered through an Amicon YC05 membrane filter (500 Dalton cut-off) before injecting a sample of the filtrate in to the column. The resulting chromatogram showed the presence of peak B at the same retention time as that observed in Fig. 1. The peaks assigned to Fulvic acids were absent in this chromatogram. The increase in baseline absorbance occurring between 8 and 10 minutes occurs due to changes in the UV absorption of the mobile phase. Superimposed on this increase is a small peak that appears to be due to concentration and subsequent elution of a hydrophobic contaminant present in the mobile phase.

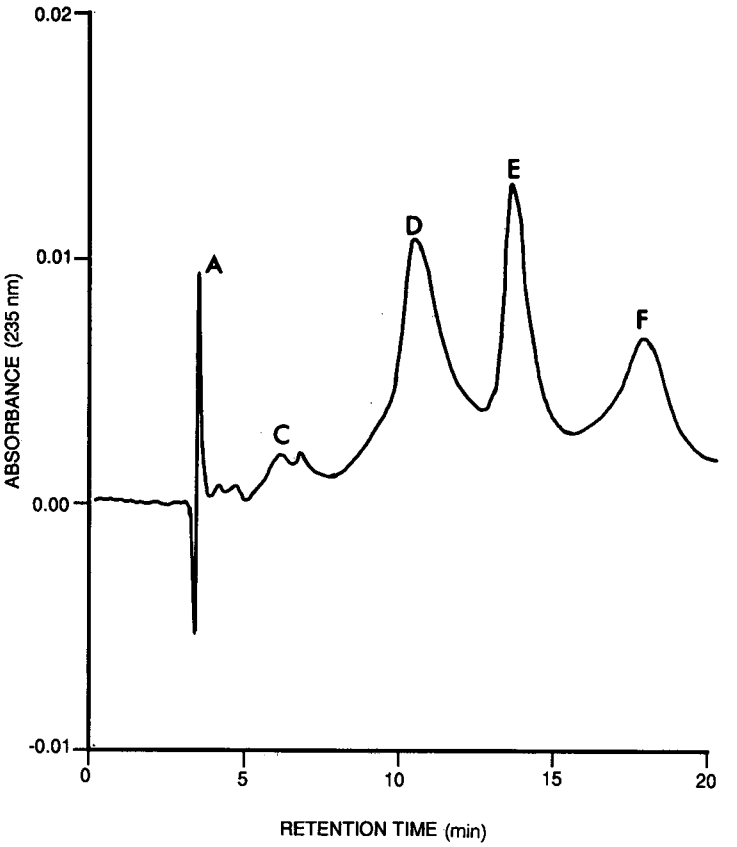

Fig. 3. Chromatogram obtained by the binary gradient separation of 20 μl of extracted fulvic acid in HPLC water (100 μg ml^{-1}) at a monitoring wavelength of 235 nm.

To illustrate the possible use of ion-pair chromatography in metal complexation studies a sample of $\times$ 10 groundwater that had been equilibrated with radioactive ^{57}Co was injected onto the column. The eluate was monitored for UV absorbance and fractions were collected at 1-min intervals for radiometric analysis. The results of this study show a close association of eluted ^{57}Co with peaks assigned as fulvic material and suggests that this methodology may be used to study the association of metals with components of fulvic acids without the need to extract the fulvic material from the groundwater.

CONCLUSIONS AND DISCUSSION

Ion-pair chromatography using a large pore stationary phase has been successfully applied to the analysis of fulvic acids in natural and concentrated groundwater samples. The method separates the organic species present in the groundwater into a number of well resolved components, the majority of which have a molecular weight

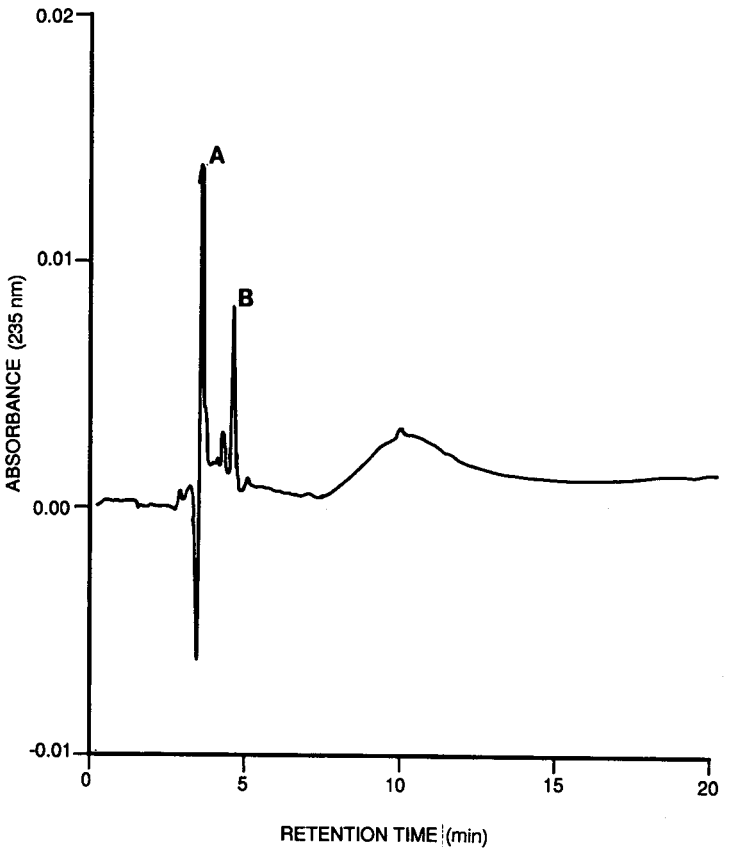

Fig. 4. Chromatogram obtained by the binary gradient separation of 20 μl of DEAE treated × 10 groundwater monitored at a wavelength of 235 nm.

of greater than 500 daltons. Separations obtained have been qualitatively analysed using a diode array spectrophotometer. The components in excess of 500 daltons show UV absorption spectra similar to humic and fulvic acids [16] whereas the component with a molecular weight of less than 500 daltons shows a sharp UV cutoff at 230 nm. It was noted that this component was not removed when the groundwater was passed through DEAE cellulose. The chromatographic separation of × 10 groundwater equilibrated with ^{57}Co has been carried out and results show that Co is associated with fulvic acid present in the groundwater.

Rotary evaporation is an efficient non-invasive method of concentrating the components in groundwater. The large (× 10) difference in the ionic strength of these injected samples does not appear to adversly effect the chromatography, indicating that equilibration of the sample with the mobile phase is rapid.

Further development work is in progress to investigate the use of ion-pair chromatography to study the extraction of organic material from groundwater.

ACKNOWLEDGEMENTS

The paper is published by permission of the Director of the British Geological Survey (Natural Environmental Research Council). This work was funded by the European Communities as part of the MIRAGE project.

REFERENCES

1 S. Boggs, D. Livermoor and M. G. Seitz, Argonne National Laboratory, Argonne, IL, *Report ANL-84-78*, 1985, p. 108.
2 J. Buffle, *Complexation Reactions in Aquatic Systems, An Analytical Approach*, Ellis Horwood, Chichester, 1988.
3 G. R. Aitken, in G. R. Aitken, D. M. McKnight, R. L. Wershaw and P. MacCarthy (Editors), *Humic Substances in Soil, Sediment and Water*, Interscience, New York, 1985, p. 692.
4 E. M. Thurmann, *Organic Geochemistry of Natural Waters*, Martinus Nijhoff and Dr. W. Junk Publishers, Dordrecht, 497 pp.
5 M. L. Adamic and D. E. Bartak, *Anal. Chem.*, 57 (1985) 279.
6 Y. Saito and S. Hayano, *J. Chromatogr.*, 177 (1979) 390.
7 C. Miles and P. L. Brezonik, *J. Chromatogr.*, 259 (1983) 499.
8 F. Y. Saleh, W. A. Ong and D. Y. Chang, *Anal. Chem.*, 61 (1989) 2792.
9 F. Y. Saleh and D. Y. Chang, *Sci. Total Environ.*, 62 (1987) 67.
10 G. P. Cartoni and F. Coccioli, *J. Chromatogr.*, 360 (1986) 225.
11 K. Hayase and H. Tsubota, *J. Chromatogr.*, 295 (1984) 530.
12 A. Hirose and D. Ishii, *J. High Resolut. Chromatogr. Chromatogr. Commun.*, 9(9) (1986) 533.
13 A. Braithwaite and F. J. Smith, *Chromatographic Methods*, Chapman and Hall, Ltd., New York, (1985).
14 G. M. Williams, J. J. W. Higgo, M. A. Sen, D. J. Noy and P. Warwick, *Radiochim. Acta*, (1990) in press.
15 M. E. Stuart, A. D. Bradley, B. Smith and D. Peachey, *Brit. Geol. Survey Technical Report WE/89/45*, 1990.
16 K. Ghosh and M. Schnitzer, *J. Soil Sci.*, 30 (1979) 735.

Journal of Chromatography, 547 (1991) 211–223
Elsevier Science Publishers B.V., Amsterdam

CHROM. 23 318

The speciation of iron, manganese, phosphorus and platinum in aqueous solutions by using ion chromatography coupled with an element selective detector

ISAI T. URASA*, WARD J. MAVURA, VALERIE D. LEWIS and SANG HO NAM
Department of Chemistry, Hampton University, Hampton, VA 23668 (USA)
(First received October 3rd, 1990; revised manuscript received March 21st, 1991)

ABSTRACT

A method is described that employs ion chromatography in combination with d.c. plasma atomic emission spectroscopy to speciate iron, manganese, phosphorus and platinum in aqueous solutions. The element selective nature of the d.c. plasma allows its use as a chromatographic detector for all species of a targeted element eluting from a chromatographic column. This procedure is not only insensitive to matrix effects but is also suitable for monitoring element transformation that can occur as a result of biological or chemical changes.

INTRODUCTION

The fundamental objective in element speciation is to identify and quantify the various forms of a targeted element in a sample. The analytical data obtained in this kind of procedure is important in the evaluation of the impact of the element on biological and environmental systems.

The existence of an element in more than one form may be due to the chemistry of that element (many transition metals can exist in nature in two or more oxidation states, manifesting quite different chemical properties); biological and/or chemical activities which may cause the element to be transformed into a different form; or man-made sources, such as industrial discharges, which may introduce into the environment a form of the element which may not have been there originally. Generally, the concentration of these species is very small so that they can only be detected by analytical techniques and methodologies having detection capabilities for low ppb concentration ranges or less.

The employment of metal species in clinical and pharmaceutical processes has considerably accelerated the development of methods which are suitable for analytical measurements in complex matrices. Every aspect of analytical chemistry has been explored in the search for efficient speciation procedures, including electrochemical [1–9], spectroscopic [10–14], chromatographic [13–17], and a combination of these techniques [18–27]. While some of these techniques have been proved to have suitable

0021-9673/91/$03.50

features for speciation work, an ideal speciation method is defined as one which can provide the desired information without altering the original sample in any way. While, in principle, techniques such as element selective electrodes have this property, they are limited by their inability to respond to all the species that might be present with good measurement sensitivity.

In the absence of such a method, the approach which appears to be most suitable for preserving analyte integrity is the one which can physically separate the species which are present and then quantify them independently. Such an approach has been employed in several laboratories, whereby chromatographic systems have been interfaced with a detector that only responds to the species of a targeted element in the sample [28–41]. In this way, all the chemical entities containing the element of interest are measured with equal efficiency. In our approach, d.c. plasma atomic emission is used as an element selective method for the detection of ion chromatographic effluents [37–41].

The use of d.c. plasma atomic emission as an element selective method of detection was first reported by Uden *et al.* who employed it in the detection of transition metal complexes separated with high-performance liquid chromatography [28]. Direct current plasma atomic emission spectroscopy has an inherent advantage in that all forms of a given element are equally excited when introduced into the excitation zone of the plasma; and that the analytical signal obtained is only based on the atoms of the targeted element. Furthermore, even when different mobile phase systems are used, representing a different sample matrix, the effect on the signals obtained are negligible. Thus, whether the element species is anionic, cationic, or neutral, the signal obtained is based only on the atomic concentration of the element.

The work presented in this paper was based on employing this approach to study the behavior of iron, manganese, platinum, and phosphorus and to evaluate the factors that influence their speciation in aqueous solutions. These elements were chosen because of their importance in biological and environmental processes. As with many other elements which can exist in more than one form, their chemical activities and their impact on biological systems are highly influenced by the form in which they exist. The data presented here can serve as a model for developing analytical measurement protocols for speciating similar elements, in particular heavy metals.

EXPERIMENTAL

Our objective was to develop speciation procedures for iron, manganese, platinum and phosphorus by using ion chromatography in combination with a d.c. plasma atomic emission spectrometer. The ion chromatograph was used to separate species of these elements in solution, while the d.c. plasma was used as an element selective detector for the ion chromatograph. The chromatographic effluents were monitored by measuring the atomic emission of each element at a selected wavelength. In this way, all the chromatographic effluents containing that element were detected with equal efficiency.

Equipment

The chromatographic system used consisted of an ion chromatograph, Dionex Model 2010i (Dionex, Sunnyvale, CA, USA) equipped with a conductivity detector

Model CDM-1, and the following separator columns: cation separator column, Model HPIC-CS2, and HPIC-CS5; and an anion separator column, Model HPIC-AS5. All separator columns were used with corresponding guard columns.

The detector consisted of a three electrode d.c. plasma atomic emission spectrometer, Model Spectraspan IV (Applied Research Instruments). Interfacing of the chromatograph and the d.c. plasma system has been described elsewhere [38].

Reagents and chemicals

Chemicals and other materials used included ACS certified ferrous ammonium sulfate, ferric nitrate, manganous chloride, potassium permanganate, sodium bicarbonate, oxalic acid, all from Fisher Scientific (Fairlawn, NJ, USA). Hydrogen hexachloroplatinate(IV) hydrate, and trilithium citrate were obtained from Aldrich Chemicals (Milwaukee, WI, USA). Redistilled hydrochloric acid and double-distilled nitric acid were obtained from GSF Chemicals (Columbus, OH, USA). A Nanopure II water purification system from Sybron (Boston MA, USA), was used in the preparation of deionized (18-MΩ) water. Sodium phosphate was obtained from Mallinckrodt (Paris, KY, USA) and adenosine triphosphate, adenosine diphosphate and adenosine monophosphate were obtained from Sigma Chemicals (St. Louis, MO, USA).

General procedure

Characterization of the solution chemistry of the elements studied in this work relied on the use of standard solutions. Analytical solutions were prepared by the dilution of appropriate volumes of 1000 ppm of Fe(II) (ferrous ammonium sulfate; Fe(III) (ferric nitrate); Mn(II) (manganous chloride); Mn(VII) (potassium permanganate); and Pt (IV) (hydrogen hexachloroplatinate(IV) hydrate. In each case, solutions were prepared in 0.1 *M* hydrochloric acid.

Samples were injected onto the chromatographic column with a 1.0-ml injection loop. The mobile phase flow-rate was kept constant at 2.0 ml per min.

Chromatographic effluents were detected by measuring the atomic emission signal of the element of interest at the respective wavelengths shown in Table I.

The chromatography was monitored using commercially obtained chromatographic software which gave data on peak areas, peak height, retention time, and the fraction of the species present. In the case of iron, the data obtained with the element selective detector approach was compared with that obtained with the classical 1,10-phenanthroline method. Measurements involving phosphorus were carried out using both the d.c. plasma approach and a conductivity detector.

TABLE I

ELEMENTS AND WAVELENGTHS USED

Element	Wavelength (nm)
Iron	373.4
Manganese	403.0
Phosphorus	213.6
Platinum	204.9

RESULTS AND DISCUSSION

Speciation of iron

In aqueous solutions, iron can exist as hexaaquairon(II) ($Fe(H_2O)^{2+}_6$), or hexaaqua iron(III) ($Fe(H_2O)^{3+}_6$), depending on the prevailing solution conditions. Since Fe(II) is the form that is more readily available to biological functions, it is important to not only know the actual concentrations of this species present in a sample, but also to be able to monitor the transformation that it may undergo. The ability to separate and quantify the iron species in which we are interested by using a detector sensitive only to iron avoids errors associated with methods that rely on the conversion of one form into the other before quantitation, such as the 1,10-phenanthroline method.

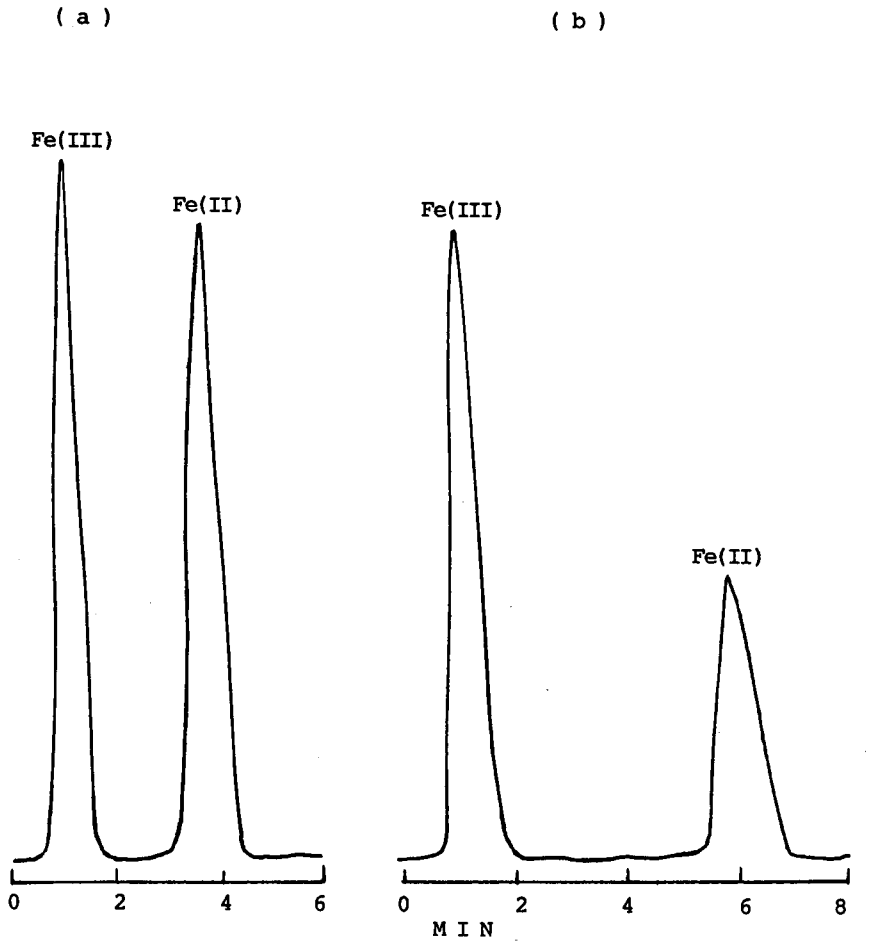

Fig. 1. Ion chromatographic separation of Fe(II)–Fe(III) obtained with d.c. plasma atomic emission spectroscopy detection; sample = 5 ppm Fe(II)–5 ppm Fe(III). (a) Eluent = 10 m*M* oxalic acid–7.5 m*M* trilithium citrate; and (b) eluent = 5.0 m*M* oxalic acid–3.75 m*M* trilithium citrate.

The chromatograms shown in Fig. 1 were obtained by injecting equal concentrations of iron(II) and iron(III) and monitoring the effluent by measuring the atomic emission of iron at 373.4 nm. The resolution between the two peaks is dependent on the concentration of the mobile phase.

This factor can be manipulated to shorten the analysis time, as required without compromising the quality of the analytical signal obtained, as can be seen in Fig. 1b. The analytical signal obtained is based on the atom population of the central metal; in this case, iron. In this way, only one analytical curve is required in the determination of both iron(II) and iron(III) species present in the sample. The analytical curves obtained for the two iron species have practically identical slopes with correlation coefficients greater than 0.9999.

Because an element selective detector responds only to the targeted element in the chromatographic effluent, it is useful in monitoring *in situ* chemical and biological changes that a sample or component of a sample may undergo. This is demonstrated in Fig. 2 which represents the oxidation of Fe(II) in dilute nitric acid. The oxidation process was monitored by injecting a small sample of the solution mixture onto a

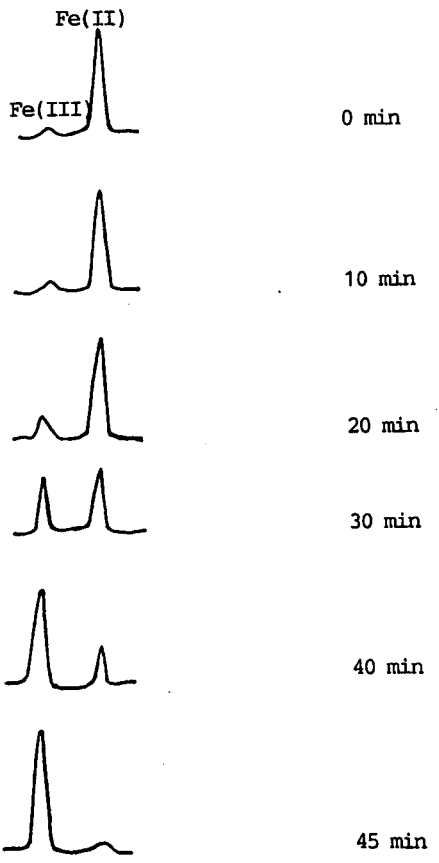

Fig. 2. Oxidation of Fe(II) in 0.5 *M* nitric acid monitored with ion chromatography–d.c. plasma atomic emission spectroscopy; sample = 1.0 ppm Fe(II); eluent = 10 m*M* oxalic acid–7.5 m*M* trilithium citrate.

cation chromatographic column and measuring the atomic emission signal obtained every several minutes. Such measurements are made possible by two features of the element selective detector approach: (1) the ability to measure species of the same element with equal efficiency; and (2) the ability to monitor these species independently without having to convert one into the other. This method is suitable for monitoring biological activity in which metal ions are involved.

The element selective detector approach for the determination of iron species was compared with the classical 1,10-phenanthroline method for the determination of iron. In this method, iron(III) is first converted into iron (II), which is then complexed with the 1,10-phenanthroline ligand, forming a colored complex. When comparing these two methods, not only is the 1,10-phenanthroline method less sensitive as is shown in Table II, but the necessity to first reduce iron(III) into iron(II) makes the method tedious, and more susceptible to errors.

Solution chemistry of manganese

Manganese has three stable oxidation states, Mn(II), Mn(IV), and Mn(VII). Manganese(IV) is insoluble in aqueous solutions; therefore the studies on manganese speciation were limited to the Mn(II) and Mn(VII) species. Manganese(VII) is a powerful oxidizing agent which, when mixed with manganese(II), will quickly oxidize the latter to the insoluble manganese(IV) species. Therefore, initial studies of the two manganese species were carried out separately in water to determine their chromatographic properties.

Manganese(II) and manganese(VII) cannot be studied together in a mixture because the former is oxidized to manganese(IV) which is insoluble, and, concurrently manganese(VII) is reduced to manganese(IV). The oxidation–reduction process was monitored by injecting a mixture of Mn(II) and Mn(VII) on the chromatographic column immediately after mixing them. This was repeated every five minutes and the ensuing chromatographic data are shown in Fig. 3. Initially, the two peaks obtained, Fig. 3a, for equal concentrations of Mn(II) and Mn(VII) were almost identical

TABLE II

SENSITIVITY COMPARISON BETWEEN ION CHROMATOGRAPHY–d.c. PLASMA ATOMIC EMISSION SPECTROSCOPY (IC–DCPAES) AND 1,10-PHENANTHROLINE METHODS FOR THE DETERMINATION OF IRON SPECIES IN ESTUARY AND RIVER SEDIMENTS

Slopes of the analytical curves for iron species Fe(II) and Fe(III) using the IC–DCPAES method are 1.21 and 1.19, respectively. Slopes of the analytical curves for iron species Fe(II) and Fe(III) using the 1,10-phenanthroline method are 0.22 and nil, respectively.

Sample	Method		
	IC–DCPAES		1,10-phenanthroline
	Fe(III)[a]	Fe(II)[a]	Fe(II)[a]
Estuary sediment	5.21 ± 0.03	9.55 ± 0.2	15.33 ± 0.43
River sediment	14.24 ± 0.84	31.12 ± 0.95	47.11 ± 1.05

[a] ppm.

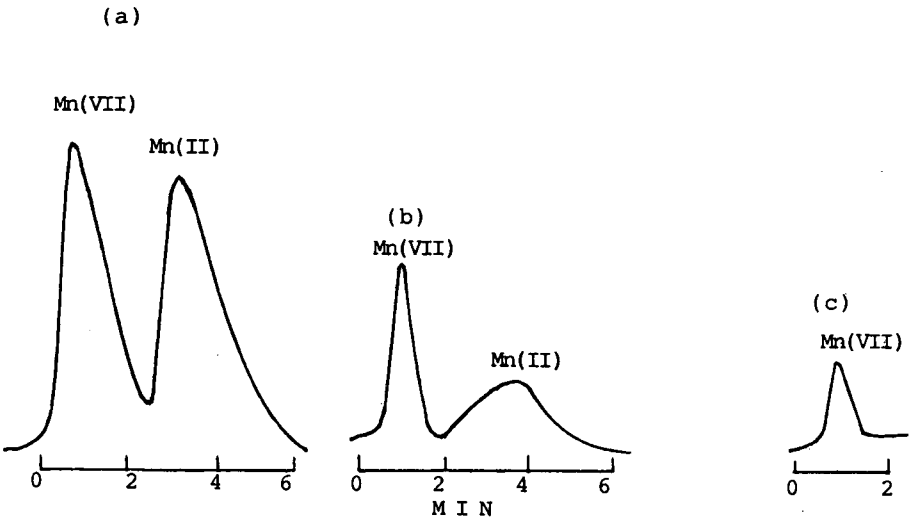

Fig. 3. Ion chromatographic separation of a mixture of manganese(II) and manganese(VII) obtained with d.c. plasma atomic emission spectroscopy detection; sample = 1.0 ppm Mn(II)–1.0 ppm Mn(VII); eluent = 20 m*M* oxalic acid–15 m*M* trilithium citrate. (a) 1 Min; (b) 5 min and (c) 10 min after mixing.

in peak area. However, as time elapsed, the oxidation of Mn(II) and the reduction of Mn(VII) continued until the stoichiometric amount of Mn(II) was used up, leaving an excess of Mn(VII), which remained unreduced, as shown by the residual peak in Fig. 3c. These data are consistent with the redox equation

$$2MnO^{-}_{4} + 3Mn^{2+} + 2H_2O \rightleftharpoons 5MnO_2(s) + 4H^{+}, \qquad E = 0.46\ V$$

in which all the Mn(II) initially present has been converted into Mn(IV) leaving the excess Mn(VII) in the mixture. This is an example of an application of the chromatographic method coupled with a spectroscopic method to study oxidation–reduction reactions. These results also point to the difficulty of studying the two manganese species together. In such cases, only total manganese can be determined by digesting the Mn(IV) with hydrochloric acid according to the equation

$$MnO_2 + 4HCl \rightleftharpoons MnCl_2 + Cl_2(g) + 2H_2O$$

Platinum

In recent years, much interest has been directed towards the application of the unique chemical activity of certain heavy metals in the treatment of ailments such arthritis, skin diseases, and, cancer [42–46]. A number of platinum compounds have been studied and tried as cancer treatment agents. Among these are the commonly known short form names such as cisplatin, carboplatin, iproplatin, and tetraplatin. The successful use of these materials has been hampered by not only chemical side effects but also by poorly understood solution chemistry. Some of them, *e.g.*, cisplatin, are known to have very poor solubility in aqueous systems. Others, such as

tetraplatin, have been found to undergo rapid degradation when placed in solution.

A commercial compound having chemical similarities with some of these materials was chosen as a model for studying the behavior of these platinum containing compounds. The compound chosen, hydrogen hexachloroplatinate(IV) (HCP), is readily soluble in water. However, when an aliquot of its solution was separated on a chromatographic column, it was observed that more than one species were present, as indicated in Fig. 4. The apparent degradation of HCP was accompanied by the dissociation of the chloride ions which, as shown in Fig. 5, appeared to reach a steady state.

The data presented above point to the utility of the d.c. plasma detector to monitor transformations that chemical species can undergo in solution. Here, the degradation of HCP, which is accompanied by a loss of chloride ions, results in at least two platinum-containing moieties, both of which can be monitored by atomic emission measurements monitored at the platinum excitation wavelength of 204.9 nm. The information obtained here is significant in that it can be used as a model for studying platinum containing compounds whose pharmaceutical and clinical use has grown steadily in recent years. Similar studies have been conducted for tetraplatin, a compound which has been shown to have potential as an anti-tumour agent [43].

Of interest is how this method can be applied in studying the interaction of these materials with biological molecules. Fig. 6 shows the chromatograms obtained

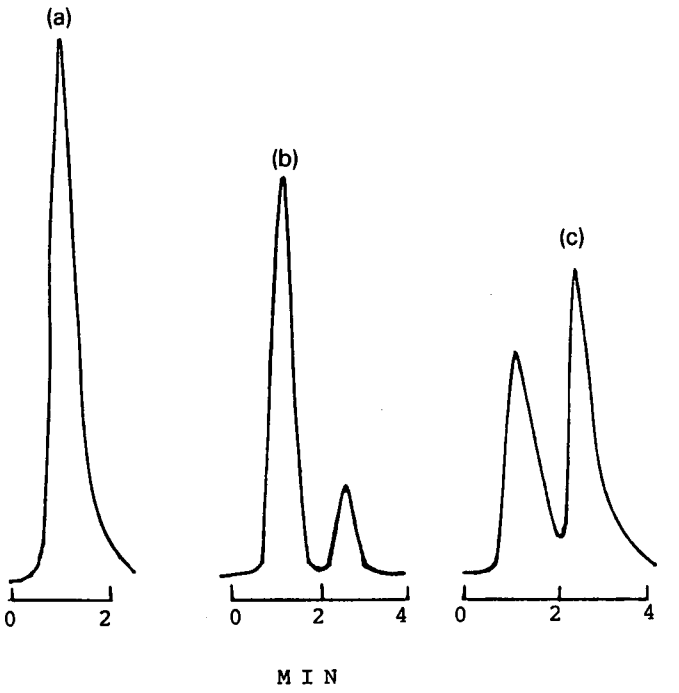

Fig. 4. Ion chromatograms of hydrogen hexachloroplatinate(IV) obtained with d.c. plasma atomic emission spectroscopy detection of platinum; eluent = 10 m*M* oxalic acid–7.5 m*M* trilithium citrate. (a) Fresh solution; (b) 14 day-old solution and (c) 28 day-old solution.

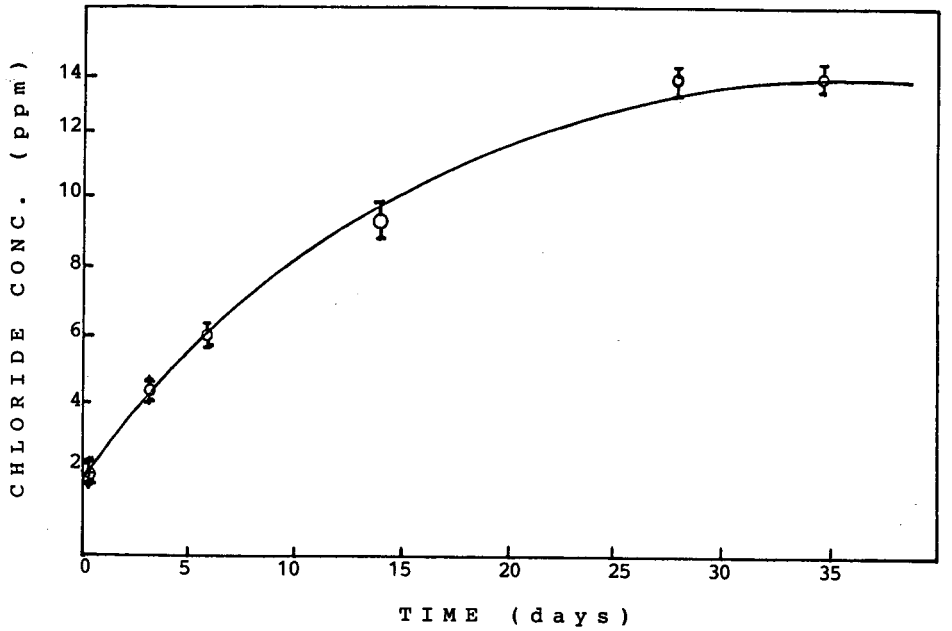

Fig. 5. Chloride content of the solution used in Fig. 4 monitored with an ion chromatograph equipped with a conductivity detector; eluent = 28 m*M* sodium bicarbonate–23 m*M* sodium carbonate.

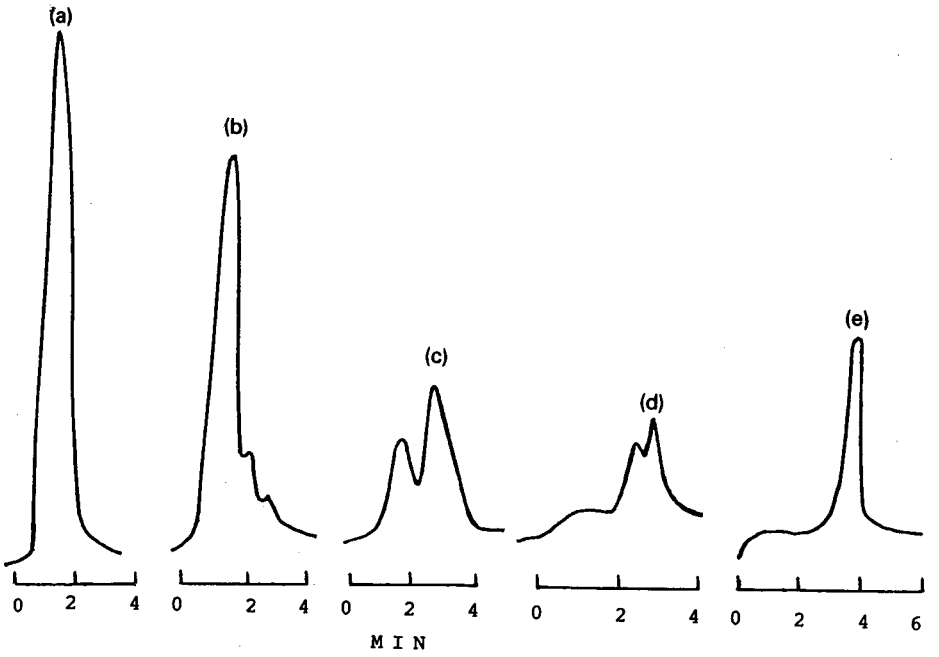

Fig. 6. Ion chromatograms of hydrogen hexachloroplatinate(IV) spiked with cysteine and monitored with d.c. plasma atomic emission spectroscopy detection of platinum. (a) Fresh unspiked solution; (b) cysteine mol ratio = 0.5; (c) cysteine mol ratio = 1.0; (d) cysteine mol ratio = 2.0; and (e) cysteine mol ratio = 10.0.

when a solution of HCP was spiked with incremental amounts of cysteine. Aliquots of the spiked solutions were injected on the cation column and the effluents were monitored by the atomic emission of platinum as was carried out earlier. The chromatograms appear to indicate that at certain concentrations of the ligand cysteine, at least three platinum-containing moieties were formed, but then this was also accompanied by a decrease in the peak size. The appearance of a third peak may correspond to the interaction of cysteine with one of the hydrated platinum species resulting from the degradation of HCP. It appears that the presence of cysteine leads to a diminishing of the platinum peaks. This is probably due to the possible complexation or precipitation of platinum via bond formation with the sulfur side of the ligand. A study of the interaction of such materials with biomolecules is essential as these materials are becoming more and more useful in clinical areas.

Solution chemistry of phosphorus

Phosphorus was included in this study to represent non-metallic elements whose chemical activities can have significant consequences on both biological and environmental systems.

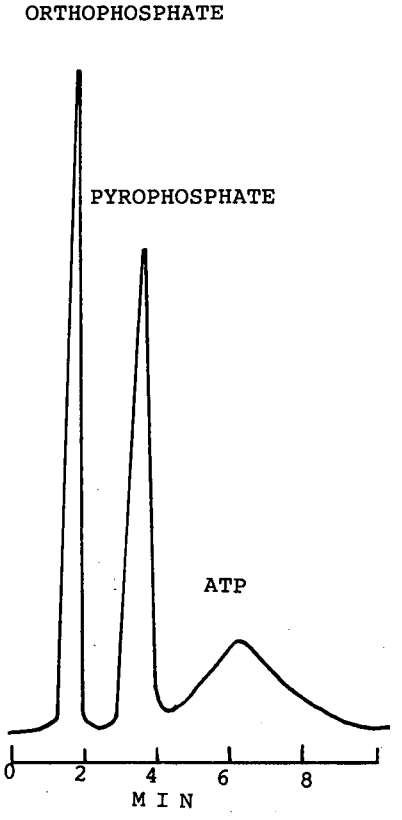

Fig. 7. Ion chromatographic separation of orthophosphate, pyrophosphate, and ATP obtained with d.c. plasma atomic emission spectroscopy detection of phosphorus; column = HPIC-AS-7; eluent = 0.5 *M* nitric acid.

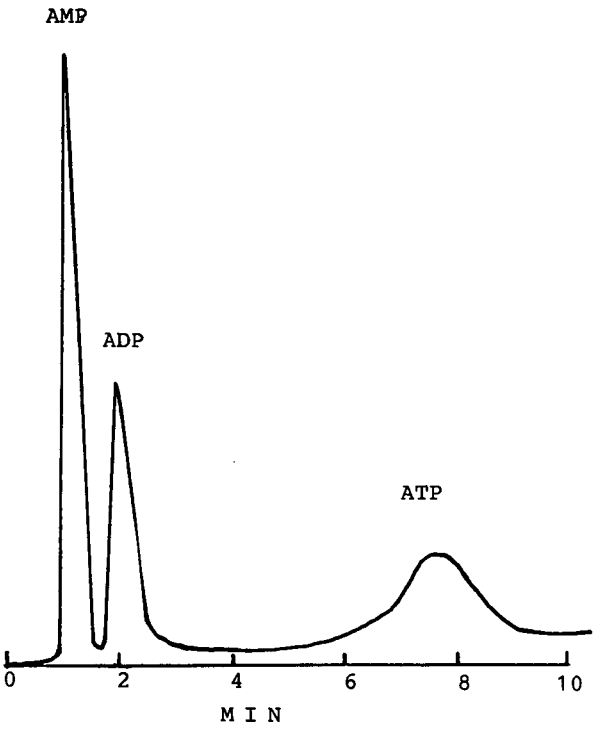

Fig. 8. Ion chromatographic separation of AMP, ADP and ATP obtained with d.c. plasma atomic emission spectroscopy detection of phosphorus; column = HPIC-AS-7; eluent = 0.5 *M* nitric acid.

The ion chromatography–d.c. plasma (IC–DCP) method was applied in the characterization of the solution chemistry of orthophosphate, pyrophosphate, AMP, ADP and ATP. Figs. 7 and 8 show the chromatograms obtained when mixtures of three of these compounds with equal phosphorus content were separated using an anion separator column. The chromatographic effluent was monitored by measuring the atomic emission of phosphorus at 213.6 nm. As with the metallic elements discussed earlier, all the phosphorus species were measured with equal efficiency. Identical linear regression lines, with a regression coefficient of 0.9999, were obtained when analytical curves for phosphorus as orthophosphate and ATP were plotted. This, as with the other elements, permits the determination of the various phosphorus species in a sample using a single analytical curve.

Fig. 9 is a chromatogram obtained when a sample of a detergent solution was injected on the column. The peak at 1.5 min corresponds to orthophosphate, followed by pyrophosphate, and the rest of the rather poorly defined peak was attributed to polyphosphates which, with time, degrade to the simplest inorganic orthophosphate form.

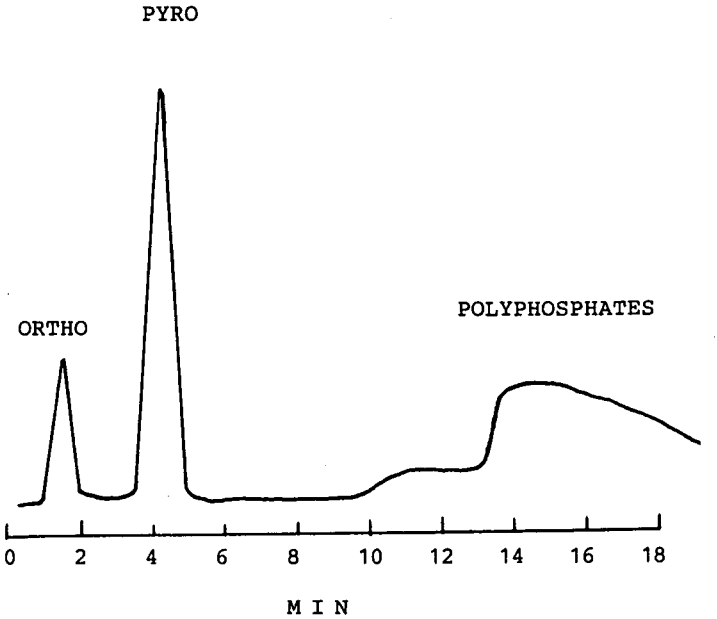

Fig. 9. Ion chromatogram of a solution of Tide detergent obtained with d.c. plasma atomic emission spectroscopy detection of phosphorus; column = HPIC-AS-7; eluent = 0.5 *M* nitric acid.

CONCLUSIONS

The work presented in this paper points to the utility of ion chromatography as a tool for studying the solution chemistry of trace elements and the speciation of these elements in aqueous samples. This capability is enhanced considerably if the chromatographic system is coupled with an element selective detector which responds only to a targeted element in the sample. The use of a d.c. plasma detector enables us to make analytical measurements on samples of varying matrix, and to monitor the element transformations that may occur in solution.

REFERENCES

1 J. Gardiner and M. Stiff, *Water Res.*, 9 (1975) 517.
2 J. C. Duinker and C. J. M. Kramer, *Mar. Chem.*, 5 (1977) 207.
3 H. E. Allen, W. R. Matson and K. H. Mancy, *J. Water Pollut. Control Fed.*, 42 (1970) 573.
4 G. E. Batley and T. M. Florence, *Anal. Lett.*, 9 (1976) 379.
5 T. M. Florence, *Water Res.*, 11 (1977) 681.
6 P. Figura and B. McDuffie, *Anal. Chem.*, 51 (1979) 121.
7 P. Figura and B. McDuffie, *Anal. Chem.*, 52 (1980) 1433–1439.
8 J. C. Thompson and H. A. Motolla, *Anal. Chem.*, 56 (1984) 755–757.
9 L. L. Stookey, *Anal. Chem.*, 42 (1970) 779–781.
10 C. R. Gibbs, *Anal. Chem.*, 48 (1976) 1197–1201.
11 A. A. Schilt, *Analytical Applications of 1,10-Phenanthroline and Related Compounds*, Pergamon, New York, 1969.

12 B. V. Stein and B. E. McClellan, *Environ. Sci. Technol.*, 14 (1980) 872–877.
13 J. C. van Loon, *Anal. Chem.*, 51 (1979) 1139A.
14 A. A. Grabinski, *Anal. Chem.*, 53 (1981) 966.
15 G. R. Ricci, L. S. Shepard, G. Coloros and N. E. Hester, *Anal. Chem.*, 53 (1981) 610.
16 D. G. Iverson, M. A. Anderson, T. R. Hohm and R. R. Stanforth, *Environ. Sci. Technol.*, 13 (1979) 1491.
17 Y. K. Chau and P. T. S. Wong, in G. W. Ewing (Editor), *Environmental Analysis*, Academic Press, New York, 1977.
18 J. C. van Loon, J. Lichwa and B. Radzuik, *J. Chromatogr.*, 136 (1977) 301.
19 R. S. Braman and M. A. Tompkins, *Anal. Chem.*, 51 (1979) 12.
20 P. C. Uden, in P. E. Brinkman and R. H. Fish (Editors), *Environmental Speciation and Monitoring Needs for Trace Metal-Containing Substances from an Energy Related Process, Special Publication No. 618*, 1981, pp. 184–196.
21 J. Lee, *Water Res.*, 15 (1981) 507.
22 R. M. Cassidy and S. Elchuck, *J. Chromatogr. Sci.*, 18 (1980) 217.
23 R. L. Smit and D. J. Pietrzyk, *Anal. Chem.*, 56 (1984) 610–614.
24 W. S. Gardner, P. F. Landrum and D. A. Yates, *Anal. Chem.*, 54 (1982) 1196–1198.
25 M. B. Colella, S. Siggia and R. M. Barnes, *Anal. Chem.*, 52 (1980) 2347–2350.
26 D. A. Roston, *Anal. Chem.*, 56 (1984) 241–244.
27 R. R. Sturgeon, S. S. Berman, S. N. Willie and J. A. H. Desauliners, *Anal. Chem.*, 53 (1981) 2337–2340.
28 P. C. Uden, B. D. Quimby, R. M. Barnes and W. G. Elliott, *Anal. Chim. Acta*, 101 (1978) 99–109.
29 L. W. Green and J. R. Woods, *Anal. Chem.*, 53 (1981) 3187.
30 J. A. Mosko, *Anal. Chem.*, 56 (1984) 629–633.
31 P. K. Dasgupta, *Anal. Chem.*, 56 (1984) 769–772.
32 J. S. Fritz, D. T. Gjerde and C. Pohlandt, *Ion Chromatography*, Hüthig, Heidelberg, 1982.
33 A. Lebel and T. F. Yen, *Anal. Chem.*, 56 (1984) 807–808.
34 H. Small, T. S. Stevens and W. C. Bauman, *Anal. Chem.*, 47 (1975) 1801.
35 K. Suzuki, H. Aruga and T. Shirai, *Anal. Chem.*, 55 (1983) 2011–2013.
36 G. J. Sevenich and J. S. Fritz, *Anal. Chem.*, 55 (1983) 12–16.
37 M. Yamamoto, H. Yamamoto and Y. Yamamoto, *Anal. Chem.*, 56 (1984) 832–834.
38 I. T. Urasa and F. Ferede, *Anal. Chem.*, 59 (1987) 1563–1566.
39 I. T. Urasa and S. H. Nam, *J. Chromatogr. Sci.*, 27 (1989) 30–37.
40 I. T. Urasa, V. D. Lewis and S. H. Nam, *J. Chromatogr. Sci.*, 27 (1989) 468–473.
41 I. T. Urasa, V. D. Lewis, J. DeZwaan, and S. E. Northcott, *Anal. Lett.*, 22 (1989) 597–619.
42 R. J. Puddephatt, *The Chemistry of Gold*, Elsevier, New York, 1978.
43 B. Rosenberg, L. Van Camp, J. E. Trosko and V. H. Mansour, *Nature (London)*, 222 (1969) 385–386.
44 C. J. F. Barnard, M. J. Cleare and P. C. Hydes, *Chem. Br.*, 22 (1986) 1001–1004.
45 S. J. Lippard, *Pure Appl. Chem.*, 59 (1987) 731–742.
46 G. Eastland, Jr., *Drugs Future*, 12 (1987) 139–141.

Journal of Chromatography, 547 (1991) 225–237
Elsevier Science Publishers B.V., Amsterdam

CHROM. 23 232

Reversed-phase liquid chromatographic retention of geometrical isomers of tris(β-diketonato)–chromium(III) and tris(β-diketonato)–cobalt(III)

Comparison with liquid–liquid partition in a dodecane–(methanol–water) system

SATOSHI TSUKAHARA, KOICHI SAITOH and NOBUO SUZUKI*
Department of Chemistry, Faculty of Science, Tohoku University, Sendai, Miyagi 980 (Japan)
(Received December 27th, 1990)

ABSTRACT

The retention of the *fac* and *mer* isomers of chromium(III) and cobalt(III) complexes with eight asymmetrical β-diketones in the octadecyl-bonded silica (ODS)–(methanol–water) system was studied. The retention order for two geometrical isomers depends on the structure of the complexing β-diketone; the retention order, *fac* < *mer*, is found for complexes of the β-diketones which possess a fluorinated functional group in each molecule, whereas the reverse order is found for complexes of β-diketones without a fluorinated moiety. The capacity factors (k') of the chromium(III) complex isomers were compared with their partition coefficients (P) between dodecane and methanol–water of an identical composition to the mobile phase used in the chromatographic separation. It was found that the transfer of a complex from a methanol–water phase occurs more easily to ODS than to dodecane. The retention sequence for the *fac* and *mer* isomers of each metal complex is the same as the increasing order of P values. The difference in k' between the *mer* and *fac* isomers is smaller than the difference in the P value.

INTRODUCTION

Metal β-diketonates have been studied intensively in gas, column liquid and thin-layer chromatography as well as in solvent extraction procedures. The first application of high-performance liquid chromatography (HPLC) to the separation of metal–β-diketonato complexes was reported by Huber *et al.* in 1972 [1]. Since that time, many papers dealing with the HPLC separation of various metal–β-diketonate complexes have been published [2–7], whereas the HPLC of the geometrical isomers of β-diketonato complexes has only rarely been described.

The octahedral complex of a trivalent metal coordinated with three molecules of an asymmetrical β-diketone possesses two geometrical isomers, with meridional (*mer*) and facial (*fac*) configurations about an octahedral coordination sphere, as illustrated in Fig. 1. Fay and Piper separated the *fac* and *mer* forms of benzoylacet-

0021-9673/91/$03.50

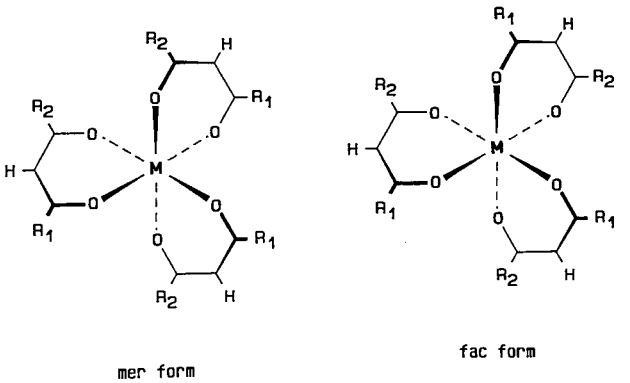

Fig. 1. Configurations of the geometrical isomers of a tris(β-diketonato) complex of a trivalent metal.

onates (1-phenyl-1,3-butanedionates) [8] and trifluoroacetylacetonates (1,1,1-trifluoro-2,4-pentanedionates) [9] of chromium(III), cobalt(III) and rhodium(III) by traditional adsorption chromatography with aluminium oxide. The successful HPLC separation of the geometrical isomers of chromium(III) and cobalt(III) complexes of asymmetrical β-diketones were carried out using a silica gel column [10] and a phenyl-bonded silica gel column [11]. The adsorption characteristics of the isomers of several chromium(III) β-diketonates on silica gel have also been reported [12]. In all these examples of chromatography with the combination of a polar stationary phase and a less polar mobile phase, the *fac* form showed a larger retention than the *mer* form with different metal β-diketonates.

The retention order, *fac* < *mer*, was reported for the chromium(III) complexes of trifluoroacetylacetone and also of 6,6,7,7,8,8,8-heptafluoro-2,2-dimethyl-3,5-octanedione, in the case of the reversed-phase HPLC with an alkyl-bonded silica gel [13].

This paper reports an investigation of the retention sequence of the *fac* and *mer* isomers of octahedral metal complexes of β-diketones in reversed-phase HPLC. Chemically inert chromium(III) and cobalt(III) complexes with eight asymmetrical β-diketones were taken as model complexes. To clarify the retention characteristics and selectivity for the *mer* and *fac* isomers on an octadecyl-bonded phase, the chromatographic retention was compared with liquid–liquid partition using dodecane as a non-polar phase. The reversed-phase chromatographic retention of several chromium(III) complexes with symmetrical β-diketones in the ODS–(methanol–water) system was previously compared with the partition coefficient in the dodecane–(methanol–water) system [7].

EXPERIMENTAL

Materials

The tris(β-diketonato) complexes of chromium(III) and cobalt(III) listed in Table I were prepared by modifying the methods reported for tris(acetylacetonato)–chromium(III) [14] and tris(acetylacetonato)–cobalt(III) [15], respectively. Prior to the preparation of these metal complexes, the β-diketones which were not commer-

TABLE I

β-DIKETONATO COMPLEXES INVESTIGATED

Complex [a]	R_1 [b]	R_2 [b]	Abbreviation	Graph symbol
Tris(acetylacetonato)–chromium(III)	CH_3	CH_3	$Cr(acac)_3$	○
Tris(propionylacetonato)–chromium(III)	CH_3	C_2H_5	$Cr(prac)_3$	●
Tris(butyrylacetonato)–chromium(III)	CH_3	C_3H_7	$Cr(buac)_3$	□
Tris(valerylacetonato)–chromium(III)	CH_3	C_4H_9	$Cr(vac)_3$	■
Tris(hexanoylacetonato)–chromium(III)	CH_3	C_5H_{11}	$Cr(hac)_3$	△
Tris(benzoylacetonato)–chromium(III)	CH_3	C_6H_5	$Cr(bzac)_3$	▲
Tris(trifluoroacetylacetonato)–chromium(III)	CF_3	CH_3	$Cr(tfa)_3$	▽
Tris(pivaroyltrifluoroacetonato)–chromium(III)	CF_3	$C(CH_3)_3$	$Cr(pfa)_3$	◑
Tris(benzoyltrifluoroacetonato)–chromium(III)	CF_3	C_6H_5	$Cr(bzfa)_3$	▼
Tris(acetylacetonato)–cobalt(III)	CH_3	CH_3	$Co(acac)_3$	○
Tris(propionylacetonato)–cobalt(III)	CH_3	C_2H_5	$Co(prac)_3$	●
Tris(butyrylacetonato)–cobalt(III)	CH_3	C_3H_7	$Co(buac)_3$	□
Tris(valerylacetonato)–cobalt(III)	CH_3	C_4H_9	$Co(vac)_3$	■
Tris(hexanoylacetonato)–cobalt(III)	CH_3	C_5H_{11}	$Co(hac)_3$	△
Tris(benzoylacetonato)–cobalt(III)	CH_3	C_6H_5	$Co(bzac)_3$	▲
Tris(trifluoroacetylacetonato)–cobalt(III)	CF_3	CH_3	$Co(tfa)_3$	▽
Tris(pivaroyltrifluoroacetonato)–cobalt(III)	CF_3	$C(CH_3)_3$	$Co(pfa)_3$	◑
Tris(benzoyltrifluoroacetonato)–cobalt(III)	CF_3	C_6H_5	$Co(bzfa)_3$	▼

[a] Geometrical isomers are not distinguished.
[b] See Fig. 1.

cially available (Hbzac, Htfa, Hbzfa and Hpfa were obtained from Wako, Osaka, or Dojin Labs., Kumamoto, Japan) were synthesized by the literature method [16].

Geometrical isomers of each metal β-diketonate were resolved by silica gel column chromatography with hexane–benzene or benzene–ethyl acetate, as shown in Table II. In the case of the cobalt(III) complexes, the early and late eluted species

TABLE II

PREPARATIVE SEPARATION OF GEOMETRICAL ISOMERS OF METAL β-DIKETONATO COMPLEXES

Complex	Column	Eluent[a]
$Cr(prac)_3$, $Co(prac)_3$ $Cr(bzac)_3$, $Co(bzac)_3$	LiChroprep Si60[b] (25 cm × 2.5 cm)	Bz–EtOAc (100:5, v/v)
$Cr(buac)_3$, $Co(buac)_3$ $Cr(vac)_3$, $Co(vac)_3$	Wakogel C-300[c] (5 cm × 2.5 cm)	Bz–EtOAc (100:4, v/v)
$Cr(hac)_3$, $Co(hac)_3$	Wakogel C-300 (4 cm × 2.5 cm)	Bz–EtOAc (100:3, v/v)
$Cr(tfa)_3$, $Co(tfa)_3$	Wakogel C-300 (10 cm × 2.5 cm)	Bz–hexane (40:60, v/v)
$Cr(bzfa)_3$, $Co(bzfa)_3$	Wakogel C-300 (15 cm × 2.5 cm)	Bz–hexane (40:60, v/v)
$Cr(pfa)_3$, $Co(pfa)_3$	Wakogel C-300 (5 cm × 2.5 cm)	Bz–hexane (10:90, v/v)

[a] Bz = Benzene; EtOAc = ethyl acetate.
[b] 40–63 μm, Merck, Darmstadt, Germany.
[c] 300 mesh; Wako, Osaka, Japan.

from the column were identified as *mer* and *fac* forms by comparing their ^{1}H-NMR spectra [8,9,17]. However, for the paramagnetic chromium(III) complexes to which ^{1}H-NMR could not be applied, the *mer* and *fac* forms were regarded as the early and late eluted fractions from the column, respectively, by reference to the elution sequence of the geometrical isomers of cobalt(III) complexes. In each instance, the yield of the *mer* form was about three to five times the yield of the *fac* form (the ratio of the statistical yields of the *mer* form to the *fac* form is 3:1).

Dodecane was distilled under reduced pressure after stirring with an equivolume mixture of fumic and concentrated sulphuric acids for 1 day. The water was doubly-distilled. Other chemicals were of analytical-reagent grade.

Equipment

A Hitachi Model 655-15 pump (Tokyo, Japan), a Rheodyne 7125 sample injection valve with a 10-μl sample loop (Cotani, CA, USA), a Shimadzu SPD-6AV UV–visible absorption detector and a C-R1A chromatographic data processor (Kyoto, Japan) were assembled into an HPLC system.

High-performance liquid chromatography

A column packed with octadecyl-bonded silica gel (TSK-Gel ODS-120T; particle size 5 μm, 15 cm × 4.6 mm I.D.; Tosoh, Tokyo, Japan) was used. The methanol–water used as the mobile phase was prepared by weighing. A sample solution of each metal complex was prepared at a concentration of about $1 \cdot 10^{-4}$ *M* in methanol, and a 1- μl aliquot of the solution was injected on to the column. The detection wavelength was set at 254 nm. The temperature was 25 ± 1°C.

Liquid–liquid partition

Aliquots (1 ml) of both dodecane and methanol–water (both of these liquids contained a metal complex at the $1 \cdot 10^{-3}$ *M* level) were agitated in a glass tube at 300 strokes per min for 30 min. After the completion of phase separation by centrifuging, a 10-μl portion of each liquid phase was injected into a reversed-phase HPLC column (5 μm Inertsil ODS, 150 mm × 4.6 mm I.D.; Gasukuro Kogyo, Tokyo, Japan) which used an appropriate methanol–water binary mobile phase for the elution of the metal complex within a few minutes. The partition coefficient was calculated as a ratio of the chromatographic peak areas measured for the metal complex in the dodecane phase to the methanol–water phase [18]. All these experiments were carried out in a thermostated room at 25 ± 1°C.

RESULTS AND DISCUSSION

Capacity factors

Every metal β-diketonato complex gave a sharp and symmetrical chromatographic peak, which implied the absence of undesirable adsorption and chemical changes, such as demetallation and isomerization, of the complex during the chromatographic process.

Prior to the calculation of the capacity factor (k') of each metal complex from its retention volume, the column void volume was determined using sodium nitrate as an unretained compound by the column. The k' values of tris(β-diketonato)–chromi-

um(III) and –cobalt(III) were determined with a relative standard deviation of less than 1% ($n=3$), with all compositions of methanol–water used [the range of the molar fraction of methanol (X_{CH_3OH}) in the binary mixture was 0.5–1.0]. The k' values are summarized in Table III. The k' value of the chromium(III) complexes are larger than those of the cobalt(III) complexes in most instances.

Figs. 2 and 3 show the variation of the retention of the chromium(III) and cobalt(III) complexes with the molar fraction of methanol in the mobile phase, respectively. The plots are restricted to the *mer* isomers of the complexes to avoid complicated illustration [no geometrical isomer is present for $Cr(acac)_3$ and Co-

TABLE III

CAPACITY FACTORS OF CHROMIUM(III) AND COBALT(III) β-DIKETONATES ON TSK-GEL ODS-120T WITH METHANOL–WATER AT 25.0°C

Complex	X_{CH_3OH}[a]					
	0.50	0.60	0.70	0.80	0.90	1.00
$Cr(acac)_3$	0.83	0.49	0.32	0.21	0.17	0.15
mer-$Cr(prac)_3$	3.47	1.59	0.84	0.48	0.31	0.23
fac-$Cr(prac)_3$	3.79	1.69	0.88	0.50	0.32	0.24
mer-$Cr(buac)_3$	13.9	4.76	2.00	0.97	0.54	0.35
fac-$Cr(buac)_3$	16.1	5.33	2.19	1.05	0.57	0.37
mer-$Cr(vac)_3$		13.9	4.70	1.91	0.91	0.52
fac-$Cr(vac)_3$		16.2	5.33	2.12	0.99	0.55
mer-$Cr(hac)_3$			11.8	3.94	1.60	0.78
fac-$Cr(hac)_3$			13.4	4.37	1.74	0.83
mer-$Cr(bzac)_3$	18.5	5.30	1.99	0.90	0.46	0.29
fac-$Cr(bzac)_3$	22.2	6.10	2.21	0.97	0.49	0.30
mer-$Cr(tfa)_3$	6.07	1.87	0.75	0.36	0.18	0.10
fac-$Cr(tfa)_3$	5.56	1.72	0.69	0.33	0.16	0.09
mer-$Cr(pfa)_3$			9.23	2.46	0.84	0.34
fac-$Cr(pfa)_3$			7.69	2.14	0.76	0.32
mer-$Cr(bzfa)_3$			7.73	2.25	0.80	0.34
fac-$Cr(bzfa)_3$			5.46	1.64	0.60	0.27
$Co(acac)_3$	0.72	0.44	0.30	0.21	0.17	0.16
mer-$Co(prac)_3$	2.89	1.39	0.77	0.46	0.31	0.24
fac-$Co(prac)_3$	3.13	1.48	0.81	0.48	0.32	0.25
mer-$Co(buac)_3$	11.5	4.13	1.83	0.93	0.54	0.36
fac-$Co(buac)_3$	13.0	4.56	1.97	0.98	0.56	0.37
mer-$Co(vac)_3$		12.0	4.24	1.79	0.89	0.52
fac-$Co(vac)_3$		13.8	4.76	1.97	0.96	0.55
mer-$Co(hac)_3$			10.6	3.68	1.56	0.78
fac-$Co(hac)_3$			11.8	4.03	1.67	0.83
mer-$Co(bzac)_3$	14.5	4.40	1.73	0.82	0.44	0.28
fac-$Co(bzac)_3$	17.8	5.14	1.94	0.88	0.47	0.29
mer-$Co(tfa)_3$	5.35	1.73	0.71	0.32	0.15	0.10
fac-$Co(tfa)_3$	5.03	1.61	0.65	0.29	0.14	0.09
mer-$Co(pfa)_3$			9.26	2.56	0.88	0.37
fac-$Co(pfa)_3$			7.62	2.21	0.79	0.35
mer-$Co(bzfa)_3$			7.06	2.13	0.78	0.34
fac-$Co(bzfa)_3$			4.99	1.56	0.59	0.27

[a] X_{CH_3OH} = molar fraction of methanol in the mobile phase.

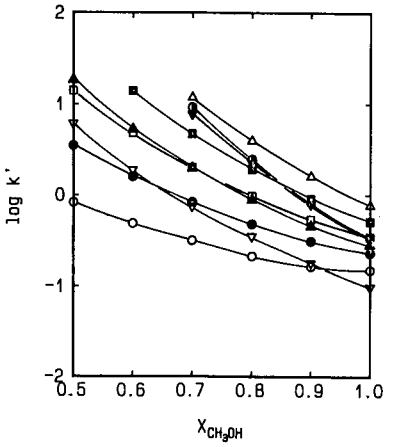

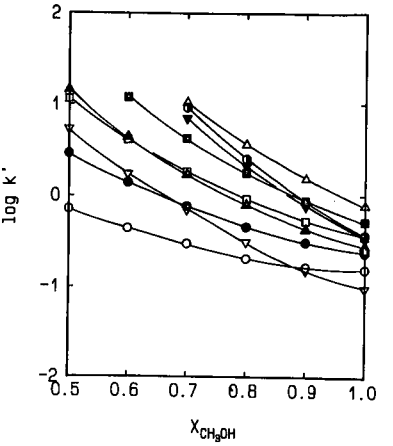

Fig. 2. Variation of the retention (log k') of tris(β-diketonato)–chromium(III) with the molar fraction of methanol (X_{CH_3OH}) in the methanol–water binary mobile phase. Symbols refer to the chromium(III) complexes as given in Table I.

Fig. 3. Variation of the retention of tris(β-diketonato)–cobalt(III) with the molar fraction of methanol (X_{CH_3OH}) in the mobile phase. Symbols refer to the cobalt(III) complexes as given in Table I.

$(acac)_3$]. The general shapes of the log k' *versus* X_{CH_3OH} curves for the chromium(III) and cobalt(III) complexes of a particular β-diketone are similar; the k' value of each metal complex decreases with increasing X_{CH_3OH}. This does not disagree with the general retention trends observed so far with many kinds of non-electrolytes in reversed-phase HPLC.

The metal complexes are classified into the following two groups with respect to the dependence of their retention on the composition of the mobile phase: (1) the complexes of the β-diketones possessing a trifluoromethyl group (fluorinated β-diketones); and (2) those of other β-diketones (non-fluorinated β-diketones). The methanol content of the mobile phase affected the retention more significantly for the complexes of fluorinated β-diketones than for the non-fluorinated compounds. Accordingly, the log k' *versus* X_{CH_3OH} plots for the complexes of these two types of β-diketones cross each other (Fig. 2 and Fig. 3). The retention order of the complexes of the fluorinated or non-fluorinated series of β-diketones was not altered by a change in the mobile phase composition; the capacity factors of both chromium(III) and cobalt(III) complexes increased in the following order of complexing β-diketones: acac < prac < buac < bzac ≈ vac < hac, in the series of non-fluorinated β-diketones, and tfa < bzfa < pfa, in the series of fluorinated compounds. It was found that for the complexes of alkyl substituted β-diketones the retention increases with increasing number of carbon atoms in the alkyl moiety of the β-diketone.

Retention difference between geometrical isomers

The *fac* forms of both the chromium(III) and cobalt(III) complexes of a fluorinated β-diketone always eluted earlier than the *mer* forms of the corresponding complexes, whereas a reversed elution sequence was always observed for the complexes of non-fluorinated β-diketone. Typical chromatograms showing these two types of

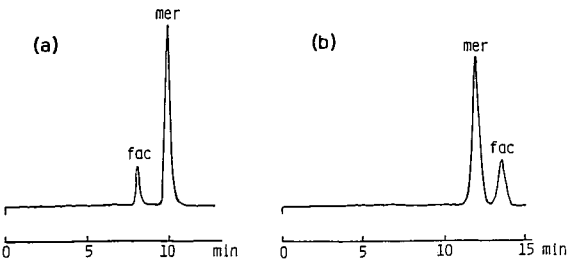

Fig. 4. High-performance liquid chromatographic separation of geometrical isomers of (a) $Cr(bzfa)_3$ and (b) $Cr(bzac)_3$. Column: TSK-gel ODS-120T, 5 μm, 150 mm × 4.6 mm I.D. Mobile phase: (a) X_{CH_3OH} = 0.8, 0.50 ml/min; (b) X_{CH_3OH} = 0.6, 0.80 ml/min.

elution sequences in the separation of the geometrical isomers studied here are illustrated in Fig. 4. A similar effect of the structure of β-diketone on the elution sequence of the geometrical isomers of its metal complex was not observed with a silica gel column from which the *fac* form always eluted later than the *mer* form, regardless of the functional groups possessed by the β-diketone.

The retention difference between the *mer* and *fac* forms of the chromium(III) and cobalt(III) complexes observed in the reversed-phase separation mode used are plotted as a function of X_{CH_3OH} of the mobile phase in Figs. 5 and 6, respectively, where

$$\Delta\log k' = \log k'_{mer} - \log k'_{fac} \quad (1)$$

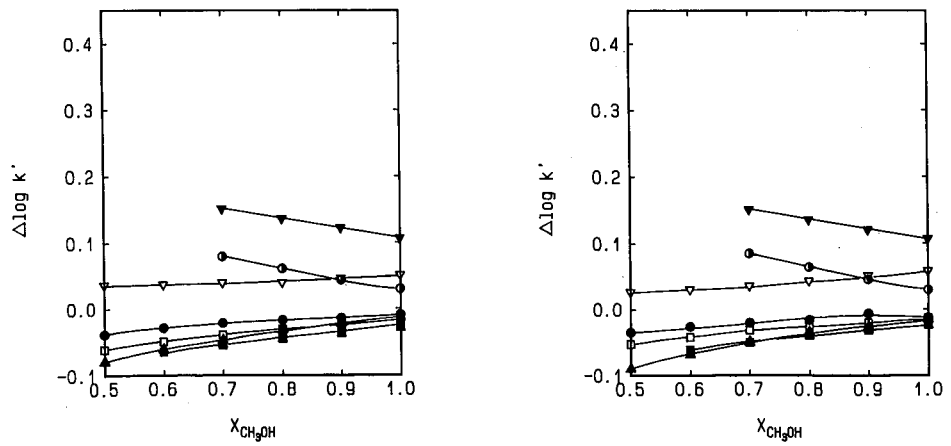

Fig. 5. Effect of the composition of the methanol–water mobile phase on the $\Delta\log k'$ value for geometrical isomers of tris(β-diketonato)-chromium(III). Symbols refer to the chromium(III) complexes as given in Table I.

Fig. 6. Effect of the mobile phase composition on the $\Delta\log k'$ value for geometrical isomers of tris(β-diketonato)–cobalt(III). Symbols refer to the cobalt(III) complexes as given in Table I.

TABLE IV

PARTITION COEFFICIENT (P) OF TRIS(β-DIKETONATO)–CHROMIUM(III) IN THE DODECANE–(METHANOL–WATER) SYSTEM AT 25.0°C

Complex	X_{CH_3OH}[b]	$(P \times 10^2)$[a]		
	0.40	0.60	0.80	1.00
$Cr(acac)_3$	3.28 ± 0.05	1.86 ± 0.04	1.64 ± 0.05	2.20 ± 0.03
mer-$Cr(prac)_3$		15.1 ± 0.4	7.96 ± 0.23	7.68 ± 0.24
fac-$Cr(prac)_3$		16.2 ± 0.3	8.32 ± 0.29	8.17 ± 0.17
mer-$Cr(buac)_3$		80.8 ± 1.1	25.7 ± 0.2	16.0 ± 0.5
fac-$Cr(buac)_3$		82.9 ± 0.4	26.8 ± 0.3	16.9 ± 0.7
mer-$Cr(vac)_3$		322 ± 2	67.9 ± 0.1	28.2 ± 0.4
fac-$Cr(vac)_3$		329 ± 4	70.5 ± 0.4	29.9 ± 0.3
mer-$Cr(hac)_3$		1410 ± 40	195 ± 4	54.4 ± 0.4
fac-$Cr(hac)_3$		1240 ± 20	191 ± 4	55.2 ± 0.6
mer-$Cr(bzac)_3$	781 ± 12	67.6 ± 0.5	15.2 ± 0.3	7.20 ± 0.13
fac-$Cr(bzac)_3$	824 ± 18	74.1 ± 1.0	16.6 ± 0.2	7.73 ± 0.09
mer-$Cr(tfa)_3$	524 ± 9	36.5 ± 0.5	6.07 ± 0.11	1.84 ± 0.06
fac-$Cr(tfa)_3$	375 ± 7	26.6 ± 0.4	4.58 ± 0.02	1.44 ± 0.02
mer-$Cr(pfa)_3$		4810 ± 70	283 ± 1	32.3 ± 0.5
fac-$Cr(pfa)_3$		2660 ± 20	161 ± 1	19.1 ± 0.5
mer-$Cr(bzfa)_3$		1970 ± 20	119 ± 0	14.1 ± 0.2
fac-$Cr(bzfa)_3$		809 ± 22	47.1 ± 0.7	6.05 ± 0.11

[a] Mean ± standard deviation ($n = 3$).
[b] X_{CH_3OH} = molar fraction of methanol in the methanol–water phase.

The $\Delta \log k'$ corresponds to the logarithmic separation factor between the isomers [= $\log (k'_{mer}/k'_{fac})$].

The magnitudes of $\Delta \log k'$ for the complexes of fluorinated β-diketones are positive regardless of the composition of methanol–water mobile phase, whereas those for the complexes of non-fluorinated β-diketones are always negative.

Liquid–liquid partition coefficients

The liquid–liquid partition coefficients (P) of the chromium(III) complexes were determined using dodecane and methanol–water as the non-polar and the polar liquid phases, respectively. P was defined as the concentration ratio of a metal complex in the non-polar to that in the polar liquid phase. The results are summarized in Table IV. The P value of each complex decreased with an increase in the methanol content of the polar liquid phase, although a slight reverese trend was found, particularly for the complexes of acac and prac when the composition of the polar phase approached pure methanol. The influence of the methanol–water composition on the partition coefficient was more significant for a complex of a fluorinated β-diketone than for that of non-fluorinated compound, so that, in some instances, the log P *versus* X_{CH_3OH} plots for the complexes of such different types of β-diketones cross each other, as shown in Fig. 7 (where the plots for *mer* forms are given in order for simplification of the illustration).

The difference in the partition coefficient between the *mer* form (P_{mer}) and *fac*

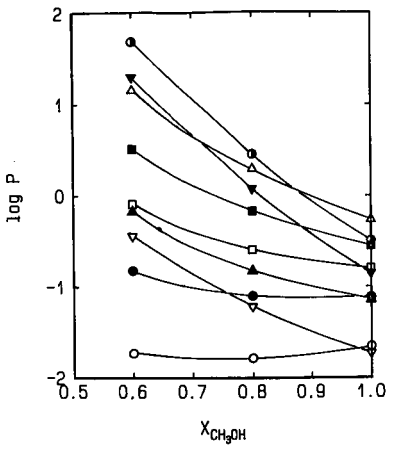

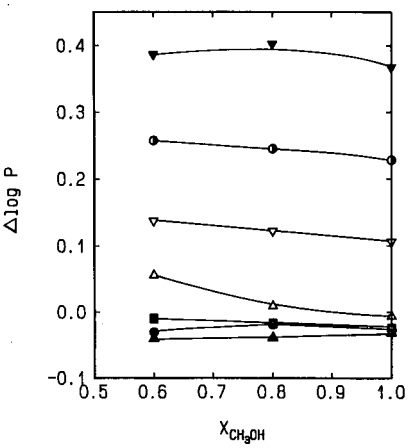

Fig. 7. Variation of the partition coefficient (P) of tris(β-diketonato)–chromium(III) with the methanol content of the mobile phase. Symbols refer to the chromium(III) complexes as given in Table I.

Fig. 8. Effect of the methanol content of the mobile phase on the $\Delta\log P$ value for geometrical isomers of tris(β-diketonato)–chromium(III) complexes. Symbols refer to the chromium(III) complexes as given in Table I.

form (P_{fac}) of each chromium(III) complex is plotted as a function of X_{CH_3OH} in the polar liquid phase in Fig. 8, where $\Delta\log P$ is defined as

$$\Delta\log P = \log P_{mer} - \log P_{fac} \tag{2}$$

The $\Delta\log P$ corresponds to the logarithmic separation factor between the isomers [log (P_{mer}/P_{fac})]. It is seen in Fig. 8 that the $\Delta\log P$ values of the complexes of fluorinated β-diketones such as tfa, pfa and bzfa are positive, regardless of X_{CH_3OH}, whereas those of non-fluorinated β-diketones are slightly negative, except for $Cr(hac)_3$ under certain conditions of X_{CH_3OH}.

Comparison of the liquid chromatographic retention with the liquid–liquid partition coefficient

Comparing Fig. 7 with both Figs. 2 and 3, it is found that the liquid–liquid partition of each metal complex in the dodecane–(methanol–water) system is similar to the chromatographic retention with respect to their dependence on the composition of the methanol–water mixture.

The capacity factor, k', in these liquid chromatography studies, is a combined function of the distribution coefficient (K), defined as a concentration ratio of a metal complex in the stationary phase to the mobile phase, and the volume ratio (φ) of these phases, represented by

$$\log k' = \log K + \log \varphi \tag{3}$$

If the partition in the dodecane–(methanol–water) system is almost equivalent to the distribution in the ODS–(methanol–water) system, K is close to P, provided that the

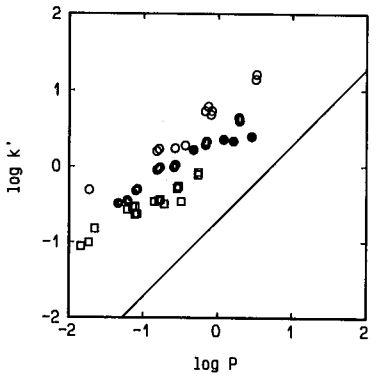

Fig. 9. Chromatographic capacity factor (log k') of tris(β-diketonato)-chromium(III) plotted against the liquid–liquid partition coefficient (log P) in the dodecane–(methanol–water) system. X_{CH_3OH}: ○ = 0.6; ● = 0.8; □ = 1.0.

methanol–water mixtures used in both systems are of identical composition. In such a case, the log k' *versus* log P plot should fall close to a straight line (equivalent line) representing

$$\log k' = \log P + \log \varphi \tag{4}$$

Fig. 9 shows the plots of log k' *versus* log P for chromium–β-diketonato complexes. The straight line shows the equivalent line (eqn. 4) obtained by the approximate calculation of φ as 0.2 from the carbon content (21%) and the bulk density (0.38 g/cm^3) of the ODS phase used, the column internal volume (2.50 cm^3), the column void volume (1.57 cm^3) and the molar volume of octadecane (327 cm^3/mol, estimated value). All the points in Fig. 9 deviate upwards from the equivalent line. It is noted that the extent of such an upward deviation tends to increase with a decrease in log P.

The solute distribution is generally a function of the energy change accompanying the transfer of a solute from one phase to another. The partition coefficient, P, in this study is given by

$$\log P = -(G_{S,np} - G_{S,p})/2.30RT \tag{5}$$

where G_S is the solution energy for a metal complex, the subscripts p an np indicate the polar liquid phase (methanol–water) and non-polar liquid phase (dodecane), respectively, R is the molar gas constant and T is the temperature. The value 2.30 is the approximate coefficient to give a $\log_{10}$ base equation instead of $\log_e$ base equation.

When the partition concept is applied to the reversed-phase chromatography studied here, the distribution coefficient, K, is discussed in an analogous manner to P and then the following equation is derived from eqn. 3:

$$\log k' = -(G_{S,S} - G_{S,m})/2.30RT + \log \varphi \tag{6}$$

where the subscripts m and s indicate the mobile phase (methanol–water) and the stationary phase (ODS), respectively. As an identical composition of methanol–water is used in the experiments of both partition and chromatography, $G_{S,p} = G_{S,m}$. The fact that all points in Fig. 9 deviate upwards from the equivalent line implies that $G_{S,S} < G_{S,np}$, which means that the transfer of the respective metal complexes from a given methanol–water phase occurs more easily to the ODS phase than to dodecane.

Comparison of the separation factor for the mer–fac pair in chromatography and the liquid–liquid partition

It has been shown in Figs. 5, 6 and 8 that both $\Delta\log k'$ and $\Delta\log P$ are positive for the complexes of fluorinated β-diketones such as tfa, pfa and bzfa, regardless of the composition of the methanol–water phase, whereas they are slightly negative for the complexes of most non-fluorinated β-diketones.

To gain an insight into the influence of the structure of the β-diketonato ligand on the $\Delta\log k'$ observed in the chromatographic separation, the $\Delta\log P$ in the liquid–liquid partition system is discussed in detail.

The solution process can be divided into the following two steps: (1) the formation of a cavity in the solvent to accommodate the solute molecule; and (2) the transfer of the solute molecule into the cavity. These two steps are accompanied by the cavity formation energy (G_C) and the solute-solvent interaction energy (G_i), respectively, which are related to the solution energy, G_s, as follows [19]:

$$G_S = G_C + G_i \tag{7}$$

The cavity formation energy, G_C, is a function of the size (diameter) of the solute and solvent molecules [19].

This concept has been successfully applied to a discussion of the liquid–liquid partition equilibria of various non-electrolytes [20–22].

When this concept is applied to the liquid–liquid partition of a metal complex, eqn. 5 is rewritten as

$$\begin{aligned}\log P &= -[(G_{C,np} - G_{C,p}) + (G_{i,np} - G_{i,p})]/2.30RT \\ &= -[\Delta G_C + \Delta G_i]/2.30RT\end{aligned} \tag{8}$$

where ΔG indicates the free energy of transferring a metal complex from the methanol–water phase into dodecane. When the *mer* and *fac* isomers of a complex are regarded as equivalent with respect to their molecular sizes (this means $\Delta G_{C,mer} = \Delta G_{C,fac}$), eqn. 2 is rewritten as

$$\Delta\log P = -[\Delta G_{i,mer} - \Delta G_{i,fac}]/2.30RT \tag{9}$$

This relationship implies that the separation factor for the *mer–fac* isomer pair depends on the difference in the interaction of the respective isomers with solvents.

In a molecule of the *fac* form of a tris complex with a fluorinated β-diketone, three trifluoromethyl groups with a higher electron withdrawing tendency than the methyl group (Hammet constant $\sigma_P = 0.54$ for $-CF_3$, -0.17 for $-CH_3$) are located at the three edges of one area of the octahedron, which makes this form more polar than

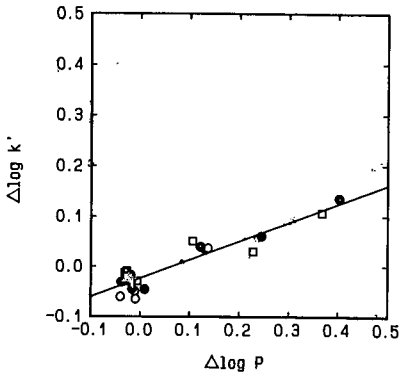

Fig. 10. Correlation between $\Delta\log k'$ and $\Delta\log P$ for geometrical isomers of tris(β-diketonato)–chromium-(III). X_{CH_3OH}: ○ = 0.6; ● = 0.8; □ = 1.0.

the *mer* form in which the fluorinated groups are distributed on different sides of the octahedron. For example, the dipole moments of the *fac* and *mer* forms of $Co(tfa)_3$ were reported to be 6.48 and 3.80 D, respectively [23]. It is considered that such a polar *fac* form, compared with the *mer* form, tends to interact strongly with the methanol and/or water which constitutes the polar liquid phase in the partition system, and this causes $\Delta\log P$ to be positive.

In the case of the isomers of a complex with a non-fluorinated β-diketone, the difference in the dipole moment between the *mer* and *fac* forms of the complex is regarded as small, because the electron withdrawing abilities of the functional groups, such as alkyl and phenyl ($\sigma_P = -0.15$ for ethyl, -0.01 for phenyl), are not so considerable as for $-CF_3$, but instead near to that of methyl. Accordingly, the negative extent of the $\Delta\log P$ observed for the complex of such a non-fluorinated β-diketone is attributed not to the dipole–dipole interaction between the complex and the polar liquid phase constituent(s) but to some other kinds of interactions. No particular interaction can be specified at this stage.

Fig. 10 shows that the $\Delta\log k'$ in the chromatography using ODS as the stationary phase is well correlated with $\Delta\log P$ in the liquid–liquid system using dodecane as the non-polar phase ($r = 0.934$; $n = 21$). The linear regression line is given by

$$\Delta\log k' = (0.37 \pm 0.07)\,\Delta\log P - (0.02 \pm 0.01) \tag{10}$$

This correlation suggests that the chromatographic retention selectivities for the *mer* and *fac* forms are governed by analogous interactions to those affecting the selectivity in the liquid–liquid partition.

It was previously found [7] in work on the retention behaviour of the β-diketonato complexes of chromium(III) and palladium(II) that the capacity factor, k', of a metal complex in the ODS–(methanol–water) system was empirically related to the partition coefficient, P (K_D in paper by Saitoh *et al.* [7]), in the dodecane–(methanol–water) system, as given by the following equations, provides that the same composition of methanol–water is used in both systems

$$\log k' = \log P - p\Delta G_i/2.3RT + q \tag{11}$$

$$\log k' = (1 + p)\log P + p\Delta G_C/2.3RT + q \tag{12}$$

where p and q are constants for a given composition of methanol–water.

When these equations are applied to geometrical isomers of the metal complexes studied here, eqn. (12) is modified for the *mer* and *fac* forms, as follows:

$$\log k'_{mer} = (1 + p) \log P_{mer} + p\Delta G_{C,mer}/2.3RT + q \quad (13)$$

$$\log k'_{fac} = (1 + p) \log P_{fac} + p\Delta G_{C,fac}/2.3RT + q \quad (14)$$

When $\Delta G_{C,mer}$ is equal to $\Delta G_{C,fac}$, the following proportional relationship is predicted:

$$\Delta \log k' = (1 + p)\Delta \log P \quad (15)$$

According to the reported values of p (-0.488 to -0.574 at X_{CH_3OH} 0.60–1.00) [7], the proportional coefficient, $(1 + p)$, is predicted in the range 0.426–0.512. It is shown by the experimental plot in Fig. 10 that $\Delta \log k'$ is nearly proportional to $\Delta \log P$. The observed proportional coefficient (strictly, the slope of the regression line), 0.37 ± 0.07, is close to the predicted value. This supports the validity of the empirical equations 11 and 12. It is noted that the slope of the plot of $\Delta \log k'$ *versus* $\Delta \log P$ is smaller than unity (see Fig. 10).

In conclusion with respect to the separation factor for the geometrical isomer pair of tris(β-diketonato)–chromium(III), chromatography in the ODS–(methanol–water) system is inferior to partition in the dodecane–(methanol–water) system, although some exceptions are found.

REFERENCES

1 J. F. K. Huber, J. C. Kraak and H. Veening, *Anal. Chem.*, 44 (1972) 1554.
2 N. Suzuki and K. Saitoh, *Bull. Chem. Soc. Jpn.*, 50 (1977) 2907.
3 C. A. Tollinche and T. H. Risby, *J. Chromatogr. Sci.*, 16 (1978) 448.
4 K. Saitoh and N. Suzuki, *Anal. Chem.*, 52 (1980) 30.
5 R. C. Gurira and P. W. Carr, *J. Chromatogr. Sci.*, 20 (1982) 461.
6 T. J. Cardwell, T. H. Lorman and Z. Z. Feng, *J. Chromatogr.*, 358 (1986) 187.
7 K. Saitoh, S. Tsukahara and N. Suzuki, *J. Chromatogr.*, 439 (1988) 245.
8 R. C. Fay and T. S. Piper, *J. Am. Chem. Soc.*, 84 (1962) 2303.
9 R. C. Fay and T. S. Piper, *J. Am. Chem. Soc.*, 85 (1963) 500.
10 P. C. Uden, I. E. Bigley and F. H. Walters, *Anal. Chim. Acta*, 100 (1978) 555.
11 C. M. Kirkman, C. Zu-Ben, P. C. Uden, W. J. Stratton and D. E. Henderson, *J. Chromatogr.*, 317 (1984) 569.
12 T. Omori, K. Hashimoto, T. Sekine and K. Yoshihara, *J. Chromatogr.*, 299 (1984) 201.
13 B. Wenclawiak, R. M. Barkley, E. J. Williams and R. E. Sievers, *J. Chromatogr.*, 349 (1985) 469.
14 W. C. Fernerius and J. E. Blanch, *Inorg. Synth.*, 5 (1957) 130.
15 B. E. Bryant and W. C. Fernerius, *Inorg. Synth.*, 5 (1957) 180.
16 F. W. Swamer and C. R. Hauser, *J. Am. Chem. Soc.*, 72 (1950) 1352.
17 R. J. York, W. D. Bonds, Jr., B. P. Cotsoradis and R. D. Archer, *Inorg. Chem.*, 8 (1969) 789.
18 K. Saitoh, S. Tsukahara and N. Suzuki, *Anal. Sci.*, 3 (1987) 309.
19 R. A. Pierotti, *Chem. Rev.*, 76 (1976) 717.
20 H. Watarai, M. Tanaka and N. Suzuki, *Anal. Chem.*, 54 (1982) 703.
21 H. Waterai, H. Oshima and N. Suzuki, *Quant. Struct.-Act. Relat.*, 3 (1984) 17.
22 K. Saitoh, S. Tsukahara and N. Suzuki, *Anal. Lett.*, 21 (1988) 599.
23 R. A. Palmer, R. C. Fay and T. S. Piper, *Inorg. Chem.*, 3 (1964) 875.

Journal of Chromatography, 547 (1991) 239–245
Elsevier Science Publishers B.V., Amsterdam

CHROM. 23 207

Temperature dependence of dead time as determined by methane retention in open-tubular capillary gas chromatography

B. KOPPENHOEFER*, G. LAUPP and M. HUMMEL
Institut für Organische Chemie der Universität, Auf der Morgenstelle 18, D-7400 Tübingen (Germany)
(First received September 4th, 1990; revised manuscript received February 13th, 1991)

ABSTRACT

The temperature dependence of the retention time of methane was determined in open-tubular capillary gas chromatography with either nitrogen or hydrogen as the carrier gas. Linear regression according to the equation $t_M = AT^B$ gave smaller standard deviations s for $0.5 < B < 1$ than for $B = 0.5$. However, the equation $t_M = Ae^{B-T}$ may fit almost equally well, the constant B being approximately independent of the column inlet pressure and of the nature of the carrier gas, which facilitates the determination of the theoretically important term $\delta \ln k'/\delta(1/T)$.

INTRODUCTION

Interest has been shown in the use of retention data for qualitative analysis ever since the advent of gas chromatography [1]. Several methods for the determination of the column dead time t_0 are currently in use. The non-coincidence [2] of gas hold-up t_0 and retention time t_M of a "non-interacting" compound such as air [3] or methane [4] has led to the determination of t_0 by a variety of computational methods based on retention data of hydrocarbons, some of which involve a high degree of sophistication [5]. Whereas significant differences between t_M and t_0 were found for packed columns showing methane adsorption [6,7], in gas–liquid chromatography with contemporary open-tubular capillary columns the methane retention time t_M in first order represents a fairly good approximation for t_0, provided that the column temperature is sufficiently high.

The temperature dependence of t_M is of interest in two fields of increasing importance, *viz.*, the determination of thermodynamic parameters of solute–solvent interactions, particularly useful for chiral recognition studies [8–10], and the prediction of retention data under temperature programming [11–14]. Ettre [15] calculated temperature-dependent viscosity data for several carrier gases that were adopted by many workers [11–13,16–19]; however, only a few experimental data on the temperature dependence of t_M have been published [17,18]. This observation prompts us to report on some previous experimental investigations on this subject [20,21].

0021-9673/91/$03.50

EXPERIMENTAL

Gas chromatography was performed on a Carlo-Erba Model 2101 gas chromatograph with hydrogen or nitrogen as the carrier gas. The inlet pressure was kept at a set of constant values, as indicated; the splitting ratio was 1:50 and detection was effected with a flame ionization detector. Retention data were measured in triplicate, using a stop-watch. Linear regression calculations were performed according to the method of Deming [22], where each data point is represented by a three-dimensional Gaussian.

Non-deactivated borosilicate glass capillaries were coated with L-Chirasil-Val [23–25], as described [26]. A stainless-steel capillary column was coated with squalane, as described [27].

RESULTS AND DISCUSSION

The capillary column may be compared with an Oswald viscometer; according to the Hagen–Poiseuille law let [28]

$$\eta = Cdt_M \tag{1}$$

where η = viscosity of the gas, d = density, C = constant for the given apparatus and t_M = gas hold-up. Neglecting the temperature dependence of C and d, it follows that

$$\frac{\delta t_M}{dT} \propto \frac{\delta \eta}{dT} \tag{2}$$

Hence the effect of the temperature dependence of dead time t_M is reduced to the well known problem of the temperature dependence of the viscosity η. Depending on the gas theory applied, several equations have been established [29]:

$$\eta \propto T^{0.5} \qquad \text{ideal gas theory} \tag{3}$$

$$\eta \propto T^{B} \qquad \text{for real gases} \tag{4}$$

where B varies from *ca.* 0.7 for hydrogen up to 1.0 for less ideal gases, and

$$\eta \propto \frac{T^{0.5}}{1 + C/T} \qquad \text{Sutherland equation} \tag{5}$$

where C is a constant specific for the particular compound, and for $C = 0$ eqn. 5 is reduced to eqn. 3. It is worth mentioning that the temperature dependence of the viscosity played a historical role in establishing a suitable model for gases, *e.g.*, Maxwell erronously predicted an exponent $B = 1.0$ in eqn. 4, assuming that the molecules would repel one another with a force inverse to the fifth power of the distance between them [29]. In contrast, the Sutherland eqn. 5, still in use today [28,30,31], is based on the assumption of a viscous action between successive gas layers.

TABLE I

TEMPERATURE DEPENDENCE OF THE RETENTION TIME OF METHANE ON SQUALANE WITH NITROGEN AS THE CARRIER GAS: COMPARISON OF EXPERIMENTAL AND CALCULATED DATA

Stainless-steel capillary column (100 m × 0.5 mm I.D.), inlet pressure 0.5 bar, splitting ratio 1:50, flame ionization detection; conditions (a) (see Table III).

T(°C)	t_M(s)				
	Experimental, $t_{M_{exp}}$	Calculated			
		t_{M_1}	t_{M_2}	t_{M_3}	t_{M_4}
50	359.3	359.22	359.28	363.42	359.16
60	367.6	367.68	367.68	369.00	367.74
70	376.0	376.02	375.96	374.52	376.08
80	384.2	384.18	384.18	379.92	384.06

In view of this discussion, we decided to determine t_M in a gas chromatographic apparatus at different temperatures. In a first experiment with nitrogen as the carrier gas (see Table I), experimental data $t_{M_{exp}}$ were compared with t_{M_1}, t_{M_2} and t_{M_4} obtained from different regression analyses:

$$t_{M_1} = AT^{0.5} + B \tag{6}$$

$$t_{M_2} = AT^B \tag{7}$$

$$t_{M_3} = AT^{0.5} \tag{8}$$

$$t_{M_4} = Ae^{B/T} \tag{9}$$

The one-parameter approximation, eqn. 8, can be ruled out by the fairly poor accordance with the experimental data for $t_{M_{exp}}$ (see Table III). However, all two-parameter approximations examined, eqns. 6, 7 and 9, agree almost equally well with $t_{M_{exp}}$. On the basis of the standard deviations s, 0.06 s for both t_{M_1} and t_{M_2} and 0.15 s for t_{M_4}, a clear distinction between the three different mathematical models is not possible.

The good description of the temperature dependence of the retention time of methane by the exponential approximation, eqn. 9 deserves particular attention. To the best of our knowledge, there is no corresponding equation for the viscosity of gases in literature. However, with respect to the viscosity of liquids, Andrade [32] published eqn. 10, which was later modified by Vogel to give eqn. 11 [33]:

$$\eta \propto e^{B/T} \tag{10}$$

$$\eta \propto e^{B/(T-C)} \tag{11}$$

The underlying model is not too different from that discussed for the viscosity of gases in the way in which a given flux is assumed, and the interaction of one layer of molecules with an adjacent layer of molecules in the liquid is used to derive the viscosity behaviour. The high predictive power of Andrade's eqn. 10 was regarded as "quite astonishing" in view of the imperfections in all the considerations involved [33].

In contrast to this statement, one may argue that an open-minded comparison of the different theoretical approaches may eventually demonstrate the arbitrariness of the multi-parameter regression analyses applied, in view of the limited accuracy of the experimental data. In order to shed some more light on the problem, an extended series of measurements were performed with hydrogen as the carrier gas. For each of four different values of the inlet pressure fourteen data points were taken (see Table II). For $p_i = 0.5$ bar hydrogen, the parabolic approximation t_{M_2}, calculated according to eqn. 7 as published previously [15], was compared with the exponential approximation t_{M_4} as proposed in eqn. 9 (see Fig. 1). No significant advantage of the former approach over the latter can be seen from this plot.

A similar observation is made for the overall set of experimental data, as judged from the standard deviation s. The relative error in the temperature coefficient B is in the range 0.9–2.2% for eqn. 7 and 1.5–2.9% for eqn. 9. However, these deviations are far below the relative errors calculated for the mean values of B, *i.e.*, 3.8% for eqn. 7 and 4.0% for eqn. 9. There is no apparent dependence of B on the inlet pressure p_i. As predicted by the classical kinetic gas theory, η of an ideal gas should be independent of its pressure p [29]. Moreover, there should be no apparent influence of the pressure drop $\Delta p = (p_i - p_0)$ on the temperature coefficient B. This prediction is justified by the

TABLE II

TEMPERATURE AND INLET PRESSURE DEPENDENCE OF THE RETENTION TIME OF METHANE ON L-CHIRASIL-VAL WITH HYDROGEN AS THE CARRIER GAS (EXPERIMENTAL DATA)

Borosilicate glass capillary column (No. H14, 20 m × 0.25 mm I.D.), splitting ratio 1:50, flame ionization detection, conditions (b) (see Table III).

T(°C)	$t_{M_{exp}}$(s)			
	0.3	0.5	0.7	1.0 [bar]
50	52.9_3	32.0_7	23.4_0	17.3_0
60	53.8_0	32.6_7	23.8_3	17.5_3
70	54.8_3	33.2_0	24.2_3	17.9_3
80	55.3_7	34.1_3	24.5_3	18.2_0
90	56.4_8	34.6_3	25.0_7	18.6_0
100	57.5_3	35.1_7	25.4_5	18.8_8
110	58.8_3	35.7_3	25.9_5	19.2_7
120	59.9_3	36.3_0	26.5_0	19.5_5
130	61.2_0	37.0_7	27.2_3	19.9_7
140	62.1_3	37.9_0	27.7_7	20.2_3
150	62.9_3	38.1_7	28.1_0	20.4_7
160	64.1_0	38.5_5	28.3_0	20.7_7
170	65.0_3	39.1_3	28.8_7	21.0_7
180	66.0_7	39.8_3	29.2_7	21.4_0

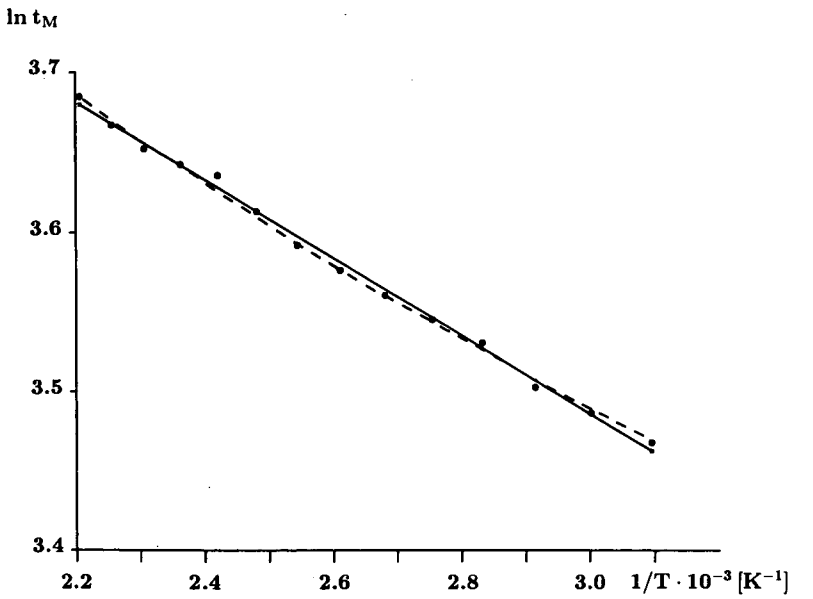

Fig. 1. Comparison of the two approaches, t_{M_2} and t_{M_4}, with the experimental data; conditions (b) (Table III), 0.5 bar H_2. Solid line, $t_{M_2} = 68.2e^{-246/T}$ s; dashed line, $t_{M_2} = 0.807T^{0.64}$ s.

TABLE III

LINEAR REGRESSION ANALYSES

Chromatographic conditions[a]	Theoretical model	Regression equation for t_M (s)	s (s)[b]
(a) 0.5 bar N_2	$t_{M_1} = AT^{0.5} + B$	$t_{M_1} = (30.55 \pm 0.09)\sqrt{T} - (190.0 \pm 1.6)$	0.06
	$t_{M_2} = AT^B$	$\ln t_{M_2} = (0.756 \pm 0.002) \ln T + (1.517 \pm 0.012)$	0.06
	$t_{M_3} = AT^{0.5}$	$t_{M_3} = (20.22 \pm 0.20)\sqrt{T}$	4.46
	$t_{M_4} = Ae^{B/T}$	$\ln t_{M_4} = -(255.2 \pm 2.2) \cdot 1/T + (6.673 \pm 0.007)$	0.15
(b) 0.3 bar H_2	$t_{M_2} = AT^B$	$\ln t_{M_2} = (0.675 \pm 0.011) \ln T + (0.059 \pm 0.063)$	0.24
0.5 bar H_2		$\ln t_{M_2} = (0.640 \pm 0.010) \ln T - (0.227 \pm 0.061)$	0.14
0.7 bar H_2		$\ln t_{M_2} = (0.688 \pm 0.015) \ln T - (0.830 \pm 0.091)$	0.15
1.0 bar H_2		$\ln t_{M_2} = (0.638 \pm 0.006) \ln T - (0.841 \pm 0.038)$	0.05
	Mean value for B	(0.660 ± 0.025)	
(b) 0.3 bar H_2	$t_{M_4} = Ae^{B/T}$	$\ln t_{M_4} = -(261.4 \pm 6.5) \cdot 1/T + (4.762 \pm 0.017)$	0.31
0.5 bar H_2		$\ln t_{M_4} = -(246.0 \pm 4.3) \cdot 1/T + (4.223 \pm 0.011)$	0.04
0.7 bar H_2		$\ln t_{M_4} = -(264.6 \pm 7.6) \cdot 1/T + (3.957 \pm 0.020)$	0.05
1.0 bar H_2		$\ln t_{M_4} = -(245.2 \pm 3.6) \cdot 1/T + (3.600 \pm 0.009)$	0.05
	Mean value for B	$-(255.3 \pm 10.2)$	

[a] As indicated in Tables I and II.

[b] Standard deviation $s = \sqrt{\frac{1}{n-2} \sum_{i=1}^{n} (t_{M_{exp}} - t_{M_j})^2}$

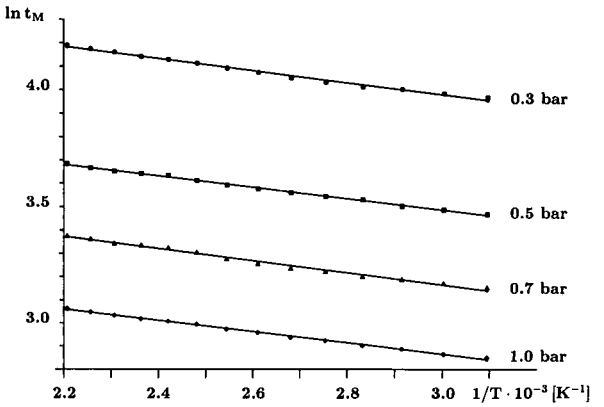

Fig. 2. Comparison of experimental and theoretical data t_{M_4}; conditions (b) (Table III), 0.3, 0.5, 0.7 and 1.0 bar H_2.

data in Table III. The entire data set of conditions (b) is depicted in Fig. 2, together with the regression analyses according to the exponential eqn. 9.

Hence this approach proves to be equally valid for gases, and not only for liquids as originally assumed. Intriguingly, both carrier gases, hydrogen and nitrogen, show a similar temperature coefficient, *i.e.*, $B = -255$. Whether this coincidence is real or an artefact remains open to further investigations. In the equation $t_M = AT^B$, a significant difference in B is found for the different gases, *i.e.*, $B = 0.756$ for nitrogen and $B = 0.660$ for hydrogen. Both values differ only slightly from those used by Ettre [15] for the temperature coefficient of the viscosity $\eta \propto T^B$ with $B = 0.725$ for nitrogen and $B = 0.680 - 0.695$ for hydrogen.

CONCLUSIONS

The temperature dependence of the retention time of methane is in good accord with both eqns. 7 and 9. As judged by the standard deviations s, both approaches are of striking resemblance. The latter, although following a viscosity theory originally established by Andrade [32] for liquids, has the advantage of fitting into the determination of thermodynamic parameters of solute–solvent interaction by gas chromatography. We found it convenient simply to determine the temperature dependence of the net retention t'_R at a constant inlet pressure [9], which yields the theoretically important term

$$\frac{\delta \ln k'}{\delta(1/T)} = \frac{\delta \ln t'_R}{\delta(1/T)} - B \tag{12}$$

where the constant B is approximately independent of the column inlet pressure and of the nature of the carrier gas. Beyond these applications in the realm of chromatography, the exponential equation $\eta \propto e^{B/T}$ proposed for the temperature dependence of the viscosity of gases may be of general interest with regard to model building in kinetic gas theory [29].

ACKNOWLEDGEMENTS

We are indebted to Professors E. Bayer and V. Schurig for helpful support.

REFERENCES

1 L. G. Blomberg, *Adv. Chromatogr.*, 26 (1987) 329.
2 J. F. Smith, *Nature (London)*, 198 (1962) 679.
3 D. A. Ambrose, A. T. James, A. I. M. Keulemans, E. Kovats, H. Röck, C. Rouit and F. H. Stross, *Pure Appl. Chem.*, 1 (1960) 177.
4 R. Feinland, A. J. Ardreatch and D. P. Cotrupe, *Anal. Chem.*, 33 (1961) 991.
5 R. J. Smith, J. K. Haken and M. S. Wainwright, *J. Chromatogr.*, 334 (1895) 95.
6 V. A. Ezrets and M. S. Vigdergauz, *Chromatographia*, 9 (1976) 205.
7 H. Becker and R. Gnauck, *J. Chromatogr.*, 366 (1986) 378.
8 U. Beitler and B. Feibush, *J. Chromatogr.*, 123 (1976) 149.
9 B. Koppenhoefer and E. Bayer, *Chromatographia*, 19 (1984) 123.
10 V. Schurig, J. Ossig and R. Link, *Angew. Chem.*, 101 (1989) 197.
11 J. Curvers, J. Rijks, C. Cramers, K. Knauss and P. Larson, *J. High Resolut. Chromatogr. Chromatogr. Commun.*, 8 (1985) 607.
12 B.-J. Chen, X.-J. Guo and S.-Y. Peng, *Chromatographia*, 23 (1987) 888.
13 J. Krupcik, D. Repka, T. Hevesi and J. Garaj, *J. Chromatogr.*, 406 (1987) 117.
14 B.-C. Lin, B.-C. Lin and B. Koppenhoefer, *Anal. Chem.*, 60 (1988) 2135.
15 L. S. Ettre, *Chromatographia*, 18 (1984) 243.
16 P. A. Leclercq and C. Cramers, *J. High Resolut. Chromatogr. Chromatogr. Commun.*, 8 (1985) 765.
17 M. Larsson, *J. High Resolut. Chromatogr. Chromatogr. Commun.*, 10 (1987) 357.
18 D. V. Crabtree, A. J. Adler and G. J. Handelman, *J. Chromatogr.*, 466 (1989) 251.
19 B.-J. Chen, X.-J. Guo and S.-Y. Peng, *Chromatographia*, 25 (1988) 888.
20 B. Koppenhoefer, *Thesis*, University of Tübingen, 1980.
21 G. Laupp, *Thesis*, University of Tübingen, 1987.
22 W. E. Deming, *Statistical Adjustment of Data*, Wiley, New York, and Chapman and Hall, London, 1948.
23 H. Frank, G. J. Nicholson and E. Bayer, *J. Chromatogr. Sci.*, 15 (1977) 174.
24 E. Bayer, *Z. Naturforsch., Teil B*, 38 (1983) 1281.
25 B. Koppenhoefer and E. Bayer, in F. Bruner (Editor), *The Science of Chromatography*, Elsevier, Amsterdam, 1985, p. 1.
26 G. J. Nicholson, H. Frank and E. Bayer, *J. High Resolut. Chromatogr. Chromatogr. Commun.*, 2 (1979) 411.
27 V. Schurig, *Chromatographia*, 13 (1980) 263.
28 *Handbuch des Chemikers*, Vol. I, VEB Verlag Technik, Berlin, 1956.
29 W. Sutherland, *London, Edinb. Dublin Philos. Mag., Ser. 5*, 36 (1883) 507.
30 M. Trautz, *Ann. Phys. (Leipzig), Folge 5*, 11 (1931) 190.
31 *Ullmanns Encyklopädie der Technischen Chemie*, Vol. 2/1, Urban Schwarzenberg, Munich, Berlin, 1961, p. 777.
32 E. N. da C. Andrade, *Nature (London)*, 125 (1930) 582.
33 U. Rost, *Kolloid-Z.*, 142 (1955) 132.

Journal of Chromatography, 547 (1991) 247–257
Elsevier Science Publishers B.V., Amsterdam

CHROM. 23 298

Topological indices as structural parameters

Structure–retention relationships for oxyethylene derivatives of alcohols, thioalcohols and alkylamines

ADAM VOELKEL

Poznań Technical University, Institute of Chemical Technology and Engineering, Pl. M. Sklodowskiej-Curie 2, 60-965 Poznań (Poland)

(First received October 24th, 1990; revised manuscript received March 13th, 1991)

ABSTRACT

A quantitative structure–retention relationship analysis is presented for the retention indices and topological parameters of a set of oligooxyethylene derivatives. The usefulness of the topological indices as structural descriptors was examined.

INTRODUCTION

Oligooxyethylene derivatives of alcohols, thioalcohols and alkylamines have been examined as solutes on typical stationary phases of various polarities [1,2] and have also been characterized by inverse gas chromatography [3]. The properties of topological indices as structural parameters for oligooxyethylene derivatives have been discussed previously [4]. It was shown that the molecular connectivity and valence molecular connectivity indices, the Balaban index and the Wiener number are all sensitive to the presence and size of alkyl group(s), oligooxyethylene chains(s) and heteroatoms, as well as position in the molecule.

The structure of molecules can be translated into numerical descriptors using chemical graph theory [5]. Trinajstič *et al.* [6] placed all the structural parameters discussed in this paper into the group of structure-explicit quantitative structure–activity relationship models. These models offer a clear mathematical characterization of the fundamental chemical structure and are non-empirical in origin. The well defined structural parameters have a precise structural interpretation. It has been pointed out [6] that a good choice of structural descriptor can produce a simple and physically valid correlation. However, a poor choice may lead to bad correlations or may not recognize a regularity in the data. Kaliszan [5] cautioned against the overfitting of the structural data, which can make the quantitative structural–retention relationship (QSRR) dubious. Special attention should be paid to the possible intercorrelations among the structural descriptors used as independent variables in the same equation. Kaliszan [5]

0021-9673/91/$03.50

recommended the presentation of results of the correlation analysis, including statistics, as given in Tables IV and VII.

It was proved that the chromatographic retention parameter should be described by at least a two-parameter equation:

$$R = aP + bNP + c \tag{1}$$

where R is the retention parameter, P is the polar interactions parameter and NP is the apolar interactions parameter; a, b and c are constants.

Lamparczyk and co-workers [7,8] derived such an equation from the general relationship for Van der Waals forces acting between the solute and liquid stationary phase in chromatographic process:

$$RI = \frac{1}{P}\left[\frac{(A\mu_{ph}^2 + \alpha_{ph})\mu_s^2 + (B_s\alpha_{ph} + \mu_{ph}^2)\alpha_s}{B_N\alpha_{ph} + \mu_{ph}^2}\right] - C \tag{2}$$

where α_{ph} and α_s are the polarizability parameters for the stationary phase and the solute, respectively; μ_{ph} and μ_s are the dipole moments for the stationary phase and the solute, respectively; $A = (2/3)kT$, where k is Boltzmann's constant and T is the absolute temperature; $B_s[(I_{ph}I_S)/(I_{ph} + I_s)$; $B_N = [(I_NI_S)/(I_N + I_s)$; I_s, I_N and I_{ph} are the first ionization potential for the solute, reference n-alkane and stationary phase, respectively; and p and C are constants.

When the respective parameters for the stationary phase are not known, eqn. 2 converts to eqn. 1. Such relationships have been used by several workers [9–11]. However, dipole moments are often not available from the literature. The method of calculation of the so-called chromatographic dipole moments has been successfully used in the QSRR analysis of alkenes [11].

QSRR with the use of topological indices has not yet been presented for oxyethylated derivatives of alcohols, thioalcohols and alkylamines. Previously reported relationships correlated the retention parameters with only the number of carbon atoms or oxyethylene units in the molecules. In this paper the appropriate chromatographic dipole moments for the examined compounds will be evaluated. Their dependence on the topological parameters used in the calculation procedure and on the chemical nature of the stationary phase will be given. The advantages and limitations of the use of topological parameters in structure–retention relationships will be illustrated.

EXPERIMENTAL

Thirty pure model oligooxyethylene derivatives of alcohols, thioalcohols and alkylamines of the general formula $RX(CH_2CH_2O)_nR'$ (where R = C_4H_9, C_6H_{13}, C_8H_{17}; R′ = H, CH_3; X = O, NH, S; n = 0–3) were used as solutes. These compounds have been characterized previously [1,2]. Retention indices and the thermodynamic solution parameters were taken from Voelkel [2]. All the retention parameters considered were estimated on four stationary phases, *i.e.* SE-30, Apiezon K, OV-17 and QF-1. The molecular connectivity indices ${}^n\chi$ and valence molecular indices of various orders ${}^n\chi^v$, the Balaban index (I_B) and the Wiener number [$W(G)$]

were used as structural parameters. The methods of their calculation have been presented by Voelkel [4].

RESULTS AND DISCUSSION

Voelkel [4] has indicated that the considered topological indices are sensitive to the presence of heteroatoms. The values of the calculated topological parameters and some structural data are summarized in Tables I and II. The increase of the number of carbon atoms in the alkyl group decreases I_B, whereas the other considered topological indices increase. An increase in the oligooxyethylene chain length increases all the structural parameters. The attachment of each oligooxyethylene group increases the molecular connectivity indices $^1\chi$, $^2\chi$ and $^3\chi$ by 1.5, 1.0606 and 0.75 I.U., respectively. The same increments for the valence molecular connectivity indices $^1\chi^v$, $^2\chi^v$ and $^3\chi^v$ are 1.0774, 0.6124 and 0.3720, respectively.

TABLE I

TOPOLOGICAL INDICES AND STRUCTURAL DATA FOR OLIGOOXYETHYLENE DERIVATIVES OF ALCOHOLS, THIOALCOHOLS AND ALKYLAMINES: $RX(CH_2CH_2O)_nR'$

No.	R	R′	X	n	Balaban index, I_B	Wiener number, $W(G)$	Rouvray index, $R(G)$
1	C_4H_9	H	O	0	2.2836	19.125	38.25
2	C_4H_9	H	O	2	3.1250	190.375	380.75
3	C_4H_9	H	O	3	3.2747	388.5	777
4	C_6H_{13}	H	S	0	2.5824	52.5625	105.125
5	C_6H_{13}	H	S	1	3.2625	135.0625	270.125
6	C_6H_{13}	H	S	2	3.4860	292.5625	585.125
7	C_6H_{13}	H	S	3	3.5535	547.5625	1095.125
8	C_6H_{13}	H	O	0	2.4996	54.625	109.25
9	C_6H_{13}	H	O	1	2.8809	151.75	303.5
10	C_6H_{13}	H	O	2	3.1116	323.871	647.75
11	C_6H_{13}	H	O	3	3.2550	593.5	1187
12	C_6H_{13}	H	NH	0	2.4748	55.2135	110.427
13	C_6H_{13}	H	NH	1	2.7882	156.5115	313.023
14	C_6H_{13}	H	NH	2	3.0192	332.8095	665.619
15	C_6H_{13}	H	NH	3	3.1785	606.6075	1213.215
16	C_8H_{17}	H	S	0	2.6792	115.3125	230.625
17	C_8H_{17}	H	S	1	3.1603	246.8125	493.625
18	C_8H_{17}	H	S	2	3.3922	468.3125	936.625
19	C_8H_{17}	H	S	3	3.4969	802.3125	1604.625
20	C_8H_{17}	H	O	0	2.6280	118.125	236.25
21	C_8H_{17}	H	O	1	2.8974	268.75	537.5
22	C_8H_{17}	H	O	2	3.0912	509.375	1018.75
23	C_8H_{17}	H	O	3	3.2266	862.5	1725
24	C_8H_{17}	H	NH	0	2.6136	118.9275	237.855
25	C_8H_{17}	H	NH	1	2.8303	275.0095	550.019
26	C_8H_{17}	H	NH	2	3.0156	521.0915	1042.183
27	C_8H_{17}	H	NH	3	3.1569	879.6735	1759.347
28	C_6H_{13}	CH_3	O	3	3.2960	707.5	1415
29	C_8H_{17}	CH_3	O	3	3.2652	1007.5	2015
30	$C_{10}H_{21}$	CH_3	O	3	3.2360	1383.5	2767

TABLE II

MOLECULAR CONNECTIVITY INDICES FOR COMPOUNDS STUDIED

No.	Molecular connectivity index			Valence molecular connectivity index		
	$^1\chi$	$^2\chi$	$^3\chi$	$^1\chi^v$	$^2\chi^v$	$^3\chi^v$
1	2.4142	1.3536	0.7071	2.0233	1.0772	0.5117
2	5.4142	3.4749	2.2071	4.1780	2.3019	1.2499
3	6.9142	4.5355	2.9571	5.2554	2.9143	1.6219
4	3.4142	2.0607	1.2071	3.5710	2.1715	1.2855
5	4.9142	3.1213	1.9571	5.2511	3.6168	2.4225
6	6.4142	4.1820	2.7071	6.3284	4.2292	2.7783
7	7.9142	5.2426	3.4571	7.4058	4.8416	3.1057
8	3.4142	2.0607	1.2071	3.0233	1.7843	1.0117
9	4.9142	3.1213	1.9571	4.1007	2.3936	1.3779
10	6.4142	4.1820	2.7071	5.1780	3.0090	1.7499
11	7.9142	5.2436	3.4571	6.2554	3.6214	2.1219
12	3.4142	2.0607	1.2071	3.1154	1.8493	1.0577
13	4.9142	3.1213	1.9571	4.2304	2.5343	1.4957
14	6.4142	4.1820	2.7071	5.3078	3.1466	1.8659
15	7.9142	5.2426	3.4571	6.3851	3.7590	2.2379
16	4.4142	2.7678	1.7071	4.5710	2.8786	1.7855
17	5.9142	3.8284	2.4571	6.2511	4.3239	2.9225
18	7.4142	4.8891	3.2071	7.3284	4.9363	3.2787
19	8.9142	5.9497	3.9571	8.4058	5.5487	3.6507
20	4.4142	2.7678	1.7071	4.0233	2.4914	1.5117
21	5.9142	3.8284	2.4571	5.1007	3.1037	1.8779
22	7.4142	4.8891	3.2071	6.1780	3.7161	2.2499
23	8.9142	5.9497	3.9571	7.2554	4.3285	2.6219
24	4.4142	2.7678	1.7071	4.1154	2.5564	1.5577
25	5.9142	3.8284	2.4571	5.2304	3.2414	1.9957
26	7.4142	4.8891	3.2071	6.3078	3.8537	2.3659
27	8.9142	5.9497	3.9571	7.3851	4.4661	2.7379
28	8.4142	5.5962	3.7071	6.6361	3.8906	2.3180
29	9.4142	6.3033	4.2071	7.6361	4.5977	2.8180
30	10.4142	7.0104	4.7071	8.6361	5.3048	3.3180

The main disadvantage of the first-order molecular connectivity indices introduced by Kier and Hall [12] is the impossibility of distinguishing between compounds containing different heteroatoms. For example, the second-order molecular connectivity index for $C_8H_{17}S(CH_2CH_2O)_2H$, $C_8H_{17}O(CH_2CH_2O)_2H$ and $C_8H_{17}NH(CH_2CH_2O)_2H$ is 4.8891 in each instance (see Tables I and II). The ability to discriminate between heteroatoms is much better for other topological parameters. Different values of parameters maybe assigned to derivatives of alcohol, thioalcohol and alkylamine. I_B arranges the examined compounds in the following order: derivatives of thioalcohols > derivatives of alcohols > derivatives of alkylamines. The value of W(G), Rouvray index and valence molecular topological indices are highest for the derivatives of thioalcohols and lowest for derivatives of alcohols. It can be stated that the considered structural parameters are generally sensitive (except $^1\chi$, $^2\chi$ and $^3\chi$) to changes in the molecule constituents.

TABLE III

RELATIONSHIPS BETWEEN RETENTION INDICES ON DIFFERENT STATIONARY PHASES AND TOPOLOGICAL PARAMETERS

L = linear, $I_R = a + bX$; M = multiplicative, $I_R = aX^b$

Topological parameter	Relationship	Liquid phase											
		Apiezon K			SE-30			OV-17			QF-1		
		a	*b*	*R*	*a*	*b*	*R*	*a*	*b*	*R*	*a*	*b*	*R*
$^1\chi^v$	L	185	222.3	0.992	129	234.5	0.991	166	258.7	0.987	226	274.6	0.977
	M	5.8	0.848	0.991	5.8	0.881	0.986	5.9	0.876	0.984	6.0	0.851	0.972
$^2\chi^v$	L	310	325.0	0.970	270	340.2	0.961	134	377.3	0.963	383	400.7	0.953
	M	6.3	0.757	0.972	6.3	0.781	0.960	6.4	0.778	0.961	6.5	0.752	0.947
$^9\chi^v$	L	471	452.4	0.938	443	471.0	0.925	503	524.2	0.931	583	556.9	0.921
	M	6.8	0.636	0.947	6.8	0.648	0.930	6.9	0.651	0.933	7.0	0.631	0.917
I_B	L	−1494	962.8	0.864	−1699	1034	0.878	−1945	1172	0.899	−1992	1237	0.884
	M	4.7	0.133	0.894	4.6	4.605	0.914	4.7	2.411	0.962	4.9	2.334	0.914
$W(G)$	L	1025	0.971	0.872	1006	1.048	0.891	1145	1.126	0.864	1267	1.190	0.852
	M	5.7	0.268	0.958	5.6	0.281	0.967	5.8	0.281	0.962	5.9	0.272	0.958

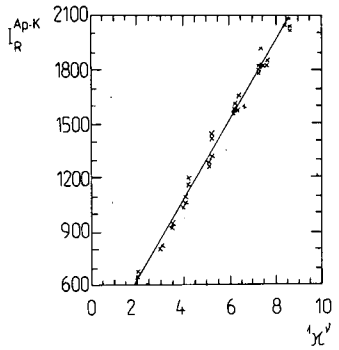

Fig. 1. Relationship between retention indices on Apiezon K and first-order valence molecular connectivity index $^1\chi^v$ for studied compounds.

The relationships between the retention indices of the examined compounds and their topological parameters are given in Table III. Both linear and multiplicative models were considered. The best results were obtained for $^1\chi^v$ used as a structural parameter (Fig. 1). All the relationships were statistically valid; the full statistical parameters for the two relationships are given in Table IV. In some instances better correlation coefficients were obtained for the multiplicative model. However, in this instance the physico-chemical interpretation of the relationship is not clear. The slopes of the linear relationships and regression coefficients a in the multiplicative model increase with an increase of the polar character of the stationary phase.

Gassiot-Mates and Firpo-Pamies [9] proposed the use of the chromatographic dipole moment, μ_{chr}, which characterizes the ability of a solute to undergo polar interactions under chromatographic conditions. Their procedure [9] was used in this work for the calculation of chromatographic dipole moments. The numerical values of such defined parameters will depend on the topological index used as structural

TABLE IV

STATISTICS FOR SELECTED QUANTITATIVE STRUCTURE–RETENTION RELATIONSHIPS BETWEEN RETENTION INDICES AND TOPOLOGICAL PARAMETERS

Statistic	Relationship			
	I_R^{Ap-K} *versus* $^1\chi^v$	I_R^{SE-90} *versus* $^2\chi^v$	I_R^{OV-17} *versus* I_B	I_R^{QF-1} *versus* $^3\chi^v$
Function	$185 + 222.3\,(^1\chi^v)$	$270 + 340.2\,(^2\chi^v)$	$4.7I_B^{2.4}$	$583 + 556.7\,(^3\chi^v)$
Correlation coefficient (R)	0.992	0.961	0.962	0.921
Standard error of estimation	47.6	110.0	218.2	185.2
F-test value	1732.2	341.5	300.1	155.9
p Significance level	0.0000	0.0000	0.0000	0.0000
Confidence intervals for regression coefficients	$121.7 < a < 248.5$ $211.3 < b < 233.2$	$143.3 < a < 404.8$ $302.4 < b < 377.9$	$4.4 < a < 4.8$ $2.3 < b < 2.5$	$379.6 < a < 787.3$ $465.3 < b < 648.1$

TABLE V

CHROMATOGRAPHIC DIPOLE MOMENTS FOR EXAMINED COMPOUNDS

$^1\chi^v$ as structural parameter.

No.[a]	Stationary phase			
	Apiezon K	SE-30	OV-17	QF-1
1	1.6245	1.7517	1.6725	1.8107
2	2.2876	2.1145	1.8114	2.2962
3	3.4942	2.3503	1.8931	2.5699
4	2.3039	1.5473	1.5257	1.2734
5	1.8889	1.8504	1.7245	2.1054
6	0.9143	2.0375	1.7997	2.4087
7	2.2966	2.2235	1.8952	2.6545
8	2.3251	1.5819	1.6672	1.5575
9	1.9915	1.8223	1.6953	2.5050
10	1.0802	2.0505	1.7402	2.2642
11	1.9977	2.2412	1.8450	2.5242
12	2.7639	1.5379	1.5582	1.4381
13	2.7873	2.0160	1.7870	2.2834
14	3.0723	2.2192	1.8017	2.4444
15	3.1738	2.3747	1.8726	2.6963
16	1.2121	1.6749	1.5366	1.4677
17	2.6850	2.0334	1.7113	2.3614
18	1.6638	2.2257	1.7936	2.7005
19	2.4368	2.4694	1.8734	2.9346
20	1.8006	1.5256	1.6452	1.8861
21	1.6856	1.8279	1.6791	2.0420
22	1.7605	2.0963	1.7889	2.4261
23	2.8486	2.3367	1.7752	2.7233
24	1.2338	1.4215	1.4431	1.5709
25	3.0774	1.9193	1.7481	2.3667
26	3.2679	2.1432	1.8173	2.6867
27	3.9327	2.4385	1.8753	2.8489
28	1.8430	2.1110	1.7361	2.1007
29	1.7823	2.2003	1.7510	2.2905
30	1.2682	2.3453	1.6744	2.4355

[a] Numbers of compounds as in Table II.

parameter and the chemical nature of the stationary phase. The chromatographic dipole moments calculated for the examined compounds ($^1\chi^v$ as a structural parameter) are reported in Table V. The value of μ_{chr} usually increases with an increase in the oxyethylene units in the solvent molecule, although some perturbations are observed (Apiezon K, and, in some instances QF-1). Statistically significant relationships have been observed between μ_{chr} values and the polarity of the stationary phase. The μ_{chr} value obtained using various connectivity indices on the same liquid phase are similar, whereas those calculated using $W(G)$ or I_B differ significantly.

The chromatographic dipole moments were used in the modified form of eqn. 1:

$$I_R = a\mu_{chr}^2 + bTP + c \tag{3}$$

TABLE VI

STATISTICS FOR RELATIONSHIPS OF TYPE $I_R = (a\mu^2_{chr}) + (bTP) + c$

Statistic	Stationary phase		
	Apiezon K	SE-30	OV-17
Function	$(8.29\mu^2_{chr}) + (220^1\varkappa^v) + 151.8$	$(72.44\mu^2_{chr}) + (266.4^2\varkappa^v) + 172.4$	$(217.1\mu^2_{chr}) + (229.6^1\varkappa^v) - 331.5$
Correlation coefficient (R)	0.991	0.998	0.999
Standard error of estimation	36.2	17.5	0.354
F-test value	1512.8	7249.5	2195904
p Significance level	0.0000	0.0000	0.0000
Confidence intervals for regression coefficients	$4.63 < a < 11.96$ $211.7 < b < 228.4$	$68.4 < a < 77.54$ $258.8 < b < 274$	$216.6 < a < 217.5$ $229.5 < b < 229.7$

TABLE VII

PREDICTION OF RETENTION INDEX FOR STUDIED COMPOUNDS ON APIEZON K

$^1\chi^v$ as structural parameter.

Compound	Retention index		Error	
	Observed	Fitted	Absolute	Relative
1	675.0	619.3	55.7	8.3
2	1150.0	1114.5	35.5	3.0
3	1437.0	1409.4	27.6	1.9
4	931.0	981.5	−50.5	5.4
5	1318.0	1336.8	−18.8	1.4
6	1564.0	1551.2	12.8	0.8
7	1829.0	1825.1	3.9	0.2
8	815.0	861.8	−46.8	5.8
9	1054.0	1087.0	−33.0	3.1
10	1325.0	1300.8	24.2	1.8
11	1576.0	1561.3	14.7	0.9
12	815.0	900.6	−85.6	10.5
13	1183.0	1147.0	36.0	3.0
14	1424.0	1398.0	26.0	1.8
15	1656.0	1640.3	15.7	1.0
16	1200.0	1169.7	30.3	2.5
17	1603.0	1587.0	16.0	1.0
18	1791.0	1787.2	3.8	0.2
19	2045.0	2050.6	− 5.6	0.3
20	1044.0	1063.9	−19.9	1.9
21	1274.0	1297.7	−23.7	1.9
22	1552.0	1536.9	15.1	1.0
23	1822.0	1815.5	6.5	0.3
24	1091.0	1057.8	33.2	3.0
25	1408.0	1381.2	26.8	1.9
26	1645.0	1628.3	16.7	1.0
27	1913.0	1905.0	8.0	0.4
28	1592.0	1679.0	−87.0	5.5
29	1837.0	1837.1	− 0.1	0.0
30	2028.0	2065.4	−37.4	1.8

where *TP* is the topological parameter and *a*, *b* and *c* are regression coefficients.

In all instances statistically significant relationships were obtained. The relevant data are given in Table VI. With the use of the known structural parameter and chromatographic dipole moment it is possible to predict the retention data of a compound (Table VII).

The problem of over-fitting the data used as independent variables in the regression equation should be taken into consideration, as a high intercorrelation among variables could cause the QSRR to be suspect. As topological parameters are to some extent used in the procedure of the estimation of μ_{chr}, the statistical independence of both variables to be used in eqn. 2 should be checked. Intercorrelation matrices were constructed for the first-order connectivity index and respective μ_{chr} values (Table VIII) as well as for $W(G)$ and the appropriate μ_{chr} values. It can be assumed that $^1\chi^v$,

TABLE VIII

INTERCORRELATION MATRIX FOR $^1\chi^v$, $^2\chi^v$ AND APPROPRIATE CHROMATOGRAPHIC DIPOLE MOMENTS

Independent variable	$^1\chi^v$	μ_{chr}^{ApK}	μ_{chr}^{SE-30}	μ_{chr}^{OV-17}	μ_{chr}^{QF-1}
$^1\chi^v$	1.0000	0.0795	0.3104	0.5707	0.4179
μ_{chr}^{ApK}		1.0000	0.3960	0.5039	0.3723
μ_{chr}^{SE-30}			1.0000	0.8655	0.8996
μ_{chr}^{OV-17}				1.0000	0.8826
μ_{chr}^{QF-1}					1.0000
	$^2\chi^v$	μ_{chr}^{ApK}	μ_{chr}^{SE-30}	μ_{chr}^{OV-17}	μ_{chr}^{QF-1}
$^2\chi^v$	1.0000	—	0.6101	0.4731	0.6568
μ_{chr}^{ApK}		—	—	—	—
μ_{chr}^{SE-30}			1.0000	0.9515	0.9015
μ_{chr}^{OV-17}				1.0000	0.9111
μ_{chr}^{QF-1}					1.0000

$^2\chi^v$ and the respective μ_{chr} values are uncorrelated whereas $W(G)$ strongly influences the values of the calculated chromatographic dipole moment with the use of this topological parameter. This will probably limit the application of $W(G)$ and I_B in QSRR analysis for gas chromatographic retention indices.

CONCLUSIONS

The best retention–structure correlations were obtained when the valence molecular connectivity indices were used as structural parameters. The Balaban index, I_B, and Wiener number, $W(G)$, are also useful as structural parameters as they are sensitive to any change in the molecule structure. However, the structure–retention relationships obtained using I_B and $W(G)$ are characterized by only moderate statistical characteristics. The chromatographic dipole moments, μ_{chr}, calculated using these topological indices are very high and their physico-chemical meaning is doubtful. In addition, μ_{chr} values are significantly influenced by I_B and $W(G)$.

The valence molecular connectivity indices of various orders can be used in the relationships of eqns. 1 and 3. Both types of relationship are statistically significant and allow the prediction of the retention index for a given oxyethylated derivative. Eqn. 3 expresses the complexity of retention in the column and is recommended for QSRR analysis. It should be also noted that the considered relationships are limited to a given group of homologues, *i.e.* herein the oxyethylene derivatives of alcohols, thioalcohols and alkylamines.

REFERENCES

1 A. Voelkel, J. Szymanowski and J. Beger, *Tenside Detergents*, 23 (1986) 135.
2 A. Voelkel, *J. Chromatogr.*, 387 (1987) 95.
3 A. Voelkel, *J. Chromatogr.*, 450 (1988) 291.
4 A. Voelkel, *J. Chromatogr.*, 464 (1989) 251.
5 R. Kaliszan, in J. D. Winefordner and I. M. Kolthoff (Editors), *High Performance Liquid Chromatography*, (*Chemical Analysis Series of Monographs*, Vol. 98), Wiley, New York, 1989, pp. 563–599.
6 N. Trinajstič, M. Randič and D. J. Klein, *Acta Pharm. Jugosl.*, 36 (1986) 267.
7 H. Lamparczyk and A. Radecki, *Chromatographia*, 18 (1984) 615.
8 H. Lamparczyk, *Chromatographia*, 20 (1985) 283.
9 A. Gassiot-Matas and G. Firpo-Pamies, *J. Chromatogr.*, 187 (1980) 1.
10 J. Bermejo and M. D. Guillen, *Chromatographia*, 17 (1983) 664.
11 A. Voelkel, *Chromatographia*, 25 (1988) 655.
12 L. B. Kier and L. H. Hall, Molecular Connectivity in Chemistry and Drug Research, Academic Press, New York, 1976.

Journal of Chromatography, 547 (1991) 259–268
Elsevier Science Publishers B.V., Amsterdam

CHROM. 23 164

Chemically bonded chelates as selective complexing sorbents for gas chromatography

I. Alkenes

W. WASIAK
Faculty of Chemistry, A. Mickiewicz University, Grunwaldzka 6, 60-780 Poznań (Poland)
(First received May 28th, 1990; revised manuscript received January 21st, 1991)

ABSTRACT

Column packings containing β-diketonate chelates of copper(II) and nickel(II) chemically bonded with silica surfaces can be used to separate nucleophilic species by metal complex formation. The investigated sorbents are capable of selectively retaining unsaturated linear and cyclic hydrocarbons. The packing properties depend on both the metal and the ligand. The influence of electronic effects on the retention of donors is discussed.

INTRODUCTION

Transition metal complexes with β-diketones are applied in gas chromatography for two different purposes. On the one hand, owing to their high volatility, they are used in the analysis of metals by gas chromatography [1,2]. On the other, these complexes can form adducts with additional ligands, so they can be employed as selective adsorption centres in complex gas chromatography.

Adduct formation is a result of coordinative unsaturation of metal ions in β-diketonates which have free energetically accessible orbitals capable of intermolecular interactions with Lewis bases [3–6]. There are copper(II) and nickel(II) adducts consisting of $ML_2 \cdot nD$ (D = donor, n = 1,2) in which copper has a coordination number of 6 and it forms distorted octahedron. The stability of such adducts depends on the nature of the β-diketonate, the base and the environment [7].

β-diketonates of transition metals may be applied as stationary phases in two different ways: by dissolving them in a liquid stationary phase [8–13] or by binding them via an appropriate ligand with the surface of silica or organic polymer [13,14]. The advantage of the latter over the former is that the thus modified carrier may be applied in both gas–solid (GSC) and high-performance liquid (HPLC) chromatography.

Sorbents modified by the β-diketonate chelates of the lanthanides have been used in initial separations of nucleophilic from non-nucleophilic species in trace anal-

0021-9673/91/$03.50

ysis [15–17]. Compounds that do not form complexes or form only very weakly bonded complexes are eluted in a normal manner and analysed by GC.

Most published papers [8,11,12,15–17] have reported on the chromatographic properties of packings containing β-diketonates of trivalent metals such as lanthanides. The packings were characterized by strong specific interactions with respect to olefins, ethers, ketones, amines and alcohols.

In this paper, we report on the binding of copper(II) and nicke(II) acetylacetonates to the surface of phosphinated silica via diphenylphosphinate groups.

EXPERIMENTAL

Reagents

1-Triethoxysilyl-2-(*m,p*-diphenylphosphinemethylphenyl)ethane was obtained from 1-trichlorosilyl-2-*m,p,*-chloromethylphenyl)ethane (Petrach Systems, Bristol, PA, U.S.A.) as described previously [18]. Toluene and tetrahydrofuran (THF) (POCh, Gliwice, Poland) of analytical-reagent grade were distilled and dried with sodium. Copper(II) and nickel(II) acetylacetonate were purchased from Ventron–Alfa Products (Karlsruhe, Germany). Porasil C (80–100 mesh) (Waters Assoc., Milford, MA, U.S.A.) was used as the support.

Apparatus

All chromatographic measurements were carried out on a GCHF 18.3 gas chromatograph manufactured by Chromatron (Berlin, Germany), equipped with a flame ionization detector, an additional thermometer for measuring the column temperature and a mercury manometer for measuring pressure at the column inlet. Argon dried over molecular sieve 4A was used as the carrier gas. Elemental compositions were determined on a Perkin-Elmer Model 240 elemental analyser. Surface-area measurements were performed on a Gravimat sorptometer (Sartorius, Göttingen, Germany). These measurements were carried out by the BET method using nitrogen as an adsorbate at −195°C. Results of the measurements are given in Table I.

Preparation of β-diketonate bonded phase

Copper(II) and nickel(II) acetylacetonates were bonded to the surface of silica (Porasil C) via diphenylphosphine groups. Phosphinated silica was obtained as described previously [19]. The reaction of 1-triethoxysilyl-2-(*m,p*-diphenylphosphinemethylphenyl)ethane with surface silanols was carried out in dry toluene. After the binding to the silica surface, an end-capping reaction was carried out with hexamethyldisilazane (HMDS) to deactivate the free hydroxyl groups remaining on the surface. This was followed by a reaction between the modified gel and corresponding acetylacetonates [$Cu(acac)_2$ or $Ni(acac)_2$] in water-free tetrahydrofuran. The excess of salt was removed by extraction in a Soxhlet apparatus using THF. The sorbent prepared in this way was placed in a stainless-steel column (2 m × 0.4 cm I.D.). The packing was conditioned at 150°C for 12 h.

The reaction scheme is as follows (Et = ethyl; Ph = phenyl):

$$\text{Si–OH} + (\text{EtO})_3\text{Si}(\text{CH}_2)_2\text{C}_6\text{H}_4\text{CH}_2\text{PPh}_2 \xrightarrow[\text{reflux}]{\text{toluene}} \text{Si–O–Si}(\text{CH}_2)_2\text{C}_6\text{H}_4\text{CH}_2\text{PPh}_2$$

$$+ \text{EtOH} \xrightarrow{\text{HMDS}} \text{Si–O–Si}(\text{CH}_2)_2\text{C}_6\text{H}_4\text{CH}_2\text{PPh}_2 + \text{Cu(acac)}_2 \xrightarrow{\text{THF}}$$

$$\text{Si–O–Si}(\text{CH}_2)_2\text{C}_6\text{H}_4\text{PPh}_2\cdot\text{Cu(acac)}_2 \xrightarrow[\text{THF}]{\text{extraction}} \text{packing}$$

The results of elemental analysis and the characterization of the packings obtained are given in Table I.

TABLE I

RESULTS OF ELEMENTAL ANALYSES AND PHYSICO-CHEMICAL CHARACTERISTICS OF THE STUDIED PACKINGS

Packing[a]	Elemental analysis (%)			Specific surface area (m^2/g)	Surface concentration of silanes ($\mu mol/mg$)[c]	Final concentration of silanes[d] ($\mu mol/m^2$)
	C	P	M[b]			
SiO_2–R–$PPh_2 \cdot Cu(acac)_2$	3.77	0.43	0.73	85	1.79	4.01
SiO_2–R–$PPh_2 \cdot Ni(acac)_2$	3.77	0.43	0.64	83	1.79	4.01

[a] R = $-SiCH_2CH_2C_6H_4CH_2-$.
[b] M = metal (Cu or Ni).
[c] From ref. 28.
[d] After end-capping with HMDS.

RESULTS AND DISCUSSION

Owing to the ability of the metal in acetylacetonates to interact coordinatively with compounds having electron-donor properties, chromatographic measurements of the retention of unsaturated (*i.e.*, containing π electrons), linear branched and cyclic hydrocarbons were carried out. The characteristics of specific interactions observed for this type of compound (metal–adsorbates with π electrons) were established on the basis of the values of capacity factors (k'), retention indices (I) molecular retention indices (ΔM_e) and specific retention volumes (V_g). The molecular retention index is a parameter particularly useful for this type of interactions. Knowing its value, we can determine the effect of substituents on the retention of a particular adsorbate [20–22].

ΔM_e values can be calculated from $\Delta M_e = M_e - M$, where M = real molecular mass, $M_e = 0.14027I + 2.016$ and I = Kováts retention index. For *n*-alkanes $\Delta M_e = 0$, which results from the definition of this value. Every additional function introduced into a molecule of *n*-alkane (substituent, unsaturated bond, heteroatom, etc.) brings about a difference between M and M_e. Positive values of the molecular retention index indicate a positive interaction, either direct or indirect, between a given functional group in the adsorbate molecule and the packing. On the other hand, negative values of ΔM_e indicate the presence of repulsive forces between the adsorbate and the packing. Thereby, in view of the above we can see that ΔM_e values

can be employed to characterize specific interactions from the point of view of both packing and the molecule of adsorbate [23–25].

Linear and branched aliphatic hydrocarbons

Specific interactions between linear and branched alkenes were compared with interactions of appropriate saturated hydrocarbons which are adsorbates incapable of π-type interactions with metals. As follows from the comparison of retention parameters for alkanes and alkenes, the presence of π electrons in the adsorbate molecule causes an increase in retention as a result of interactions with the electron-acceptor centre which binds them in a metal complex.

TABLE II

RETENTION PARAMETERS FOR LINEAR AND BRANCHED HYDROCARBONS AT 141°C

Adsorbate	$-P-Ph_2 \cdot Cu(acac)_2$			$PPh_2 \cdot Ni(acac)_2$		
	k'	V_g	ΔM_c	k'	V_g	ΔM_c
Pentane	0.63	1.21	0	0.66	2.29	0
1-Pentene	0.63	1.22	1.86	0.70	2.45	3.57
cis-2-Pentene	0.67	1.28	3.40	0.80	2.80	6.88
trans-2-Pentene	0.66	1.26	2.98	0.76	2.65	5.62
2-Methyl-1,3-butadiene	0.68	1.30	5.84	0.89	3.09	11.62
1-Pentyne	0.76	1.46	9.07	1.32	4.59	22.73
Hexane	1.00	1.92	0	1.10	3.83	0
1-Hexene	1.00	1.92	1.87	1.22	4.24	4.60
cis-2-Hexene	1.04	1.99	2.99	1.37	4.77	7.66
trans-2-Hexene	1.01	1.94	2.85	1.29	4.50	6.09
1,3-Hexadiene	1.13	2.17	7.66	1.74	6.07	16.65
1,4-Hexadiene	1.00	1.91	3.74	1.53	5.33	12.80
2,3-Hexadiene	1.14	2.19	7.80	1.73	6.03	16.46
2,4-Hexadiene	1.26	2.41	10.89	2.16	7.53	22.57
1,3,5-Hexatriene	1.26	2.43	12.91	2.11	7.35	23.91
Heptane	1.55	2.98	0	1.83	6.36	0
1-Heptene	1.55	2.99	1.86	2.10	7.30	5.68
cis-2-Heptene	1.61	3.09	3.27	2.36	8.22	9.00
trans-2-Heptene	1.58	3.03	2.56	2.23	7.75	7.30
cis-3-Heptene	1.57	3.02	2.42	2.19	7.60	6.81
trans-3-Heptene	1.55	2.98	2.14	2.17	7.55	6.63
2,3-Dimethylbutane	0.91	1.75	−3.23	0.99	3.46	−3.07
2,2-Dimethylbutane	0.85	1.64	−4.21	0.91	3.16	−5.71
2,3-Dimethyl-1-butene	0.90	1.79	−1.49	1.26	4.39	5.42
2,3-Dimethyl-2-butene	1.05	2.01	3.27	1.56	5.43	11.39
3,3-Dimethyl-1-butene	0.79	1.52	−5.70	1.02	3.56	−0.31
2-Methylpentane	0.92	1.78	−2.81	0.99	3.45	−3.14
3-Methylpentane	0.95	1.82	−1.97	1.01	3.54	−2.49
2-Methyl-1-pentene	0.98	1.87	1.03	1.33	4.64	6.92
4-Methyl-1-pentene	0.91	1.74	1.35	1.16	4.03	3.24
2-Methyl-2-pentene	1.00	1.93	2.15	1.41	4.91	8.50
cis-3-Methyl-2-pentene	1.01	1.94	2.15	1.43	4.98	8.98
trans-3-Methyl-2-pentene	1.05	2.01	3.13	1.47	5.11	9.61
cis-4-Methyl-2-pentene	0.91	1.76	−1.07	1.21	4.28	4.42
trans-4-Methyl-2-pentene	0.92	1.77	−0.93	1.23	4.22	4.83

For a packing containing $Ni(acac)_2$, the specific interactions with alkenes are stronger than for the packing with $Cu(acac)_2$ (Table II). This can be accounted for by the formation of a back-donating bond between a metal, in this case Ni^{2+}, and an atom of phosphorus in a diphenylophosphine group [26]. As a result, nickel becomes a stronger acceptor of π electrons coming from additional ligands, which in this instance are alkene molecules. For comparison, Table III gives the values of I and ΔI for packings modified with acetylacetonates of copper(II) and nickel(II) and for phosphinated silica, where $\Delta I = I_{Cu(II) \text{ or } Ni(II)} - I_{\text{phosphinated silica}}$.

The differences in values of the interactions of particular alkenes with the studied packings results from at least three causes: (i) substitution at the double bond, (ii) localization of the double bond and (iii) influence of the chain length and branching. The substitution at the double bond may be considered from the point of view of electric and steric effects. For alkyl substituents, owing to an induction effect an

TABLE III

VALUES OF RETENTION INDICES (I_R) AND ΔI_R OF ALIPHATIC HYDROCARBONS

Adsorbate	$-PPh_2$,	$-PPh_2 \cdot Cu(acac)_2$		$-PPh_2 \cdot Ni(acac)_2$	
	I_R	I_R	ΔI_R	I_R	ΔI_R
1-Pentene	501	499	−2	511	10
cis-2-Pentene	505	510	5	534	29
trans-2-Pentene	502	507	5	525	23
2-Methyl-1,3-butadiene	507	513	6	554	47
1-Pentyne	514	536	22	633	119
1-Hexene	600	599	−1	618	18
cis-2-Hexene	604	607	3	640	36
trans-2-Hexene	602	606	4	629	27
1,3-Hexadiene	614	626	12	690	76
1,4-Hexadiene	600	598	−2	662	62
2,3-Hexadiene	614	627	13	688	74
2,4-Hexadiene	617	649	32	732	115
1,3,5-Hexatriene	620	649	29	727	107
1-Heptene	700	699	−1	726	26
cis-2-Heptene	703	709	6	749	46
trans-2-Heptene	702	704	2	737	35
cis-3-Heptene	701	703	2	734	33
trans-3-Heptene	700	701	1	733	33
2,3-Dimethylbutane	579	577	−2	578	−1
2,2-Dimethylbutane	566	570	4	559	−7
2,3-Dimethyl-1-butene	570	575	5	624	54
2,3-Dimethyl-2-butene	595	609	14	666	71
3,3-Dimethyl-1-butene	540	545	5	583	43
2-Methylpentane	575	580	5	577	2
3-Methylpentane	580	586	6	582	2
2-Methyl-1-pentene	580	593	13	635	55
4-Methyl-1-pentene	570	576	6	608	38
2-Methyl-2-pentene	590	601	11	646	56
cis-3-Methyl-2-pentene	598	601	3	649	51
trans-3-Methyl-2-pentene	599	608	9	654	55
cis-4-Methyl-2-pentene	570	578	8	617	47
trans-4-Methyl-2-pentene	571	579	8	620	49

increase in the density of π electrons takes place, which should lead to an increase in the value of specific interactions. On the other hand, the presence of the substituent hinders access to the unsaturated bonds. Therefore, the observed effect should be considered as a resultant of these two factors.

This is illustrated by three isomers of methylpentene, which are eluted in the following order:

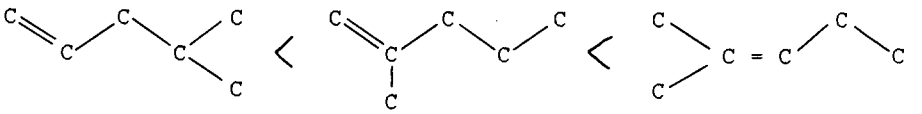

4-methyl-1-pentene 2-methyl-1-pentene 2-methyl-2-pentene

4-Methyl-1-pentene was eluted first. For this compound, because of the considerable distance of the substituent from the unsaturated bond, the induction effect cannot be taken into consideration, unlike the case for the other two compounds, where the effect influences the values of the retention parameters.The influence of the surroundings of the unsaturated bond is also evident in the case of geometric isomers, for which the *cis* isomers of *n*-alkenes are eluted after the corresponding *trans* isomers owing to less steric hindrance of the substituent.

The situation is different for branched *cis* and *trans* isomers of methyl-2-pentene. Here the order of elution of the isomers is reversed, the *cis* isomers being eluted first. A similar effect was observed by Hively [27], who studied 14 pairs of *cis-trans* isomers on packings with liquid phases of different polarity.

The influence of the number of unsaturated bonds or the degree of their unsaturation (double or triple bonds) may be observed for hexadienes and 1-pentyne. The molecular retention index for the latter was almost four times higher than those for pentenes. Moreover, localization of the double bonds significantly affected specific interactions. Hence the strongest interactions occurred for 1,3- and 2,4-hexadiene, that is, for conjugated bonds. There were stronger than those for 2,3-hexadiene, *i.e.*, for cumulated bonds, which may be related to considerable stiffening of the 2,3-hexadiene molecule. The influence of the presence of isolated bonds (1,4-hexadiene) on the specific interaction was the weakest, although stronger than for hexenes.

For C_5–C_7 alkenes, the length of the hydrocarbon chain did not significantly influence the retention, whereas chain branching led, owing to steric effects, to a reduction in interactions in comparison with linear alkenes. This is particularly well illustrated for the packing containing copper(II) acetylacetonate. Interactions for this packing, although generally weaker, were more sensitive to all additional effects inhibiting the contact between an alkene and the metal. This is evidenced by negative values of ΔM_e for branched derivatives of butenes and 4-methyl-1-pentene. For the latter, the CH_3 substituent, being a significant distance from the unsaturated bond, yields only a negative steric effect, and does not lead to an increase in electron density as a result of an induction effect. Negative values of ΔM_e were also reported for branched C_6 alkanes (methylcyclopentanes and dimethylbutanes) for both of the studied packings.

Cyclic alkenes

Interactions of cyclic alkenes with the studied packings were stronger than those of linear alkenes (Tables IV and V).

TABLE IV

RETENTION PARAMETERS FOR CYCLIC HYDROCARBONS AT 140°C

Adsorbate	$-PPh_2 \cdot Cu(acac)_2$			$-PPh_2 \cdot Ni(acac)_2$		
	k'	V_g	ΔM_e	k'	V_g	ΔM_e
Cyclopentane	0.56	1.16	4.25	0.79	1.77	5.54
Cyclohexane	0.92	1.97	4.53	1.21	2.74	4.55
Cycloheptene	1.62	2.41	7.19	2.24	5.06	7.63
Cyclooctane	2.74	6.22	8.73	3.88	8.76	9.01
Cyclopentene	0.56	1.18	5.98	0.89	2.02	11.30
Cyclohexene	0.97	2.07	8.08	1.68	3.79	15.76
Cycloheptane	1.62	2.55	9.35	2.83	6.39	16.34
Cyclooctene	2.65	6.55	9.91	4.53	10.22	15.42
Methylcyclopentane	0.83	2.79	1.87	1.15	2.59	3.12
Methylcyclohexane	1.34	3.85	2.14	1.86	4.20	2.65
Ethylcyclohexane	2.18	5.58	2.14	3.11	7.01	2.91
1-Methyl-1-cyclopentene	0.90	2.93	5.98	1.52	3.43	12.78
1,3-Cyclohexadiene	1.01	4.06	11.37	2.01	4.55	22.76
1,4-Cyclohexadiene	1.10	4.34	13.75	2.35	5.31	26.99
Benzene	1.02	4.18	13.53	2.32	5.24	2.60
1,3,5-Cycloheptatriene	1.76	5.70	15.63	4.25	9.59	31.64
1,5-Cyclooctadiene	3.12	8.52	16.84	7.96	17.98	33.19
Cyclooctatetraene	3.02	8.31	19.87	7.45	16.82	35.33

TABLE V

VALUES OF RETENTION INDICES (I_R) AND ΔI_R OF CYCLIC HYDROCARBONS

Adsorbate	$-PPh_2$,	$-PPh_2 \cdot Cu(acac)_2$		$-PPh_2 \cdot Ni(acac)_2$	
	I_R	I_R	ΔI_R	I_R	ΔI_R
Cyclopentane	509	516	7	525	14
Cyclohexane	608	618	10	618	10
Cycloheptane	712	737	25	740	28
Cyclooctane	816	848	32	850	34
Cyclopentene	504	516	12	551	47
Cyclohexene	614	629	15	683	69
Cycloheptene	710	738	28	787	77
Cyclooctene	814	842	28	881	67
Methylcyclopentane	594	599	5	608	14
Methylcyclohexane	698	701	3	704	6
Ethylcyclohexane	799	801	2	806	7
1-Methyl-1-cyclopentene	589	614	25	662	73
1,3-Cyclohexadiene	612	638	26	719	107
1,4-Cyclohexadiene	622	655	33	749	127
Benzene	628	639	11	746	118
1,3,5-Cycloheptatriene	703	754	51	868	165
1,5-Cyclooctadiene	814	871	57	993	179
Cyclooctatetraene	822	869	47	980	158

The presence of methyl or ethyl substituent in a ring caused a decrease in the interactions. This is evidenced by methylcyclopentane and methylcyclohexane, the ΔM_e values of which are lower than those for cyclopentane and cyclohexane. This testifes again to the fact that with acetylacetonates the steric effect plays a decisive role in the donor electron–metal interactions.

With cyclic compounds containing more than one unsaturated bond, a change in elution sequence with respect to linear alkenes was observed. Whereas for acyclic alkenes specific interactions increased in the sequence isolated bonds < cumulated bonds < conjugated bonds, for cyclic hydrocarbons the strongest effect was observed for isolated bonds. Elution of 1,3-cyclohexadiene preceded that of 1,4-cyclohexadiene, and that of 1,3-cyclooctadiene preceded that of 1,5-cyclooctadiene.

The slight difference between 1,5-cyclooctadiene and cyclooctatetraene is due to the structure of the latter, which allows for simultaneous interaction only with two π-bonds. The weaker interaction of the benzene molecule in comparison with that of 1,4-cyclohexadiene results from the fact, among others, that the benzene molecule, owing to its structure, interacts with its whole area, whereas 1,4-cyclohexadiene may assume a position perpendicular to the metal, thus having better access to the electron-acceptor centre.

The results in Table IV indicate a high sensitivity of ΔM_e. Differences in the values of ΔM_e are prominent, even for cases where the values of k' and I are the same for two different adsorbates. For example, for cyclopentane and cyclopentene, the values of k' and I are 0.56 and 516, whereas those of ΔM_e are 4.25 and 5.98, respectively.

As follows from a comparison of the retention parameters for cyclopentane, cyclopentene and 1-methyl-1-cyclopentene, for the last compound the positive induction effect of the substituent is counterbalanced by a negative steric effect of the substituent, as the ΔM_e values are very close. On the other hand, the presence of a substituent in cyclopentane causes a considerable decrease in this value (ΔM_e) in comparison with cyclopentane and 1-methyl-1-cyclopentene.

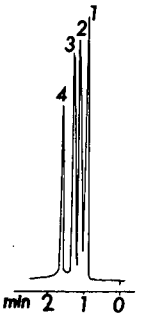

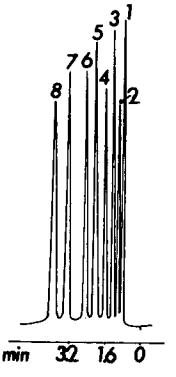

Fig. 1. Separation of C_5 hydrocarbons. Packing, $-PPh_2 \cdot Ni(acac)_2$; column temperature, 115°C; carrier gas (argon) flow-rate, 21 ml/min. Peaks: 1 = pentane; 2 = *trans*-2-pentene; 3 = *cis*-2-pentene; 4 = 1-pentyne.

Fig. 2. Analysis of a mixture of cycloakanes and cycloalkenes. Packing as in Fig. 1. Column temperature, 125°C; carrier gas flow-rate 22.2 ml/min. Peaks: 1 = cyclopentane; 2 = cyclopentene; 3 = cyclohexane; 4 = cyclohexene; 5 = cycloheptane; 6 = cycloheptene; 7 = cyclooctane; 8 = cyclooctene.

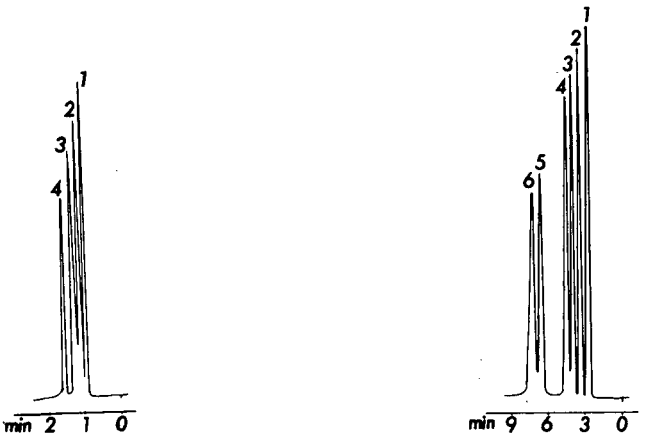

Fig. 3. Separation of a mixture of cyclic hydrocarbons (C_5 and C_6). Packing as in Fig. 1. Column temperature, 124.4°C; carrier gas flow-rate, 22.1 ml/min. Peaks: 1 = cyclopentane; 2 = cyclopentene; 3 = methylcyclopentane; 4 = 1-methyl-1-cyclopentene.

Fig. 4. Analysis of cyclic C_8 hydrocarbons. Packing as in Fig. 1. Column temperature, 124.5°C; carrier gas flow-rate, 22.1 ml/min. Peaks: 1 = ethylcyclohexane; 2 = cyclooctane; 3 = cyclooctene; 4 = 1,3-cyclooctadiene; 5 = cyclooctatetraene; 6 = 1,5-cyclooctadiene.

ANALYTICAL APPLICATIONS

The practical value of the studied packings is illustrated by the chromatograms presented for mixtures of linear (Fig. 1) and cyclic (Figs. 2–4) hydrocarbons. Sharp and symmetrical peaks testify to the high rate and complete reversibility of the reaction of alkene complexation. It is worth mentioning the separation of the mixture of C_5 alkenes because of the separation of *cis–trans* isomers of 2-pentene.

Fig. 2 illustrates a chromatogram for a mixture of four cycloalkane–cycloalkene pairs. It is characterized by sharp and symmetrical peaks and complete separation of the mixture in a relatively short time. Fig. 3 demonstrates the separation of a mixture of cycloalkanes and cycloalkenes, where the separation of methylcyclopentane from 1-methyl-1-cyclopentene is worth emphasizing. Fig. 4 shows the separation of mixture of cyclic C_8 hydrocarbons, including two isomers of cyclooctadiene.

The above examples confirm the possibility of employing these types of packings and, in particular, those containing nickel(II) acetyloacetonate, in everyday laboratory practice.

REFERENCES

1 S. Dilli and E. Patsalides, *Aust. J. Chem.*, 29 (1986) 2369 and 2381.
2 K. Robards, E. Patsalides and S. Dilli, *J. Chromatogr.*, 411 (1987) 1.
3 R. P. Houghton, *Metal Complexes in Organic Chemistry*, Cambridge University Press, Cambridge, 1979.
4 V. E. Spitsyn (Editor), *β-Diketony Metallov (β-Diketonates of Metals)*, Nauka, Moscow, 1978.
5 J. J. Brooks and R. E. Sievers, *J. Chromatogr. Sci.*, 11 (1973) 303.
6 R. E. Rondeau and R. E. Sievers, *J. Am. Chem. Soc.*, 93 (1971) 1522.

7 E. N. Marov, O. M. Petrukhin, B. B. Zhukov and N. B. Kalinichenko, *Koord. Khim.*, 1 (1975) 1398.
8 B. Feibush, M. F. Richardson, R. E. Sievers and C. S. Springer, Jr., *J. Am. Chem. Soc.*, 94 (1972) 6717.
9 E. Gil-Av and V. Schurig, *Anal. Chem.*, 43 (1971) 2030.
10 V. Schurig and E. Gil-Av, *Chem. Commun.*, (1971) 650.
11 E. T. Kowalska and W. J. Kowalski, *Chromatographia*, 19 (1984) 301.
12 W. J. Kowalski, *J. Chromatogr.*, 349 (1985) 457.
13 T. Seshadri, U. Kampschulze and A. Kettrup, *Fresenius' Z. Anal. Chem.*, 300 (1980) 124.
14 G. P. Potapov, E. I. Kazakova, V. A. Poluboyarov and V. Anutrienko, *React. Kinet. Catal. Lett.*, 25 (1984) 237.
15 J. E. Picker and R. E. Sievers, *J. Chromatogr.*, 203 (1981) 29.
16 J. E. Picker and R. E. Sievers, *J. Chromatogr.*, 217 (1981) 275.
17 T. J. Wenzel, L. W. Yarmaloff, L. Y. St. Cyr, L. J. O'Meara, M. Donatelli and R. W. Bauer, *J. Chromatogr.*, 396 (1987) 51.
18 W. Urbaniak, W. Wasiak and B. Marciniec, *Pol. Pat.*, 140 182 (1986).
19 W. Wasiak, W. Urbaniak and W. Szczepaniak, *Pol. Pat.*, 140 532 (1986).
20 M. B. Evans, *Chromatographia*, 2 (1969) 397.
21 M. B. Evans, *Chromatographia*, 11 (1978) 183.
22 M. B. Evans and J. F. Smith, *J. Chromatogr.*, 30 (1967) 325.
23 J. K. Haken and S. Srisukh, *J. Chromatogr.*, 219 (1981) 45.
24 W. Wasiak, *Chromatographia*, 18 (1984) 205.
25 W. Wasiak, *Chromatographia*, 22 (1986) 147.
26 F. A. Cotton and G. Wilkinson, *Advanced Inorganic Chemistry*, Wiley, New York, 1988.
27 R. A. Hively, *Anal. Chem.*, 35 (1983) 1921.
28 G. E. Berendsen and L. de Galan, *J. Liq. Chromatogr.*, 1 (1978) 561.

Journal of Chromatography, 547 (1991) 269–282
Elsevier Science Publishers B.V., Amsterdam

CHROM. 23 206

Evaluation of the effect of the cyanopropyl radical on the interaction of the methylene group with silicone stationary phases

M. R. BECERRA, E. FERNÁNDEZ-SÁNCHEZ, A. FERNÁNDEZ-TORRES, J. A. GARCÍA-DOMÍNGUEZ* and J. M. SANTIUSTE

Instituto de Química Física "Rocasolano", CSIC, Serrano 119, 28006 Madrid (Spain)

(First received September 25th, 1990; revised manuscript received January 24th, 1991)

ABSTRACT

Values of the solute–polymer interaction parameter of *n*-alkanes and polar substances between 90 and 200°C were obtained on two packed columns (OV-101 and OV-105). Experiments carried out with a capillary column confirmed that with non-polar solute–polymer systems the values of both the specific retention volumes and the thermodynamic parameters derived from them are equivalent to those obtained with packed columns. The results showed that *n*-alkanes mix better with OV-101 and polar substances are better solvents of OV-105. The differences are small, however. Partial molar enthalpies and free energies of solution and mixing were calculated. The contribution of the methylene group of the *n*-alkanes to the thermodynamic parameters of solution was evaluated. The effect of cyanopropyl group substitution on the contribution of the methylene group to the partial molar free energy of solution of *n*-alkanes was found to be roughly linear with the cyanoalkyl group content, decreasing as the polarity of the polymer increases. The solubility parameter of the stationary phase increases only slightly when a 5% substitution of cyanopropyl groups is introduced in the polymer.

INTRODUCTION

The cyanoalkylsilicones form one of the most interesting families of stationary phases in gas chromatography (GC). Their selectivity varies with the cyanoalkyl group content of the polymer, which ranges from 5 to 100% substitution [1]. They have been considered as "preferred stationary phases" by Stark *et al.* [2] and Sandra *et al.* [3]. The presence of the cyano group in their structure confers on them certain characteristics which make them particularly suitable for some chromatographic separations. GC is a useful technique in the study of solute–polymer and polymer–polymer interactions [4], as shown by the increasing number of publications in the field. The technique is normally called inverse gas chromatography (IGC) because interest is focused on the stationary phase rather than on the solutes being eluted. In this sense, the results offer information on the expected behaviour of the solutes when they are used as solvents of the stationary phase, and conclusions may be drawn regarding the behaviour of other substances of the same or a similar chemical type, and the behaviour of mixtures of the liquids used as stationary phases. Many polymers have been studied by IGC, but data

0021-9673/91/$03.50

on cyanoalkylsilicones are scarce [5]. In this paper, two stationary phases, OV-101, polydimethylsiloxane, and OV-105, polymethylcyanopropylsiloxane, 5% substitution, are compared. Results reported for other cyanopropylsilicones are taken into account in the discussion section. Our interest was focused on an evaluation of the cyanopropyl group and its effect on the chromatographic behaviour of the polymer, on the study of the interaction of the methylene group of the *n*-alkanes with the polymers and on the effect of the cyanopropyl group on that interaction. The study might also allow a prediction of the degree of miscibility of each polymer with other stationary phases of different chemical types. The latter point would help in the understanding of the problem of modification of the selectivity of chromatographic columns by making use of mixtures of stationary phases.

EXPERIMENTAL

For packed columns the stationary phases were deposited on Chromosorb W AW DMCS (80–100 mesh) in the usual way, using methylene chloride (OV-101) or acetone (OV-105) as solvents. A Stainless-steel tube (1/8 in. O.D.) was employed. Other characteristics of the columns were as follows: OV-101, stationary phase loading 14.8% (w/w) and length 3 m; OV-105, loading 16.6% (w/w) and length 2 m. Stationary phase percentages were determined by an extraction method [6]. A capillary column was prepared with OV-101 by the static method described by Grob [7] on borosilicate glass silanized with hexamethyldisilazane and without any immobilization. The characteristics of the column were I.D. 0.2475 mm, length 21.42 m, weight of stationary phase in the column $5.647 \cdot 10^{-3}$ g and film thickness 0.34 μm. The density of OV-101 was measured by a pycnometric procedure and that of OV-105 was taken from the literature [8]. The gas chromatographs used were a Shimazdu R1A and a Perkin-Elmer Sigma 2 (packed columns) and a Hewlett-Packard 5890 (capillary column). Temperatures were checked with the help of a thermocouple placed close to the column, and head pressures were measured with precision manometers (packed columns) or a presure transducer (capillary column). Chromatograms were carried out between 90 and 200°C. Sample injection was always of the order of 0.1 μl (splitting ratio 1:20 in the capillary column). The high percentage of stationary phase in the packed columns ensured that the contribution of adsorption phenomena to the retention of solutes was negligible.

DATA REDUCTION

Specific retention volumes were calculated in the usual manner, using a mathematical dead time method [9] to correct retention times.

Activity coefficients at infinite dilution based on weight fraction, Ω_1^∞, were calculated [10,11] according to the expression

$$\ln \Omega_1^\infty \equiv \ln\left(\frac{a_1}{w_1}\right) = \ln\left(\frac{273.15\,R}{P_1^0 V_g M_1}\right) - \frac{P_1^0}{RT}(B_{11} - V_1^0) \tag{1}$$

where a_1 and w_1 are the activity and weight fraction, respectively, of the solute in the polymer and M_1, P_1^0, B_{11} and V_1^0 are the molecular weight, saturated vapour pressure,

second viral coefficient and molar volume respectively, of the solute at the column temperature T; R is the gas constant.

Vapour pressures were deduced using Antoine coefficients from various sources [12,13]. Second viral coefficients of *n*-alkanes were calculated by the method of O'Connell and Prausnitz [14]; for other substances, values were inter- or extrapolated from literature values corresponding to other temperatures [15]. Densities were calculated according to the pertinent equation [16,17]. Molar volumes were deduced from molecular weight and density values.

Flory–Huggins interaction parameters were calculated according to the expression [10,11,18]

$$\chi^{\infty} = \ln \Omega_1^{\infty} + \ln\left(\frac{\rho_1}{\rho_2}\right) - \left(1 - \frac{V_1^0}{V_2^0}\right) \tag{2}$$

where ρ_1 and ρ_2 are the densities of the solute and the polymer, respectively, and V_1^0 and V_2^0 the corresponding molar volumes. Considering that $V_1^0 \ll V_2^0$, the ratio V_1^0/V_2^0 was taken as zero.

Partial molar enthalpies of solution, ΔH_s were deduced in each instance from experimental values, according to the expression

$$\Delta H_s = -R \cdot \frac{\partial(\ln V_g)}{\partial(1/T)} \tag{3}$$

Partial molar enthalpies of mixing of the solutes at infinite dilution, ΔH_m^{∞}, were calculated from

$$\Delta H_m^{\infty} = R \cdot \frac{\partial(\ln \Omega_1^{\infty})}{\partial(1/T)} \tag{4}$$

The partial molar enthalpy of vaporization of the solutes may be calculated [18] as the difference:

$$\Delta H_v = \Delta H_m^{\infty} - \Delta H_s \tag{5}$$

Solubility parameters of the solutes were deduced from the expression

$$\delta_1 = [(\Delta H_v - RT)/V_1^0]^{1/2} \tag{6}$$

Partial molar free energies of mixing were calculated from activity coefficients at infinite dilution [18,19]. Partial molar free energies of solution at infinite dilution were calculated from

$$\Delta G_s = -RT \ln(M_1 V_g/273.15R) \tag{7}$$

Solubility parameters of the stationary phases were deduced from the expression [5,11]

$$\frac{\delta_1^2}{RT} - \frac{\chi^{\infty}}{V_1^0} = \frac{2\delta_2}{RT} \cdot \delta_1 - \left(\frac{\delta_2^2}{RT} + \frac{\chi_S^{\infty}}{V_1^0}\right) \tag{8}$$

where δ_2 is the solubility parameter of the polymer and χ_S^∞ is the entropic contribution to the interaction parameter χ^∞. On plotting the left-hand side term of eqn. 8 *versus* δ_1, a straight line was obtained, and from its slope the value of δ_2 was deduced.

A personal computer was used to run the FORTRAN programs necessary to obtain the values of the different parameters.

RESULTS AND DISCUSSION

Specific retention volumes

Table I gives the values of the specific retention volumes of the solutes on both stationary phases at various temperatures. The least mean squares (l.m.s.) method, applied to the straight line obtained by plotting ln V_g *versus* the inverse of the absolute temperature, gave in all instances correlation coefficients of 0.9998 or better. The

TABLE I

SPECIFIC RETENTION VOLUMES (V_g)

Stationary phase	Solute	Temperature (K)						
		363.15	383.15	403.15	423.15	453.15	473.15	
OV-101	*n*-Hexane	26.2	16.5	10.9	7.5	4.5	3.3	
	n-Heptane	53.3	31.7	19.9	13.0	7.4	5.3	
	n-Octane	108.2	59.4	34.4	21.0	10.7	7.2	
	n-Nonane	219.2	111.7	60.6	34.4	16.5	10.5	
	n-Decane	372.7	188.4	100.4	56.7	25.2	17.0	
	n-Undecane	732.6	348.0	174.7	93.1	38.7	24.9	
	n-Dodecane	1484.2	657.3	309.2	155.3	59.4	36.7	
	Benzene	39.4	24.5	16.0	10.7	6.5	4.8	
	Toluene	82.0	47.2	28.8	18.1	10.1	7.0	
	2-Pentanone	42.3	26.0	16.5	10.9	6.2	4.5	
	Ethyl acetate	25.1	16.0	10.6	7.2	4.4	3.2	
	Pyridine	65.2	38.6	24.1	15.6	8.9	6.3	
	n-Butanol	36.5	22.0	14.0	9.4	5.4	3.9	
	1-Octanol	517.1	255.0	132.6	72.9	31.8	20.8	
	Dimethylaniline	615.9	306.1	160.4	88.8	39.1	25.8	
		372.9	383.35	393.55	403.6	413.5	453.15	473.15
OV-105	*n*-Hexane	19.3	15.1	12.7	10.4	8.6	4.6	3.4
	n-Heptane	36.5	27.5	22.3	17.8	14.2	6.8	4.9
	n-Octane	69.3	50.6	39.9	30.9	23.9	10.4	7.2
	n-Nonane	131.0	92.8	70.6	53.0	40.0	15.7	10.4
	n-Decane	248.2	169.7	125.4	91.1	67.1	24.0	15.1
	n-Undecane	469.9	310.7	222.2	156.7	112.0	36.2	21.7
	n-Dodecane	888.0	566.1	392.2	269.5	186.2	54.6	31.4
	Benzene	33.0	25.7	21.0	17.2	14.0	7.2	5.3
	2-Pentanone	35.0	30.9	24.8	19.8	15.8	7.5	5.4
	Pyridine	61.7	47.4	36.8	29.6	23.6	11.0	7.8
	n-Butanol	33.0	26.7	21.6	17.0	13.6	6.5	4.6

experimental values of the specific retention volumes of the *n*-alkanes with 7–12 carbon atoms, obtained on the OV-101 capillary column at 120°C, when compared with the corresponding values calculated for the packed column with the same stationary phase at the same temperature, as deduced from the l.m.s. equation (no experimental values available at that temperature), gave absolute errors with an average value of 1.87%, with the highest difference corresponding to *n*-decane (4.1%). This indicates that the adsorption phenomena in the packed column, if any, are negligible, and confirms the finding of Korol *et al.* [20] in the sense that for non-polar stationary phases and solutes, retention data obtained on packed and capillary columns are interchangeable.

Interaction parameters

Table II lists the corresponding solute–polymer interaction parameters (χ^{∞}). The variation of the interaction parameters with temperature may best be observed from Figs. 1–4. The curves show the parabolic dependence of χ^{∞} on temperature

TABLE II

SOLUTE–POLYMER INTERACTION PARAMETERS (χ^{∞})

Stationary phase	Solute	Temperature (K)						
		363.15	383.15	403.15	423.15	453.15	473.15	
OV-101	*n*-Hexane	0.17	0.08	−0.01	−0.10	−0.19	−0.26	
	n-Heptane	0.25	0.16	0.07	0.02	−0.12	−0.20	
	n-Octane	0.32	0.25	0.19	0.14	0.09	0.04	
	n-Nonane	0.37	0.30	0.26	0.23	0.19	0.17	
	n-Decane	0.59	0.46	0.37	0.31	0.28	0.17	
	n-Undecane	0.66	0.52	0.44	0.38	0.35	0.26	
	n-Dodecane	0.70	0.56	0.47	0.42	0.41	0.33	
	Benzene	0.51	0.42	0.33	0.27	0.14	0.10	
	Toluene	0.55	0.47	0.41	0.37	0.27	0.24	
	2-Pentanone	0.93	0.79	0.67	0.58	0.48	0.41	
	Ethyl acetate	0.73	0.59	0.48	0.39	0.30	0.27	
	Pyridine	1.23	1.11	1.00	0.92	0.79	0.74	
	n-Butanol	1.99	1.67	1.40	1.18	0.91	0.77	
	1-Octanol	1.98	1.59	1.31	1.11	0.93	0.79	
	Dimethylaniline	−0.80	−0.82	−0.80	−0.78	−0.69	−0.71	
		372.9	383.35	393.55	403.6	413.5	453.15	473.15
OV-105	*n*-Hexane	0.21	0.17	0.09	0.05	0.01	−0.16	−0.23
	n-Heptane	0.34	0.31	0.24	0.20	0.18	0.02	−0.04
	n-Octane	0.44	0.42	0.35	0.31	0.30	0.16	0.11
	n-Nonane	0.53	0.50	0.43	0.40	0.39	0.28	0.25
	n-Decane	0.61	0.58	0.51	0.48	0.47	0.38	0.35
	n-Undecane	0.67	0.65	0.58	0.56	0.55	0.47	0.46
	n-Dodecane	0.73	0.71	0.65	0.62	0.62	0.55	0.55
	Benzene	0.42	0.38	0.33	0.28	0.26	0.11	0.06
	2-Pentanone	0.67	0.67	0.55	0.50	0.47	0.33	0.29
	Pyridine	0.98	0.91	0.87	0.81	0.78	0.64	0.59
	n-Butanol	1.62	1.48	1.32	1.21	1.12	0.78	0.66

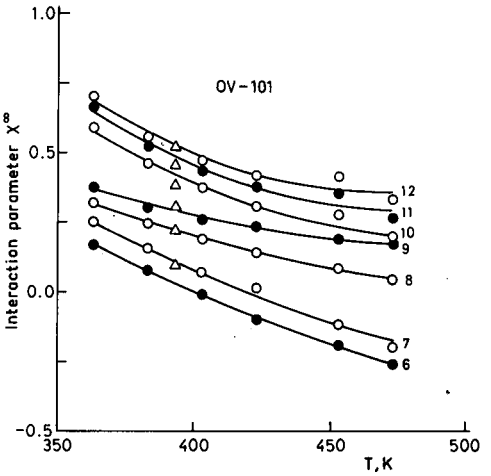

Fig. 1. Interaction parameters of the *n*-alkanes in OV-101. The numbers on the right represent the number of carbon atoms in the *n*-alkane. △, Values obtained from experiments on the capillary column.

predicted by theory [21–23]. They show, in all instances except for dimethylaniline, that as the temperature increases in the range studied, the systems leave the upper critical solution temperature (UCST), therefore increasing the solubility of the solute in the polymer (the curves tend to reach lower values of χ^{∞}). The UCST is a temperature below which complete miscibility of solute and polymer does not occur. It is important to realize that the concentration conditions met in IGC, where infinite dilution is the norm, are far from those where the critical conditions are satisfied (high concentration). However, the trends of the curves do indicate whether solubility increases or decreases. With dimethylaniline in OV-101 (Fig. 2), the temperature range

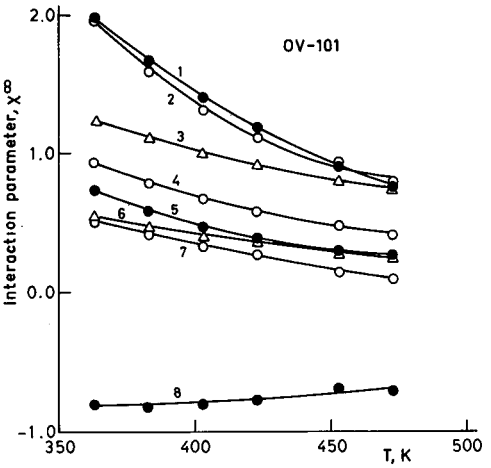

Fig. 2. Interaction parameters in OV-101. Substances: 1 = *n*-butanol; 2 = 1-octanol; 3 = pyridine; 4 = 2-pentanone; 5 = ethyl acetate; 6 = toluene; 7 = benzene; 8 = dimethylaniline.

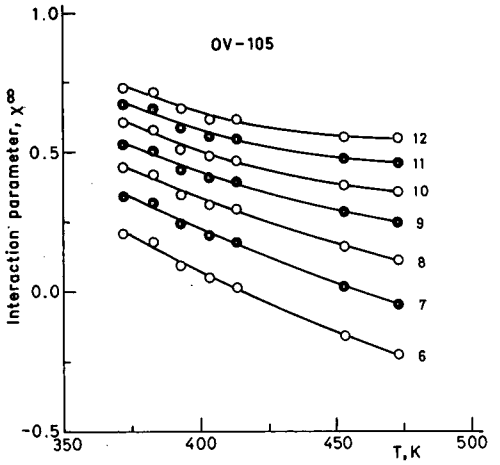

Fig. 3. Interaction parameters of the *n*-alkanes in OV-105. The numbers on the right represent the number of carbon atoms in the *n*-alkane.

considered is close to the zone of maximum solubility, the trend of the curve indicating that, as the temperature increases, the system is approaching its lower critical solution temperature (LCST), above which phase separation should occur under conditions of high solute concentration.

From the values in Table II, it may be deduced that the best solvents for the polymers are the alkanes and aniline (low values of χ^∞), whereas alcohols are clearly bad solvents, especially at low temperatures. The carbonyl compounds may be considered as medium solvents. The expected behaviour of aromatic compounds as solvents of OV-101 and OV-105 is not clear. Whereas benzene and toluene show low values of χ^∞ (good solvents), pyridine presents values of the interaction parameter that are closer to those of the alcohols, indicating poorer solubility.

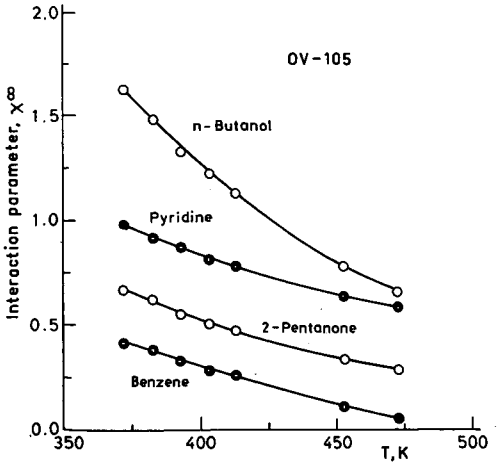

Fig. 4. Interaction parameters in OV-105.

On comparing the values of the interaction parameter of those solutes that were run on both polymers (Table II), we find that *n*-alkanes are more soluble in polydimethylsiloxane than they are in polymethylcyanopropylsiloxane. On the other hand, polar solutes mix better with the polymer OV-105, because the cyano group, with a high electronic attraction and dipolar moment, interacts with π electron-containing substances, increasing their solubility in the stationary phase, thus producing higher values of V_g and consequently lower values of Ω_1^∞ (eqn. 1). This results in lower values of χ^∞ (eqn. 2).

Values of the interaction parameters of a few *n*-alkanes, deduced from experimental measurements carried out in the capillary column at 120°C, were compared with those calculated for the packed column OV-101 for the same temperature. The results are included in Fig. 1. Again, it is shown that the values deduced from experiments with capillary columns are comparable to those obtained with packed columns.

Partial molar enthalpies and free energies

Table III presents the results obtained for the partial molar enthalpies of solution and mixing (eqns. 3 and 4) on both stationary phases. The values of ΔH_m for the *n*-alkanes are lower in both polymers than those corresponding to more polar solutes, the difference being highest with alcohols. An exception is dimethylaniline, as observed when considering interaction parameters. Comparing values for the same solutes, it might be said that *n*-alkanes are not as good solvents and the polar substances are slightly better solvents of OV-105 than they are of the polymer OV-101. The cyanopropyl content of OV-105 is low, so it is not surprising that the values of ΔH_s

TABLE III

PARTIAL MOLAR ENTHALPIES OF SOLUTION AND MIXING (kcal mol^{-1})

Errors based on a 95% confidence limit.

Solute	OV-101		OV-105	
	ΔH_s	ΔH_m	ΔH_s	ΔH_m
n-Hexane	−6.40 ± 0.05	0.88 ± 0.11	−6.01 ± 0.11	1.30 ± 0.12
n-Heptane	−7.16 ± 0.06	0.99 ± 0.06	−7.02 ± 0.11	1.10 ± 0.12
n-Octane	−8.42 ± 0.06	0.53 ± 0.16	−7.91 ± 0.12	1.01 ± 0.15
n-Nonane	−9.43 ± 0.05	0.41 ± 0.17	−8.85 ± 0.10	0.94 ± 0.14
n-Decane	−9.69 ± 0.25	1.03 ± 0.34	−9.78 ± 0.10	0.89 ± 0.18
n-Undecane	−10.60 ± 0.23	1.02 ± 0.37	−10.73 ± 0.12	0.81 ± 0.21
n-Dodecane	−11.59 ± 0.26	0.95 ± 0.45	−11.67 ± 0.11	0.74 ± 0.22
Benzene	−6.55 ± 0.08	1.02 ± 0.11	−6.39 ± 0.07	1.17 ± 0.09
Toluene	−7.63 ± 0.07	0.82 ± 0.08	–	–
2-Pentanone	−7.01 ± 0.10	1.29 ± 0.26	−7.06 ± 0.08	1.20 ± 0.17
Ethyl acetate	−6.38 ± 0.05	1.55 ± 0.16	–	–
Pyridine	−7.25 ± 0.04	1.47 ± 0.12	−7.23 ± 0.05	1.46 ± 0.10
n-Butanol	−6.93 ± 0.03	3.69 ± 0.34	−7.07 ± 0.10	3.45 ± 0.25
1-Octanol	−10.06 ± 0.21	3.51 ± 0.85	–	–
Dimethylaniline	−9.94 ± 0.21	−0.45 ± 0.29	–	–

reported in Table III are similar in both polymers for all the solutes considered, polar and apolar.

Discussion on the solution parameters ΔG_s, ΔH_s and $T\Delta S$

The values of the partial molar free energies of mixing are given in Table IV. The thermodynamic parameters of solution, ΔG_s, ΔH_s and $T\Delta S$, were calculated for the *n*-alkanes on both stationary phases. The process of solution implies the transfer of solute molecules from the gas to the liquid phase. The solute–polymer interaction is closely related to this process, and therefore the enthalpy of solution will also depend on the interaction. Fig. 5 presents results obtained at 200°C for the different parameters *versus* the number of carbon atoms of the *n*-alkane in OV-105. The lines corresponding to the polymer OV-101 are similar. The slope of the lines represents the contribution of the methylene group to the corresponding parameter. Values are

TABLE IV

PARTIAL MOLAR FREE ENERGIES OF MIXING, ΔG_m (kcal mol^{-1})

Stationary phase	Solute	Temperature (K)						
		363.15	383.15	403.15	423.15	453.15	473.15	
OV-101	*n*-Hexane	1.16	1.17	1.18	1.19	1.23	1.25	
	n-Heptane	1.19	1.20	1.20	1.22	1.24	1.25	
	n-Octane	1.21	1.23	1.26	1.30	1.37	1.42	
	n-Nonane	1.23	1.26	1.29	1.34	1.42	1.48	
	n-Decane	1.37	1.36	1.36	1.38	1.47	1.44	
	n-Undecane	1.41	1.39	1.40	1.42	1.51	1.50	
	n-Dodecane	1.43	1.40	1.41	1.44	1.54	1.54	
	Benzene	1.19	1.20	1.20	1.23	1.22	1.25	
	Toluene	1.22	1.23	1.25	1.28	1.31	1.34	
	2-Pentanone	1.56	1.54	1.55	1.56	1.61	1.63	
	Ethyl acetate	1.34	1.31	1.29	1.28	1.27	1.27	
	Pyridine	1.62	1.62	1.62	1.63	1.64	1.67	
	n-Butanol	2.30	2.19	2.09	2.01	1.92	1.88	
	1-Octanol	2.28	2.11	2.00	1.93	1.92	1.87	
	Dimethylaniline	0.16	0.16	0.19	0.22	0.32	0.32	
		372.9	383.35	393.55	403.6	413.5	453.15	473.15
OV-105	*n*-Hexane	1.22	1.24	1.21	1.21	1.22	1.21	1.22
	n-Heptane	1.28	1.30	1.28	1.29	1.30	1.32	1.34
	n-Octane	1.33	1.35	1.33	1.34	1.36	1.39	1.42
	n-Nonane	1.37	1.39	1.38	1.39	1.41	1.45	1.49
	n-Decane	1.42	1.43	1.42	1.43	1.45	1.51	1.56
	n-Undecane	1.45	1.48	1.46	1.47	1.50	1.57	1.62
	n-Dodecane	1.48	1.51	1.50	1.51	1.54	1.62	1.69
	Benzene	1.15	1.16	1.14	1.14	1.15	1.14	1.15
	2-Pentanone	1.40	1.41	1.39	1.39	1.40	1.42	1.46
	Pyridine	1.46	1.46	1.44	1.44	1.45	1.45	1.46
	n-Butanol	2.09	2.04	1.97	1.93	1.90	1.76	1.71

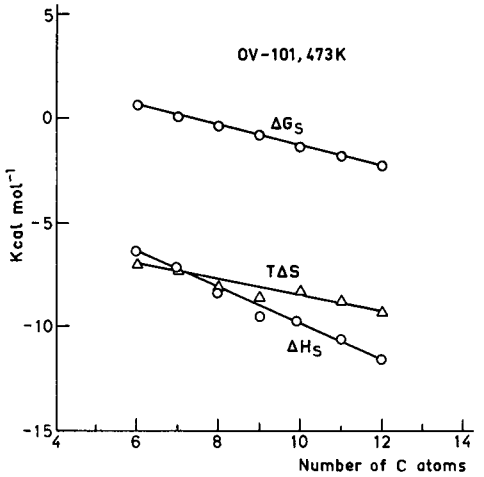

Fig. 5. Thermodynamic parameters of solution of the *n*-alkanes in OV-105 at 473.15 K.

presented in Table V. The difference between the values obtained for the two stationary phases for the slopes of the lines corresponding to ΔH_s (0.07 kcal mol^{-1}) may be attributed to the effect of the 5% substitution of methyl groups by cyanopropyl groups in the polymer, indicating that the solution of the methylene group in the OV-105 polymer is slightly more exothermic. The contribution of the methylene group to the interaction parameter χ^{∞} at 200°C may be deduced from Table II as *ca.* 0.10 for OV-101 and 0.13 for OV-105. The lower value found for OV-101 is indicative of the fact that in this stationary phase, the solubility of *n*-alkanes of longer chain length is more similar to the solubility of those of lower molecular weight than it is in the polymer OV-105, where the solubility decreases more rapidly with increasing chain length. On the other hand, the variation with temperature of the contribution of the CH_2 group to χ^{∞}, as deduced from Table II, is small in both instances, but smaller for OV-101, indicating less deterioration of solubility of the *n*-alkanes with temperature in this instance.

Results obtained on additional stationary phases, and not only those corresponding to the two polymers so far considered, have been taken into account for the purpose of the following discussion on the partial molar free energy of solution. This discussion is concerned with the effect of the presence of the cyanopropyl group in the polymers, and this should be deduced from data obtained on cyanoalkylsilicones.

TABLE V

CONTRIBUTIONS OF THE METHYLENE GROUP TO ΔG_s, ΔH_s AND $T\Delta S$ (kcal mol^{-1}) AT 473.15 K

Errors based on a 95% confidence limit.

Stationary phase	ΔG_s	ΔH_s	$T\Delta S$
OV-101	−0.483 ± 0.017	−0.868 ± 0.082	−0.385 ± 0.097
OV-105	−0.452 ± 0.012	−0.938 ± 0.011	−0.487 ± 0.017

TABLE VI

COMPOSITION OF SILICONE STATIONARY PHASES

Stationary phase	Group substitution (%)		
	Methyl	Phenyl	Cyanopropyl
Methylphenylsilicones			
OV-101	100	0	0
OV-3	90	10	0
OV-7	80	20	0
OV-11	65	35	0
OV-17	50	50	0
OV-22	35	65	0
OV-25	25	75	0
Cyanopropylsilicones			
OV-105	95	0	5
SP-2300	0	50	50
SP-2310	0	25	75
SP-2330	0	5	95
SP-2340	0	0	100

However, some of the commercially available stationary phases containing this group also contain the phenyl group, so the effect of the latter must also be considered. The percentage substitutions of the various groups in the polymers are presented in Table VI.

Using V_g data for *n*-alkanes at 120°C [24], values of the partial molar free energy of solution were calculated for the methylphenylsilicones listed in Table VI. For each stationary phase, ΔG_s was plotted *versus* the number of carbon atoms in the *n*-alkane. In all instances, the correlation coefficients obtained were 0.9997 or higher. The slopes of these straight lines represent, in each instance, the contribution of the methylene group of the *n*-alkanes to the partial molar free energy of solution [$\Delta G_s(CH_2)$] of those substances in the polymer at that temperature. A representation of the slope of the straight lines just mentioned *versus* percentage substitution of the phenyl group is presented in Fig. 6. It can be seen that, taking OV-101 as a reference, the value of $\Delta G_s(CH_2)$ decreases as the phenyl group content increases (-10.6 cal mol^{-1} at *ca.* 30% substitution), and later increases ($+1.4$ cal mol^{-1} at *ca.* 60% substitution; $+15.5$ cal mol^{-1} at 75% substitution). We found that the points fit a parabola very well. The equation is

$$\Delta G_s(CH_2)_{MPS} = 0.0125\,x^2 - 0.7273\,x - 548 \tag{9}$$

where MPS refers to methylphenylsilicones, x represents the percentage substitution of phenyl groups in the silicone and the result is given in cal mol^{-1} (sum of squares of residuals = 2.5). Although the effect of the phenyl group on $\Delta G_s(CH_2)$ is not uniform, it is in any case small.

The same kind of representations of values of V_g for the *n*-alkanes in the cyanopropylsilicones in Table VI [25] plus the polymer OV-101 produced values of the dependence of $\Delta G_s(CH_2)$ on the cyanopropyl percentage substitution which are also

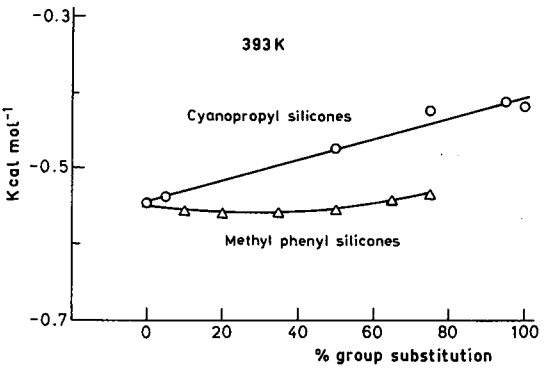

Fig. 6. Contribution of the methylene group of the *n*-alkanes to the partial molar free energy of solution [$\Delta G_s(CH_2)$] of the *n*-alkanes in methylphenyl- and cyanopropylsilicones with different contents of the active group.

shown in Fig. 6. The correlation coefficient obtained was 0.989, indicating that with cyanopropylmethylsilicones there is a linear dependence of the contribution of the methylene group to ΔG_s with the cyanopropyl group substitution of the polymer, given by the expression

$$\Delta G_s(CH_2)_{CPS} = 1.405\,x - 543 \tag{10}$$

where CPS refers to cyanopropylsilicones, x now represents the percentage of cyanopropyl substitution in the polymer and $\Delta G_s(CH_2)$ is given in cal mol^{-1}. In view of the low contribution of the phenyl group, eqn. 10 may be considered as a good approximation for the determination of the effect of cyanopropyl substitution in the polymer. The slope of the line (1.405 cal mol^{-1}) represents the contribution of the methylene group to the partial molar free energy of solution per unit cyanopropyl substitution (expressed as a percentage).

Fig. 6 shows that the value of $\Delta G_s(CH_2)$ increases (becomes less negative) with increasing cyanopropyl content of the polymer, indicating a decrease in the interaction of the methylene group with the polymers of higher cyanopropyl group content. This explains the high values of the solute–polymer interaction parameter of the *n*-alkanes, χ^{∞}, of between 2.4 and 3.8 for *n*-hexane to *n*-dodecane at 120°C, reported for the stationary phase SP-2340 (100% cyanopropyl) [5].

Solubility parameters of the stationary phases

GC has proved to be a good experimental technique to deduce values of solubility parameters of polymers [5,11,18,26–28]. In the case of the two stationary phases considered here, the straight lines obtained with the help of eqn. 2 produced values for δ_2 of 6.49 $\pm$ 0.04 (cal cm^{-3})$^{1/2}$ for OV-101 and 6.83 $\pm$ 0.04 (cal cm^{-3})$^{1/2}$ for OV-105. In neither instance was the dependence of δ_2 on temperature significant, with perhaps slightly lower values at higher temperatures. The value found for OV-101 agrees well with that reported by Roth [29] for polydimethylsiloxane [6.53 (cal cm^{-3})$^{1/2}$ at 90°C].

CONCLUSIONS

The introduction of a small proportion of cyanopropyl groups in the molecule of a dimethylsilicone stationary phase decreases the solubility of *n*-alkanes and improves that of polar compounds. At the same time, it increases the value of the solubility parameter of the polymer, although only slightly.

It has been confirmed that with non-polar solute–polymer systems, specific retention volumes, and therefore the thermodynamic parameters derived from them, may be obtained either from chromatograms carried out in packed or in capillary columns.

The values of the solute–polymer interaction parameters presented here suggest the behaviour that could be expected in the preparation of columns with mixed stationary phases. Polymers containing cyanoalkyl groups should not mix well with hydrocarbon-type stationary phases (hydrocarbons or silicones with alkyl groups), or with those of alcoholic type. They should mix better with polymers containing the phenyl group in their structure.

ACKNOWLEDGEMENTS

The authors thank Dr. M. D. Salvador Moya for her interest and collaboration in the course of the work. This study was carried out under Project PB87-0393 of the Dirección General de Investigación Científica y Técnica of Spain.

REFERENCES

1 J. A. Yancey, *J. Chromatogr. Sci.*, 23 (1985) 161.
2 T. J. Stark, P. A. Larson and R. Dandeneau, *J. Chromatogr.*, 279 (1983) 31.
3 P. Sandra, F. David, M. Proot, G. Diricks, M. Verstape and M. Verzele, *J. High Resolut. Chromatogr. Chromatogr. Commun.*, 8 (1985) 782.
4 J. Conder and C. L. Young, *Physicochemical Measurements by Gas Chromatography*, Wiley, New York, 1979.
5 E. Fernández-Sánchez, A. Fernández-Torres, J. A. García-Domínguez, J. M. Santiuste and E. Pertierra-Rimada, *J. Chromatogr.*, 457 (1988) 55.
6 E. Fernández-Sánchez, J. A. García-Domínguez, J. García-Muñoz and M. J. Molera, *J. Chromatogr.*, 299 (1984) 151.
7 K. Grob, *Making and Manipulating Capillary Columns for Gas Chromatography*, Hüthig, Heidelberg, 1986.
8 B. R. Kersten, S. K. Poole and C. F. Poole, *J. Chromatogr.*, 468 (1989) 235.
9 J. A. García-Domínguez, J. García-Muñoz, E. Fernández-Sánchez and M. J. Molera, *J. Chromatogr. Sci.*, 15 (1977) 520.
10 D. Patterson, Y. B. Tewari, H. P. Schreiber and J. E. Guillet, *Macromolecules*, 4 (1971) 356.
11 G. J. Price, J. E. Guillet and J. H. Purnell, *J. Chromatogr.*, 369 (1986) 273.
12 R. C. Wilhoit and B. J. Zwolinski, *Handbook of Vapour Pressures and Heats of Vaporization of Hydrocarbons and Related Compounds*, Thermodynamics Research Center, Texas, A&M University, College Station, TX, 1971.
13 T. Boublík, V. Fried and E. Hála, *The Vapour Pressures of Pure Substances*, Elsevier, Amsterdam, 1975.
14 J. P. O'Connell and J. M. Prausnitz, *Ind. Eng. Chem., Process Des. Dev.*, 6 (1976) 245.
15 J. H. Dymond and E. B. Smith, *The Viral Coefficients of Pure Gases and Mixtures. A Critical Compilation*, Clarendon Press, Oxford, 1980.
16 National Research Council of the USA, *International Critical Tables of Numerical Data. Physics, Chemistry and Technology*, Vol. III, McGraw-Hill, New York, 1928.
17 *TRC Thermodynamic Tables*, Thermodynamics Research Center, Texas Engineering Experiment Station, The Texas A & M University System, College Station, TX.

18 G. DiPaola-Baranyi and J. E. Guillet, *Macromolecules*, 11 (1978) 228.
19 R. Sanetra, B. N. Kolarz and A. Wlochowicz, *Polymer*, 28 (1987) 1753.
20 A. N. Korol, N. N. Solodchenko and A. A. Ernakov, *J. High Resolut. Chromatogr. Chromatogr. Commun.*, 6 (1983) 279.
21 P. I. Freeman and J. S. Rowlinson, *Polymer*, 1 (1960) 20.
22 T. Bohossian, G. Charlet and G. Delmas, *Polymer*, 30 (1989) 1695.
23 J. I. Iribarren, M. Iriarte, C. Uriarte and J. J. Iruin, *J. Appl. Polym. Sci.*, 37 (1989) 3459.
24 E. Fernández-Sánchez, J. A. García-Domínguez and J. García-Muñoz, *Anal. Quim.*, 83A (1987) 59.
25 E. Fernández-Sánchez, A. Fernández-Torres, J. A. García-Domínguez and J. M. Santiuste, in preparation.
26 J. E. Guillet, *J. Macromol. Sci. Chem.*, 4 (1970) 1669.
27 J. H. Hildebrand, J. M. Prausnitz and R. L. Scott, *Regular and Related Solutions. The Solubility of Gases, Liquids and Solids*, Van Nostrand Reinhold, New York, 1970.
28 P. J. Flory, *Discuss. Faraday Soc.*, 49 (1970) 7.
29 M. Roth, *Macromolecules*, 23 (1990) 1696.

Journal of Chromatography, 547 (1991) 283–289
Elsevier Science Publishers B.V., Amsterdam

CHROM. 23 228

Stereoselectivity of α-, β- and γ-cyclodextrin complexation relative to *cis–trans* acyclic alkenes and cyclooctenes under conditions of gas–liquid chromatography

L. OSSICINI*, G. PEREZ, G. CAPONECCHI and A. CRISTALLI
Istituto di Cromatografia del CNR, Area della Ricerca di Roma, 00016 Monterotondo Stazione (Italy)
and
D. SYBILSKA, T. KOSCIELSKI[a] and J. GORONOWICZ
Institute of Physical Chemistry, Polish Academy of Science, Kasprzaka 44/52, 01-224 Warsaw (Poland)
(First received April 4th, 1990; revised manuscript received February 19th, 1991)

ABSTRACT

Solutions of α-, β- and γ-cyclodextrins in formamide were used as stationary phases in gas–liquid chromatographic systems to observe the effects of complexation on the retentions of acyclic (C_6–C_9) alkenes and cyclooctenes which differ in structure and geometry. On adding β-cyclodextrin to a liquid stationary phase, substantial stereoselectivity with respect to *cis–trans* geometry of acyclic alkenes was found, whereas double bond positions were less recognizable. Almost all the investigated isomers of acyclic alkenes were separated using β-cyclodextrin under appropriate conditions. Small, but distinguishable, effects of γ-cyclodextrin complexation, improving the resolution of *cis–trans* isomers, were observed for 2-octenes and 2-onenes. α-Cyclodextrin influences the resolution of cyclooctenes, enhancing the separation factors for *cis–trans* geometrical isomers and showing substantial enantioselectivity towards optical isomers of *trans*-cyclooctene. Baseline resolutions were achieved for mixtures of *cis*-cyclooctene and two enantiomeric *trans*-cyclooctenes.

INTRODUCTION

The behaviour of alkenes on conventional gas chromatographic stationary phases has been the subject of many studies which have provided some qualitative information [1–3]. It has been established that the retention of alkenes depends on the length of the alkene chain, the double bond position, the *cis*–trans geometry and the stationary phase polarity. Recently, attemps have been made to find some quantitative descriptions, *i.e.*, to evaluate relationships between retention indices of alkenes (determined on different commonly used stationary phases) and the parameters describing their structure [4].

Nevertheless, resolutions of isomeric alkenes on known conventional phases are very poor and thus the separations are not easy to perform. More promising selectivities have been observed recently for alkenes by applying some special gas

[a] Present address: Petroleum Research Centre, P.O. Box 6431, Tripoli, Libya.

0021-9673/91/$03.50

chromatographic systems, *e.g.*, using liquid crystal glass capillaries [5–11] and copper complexes bonded to silica [12–14].

On the other hand, cyclodextrin (CD) complexation [15,16] may be considered as a possible choice for the separation of various isomers [17–20], which can distinguish their shape more than their polarity under gas–liquid chromatographic conditions [21–23]. Therefore, it is of interest to investigate how such steroselective CD inclusion will recognize isomers of alkenes.

In this work we studied agents that improve the differentiation of isomeric alkenes and the relationship between the structure of a guest molecule (double bond position, *cis*–trans geometry, cyclization and chirality) and its ability to form inclusions in α-, β- and γ-CD cavities.

EXPERIMENTAL

Reagents

α-, β- and γ-CD were supplied by Chinoin (Budapest, Hungary). Celite was obtained from BDH (Poole, UK), Chromosorb P AW from Chrompak (Netherlands) and pure formamide from Merck (Darmstadt, Germany).

All the investigated compounds, except *trans*-cyclooctene, were commercial products from different sources and were used without further purification.

Racemic *trans*-cyclooctene was generated in methanolic solution by singlet photosensitized isomerization of *cis*-cyclooctene, according to the procedure described in detail by Inoue *et al.* [24]; methyl benzoate was used as an active sensitizer.

Apparatus and procedures

Chromatographic studies were performed using Hewlett-Packard Model 5890 and Carlo Erba Model 4200 gas chromatographs, both equipped with flame ionization detectors. Glass columns (2 m × 4 mm I.D. and 1 m × 3.2 mm I.D.) were used. The peaks areas and the retention times were measured with a Hewlett-Packard Model 3390 integrator. The compounds were injected separately (0.02 μl) or as mixtures with Hamilton microsyringes.

The stationary phases were prepared as follows. Celite (30–80 mesh) and Chromosorb P AW (80–100 mesh) were coated with α-, β-, γ-CD dissolved in formamide. In order to obtain a good separation, the α-CD column contained 4% of water together with lithium nitrate (0.45 g) used as a stabilizing agent.

The amounts of CDs in stationary phases containing 4.5 g of formamide and 20 g of Celite were as follows: column I, none; column II, 0.6 g of α-CD; column III, 1.2 g of β-CD and column IV, 1.2 g of γ-CD. The contents of formamide and water in each stationary phase were determined by thermogravimetric analyses using a DuPont Thermal Analysis System 1090. The amount of coated support contained in the 2-m columns was 11.5 ± 0.5 g.

The column used for special separations of hexenes and heptenes is described in the caption of Figure 1.

In all experiments special care was devoted to maintaining a constant helium inlet pressure (2.75 ± 0.05 atm) and flow-rate (50 ± 0.5 ml/min) in order to make possible a comparison between the stability constants of CD complexes if the isomeric alkenes, although their exact values could not be determined [25,26].

RESULTS AND DISCUSSION

The relative stabilities of CD complexes can be compared on the assumption that only 1:1 stoichiometric complexes are formed using the following equation:

$$t'_R = t'_{Ro}(1 + k[CD])$$

were t'_R and t'_{Ro} are the adjusted retention times of the solute on the column containing CD in formamide and on the reference column containing pure formamide, respectively, k is the stability constant of the solute–CD complex and [CD] is the CD concentration (molar fraction) in formamide solution.

The separation factor, α, for two solutes, A and B, can be calculated by the ratio of their adjusted retention times when the same column and identical separation conditions are used:

$$\alpha = t'_{R(B)}/t'_{R(A)}$$

The adjusted retention times of *n*-alkenes, reported in Table I, show the influence of their structure on their ability to be complexed by α-, β- and γ-CD. The selectivities are increased when β-CD in formamide is used as a stationary phase. Chromatograms of the elutions of *cis* and *trans* isomers (Fig. 1) exemplify the behaviours of α-, β- and γ-CD with respect to *n*-alkenes.

It can be observed that α-CD influences very slightly the retentions of *n*-alkenes as an index of the low stability of the complex formed. Small but distinguishable effects of γ-CD activity, which improves the resolution of *cis–trans* isomers, can be

TABLE I

ADJUSTED RETENTION TIMES (t'_R) OF ACYCLIC ALKENES DETERMINED ON COLUMNS (2 m × 4 mm I.D.) FILLED WITH CELITE (30–80 mesh) COATED WITH FORMAMIDE (F, COLUMN I) AND FORMAMIDE SOLUTIONS MODIFIED BY α-CD (COLUMN II), β-CD (COLUMN III) AND γ-CD (COLUMN IV) AT 40°C AND A HELIUM FLOW-RATE OF 40 ml/min

Compound	t'_R			
	Column I, F	Column II, F, α-CD	Column III, F, β-CD	Column IV, F, γ-CD
cis-2-Hexene	0.09	0.11	1.8	0.39
trans-2-Hexene	0.06	0.12	0.9	0.27
cis-3-Hexene	0.09	0.09	1.2	0.28
trans-3-Hexene	0.09	0.06	0.6	0.17
cis-2-Heptene	0.19	0.47	3.8	0.7
trans-2-Heptene	0.16	0.42	2.1	0.7
cis-3-Heptene	0.20	0.43	3.3	0.6
trans-3-Heptene	0.16	0.34	1.7	0.4
cis-2-Octene	0.42	0.58	7.9	1.3
trans-2-Octene	0.25	0.62	4.4	0.9
cis-2-Nonene	1.1	1.1	15.2	2.5
trans-2-Nonene	0.9	1.6	8.9	1.8

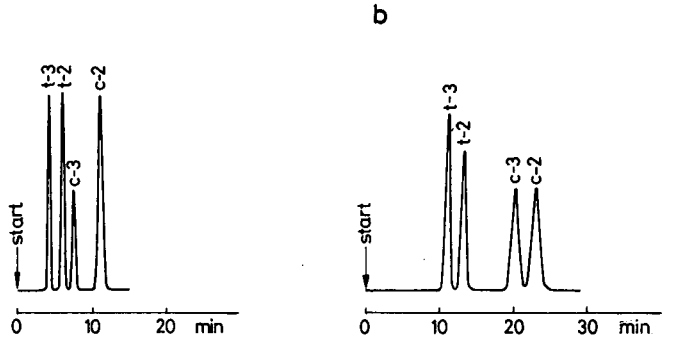

Fig. 1. Chromatograms of mixtures of (a) *cis*- and *trans*-2- and -3-hexenes and (b) *cis*- and *trans*-2- and -3-heptenes obtained under optimum conditions: β-CD column (2 m × 4 mm I.D.) containing 15.7 g of filling prepared using 20 g of Chromosorb P AW, 80–100 mesh, 1.5 g of β-CD and 4.5 g of formamide; temperature, 30°C; helium flow-rate, 40 ml/min; injected samples, 0.08 × 0.1 μl.

observed for 2-octenes and 2-nonenes. This behaviour may suggest that a major selectivity of γ-CD might appear towards larger molecules of *n*-alkenes ($> C_9$).

In contrast to α-CD and γ-CD, β-CD appears to be a true powerful selector for *n*-alkenes. The stereoselectivity imparted to a liquid stationary phase by β-CD complexation is considerable with respect to both *cis–trans* geometry and alternation of the double bond position. The data in Table I indicate that the *cis–trans* geometry is better recognized than double bond position by β-CD . Nevertheless the differentiation of all the investigated isomers was sufficient to perform the analyses, as is exemplified by the chromatograms of 2- and 3-hexenes and -heptenes.

The relatively indifferent behaviour of β-CD towards homologous compounds seems worth mentioning. The mean value of the separation coefficient for homologous series (C_{n+1}/C_n) on a β-CD estimated from the retention of C_6–C_9 alkenes of corresponding configuration is about 2 both for the compounds of *cis*-2 and for those of *trans*-2 configuration. Its comparison with the corresponding $\alpha_{(C_{n+1}-C_n)}$ values observed with pure matrix solvent (2–3) leads to the conclusion that the separation of homologous series achieved using the applied systems with β-CD is mainly due to the matrix solvent contribution, *i.e.*, formamide used in this study. This suggestion was confirmed in a separate set of experiments performed with C_5–C_9 1-alkenes, where $\alpha_{(C_{n+1}-C_n)}$ was found to be *ca.* 2 for the columns containing either formamide or β-CD formamide solution.

Resolution of cyclooctenes

Cyclooctenes are interesting compounds because of the considerable difference (9.3 kcal/mol) in the strain energy between *trans* and *cis* isomers [27]. One of the most fascinating aspects of their structure is the inherent chirality of *trans*- or (*E*)-cyclooctene [28]. Therefore, it seemed interesting to establish how the cyclization and the difference in the structures of stereoisomers and enantiomers of cyclooctene will be reflected in their abilities to form CD inclusion complexes.

Fig. 2 shows chromatograms of *cis*-cyclooctene and of its mixtures with racemic *trans*-cyclooctene, generated in solution via a sensitized photoisomerization process [25]. Stereoselective inclusions in α-, β- and γ-CD cavities are confirmed.

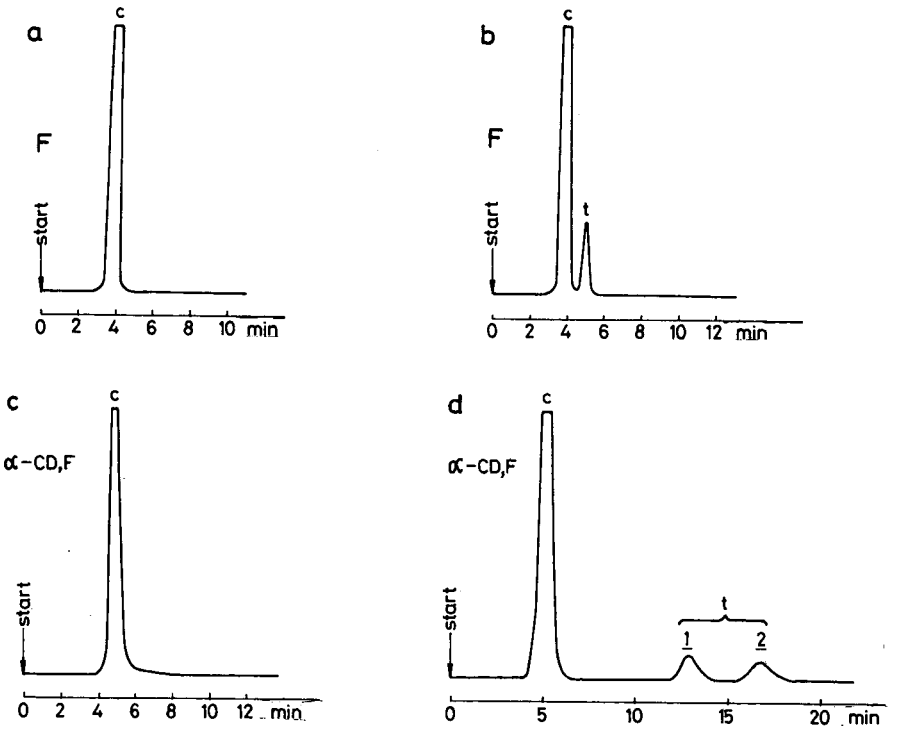

Fig. 2. Chromatograms of methanolic solution of *cis*-cyclooctene (a and c) unirradiated and (band d) afer *ca.* 16 h of irradiation performed at 40°C on (c and d) column II with α-CD in formamide and (a and b) on the reference column I with formamide. Helium flow-rate, 40 ml/min; injected samples, 0.1 μl. Peaks of methanol, which eluted much later than cyclooctene, are not shown.

It should be explained that for chromatographic studies of *trans*-cyclooctene behaviour we used the mixtures of *cis–trans* cyclooctenes obtained directly after the irradiation period (*ca.* 18 h). Under the conditions of the sensitized photoisomerization process applied in this work, the content of *trans* form in the stationary state was *ca.* 12% (*cis ca.* 88%).

These data indicate a high stereoselectivity of α-CD complexation with respect in the isomeric cyclooctenes, which leads to efficient baseline separations of (+)- and (−)-*trans*-cyclooctenes and their mixtures with *cis*- cyclooctene.

The kinetic data, reported in Table II show that the racemic *trans*-cyclooctene, determined on column I, is split into equal peaks on column II. This supports the hypothesis that the α-CD column really works for the separation of racemic *trans*-cyclooctene into enantiomers. To the best of our knowledge, this is the first example of the direct chromatographic resolution of *cis*-syclooctene and enantiomeric *trans*-cyclooctenes.

Further studies aimed at the determination of the absolute configuration of enantiomer 1 and 2 (indicated here according to the sequence of their elution) are in progress. Attempts have also been made to elaborate an assay method for monitoring chiral sensitized photoisomerization processes using optically active sensitizers.

TABLE II

CHANGES IN COMPOSITION OF *CIS*- AND *TRANS*-CYCLOOCTENE MIXTURE (CALCULATED FROM CHROMATOGRAPHIC DATA, IN %) DURING IRRADIATION PROCESSES

Sample	Time of irradiation (h)	Composition determined at 40°C on the achiral column I covered with formamide		Composition determined at 40°C on column II covered with α-CD solution in formamide		
		cis, t'_R = 3.8 min	*trans*, t'_R = 5.6 min	*cis*, t'_R = 4.2 min	*trans* 1, t'_R = 12.2 min	*trans* 2, t'_R = 16.3 min
Initial solution[a]	0	97.4	–	99.9	–	–
Sample 1	6	93.1	4.4	94.8	2.4	2.3
Sample 2	12	87.2	9.2	89.4	5.1	4.8
Sample 3	18	83.9	12.8	86.7	6.7	6.6
Sample 4	24	82.4	13.9	84.9	7.6	7.7
Sample 5	32	82.0	13.4	86.8	6.6	6.5

[a] Initial solution containing 0.4 g of *cis*-cyclooctene dissolved in 5 ml of methanol and 50 mg of methyl benzoate used as a sensitizer. Irradiation process was performed following strictly ref. 24. Each value quoted is a mean value of three determinations. The peak of methanol, eluted at a retention time of 50 min from column I and 60 min from column II was not taken into account.

In contrast with the acyclic alkenes investigated, efficient separations of *cis*- and racemic *trans*-cyclooctene can be simply acieved on conventional liquid polar stationary phases, as has been reported elsewhere [29,30] and confirmed in this work using pure formamide liquid stationary phase ($\alpha_{trans-cis}$ = 1.46). This phenomenon is due to the substantial polarity of the *trans*-cyclooctene molecule. For this reason, the sequence of elution from the reference formamide column, first *cis* and then *trans*, is the opposite of that observed for acyclic *trans*- and *cis*-2-octenes.

Although γ-CD and espacially β-CD form much more stable complexes than α-CD with cyclooctenes, their discrimination of *cis–trans* geometry is very poor and there is no chiral recognition of *trans*-cyclooctene optical isomers. The very weak discrimination of *cis–trans* geometry arising from β-CD or γ-CD complexation is the opposite in direction to that imposed by formamide medium. As a consequence, the stereoselectivity towards *cis–trans* geometry exhibited by pure formamide ($\alpha_{trans-cis} \approx$ 1.46) can be annihilated by β- or γ-CD complexation, as has been found for columns III ($\alpha_{trans-cis} \approx 1$) and IV ($\alpha_{trans-cis} \approx 1$). On increasing the β-CD concentration a decrease in selectivity is observed, which leads to a change in $\alpha_{trans-cis}$ values from 1.46 to 1.0.

This behaviour confirms again the suggestion that there is no relationship between strength of α-, β- and γ-CD complexation of various organic compounds and their ability to differentiate selectively the isomers of these compounds.

ACKNOWLEDGEMENT

The work was supported in part by Grant CPBP 3.20 from the Polish Academy of Sciences.

REFERENCES

1 L. Sojak, J. Hrivnak, P. Majer and J. Janak, *Anal. Chem.*, 45 (1973) 293.
2 C. F. Chien, D. L. Furio, M. M. Kopecni and R. J. Raub, *J. High Resolut. Chromatogr. Chromatogr. Commun.*, 6 (1983) 577.
3 S. Rang, K. Kuningas, T. Strenze, A. Orav and O. Eisen, *J. Chromatogr.*, 406 (1987) 75.
4 A. Voelkel, *Chromatographia*, 25 (1988) 655.
5 L. Sojak, G. Kraus, I. Ostrovsky, E. Kralovicova and J. Krupcik, *J. Chromatogr.*, 206 (1981) 463.
6 L. Sojak, G. Kraus, I. Ostrovsky, E. Kralovicova and J. Krupcik, *J. Chromatogr.*, 206 (1981) 475.
7 L. Sojak, G. Kraus, I. Ostrovsky, E. Kralovicova and P. Farkas, *J. Chromatogr.*, 217 (1981) 225.
8 L. Sojak, G. Kraus, I. Ostrovsky and E. Kralovicova, *J. Chromatogr.*, 234 (1982) 347.
9 L. Sojak, G. Kraus, P. Farkas and I. Ostrovsky, *J. Chromatogr.*, 238 (1982) 51.
10 L. Sojak, G. Kraus, P. Farkas and I. Ostrovsky, *J. Chromatogr.*, 249 (1982) 29.
11 W. A. Konig, *The Practice of Enantiomer Separation by Capillary Gas Chromatography*, Hüthig, Heidelberg, 1987.
12 W. Wasiak and W. Szczepaniak, *J. Chromatogr.*, 364 (1986) 259.
13 W. Wasiak, *Chromatographia*, 23 (1987) 423.
14 W. Wasiak, *Chromatographia*, 23 (1987) 427.
15 J. Szejtli, *Cyclodextrins and Their Inclusion Complexes*, Akadémiai Kiadó, Budapest, 1982.
16 V. Schurig, *J. Chromatogr.*, 13 (1988) 135.
17 W. L. Hinze, *Sep. Purif. Methods*, 10 (1981) 159.
18 E. Smolkova-Keulemansova, *J. Chromatogr.*, 251 (1982) 17.
19 V. Schurig and H. P. Nowotny, *J. Chromatogr.*, 441 (1988) 155.
20 V. Schurig, *Chromatographia*, 13 (1980) 263.
21 T. Koscielski, D. Sybilska, J. Lipkowski and A. Miediokritskaja, *J. Chromatogr.*, 351 (1986) 512.
22 T. Koscielski, D. Sybilska and J. Jurczak, *J. Chromatogr.*, 364 (1986) 299.
23 T. Koscielski, D. Sybilska, S. Belniak and J. Jurczak, *Chromatographia*, 21 (1986) 413.
24 Y. Inoue, S. Takamaku, Y. Kunitomi and H. Sakurai, *J. Chem. Soc., Perkin Trans.*, 2 (1980) 1672.
25 J. H. Purnell, in A. B. Littlewood (Editor), *Gas Chromatography*, Institute of Petroleum, London, 1966, pp. 3–20.
26 C. Eon, C. Pommier and G. Guiochon, *J. Phys. Chem.*, 75 (1971) 2632.
27 P. v. R. Schleyer, J. E. Williams and K. R. Branchard, *J. Am. Chem. Soc.*, 92 (1970) 2377.
28 R. P. Johnson, in J. F. Liebman and A. Greenberg (Editors), *Molecular Structure and Energetics, Vol. 3, Studies of Organic Molecules*, VCH, Deerfield Beach, FL, 1986, p. 91.
29 Y. Inoue, S. Takamaku and H. Sakurai, *J. Chem. Soc., Chem. Commun.*, (1976) 423.
30 Y. Inoue, S. Takamaku and H. Sakurai, *J. Phys. Chem.*, 81 (1977) 7.

Journal of Chromatography, 547 (1991) 291–298
Elsevier Science Publishers B.V., Amsterdam

CHROM. 23 216

Determination of volatile aliphatic aldehydes in the headspace of heated food oils by derivatization with 2-aminoethanethiol

AKIO YASUHARA*

Regional Environment Division, National Institute for Environmental Studies, 16–2 Onogawa, Tsukuba, Ibaraki 305 (Japan)

and

TAKAYUKI SHIBAMOTO

Department of Environmental Toxicology, University of California, Davis, CA 95616 (USA)

(Received December 10th, 1990)

ABSTRACT

Reaction conditions for the derivatization of volatile aliphatic aldehydes with 2-aminoethanethiol (cysteamine) were investigated. Reaction at room temperature for 1 h at pH 8 was sufficient and the recovery was quantitative for all the aldehydes tested. The detection limits were very low with a nitrogen–phosphorus detector. Concentration of the extract solution cannot be used because of the high volatility of the derivatization products, thiazolidines. Eleven aldehydes in the headspace of heated food oils were determined by this derivatization method. The concentration of hexanal was very high in all samples. It is noteworthy that the contents of isoalkanals were very low.

INTRODUCTION

The formation of many carbonyl compounds, particularly volatile aldehydes, by oxidation or decomposition of foodstuffs which contain lipids has already been reported [1–5]. As volatile aliphatic aldehydes have offensive smells, great attention has been paid to analytical methods for these aldehydes with regard to the odour control of exhaust gases from the paint and printing industries which include heating processess [6].

Many analytical methods for volatile aldehydes have been developed. Derivatization with 2,4-dinitrophenylhydrazine [7–9], benzyloxyamine [10], pentafluorobenzyloxyamine [11,12], or N-benzylethanolamine [13,14] are well known. However, peak identification is extremely difficult because the formation of both *syn* and *anti* forms is inevitable. Therefore, it is almost impossible to determine different aldehydes simultaneously by these derivatization methods. Derivatization with 2-hydroxy methylpiperidine has been recommended in the OSHA method for the determination of both formaldehyde and acrolein [15]. However, this method is not applicable to the determination of other aldehydes because excess of the reagent, 2-hydroxymethyl-

0021-9673/91/$03.50

piperidine, interferes. Recently, Shibamoto and co-workers [16–18] developed a new derivatization method with 2-aminoethanethiol (cysteamine). This method has several characteristics compared with other derivatization methods: (1) only one derivative is formed from one aldehyde; (2) the derivatization reaction proceeds under very mild conditions, rapidly and with almost quantitative yield; (3) the derivatives, thiazolidines, can be separated perfectly with fused-silica capillary column and detected selectively with a nitrogen–phosphorus detector; and (4) excess of the reagent, 2-aminoethanethiol, does not interfere with gas chromatographic (GC) analysis.

We have already reported results for aldehydes and ketones in the headspace of heated pork fat, obtained using the derivatization method with cysteamine [19]. However, details of this analytical method have not been reported previously. This paper describes the reliability of this method and its application to the headspace analysis of heated food oils.

EXPERIMENTAL

Reagents

Cysteamine hydrochloride was purchased from Aldrich and aldehydes from Wako. Pure thiazolidines as derivatization products were synthesized according to the literature.

Sampling and analytical procedure

Cysteamine hydrochloride (0.5 g) was dissolved in 15 ml of distilled water and the pH was adjusted to 8.0 with 0.1 *M* sodium hydroxide solution. The final volume of the solution was set at 20 ml. This solution was sucked through a sample gas inlet into a sampling bottle, which was evacuated by a vacuum pump before sampling. The volume of the sampling bottle was 1020 ml. The set-up is shown in Fig. 1.

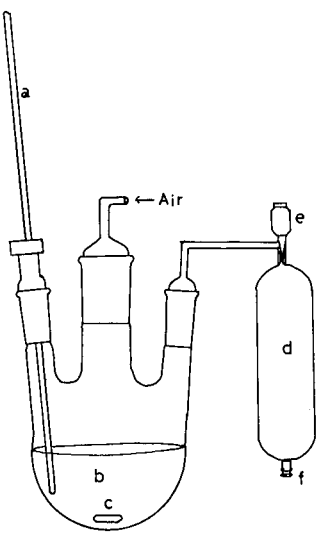

Fig. 1. Apparatus for sampling headspace of heated food oil. a = Thermometer; b = food oil; c = bar for magnetic stirrer; d = sampling bottle; e = needle valve; f = glass stopper.

Food oils used as samples were corn oil, corn oil used for a long period, cottonseed oil, a mixture of soybean oil and sesame oil and safflower oil. All these oils are widely used in most Japanese homes for cooking. A 100-g amount of each oil was placed in a 2-l three-necked round flask and heated at 200°C with magnetic stirring. The sampling bottle containing cysteamine solution prepared as described above was connected to the flask as shown in Fig. 1. Headspace was sucked into the bottle by loosening a needle valve. After sampling, the bottle was shaken vigorously for 5 min and then kept for 1 h at room temperature for completion of derivatization. Next, the solution was transferred to a separating funnel and extracted twice with dichloromethane (10 and 5 ml). The combined organic layer was passed through a small amount of anhydrous sodium sulphate for removal of water and the sodium sulphate was washed with dichloromethane (5 ml). Both dichloromethane solutions were combined. A 20-μl volume internal standard (N-methylacetamide) solution (12.2 mg/ml in dichloromethane) was added to the solution and the final volume was adjusted to 20 ml.

Gas chromatography

A Hewlett-Packard Model 5890A gas chromatograph equipped with a DB-WAX (0.25 μm) fused-silica capillary column (30 m $\times$ 0.25 mm I.D.) and a nitrogen–phosphorus detector was used. The column oven temperature was held at 40°C for 2 min and then programmed to 180°C at 4°C/min. The GC peak areas were integrated with a System Instruments Model 7000B integrator. The injector temperature was 250°C and the detector temperature 300°C. The carrier gas (helium) flow-rate was 33.7 cm/s. The injector splitting ratio was 1:20.

Gas chromatography–mass spectrometry

The GC conditions were similar to those described above. A JEOL Model DX-300 mass spectrometer equipped with a Hewlett-Packard Model 5710A gas chromatograph and a JEOL Model JMA-3500 data acquisition and analysis system was used for measurements of mass spectra. The mass spectrometric conditions were as follows: ion-source pressure, $3 \cdot 10^{-6}$ Torr; ion-source temperature, 190°C; ionization energy, 70 eV; ionization current, 300 μA; accelerating voltage, 3 kV; scan range, m/z 10–400; scan speed, 1.4 per scan; repetition time, 2 s; coupling mode for gas chromatograph and mass spectrometer, direct.

RESULTS AND DISCUSSION

Effect of pH on derivatization

Recovery was measured by reacting 100 μg of each aldehyde with 0.5 g of cysteamine for 3 h at various pH values and the results are shown in Table I, with blank values substracted for formaldehyde and acetaldehyde. The reaction seems to proceed completely at pH $\geqslant$ 8. As alkaline conditions are not favourable for sample preparation, pH 8 was adopted.

Effect of reaction time on derivatization

Recovery was investigated by reacting 100 μg of each aldehyde with 0.5 g of cysteamine at pH 8 for various reaction times and the results are shown in Table II,

TABLE I

RECOVERY ON DERIVATIZATION WITH CYSTEAMINE AT VARIOUS pH VALUES

Blank values were subtracted for formaldehyde and acetaldehyde.

pH	Recovery (%)										
	C_1	C_2	C_3	*i*-C_4	C_4	*i*-C_5	C_5	C_6	C_7	C_8	C_9
6	37	54	93	96	94	96	96	72	85	89	81
7	95	90	99	98	98	98	97	81	87	98	88
8	94	103	104	101	103	99	102	95	91	99	94
9	100	103	101	100	102	99	101	95	87	99	99
10	99	104	102	101	103	101	104	99	95	99	97
11	99	103	101	102	104	99	103	98	97	99	98

with blank values subtracted for formaldehyde and acetaldehyde. The necessary reaction time is 1 h, as the reaction rate is fast.

Blank test

Blank values were observed only for formaldehyde and acetaldehyde, probably present in the solvent and distilled water. The values were 7.21 μg for formaldehyde and 9.63 μg for acetaldehyde when 15 ml of dichloromethane and 20 ml of distilled water were used for extraction and dissolution of cysteamine hydrochloride, respectively.

Reliability of analytical procedure

Replicate recoveries were measured by reacting 0.5 g of cysteamine and 100 μg of each aldehyde at pH 7 for 3 h and the results are given in Table III with blank values substracted for formaldehyde and acetaldehyde. The high standard deviations for formaldehyde and acetaldehyde seem to be due to the deviation of the blank values.

Detection limit

Detection limits, shown in Table IV, were calculated from the peak height with a signal-to-noise ratio of 3 using split-mode injection. The detection limits were

TABLE II

EFFECT OF REACTION TIME ON DERIVATIZATION

Blank values were subtracted for formaldehyde and acetaldehyde

Time (h)	Recovery (%)										
	C_1	C_2	C_3	*i*-C_4	C_4	*i*-C_5	C_5	C_6	C_7	C_8	C_9
1	91	99	93	89	89	90	88	83	88	99	93
2	92	101	95	92	91	93	90	88	89	100	94
3	94	92	97	96	94	98	93	90	91	101	95
4	94	92	96	95	95	97	92	91	90	99	96

TABLE III

REPRODUCIBILITY OF RECOVERY ON DERIVATIZATION

Blank values were subtracted for formaldehyde and acetaldehyde.

Run No.	Recovery (%)										
	C_1	C_2	C_3	*i*-C_4	C_4	*i*-C_5	C_5	C_6	C_7	C_8	C_9
1	108	109	98	95	94	96	97	98	97	96	91
2	88	92	97	95	93	95	95	97	94	95	88
3	93	95	98	95	94	95	95	98	98	91	90
4	99	98	100	97	97	99	99	104	99	100	99
5	90	90	98	95	97	98	97	101	95	99	90
Av.	96	97	98	95	95	97	97	100	97	96	92
R.S.D. (%)[a]	8	8	1	1	2	2	2	3	2	4	5

[a] Relative standard deviation.

roughly proportional to molecular weight, as the relative nitrogen content in the molecules decreases with increasing molecular weight.

Loss of thiazolidines by concentrating dichloromethane solution

A 10-μg amount of each thiazolidine was dissolved in 80 ml of dichloromethane and the solution was concentrated to 2 ml by distillation under atmospheric pressure. Losses of thiazolidines in this procedure are shown in Table V. These results suggest that concentration by distillation should not be adopted.

Application to headspace of heated food oil

Typical gas chromatograms are shown in Figs. 2 and 3. Table VI gives the analytical results. The contents of isoalkanals such as isobutyraldehyde and isovaleraldehyde were low compared with the *n*-alkanals. The abundance of hexanal was the highest in every instance. These trends were the same as the results for the headspace

TABLE IV

DETECTION LIMITS OF THIAZOLIDINES AND CORRESPONDING ALDEHYDES

Substance	Detection limit (pg)	Corresponding aldehyde (pg)
Thiazolidine	17.2	5.8
2-Methylthiazolidine	16.7	7.1
2-Ethylthiazolidine	20.2	10.0
2-Isopropylthiazolidine	22.7	12.5
2-Propylthiazolidine	26.1	14.4
2-Isobutylthiazolidine	30.4	18.0
2-Butylthiazolidine	32.8	19.5
2-Pentylthiazolidine	39.2	24.7
2-Hexylthiazolidine	42.8	28.2
2-Heptylthiazolidine	53.3	36.5
2-Octylthiazolidine	51.3	36.2

TABLE V

LOSS OF THIAZOLIDINES DURING CONCENTRATION PROCESS

Substance	Loss (%)	Substance	Loss (%)
Thiazolidine	59	2-Butylthiazolidine	37
2-Methylthiazolidine	46	2-Pentylthiazolidine	31
2-Ethylthiazolidine	42	2-Hexylthiazolidine	19
2-Isopropylthiazolidine	35	2-Heptylthiazolidine	8
2-Propylthiazolidine	39	2-Octylthiazolidine	3
2-Isobutylthiazolidine	34		

of heated pork fat [19]. These results suggest that the oxidative cleavage of the double bond in natural unsaturated fatty acid esters such as linoleic acid esters produces hexanal [2]. It is noteworthy that large amounts of these saturated aliphatic aldehydes (C_1-C_9) were formed by heating food oils. It has been confirmed by mass spectrometry that mass spectra at peaks corresponding to thiazolidines in GC were coincident with the reported values [20,21]. As a strong common peak exists at *m/z* 88 in the mass spectra of 2-alkylthiazolidines, mass chromatography at *m/z* 88 is very effective for the detection of thiazolidines derived from aldehydes. Fig. 4 shows a typical example. Mass chromatography at *m/z* 102 is performed for detection of 2-alkanones,

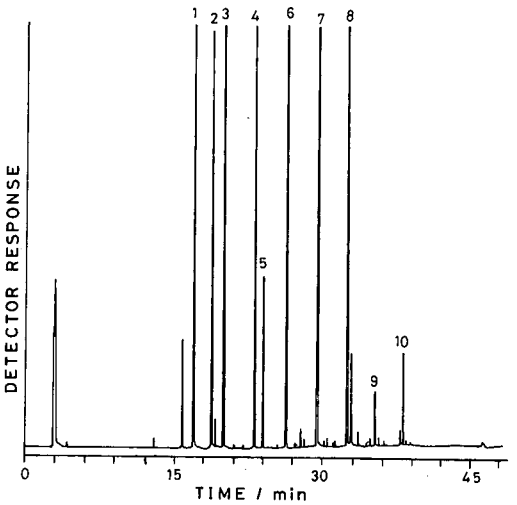

Fig. 2. Gas chromatogram of derivatives from aldehydes in headspace of heated safflower oil. Peaks: 1 = 2-methylthiazolidine from acetaldehyde; 2 = thiazolidine from formaldehyde; 3 = 2-ethylthiazolidine from propionaldehyde; 4 = 2-propylthiazolidine from butyraldehyde; 5 = internal standard (N-methylacetamide); 6 = 2-butylthiazolidine from valeraldehyde; 7 = 2-pentylthiazolidine from hexanal; 8 = 2-hexylthiazolidine from heptylaldehyde; 9 = 2-heptylthiazolidine from octylaldehyde; 10 = 2-octylthiazolidine from nonylaldehyde.

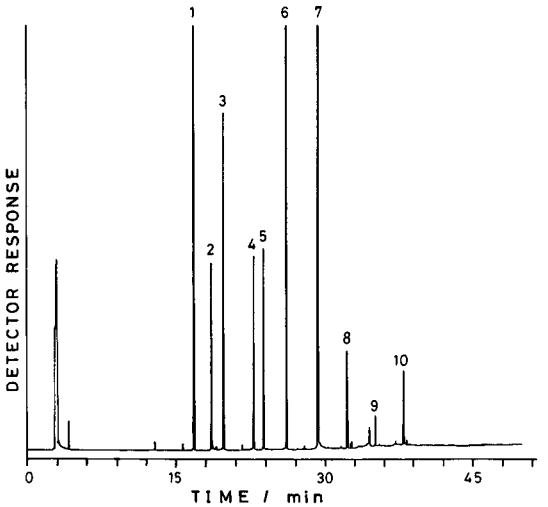

Fig. 3. Gas chromatogram of derivatives from aldehydes in headspace of heated corn oil. Peaks: 1 = 2-methylthiazolidine from acetaldehyde; 2 = thiazolidine from formaldehyde; 3 = 2-ethylthiazolidine from propionaldehyde; 4 = 2-propylthiazolidine from butyraldehyde; 5 = internal standard (N-methylacetamide); 6 = 2-butylthiazolidine from valeraldehyde; 7 = 2-pentylthiazolidine from hexanal; 8 = 2-hexylthiazolidine from heptylaldehyde; 9 = 2-heptylthiazolidine from octylaldehyde; 10 = 2-octylthiazolidine from nonylaldehyde.

TABLE VI

CONCENTRATIONS OF ALDEHYDES IN HEADSPACE OF HEATED FOOD OILS

Unit of concentration is μg/l of headspace on 100 g of heated food oil. Concentration values are averages of three replicate measurements.

Aldehyde	Food oil				
	Fresh corn	Used corn	Cotton-seed	Safflower	Mixed oil[a]
C_1	53	72	99	85	46
C_2	583	859	576	1130	572
C_3	286	745	232	797	475
i-C_4	2	4	ND	3	ND
C_4	174	317	161	622	140
i-C_5	3	4	ND	ND	ND
C_5	714	548	630	1550	413
C_6	2570	1480	2220	4700	1390
C_7	179	326	180	1230	165
C_8	77	147	77	143	72
C_9	162	513	181	251	263

[a] Mixture of soybean oil and sesame oil.

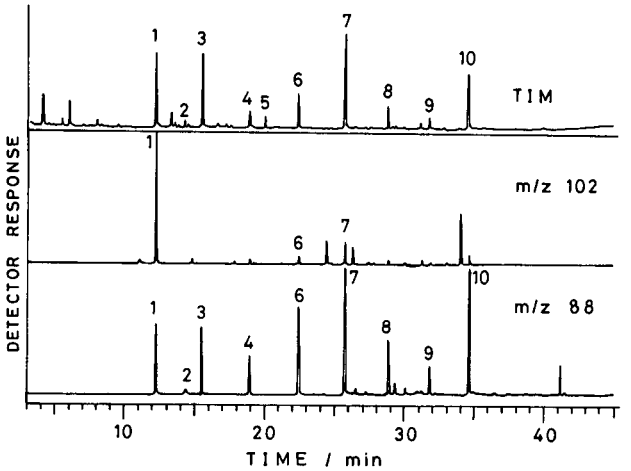

Fig. 4. Mass chromatogram of derivatives from aldehydes in headspace of heated mixture of soybean oil and sesame seed oil. TIM = total ion monitoring. Peaks: 1 = 2-methylthiazolidine from acetaldehyde; 2 = thiazolidine from formaldehyde; 3 = 2-ethylthiazolidine from propionaldehyde; 4 = 2-propylthiazolidine from butyraldehyde; 5 = internal standard (N-methylacetamide); 6 = 2-butylthiazolidine from valeraldehyde; 7 = 2-pentylthiazolidine from hexanal; 8 = 2-hexylthiazolidine from heptylaldehyde; 9 = 2-heptylthiazolidine from octylaldehyde; 10 = 2-octylthiazolidine from nonylaldehyde.

because thiazolidines derived from 2-alkanones show a strong common peak at m/z 102 in their mass spectra.

It is concluded that the described method is very effective for the determination of aldehydes.

REFERENCES

1 T. Yamamoto, T. Kurata, H. Kato and M. Fujimaki, *Agric. Biol. Chem.*, 34 (1970) 88.
2 D. S. Mottram, R. A. Edwards and H. J. H. MacFie, *J. Sci. Food Agric.*, 33 (1982) 934.
3 B. Reindl and H. J. Stan, *J. Agric. Food Chem.*, 30 (1982) 849.
4 D. S. Mottram, S. E. Croft and R. L. S. Patterson, *J. Sci. Food Agric.*, 35 (1984) 233.
5 S. Ohnishi and T. Shibamoto, *J. Agric. Food Chem.*, 32 (1984) 987.
6 Japan Environment Agency, *Personal communication.*
7 D. Grosjean, *Environ. Sci. Technol.*, 16 (1982) 254.
8 K. Kuwata, M. Uebori, H. Yamasaki and Y. Kuge, *Anal. Chem.*, 55 (1983) 2013.
9 S. B. Tejada, *Int. J. Environ. Anal. Chem.*, 26 (1986) 167.
10 S. P. Levine, T. M. Harvey, T. J. Waeghe and R. H. Shapiro, *Anal. Chem.*, 53 (1981) 805.
11 H. Nishikawa, Y. Takahara, H. Mori and T. Hayakawa, *J. Jpn. Soc. Air Pollut.*, 19 (1984) 387.
12 H. Nishikawa, T. Hayakawa and T. Sakai, *Bunseki Kagaku*, 36 (1987) 381.
13 E. R. Kennedy and R. H. Hill, Jr., *Anal. Chem.*, 54 (1982) 1739.
14 *NIOSH Manual of Analytical Methods*, US National Institute for Occupational Safety and Health, 1984, Method 2502.
15 *OSHA Manual of Analytical Methods*, US Department of Labor–Occupational Safety and Health Administration, 1985, Method 52.
16 T. Hayashi and T. Shibamoto, *J. Agric. Food Chem.*, 33 (1985) 1000.
17 T. Hayashi, C. A. Reece and T. Shibamoto, *J. Assoc. Off. Anal. Chem.*, 69 (1986) 101.
18 K. Umano and T. Shibamoto, *J. Agric. Food Chem.*, 35 (1987) 14.
19 A. Yasuhara and T. Shibamoto, *J. Food Sci.* 54 (1984) 1471.
20 A. Yasuhara and T. Shibamoto, *Agric. Biol. Chem.*, 53 (1989) 2273.
21 A. Yasuhara, H. Ito, T. Mizoguchi, T. Uehiro, J. Shindo, R. Shinohara, Y. Shirane, K. Kenmotsu, T. Okumura and K. Imamura, *NIES Mass Spectral Data Base for Environmental Analysis*, Techno Culture Tsukuba, Tsukuba, 2nd ed., 1990, p. 1148.

Journal of Chromatography, 547 (1991) 299–306
Elsevier Science Publishers B.V., Amsterdam

CHROM. 23 280

Gas chromatographic–mass spectrometric separation and characterization of methyl trimethylsilyl monosaccharides obtained from naturally occurring glycosides and carbohydrates

A. DE BETTIGNIES-DUTZ, G. REZNICEK, B. KOPP and J. JURENITSCH*
Institut für Pharmakognosie, Universität Wien, Währinger Strasse 25, A-1090 Vienna (Austria)
(First received November 2nd, 1990; revised manuscript received March 7th, 1991)

ABSTRACT

Gas chromatographic–mass spectrometric (GC–MS) analysis of different methyl trimethylsilyl derivatives of aldohexoses, 6-deoxyaldohexoses and aldopentoses obtained after hydrolysis and trimethylsilylation of permethylated natural glycosides (*e.g.*, cardiac glycosides and saponins) is shown to be a reliable alternative method to the commonly applied analysis via partially methylated alditol acetates. GC and MS reference data for 25 monosaccharide derivatives are given, which allow the determination of the linkages in sugar chains of glycosides and polysaccharides. Mass spectra are characterized by fragmentation patterns, permitting conclusions even if reference substances or data are not available.

INTRODUCTION

In addition to other methods (*e.g.*, NMR techniques) gas chromatography–mass spectrometry (GC–MS) still remains an important method for the determination of the sugar moieties and their specific linkages in naturally occurring glycosides and carbohydrates. Normally the alditol acetates, obtained by hydrolysis of the permethylated compounds, reduction and acetylation, are analysed [1,2]. The preparation of the trimethylsilyl (TMS) derivatives of the hydrolysed products of permethylation so far is uncommon, although this method offers certain advantages. Direct trimethylsilylation without reduction results in two representative GC peaks corresponding to both anomeric sugar configurations with a constant relation of the peak areas [3,4]. Therefore, this method allows a more reliable identification of the particular monosaccharides.

This paper describes the GC–MS characterization of 25 TMS derivatives of monosaccharides after hydrolysis of various permethylated glycosides and oligosaccharides. The resulting reference data and the interpretation of the GC and MS data of the methyl TMS aldoses are given.

0021-9673/91/$03.50

EXPERIMENTAL

Methylation [5]

Approximately 2 mg of glycoside or carbohydrate are dried over phosphorus pentoxide and dissolved in 1 ml of dimethyl sulphoxide (DMSO), then 750 μl of methylsulphinyl carbanion are slowly added and stirred under nitrogen for 1 h at ≤30°C. (Preparation of methylsulphinyl carbanion [6]: 4.2 g of potassium *tert.*-butylate are dissolved in 12.5 ml of DMSO under nitrogen while stirring; the solution turns light yellow and stiffens when stored in the cool; for use, warm to 60°C). Then the solution is frozen in an ice-bath [sodium chloride–ice (1:3), −20°C] and 500 μl of iodomethane are slowly added. After thawing, the solution is stirred for 75 min under nitrogen and then diluted with 10 ml water. The solution is extracted five times with 10 ml of chloroform, the organic layer is washed three times with 10 ml water and dried with sodium sulphate and the chloroform is removed under reduced pressure [7].

Hydrolysis

A 0.5–1.0-mg amount of permethylated glycoside is heated with 0.3 ml of Kiliani mixture [8] (3.5 ml of concentrated acetic acid + 1.0 ml of concentrated hydrochloric acid + 5.5 ml of water) at 100°C for 2 h. The solution is neutralized on a Dowex 44 (OH^-) column (10 × 1 cm I.D.) with water and the eluate is dried with 2-butanone–1-propanol (1:1) under reduced pressure at ≤40°C [3,4].

Trimethylsilylation

The sugar derivatives are dissolved in dry pyridine (100 μl per 0.2 mg of sugar). To 100 μl of pyridine, 10 μl of hexamethyldisilazane and 10 μl trimethylchlorsilane are added [9] and 1 μl of this suspension is injected into the GC–MS system. The solution remains stable for several days (desiccator, 4°C).

GC–MS apparatus and conditions

A Shimadzu QP-1000 fused-silica capillary column (50 m × 0.25 mm I.D.) coated with SE-54-CB, film thickness 0.45 μm, was used, the split (1:10) being opened 0.5 min after injection, with a helium flow-rate of 2.5 ml/min, temperature programming from 100 to 250°C at 3°C/min, injection temperature 250°C, interface temperature 250°C, ion source temperature 170°C, ionization energy 20 eV, vacuum 3×10^{-6} Torr and mass range *m/z* 40–600 in 2 s.

Reagents

Potassium *tert.*-butylate, DMSO (distilled at 190°C with exclusion of water and stored over 4-nm molecular sieve under a nitrogen atmosphere), iodomethane (CH_3I) (distilled at 44°C and stored under nitrogen in the dark) (all of analytical-reagent grade from Merck, Darmstadt, Germany), trimethylchlorosilane and hexamethyldisilazane (Pierce, Rockford, IL, USA), β-D-allose, D-(+)-mannose (Sigma, St. Louis, MO, USA), D-(+)-glucose, D-(+)-galactose, L-(+)-arabinose, L-(−)-xylose, L-(+)-rhamnose (Merck), hyperoside, quercetrin dihydrate, α-sophorose monohydrate, gentiobiose (Roth, Karlsruhe, Germany), 1-(−)-fucose, cellobiose (Schuchardt, Munich, Germany) were used.

The glycosides were isolated in this institute and their structures were determined by fast atom bombardment MS and NMR spectroscopy: convalloside [10], neo-convalloside [10], glucoalliside [11], sarmentogenin-3-β-O-(β-D-6′-deoxyallopyranosido-4′-β-D-xylopyranosido-4″-α-L-rhamnopyranoside) [12], sarmentogenin-3-β-O-(β-D-6′-deoxyallopyranosido-4′-β-D-xylopyranosido-3″-β-D-apiofuranoside) [12], scilliphäosidin-3-O-(α-L-rhamnopyranosido-4′-D-glucopyranosido-3″-β-D-glucopyranoside) [13], 5α-4,5-dihydroscillirosidin-3-O-(α-L-6′-deoxyglucopyranosido-4′-β-D-glucopyranosido-4″-β-D-glucopyranoside) [14], 16β-O-acetylscillarenin-3-O-(β-D-glucopyranosido-4′-β-D-glucopyranoside) [15], scillarenin-3-O-(β-D-glucopyranosido-4′-β-D-glucopyranoside) [15], cyclamin [16], isocyclamin [16], giganteasaponin-1 [17] and -4 [18] and canadensissaponin A and B [19].

RESULTS AND DISCUSSION

After hydrolysis of the previously permethylated glycosides or carbohydrates, 25 different derivatives of the aldoses were trimethylsilylated. It was possible to separate all derivatives with high efficiency by GC using a specially adapted temperature programme. Identical monosaccharide derivatives obtained from different substances always showed identical retention times. Standard conditions during hydrolysis and trimethylsilylation resulted in constant ratios of the peak areas of the corresponding anomers. Therefore, the ratio may be used as additional tool for identification of a specific monosaccharide (Table I). As an example, the total ion current chromatogram of aldose derivatives obtained from giganteasaponin 4 [18] is given in Fig. 1.

Optimization of the MS parameters was necessary to obtain a high response for the most relevant fragment ions: reduction of the ion source temperature to 170°C and consequent use of a 20-eV ionization energy [7] caused a significant depression of the ions at *m/z* 73 and 147 corresponding to the TMS functions, whereas the fragment ions essential for interpretation increased at the same time.

The MS data showed high reproducibility and therefore results regarding the identity of each sugar obtained by GC were confirmed. As differently substituted sugar monomers were represented by distinct MS fragmentations, information about the substitution of sugars that were not examined could also be obtained.

The sample preparation scheme (permethylation, hydrolysis and trimethylsilylation) results in the substitution of the glycosidic hydroxyl group with TMS in each instance. Therefore, the interpretation of the mass spectra is simple and we recommend a step-by-step procedure to define the residues at C-1 to C-4 for all aldoses (hexoses, 6-deoxyhexoses and pentoses) and at C-6 for hexoses. For this purpose, it is sufficient to compare the intensities of some specific fragment series (J, F/G, H and K series, following the nomenclature of Kochetkov and Chizhov [20] and Petersson and Samuelson [21,22]) (Table I). The most intensive fragment in each of these series represents the substituent of a particular carbon atom.

The stepwise interpretation is performed as follows:

C-1: $-$O-TMS in all instances.

C-3: if the ion at *m/z* at 133 is more intense than that at *m/z* 191 (J series), C-3 must be substituted by $-O-CH_3$, whereas if the ion at *m/z* 191 is more intense than that of *m/z* 133, C-3 must be substituted by $-$O-TMS.

C-2: the fragments at *m/z* 88, 146 or 204 (H series) must be compared. A

TABLE I

GC AND MS DATA FOR ALL THE SUGARS ANALYSED

The C atoms with −O-TMS groups are listed; all others are $-O-CH_3$ substituted. FV (%) = ratios of the two GC peak areas of one sugar. Abundances of 0% represent traces less than 0.49%; dashes indicate not detected. Values are the averages of all measurements for each sugar. The fragment series (J, H, F/G and K) are assigned according to refs. 20–22.

Assignment		GC data		Abundance of MS fragments as % of the base peak															
Position of −O-TMS	Sugar	FV (%)	Retention time (min:s)	J series			H series			F/G series			K series						
													Hexoses			6-Deoxy hexoses		Pentoses	
				m/z 75	*m/z* 133	*m/z* 191	*m/z* 88	*m/z* 146	*m/z* 204	*m/z* 101	*m/z* 159	*m/z* 217	*m/z* 102	*m/z* 160	*m/z* 218	*m/z* 72	*m/z* 130	*m/z* 58	*m/z* 116
1	Allose	100	32:32	10	100	–	71	1	–	59	4	–	5	2	–	3	–	–	1
		20	34:10	10	100	–	61	2	–	46	20	–	8	–	–	6	–	–	1
	Glucose	74	31:52	11	100	0	69	2	0	42	6	0	11	1	0	3	1	0	1
		100	32:06	9	100	0	72	2	0	32	13	1	8	2	1	2	1	0	1
	Mannose	100	32:54	8	100	0	70	2	–	30	3	0	4	0	0	1	0	0	0
		10	33:24	5	100	–	47	6	2	22	2	1	3	–	–	1	–	–	–
	Galactose	100	32:46	5	100	0	58	1	0	34	4	0	6	0	–	4	0	2	2
		78	33:26	6	100	–	51	0	–	32	5	0	6	1	0	–	2	1	1
	Rhamnose	100	25:50	14	79	0	100	11	–	14	2	0	3	1	–	14	3	1	2
		10	26:10	11	72	0	100	6	0	55	3	0	1	1	–	17	1	1	1
	Fucose	86	24:34	11	53	–	100	6	0	23	1	–	2	1	–	19	1	2	1
		100	25:08	14	62	–	100	3	–	29	2	–	2	1	–	22	3	4	3
	Arabinose	100	26:44	0	100	1	26	1	1	72	1	1	–	–	–	3	0	6	2
		52	27:26	0	100	2	36	21	2	45	8	7	4	2	2	1	–	7	–
	Xylose	100	24:28	5	100	1	60	3	1	53	2	2	3	1	1	–	1	7	2
		83	24:40	9	100	2	68	2	–	40	3	3	5	1	0	1	1	9	2
	Apiose	–	25:46	100	7	–	–	–	–	20	5	–	–	–	–	3	–	–	–
1,2	Glucose	100	36:24	7	100	2	25	84	1	14	77	0	1	12	1	7	3	0	1
		60	37:30	2	100	2	2	68	3	2	88	14	–	15	3	8	3	0	1
	Rhamnose	100	27:20	–	100	2	17	59	4	0	22	1	0	3	1	7	1	0	1

		45	28:36	0	100	3	11	46	2	0	22	2	2	0	4	6	1	1	1
1,3	Glucose	100	36:40	5	1	82	–	100	–	8	3	3	3	1	1	1	–	–	1
		64	37:38	7	0	100	–	91	–	15	3	1	3	–	1	1	–	–	1
	Xylose	100	29:08	11	6	81	1	100	–	21	7	2	2	1	1	1	1	0	1
		68	30:18	8	4	75	–	100	–	22	6	6	1	1	1	–	3	2	3
1,4	Glucose	100	36:50	3	99	–	74	4	1	8	60	4	2	23	3	1	2	0	2
		76	37:06	1	100	1	50	4	3	7	44	5	1	17	3	1	1	0	1
	6-Deoxy-	25	31:30	6	100	6	95	2	–	8	68	–	2	5	–	–	13	–	3
	allose	100	31:50	1	100	3	80	8	–	4	61	–	–	6	1	–	24	–	–
	6-Deoxy-	100	30:34	2	84	6	100	21	4	4	19	4	0	12	1	0	26	1	2
	glucose	85	31:02	1	100	5	84	14	2	6	29	2	0	4	1	–	27	1	1
	Rhamnose	100	30:50	5	16	6	100	19	2	5	16	6	2	5	1	1	23	–	1
		65	31:10	8	22	5	87	7	3	8	22	5	–	4	6	–	22	–	–
	Xylose	100	29:36	–	68	–	50	10	–	12	100	7	4	96	2	11	1	2	10
		92	29:58	5	83	5	68	5	2	15	100	6	1	81	6	23	4	–	17
1,6	Glucose	100	35:22	8	100	2	58	3	1	25	8	2	3	6	0	2	2	0	1
		90	36:12	7	100	9	57	2	21	24	8	2	3	6	–	0	2	0	1
1,2,3	Glucose	100	41:38	1	14	79	2	11	46	3	18	1	1	2	4	0	0	0	0
		93	43:52	0	11	75	3	5	68	3	15	14	1	1	20	1	2	1	2
	6-Deoxy-	38	34:58	3	6	49	1	31	100	1	7	4	1	2	1	3	2	1	1
	glucose	100	37:54	2	6	100	0	18	97	1	7	3	1	1	1	2	0	–	–
	Arabinose	85	34:36	0	10	65	0	61	100	–	42	5	1	9	1	0	0	1	5
		100	36:50	3	7	64	1	33	100	–	36	6	0	7	1	0	0	–	1
1,2,4	Arabinose	100	33:02	2	20	1	4	31	2	3	6	100	0	0	20	0	1	0	3
		94	33:18	3	20	2	2	36	1	3	10	96	0	1	80	1	1	1	4
1,2,6	Glucose	75	38:46	12	88	5	3	100	4	3	95	6	1	24	1	1	2	0	3
		100	41:20	5	59	1	6	100	4	2	57	0	1	14	3	1	1	1	4
1,3,4	Rhamnose	100	35:00	2	7	87	0	100	68	1	14	3	–	2	1	2	11	0	1
		15	37:02	1	2	60	–	100	10	–	10	2	–	1	1	1	10	–	0

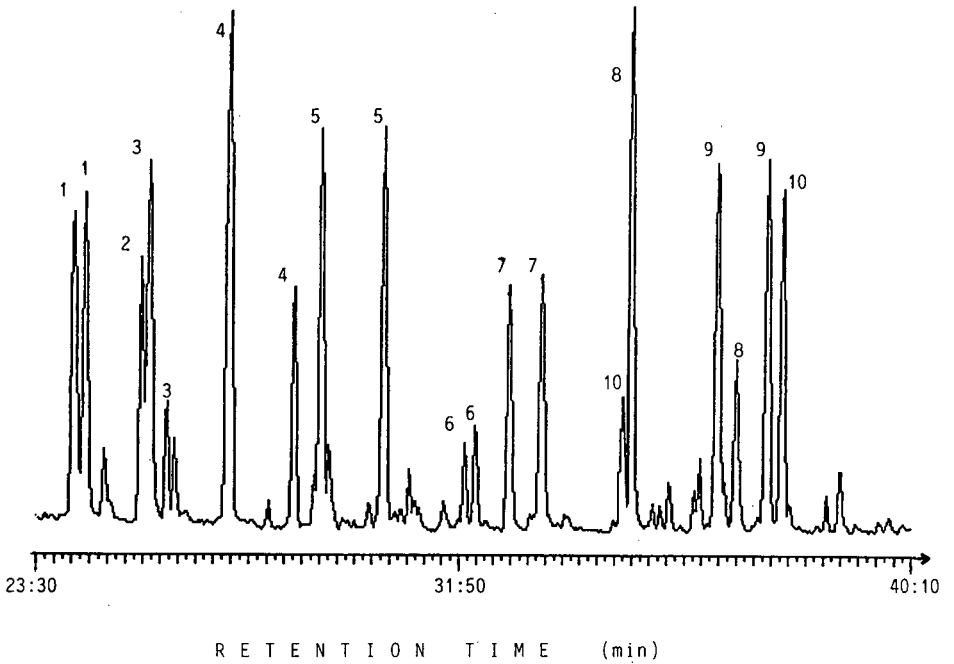

Fig. 1. Total ion chromatogram from 23 min 30 s to 40 min 10 s of partially methylated trimethylsilylated monosaccharides obtained from giganteasaponin 4 [18] on SE-54-CB with temperature programming from 100 to 250°C at 3°C/min. Identified peaks: 1 = 2,3,4,-trimethyl-1-TMS-xylose; 2 = 2,3,3′-trimethyl-1-TMS apiose; 3 = 2,3,4-trimethyl-1-TMS-rhamnose; 4 = 3,4-dimethyl-1,2-TMS-rhamnose; 5 = 2,4-dimethyl-1,3-TMS-xylose; 6 = 2,3,4,6-tetramethyl-1-TMS-glucose; 7 = 2,3,4,6-tetramethyl-1-TMS-galactose; 8 = 2-methyl-1,3,4-TMS-rhamnose; 9 = 2,4,6-trimethyl-1,3-TMS-glucose; 10 = 4-methyl-1,2,3-TMS-6-deoxyglucose.

dominant ion at *m/z* 88 represents $-O\text{-}CH_3$ and at *m/z* 204 −O-TMS groups at C-2 and C-3, respectively. A most abundant ion at *m/z* 146 shows one $-O\text{-}CH_3$ and one −O-TMS at these positions; considering the apparent substituent at C-3, one can determine the substituent at C-2.

C-4: the fragments at *m/z* 101, 159 or 217 (F/G series) must be compared. A dominant ion at *m/z* 101 represents $-O\text{-}CH_3$ and at *m/z* 217 −O-TMS groups on C-2 and C-4, respectively. A most abundant ion at *m/z* 159 shows one $-O\text{-}CH_3$ and one −O-TMS at these positions; considering the apparent substituent at C-2, one can determine the substituent at C-4.

C-6: depending on the substitution pattern of C-4 and C-6 of hexoses (two $-O\text{-}CH_3$ or one $-O\text{-}CH_3$ + one −O-TMS or two −O-TMS groups), the most intensive ion of a series of three must be considered (K series): *m/z* 102 or 160 or 218. As the substituent at C-4 is known, one can determine the substituent at C-6.

With 6-deoxyhexoses the K series (*m/z* 72 for C-4 $-O\text{-}CH_3$ or *m/z* 130 for C-4 −O-TMS) gives further confirmation of the substituent at C-4.

In addition, all results were confirmed by analysis of permethylated (the dominant J series peak is at *m/z* 75) and pertrimethylsilylated sugars which showed analogous fragmentation patterns [7].

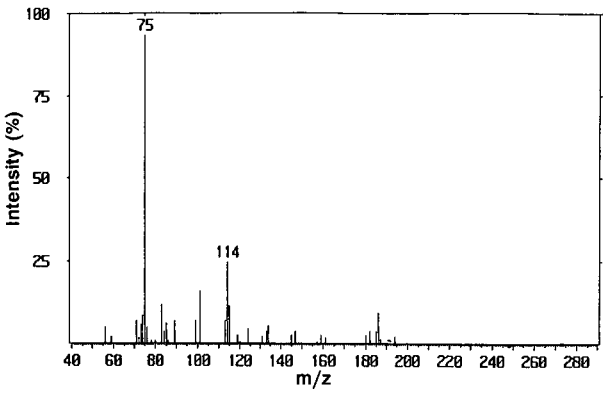

Fig. 2. Mass spectrum of the artifact representing 2,3,3′-trimethyl-1-TMS-apiofuranoside after GC. For details, see text.

It should be stated that the given procedure is only suitable for pyranosides, but we found all sugars investigated to be pyranoses; furanosides are recognized according to the literature [20–22] by a base peak in the F/G series and very weak H series ions (maximum *ca.* 10%). The occasional occurrence of genuine partially methylated sugars in natural products must also be taken into consideration: a parallel analysis without prior methylation (only hydrolysis and pertrimethylsilylation) gives the respective information [3,4]. The differentiation of hexoses, 6-deoxyhexoses and pentoses by comparison of the intensities of the seven K series ions (for pentoses *m/z* 58 if C-4 $-O-CH_3$ or *m/z* 116 if C-4 $-O$-TMS) was not possible because five sugars (3-methyl-1,2,4-TMS-arabinose, 4-methyl-1,2,3-TMS-arabinose, 4,6-dimethyl-1,2,3-TMS-glucose, 2,4-dimethyl-1,3-TMS-xylose and 2,3-dimethyl-1,4-TMS-xylose) gave contradictory results.

As an exceptional case the 2,3,3′-O-trimethyl-1-O-TMS-apiofuranoside should be mentioned; this derivative is destroyed by acid hydrolysis, but always appears as the same reproducible artifact represented by a GC peak at 25 min 46 s. The corresponding mass spectrum shows fragments at *m/z* 75 (base peak), 114 (23%), 101 (20%), 115 (6%) and 83 (5%) (Fig. 2).

However, it should be pointed out that the MS results must be evaluated very carefully. The few exceptions found during these investigations show that the use of MS data as the only method for identification is not always reliable. On the other hand, it is definitely possible to determine sugars and their substitution patterns as long as reference data for retention times, peak area relationships and MS fragmentations are available.

ACKNOWLEDGEMENTS

We thank M. Daxner and Ch. Klostermann for preliminary studies (M.Ph. Thesis, University of Vienna, 1983). The GC–MS apparatus was financed by support from the Austrian Bundesministerium für Wissenschaft und Forschung.

REFERENCES

1 S. C. Churms, *J. Chromatogr.*, 500 (1990) 555.
2 K. B. Hicks, *Adv. Carbohydr. Chem.*, 46 (1988) 17.
3 B. Kopp, J. Jurenitsch and W. Kubelka, *J. Chromatogr.*, 210 (1981) 291.
4 J. Jurenitsch, B. Kopp, I. Gabler-Kolacsek and W. Kubelka, *J. Chromatogr.*, 210 (1981) 337.
5 S. Hakamori, *J. Biochem. (Tokyo)*, 55 (1964) 205.
6 J. Finne, T. Krusius and H. Rauvala, *Carbohydr. Res.*, 80 (1980) 336.
7 A. de Bettignies-Dutz, *M.Ph. Thesis,* University of Vienna, 1989.
8 H. Kiliani, *Ber. Dtsch. Chem. Ges.*, 63 (1930) 2866.
9 C. Sweeley, R. Bentley, M. Makita and W. Wells, *J. Am. Chem. Soc.*, 85 (1963) 2497.
10 B. Kopp and W. Kubelka, *Planta Med.*, 45 (1982) 195.
11 J. B.-S. Park, W. Kubelka and J. Jentzs, *Sci. Pharm.*, 57 (1989) 445.
12 U. Ghannamy, B. Kopp, W. Robien and W. Kubelka, *Planta Med.*, (1987) 121.
13 L. Krenn, M. Jambritz and B. Kopp, *Planta Med.*, (1988) 191.
14 A. Hoyer, *M.Ph. Thesis*, University of Vienna, 1990.
15 R. Terkola, *M.Ph. Thesis*, University of Vienna, 1990.
16 G. Reznicek, J. Jurenitsch, W. Robien and W. Kubelka, *Phytochemistry*, 28 (1989) 825.
17 G. Reznicek, J. Jurenitsch, G. Michl and E. Haslinger, *Tetrahedron Lett.*, 30 (1989) 4097.
18 G. Reznicek, J. Jurenitsch, W. Kubelka, G. Michl, S. Korhammer and E. Haslinger, *Liebigs Ann. Chem.*, (1990) 989.
19 G. Reznicek, J. Jurenitsch, W. Kubelka, S. Korhammer, E. Haslinger and K. Hiller, *Planta Med.*, 56 (1990) 554.
20 N. K. Kochetkov and O. S. Chizhov, *Adv. Carbohyd. Chem.*, 21 (1966) 39.
21 G. Petersson and O. Samuelson, *Sven. Papperstidn*, 71 (1968) 77.
22 G. Petersson and O. Samuelson, *Sven. Papperstidn.*, 71 (1968) 731.

Journal of Chromatography, 547 (1991) 307–314
Elsevier Science Publishers B.V., Amsterdam

CHROM. 23 224

Derivatization and gas chromatographic determination of hydroxycarboxylic acids treated with chloroformates[a]

PETR HUŠEK
Institute of Endocrinology, Národní 8, 116 94 Prague 1 (Czechoslovakia)
(First received November 27th, 1990; revised manuscript received February 18th, 1991)

ABSTRACT

Hydroxymonocarboxylic acids with a hydroxyl group in position 2, 3 or 4 can be converted into derivatives amenable to capillary gas chromatography by treatment with alkyl chloroformates instantaneously. The carboxylic group is esterified to the corresponding alkyl ester, and the hydroxyl group adjacent to the carboxylic group is converted to the alkoxycarbonyl ether. Hydroxyl groups in other positions remain free. The yield of 2-hydroxyl group alkylation proved to be strongly influenced by the presence of the corresponding alkyl alcohol in the reaction medium and optimization of the reaction conditions was necessary.

INTRODUCTION

Hydroxymonocarboxylic acids (HA) and dicarboxylic acids are the predominant excretion products among the urinary aliphatic organic acids. They originate mainly from ketogenesis and from the metabolism of branched-chain aliphatic amino acids [1] and are mostly determined together with other urinary organic acids to scan metabolic profiling. Because of the polyfunctional nature of the pattern, reagents of general use are required to prepare the sample for high-resolution capillary gas chromatographic (cGC) analysis. Almost exclusively silylating reagents are the choice, as they are able to convert groups with active hydrogen into trimethylsilyl esters, ethers and amides at room or elevated temperature in 30–60 min [2–5]. This chemical approach is preferred even for the treatment of HA as a group or individual components [6–9]. As an alternative, methylation of the acids with diazomethane is carried out [1,10,11], which is easy to perform but results in various problems such as double peaks and side-product formation. Two-step procedures, using an alcohol (or diazomethane) for esterification of the carboxylic groups and another reagent for treatment of the hydroxyl group, have been elaborated, *e.g.*, for analysis of optical isomers in form of isopropylurethane isopropyl esters [12] or for purposes of electron-capture detection after converting HA into pentafluorobenzoyl [13] or heptafluorobutyryl methyl esters [14].

[a] Dedicated to Luboslav Stárka, Head of the Institute of Endocrinology, on the occasion of his 60th birthday.

0021-9673/91/$03.50

High-performance liquid chromatography (HPLC) has also been applied to the determination of HA [15], involving precolumn derivatization of the carboxylic group with 2-nitrophenylhydrazine to form a highly absorbing compound, with a detection limit down to picomoles in the visible range of the spectrum. This procedure was used successfully for monitoring HA and dicarboxylic acids in urine samples after two-step extraction of the derivatives with diethyl ether. The derivatization step, however, required heating of the sample at 60°C for 30 min so that no time gain in comparison with silylation procedure and cGC, which gives a more efficient separation, was achieved.

In this work we examined the possibility of whether the reaction conditions used for the esterification of carboxylic groups with chloroformates [16] would be suitable even for the derivatization of HA. It was found that optimization of the reaction conditions was a complex problem, as the derivatization of the hydroxyl group was far from smooth, being markedly influenced by the necessary presence of alcohol in the reaction medium. The results of this study show that carboxylic acids with hydroxyl groups in the aliphatic chain can be determined satisfactorily and instantaneously by cGC after a chloroformate treatment.

EXPERIMENTAL

Apparatus

A Hewlett-Packard HP 5890 gas chromatograph with a flame ionization detector and a Model 3392A integrator was employed. The injector and detector temperatures were 200 and 250°C, respectively. The analysis was carried out on a 10 m × 0.25 mm I.D. CP-Sil 19 CB fused-silica capillary column with a 0.2-μm thick layer of OV-1701 (Chrompack, Middelburg, Netherlands) in the temperature range 50–200°C programmed at 15°C/min. Helium was used as the carrier gas with a head pressure of 70 kPa.

Chemicals

Methyl and ethyl chloroformate (MCF, ECF) and the organic solvents, *i.e.*, pyridine, acetonitrile, chloroform, methanol and ethanol, were obtained from Fluka (Buchs, Switzerland). HA were obtained from Sigma (St. Louis, MO, USA) and an equimolar mixture of (1) 2-hydroxyacetic (glycolic), (2) 2-hydroxypropionic (lactic), (3) 2-hydroxybutyric (HB), (4) 2-hydroxyisovaleric (HIV), (5) 2-hydroxyvaleric (HV), (6) 2-hydroxyisocaproic (HIC), (7) 2-hydroxycaproic (HC), (8) 3-hydroxybutyric (3-HB) and (9) 4-hydroxybutyric acid (4-HB) was prepared in water (25 μmol/ml).

Procedures

A 2-μl volume of the aqueous HA solution was covered with 100 μl of a medium composed of acetonitrile, alcohol (methanol or ethanol), water and pyridine in various proportions and 5 μl of the corresponding chloroformate were added. Subsequently, 100 μl of chloroform were added and, after brief shaking the tube by striking it against a pad for about 5 s, an aliquot of the chloroform layer was injected into the capillary column.

Optimum compositions of the reaction media were as follows: (a) for the formation of O-methoxycarbonyl (MOC) methyl esters, acetonitrile–pyridine–methanol

(22:2:1 or, in the presence of 10% of water, 7:1:1), 100 μl of solvent treated with 5 μl of MCF; (b) for the formation of O-ethoxycarbonyl (EOC) ethyl esters, acetonitrile–ethanol–water–pyridine (5:2:2:1 or 4:3:2:1), 100 μl of solvent treated with 7 μl of ECF; and (c) for the formation of O-MOC (EOC) ethers MOC (EOC) esters ("mixed anhydrides"), acetone–acetonitrile–water (6:3:1, containing 4% of pyridine in), 100 μl of solvent treated with 5 μl of the corresponding chloroformate.

RESULTS AND DISCUSSION

Earlier studies with amino acids [17] and biogenic amines treated with chloroformates [18] and our recent examinations with the same kind of compounds [19–20] revealed that hydroxyl groups not neighbouring the carboxylic group are not derivatized by the action of the reagents mentioned. In a preceding paper [16], conditions for the rapid esterification of carboxylic groups with alkyl chloroformates were given. In view of these findings, the treatment of HA with this kind of reagent can represent a complex problem.

Our first experiments with the derivatization of HA under conditions close to those for carboxylic acids showed that four possible derivatives with 2-hydroxy acids are formed:

Alkoxycarbonyl esters:

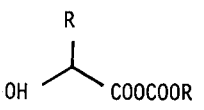

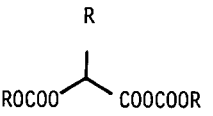

alkyl esters:

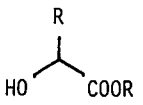

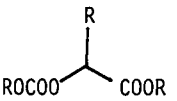

Because with a well deactivated capillary column all of the presented forms can be eluted, one will obtain a blend of peaks and a complicated baseline.

The aim of the subsequent experiments was to find reaction conditions under which the formation of esterified alkyl esters, the prevailing and desired form, is promoted.

The experiments revealed that the presence of an alcohol in the reaction medium, necessary for esterification of the carboxylic group, prevented the effective esterification of the 2-hydroxyl group. This is apparent from Fig. 1, where the treatment with chloroformates was done in alcohol alone. The amount of side-products with the shortest retention, *i.e.*, alkyl esters with a free hydroxyl group, is highest under these conditions and higher with methanol than with ethanol. With ethanol, on the other hand, the decarboxylation of the alkoxycarbonyl esters (mixed anhydrides) does not proceed smoothly and this results in a complicated baseline at the rear of the chromatogram.

In a second series of experiments, the alcohol was partially replaced with acetonitrile, water or a mixture of the two (Fig. 2). Comparing the chromatograms, it can be seen that the methanol–MCF and ethanol–ECF systems behave differently. In the former system the use of water in combination with methanol is clearly disadvanta-

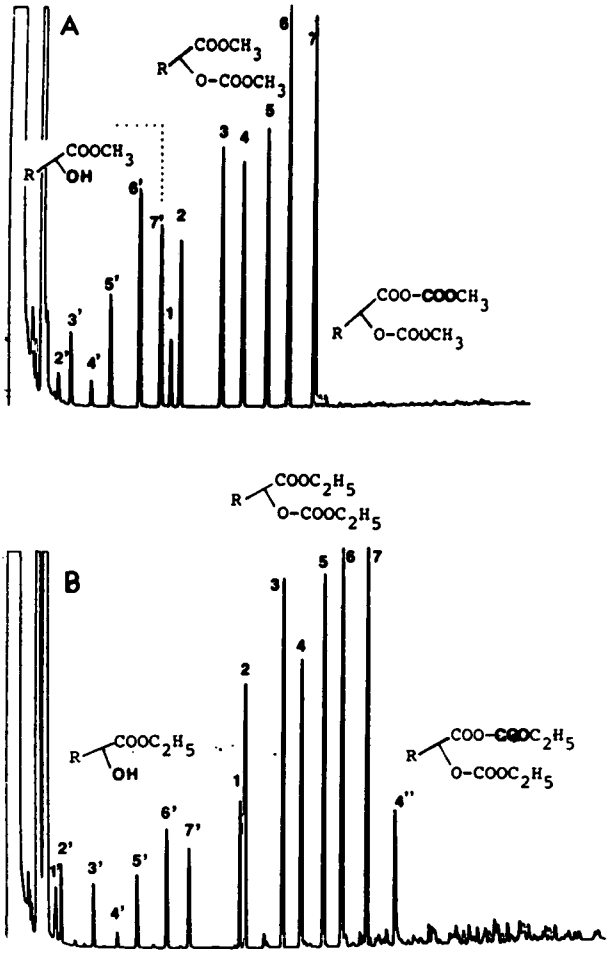

Fig. 1. HA 1–7 analysed after treatment with (A) MCF in methanol and (B) ECF in ethanol in the presence of 8% (v/v) of pyridine in the medium. Primed numbers represent side-products with a free hydroxyl group and the double-primed number (and baseline impurities) are non-decarboxylated side-products, *i.e.*, alkoxycarbonyl esters.

geous: the amount of the volatile side-products does not decline (dotted line) and the dashed line shows a decrease in yield of straight-chain HA in comparison with the branched HIV acid, which reacts differently to the others. The same phenomenon, *i.e.*, decrease in the yield of unbranched HA, can be observed to a lesser extent with ECF in the ethanol–water system; however, the difference between water and acetonitrile is not as pronounced as in the former instance; this concerns even the formation of the side-products with a free hydroxyl group.

In order to suppress the formation of products with a free 2-hydroxyl group, it was clear that the amount of alcohol (methanol more than ethanol) should be held as low as possible. Moreover, in accordance with the previous findings [17–20], hydroxyl

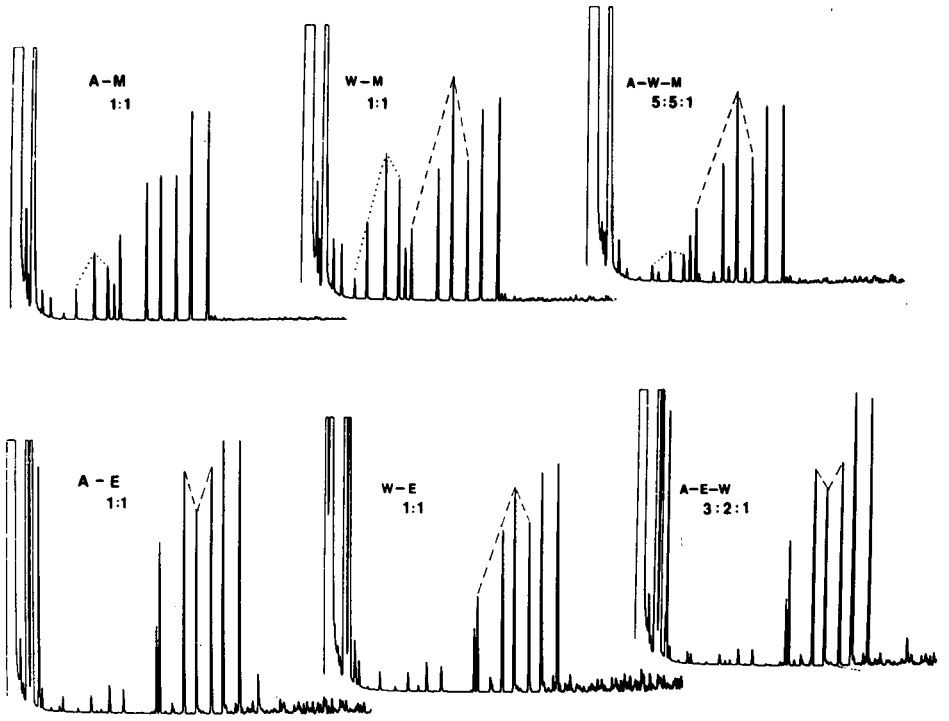

Fig. 2. Influence of composition of the reaction medium on the derivatization of HA 1–7 with (top) MCF and (bottom) ECF. Pyridine (P) (8 vol.%) was added to each medium. A = Acetonitrile; M = methanol; E = ethanol; W = water. Side-products with a free hydroxyl group are marked with the dotted line and the decline of unbranched HA in comparison with HIV acid is marked by the dashed line.

groups in positions 3 and 4 are not derivatized, *i.e.*, 3-HB and 4-HB acids are eluted first and do not form side products. They were therefore used as "internal standards" in a further study dealing with influence of water on the derivatization yields (Figs. 3 and 4).

From both figures it appears that an increase in the water content in the medium has a deteriorating effect on the yield of straight-chain HA; the decline is marked by the dotted line and even by the dashed line when compared with HIV acid. At the same time, the degradation of the baseline, *i.e.*, the amount of non-decarboxylated products, increases. The composition of the medium designated D is close to that used for esterification of fatty acids under aqueous conditions [16]; being optimum for fatty acids is far from optimum for HA. In all these studies, 100 μl of the medium (containing 8% pyridine) were treated with 5 μl of MCF or ECF.

Finally, as a result of numerous experiments, the most favourable reaction conditions were found under which the formation of O-alkoxycarbonyl alkyl esters is promoted and the amount of side-products is suppressed. The optimum reaction conditions are given under Experimental and the corresponding chromatograms are shown in Fig. 5. With MCF, exclusion of water from the medium afforded the best results, but a water content up to 10 vol% was found to be acceptable. With ECF the

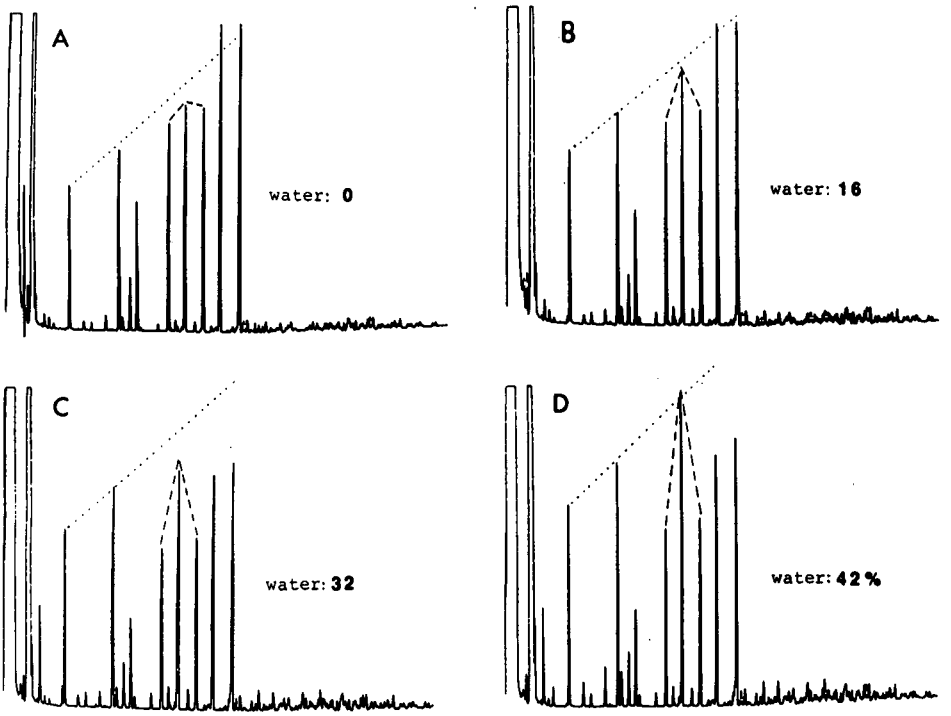

Fig. 3. Influence of the presence of water in the reaction medium on HA 1–9 derivative formation with MCF. Acetonitrile in the reaction medium (with 8% of pyridine and 4% of methanol) was partially replaced with water as indicated.

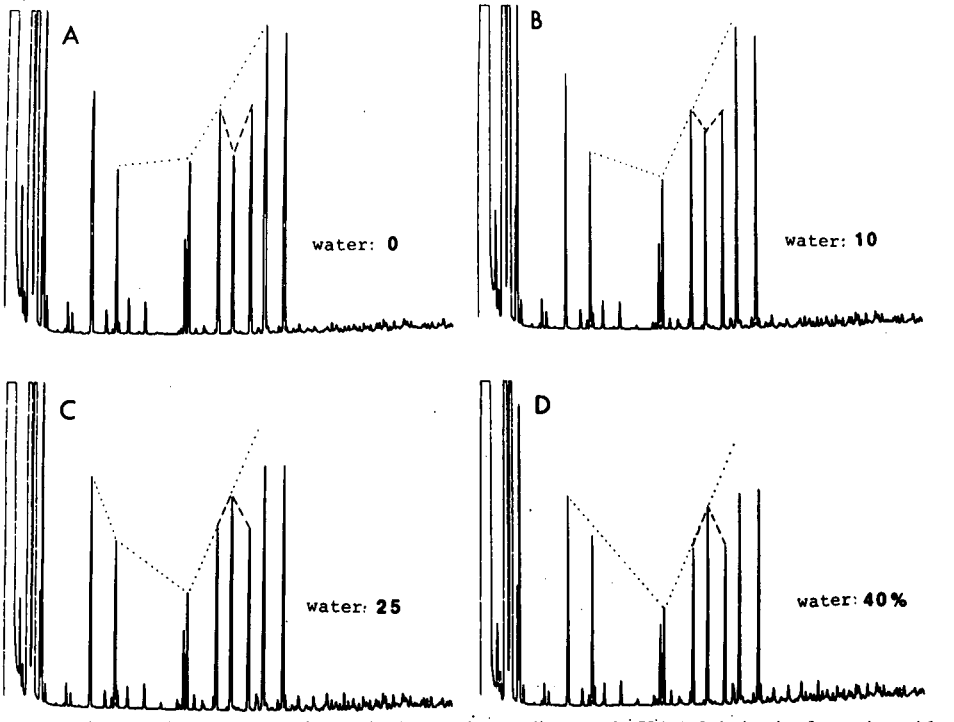

Fig. 4. Influence of the presence of water in the reaction medium on the HA 1–9 derivative formation with ECF. Acetonitrile in the reaction medium (1:1 with ethanol and containing 8% of pyridine) was partially replaced with water as indicated.

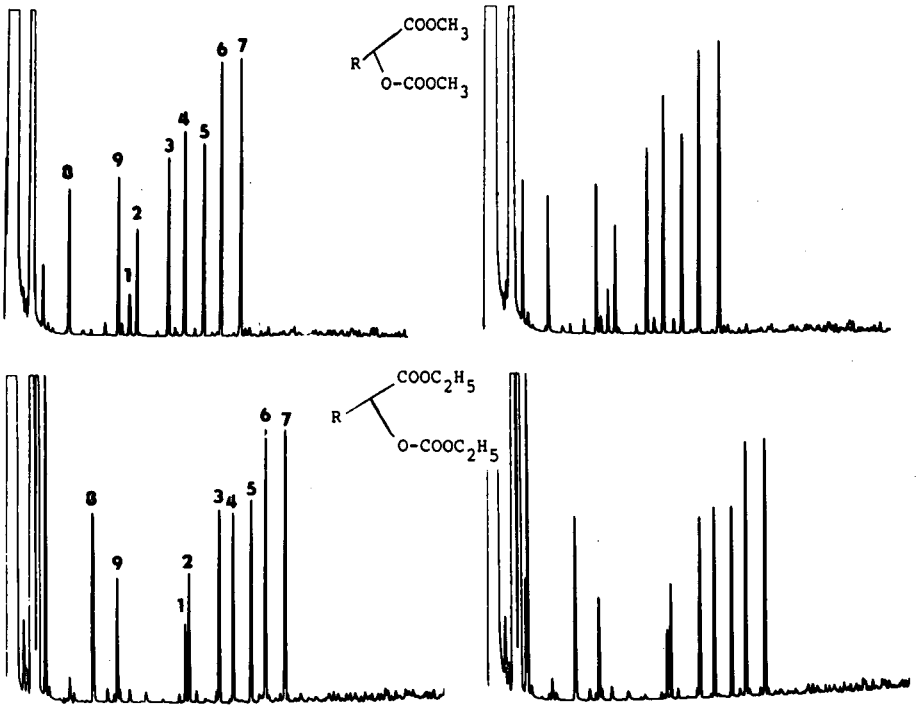

Fig. 5. HA 1–9 analysed as O-MOC methyl esters after treatment with MCF in A–P–M (22:2:1) (top left) or in A–P–M–W (7:1:1:1) (top right) and as O-EOC ethyl esters after treatment with ECF in A–E–W–P (5:2:2:1) (bottom left) or in the same solvent with ratios 4:3:2:1 (bottom right). For abbreviations, see Fig. 2.

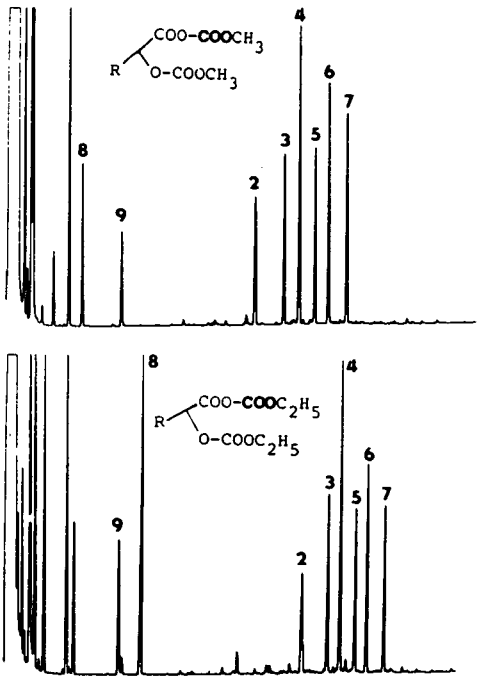

Fig. 6. HA 1–9 analysed as (top) O-MOC ethers MOC esters or (bottom) O-EOC ethers EOC esters after treatment with the corresponding chloroformate under optimum conditions for their formation. The 4-HB acid is analysed as the methyl or ethyl ester, respectively.

pyridine content in the medium was increased to 10% and the amount of reagent to 7 μl; under these conditions a water content of 20% was tolerable and two different mixing ratios gave virtually identical results.

Similarly to the formation of "mixed anhydrides" with fatty acids [16], it was possible to maintain and determine HA in the form of non-decarboxylated products, the alkoxycarbonyl ethers/esters (Fig. 6). For this purpose, the polarity of the medium was diminished by addition of acetone and the amount of pyridine was lowered below that of the reagent. However, the yield, compared with HIV acid, was not quantitative. As the 4-HB acid does not alter its retention time in comparison with the chromatogram in Fig. 5, it is measured as the alkyl ester, *i.e.*, it decarboxylates immediately even under reaction conditions convenient for the formation of the alkoxycarbonyl esters. Both 3-HB and 4-HB acids have the hydroxyl group underivatized.

In conclusion, if chloroformates are to be used as general-purpose reagents, *e.g.*, for metabolic profiling of urinary organic acids, the dissimilar reaction conditions for treatment with MCF and ECF on the one hand and for fatty acids and hydroxy acids on the other have to be taken in account. Attempts to unify the conditions in order to use the procedure in a broader range of applications are under study.

REFERENCES

1 H. M. Liebich and C. Först, *J. Chromatogr.*, 309 (1984) 225.
2 P. Englmaier, *J. Chromatogr.*, 194 (1980) 33.
3 T. Niwa, *J. Chromatogr.*, 379 (1986) 313.
4 M. F. Lefevere, B. J. Verhaeghe, D. H. Declerck, J. F. van Bocxlaer, A. P. De Leenheer and R. M. De Sagher, *J. Chromatogr. Sci.*, 27 (1989) 23.
5 G. Hoffmann, S. Aramaki, E. Blum-Hoffmann, W. L. Nyhan and L. Sweetman, *Clin. Chem.*, 35 (1989) 587.
6 T. Hyppanen, E. Sjöström and T. Vuorinen, *J. Chromatogr.*, 261 (1983) 320.
7 R. Alen, K. Niemela and E. Sjöström, *J. Chromatogr.*, 301 (1984) 273.
8 W. Yu, T. Kuhara, Y. Inoue, I. Matsumoto, R. Iwasaki and S. Morimoto, *Clin. Chim. Acta*, 188 (1990) 161.
9 S. Nissen, M. Van Koevering and D. Webb, *Anal. Biochem.*, 188 (1990) 17.
10 H. M. Liebich, *J. Chromatogr.*, 379 (1986) 347.
11 H. M. Liebich and C. Först, *J. Chromatogr.*, 525 (1990) 1.
12 W. A. Konig, I. Benecke and S. Sievers, *J. Chromatogr.*, 238 (1982) 427.
13 D. V. Crabtree, A. J. Adler and G. J. Handelman, *J. Chromatogr.*, 466 (1989) 251.
14 M. Scheutwinkel-Reich and H. J. Stan, *Fresenius Z. Anal. Chem.*, 303 (1980) 126.
15 H. Miwa, M. Yamamoto and T. Asano, *Anal. Biochem.*, 185 (1990) 17.
16 P. Hušek, J. A. Rijks, P. A. Leclerg and C. A. Cramers, *J. High Resolut. Chromatogr.*, 13 (1990) 633.
17 M. Makita, S. Yamamoto and S. Kiyama, *J. Chromatogr.*, 237 (1982) 279.
18 O. Gyllenhaal, L. Johansson and J. Vessman, *J. Chromatogr.*, 190 (1980) 347.
19 P. Hušek, *J. Chromatogr.*, 552 (1991) in press.
20 P. Hušek, Z. H. Huang and C. C. Sweeley, *Anal. Chim. Acta*, submitted for publication.

Journal of Chromatography, 547 (1991) 315–323
Elsevier Science Publishers B.V., Amsterdam

CHROM. 23 282

Determination of resin and fatty acids in sediments near pulp mill locations

HING-BIU LEE* and THOMAS E. PEART
Research and Applications Branch, National Water Research Institute, Canada Centre for Inland Waters, 867 Lakeshore Road, P.O. Box 5050, Burlington, Ontario L7R 4A6 (Canada)
(First received December 10th, 1990; revised manuscript received February 28th, 1991)

ABSTRACT

A gas chromatographic method for the determination of resin and fatty acids in sediments is described. In this procedure, the sediment sample was air-dried and soxhlet-extracted with a mixture of acetone—methanol (88:12, v/v) in the presence of hydrochloric acid. The acids extracted were converted into their pentafluorobenzyl esters and were then cleaned up on a deactivated silica gel column. Final analysis was performed on either a DB-17 or a DB-5 capillary column with electron-capture detection. Quantitative recovery was obtained from fortified sediments for all acids except palustric, neoabietic and levopimaric acids. The detection limit of all acids in this method was 0.1 μg/g based on 1 g of sample. This procedure has been successfully applied to the monitoring of resin and fatty acids in sediment samples collected in the vicinity of several Canadian pulp mill locations.

INTRODUCTION

Pulp and paper mill effluents contain a large number of environmental contaminants. During the past twenty years, extensive research has been carried out in the identification of those toxic components present in various pulp mill discharges [1–5]. In general, diterpene resin acids (Fig. 1), fatty acids, diterpene alcohols and other neutral lignin degradation products can be found in nearly all effluents [3,4]. In addition, chlorinated phenols, guaiacols, catechols, vanillins and resin acids as well as other volatile chlorinated acids and aliphatics are also present in chlorobleaching kraft mill effluents [6–8]. Resin acids, which are commonly found in the debarker and woodroom effluents from pulp mills, have been identified as the major contributor to the toxicity in effluents to fish [9–11]. The levels of these acids are generally higher if there is no secondary waste treatment on the effluents. In some cases, the effluents are acutely toxic to fish if undiluted. Therefore, chemical analysis for resin and fatty acids (RFAs) has been one of the core components in the Canadian pulp mill water quality monitoring program.

Several methods have been developed and used in the determination of RFAs in effluents [12,13]. They involved extraction of the acids either by solvent or by a ion-exchange column then followed by the flame ionization detection (FID) of the methyl or ethyl derivative of the acids. Very little information regarding the levels of

0021-9673/91/$03.50

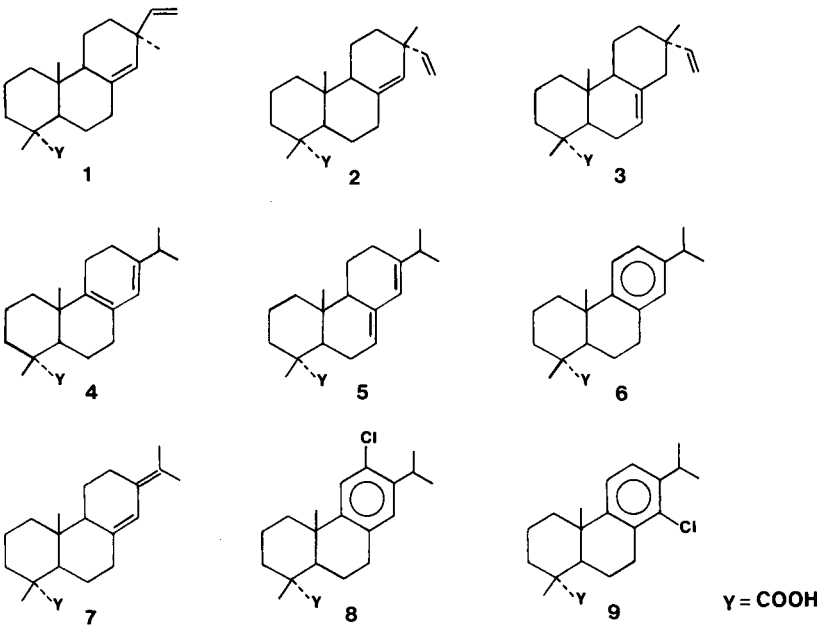

Fig. 1. Molecular structures for selected resin acids. Acids: 1 = pimaric; 2 = sandaracopimaric; 3 = isopimaric; 4 = palustric; 5 = abietic; 6 = dehydroabietic; 7 = neoabietic; 8 = 12-chlorodehydroabietic; 9 = 14-chlorodehydroabietic. Dichlorodehydroabietic acid has chlorine substitutions at both 12 and 14 positions.

RFAs in sediments at pulp mill locations is available, and few methods have been reported in the literature for the determination of RFAs in such samples. In one paper describing the distribution of dehydroabietic acid in sediments adjacent to a kraft pulp and paper mill, the resin acid was soxhlet-extracted by acetone, methylated and analyzed by gas chromatography (GC)–FID with a packed column [14].

In the past two years, we have been working on new and improved methods for the analysis of RFAs in various matrices. Our approach involves the conversion of the acids into their pentafluorobenzyl (PFB) esters. With these esters, an electron-capture detection (ECD) instead of FID is used for analysis. In addition, negative-ion chemical ionization mass spectrometry (NICI-MS) can be applied to the quantitation and positive identification of RFAs. This new approach has been succesfully applied to the determination of RFAs in many final effluents [15]. Based on the same derivatization and detection technique, a method for the quantitative analysis of RFAs in sediment samples is presented. Factors affecting the extraction recoveries of RFA in sediments are also discussed.

EXPERIMENTAL

Reagents and chemicals

All solvents used were of distilled-in-glass grade supplied by Burdick and Jackson (Muskegon, MI, USA).

Resin acids were purchased from Helix-Biotech Scientific (Vancouver, Canada)

and used without further purification. All fatty acids and pentafluorobenzyl bromide (PFBBr) were acquired from either Aldrich (Milwaukee, WI, USA) or Sigma (St. Louis, MO, USA).

Stock solutions of individual RFAs at 1000 μg/ml were prepared in acetone and kept at −20°C in crimped top vials. Spiking solutions of the mixed RFAs at 50 μg/ml in acetone were kept at 4°C in the dark. Because of the gradual decomposition of neoabietic acid, a new stock solution of this acid and fresh RFA mixtures were made up once every two months.

A PFBBr solution was prepared by dissolving 1 g of the reagent in 20 ml of acetone with a water content of 0.2% or less by volume and kept at −20°C until use. A 30% (w/v) potassium carbonate solution was made by dissolving 3 g of the anhydrous base in 10 ml of water. Anydrous sodium sulfate was heated at 600°C overnight before use.

Sampling of sediment samples

Grab river sediments were collected and excess water was decanted off. The samples were kept in 500-ml wide-mouth, brown, screw-capped bottles with aluminium foil liners and frozen at −20°C in the dark until analysis.

Fortified sediment samples for the recovery runs were prepared by spiking known amounts of RFAs to a wet sediment which was known to have negligible amounts of native resin acids and low levels of fatty acids. The sediment was then thoroughly mixed, air-dried and extracted as described below.

Extraction, derivatization and clean-up

The wet sediment was homogenized before a 5.00-g subsample was air-dried in a fumehood at room temperature. Another sample was taken for moisture content determination. An aliquot of 25 μg of tricosanoic acid in 100 μl of acetone was evenly applied to the sediment, and the sample was quantitatively transferred to the top of a 5-cm Celite 545 layer in a glass thimble with a coarse fritted disc. The sediment was then soxhlet-extracted for 7 h with 300 ml of methanol–acetone (12:88, v/v) in the presence of 100 μl of concentrated hydrochloric acid. The sample extract was evaporated to dryness with a rotary evaporator using a 40°C bath and redissolved in three 2-ml aliquots of acetone. This acetone extract was passed through a column made up of 3 cm of Celite in a disposable Pasteur pipet with a glasswool plug for the removal of particulate matters. The extract was then adjusted to a volume of 10.0 ml in a calibrated centrifuge tube.

A 2-ml volume of the filtered acetone extract was transferred to a centrifuge tube and evaporated to 1 ml. A 100-μl volume of 30% K_2CO_3 and 250 μl of PFBBr solution were added and the mixture was heated at 60°C for 2 h. After reaction, the acetone was evaporated and the residue redissolved in hexane. The derivatized products were then cleaned up by passing the above hexane solution through a 5.00-g 5% deactivated silica gel column, as described for the effluent samples [15]. The final volume was adjusted to 2.0 ml in isooctane. Depending on the concentrations of RFAs in the sample, further dilution or concentration of this extract could be required.

Chromatographic analyses

Sediment extracts were analyzed with a Hewlett-Packard 5880A gas chromatograph equipped with an electron-capture detector and a 30 m × 0.25 mm I.D. fused-silica DB-17 or a DB-5 capillary column (J&W Scientific). The chromatographic conditions used were as follows: the initial temperature of the column oven was held at 70°C for 0.75 min and then programmed to 160°C at 30°C/min. It was further raised to 290°C at 2°C/min. Injector and detector temperatures were 250 and 300°C, respectively. Helium was used as carrier gas and the column head pressure was 105 kPa. Samples of 2 μl were injected in the splitless mode with a valve time of 0.75 min. Known amounts of RFAs were directly derivatized and cleaned up as described above alongside the sediment samples and used as external standards for the quantitation of the acids.

Confirmation of peak identity was achieved by electron-impact (EI) MS in the full-scan mode [15]. For samples of low RFA concentrations, selected-ion monitoring (SIM) using NICI-MS as described before [15] can be applied. In this case, the characteristic $[M-181]^-$ ions monitored were *m/z* 199 for lauric acid, *m/z* 227 for myristic acid, *m/z* 255 for palmitic acid, *m/z* 283 for stearic acid, *m/z* 281 for oleic acid, *m/z* 279 for linoleic acid, *m/z* 277 for linolenic acid, *m/z* 311 for eicosanoic acid, *m/z* 339 for behenic acid, *m/z* 299 for dehydroabietic acid, *m/z* 333 for chlorodehydroabietic acids, *m/z* 367 for dichlorodehydroabietic acid and *m/z* 301 for the other resin acids.

RESULTS AND DISCUSSION

Comparison of the PFB and methyl esters of RFAs

In the past, nearly all information regarding the levels of RFAs in pulp mill effluents and related samples was obtained by GC analysis of their methyl esters using a flame ionization detector. Although this technique is applicable in many cases, it lacks the sensitivity required for the monitoring of RFAs in final effluents and other environmental samples collected further downstream from the mills. This problem can be solved by the conversion of the RFAs into their PFB ester derivatives [15] so that the more sensitive electron-capture detector can be used in the final analysis. Aside from an over 100-fold enhancement in sensitivity, the PFB esters of RFAs have the following advantages over the corresponding methyl ester derivatives. (1) Formation of methyl esters requires diazomethane, a toxic, carcinogenic, explosive and unstable reagent which has to be generated each time before use. For the PFB esters, a less hazardous and readily available reagent, PFBBr, which does not have the other undesirable properties, is used. (2) Methyl esters of some resin acids are unstable in hydrocarbon and chlorinated solvents for an extended period of time [13]. In contrast, the PFB esters are stable for months in hydrocarbon solvents so that the derivatized extract can be stored for a long time for further analysis or confirmation if necessary. (3) The presence of methyl esters of RFAs has been reported in pulp mill effluent samples [4]. Thus with the methyl ester method, the RFA results would have a high bias unless the native methyl esters are removed from the effluent extract before methylation of the free acids takes place. However, this partitioning step is unnecessary in the PFB ester procedure. (4) Since the characteristic $[M-181]^-$ ion is the base peak for the PFB ester of every RFA under the NICI condition, RFA can be quantitated and positively identified by this MS technique with a sensitivity similar to ECD [15].

Extraction of RFAs in sediments

At the early stages of method development, we investigated three techniques commonly used for the extraction of organics in sediments. Using a freeze-dried and homogenized sediment obtained from a pulp mill as a reference sample and acetone as the extraction solvent, the recoveries of RFAs obtained by soxhlet, polytron (a high-speed sample homogenizer) and ultrasonic extraction techniques were compared. In each case, the RFA concentrations obtained were summed. Since soxhlet extraction produced 10–30% higher recoveries for total acids than the other two techniques, this method was chosen for the subsequent experiments.

The choice of extraction solvent also played an important role in the recovery of RFAs. Although acetone–hexane mixtures and pure acetone are usually adequate for the extraction of most neutral pesticides and organics in sediments, an increase of 30–40% for the recovery of RFAs in the reference sample was obtained by using the azeotropic mixture of 12% methanol in acetone (v/v) instead of pure acetone. The use of higher methanol content or pure methanol did not further improve the recovery. On the other hand, the addition of 100 μl of hydrochloric acid to the solvent prior to extraction had an even greater (*ca.* 200–300%) improvement on the recovery of all RFAs in the reference sample except for palustric and neoabietic acids. Further increase in the amount of hydrochloric acid gave even lower recovery of palustric and neoabietic acids and no improvement of the other resin acids. Using the results for five representative acids, namely palmitic, oleic, isopimaric, dehydroabietic and palustric acids, the effect of various solvent systems on the recovery of RFAs in sediments is depicted in Fig. 2.

In light of the reported isomerization of palustric and neoabietic acids under acidic conditions, it is not surprising to find that an extraction procedure using an acidified solvent mixture is not ideal for the recovery to those unstable resin acids. Since the use of non-acidified solvent systems produced much lower recoveries for all other acids, soxhlet extraction using 12% methanol in acetone with 100 μl of concentrated hydrochloric acid was chosen as a compromise for the optimal recovery of most RFAs in sediments.

Chromatographic separations of RFA-PFB esters

The DB-5 and DB-17 capillary columns were both used in the GC analysis of sediment extracts since the different elution patterns of the RFA esters on these columns allow tentative identification of peaks in the absence of a mass spectrometer. In general, the more polar DB-17 column had slightly better overall resolution of the esters. For instance, it was observed that the PFB esters of dehydroabietic acid and *o*-methylpodocarpic acid, a surrogate used by some workers for pulp and paper mill samples, as well as those of 12-chlorodehydroabietic acid and erucic acid (*cis*-13-22:1), could not be resolved on the DB-5 column.

Method performance and interference

Using fortified subsamples of a lake sediment containing non-detectable amounts or low levels of native RFAs, the precision and accuracy of our method were determined by the recovery of the acids in replicate runs. For sediments fortified at 10 and 1 μg/g, the recoveries were between 85 and 105%, with relative standard deviations ranging from 3 to 8% in nearly all cases (Table I). It should be noted that the

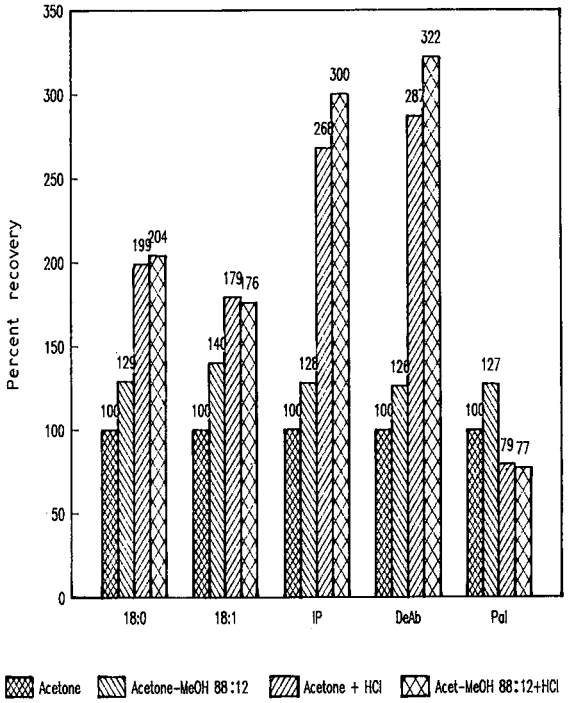

Fig. 2. Effect of methanol and acid on the recovery of resin and fatty acids. Legend: 18:0 = stearic acid; 18:1 = oleic acid; IP = isopimaric acid; DeAb = dehydroabietic acid; Pal = palustric acid; MeOH = methanol; Acet = acetone.

TABLE I

RECOVERIES OF REPLICATE DETERMINATION OF RESIN AND FATTY ACIDS IN FORTIFIED SEDIMENT SAMPLES

RFA	Recovery (mean ± S.D., $n=6$) (%)	
	10 μg/g	1 μg/g
Lauric (12:0)	97 ± 2.9	86 ± 6.7
Myristic (14:0)	103 ± 3.9	100 ± 8.8
Palmitic (16:0)	97 ± 4.0[a]	90 ± 7.9[a]
Stearic (18:0)	93 ± 5.3[a]	86 ± 7.5[a]
Oleic (18:1)	98 ± 5.7	88 ± 8.0
Linoleic (18:2)	95 ± 6.4	76 ± 8.1
Linolenic (18:3)	94 ± 5.7	77 ± 6.4
Arachidic (20:2)	91 ± 4.8[a]	86 ± 10[a]
Behenic (22:0)	96 ± 7.9	92 ± 12[a]
Pimaric	93 ± 6.2	101 ± 5.1
Sandaracopimaric	96 ± 7.9	105 ± 5.7
Isopimaric	93 ± 5.1	103 ± 5.3
Abietic	98 ± 5.2	90 ± 5.1
Dehydroabietic	101 ± 7.1	103 ± 6.0
14-Chlorodehydroabietic	95 ± 7.5	103 ± 5.7
12-Chlorodehydroabietic	96 ± 6.7	106 ± 5.7
12,14-Dichlorodehydroabietic	91 ± 7.0	102 ± 6.1

[a] After correction for sample blanks.

data presented in this table were obtained in the absence of levopimaric, palustric and neoabietic acids. The recoveries of palustric and neoabietic were low (between 15 and 25%), if they were also spiked to the sediment. At the same time, their recoveries could not be improved even if polytron extraction with a non-acidified solvent was performed at room temperature. Therefore, this method is only semi-quantitative for palustric and neoabietic acids and would have a high bias for abietic acid due to the conversion of palustric and neoabietic acids into the former. The present method was not applicable to levopimaric acid since it was never recovered from any fortified or naturally contaminated samples. The method detection limit, estimated to be 0.05 μg/g for the RFAs based on 1 g of sample, is sensitive enough for purposes such as environmental monitoring and toxicity evaluation.

Anhydrous sodium sulfate is often used for the removal of water in organic extracts of wet sediments. However, we found that a large number of fatty acids was present at high ng/g levels in analytical-reagent-grade anhydrous sodium sulfate from several suppliers (Fisher, BDH and Baker). The use of this adsorbent must therefore be avoided before the derivatization step of our procedure, and it should be substituted by air-drying of the sediment prior to extraction. Also, a method blank for the fatty acids should be run for each set of samples if the levels are lower than 1 μg/g.

Application to sediment samples

The present method has been applied to dozens of sediment samples collected in the vicinity of pulp and paper mill sites. The results of a few examples are given in Table II. Qualitatively, all RFAs except levopimaric acid were found in all or most sediment samples collected downstream of paper mills. Sample 1 was a river sediment collected from a site approximately 2 km upstream of a paper mill located in Ontario. Other than low levels of some native fatty acids and a trace amount of dehydroabietic acid, no other resin acids were found in this sample. Sample 2, collected from a site about 2 km downstream of the same paper mill, was quite heavily contaminated with RFAs, and the total amount of fatty and resin acids on dry weight basis were 58 and 211 μg/g, respectively. RFAs were still readily detected at a site about 5 km downstream of the same paper mill (sample 3). The presence of chlorinated dehydroabietic acids in samples 2 and 3 is consistent with the fact that this paper mill employs chlorobleaching of the pulps and that chloro- and dichlorodehydroabietic acids are formed by the chlorination of dehydroabietic acid under pulp bleaching conditions [16]. A GC–ECD profile of sample 2 is shown in Fig. 3. Sample 4 was a sludge sample collected from another pulp mill. This sample contained nearly 1 mg/g total resin acids and the concentration of dehydroabietic acid was over 400 μg/g.

Other acidic components in pulp mill sediments

Although this method was tested with the RFAs listed in Table I, the procedure is applicable to other fatty and resin acids occurring in pulp mill samples. Indeed, a large number of saturated and unsaturated fatty acids from C_6 to C_{24} were found in the sediment samples tested. Among them, the predominant ones were those saturated fatty acids from C_{16} to C_{24} with an even number of carbon atoms with the exception of *anteiso*-heptadecanoic (14-methylhexadecanoic) acid. Straight-chain fatty acids with an odd number of carbons such as pentadecylic (15:0), margaric (17:0) and tricosanoic (23:0) were also present in all samples, albeit at much lower concen-

TABLE II

LEVELS OF RESIN AND FATTY ACIDS IN SEDIMENTS COLLECTED FROM PULP MILL LOCATIONS

RFA	Concentration (μg/g dry weight)			
	Sample 1	Sample 2	Sample 3	Sample 4
Lauric (12:0)	0.77	1.44	1.27	6.83
Myristic (14:0)	0.85	2.87	1.53	11.72
Palmitic (16:0)	2.70	13.95	6.90	41.90
Stearic (18:0)	1.19	5.82	3.68	23.32
Oleic (18:1)	0.59	7.73	3.83	40.82
Linoleic (18:2)	<0.05	7.76	3.95	21.68
Linolenic (18:3)	<0.05	<0.05	<0.05	<0.05
Arachidic (20:0)	0.38	5.00	2.66	15.32
Behenic (22:0)	1.25	13.12	9.50	71.14
Pimaric	<0.05	11.62	6.84	72.02
Sandaracopimaric	<0.05	5.14	3.21	28.91
Isopimaric	<0.05	27.46	12.09	112.35
Palustric	<0.05	4.60	<0.05	60.73
Abietic	<0.05	12.38	5.18	87.47
Dehydroabietic	0.76	121.2	36.60	405.51
Neoabietic	<0.05	<0.05	<0.05	7.91
14-Chlorodehydroabietic	<0.05	9.45	5.74	10.65
12-Chlorodehydroabietic	<0.05	20.03	14.94	21.08
12,14-Dichlorodehydroabietic	<0.05	3.70	3.20	68.48
Total fatty acids	6.46	44.58	23.80	232.72
Total resin acids	0.76	210.98	87.78	875.09

trations. The major unsaturated fatty acids found were entirely straight-chained with an even carbon number and in the *cis* form, namely myristoleic (14:1), palmitoleic (16:1), eicosenoic (20:1), erucic (22:1) and nervonic (24:1) acids in addition to oleic (18:1) and linoleic (18:2) acids. Chlorinated stearic acids were not found in the sediments analysed in this study. A resin acid metabolite, 7-isopimarenoic (dihydroisopimaric) acid, resulting from the anaerobic reduction of isopimaric acid [17], was also found in a few sediments. Several other smaller peaks of m/z 301 and 303 observed in the NICI mass spectra of the derivatized extracts were presumably derived from other resin acids. Because of the lack of authentic standards in our laboratory, they could not be identified.

CONCLUSIONS

As demonstrated above, the analytical method described here is applicable to the determination of the major RFAs in sediments at the μg/g level. Presumably due to their stability and low water solubility, many RFAs could readily accumulate in river sediments. Indeed, high levels of the toxic RFAs were found in many sediment

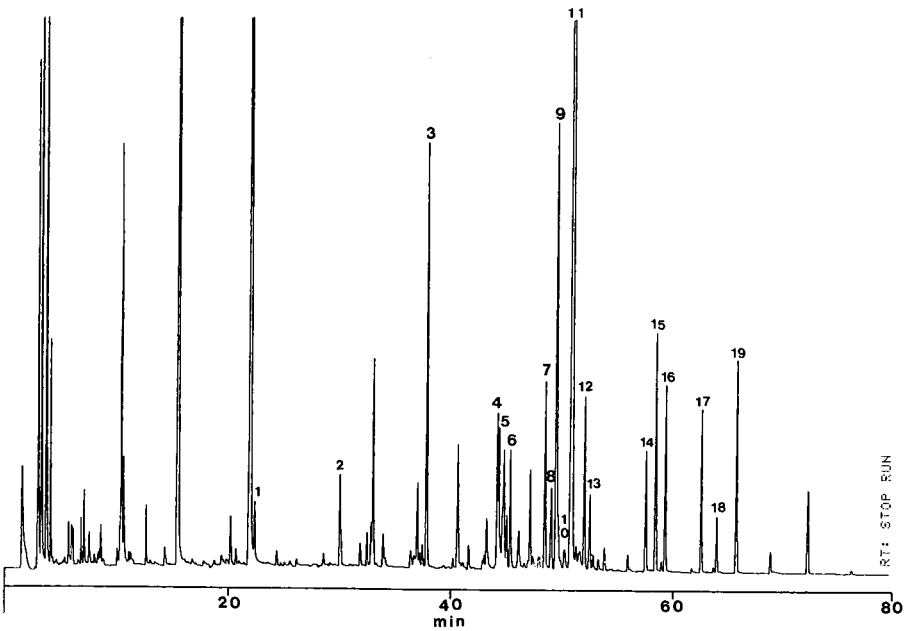

Fig. 3. GC–ECD profile of the PFB esters of resin and fatty acids in sediment sample 2 as chromatographed on a 30-m DB-5 column. Acids: 1 = lauric; 2 = myristic; 3 = palmitic; 4 = linoleic; 5 = oleic; 6 = stearic; 7 = pimaric; 8 = sandaracopimaric; 9 = isopimaric; 10 = palustric; 11 = dehydroabietic; 12 = abietic; 13 = arachidic; 14 = 14-chlorodehydroabietic; 15 = 12-chlorodehydroabietic; 16 = behenic; 17 = tricosanoic; 18 = dichlorodehydroabietic; 19 = lignoceric.

samples collected downstream of pulp and paper mills. Therefore, regular monitoring of RFAs in such locations is a high priority for the protection of fish and the aquatic environment.

REFERENCES

1 I. H. Rogers, *Tappi*, 58, No. 7 (1975) 136.
2 J. M. Leach and A. N. Thakore, *Tappi*, 59, No. 2 (1976) 123.
3 A. B. McKague, J. M. Leach, R. N. Soniassy and A. N. Thakore, *Pulp Pap. Can. Trans. Tech. Sect.*, 3, No. 3 (1977) TR75.
4 I. Rogers, H. Mahood, J. Servizi and R. Gordon, *Pulp Pap. Can.*, 80, No. 9 (1979) T286.
5 I. H. Rogers in D. F. Zinkel and J. Russell (Editors), *Navel Stores – Production, Chemistry, Utilization*, Pulp Chemicals Association, New York, 1989, Ch. 28, pp. 942–973.
6 R. H. Voss, J. T. Wearing, R. D. Mortimer, T. Kovacs and A. Wong, *Pap. Puu*, 62 (1980) 809.
7 K. P. Kringstad, P. O. Ljungquist, F. de Sousa and L. M. Strömberg, *Environ. Sci. Technol.*, 15 (1981) 562.
8 K. Lindström and F. Österberg, *Environ. Sci. Technol.*, 20 (1986) 133.
9 C. C. Walden and T. E. Howard, *Tappi*, 60, No. 1 (1977) 122.
10 C. C. Walden and T. E. Howard, *Pulp Pap. Can.*, 82, No. 4 (1981) T143.
11 M. H. Priha and E. T. Talka, *Pulp Pap. Can.*, 87, No. 12 (1986) T447.
12 R. H. Voss and A. Rapsomatiotis, *J. Chromatogr.*, 346 (1985) 205.
13 L. LaFleur, *Natl. Conc. Pap. Ind. Air Stream Improv. Tech. Bull.*, No. 501 (1986).
14 B. Brownlee, M. E. Fox, W. M. J. Strachan and S. R. Joshi, *J. Fish. Res. Board Can.*, 34 (1977) 838.
15 H. B. Lee, T. E. Peart and J. M. Carron, *J. Chromatogr.*, 498 (1990) 367.
16 G. S. Furman and D. B. Easty, *Tappi*, 67, No. 3 (1984) 89.
17 P. N. McFarlane and T. A. Clark, *Water Sci. Technol.*, 20 (1988) 273.

Journal of Chromatography, 547 (1991) 325–334
Elsevier Science Publishers B.V., Amsterdam

CHROM. 23 204

Determination of 19-nortestosterone, testosterone and trenbolone by gas chromatography–negative-ion mass spectrometry after formation of the pentafluorobenzylcarboxymethoxime–trimethylsilyl derivatives

RENZO BAGNATI* and ROBERTO FANELLI
Istituto di Ricerche Farmacologiche "Mario Negri", Via Eritrea 62, 20157 Milan (Italy)
(First received July 6th, 1990; revised manuscript received February 11th, 1991)

ABSTRACT

The known reaction of 3-ketosteroids with carboxymethoxylamine (to form the corresponding carboxymethoximes), followed by esterification of the carboxyl group with pentafluorobenzyl bromide, has been used to obtain derivatives of 19-nortestosterone, testosterone and trenbolone suitable for high-sensitivity detection with gas chromatography–negative-ion chemical ionization mass spectrometry. These derivatives, after further silylation of the alcoholic groups of the steroids, showed excellent chromatographic and spectrometric characteristics and were detectable in the low picogram range. The derivatization gave rise to the formation of two isomers which were distinguishable by gas chromatography. The existence of the two isomers was also confirmed by high-performance liquid chromatography. Examples of the usefulness of this derivatization procedure are given for the analysis of 19-nortestosterone, testosterone and trenbolone in meat and urine samples. By the use of immunoaffinity extraction and addition of deuterated internal standards (synthesized by isotopic exchange), the new derivatization procedure allowed a correct identification and quantitation of the steroids and reached very low detection limits [0.02 ppb (10^9) for 19-nortestosterone and testosterone, 0.06 ppb for trenbolone].

INTRODUCTION

The determination of steroids in biological samples is an analytical problem of great importance. In fact, several immunological and instrumental methods [radioimmunoassay (RIA), enzyme-linked immunosorbent assay (ELISA), high-performance liquid chromatography (HPLC), gas chromatography (GC) and GC–mass spectrometry (MS)] have been developed for this purpose [1–8]. GC–MS is considered the most effective technique to obtain a selective and accurate measurement of these substances, but all the methods reported in the literature require derivatization of the molecules to achieve good chromatographic and spectrometric characteristics [4–8]. The most widely used derivatizing agents are methoxyamine (for the reaction with keto groups), silylating compounds (for alcoholic groups) and aliphatic fluorinated anhydrides (for both). Depending on the derivatization method, MS detection has been done with electron-impact (EI) ionization mode or negative-ion chemical ion-

0021-9673/91/$03.50

ization (NICI) mode, obtaining different sensitivities and specificities during the analysis of samples.

To extend the choice of derivatizing agents, we describe here the use of carboxymethoxylamine (a compound already used to introduce a carboxyl group into steroid molecules, for their subsequent conjugation to proteins [9]) as a derivatizing agent of the 3-keto groups of 19-nortestosterone, testosterone and trenbolone, followed by pentafluorobenzylation of the carboxyl group of the resulting carboxymethoximes. This attempt at introducing a pentafluorobenzyl ester moiety into the steroid molecules was made to exploit the high-sensitivity detection achievable for the compounds containing this group by GC–NICI-MS [10,11].

EXPERIMENTAL

Materials

19-Nortestosterone (19-norT) and testosterone (T) were from Sigma (St. Louis, MO, USA). Trenbolone (TBOH) was extracted and purified from pharmaceutical formulations. Carboxymethoxylamine hemihydrochloride (CMOA), pentafluorobenzyl bromide (PFBBr), deuterium oxide (^2H_2O), potassium deuteroxide (KO^2H, 40% solution in ^2H_2O), and monodeuteromethanol (CH_3O^2H) were from Aldrich (Milwaukee, WI, USA). N,O-Bis(trimethylsilyl)trifluoroacetamide (BSTFA) and methoxyamine hydrochloride, 2% solution in pyridine (MOX), were from Pierce (Oud Beijerland, Netherlands). Diisopropylethylamine (DIPEA) was from Fluka (Buchs, Switzerland). N,O-Bis(trimethylsilyl-$^2H_{18}$)acetamide (BSA-D_{18}) was from ICN Biomedicals (Cambridge, MA, USA). Immunoaffinity columns and extraction kits (Multi-Prep II) were from Genego (Gorizia, Italy).

Derivatization

Derivatization was done as follows. To dried standards or samples, in conical glass tubes, 100 μl of a solution of 1 mg/ml CMOA in acetonitrile–DIPEA (100:1, v/v) were added. The tubes were capped and heated at 60°C for 2 h. Then, 10 μl of a solution of PFBBr in acetonitrile (1:40, v/v) were added and the tubes were heated at 40°C for 10 min. Finally, after evaporating the solvents, 20 μl of BSTFA were added and the tubes heated at 60°C for 30 min.

The reagent solutions were prepared fresh every month.

Gas chromatography–mass spectrometry

A VG TS-250 mass spectrometer coupled to a HP 5890 gas chromatograph and equipped with an 11-250J data system was used for EI mode, and a Finnigan 4000 mass spectrometer coupled to a DANI 6500 gas chromatograph and equipped with a Teknivent 1050 data system (St. Louis, MO, USA) was used for NICI mode. Source conditions in NICI mode were: temperature, 250°C; emission current, 250 μA; electron energy, 100 eV. Ammonia was used as the reactant gas for electron-capture ionization at a source pressure of 0.2 Torr.

Samples were injected in 2-μl aliquots with the following GC conditions: column, CP Sil 5 CB, 25 m × 0.32 mm I.D., film thickness, 0.12 μm (Chrompack Italia, Cernusco sul Naviglio, Italy); oven temperature raised from 160°C (1 min) to 220°C at 25°C/min, then to 300°C (4 min hold) at 15°C/min; helium head pressure of the column, 0.4 bar.

The HP 5890 gas chromatograph was equipped with a split–splitless injector (operated in splitless mode at 240°C), and with an 'on-column' injector; the DANI gas chromatograph was equipped with a programmable temperature vaporizer (PTV) injector (Dani, Monza, Italy) which was initially kept at 60°C and then heated quickly to 275°C immediately after injection. The split–splitless injector gave sensitivity problems when injecting the pentafluorobenzylcarboxymethoxime–trimethylsilyl (PFBCMO–TMS) derivatives, probably because of thermal instability during the flash heating. The PTV injector and the on-column injector did not suffer such problems and sensitivity was always good.

High-performance liquid chromatography

HPLC injections were done on a Beckman System Gold chromatograph, equipped with a 20-μl loop injector and with a UV detector (set at 266 nm). The column was a Chromspher C_{18}, 100 × 3.0 mm (Chrompack Italia) operated at a flow-rate of 0.5 ml/min of methanol–water (60:40).

Deuterium exchange of 19-nortestosterone, testosterone and trenbolone

Deuterated analogues of 19-norT, T and TBOH, to be used as internal standards in GC–MS quantitation, were obtained by isotopic exchange in deuterated solvents under alkaline conditions. Briefly, 1 mg of 19-norT and T and 0.1 mg of TBOH were incubated, at room temperature, with a mixture of 10 μl of 10% KO^2H in ^2H_2O and 200 μl of CH_3O^2H. The isotopic exchange of the weakly acidic protons adjacent to the 3-keto group and to the double bond in the 4–5 position was monitored by GC–MS. After 10 days for 19-norT and TBOH and 20 days for T the incubation was stopped. The mixtures were diluted with 2 ml of ^2H_2O and the steroids were extracted with three 2-ml volumes of ethyl acetate. T and TBOH were found by GC–MS to have exchanged five protons, giving [$^2H_5$]testosterone (T-D_5) and [$^2H_5$]trenbolone (TBOH-D_5), while 19-norT exchanged six protons, giving [$^2H_6$]19-nortestosterone (19-norT-D_6). The isotopic purity of these compounds was about 80%, owing, mainly, to the presence of pentadeuterated 19-norT and tetradeuterated T and TBOH. However, the amount of completely non-deuterated molecules was negligible (<0.1%), as measured by GC–MS. The deuteration mixtures also contained other minor unidentified substances which were separated by GC and did not interfere in the quantitation procedure of the non-deuterated compounds.

Immunoaffinity extraction

The immunoaffinity purification of urine samples was performed using Multi-Prep II columns and buffers and following the manufacturer's instructions. Briefly, the procedure was as follows: the samples were diluted to 8 ml with extraction buffer, loaded on the columns and gently mixed with the gel for 1 min; the columns were then left to elute by gravity and washed with washing buffer (2 × 10 ml) and distilled water (2 ml); finally, immunoabsorbed substances were recovered by elution with acetone–water (95:5 v/v; 2 × 1.5 ml). The eluates were dried with a stream of air at 60°C and derivatized as described.

RESULTS AND DISCUSSION

The efficiency of the derivatization procedure described was tested by full-scan GC–MS injections of pure steroid standards. The chromatograms did not show any peak corresponding to underivatized or partially derivatized steroids, indicating that the derivatization reactions were complete.

The derivatization of 19-norT, T, and TBOH with CMOA can give rise to the formation of two isomers for each substance, because of the possible *cis–trans* conformation relative to the nitrogen atom of the oxime group. The same kind of isomerization has been described in the literature after the derivatization of 3-ketosteroids with methoxyamine [12]. Indeed, the injection of the PFBCMO–TMS derivatives of either 19-norT, T or TBOH, by GC–MS, showed the presence of two peaks (Fig. 1) with identical mass spectra in both EI and NICI modes (Fig. 3). To confirm the existence of the two isomers and to exclude the possibility of GC artifacts (*e.g.* false double peaks [13]), the derivatized steroids were also analyzed by HPLC. Each steroid (50 μg) was derivatized by the method described but omitting the silylation reaction (because of incompatibility of silyl ethers with HPLC eluents), dissolved in methanol (0.5 ml) and injected (5 μl) into a liquid chromatograph under the conditions described in the Experimental section. The results confirmed the presence of two isomers for all of the three steroids considered. The isomers eluted in reverse order with respect to GC (the minor isomers eluted after the major isomers) and had retention times distinguisable from those of the underivatized compounds (Fig. 2).

The ammonia NICI spectra of the PFBCMO–TMS derivatives of steroids (Fig. 3) are characterized by three major peaks: one is the usual fragment of PFB esters, corresponding to the loss of the PFB group (M − 181, carboxylate anion [11,14,15]), and the other two (common to all derivatives) probably correspond to the fragments $CHOCOO^-$ (*m/z* 73) and $HOCH_2COO^-$ (*m/z* 75), resulting from further cleavage of

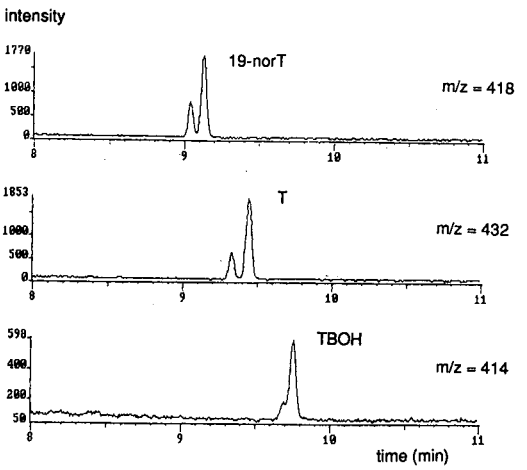

Fig. 1. GC–NICI–SIM tracings of 16 pg of each of the PFBCMO–TMS derivatives of 19-norT, T and TBOH, showing total or partial separation of the *cis–trans* isomers relative to the nitrogen atom of the oxime group. Conditions were as described in the Experimental section.

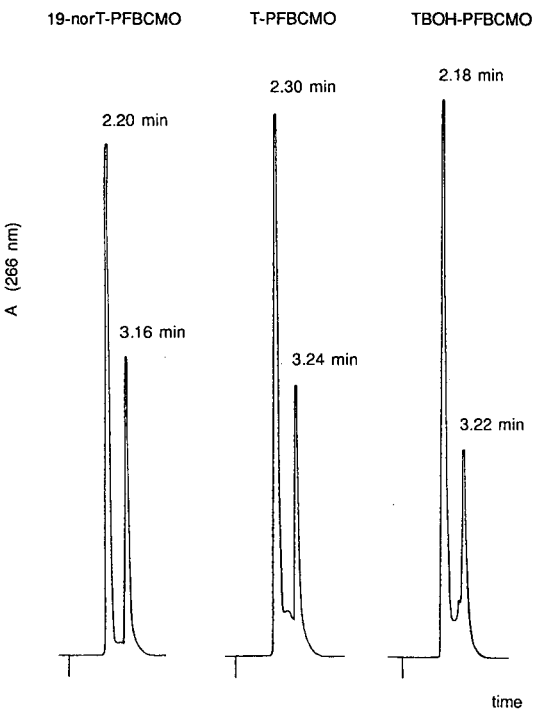

Fig. 2. HPLC profiles of the PFBCMO derivatives of 19-norT, T and TBOH, with retention times of the two isomers of each compound. The retention times of underivatized 19-norT, T and TBOH, under the same conditions (see Experimental section), were 2.90, 2.96 and 2.92 min, respectively. See also Fig. 1 and text for other explanations.

the oxygen–nitrogen bond of the carboxymethoxime group, with rearrangements involving a hydrogen atom. The possibility that these last two peaks could originate from the silyl groups was excluded by taking NICI spectra of PFBCMO derivatives in which the hydroxyl groups were reacted with deuterated BSA (BSA-D_{18}) to form the nonadeutero-trimethylsilyl (TMS-D_9) derivatives. These derivatives had the same peaks at *m/z* 73 and *m/z* 75, indicating that the silyl groups were not involved in the fragmentation.

The NICI mass spectra of the deuterated analogues of the steroids (19-norT-D_6, T-D_5 and TBOH-D_5) showed the corresponding carboxylate anions (with complete conservation of the isotopic abundances) and the same *m/z* 73 and *m/z* 75 ions as the non-deuterated compounds.

Selected-ion monitoring (SIM) of the carboxylate anions of the PFBCMO–TMS derivatives (*m/z* 418 for 19-norT, *m/z* 424 for 19-norT-D_6, *m/z* 432 for T, *m/z* 437 for T-D_5, *m/z* 414 for TBOH and *m/z* 419 for TBOH-D_5), during GC injections, gave highly specific and sensitive detection. The injection of pure standards of derivatized steroids produced chromatograms free of interferences for all the compounds tested, and the detection limit was about 1 pg injected into the gas chromatograph.

However, the advantages of the use of these derivatives are more clearly shown

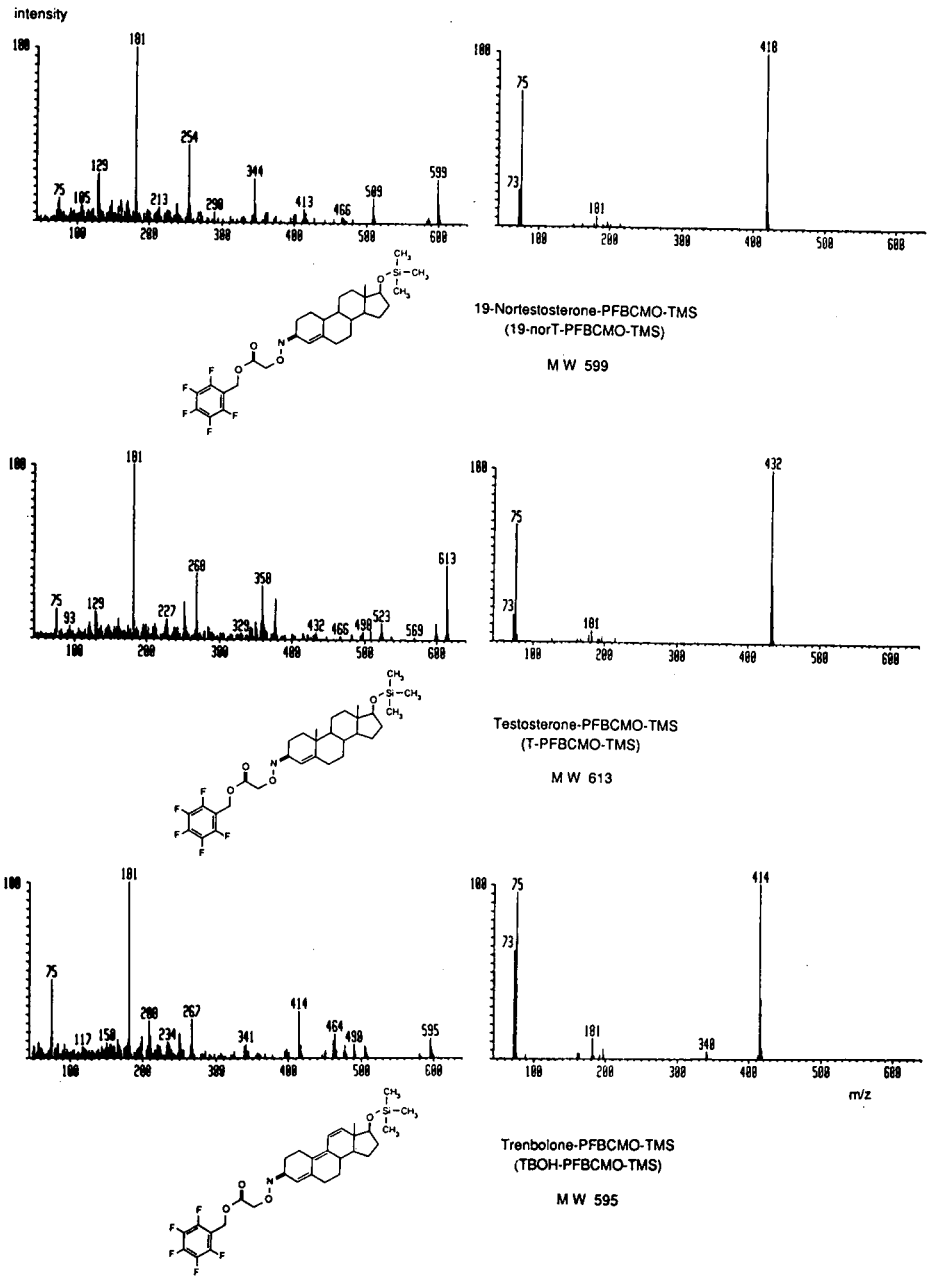

Fig. 3. EI (left) and NICI (right) mass spectra of the PFBCMO–TMS derivatives of the steroids indicated. MS conditions were as described in the Experimental section. MW = Molecular weights.

by the analysis of biological samples. Two extraction procedures of such samples, one using conventional methods (liquid–liquid and solid–phase extractions, HPLC) and one using an immunoaffinity method, were used to evaluate the detection improvements which could be obtained.

As a first case, a meat sample from a commercial food, suspected of being contaminated by 19-norT and which was extracted and purified by solid-phase extraction and HPLC, was divided into two aliquots to be examined by different GC–

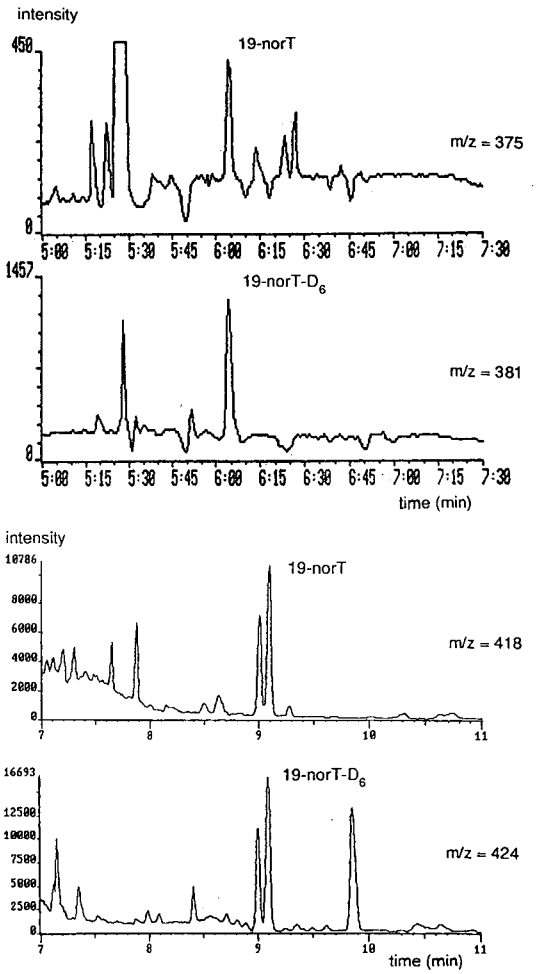

Fig. 4. GC–SIM tracings of an extracted meat sample, contaminated by 19-norT, after two different derivatization and ionization techniques. (A) Tracings obtained after conversion of steroids to the MO–TMS derivatives and after detection with EI mode; 2.5 ng of 19-norT-D_6 were added as external standard. Upper trace: molecular ion of 19-norT–MO–TMS. Lower trace: molecular ion of 19-norT-D_6–MO–TMS. (B) Tracings obtained after conversion of steroids to the PFBCMO–TMS derivatives and after detection with NICI mode; 1 ng of 19-norT-D_6 was added as external standard. Upper trace: carboxylate ion of 19-norT–PFBCMO–TMS. Lower trace: carboxylate ion of 19-norT-D_6–PBFCMO–TMS. The chromatograms of the PFBCMO–TMS derivatives show the separation of the two derivatization isomers of the steroids. See Fig. 1 and text for other explanations.

MS detection procedures. An aliquot was derivatized with MOX and BSTFA to give the methoxime–trimethylsilyl (MO–TMS) derivatives [12], and the other was derivatized by the method described. To both samples was added, before derivatization, 19-norT-D_6 as external standard (2.5 ng for the aliquot derivatized with MOX and 1 ng for the aliquot derivatized with CMOA). The MO–TMS derivatives were detected by GC–SIM using EI mode and monitoring the molecular ions (*m/z* 375 for 19-norT and *m/z* 381 for 19-norT-D_6), while the PFBCMO–TMS derivatives were detected, as described, using NICI mode. The same GC conditions (see Experimental section) were used for both samples. The use of the latter derivatization and ionization technique considerably increased the specificity and sensitivity of detection (Fig. 4). The improved sensitivity can be attributed to the increase in the absolute signal given by the analytes and to the reduced interferences in the chromatograms. In fact the PFBCMO–TMS derivatives of 19-norT and 19-norT-D_6 had longer retention times than MO–TMS derivatives and eluted into clean zones of the chromatograms. (The MO–TMS derivatives, unlike the PFBCMO–TMS derivatives, did not show the separation of two isomers with the GC conditions which were used.) For the meat sample analysed, a more certain identification and a more accurate quantitation of 19-norT could be obtained from the chromatograms of the PFBCMO–TMS derivatives. The quantitation of these samples, based on calibration curves made with standards containing known amounts of non-deuterated and deuterated analytes

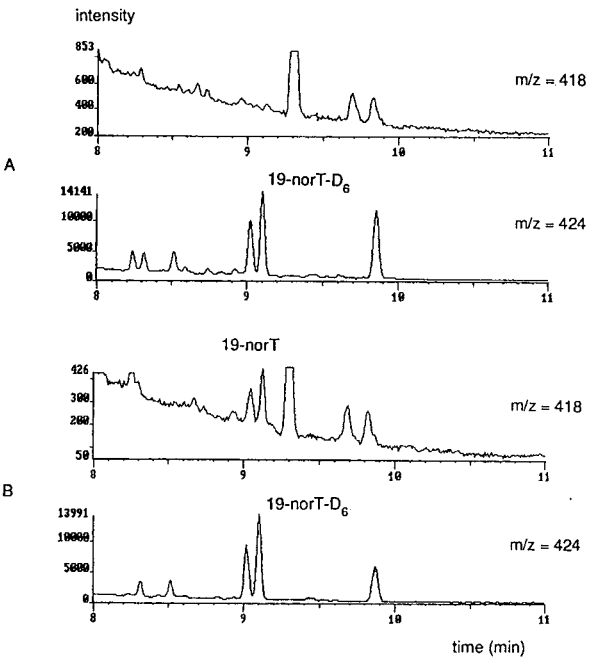

Fig. 5. GC–NICI-SIM tracings of two blank urine samples (1 ml) spiked with 19-norT and 19-norT-D_6, extracted with immunoaffinity columns and derivatized to form the PFBCMO–TMS derivatives of the two compounds. (A) Sample spiked with 1 ng of 19-norT-D_6 (lower trace) and not spiked with 19-norT (upper trace). (B) Sample spiked with 1 ng of 19-norT-D_6 (lower trace) and 20 pg of 19-norT (upper trace). The chromatograms show the separation of the two derivatization isomers of the steroids. See Fig. 1 and text for other explanations.

[15], gave values of 0.70 and 0.64 ppb (10^9) of 19-norT for the MO–TMS and PFBCMO–TMS derivatives respectively.

A second application of the derivatization procedure was performed to evaluate exactly the accuracy and the sensitivity achievable in the determination of 19-norT, T and TBOH. Several samples of female calf urine, spiked with known amounts of these steroids, were analysed after purification with immunoaffinity columns (IACs). The IACs (Multi-Prep II) contained anti-19-norT antibodies immobilized to a Sepharose gel and could also recover other similar steroids as T and TBOH. (Recovery efficiencies claimed by the manufacturer are 87% for 19-norT, 85% for T and 35% for TBOH.) The samples (1 ml urine, in triplicate) were spiked with 0, 20, 100 and 1000 pg of 19-norT, T and TBOH and with a constant amount (1000 pg) of 19-norT-D_6, T-D_5 and TBOH-D_5 and then extracted using the procedure described in the Experi-

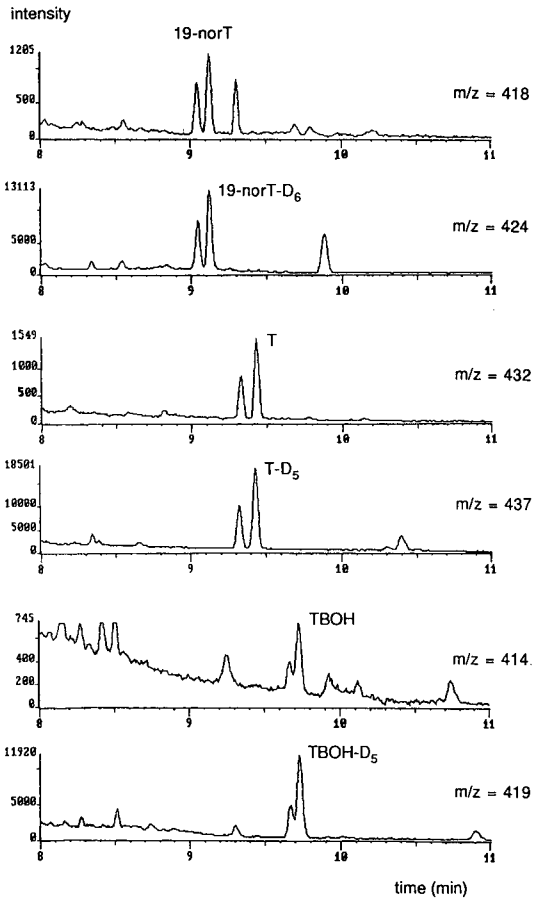

Fig. 6. GC–NICI–SIM tracings of a sample of female calf urine (1 ml) spiked with 100 pg of 19-norT, T and TBOH and with 1 ng of 19-norT-D_6, T-D_5 and TBOH-D_5. The sample was extracted with an immunoaffinity column containing antibodies raised against 19-norT and derivatized to obtain the PFBCMO–TMS derivatives of the steroids indicated. The chromatograms show the separation of the two derivatization isomers of every compound. See Fig. 1 and text for other explanations.

mental section. Injections by GC–NICI–SIM showed that urines spiked with deuterated standards only did not show any peak corresponding to unlabelled 19-norT and TBOH. The lowest level of 19-norT which could be detected corresponded to a concentration of 0.02 ppb (Fig. 5). The detection limit of TBOH, instead, was estimated to be about 0.06 ppb, because of the lower recovery from the IACs. For T the detection limit was not measurable in that way, because of its natural presence in urine at these low levels; however a detection limit of 0.02 ppb was obtained by extracting, in the same way, pure buffer samples spiked with T and T-D_5. The coefficients of variation for these determinations, obtained by extracting three urine samples spiked at the 0.1 ppb level, were 5.6% for 19-norT, 8.7% for TBOH and 6.3% for T. The complete chromatograms of one of these samples are shown in Fig. 6.

CONCLUSIONS

We have introduced a new derivatization procedure which expands the possibilities of choice for GC–MS detection of some 3-ketosteroids. This procedure was useful for the detection of 19-norT, T and TBOH at very low levels in biological samples. The method is suitable for extension to other similar steroids.

REFERENCES

1 A. Turkes, A. O. Turkes, B. G. Joyce, G. F. Read and D. Riad-Fahmy, *Steroids*, 33 (1979) 347.
2 B. Hoffmann and G. Oettel, *Steroids*, 27 (1976) 509.
3 M. W. Phillips and D. J. Harvood, *J. Vet. Pharmacol. Ther.*, 5 (1982) 285.
4 V. J. Gould, A. O. Turkes and S. J. Gaskell, *J. Steroid Biochem.*, 24 (1986) 563.
5 M. Axelson and J. Sjovall, *J. Chromatogr.*, 126 (1976) 705.
6 L. A. van Ginkel, R. W. Stephany, H. J. van Rossum, H. M. Steinbuch, G. Zomer, E. Van De Heeft and A. P. J. M. de Jong, *J. Chromatogr.*, 489 (1989) 111.
7 S. Hsu, R. H. Eckerlin and J. D. Henion, *J. Chromatogr.*, 424 (1988) 219.
8 M. H. Baker, I. Howe, M. Jarman and R. McCague, *Biomed. Environ. Mass Spectrom.*, 16 (1988) 211.
9 B. F. Erlanger, F. Borek, S. M. Beiser and S. Liebermann, *J. Biol. Chem.*, 228 (1957) 713.
10 E. A. Stemmler and R. A. Hites, *Biomed. Environ. Mass Spectrom.*, 17 (1988) 311.
11 K. A. Waddel, I. A. Blair and J. Wellby, *Biomed. Mass Spectrom.*, 10 (1983) 83.
12 M. G. Horning, A. M. Moss and E. C. Horning, *Anal. Biochem.*, 22 (1968) 284.
13 A. D. Sauter, L. D. Betowski, T. R. Smith, V. A. Strickler, R. G. Beimer, B. N. Colby and J. E. Wilkinson, *J. High Resolut. Chromatogr. Chromatogr. Commun.*, 4 (1981) 366.
14 T. M. Trainor and P. Vouros, *Anal. Chem.*, 59 (1987) 601.
15 R. Bagnati, M. G. Castelli, L. Airoldi, M. Paleologo Oriundi, A. Ubaldi and R. Fanelli, *J. Chromatogr.*, 527 (1990) 267.

Journal of Chromatography, 547 (1991) 335–344
Elsevier Science Publishers B.V., Amsterdam

CHROM. 23 262

Use of a liquid crystal stationary phase at temperatures below its melting point for the gas chromatographic study of some volatile oil constituents

T. J. BETTS*, CHARMAINE M. MOIR and A. I. TASSONE
School of Pharmacy, Curtin University of Technology, G.P.O. Box U1987, Perth, Western Australia 6001 (Australia)

(First received January 9th, 1991; revised manuscript received February 25th, 1991)

ABSTRACT

The liquid crystal bismethoxybenzilidine-bitoluidine (BMBT), used as the stationary phase for the gas chromatographic study of some aromatics and a monoterpenoid constituent of volatile oils, gave best results used below its melting point of about 180°C. At these temperatures (120–175°C), relative retention times to linalol were dependent on whether the column was heated from ambient conditions, or cooled from above the melting point. Changes in the sequence of retentions (terpineol–estragole and anethole–thymol "shifts") suggested this liquid crystal may operate by three different mechanisms, dependent on the column treatment. Results are given for fennel and tea-tree oils.

INTRODUCTION

Betts [1] has recorded introductory studies of bismethoxybenzilidineanil-chloroaniline $(MBCA)_2$ liquid crystal stationary phase for the gas chromatographic (GC) examination of aromatic constituents of essential oils. The observed melting point of the commercial $(MBCA)_2$ used was 142°C, and he logically used it after heating to 190°C (the maximum before decomposition became likely) and cooling it down to operational conditions. However, Betts also recorded "normal" results for three aromatic oil constituents and two mono-terpenes at 135°C, below the liquid crystal melting point when it should, theoretically, no longer function as a liquid stationary phase. He remarked [1] "it is amazing that $(MBCA)_2$ ... functions as a stationary phase ... even as low as 50°C". This penomenon was noticed originally by Dewar and Schroeder [2], who were jointly the first in 1964 to publish on liquid crystal GC. Their liquid crystal had a melting point of 120°C, but still resolved methyl isomers of methyl benzoate at 115°C, and they suggested that the "stationary liquid phase had supercooled and was still in the nematic (liquid crystal) form". Two years later Barrall *et al.* [3] obtained good separations of benzene derivatives and paraffins operating liquid crystals at well below their melting points (*e.g.*, at 49°C using a liquid crystal melting at 88°C) and explained this by the mixed liquid crystal and support "substrate results in a general lowering of all transition temperatures" (*i.e.*, melting point of the liquid

0021-9673/91/$03.50

crystal). This phenomenon was confirmed by others [4,5], and Lester and Hall [6] went so far as to say "it is clear that the liquid crystal stationary phase must be used in the supercooled state ... (which) dramatically improves the resolution" for dodecadienyl acetates. Their liquid crystal had a melting point of 167.5°C, but was used down to 100°C after being "conditioned" just above this at 180°C.

"The properties of the supercooled region" were studied by Wasik and Chesler [7] using as liquid crystal a non-chlorinated dimer of a di-aromatic anil BMBT or $(MBT)_2$ with a higher melting point than that used by Betts [1]. Plotting retention data against temperature they observed a hysteresis loop for dimethylnaphthalenes in which retention values at a particular temperature (below the liquid crystal melting point of 181°C) were higher if the column was cooled to this point rather than heated to it. This applied down to 120°C, which they commented "essentially extends the temperature range of the liquid crystal column (downwards, with) no abrupt change in (the separation factor) α (values) at or near 181°C." They gave results at 130°C. Haky and Muschik [8] recorded that $(MBT)_2$ could be used down to 115°C for resolving dimethylnaphthalenes and commented that "interactions of the support with the liquid crystal ... and the existence of supercooled nematic thermal regions ... lower the minimum operating temperatures (so that) the versatility of such columns is increased."

In the course of our GC studies of essential oils it seemed of interest to see how this 'supercooled' dimer $(MBT)_2$ behaved with them. Witkiewicz and Waclawczyk [9] classify this as a "high-temperature" liquid crystal and found that similar liquid crystal dimers gave retention times for dimethylnaphthalenes which were "longer during cooling of the column than during heating". Plots of retention time versus increasing column temperature revealed, in some cases, transition temperatures by changing in direction. With about 2.5% liquid crystal column loading "the relative retention times are highest in the solid-state temperature region... In some instances they are similar to those observed with conventional stationary phases".

EXPERIMENTAL

Apparatus

A Pye Unicam GCD gas chromatograph fitted with flame-ionisation detector and wide-range amplifier with a Hewlett-Packard 3380A recorder/integrator were used. Three glass columns (1.5 m × 4 or 2 mm I.D.) were packed with Supelco Chromasorb WAW 80/100 mesh coated with 3% $(MBT)_2$ which was purchased as N,N'-bis(*p*-methoxy-benzylidine)-α,α'-bi-*p*-toluidine (BMBT) from TCI (Tokyo, Japan) (melting point observed 179°C). This is the di-(anisole-anil) derivative (CH_3O–C_6H_4–$CH=N$–C_6H_4–CH_2–)$_2$. No preliminary 'conditioning' heating was applied to obtain the values given in the lowest portion of Table I (see Results below). Nitrogen was used as mobile phase at a slow flow of about 7.5–10 ml min^{-1}.

A Technoterm 7300 probe was used to observe oven temperatures with a reading to 0.1°C if below 200°C, and to 1°C if above.

Materials and methods

Anethole, estragole (4-allylanisole), linalol and thymol were obtained from Sigma. Also used were α-terpineol (TCI), safrole (Fritzsche), and cuminal (*p*-isopropyl-

benzaldehyde, Eastman). These were injected from a micro-syringe which had been filled and then "emptied" of the substances. The solid thymol was injected in strong solution in ethanol. Retention times were determined, after deducting hold-up time. Various isothermal conditions were used, as detailed in Table I.

About 0.1 μl was injected of a Western Australian fennel oil, which is an old specimen donated by a Perth pharmacy, of unknown origin. The same volume was injected of the Australian antiseptic 'Thurday Plantation' tea-tree oil (distilled from *Melaleuca alternifolia*).

RESULTS AND DISCUSSION

Average results are presented in Table I and Figs. 1 and 2. They are calculated as retentions relative to linalol, which is preferable to using simple retention times or more complex presentations. Linalol once again proved an ideal GC standard, as it has in the past for conventional and liquid crystal phase work [1,10]. Linalol has a reasonably short retention time, giving sharp, sensitive peaks, and is easy to fill and empty from the micro-syringe, for it is not viscous.

These results reflect trends rather than absolute values, as some variation is found from one run to another, particularly in the region of the liquid crystal melting

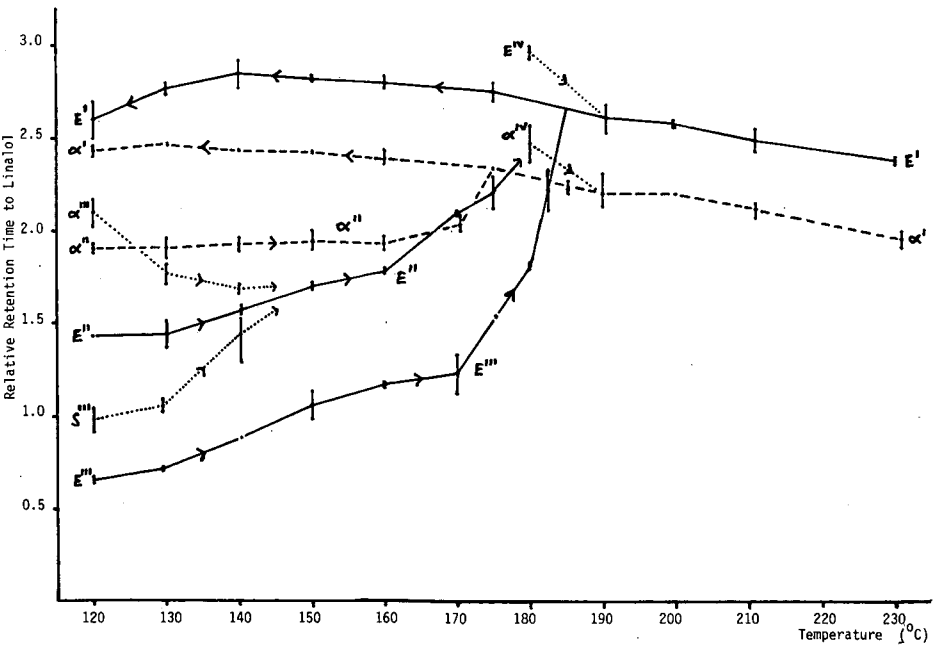

Fig. 1. Average relative retention times to linalol for some test solutes over a range of isothermal column temperatures in °C. Vertical bars depict range of observations. α = α-Terpineol; E = estragole; S = safrole. Suffix [i]: results after the liquid crystal was heated above 190°C; [ii]: results on heating from cold the liquid crystal which had been previously heated above 190°C; [iii]: results on a 'naive' liquid crystal which had not been previously taken above 190°C; [iv]: results are unusually high and sometimes obtained on heating the liquid crystal.

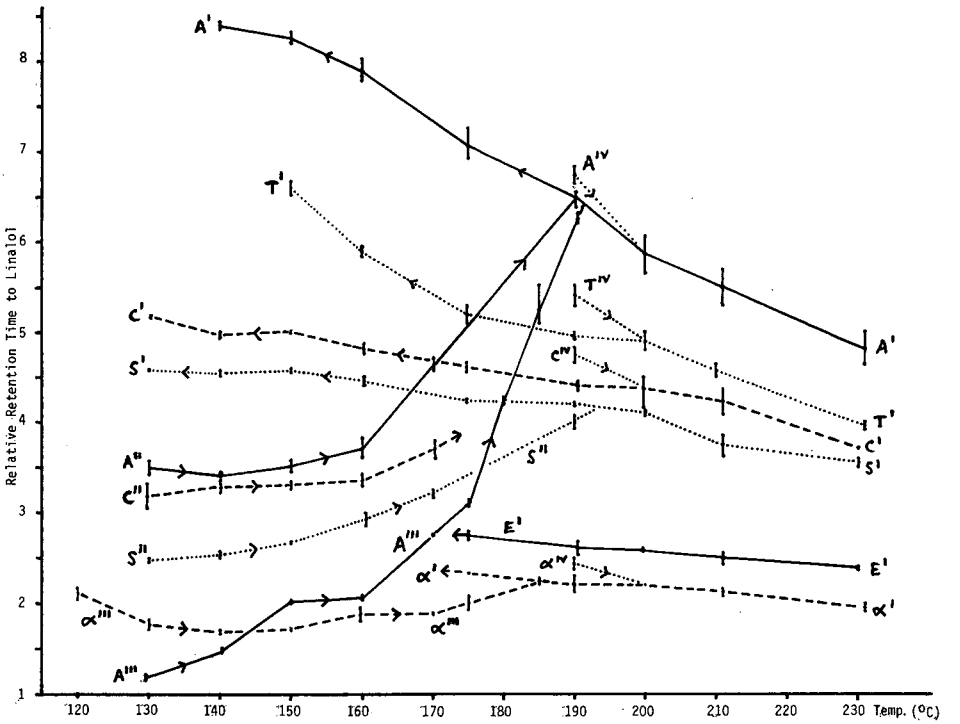

Fig. 2. As for Fig. 1. A = Anethole; C = cuminal; T = thymol. For clarity, the full results from Table I are not shown.

point. However, close agreement was observed in some cases, *e.g.*, estragole at 160°C. Celsius rather than absolute temperatures were used as being more practical for chromatographers.

In Table I, some aromatic substances always emerge in the same sequence: estragole (quickest)–safrole–cuminal–thymol (slowest). The positions of α-terpineol and anethole change in relation to this sequence, and are noteworthy.

Fig. 1 displays average results for the linear aromatic substance estragole, which typify the characteristics of this $(MBT)_2$ liquid crystal column. A newly prepared, never-before heated column behaves in a different way from one which has been used above the melting point of the liquid crystal. At temperatures up to about 150°C with the new column, estragole shows shorter retention time than linalol, slowly increasing to about 170°C, after which retention quickly increases to almost three times that of linalol by 185°C. It then settles down with further temperature increase to about 2.6–2.4 times the retention of linalol. If the liquid crystal column is now cooled, estragole retention time gradually increases to about 2.8 times linalol from 175 down to 140°C, below which temperature estragole retention decreases towards that of linalol at about 85°C. Either this procedure, or just cooling overnight, gives a return to initial lower relative retention times, but not to the 'naive' values below unity seen with the freshly prepared column. These very low values cannot be obtained again, even though the column is kept in a freezer for 16 h. Retention times

in the 'mature' used column are more than 1.4 times linalol from 120°C up, rising to more than two times at 170°C before climbing to the levels given above. This suggests that the effect of estragole on the melting point of this liquid crystal on the GC support is apparent from 170°C or less, and below its melting-point-apparatus value (179°C). If the liquid crystal column is pre-heated at 210°C, and the relative retention time of estragole observed with gradual increase of temperature from 170°C, there is a slight increase in value at 180°C, confirming this as the melting point. Near this temperature, estragole, like most of the solutes studied, sometimes gave relative retention times above the normal. They are shown in Table I and Figs. 1 and 2. With estragole and α-terpineol these occurred at the liquid crystal melting point, but above this with other solutes, at 190°C.

The propenyl isomer of estragole, anethole, shows a more extreme form of this cycle of behaviour (Fig. 2). The naive column at 130–160°C shows retention times for anethole just over one to two times linalol, rising quite sharply then to over six times linalol at 190°C. Retention now drops away, with further temperature increase, to less than five times that of linalol at 230°C. Cooling this hot column gives an increase in relative retention times to over eight, below 155°C. With the 'mature' column left to cool overnight, the 'unmelted' liquid crystal now gives initial relative retention times increased to about three-and-a-half from 130 to 160°C, before climbing rapidly to joint the cooling plot.

The monocyclic monoterpenoid α-terpineol (Table I and Fig. 1) shows these changes apply to this non-aromatic too, although with a shallower behaviour cycle than estragole. There is an interesting 'cross-over' response, in that with the column heated up to only 160°C or less, α-terpineol has higher retention times than estragole, as with conventional GC phases [10], but that above this temperature estragole shifts to show higher retention times which are maintained during subsequent heating and supercooling. This 'terpineol–estragole shift' is reversed if the column is cooled below 85°C, and so indicates the 'condition' of true or pseudo liquid crystal. Results in Table I show that with a 'naive' column, as well as estragole, some other aromatics like safrole and anethole, also with unbranched side chains, have shorter retention times than α-terpineol up to about 145°C, but these cannot be reobtained if the liquid crystal has been melted once.

As was previously observed with the $(MBCA)_2$ column [1], the sequence of certain aromatics above the liquid crystal melting point is estragole (always first), then safrole–thymol–anethole (last). On a polyethylene glycol column anethole precedes safrole [10]. If the liquid crystal column is not heated above 165°C, thymol is always 'conventionally' behind anethole (Table I) although safrole does not shift. This 'anethole–thymol shift' was previously detected on $(MBCA)_2$ [1], although this liquid crystal has a lower melting point than $(MBT)_2$. Only above the melting point does the matching anisole character of the liquid crystal preferentially retain anethole. This 'shift' provides a second check on the liquid crystal condition. Cuminal has a branched isopropyl side chain, like thymol, but does not show any 'shift' in the mature column. Cuminal behaves like safrole (Fig. 2), which has an allyl side chain. Oddly, this GC system seems less sensitive to injections of cuminal than of other aromatics.

An interesting observation is that thymol behaves differently to cuminal and to the other aromatic solutes studied, which must reflect not so much its molecular

TABLE I

RELATIVE RETENTION TIMES (LINALOL = 1.00)[a] ON A PACKED COLUMN OF 3% $(MBT)_2$

Mobile phase, nitrogen at a flow-rate of 7.5 to 10.0 ml min^{-1} at the flame ionisation detector outlet. Averages of two observations, or in parentheses, the number of observations made.

Solute	Nominal column temperature (°C)												
	120	130	140	150	160	170	175	180	185	190	200	210	230
After heating of liquid crystal above 190°C													
Anethole[b]			8.39	8.26	7.88 (3)		7.06 (3)			6.49 (3)	5.87 (3)	5.49 (4)	4.81 (3)
Thymol				6.60	5.88		5.19			4.95 (3)	4.90	4.57	3.96
Cuminal		5.08	4.98	5.01	4.82		4.62			4.41 (3)	4.38 (4)	4.22	3.71
Safrole		4.59	4.55	4.58	4.46		4.24			4.20	4.10	3.74 (5)	3.55
Estragole	2.60	2.77	2.85	2.83	2.80 (5)		2.75 (3)			2.61 (7)	2.58	2.49 (4)	2.38
α-Terpineol[b]	2.43	2.47	2.44	2.43 (3)	2.39 (3)		2.34			2.20 (6)	2.20	2.12 (3)	1.96
"Mature" liquid crystal heated from cold with a history of heating above 190°C													
Thymol		5.49	5.02	4.71	4.53 (3)	4.58				5.40[c]			
Anethole[b]		3.50	3.41	3.53	3.72	4.65				6.74[c]			
Cuminal		3.18	3.28 (3)	3.30	3.35	3.70				4.72[c]			
Safrole		2.47	2.53	2.67	2.93	3.21				4.00			
α-Terpineol[b]	1.90	1.90	1.92	1.94 (4)	1.94	2.03 (3)		2.47[c]					
Estragole	1.43	1.44	1.57 (3)	1.70	1.79	2.09 (3)	2.21	2.97[c]					
"Naive" liquid crystal never heated to 190°C													
Thymol				3.21	3.17 (3)	3.41	3.73						
Cuminal					2.76	2.98							
α-Terpineol[b]	2.10	1.77	1.69	1.71	1.87	1.88	2.00		2.23	2.43[c] (3)			
Anethole[b]		1.18	1.46	2.02 (3)	2.07	2.75	3.10	4.25	5.25 (3)	6.25 (4)			
Safrole	0.97	1.05	1.44	1.70	1.80	2.06	2.38	2.81					
Estragole	0.65	0.71	0.88	1.05	1.16	1.23	1.54	1.81	2.22				

[a] After subtraction of holdup time, retention times for linalol were approx. 1.0 min at 120°C (from cold), 0.25 min at 190°C, 0.1 min at 230°C; then on cooling 0.4 min at 160°C, and 1.3 min at 120°C.

[b] Anethole and α-terpineol shift in retention position in relation to the other constant solutes.

[c] These unusually high values are sometimes seen.

shape, which is like cuminal, but its polar phenolic nature. With a mature column heated from 130°C upwards there is a drop from initial high relative retention times (Table I) to a minimum at about 160°C. This is unlike the continuous slow initial increase shown by the others. Cooling from above the liquid crystal melting point gives only a limited usable temperature range for thymol down to 150°C, below which a rapid increase in relative retention time occurs. Other substances studied level off in such values at this temperature, and estragole then shows a decline at lower temperatures, as does safrole.

This $(MTB)_2$ column could certainly be used at 120°C or lower for some solutes, but gave best results for the aromatic substances studied at 130°C or above, as noted by Haky and Muschik [8]. Use above the melting point of the liquid crystal (*i.e.*, above 180°C) gave retention times that were too short, and generally best results were found on cooling down to 140–175°C after preliminary heating at 210°C. As safrole is always ahead of anethole, this indicates that the liquid crystal is not like a conventional GC stationary phase whether melted or not. This is confirmed by the terpineol–estragole and anethol–thymol shifts. Another solute shift, of anethole–terpineol, is seen only in the naive column (Fig. 2) at 145°C, and may indicate some change in the liquid crystal condition then. These pairs of substances do not occur together in natural volatile oils, and peaks from such oils can be anticipated to emerge in the sequence seen from a conventional phase. Thus, the bicyclic monoterpenoid fenchone in fennel oil appears after the monoterpene hydrocarbons present and before estragole, as usual (Fig. 3). This is an atypical oil, yielded by an unusual chemovar [11], rich in estragole.

The $(MBT)_2$ column did not yield peaks of cinnamal, eugenol or vanillin after their injection, even at 290°C, so it firmly retains some aromatics, and would be no use for analysis of cinnamon, clove or pimento oils. However, it does handle some monoterpenoids well such as the fenchone in fennel oil (Fig. 3), and it resolves α-terpineol from terpinen-4-ol (α value 1.25 or more) in tea-tree oil (Fig. 4), which is not well achieved by a programmed methylpolysiloxane capillary (α value found only 1.04). Best resolution of fenchone is obtained if the liquid crystal column is directly heated to 140°C from cold, and not melted. Similarly, the *ca.* 3% α-terpineol in tea-tree oil is better resolved from the *ca.* 40% terpinen-4-ol just preceding it on the unmelted liquid crystal at 120°C.

The liquid crystal column was evaluated for its polarity by the method in use in these laboratories [12], utilising the average of retention indices for linalol, estragol and carvone against both *n*-alkanes and *n*-alcohols. Against the standard phenylmethylpolysiloxane-packed column the liquid crystal gave a value of −41 when heated (as a 'mature' column) from ambient conditions to 160°C; then only −24 when cooled to 160°C from 230°C. These values are between those of a fully methylpolysiloxane column and the standard column, so this liquid crystal behaves as a non-polar GC phase which becomes less non-polar after heating above its melting point. This agrees with the observations of Isenberg *et al.* [13], who found that some di-ester aromatic liquid crystals "correspond to silicone phases of low polarity" using Rohrschneider solute probes.

The $(MBT)_2$ was clearly a better liquid crystal column than the previously used $(MBCA)_2$ [1] for the GC analysis of many volatile oils, due to its higher melting point allowing the use of a range of temperatures below this, both cooled from above it, or

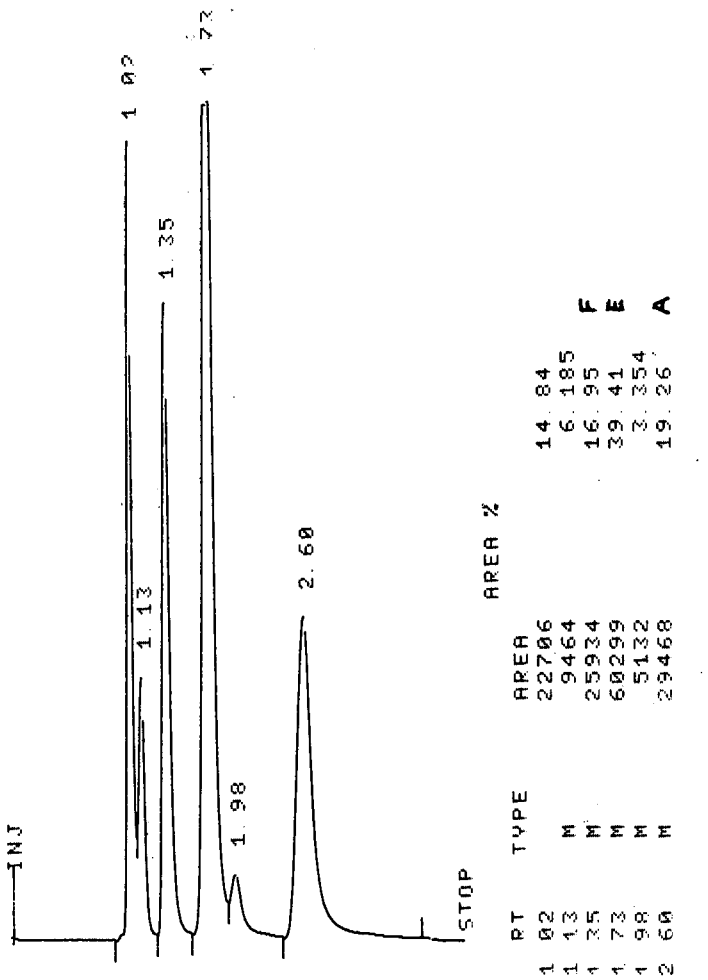

Fig. 3. Gas chromatogram of Western Australian fennel oil on $(MTB)_2$ at 140°C on a mature liquid crystal heated from cold. A = Anethole; E = estragole; F = fenchone. Early peaks are monoterpene hydrocarbons. RT = Retention time in minutes; type = peak merged (M) with previous one and tangent (T) skimmed baseline; area% given at right.

heated from ambient conditions. From the different sequences of the substances indicated in Table I, three different separation mechanisms may be involved, depending on the liquid crystal column temperature and its history. After the liquid crystal has melted, it is able to 'supercool' to a considerable extent due to interaction with the column support [3,8]. The lower temperature use of this column is restricted more by excessively long retention times producing broad peaks than by any sudden change in physical condition by the liquid crystal. Before melting, it is still a useful GC stationary phase, and we suggest that the moving band of solute traversing the column is able to form a temporary eutectic liquid mixture with the unmelted liquid crystal. If it has been previously heated above its melting point, the liquid crystal has left a more

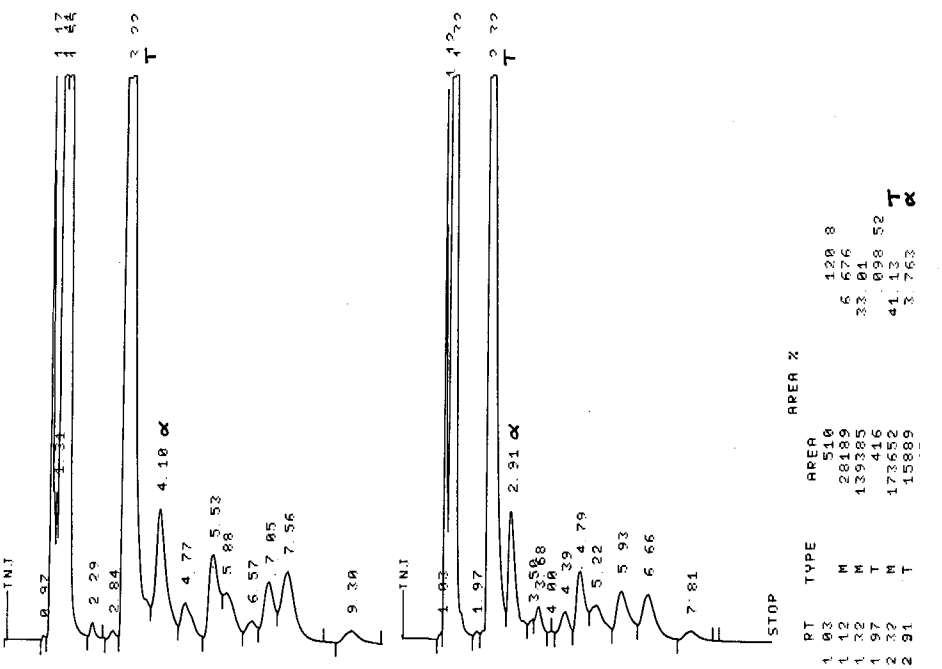

Fig. 4. Gas chromatograms of Australian tea-tree oil on $(MBT)_2$. Left: 120°C after 'supercooling' from 210°C (no printout). Right: 120°C on a mature liquid crystal heated from cold. α = α-Terpineol; T = terpinen-4-ol. Early peaks are monoterpene hydrocarbons, particularly terpinenes. See Fig. 3 for abbreviations. The complete area% printout is not shown, and at the temperature used *ca.* 5% of slow-moving oil constituents are retained on the liquid crystal.

organised stationary phase than that in a never-melted column, and this resembles the true liquid crystal condition during the transient eutectic state with passing bands of estragole, safrole, cuminal and thymol, although not for α-terpineol or anethole. If an 'overload' of a solute is injected it usually gives a delay in retention, as seen on conventional GC phases, when the liquid crystal has not been heated to its melting point. If this occurs after melting, the 'overload' causes a decrease in retention, typical of liquid crystals. This was noted by Betts [1] on another liquid crystal.

A general conclusion from this is that, for GC work, the nematic temperature range of a liquid crystal (from its melting point, to when it becomes a normal isotropic liquid) is irrelevant, as it functions well at lower temperatures. More important to the analyst is knowledge of the particular behaviour of each test solute on the liquid crystal, and details of 'solute shifts' which indicate a change of liquid crystal condition. There should be no hesitation in using a liquid crystal column below its melting point, although temperatures approaching the melting point in a column heated from cold should be avoided, as relative retention times can undergo rapid increase.

ACKNOWLEDGEMENT

Thanks to Mr. B. MacKinnon for preparing the liquid crystal columns.

REFERENCES

1 T. J. Betts, *J. Chromatogr.*, 513 (1990) 311.
2 M. J. S. Dewar and J. P. Schroeder, *J. Am. Chem. Soc.*, 86 (1964) 5235.
3 E. M. Barrall, R. S. Porter and J. F. Johnson, *J. Chromatogr.*, 21 (1966) 392.
4 G. Osterhelt, P. Maragg, R. Rueher and A. Germann, *J. Chromatogr.*, 234 (1982) 99.
5 K. P. Naikwadi, S. Rokushika, H. Hatano and M. Ohshima, *J. Chromatogr.*, 331 (1985) 69.
6 R. Lester and D. R. Hall, *J. Chromatogr.*, 190 (1980) 35.
7 S. Wasik and S. Chesler, *J. Chromatogr.*, 122 (1976) 451.
8 J. E. Haky and G. M. Muschik, *J. Chromatogr.*, 238 (1982) 367.
9 Z. Witkiewicz and A. Waclawczyk, *J. Chromatogr.*,173 (1979) 43.
10 P. N. Breckler and T. J. Betts, *J. Chromatogr.*, 53 (1970) 163.
11 T. J. Betts, *Austr. J. Pharm. Sci.*, 5 (1976) 78.
12 T. J. Betts, K. A. Allan and C. A. Donovan, *J. Chromatogr.*, 291 (1984) 361.
13 A. Isenberg, G. Kraus and H. Zaschke, *J. Chromatogr.*, 292 (1984) 67.

Journal of Chromatography, 547 (1991) 345–353
Elsevier Science Publishers B.V., Amsterdam

CHROM. 23 258

Determination of carbaryl and 1-naphthol in English apples and strawberries by combined gas chromatography–fluorescence spectrometry

H. BAGHERI and C. S. CREASER*
School of Chemical Sciences, University of East Anglia, Norwich NR4 7TJ (UK)
(First received November 20th, 1990; revised manuscript received March 5th, 1991)

ABSTRACT

A rapid and selective method is reported for the determination of carbaryl (1-naphthalenol methyl carbamate) and its hydrolysis product, 1-naphthol, using combined gas chromatography–fluorescence spectrometry (GC–FS). The title compounds were detected and quantified as 1-methoxynaphthalene (λ_{ex} 282 nm, λ_{em} 334 nm) after derivatisation with trimethyl anilinium hydroxide. The method has been demonstrated for the analysis of English apples and strawberries. The limit of detection for carbaryl by GC–FS was 0.14 mg kg^{-1}.

INTRODUCTION

N-methyl carbamates are widely used as insecticides and maximum residue limits for carbaryl (1-naphthalenol methyl carbamate, **I**) in fruit and vegetables in the UK range from 0.2 to 10 mg/kg. A fast and efficient method for monitoring residues of these compounds in different agricultural products is therefore required. Carbamate pesticides have been determined using a variety of methods including gas chromatography (GC) [1–18], high-performance liquid chromatography (HPLC) [19–21] and combinations of these techniques with mass spectrometry [22–24]. Multiple residue methods for liquid chromatographic determination of N-methyl carbamates in crops [25], fruits and vegetables [26] have also been reported.

Ebing [1] reported that N-monomethyl carbamates were unstable during GC and carbaryl, which falls in this category, was degraded to 1-naphthol at a column temperature of 240°C. Nevertheless the direct GC detection of the intact carbamate has been carried out by minimising the effects of thermal instability and column substrate interaction [2,3], although some carbamate decomposition can occur even with careful selection of column conditions. The instability of the carbamates led to the development of thermally stable derivatives for quantitative gas chromatographic analysis. The trimethylsilyl (TMS) derivatives of several carbamates were prepared by Fishbein and Zielinski [4], by reaction with hexamethyldisilazane in pyridine in the presence of trimethylchlorosilane. Low levels of carbamates have also been measured by GC with electron-capture detection as N-perfluoroacyl [5] and N-trifluoroacetyl

0021-9673/91/$03.50

[6] derivatives. These derivatization procedures were applied to the detection of either the methyl amine moiety [7–11] or the liberated phenol moiety [12–16] of N-methylcarbamates. On-column transesterification of N-methylcarbamate with methanolic sodium hydroxide was investigated by Moye [17], who used a nitrogen/phosphorus detector to analyse mobam extracted from lettuce. Bowman and Beroza [18] hydrolysed carbaryl completely to 1-naphthol. They determined carbaryl (as 1-naphthol) in grass and milk using packed column GC combined with solution-phase fluorimetry.

The application of combined gas chromatography–vapour-phase fluorescence spectrometry has been demonstrated for the determination of polycyclic aromatic hydrocarbons [27,28] and the indirect detection of fluorescence quenchers [29]. In this paper, we report a rapid method for the determination of carbaryl, and its hydrolysis product 1-naphthol, as 1-methoxynaphthalene using combined gas chromatography–fluorescence spectrometry (GC–FS). The method is demonstrated for the analysis of English apples and strawberries.

EXPERIMENTAL

Instrumentation

A Perkin Elmer LS-5 luminescence spectrometer was interfaced to a Pye 104 gas chromatograph using a heated transfer line [27,28,30]. The column effluent was passed to a heated quartz flow cell (48 μl) via a zero dead volume coupling (SGE) located inside the oven of the gas chromatograph, and a length of fused-silica capillary tubing (60 cm × 0.3 mm I.D.) contained in the transfer line. A wide bore capillary column adaptor (SGE) was fitted to the injection port of the gas chromatograph. The column (25 m × 0.53 mm I.D. BP-5, SGE) was maintained isothermally at 170°C or programmed from 50°C to 180°C at 6°C min^{-1}, the transfer line at 200°C, the flow cell at 160°C and the injector at 235°C. The column head pressure was set at 53 kPa of oxygen free nitrogen. Data acquisition and processing was carried out using a Philips 3105 data station with Chromate PC software. The fluorescence spectrometer was operated in the time-drive mode for chromatographic analysis, with slit widths set to 15 and 20 nm at the excitation and emission monochromators respectively. Vapour-phase fluorescence excitation and emission spectra were recorded by the method described previously [30].

Reagents

The solvents, methanol (Fisons), chloroform (May & Baker) and dichloromethane (Fisons), were of HPLC grade, Analar and Pesticide grade respectively. Carbaryl (Prochem), 1-naphthol (Interchem) and 1-methoxynaphthalene (Aldrich) were obtained at 98% purity or better. Trimethylanilinium hydroxide (Methelute®) was purchased as a 0.2 *M* methanolic solution from Pierce.

Sample preparation and extraction

Apples (250–300 g) were chopped and blended with 100 ml Analar water, to form a homogenous mixture. Approximately 60 g of the resulting aqueous slurry (equivalent to 45–50 g of apple) was transfered to a 750-ml conical flask containing 50 grams of anhydrous sodium sulphate. To this slurry was added 150 ml of chloroform and the mixture was vigorously shaken for 10 min, before being filtered through

Whatman No. 1 paper. Four drops of diethylene glycol were added to the extract and the chloroform was removed by evaporation in a stream of dry air at room temperature. The residue was diluted to 1 ml with methanol. For the recovery experiments, the apple mixture was fortified with 1 ml of a 275-μg/ml solution of carbaryl in chloroform prior to extraction. Carbaryl and its hydrolysis product 1-naphthol were determined individually after separation by column liquid chromatography [31]. A 30 cm × 20 mm I.D. column was packed from the bottom with 5 g of anhydrous sodium sulphate, 10 g of alumina (70–230 mesh) and 10 g of anhydrous sodium sulphate. The column was prewashed with 50 ml of chloroform and the eluate discarded. A volume of 60 ml of the chloroform extract was added to the column and the carbaryl eluted with an additional 50 ml solvent to give a total volume of 110 ml. The column was then washed with 100 ml of methanol to elute the 1-naphthol. Four drops of diethylene glycol were added to the chloroform fraction, and the mixture was concentrated to near dryness. The residue was diluted to 1 ml with methanol. The methanol fraction was transferred to a 500-ml separatory funnel containing 50 ml of saturated aqueous sodium chloride. The container was washed with Analar water, and the washings were added to the separatory funnel. This solution was extracted twice with 100 ml of dichloromethane, and the extract dried through a plug of anhydrous sodium sulphate (3.5 cm × 2 cm I.D.). Four drops of diethylene glycol were added, the dichloromethane was removed and the residue dissolved in 1 ml of methanol.

Strawberry samples (150 g) were blended with 50 ml Analar water and 66 g of the resulting slurry (equivalent to 50 g strawberries) was extracted and pretreated by the same procedure as that used for apple.

Methylation procedure

A volume of 25 μl methelute (0.2 *M* trimethylanilinum hydroxide, TMAH, in methanol) was added to 50 μl of methanol extract and the mixture was shaken for a few seconds. Aliquots of 1.5 μl of each mixture were analysed directly by GC–FS.

RESULTS AND DISCUSSION

The fluorescence excitation and emission spectra of carbaryl in 95% ethanol solution show maximum intensity at 285 nm and 340 nm respectively, whilst for the hydrolysis product, 1-naphthol, the maximum excitation and emission wavelengths are shifted toward the red (λ_{ex} = 306 nm, λ_{em} = 362 nm) [32]. However, the vapour-phase fluorescence excitation and emission maxima of carbaryl in nitrogen at 160°C (λ_{ex} = 283 nm, λ_{em} = 338 nm) were found to be identical to that of 1-naphthol (Fig. 1a), probably as a result of the decomposition of carbaryl to 1-naphthol at high temperature in the vapour-phase. The difference between the maximum excitation and emission wavelengths of 1-naphthol on going from solution (95% ethanol) to vapour (nitrogen) may be attributed to matrix effects. Fluorescence excitation and emission wavelengths were therefore set at 283 nm and 338 nm respectively for the detection of 1-naphthol and carbaryl (Table I).

The direct analysis of carbaryl by GC with vapor-phase fluorescence detection yields two chromatographic peaks with retention times of 20.3 and 35.4 min (Fig. 2a). The longer retention time peak is assigned to the intact carbaryl, while the peak at 20.3 min arises from thermal decomposition of a portion of carbaryl (approximately

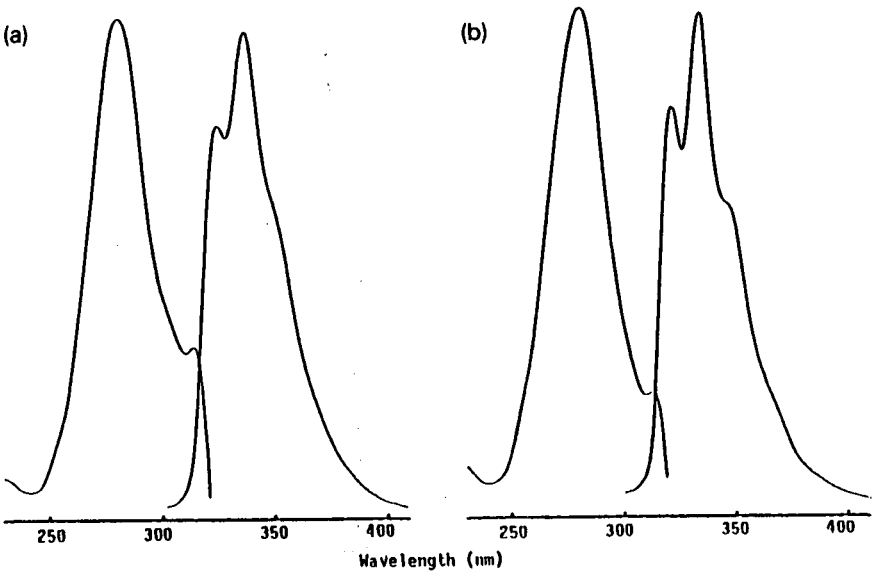

Fig. 1. Vapour-phase fluorescence excitation and emission spectra of (a) 1-naphthol and (b) 1-methoxynaphthalene.

45%) to 1-naphthol during GC (injector temperature at 235°C). The thermal decomposition of carbaryl to 1-naphthol, the high limit of detrection (115 ng) and long retention time (35 min) therefore make the direct determination of carbaryl at residue levels unreliable.

The possibility of the detection of intact carbaryl using cold on-column injection (temperature programming 50–180°C at 6°C/min) was investigated, using the combined GC–FS technique, but carbaryl was still partially hydrolysed to 1-naphthol under these conditions. Lowering the flow cell and transfer line temperatures resulted in increased tailing of the carbaryl peak with little change in the decomposition to 1-naphthol. However, quantitative conversion of carbaryl to the 1-naphthol was ob-

TABLE I

CHROMATOGRAPHIC AND VAPOUR-PHASE FLUORESCENCE CHARACTERISTICS FOR CARBARYL, 1-NAPHTHOL AND 1-METHOXYNAPHTHALENE

Compound	Retention time (t_R, min:s)[a]	limit of detection (LOD) (ng)	Tailing factor (TF)	$\lambda_{ex}/\lambda_{em}$
Carbaryl	35:42	115	1.6	283/338[b]
1-Naphthol	20:30	7.5	1.6	283/338
1-Methoxynaphthalene	19:18	2.5	1.1	282/334

[a] Conditions: temperature programming from 50 to 180°C at 6°C/min.
[b] Possible decomposition of carbaryl to 1-naphthol in the vapour phase.

served when a small piece of glass wool was inserted into the hot capillary injector. Fig. 2a and b compares the chromatograms obtained from the analysis of a carbaryl solution (λ_{ex} 283 nm, λ_{em} 338 nm) with, and without the presence of the glass wool in

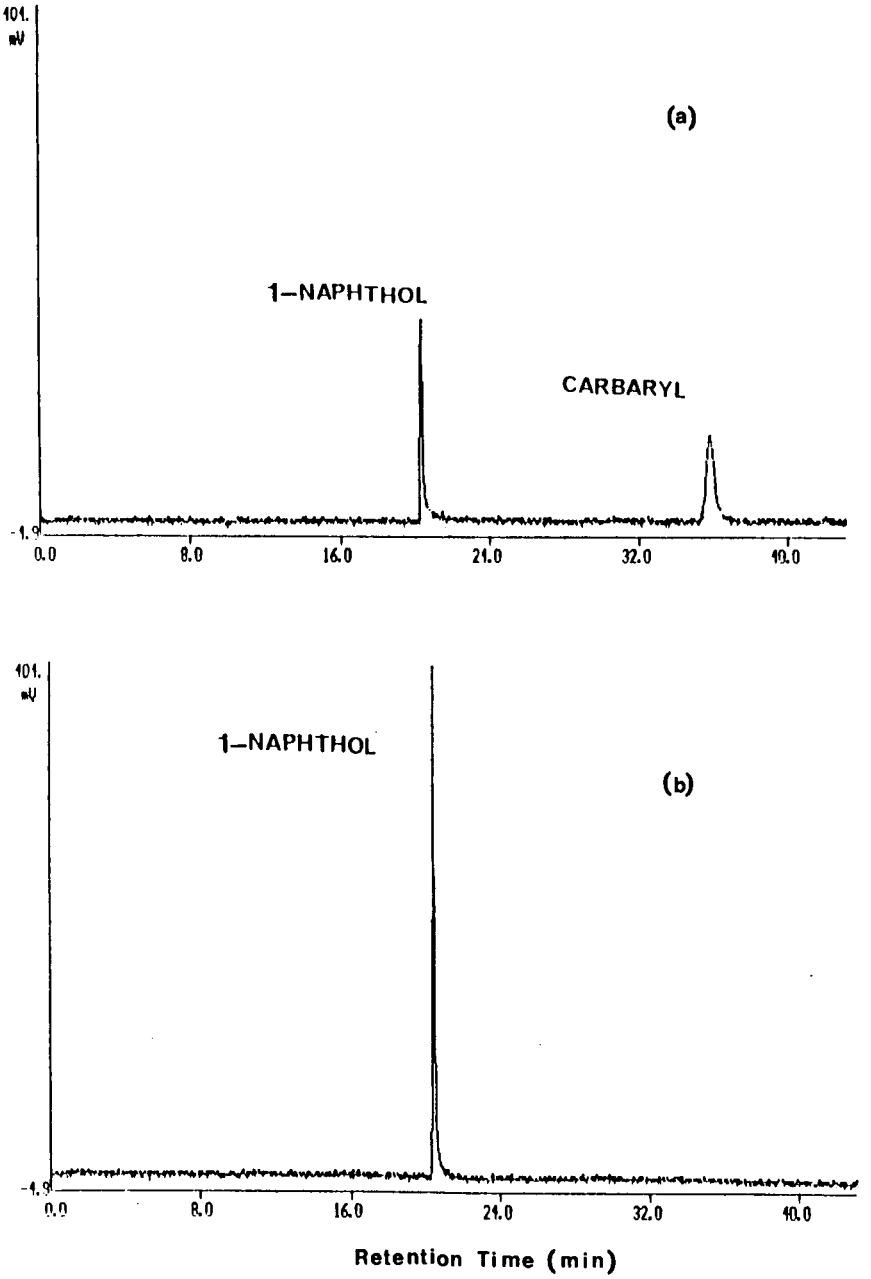

Fig. 2. GC–FS chromatograms of carbaryl without (a) and with (b) glass wool in the injector port (λ_{ex} 283 nm, λ_{em} 338 nm). Conditions: temperature programmed from 50°C at 6°C/min to a final temperature of 180°C.

the hot injector. A similar result was obtained by Bowman and Beroza [18] using a short plug containing 85% phosphoric acid at the head of a packed GC column. This suggested a convenient method for the determination of carbaryl after complete hydrolysis.

The thermal methylation of N-methyl and N-aryl carbamates with TMAH was investigated by Wien and Tanaka [33]. The reaction of N-aryl carbamates containing a single N–H group (*e.g.* propham) yielded the thermally stable N-methyl analogue, but the product of the thermal reaction of N-methyl carbamates (*e.g.* carbaryl) with TMAH was the aryl methyl ether. The methylation of 1-naphthol following carbaryl hydrolysis was therefore investigated for the detection of carbaryl as 1-methoxynaphthalene by GC–FS.

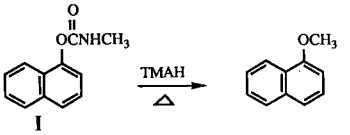

I

The vapour-phase fluorescence spectrum of 1-methoxynaphthalene shows maximum excitation and emission wavelengths at 282 and 334 nm (Fig. 1b) which were selected for subsequent quantitative detection. Table I gives data on retention times, limits of detection, tailing factors and maximum fluorescence excitation and emission wavelengths for carbaryl, 1-naphthol and 1-methoxynaphthalene. The limit of detection for 1-methoxynaphthalene (2.5 ng) was found to be lower than for 1-naphthol (7.5 ng) and a much improved peak shape was observed. A wide linear range for the detection of 1-methoxynaphthalene from the carbaryl/TMAH reaction (0.010–6.8 μg) was established.

The apple and strawberry extracts were prepared by a simple homogenisation and extraction procedure and the resulting methanol solution (1 ml) was mixed with the TMAH derivatizing reagent immediately prior to analysis by GC–FS. Detection of total carbaryl and 1-naphthol, as 1-methoxynaphthalene (λ_{ex} 282 nm, λ_{em} 334 nm) in a strawberry extract fortified with carbaryl (5.5 ppm) is shown in Fig. 3. The first peak is due to the presence of N,N-dimethylaniline from the derivatizing reagent, which fluoresces strongly, whilst the peak at 4:06 min arises from 1-methoxynaphthalene. This confirms the high selectivity of combined GC–FS for the rapid screening of total carbaryl/1-naphthol in sample extracts without pre-treatment. In order to quantify carbaryl and 1-naphthol separately in the apple and strawberry samples, 1-naphthol and carbaryl were separated on alumina using the method of Bowman and Beroza [31]. The analytical method recoveries for spiked samples of English apples and strawberries are given in Table II. The coefficients of variation (C.V.) for carbaryl and 1-naphthol are 11% and 8%, respectively. The results obtained from samples fortified with carbaryl and 1-naphthol at the 5.5-ppm level indicated that a total of 110 ml of chloroform (rather than 160 ml [31]) was sufficient to elute the carbaryl. A low recovery (31%) was observed for 1-naphthol for the apple samples, which may arise either from incomplete extraction or losses during the evaporation process. Recoveries of 73–78% have been reported [18] for 1-naphthol in milk which were lower than those for carbaryl (95–100%). Recoveries from corn samples were 89–93% and 16–34% for carbaryl and 1-naphthol, respectively. This indicates that the recovery is matrix dependent and varies between different samples. The recovery of

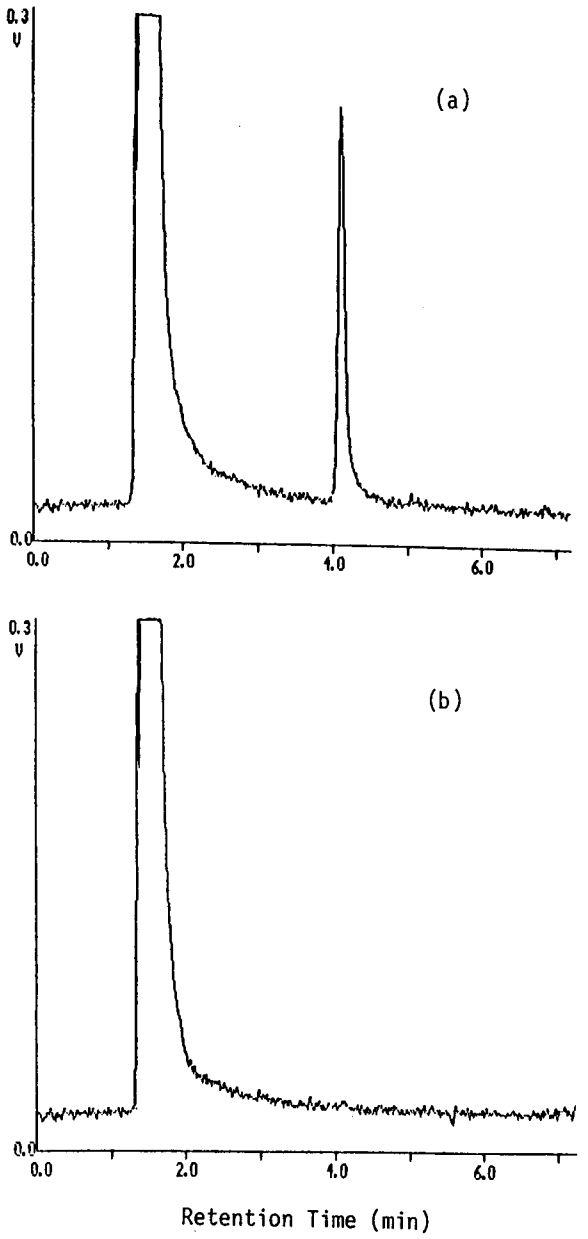

Fig. 3. Detection of carbaryl as 1-methoxynaphthalene in crude strawberry extract sample by GC–FS. (a) Sample spiked at 5.5 ppm, (b) unspiked sample; λ_{ex} 282 nm, λ_{em} 334 nm. Conditions: isothermal at 170°C.

TABLE II

RECOVERIES FOR CARBARYL AND 1-NAPHTHOL IN ENGLISH APPLES AND STRAWBERRIES USING GC–FS DETECTION

Compound[a]	Amount added (μg)	Amount recovered (μg)		Recovery (%)	
		Apple	Strawberry	Apple	Strawberry
Carbaryl	275 (5.5 ppm)	212	198	77	72
1-Naphthol	260 (5.5 ppm)	81	156	31	60

[a] Detected as 1-methoxynaphthalene (λ_{ex} 282 nm, λ_{em} 334 nm).

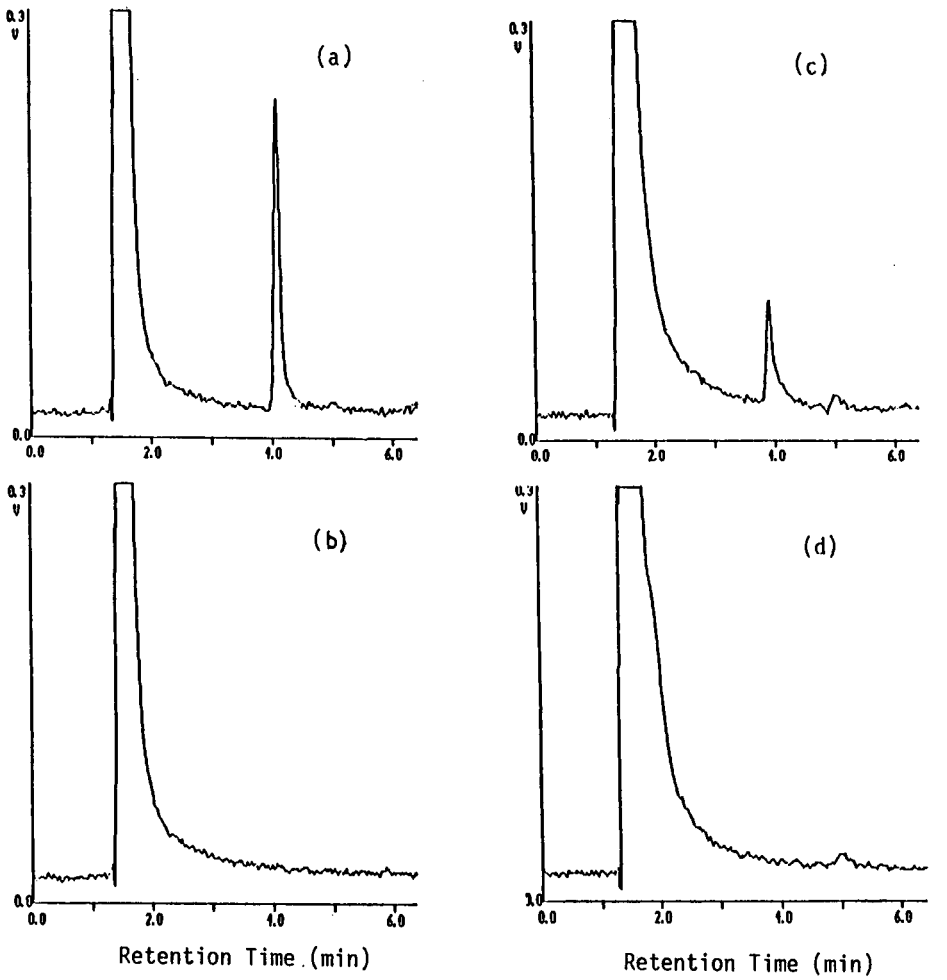

Fig. 4. Detection of carbaryl (a: spike, b: sample) and 1-naphthol (c: spike, d: sample) as 1-methoxynaphthalene in apple extract by GC–FS (λ_{ex} 282 nm, λ_{em} 334 nm). Conditions: isothermal at 170°C.

carbaryl from both fruit extracts is, however, satisfactory (>70%). The chromatograms obtained from the GC–FS analysis of an apple sample are shown in Fig. 4. The presence of carbaryl and 1-naphthol in this sample is not confirmed (Fig. 4b and d), although their levels may be below the GC–FS limit of detection (0.14 ppm). Samples spiked at the 5.5-ppm level were easily detected without interference (Fig. 4a and c). Maximum residue limits (MRL) for apple and strawberry in the UK are 5 and 7 mg/kg respectively.

The quantitative determination of carbaryl and 1-naphthol in real samples can be carried out with high sensitivity and selectivity using the combined GC–FS technique. The extracts examined in this study show no matrix interferences and require short analysis times (< 5 min at an isothermal column temperature of 170°C), providing a rapid and novel screening procedure for total carbaryl/1-naphthol, whilst both may be determined separately after alumina column separation.

ACKNOWLEDGEMENT

The authors thank the committee of Vice Chancellors and Principals for an ORS award to H.B.

REFERENCES

1 W. Ebing, *Chimia*, 19 (1965) 501.
2 L. Wheeler and A. Strother, *J. Chromatogr.*, 45 (1969) 362.
3 E. J. Lorah and D. D. Hemphill, *J. Assoc. Off. Anal. Chem.*, 57 (1974) 570.
4 L. Fishbein and W. L. Zielinski, *J. Chromatogr.*, 20 (1965) 9.
5 J. N. Seiber, *J. Agric. Food Chem.*, 20 (1972) 443.
6 L. Wong and F. M. Fisher, *J. Agric. Food Chem.*, 23 (1975) 315.
7 I. C. Cohen and B. B. Wheals, *J. Chromatogr.*, 43 (1969) 233.
8 E. R. Holden, *J. Agric. Food Chem.*, 56 (1973) 713.
9 C. E. Mendoza and J. B. Shields, *J. Agric. Food Chem.*, 22 (1974) 255.
10 R. L. Tilden and C. H. Van Middelem, *J. Agric. Food Chem.*, 18 (1970) 154.
11 D. G. Crosby and J. B. Bowers, *J. Agric. Food Chem.*, 16 (1968) 839.
12 M. C. Bowman and M. Beroza, *J. Assoc. Off. Anal. Chem.*, 50 (1967) 926.
13 L. I. Bulter and L. M. McDonough, *J. Agric. Food Chem.*, 16 (1968) 403.
14 C. W. Stanely, J. S. Thornton and D. B. Katague, *J. Agric. Food Chem.*, 20 (1972) 1265.
15 I. C. Cohen, J. Norcup, J. H. A. Ruzicka and B. B. Wheals, *J. Chromatogr.*, 44 (1969) 251.
16 J. N. Seiber, D. G. Crosby, H. Fouda and C. J. Soderquist, *J. Chromatogr.*, 73 (1972) 89.
17 H. A. Moye, *J. Agric. Food Chem.*, 19 (1971) 452.
18 M. C. Bowman and M. Beroza, *Anal. Chem.*, 40 (1968) 535.
19 R. T. Krause, *J. Chromatogr. Sci.*, 16 (1978) 281.
20 R. T. Krause, *J. Chromatogr.*, 185 (1979) 615.
21 K. M. Hill, R. H. Hollowell and L. A. DalCortivo, *Anal. Chem.*, 56 (1984) 2465.
22 B. S. Clegg and R. Frank, *J. Agric. Food Chem.*, 36 (1988) 502.
23 G. C. Mattern, G. M. Singer, J. Louis, M. Robson and J. D. Rosen, *J. Agric. Food Chem.*, 38 (1990) 402.
24 K. S. Chiu, A. Van Langenhove and C. Tanaka, *Biomed. Environ. Mass Spectrom.*, 18 (1989) 200.
25 R. T. Krause, *J. Assoc. Off. Anal. Chem.*, 63 (1980) 1114.
26 D. Chaput, *J. Assoc. Off. Anal. Chem.*, 71 (1988) 542.
27 H. Bagheri and C. S. Creaser, *Analyst*, 113 (1988) 1175.
28 H. Bagheri and C. S. Creaser, in C. S. Creaser and A. M. C. Davis (Editors), *Analytical Application of Spectroscopy*, Royal Society of Chemistry, London, 1988, p. 388.
29 H. Bagheri and C. S. Creaser, *Anal. Chimica Acta*, 233 (1990) 303.
30 C. S. Creaser and A. Stafford, *Analyst (London)*, 112 (1987) 423.
31 M. C. Bowman and M. Beroza, *J. Agric. Food Chem.*, 15 (1967) 894.
32 M. C. Bowman and M. Beroza, *Residue Rev.*, 17 (1967) 23.
33 R. G. Wien and F. S. Tanaka, *J. Chromatogr.*, 130 (1977) 55.

Journal of Chromatography, 547 (1991) 355–365
Elsevier Science Publishers B.V., Amsterdam

CHROM. 23 301

Gas chromatographic system for the identification of halogenated pesticides by retention indices using *n*-alkanes as standards

MAURO DE PAOLI and MARIA TACCHEO-BARBINA
Regional Centre for the Experimental Agriculture of Friuli-Venezia Giulia, Via Sabbatini 5, I-33050 Pozzuolo del Friuli (Italy)
and
GINO BONTEMPELLI*
Institute of Chemistry, University of Udine, Via Cotonificio 108, I-33100 Udine (Italy)
(First received November 28th, 1990; revised manuscript received March 15th, 1991)

ABSTRACT

A gas chromatographic system for the evaluation of linear temperature-programmed retention indices allowing *n*-alkanes to be adopted as the reference retention markers for any type of analyte, irrespective of the atoms present in their molecules, is described. It is based on the simultaneous use of two different detectors (a flame ionization detector and a specific detector suitable for the sample components), both connected (in parallel) to the same column outlet. The performance of this system has been tested by measuring the retention indices of fifteen chlorinated pesticides under conditions of linear programming temperature, by adopting an electron-capture detector as the specific detector. The reliability of the retention indices thus determined has been proven by verifying that they can be reproduced under different chromatographic conditions.

INTRODUCTION

It is a common practice in gas chromatography (GC) to perform qualitative analyses by comparing retention times (RT) or relative retention times (RRT) of unknown analytes with those of standard substances. Nevertheless, this method is adequate only for simple mixtures. As the complexity of the sample increases, analyte identification becomes more doubtful, even though the margin of uncertainty can be reduced by repeating chromatographic runs after suitable changes of either the temperature or the stationary phase or after chemical derivatization of the analytes.

A decided improvement is offered by Kováts indices [1,2] which relate retention times of unknown compounds (RT_x) to those of *n*-alkanes eluting immediately before (RT_n) and after (RT_{n+1}) them. The considerable progress made in analyte identification thanks to the adoption of these indices has been reviewed recently [3,4].

They depend only on the nature of the liquid phase employed and this is the reason why their use for the characterization of stationary phases has been suggested

0021-9673/91/$03.50

[5]. Moreover, they present a uniform scale rather than a single fixed point for comparison and can also yield supporting information on the analyte structure [6].

This notwithstanding, their use is limited by two main drawbacks which make Kováts indices inapplicable in some cases. The former is that they are defined for isothermal chromatography, *i.e.* for experimental conditions which are not the most appropriate to separate complex samples containing analytes with quite different chromatographic behaviour. The second drawback comes from the need to employ a flame ionization detector (FID) to gain a satisfactory sensitivity in the evaluation of these indices referred to *n*-alkanes, thus precluding the application of this approach to analytes detectable at trace levels only by specific detectors.

The first limitation can be overcome by using retention indices calculated under conditions of linear programming temperature [7]:

$$I_{px} = 100\left(n + \frac{T_x - T_n}{T_{n+1} - T_n}\right) \tag{1}$$

where T_x, T_n and T_{n+1} are the retention temperatures of the unknown analyte (x) and of the n-alkanes eluting immediately before (n) and after it ($n + 1$), respectively.

As a matter of fact, the application of this equation requires careful evaluation of retention temperatures, which is not a problem when retention times are linearly dependent on them. Sometimes, however, the temperature programmes installed into commercially available instruments may deviate from linearity, especially at the beginning and at the end of the temperature programme. In these cases it appears convenient to resort to a cubic spline interpolation procedure [8] of the points describing the plot of the retention temperature *versus* the retention time, by using the following equation:

$$I_{px} = I_{pn} + a(\mathrm{RT}_x - \mathrm{RT}_n) + b(\mathrm{RT}_x - \mathrm{RT}_n)^2 + c(\mathrm{RT}_x - \mathrm{RT}_n)^3 \tag{2}$$

where a, b and c are coefficients calculated by a regression program and other symbols have the meaning reported above, except for n, which indicates in this case a general term of the homologous series. This last relationship offers the additional advantage of allowing temperature-programmed retention indices (I_{px}) to be calculated directly from retention times found under conditions of linear programming temperature even when the dependence of retention times on elution temperatures is not completely linear.

To overcome the second drawback, the use as standards of series of organic compounds suitable for specific detectors, in that they contain atoms such as nitrogen [9–11], sulphur [11,12] or more hetero elements simultaneously [11], has been suggested. Such an expedient does not appear, however, as a remedy since many components of these homologous series are either not commercially available (and hence must be synthesized) or poorly stable with time (and hence cannot be stored). Moreover, these series of standards are usually chosen arbitrarily and this makes an interlaboratory comparison and transfer of the indices thus determined impractical.

This paper describes the evaluation of I_{px} by adopting n-alkanes as the retention standards for any type of unknown analytes, irrespective of the atoms contained in their molecules. These indices are acquired using a gas chromatograph equipped with

a single column but two different detectors, one of which is a FID while the other is a specific detector. The suitability of this system for the retention index evaluation under conditions of linear programming temperature has been proven for a standard mixture of fifteen chlorinated pesticides. Moreover, the possibility of reproducing the temperature-programmed retention indices obtained by this approach under different chromatographic conditions has also been considered.

EXPERIMENTAL

All samples were analyzed under temperature-programmed conditions by a Mega Series 5300 gas chromatograph (Carlo Erba, Milan, Italy) equipped with both a Model 40 FID (Carlo Erba) for standard *n*-alkanes and a Model HT25 electron-capture detector (ECD) (Carlo Erba), for chlorinated pesticides. Simultaneous detection of these two classes of compounds was accomplished by clamping an Y-shaped glass press-fit (Carlo Erba) at the end of the chromatographic column so as to split the column outlet into two equivalent channels connected to the mentioned detectors by equal 10-cm pieces of silanized fused-silica, as shown in Fig. 1.

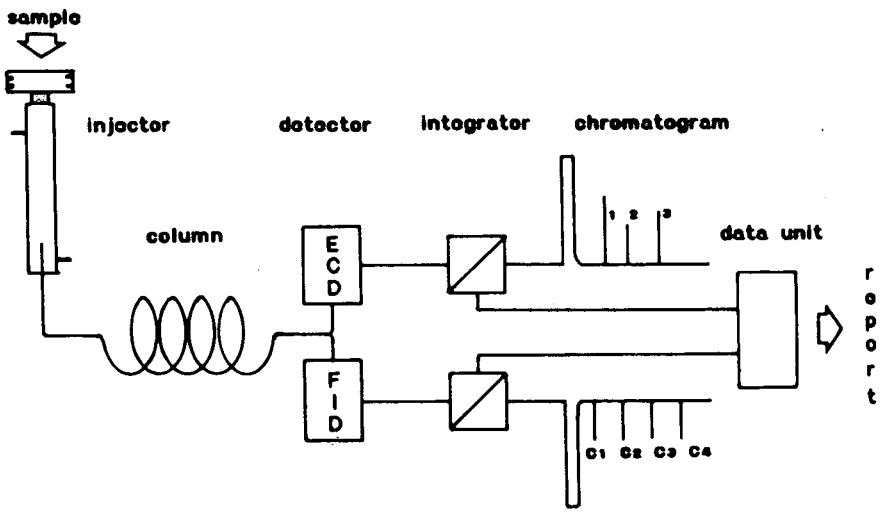

Fig. 1. Schematic view of the gas chromatographic apparatus employed.

Two 25 m × 0.32 mm I.D. methyl silicone (OV-1) on fused-silica capillary columns (Mega, Legnano, Italy) coated with different film thicknesses were employed for sample separations. Both these columns were used under different flow-rates of the carrier gas and different conditions of programming temperature. Operation parameters together with column characteristics are given in Table I.

Samples (1 μl) were introduced with a split injector maintained at 250°C (split ratio 1:20). A constant current of 200 μA with pulse duration of 0.5 μs was used for the ECD whose temperature was set at 275°C, while the temperature of the FID block was

TABLE I

OPERATION PARAMETERS AND CHARACTERISTICS OF THE TWO OV-1 CAPILLARY COLUMNS EMPLOYED, BOTH HAVING DIMENSIONS OF 25 m × 0.32 mm I.D.

Column	Operation condition	ft[a] (μm)	β[b]	fr[c] (ml/min)	t_0[d] (min)	r[e] (°C/min)	rt_0/β (°C)
A	A-a	0.10	800	1	1.6	1.5	0.0030
A	A-b	0.10	800	1	1.6	2.0	0.0040
A	A-c	0.10	800	2	0.8	1.5	0.0015
A	A-d	0.10	800	2	0.8	2.0	0.0020
B	B-a	0.15	530	1	1.6	1.0	0.0030
B	B-b	0.15	530	1	1.6	1.3	0.0040
B	B-c	0.15	530	2	0.8	1.0	0.0015
B	B-d	0.15	530	2	0.8	1.3	0.0020

[a] Film thickness of the stationary phase.
[b] Phase ratio defined as the ratio between I.D. and 2 ft.
[c] Carrier gas flow-rate.
[d] Gas hold-up time of the column measured as the methane elution time at 160°C.
[e] Temperature programme rate from 160°C (hold for 1 min) to 240°C.

set at 250°C. Data handling was performed by a dual-channel Spectra-Physics SP4270 (Santa Clara, CA, USA) integrator connected to an IBM XT computer (Valhalla, NY, USA).

Pure chlorinated pesticides were obtained from Riedel de-Häen (Seelze, Germany); their formulae, as well as their basic characteristics, are reported in Table II. Stock solutions of these test compounds were prepared at a concentration of 0.1 ppm in *n*-hexane by diluting successively the pure products, while stock mixtures of C_{11}–C_{24} n-alkanes at a concentration of 20 ppm in *n*-hexane were prepared by diluting the pure compounds obtained from Fluka Chemie (Buchs, Switzerland). These last mixtures of reference retention markers were mixed with the pesticide samples prior to chromatographic analysis.

RESULTS AND DISCUSSION

ECD and FID responses relative to each injection were simultaneously recorded by the dual-channel integrator and then compared by the connected computer so as to obtain the relevant difference, as shown in Fig. 2. This last step allowed us to show the possible coincidence of retention times for pesticides with those for the reference retention markers (see the coincidence in Fig. 2 between retention time for the alkane C_{21} and that for heptachlorepoxid). Retention indices (I_{px}) for all pesticides employed were then calculated by inserting the corresponding retention times, evaluated from chromatograms like those in Fig. 1, in a computation program written on the basis of eqn. 2 which is available on request.

In order to test the reliability of these indices, their independence from the particular chromatographic conditions employed has been verified following the criterion reported recently by Yin and Sun [13]. These authors point out that capillary columns of different sizes (length and inner diameter), working under different heating

TABLE II

CHLORINATED PESTICIDES EMPLOYED

No.	Compound	Structure	Characteristics
1.	α-1,2,3,4,5,6-Hexachlorocyclohexane (α-HCH)		Insecticide $C_6H_6Cl_6$ M = 290.83 g/mol CAS 319-84-6
2.	β-1,2,3,4,5,6-Hexachlorocyclohexane (β-HCH)		Insecticide $C_6H_6Cl_6$ M = 290.83 g/mol CAS 319-85-7
3.	Hexachlorobenzene (HCB)		Fungicide C_6Cl_6 M = 284.78 g/mol CAS 118-74-1
4.	γ-1,2,3,4,5,6-Hexachlorocyclohexane (lindane)		Insecticide $C_6H_6Cl_6$ M = 290.83 g/mol CAS 58-89-9
5.	1,4,5,6,7,8,8-Heptachloro-3a,4,7,7a-tetrahydro-4,7-methanoindene (heptachlor)		Insecticide $C_{10}H_5Cl_7$ M = 373.32 g/mol CAS 76-44-8
6.	1,2,3,4,10,10-Hexachloro-1,4,4a,5,8,8a-hexahydro-1,4-*endo-exo*-5,8-dimethanonnaphthalene (aldrin)		Insecticide $C_{12}H_8Cl_6$ M = 364.91 g/mol CAS 309-00-2
7.	1,4,5,6,7,8,8-Heptachloro-2,3- epoxy-4,7-endomethano-3a,4,7,7a-tetrahydroindene (Heptachlorepoxid)	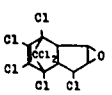	Insecticide $C_{10}H_5Cl_7O$ M = 389.32 g/mol CAS 1024-57-3
8.	2-(2-Chlorophenyl)-2-(4-chlorophenyl)-1,1-dichloroethene (2,4'-DDE)	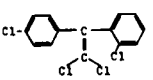	Metabolite $C_{14}H_8Cl_4$ M = 318.03 g/ml CAS 3424-82-6
9.	1,2,3,4,10,10-Hexachloro-6,7-epoxy-1,4,4a,5,6,7,8,8a-octahydro-1,4-*endo*-5,8-*exo*-dimethanonaphthalene (dieldrin)	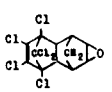	Insecticide $C_{12}H_8Cl_6O$ M = 380.91 g/mol CAS 60-57-1

(*Continued on p. 360*)

TABLE II (*continued*)

No.	Compound	Structure	Characteristics
10.	2,2-Bis-(4-chlorophenyl)-1,1-dichloroethene (4,4′-DDE)	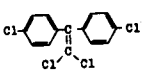	Metabolite $C_{14}H_8Cl_4$ M = 318.03 g/mol CAS 72-55-9
11.	2,(2-Chlorophenyl)-2-(4-chlorophenyl)-1,1-dichloroethane (2,4′-DDD)	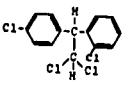	Insecticide $C_{14}H_{10}Cl_4$ M = 320.05 g/mol CAS 53-19-0
12.	1,2,3,4,10,10-Hexachloro-6,7-epoxy-1,4,4a,5,6,7,8,8a-octahydro-1,4-*endo*-*endo*-5,8-dimethanonaphthalene (endrin)	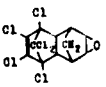	Insecticide $C_{12}H_8Cl_6O$ M = 380.91 g/mol CAS 72-20-8
13.	2-(2-Chlorophenyl)-2-(4-chlorophenyl)-1,1,1-trichloroethane (2,4′-DDT)	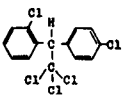	Insecticide $C_{14}H_9Cl_5$ M = 354.49 g/mol CAS 784-02-6
14.	2,2-Bis-(4-chlorophenyl)-1,1-dichloroethane (4,4′-DDD)	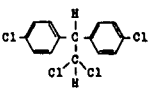	Insecticide $C_{14}H_{10}Cl_4$ M = 320.05 g/mol CAS 72-54-8
15.	2,2-Bis-(4-chlorophenyl)-1,1,1-trichloroethane (4,4′-DDT)	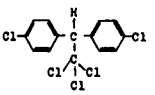	Insecticide $C_{14}H_9Cl_5$ M = 354.51 g/mol CAS 50-29-3

rates and/or carrier gas flow-rates and characterized by different phase ratios β are able to reproduce the same values of retention indices (within $\pm$ 2 index units), provided that their ratios rt_0/β are kept unchanged (the meaning of the symbols is defined in Table I).

Consequently, retention indices for the fifteen chlorinated pesticides here analyzed have been determined on two different columns (A and B in Table I) having the same size but different phase ratios β. They have been used under the different experimental conditions (*fr* and *r*) reported in Table I. Both flow-rate and temperature programme rate were chosen in such a way that same values of the ratio rt_0/β could be attained for both columns A and B.

Tables III–VI list the temperature-programmed retention indices found for all

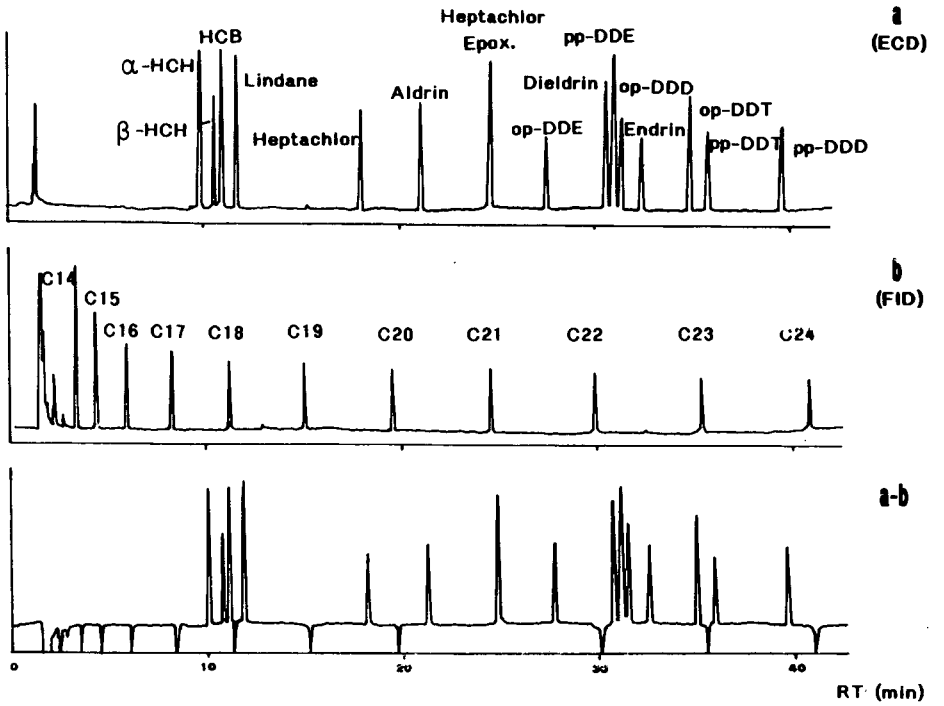

Fig. 2. Analysis of a mixture containing the fifteen chlorinated pesticides listed in Table II and the C_{11}–C_{24} reference retention markers. Gas chromatograms were recorded on the capillary column A under the experimental conditions A-c in Table I.

TABLE III

TEMPERATURE-PROGRAMMED RETENTION INDICES (I_{px}) FOUND WITH A RATIO rt_0/β = 0.0030 (OPERATION CONDITIONS A-a AND B-a IN TABLE I)

Pesticide	Column A[a] (A-a)	Column B[a] (B-a)	Difference ($I_{A\text{-}a}$–$I_{B\text{-}a}$)
1. α-HCH	1657.62 (0.14)	1657.16 (0.25)	0.46
2. β-HCH	1678.72 (0.17)	1678.74 (0.32)	−0.02
3. HCB	1690.43 (0.23)	1690.58 (0.21)	−0.15
4. Lindane	1710.92 (0.09)	1710.78 (0.07)	0.14
5. Heptachlor	1863.41 (0.27)	1862.70 (0.18)	0.71
6. Aldrin	1928.13 (0.25)	1927.87 (0.26)	0.26
7. Heptachlorepoxid	1997.42 (0.32)	1997.03 (0.09)	0.39
8. 2,4′-DDE	2053.43 (0.20)	2053.68 (0.29)	−0.25
9. Dieldrin	2107.58 (0.12)	2107.37 (0.06)	0.21
10. 4,4′-DDE	2116.56 (0.07)	2116.04 (0.05)	0.52
11. 2,4′-DDD	2122.95 (0.17)	2123.07 (0.11)	−0.12
12. Endrin	2140.77 (0.17)	2140.55 (0.09)	0.22
13. 2,4′-DDT	2186.01 (0.23)	2186.57 (0.06)	−0.56
14. 4,4′-DDD (TDE)	2202.69 (0.30)	2202.72 (0.10)	−0.03
15. 4,4′-DDT	2270.20 (0.29)	2269.95 (0.08)	0.25

[a] Mean values of five replicate measurements; standard deviation in parentheses.

TABLE IV

TEMPERATURE-PROGRAMMED RETENTION INDICES (I_{px}) FOUND WITH A RATIO $rt_0/\beta = 0.0040$ (OPERATION CONDITIONS A-b AND B-b IN TABLE I)

Pesticide	Column A[a] (A-b)	Column B[a] (B-b)	Difference ($I_{A-b}-I_{B-b}$)
1. α-HCH	1659.47 (0.67)	1658.95 (0.05)	0.52
2. β-HCH	1681.68 (0.52)	1681.66 (0.73)	0.02
3. HCB	1692.68 (0.53)	1692.71 (0.11)	−0.03
4. Lindane	1713.18 (0.43)	1713.27 (0.07)	−0.09
5. Heptachlor	1867.26 (0.35)	1866.69 (0.17)	0.57
6. Aldrin	1932.91 (0.24)	1932.73 (0.16)	0.18
7. Heptachlorepoxid	2002.67 (0.36)	2002.27 (0.19)	0.40
8. 2,4′-DDE	2057.70 (0.13)	2058.02 (0.25)	−0.32
9. Dieldrin	2114.37 (0.17)	2114.33 (0.11)	0.04
10. 4,4′-DDE	2120.93 (0.14)	2120.24 (0.06)	0.69
11. 2,4′-DDD	2127.97 (0.12)	2128.09 (0.15)	−0.12
12. Endrin	2148.33 (0.31)	2148.35 (0.13)	−0.02
13. 2,4′-DDT	2191.38 (0.28)	2191.69 (0.16)	−0.31
14. 4,4′-DDD (TDE)	2208.38 (0.36)	2208.27 (0.08)	0.11
15. 4,4′-DDT	2276.91 (0.49)	2276.81 (0.28)	0.10

[a] Mean values of five replicate measurements; standard deviation in parentheses.

TABLE V

TEMPERATURE-PROGRAMMED RETENTION INDICES (I_{px}) FOUND WITH A RATIO $rt_0/\beta = 0.0015$ (OPERATION CONDITIONS A-c AND B-c IN TABLE I)

Pesticide	Column A[a] (A-c)	Column B[a] (B-c)	Difference ($I_{A-c}-I_{B-c}$)
1. α-HCH	1655.40 (0.24)	1654.61 (0.75)	0.79
2. β-HCH	1676.31 (0.12)	1676.70 (0.17)	−0.39
3. HCB	1687.93 (0.22)	1688.22 (0.07)	−0.29
4. Lindane	1709.35 (0.05)	1709.46 (0.07)	−0.11
5. Heptachlor	1861.10 (0.33)	1860.62 (0.05)	0.48
6. Aldrin	1925.83 (0.08)	1925.43 (0.12)	0.40
7. Heptachlorepoxid	1993.13 (0.18)	1992.64 (0.11)	0.49
8. 2,4′-DDE	2050.46 (0.13)	2051.22 (0.21)	−0.76
9. Dieldrin	2104.43 (0.12)	2104.24 (0.12)	0.19
10. 4,4′-DDE	2113.18 (0.11)	2112.76 (0.09)	0.42
11. 2,4′-DDD	2118.56 (0.10)	2118.78 (0.29)	−0.22
12. Endrin	2135.27 (0.11)	2135.17 (0.06)	0.10
13. 2,4′-DDT	2180.51 (0.09)	2181.05 (0.10)	−0.54
14. 4,4′-DDD (TDE)	2196.31 (0.52)	2195.92 (0.12)	0.39
15. 4,4′-DDT	2263.77 (0.07)	2263.43 (0.45)	0.34

[a] Mean values of five replicate measurements; standard deviation in parentheses.

TABLE VI

TEMPERATURE-PROGRAMMED RETENTION INDICES (I_{px}) FOUND WITH A RATIO rt_0/β = 0.0020 (OPERATION CONDITIONS A-d AND B-d IN TABLE I)

Pesticide	Column A[a] (A-d)	Column B[a] (B-d)	Difference ($I_{A\text{-}d}-I_{B\text{-}d}$)
1. α-HCH	1657.15 (0.28)	1656.85 (0.24)	0.30
2. β-HCH	1679.10 (0.22)	1679.50 (0.60)	−0.40
3. HCB	1690.81 (0.43)	1691.04 (0.09)	−0.23
4. Lindane	1711.33 (0.30)	1711.20 (0.05)	0.13
5. Heptachlor	1865.81 (0.34)	1865.45 (0.44)	0.36
6. Aldrin	1929.71 (0.34)	1929.41 (0.46)	0.30
7. Heptachlorepoxid	1999.40 (0.44)	1998.95 (0.10)	0.45
8. 2,4′-DDE	2054.26 (0.33)	2054.76 (0.10)	−0.50
9. Dieldrin	2111.28 (0.15)	2111.04 (0.07)	0.24
10. 4,4′-DDE	2116.40 (0.09)	2115.83 (0.08)	0.57
11. 2,4′-DDD	2124.24 (0.15)	2124.26 (0.05)	−0.02
12. Endrin	2142.85 (0.16)	2143.09 (0.06)	−0.24
13. 2,4′-DDT	2186.33 (0.09)	2186.87 (0.35)	−0.54
14. 4,4′-DDD (TDE)	2202.22 (0.25)	2201.93 (0.06)	0.29
15. 4,4′-DDT	2269.69 (0.17)	2269.23 (0.51)	0.46

[a] Mean values of five replicate measurements; standard deviation in parentheses.

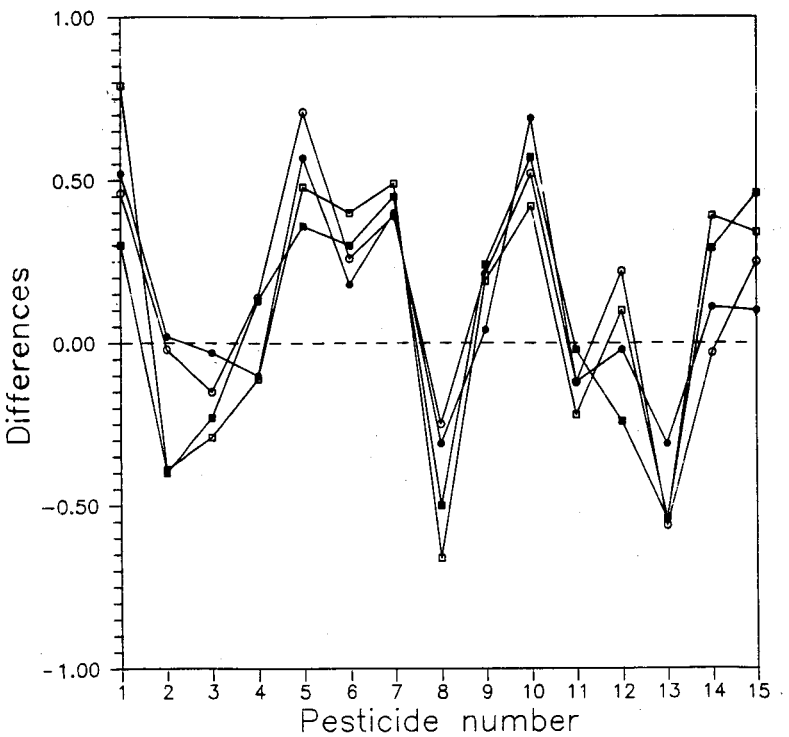

Fig. 3. Differences found between retention indices, evaluated under different operation conditions (see Table I) but with the same value of rt_0/β, plotted against the number attributed to each chlorinated pesticide in Table II. (○) $I_{A\text{-}a} - I_{B\text{-}a}$; (●) $I_{A\text{-}b} - I_{B\text{-}b}$; (□) $I_{A\text{-}c} - I_{B\text{-}c}$; (■) $I_{A\text{-}d} - I_{B\text{-}d}$.

the pesticides analyzed under the experimental conditions entailing the values of the rt_0/β parameter listed in Table I. Each of these tables reports retention indices, always calculated as the means of five replicate measurements, obtained on the two columns employed when they are characterized by the same value of rt_0/β. The quite negligible standard deviation affecting these indices shows that reproducibility is virtually the same for all pesticides analyzed.

Comparison between the indices obtained on the two chromatographic columns shows that a very small discrepancy is observed in any case which is comparable with the standard deviation peculiar to our measurements and that the I_{px} values obtained are reproduced well, within $\pm$ 1 index unit, as also shown by the plot reported in Fig. 3, giving a comprehensive view of this finding.

Such a result confirms the possibility of transferring these indices from one set of conditions to another, thus giving an indirect proof of the reliability of our approach for the evaluation of temperature-programmed retention indices.

CONCLUSIONS

The results obtained in this investigation indicate that the method of calculating retention indices under conditions of linear programming temperature based on the simultaneous and parallel use of an FID and a specific detector is an effective and profitable approach suitable for rather general applications. It allows *n*-alkanes to be adopted as the reference retention markers for any type of unknown analyte, irrespective of the atoms present in their molecules, provided that the specific detector to be coupled with an FID is chosen appropriately.

It allows retention indices of eluting components undetectable with an FID to be calculated from a single injection, without resorting to retention index standards containing specific elements. Moreover, it offers the quite important advantage over most currently employed procedures of avoiding any possible and undesired overlap of analyte peaks with peaks due to the reference markers, thus preventing the collection of unreliable responses for both identification and quantitative determination purposes.

ACKNOWLEDGEMENTS

The financial aid of the Italian National Research Council (C.N.R.) and of the Ministry of the University and of the Scientific and Technological Research (M.U.R.S.T.) is gratefully acknowledged.

REFERENCES

1 E. Kováts, *Helv. Chim. Acta*, 41 (1958) 1951.
2 E. Kováts, *Adv. Chromatogr.*, 1 (1965) 229.
3 G. Tarjan, S. Nyiredy, M. Gyor, E. R. Lombosi, T. S. Lombosi, M. V. Budshegyl, S. Y. Meszaros and J. M. Takacs, *J. Chromatogr.*, 472 (1989) 1.
4 M. B. Evans and J. K. Haken, *J. Chromatogr.*, 472 (1989) 93.
5 W. O. McReynolds, *J. Chromatogr. Sci.*, 8 (1970) 685.
6 W. O. McReynolds, *Gas Chromatographic Retention Data*, Preston Industries, Niles, IL, 5th ed., 1987.
7 H. Van Den Dool and P. D. Kratz, *J. Chromatogr.*, 11 (1963) 463.
8 W. A. Halang, R. Langlais and E. Kugler, *Anal. Chem.*, 50 (1978) 1829.

9 G. L. Hall, W. E. Whitehead, C. R. Mourer and T. Shibamoto, *J. High Resolut. Chromatogr. Chromatogr. Commun.*, 9 (1986) 266.
10 W. Vickie and F. T. Simonick, *J. Anal. Toxicol.*, 11 (1987) 210.
11 A. Manninen, M. L. Kuitunen and L. Julin, *J. Chromatogr.*, 394 (1987) 210.
12 L. N. Zotov, G. V. Golovkin and R. V. Golovnya, *J. High Resolut. Chromatogr. Chromatogr. Commun.*, 4 (1981) 6.
13 H. F. Yin and Y. L. Sun, *Chromatographia*, 29 (1990) 39.

Journal of Chromatography, 547 (1991) 367–376
Elsevier Science Publishers B.V., Amsterdam

CHROM. 23 256

Chemical characteristics of herbivore defenses in *Betula pendula* winter-dormant young stems

P. VAINIOTALO
Department of Chemistry, University of Joensuu, Box 111, SF-80101 Joensuu 10 (Finland)
R. JULKUNEN-TIITTO* and M.-R. JUNTHEIKKI
Department of Biology, University of Joensuu, Box 111, SF-80101 Joensuu 10 (Finland)
P. REICHARDT
Department of Chemistry, University of Alaska, Fairbanks, Alaska 99775-0180 (USA)
and
S. AURIOLA
Department of Pharmaceutical Chemistry, University of Kuopio, Box 6, SF-70211 Kuopio (Finland)
(First received January 9th, 1991; revised manuscript received March 1st, 1991)

ABSTRACT

Aqueous acetone-soluble phenolic glucosides, phenolic aglycones and triterpenoic components were extracted from winter-dormant *Betula pendula* twigs. The chemical composition was analyzed using gas chromatography for triterpenoids and most phenolics and high-performance liquid chromatography with ultraviolet–visible detection for phenolics, especially for platyfylloside. Gas chromatography–mass spectrometry and thermospray high-performance liquid chromatography–mass spectrometry were used for complete identification and structural elucidation. The analysis revealed five new components, salidroside, dehydrosalidroside, catechin pentoside, an isomer of catechin and deacetylpapyriferic acid, which have not previously been reported in the twigs of this species.

INTRODUCTION

In Finland, European white birch (*Betula pendula*, Betulaceae) is one economically promising deciduous tree species used in reforestation, and its demand in the plywood and pulp industry is increasing [1]. White birch is not preferred by forest owners, however, because they think it is very vulnerable to browsing mammals. Thus, to increase the distasteful or potentially toxic deterrent components in birch tissues and thereby their resistance to herbivore feeding (*e.g.* ref. 2), researchers and plant breeders have focused on the secondary phytochemicals in birch. More recently, studies on the Alaskan paper birch, *Betula resinifera*, have shown that a triterpene, papyriferic acid, is the main anti-feeding component in winter-dormant twigs [3]. On the other hand, a phenolic glucoside, platyfylloside, has been claimed to cause most of the low digestibility of *B. pendula* twigs in ruminants and to be responsible for sodium losses in hares and rabbits feeding on birch twigs [4].

In this paper we characterize phenolic and terpenoic components extracted

0021-9673/91/$03.50

from winter-dormant twigs of *B. pendula*. Our hare-feeding studies have indicated that several of these components may be negatively correlated with feeding by hares [5]. Betuloside, platyfylloside, (+)-catechin, papyriferic acid and deacetylpapyriferic acid have previously been identified by nuclear magnetic resonance (NMR) spectroscopy [4,6,7]; but there are no analytical data on papyriferic and deacetylpapyriferic acid identified by gas–liquid chromatography (GC) in any tree species. Moreover, the ultraviolet–visible (UV–VIS) spectral analysis of betuloside, platyfylloside and catechins are not found in previous publications. Throughout this study we have emphasized the use of gas chromatography–mass spectrometry (GC–MS) and thermospray high-performance liquid chromatography–mass spectrometry (HPLC–TSP-MS) systems for identification of compounds in birch. It should be noted that fragmentation routes presented are only tentative and based on the elemental principles of mass spectral fragmentations because it was not possible to perform metastable ion analyses. We describe the analysis of nine young stem components, of which four phenolic and one terpenoic phytochemical have not previously been reported in *B. pendula*.

EXPERIMENTAL

Materials

Stems from one-year-old seedlings of *B. pendula* were collected for phytochemical extractions. These seedlings were cultivated in a greenhouse on prefertilized commercial peat (VAPO) and allowed to remain in the unheated greenhouse until December in order to reach winter dormancy. The young stems were stored in sealed plastic bags at −20°C for a few months until extracted.

Equipment and chromatographic conditions

A Hewlett-Packard HPLC system (Hewlett-Packard, Avondale, PA, USA) was used which consisted of a quaternary solvent delivery system (HP 1050 Series) and an autosampler (HP 1050 Series). A photodiode array detector (HP 1040A Series) coupled with an HP data system–personal computer was used for recording chromatograms and UV–VIS spectra. The compounds were separated on a 60 mm × 4.6 mm I.D. column filled with HP Hypersil ODS II (3 μm) particles as the stationary phase. The samples were eluted (flow-rate 2 ml/min) using the gradient shown in Table I. To avoid the tailing of phenolic compounds, orthophosphoric acid was added to the solvent in order to adjust the pH to about 3. Before analysis, the samples were dissolved in water–methanol (1:1, v/v). The autoinjected volume was 10 μl. All runs were processed at the room temperature.

A capillary gas chromatograph (Hewlett-Packard Model 5890) equipped with a flame ionization detector and auto-injector (Model 7673A) was used. An OV-1 fused-silica capillary column (20 m × 0.32 mm I.D.) with a phase thickness of 0.25 μm was used throughout. The temperature programme was started at 210°C, and the temperature was raised to 318°C at a rate of 14°C/min. The detector and injector temperatures were 300 and 260°C, respectively. Helium was used as a carrier gas and the split-ratio was 1:15. The samples were derivatized with trimethylsilylimidazole in pyridine (Aldrich-Chemie, Steinheim, Germany). The sample vial was shaken vigorously for about 1 min and allowed to react for 10 h at 4°C. The autoinjected volume was 1 μl.

TABLE I

CONDITIONS USED IN HPLC GRADIENT ELUTION

Solvent A = aqueous 2% tetrahydrofuran + 0.25% orthophosphoric acid; solvent B = 100% methanol.

Time (min)	Solvent A (%)	Solvent B (%)
Initial	100	0
5	100	0
10	80	20
20	60	40
40	50	50
45	50	50
Rinsing	0	100
Equilibration	100	0

Sample preparation

Fresh-frozen stems (300–400 mg) were extracted in a clipping homogenisator three times for 5 min with 30 ml of 80% aqueous acetone (Merck, Darmstadt, Germany). The acetone was filtered, the residue washed with 20 ml of acetone and the whole extract evaporated using a vacuum evaporator. Aqueous acetone was shown to be the most effective and reproducible solvent for extracting both phenolic and terpenoic secondary components during the same extraction. Quantitatively, the solvent for slightly more complete extraction of terpenoic chemicals is 96% ethanol but it is a poor solvent for the phenolic components studied [8]. The sample was redissolved in methanol (Lab-Scan, Dublin, Ireland) and purified on Bond Elut C_{18} octadecyl (500 mg) solid-phase extraction columns. The eluent was used for HPLC, GC and GC–MS and HPLC–TSP–MS. All solvents used were HPLC grade.

Mass spectrometric measurements

GC–MS experiments were performed on a Jeol JMS D300 mass spectrometer coupled with a Carlo Erba Fractovap 4160 gas chromatograph and controlled by a Jeol JMA 2000H data system (Jeol, Tokyo, Japan). The column used was fused-silica capillary column with a chemically bonded SE-52 liquid phase (film thickness, 0.25 μm). Electron ionization spectra were obtained with an acceleration voltage of 3 kV, electron energy of 70 eV, ionization current of 300 μA and source temperature of 170°C. The following mass spectra of the trimethylsilyl (TMS) derivatives of the compounds identified were observed (m/z, relative intensity): salidroside, $M^{+\cdot}$ 660(0), 217(13), 206(9), 205(20), 204(100), 194(13), 193(67), 192(61), 147(9), 74(6), 73(53); dehydrosalidroside, $M^{+\cdot}$ 658(0), 361(11), 217(19), 206(9), 205(21), 204(100), 192(6), 191(36), 147(10), 129(14), 103(6), 73(40); betuloside, $M^{+\cdot}$ 688(0), 363(6), 362(65), 361(19), 221(15), 220(15), 206(10), 205(24), 204(100), 180(5), 179(34), 147(8), 103(8), 73(53); (+)-catechin $M^{+\cdot}$ 650(13), 383(10), 370(16), 369(34), 368(100), 357(5), 356 (12), 355(35), 297(7), 267(12), 179(8), 74(6), 73(72); pentose derivative of (+)-catechin, 577(6), 370(10), 369(20), 368(60), 355(6), 350(15), 349(33), 348(100), 283(10), 267(8), 259(11), 232(5), 218(6), 217(30), 179(5), 146(10), 129(10), 103(12), 75(6), 74(9), 73(89). Peaks with a relative intensity less than 5% are omitted. The 70-eV mass spectra of the TMS derivatives of papyriferic acid and deacetylpapyriferic acid are presented in Fig. 3 below.

The direct inlet probe at 200°C was used to introduce the isolated underivatized samples. The mass spectra obtained in this way were: papyriferic acid, $M^{+\cdot}$ 604(0), 442(8), 381(9), 191(9), 189(6), 144(10), 143(100), 135(7), 125(14), 109(6), 107(7), 95(7), 93(7), 85(14), 84(6), 81(8), 71(8), 69(7), 55(6), 44(17), 43(26); deacetylpapyfiferic acid, $M^{+\cdot}$ 562(0), 442(9), 381(8), 191(12), 189(8), 147(6), 144(10), 143(100), 135(10), 133(5), 125(17), 121(8), 119(6), 109(8), 108(5), 107(11), 105(6), 95(10), 93(10), 85(16), 84(6), 83(5), 81(11), 71(9), 69(10), 59(6), 55(8), 44(15), 43(31), 41(6).

LC–MS measurements were carried out using a VG thermospray–plasmaspray probe coupled to a VG Trio-2 quadrupole mass spectrometer. The measurements were run using the instrument in the thermospray ionization mode. The ion source temperature was 180°C, the vaporizer tip temperature 150°C and the repeller electrode potential 180 V. The HPLC system consisted of a Spectra-Physics Model SP8810 pump and Rheodyne 7125 injector with a 20-μl loop. The HPLC column was a HP Hypersil ODS (3 μm, 60 mm × 4.6 mm I.D.). The isocratic eluent system consisted of 0.1 *M* ammonium acetate–methanol (85:15, pH 7.2). The flow-rate was 1.0 ml/min.

RESULTS AND DISCUSSION

GC and GC–MS

The analysis of the aqueous acetone extract from winter-dormant *B. pendula* young stems by GC is shown in Fig. 1. The capillary column of fused silica coated with OV-1 used in this study gave satisfactory separation of TMS derivatives of phenolic aglycones, phenolic glucosides and triterpenoic compounds (Fig. 2). Simple soluble sugars, fructose (A), glucose (B, C), sucrose (D) and raffinose (E) (Fig. 1), could also be analyzed in the same run. All secondary components of birch stems, including salidroside, betuloside, (+)-catechin, catechin glycosides, dehydrosalidroside, papyriferic acid and deacetylpapyriferic acid, were eluted within 20 min. Only platyfylloside, found previously in *B. pendula* twigs, could not be analyzed by the GC

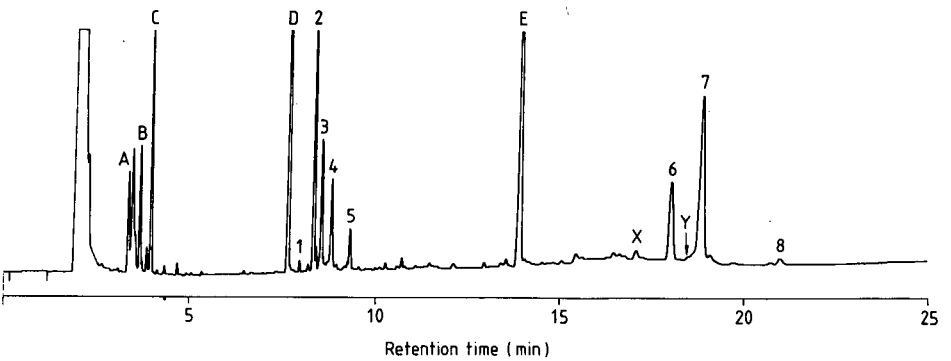

Fig. 1. GC trace of TMS derivatives of phenolic and terpenoic phytochemicals and sugars in the winter-dormant twigs of *B. pendula*. Peaks: 1 = salidroside; 2 = betuloside; 3 = (+)-catechin; 4 = isomer of (+)-catechin; 5 = dehydrosalidroside; 6 = catechin pentoside; 7 = papyriferic acid; 8 = deacetylpapyriferic acid; A = fructose; B and C = glucose; D = sucrose; E = raffinose; X and Y = unknown triterpenoic components.

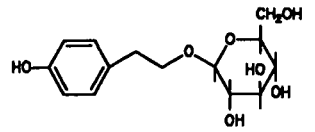

Salidroside

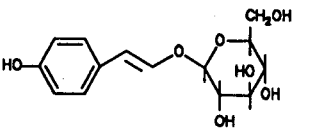

Dehydrosalidroside

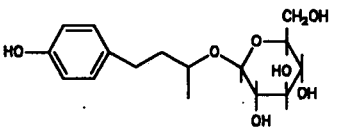

Betuloside

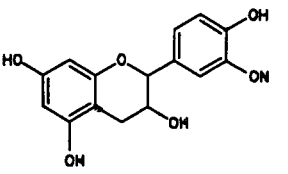

(+)-Catechin

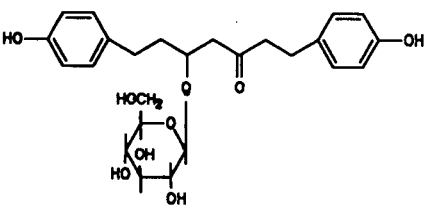

Platyfylloside

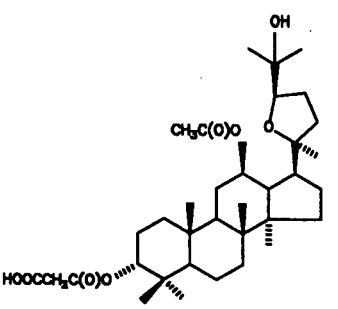

Paryriferic acid

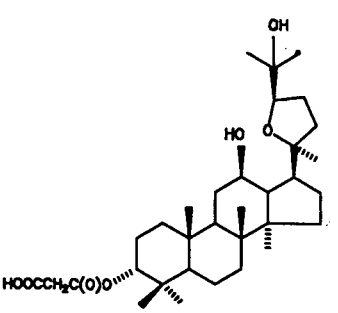

Deacetylpapyriferic acid

Fig. 2. Structures of the compounds identified in the aqueous acetone extracts of *B. pendula* twigs.

method. In addition to the identified components, the GC pattern also indicated the presence of minor unknown constituents.

The initial identification of the extracted components was based on their retention times. Identification was confirmed by GC–MS, which also allowed verification of some new components. Although the mass spectra did not always allow complete

assignment of structure, certain structural features were easy to identify. At least in cases where authentic reference compounds were available (sugars, Merck; salidroside; (+)-catechin, Sigma, St. Louis, MO, USA; papyriferic acid and deacetylpapyriferic acid) identification was simple and unambiguous.

Several of the most intense fragment ion peaks in the mass spectra of the phenolic glucosides, salidroside and betuloside (Fig. 1, components 1 and 2, respectively) were connected to the glucose part of the molecule and existed at *m/z* 451, 361, 217, 204 and 147. The intensity of these peaks varied considerably from compound to compound. The base peak, however, was always at *m/z* 204 representing the $[C_8H_{20}Si_2O_2]^+$ ion. Analogous fragmentations have previously been observed for platyphylloside [9]. Although no molecular ion peaks were present, it was possible to identify the aglycone moiety by means of the ions formed from the inductive cleavage of the acetal bond. The same bond was also cleaved with a simultaneous hydrogen transfer to the oxygen atom. These ions existed at mass numbers *m/z* 193 and 192 for salidroside and at *m/z* 221 and 220 for betuloside. In the case of betuloside, the length of the carbon chain allowed further elimination of propene from the *m/z* 193 ion, which led to formation of the *m/z* 179 ion. In the case of salidroside, the identification was verified by comparing its spectrum with that of the authentic compound.

The general appearance of the spectrum of component 5 (Fig. 1) resembled closely that of salidroside and betuloside. The spectrum was best rationalized as representing dehydrogenated salidroside, because the ion connected to the aglycone unit now existed at *m/z* 191 and the ion formed through a hydrogen atom rearrangement was totally absent. This is in agreement with the proposed structure since it is improbable that the necessary hydrogen would have been transferred from an ethylenic carbon.

Component 3 (Fig. 1) had a retention time and mass spectrum identical to that of authentic (+)-catechin. The molecular ion peak was clearly visible, accompanied with the $[M - 15]^+$ ion typical of TMS ethers. The main fragmentation was cleavage of the heterocyclic ring so that O–C-1 and C-2–C-3 bonds were broken, giving rise to the *m/z* 368 ion, which formed the base peak in the spectrum. Component 4 (Fig. 1) must be very similar to (+)-catechin. It is most probably an isomer of (+)-catechin because its spectrum was almost identical to that of (+)-catechin. It is noteworthy that this isomer was not (−)-epicatechin as the measurements with an authentic sample (Sigma) pointed out. In addition to the free catechin, a pentose derivative was also present (component 6, Fig. 1). Almost all the peaks present in the spectrum of the TMS derivative of (+)-catechin were also found in the spectrum of component 6. This can be rationalized as a formation of (+)-catechin tetra-TMS ether from its pentoside as a consequence of $OSi(CH_3)_3$ group migration from the pentose ring to the catechin moiety to replace the broken acetal bond. Related migrations have previously been observed for oligosaccharide TMS ethers [10]. Parallel to the fragmentations of phenolic glucosides (*cf.* salidroside and betuloside) the most abundant ions originated from the pentose moiety existing at *m/z* 349, 348 and 217.

As in Alaskan paper birch (*B. resinifera*) our samples also contained a triterpenoid papyriferic acid [6] (component 7, Fig. 1). The 70-eV mass spectrum of its TMS derivative (Fig. 3) resembled that of the underivatized acid in many respects and was identical to the spectrum of the compound isolated from Alaskan paper birch. With the underivatized compound, the tetrahydrofuran ring dominated the fragmentation

behavior, leading to formation of the *m/z* 143 ion as a consequence of α-cleavage reaction with respect to the ring oxygen atom. The related ion was also present in the spectrum of the TMS derivative at *m/z* 215. Silylation, however, altered the fragmentation behavior so that now the most important reaction was the α-cleavage reaction with respect to the tertiary alcohol group, which gave rise to formation of the ion at *m/z* 131. Other major fragment ions were practically the same for both the derivatized and underivatized compound. This is to be expected because they were formed by loss of the substituents in the ring system. Therefore the ions at *m/z* 442 and 381 can be rationalized as being formed through successive elimination of the malonyl and $C(OH)(CH_3)_2$ groups and the malonic acid, acetic acid and $C(OH)(CH_3)_2$ group, respectively.

Another triterpenoic compound with the longest retention time and hitherto unknown in *B. pendula* twigs was also found in GC analysis (component 8, Fig. 1). Its spectral similarity to papyriferic acid indicated that their structures are closely related. Based on comparison with an authentic sample, that component was identified as deacetylpapyriferic acid [7]. In the spectrum of the derivatized compound the only discernible difference from derivatized papyriferic acid (Fig. 3) was that the *m/z* 442 ion was now shifted to *m/z* 472. This is just the difference caused by substitution of the acetyl group in the molecule with the trimethylsilylated hydroxy group. The first suggestion was that this exchange took place during the derivatization process and that no deacetylpapyriferic acid was present in the original samples. This phenomenon was, however, never observed when authentic papyriferic acid was derivatized. So the compound detected must originate from the birch twigs. It is interesting to note that deacetylpapyriferic acid itself gave rise to a spectrum virtually identical to that of papyriferic acid. This was not expected because, analogous to the behavior described above, the *m/z* 442 ion now should exist at mass number *m/z* 400. The

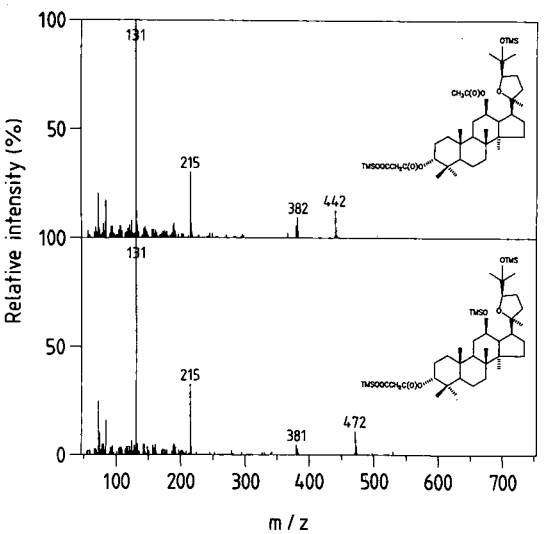

Fig. 3. Mass spectra (70 eV) of the TMS derivatives of papyriferic acid (top) and deacetylpapyriferic acid (bottom).

reason for this unexpected behavior is most probably explained by the effects of high temperature. At the elevated temperatures required to get the compound into the gas phase decarboxylation of the malonyl group took place, which led to the situation where there was an acetyl group at position 3 instead of the malonyl group. In this case the *m/z* 442 ion was formed by consecutive eliminations of hydroxy and $C(OH)(CH_3)_2$ groups. Of course, the same decarboxylation could also occur with papyriferic acid itself. Verification of this last assumption was, however, not possible. In both cases the relative intensity of the *m/z* 44 ion was decreased when the temperature of the direct inlet probe was programmed from 170 to 210°C, indicating that decarboxylation does take place.

In the GC–MS analysis two other unknown triterpenoic components were detected. The retention times of these were shorter than that of papyriferic acid, possibly indicating a shorter side-chain at position 3 (components X and Y, Fig. 1). The mass spectra of these components were identical to that of the TMS derivative of deacetyl papyriferic acid. As these components were not isolated, complete structural elucidation was not possible.

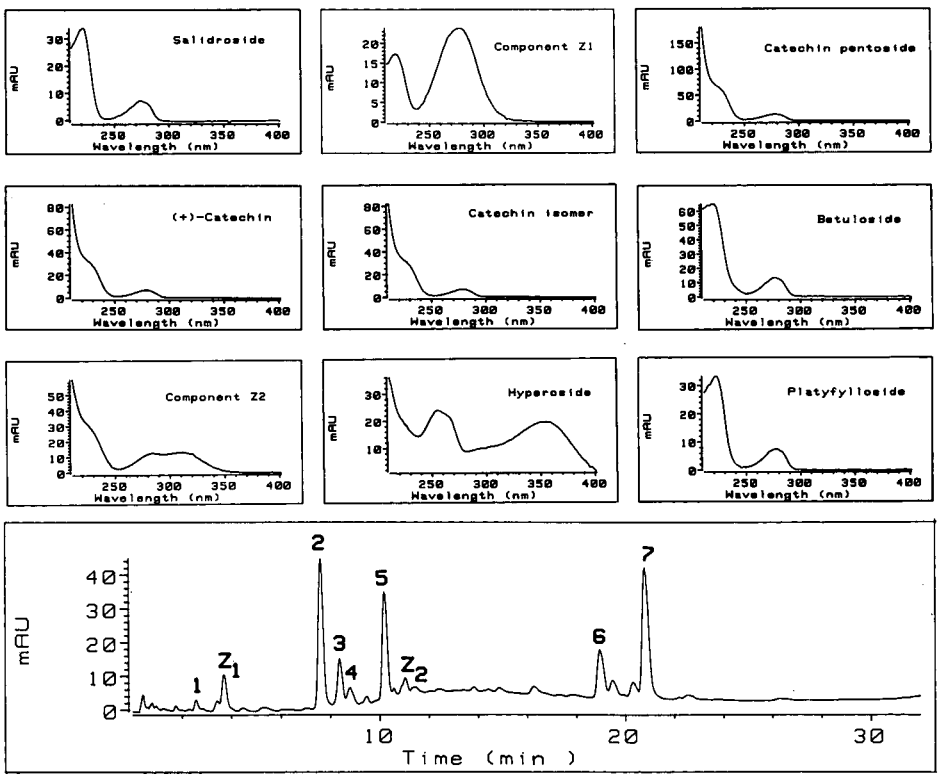

Fig. 4. HPLC trace and UV spectra of phenolic phytochemicals in the winter-dormant twigs of *B. pendula*. Peaks: 1 = salidroside; 2 = catechin pentoside; 3 = (+)-catechin; 4 = catechin isomer; 5 = betuloside; 6 = hyberoside; 7 = platyfylloside; Z_1 and Z_2 = unknowns.

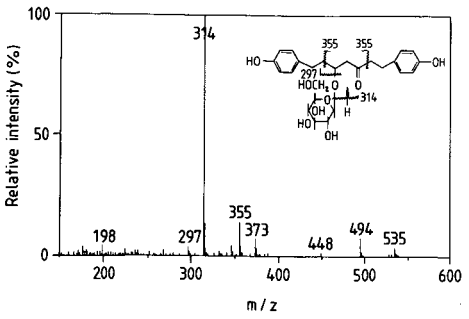

Fig. 5. Thermospray ionization mass spectrum of platyfylloside.

HPLC and HPLC–TSP-MS

An HPLC–UV–VIS profile and UV spectra of the components of the birch young stems extract are presented in Fig. 4. Most of the phenolic components in *B. pendula* winter-dormant stems found by GC are also easily detected and distinguished by their characteristic UV spectra. However, a more complete identification of the components in a chromatogram is possible by comparing their retention times and UV spectra with those of authentic and library components. Consequently, betuloside, platyfylloside, (+)-catechin and salidroside can easily be recognized as components of the extract (Fig. 4). The HPLC profile also indicated the presence of a few minor unknown components (Z_1, Z_2 and 6, Fig. 4), of which component 6 could be identified as the flavonoid glucoside hyperoside (Aldrich-Chemie). Based on retention time and spectral behavior, component Z_1 could be dehydrosalidroside.

LC–TSP-MS offers another possibility for the analysis of non-volatile and polar compounds directly without derivatization [11,12]. As platyfylloside was not detected by GC–MS this method was used to confirm its presence. The HPLC measurements, on the other hand, strongly indicated the presence of platyphylloside. The HPLC–TSP mass spectrum obtained (Fig. 5) shows an abundant ammonium adduct $[M + NH_4]^+$ ion peak at *m/z* 494. The ion at *m/z* 314 giving rise to the base peak and the *m/z* 297 ion were formed by cleavage of the glucosidic bonds. Corresponding fragmentations for a cyanogenic glucoside have been reported previously [13]. The ion at *m/z* 535 was presumably $[M + NH_4 + CH_3CN]^+$.

LC–TSP-MS was also used to verify the molecular weight of betuloside. In this case, almost the only adduct ions at *m/z* 346 and 387 were $[M + NH_4]^+$ and $[M + NH_4 + CH_3CN]^+$, respectively.

ACKNOWLEDGEMENTS

This research was supported by the Academy of Finland. Technical assistance was provided by Ms. Sinikka Sorsa. We thank Professor Heinz Thieme for the purified salidroside, Professor Jorma Tahvanainen for helpful comments on the manuscript and Dr. R. Ekman for generous discussions at the very beginning of this study.

REFERENCES

1 M. J. Oksanen, *Sorbifolia*, 18 (1987) 195.
2 M. Rousi, *Ph.D. Thesis*, University of Helsinki, Helsinki, 1990.
3 P. B. Reichardt, J. P. Bryant, T. P. Clausen and G. D. Wieland, *Oecologia*, 65 (1984) 58.
4 T. Palo, *Ph.D. Thesis*, University of Uppsala, Uppsala, 1987.
5 J. Tahvanainen, R. Julkunen-Tiitto and M. Rousi, *J. Chem. Ecol.*, submitted for publication.
6 P. B. Reichardt, *J. Org. Chem.*, 46 (1981) 4576.
7 P. B. Reichardt, T. P. Green and S. Chang, *Phytochemistry*, 26 (1987) 855.
8 R. Julkunen-Tiitto, unpublished results.
9 M. Terazawa, T. Koga, H. Okuyama and M. Miyake, *Mokuzai Gakkaishi*, 30 (1984) 391.
10 T. Radford and D. C. Dejongh, in G. R. Walter and O. C. Dermer (Editors), *Biochemical Applications of Mass Spectrometry*, 1st Suppl. Vol., Wiley, New York, 1980, p. 255.
11 T. R. Covey, J. B. Crowther, E. A. Dewey and J. D. Henion, *Anal. Chem.*, 57 (1985) 474.
12 R. D. Voyksner and C. A. Haney, *Anal. Chem.*, 57 (1985) 991.
13 G. Stenhagen and H. Alborn, *J. Chromatogr.*, 474 (1989) 285.

Journal of Chromatography, 547 (1991) 377–392
Elsevier Science Publishers B.V., Amsterdam

CHROM. 23 277

Role of additives in packed column supercritical fluid chromatography: suppression of solute ionization

TERRY A. BERGER* and JEROME F. DEYE
Hewlett-Packard Co., P.O. Box 900, Avondale, PA 19311-0900 (USA)
(First received November 5th, 1990; revised manuscript received February 26th, 1991)

ABSTRACT

Tailing of polycarboxylic acids in packed column supercritical fluid chromatography (SFC) is primarily due to solute ionization. Very acidic additives improve the peak shape of acidic solutes by suppressing solute ionization. Coverage of active sites appears to be a secondary function of additives. The sorption of acidic additives was measured on five stationary phases used in packed column SFC. Surface coverages (at constant mobile phase composition) varied by more than 50-fold (0.4 to 21%), depending on the stationary phase identity. Within the group of additives used, coverage was independent of additive identity or concentration but was inversely proportional to modifier concentration. Chromatographic peak shapes of polyfunctional acidic solutes were also observed under the same conditions as used for the surface coverage measurements. Solute peak shapes depended on the acid strength of the additives but were unrelated to the amount of additive retained on the column.

INTRODUCTION

Supercritical fluid chromatography (SFC) is a transitional technique between gas chromatography (GC) and liquid chromatography (LC) in that the mobile fluid is a gas that solvates. The most widely used fluid, carbon dioxide, is similar to liquid pentane or liquid hexane in solvent strength [1–3]. The polarity of carbon dioxide can be increased by adding small amounts of a polar organic modifier, but modifiers that are miscible with carbon dioxide are also only moderately polar (*i.e.*, $p' = 5.1$ for methanol *vs.* 0 for pentane and 10.2 for water [4,5]). Solvatochromic dye studies suggest [6] that very polar compounds, such as trifluoroacetic acid (TFA), when added to modifiers can significantly increase the polarity of modified mobile phases. Small concentrations (*i.e.*, 10^{-4} *M*) of such very polar compounds improve chromatographic peak shapes [7–11] and elute solutes that are normally retained. Such small concentrations cannot be directly added to non-polar supercritical fluids. Instead, they are added to a modifier of intermediate polarity, such as methanol. We differentiate them from modifiers by calling them additives. Additives provide a key to the separation of more polar solutes by SFC.

While it has been demonstrated that additives affect retention and peak shapes, the mode of operation of additives is unknown, although many workers assume that additives function by covering active sites. If additives function by covering active

0021-9673/91/$03.50

sites, then the peak shape should be related to the amount of an additive retained and the intensity with which it is held. Such measurements have not been made. The effect of additive polarity on additive retention and solute chromatographic peak shape have not been systematically studied. In this work we measured the retention of a series of progressively more polar additives on a series of progressively more polar stationary phases, and compared the amount of additive retained and additive polarity with solute chromatographic retention and peak shape. The number of active sites was also determined and compared with the amount of additive retained.

EXPERIMENTAL

Instrumentation

The chromatographic system included a Hewlett-Packard (HP) Model 1082 liquid chromatograph, modified to pump carbon dioxide, and an HP Model 1050 pump for modifier addition. Flow-rates and modifier concentrations (%, v/v) are based on volumetric flow-rates at the pumps. The carbon dioxide pump head temperature was 4.0°C. Detection was effected with an HP Model 1050 UV–VIS photodiode-array detector with a high-pressure flow cell. A low-volume electronic back-pressure regulator, built in-house, was used to control the system pressure. Additive concentration is expressed in terms of its concentration in the modifier, not in the complete mobile phase.

Breakthrough experiments used the three-pump system shown in Fig. 1. All three pumps ran continuously. A modified HP Model 1050 pump delivered a fixed flow of carbon dioxide. One of the remaining Model 1050 pumps delivered a fixed flow of pure modifier while the other Model 1050 pump delivered the same flow of modifier containing a small concentration of a very polar additive. A switching valve allowed the flow from either one of the modifier pumps to be mixed with the carbon dioxide at the head of the column. The other modifier flow was added downstream of the column and detector but upstream of the back-pressure regulator so that both modifier pumps were always pressurized to nearly the same pressure. Switching the valve interchanged the two liquid flows. The baselines in the figures demonstrating breakthrough measurements appear noisy. This noise has many sources. Most of the additives have low molar absorptivities, producing little change in signal for a few percent change in modifier concentration. The detection wavelength was 210 nm, where both methanol and the additives adsorb. Most of the mixing apparatus used in chromatography was removed, allowing larger than normal short-term composition and pressure variations.

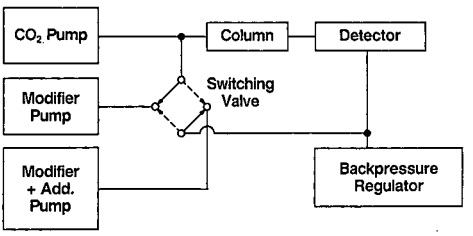

Fig. 1. Schematic diagram of instrumentation used for breakthrough experiments.

Columns

The columns were 100 mm × 2 or 2.1 mm I.D. standard packed columns for liquid chromatography (LC), which were washed overnight with pure methanol at 80°C before use. The 2 mm I.D. columns were purchased from Keystone Scientific (Bellefonte, PA, USA). The Phenyl and Cyanopropyl (CN) phases were on 5-μm Hypersil. The sulfonic acid (SA) packing was 5-μm Nucleosil. The Diol packing was 7-μm Nucleosil. The MOS (C_8) columns were 100 mm × 2.1 mm I.D. with 5-μm Hypersil, packed by Hewlett-Packard.

Column pretreatment

Two different column preparations were used, a methanol wash and a base wash. The methanol wash involved flushing the column with a low concentration (usually 4 or 6%) of methanol (without an additive) in carbon dioxide, for some fixed time (usually 20 min). After such washes, the additive was re-introduced into the mobile phase while keeping the modifier concentration constant. The time between the re-introduction of additive at the column inlet and the appearance of the additive in the column effluent constitutes a breakthrough time proportional to the amount of additive retained on the column. Methanol washes probably remove only weakly retained additives.

The base wash consisted of 10 ml each of (1) 1% N-*tert.*-butylammonium hydroxide in methanol, (2) methanol, (3) 1% acetic acid in methanol and (4) methanol; all four wash fluids contained 10% carbon dioxide. Base washes were followed by a methanol wash before breakthrough measurements. Base washes probably produce a "bare" column with no strongly adsorbed acidic additives.

Chemicals

Carbon dioxide was of supercritical grade in aluminium cylinders, purchased from Scott Specialty Gases (Plumsteadville, PA, USA). Methanol was of high-purity grade from Burdick & Jackson Labs. (Muskegon, MI, USA). Additives were purchased from Eastman Kodak (Rochester, NY, USA). Other chemicals were purchased from Aldrich (Milwaukee, WI, USA).

RESULTS AND DISCUSSION

Determination of active sites

There are *ca.* 8 μmol/m^2 of silanol groups on hydrolyzed bare silica particles [12–14]. The theoretical pH of silanol in water is 7.1 [15,16], but experimentally measured values can be much higher or lower [17]. Up to 5% of the total silanols are chemically distinct with a lower pH [18]. Other investigators have suggested that the fraction of more "reactive" silanols is less than 0.1–0.3%, which correlates with the concentration of metal ions in the silica [19–21]. Bonded stationary phases typically cover 40–60% of silica surfaces [22–24], so the total available silanol concentration would be reduced to 3.2–4.8 μmol/m^2, and reactive silanols would be reduced to 0.04–0.18 μmol/m^2. The total surface areas of several of the columns were measured using a modification [25] of tracer pulse chromatography [26]. The 300 Å Diol column had a measured surface area of 15 m^2 and the 4000 Å Diol column 3.0 m^2.

Breakthrough experiments

Column transit times were *ca.* 0.15 min, but as long as 45 min passed with no measurable additive in the column effluent after additives were introduced into the mobile phase at the column inlet. After such delays, the baseline undergoes a step change to a higher absorbance, as seen in Fig. 2. These breakthrough times, the flow-rate and the concentration of additive indicate the moles of additive retained on the column. Such breakthrough times, from each type of wash, could be reproduced to within *ca.* ±5% within one day and *ca.* ±20% over several months.

The amounts of additive retained on various columns are presented in Table I. Loading factors (μmol/m^2) were obtained by dividing the number of micromoles retained by the measured surface areas of representative columns. Loading factors were converted to surface coverage (%) by dividing by the total surface concentration of silanols on an uncoated packing (8 μmol/m^2) and multiplying by 100. A 100% coverage would be equivalent to a monolayer of additive on both bonded phase and exposed silica.

Loading factors and surface coverages are presented in Table II. Surface coverage was independent of the additive identity or acid strength, as similar coverages were measured using trifluoroacetic acid, dichloroacetic acid and citric acid. The retention of an additive is a strong function of stationary phase identity.

On the least polar columns (*i.e.*, MOS) the amount of additive retained was about the same after both the base wash and the methanol wash (the additive is easily removed), and the absolute amount was very small. The additive surface coverage of 0.4% was much lower than most estimates of the surface coverage of silica by all

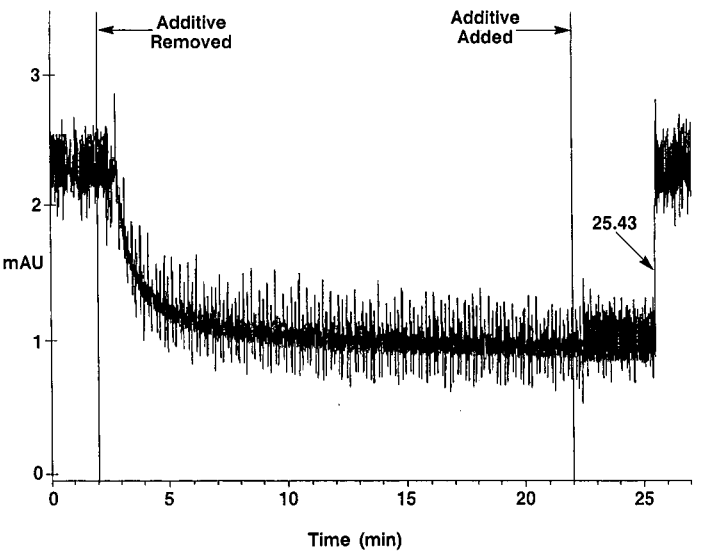

Fig. 2. Results from a typical breakthrough experiment. From 0 to 2 min: 6% (v/v) methanol containing 0.1% dichloroacetic acid in carbon dioxide; 2 to 22 min, 6% methanol in carbon dioxide (methanol wash); 22 to 27 min, 6% methanol containing 0.1% dichloroacetic acid, in carbon dioxide. Breakthrough time = 3.43 min. Column, 100 mm × 2 mm I.D., 7-μm Nucleosil, 4000 Å Diol, flow-rate 1 ml/min (at pumps; CO_2 at 4°C), 40°C, 207 bar.

TABLE I

MICROMOLES OF ADDITIVE SORBED ON COLUMNS FROM METHANOL–CARBON DIOXIDE MIXTURES AT 40°C AND 200 BAR

Columns, 100 × 2 mm I.D.

Stationary phase	Additive	After base wash	20-min methanol wash	Other methanol wash
MOS (C_8), 120Å, Hypersil	DCA		0.622[a],0.500[b]	
	TFA		0.75[a],0.57[b]	
CN, 120 Å, Hypersil	DCA	0.493[a]	0.590[a] 0.60[b]	
SA, 300 Å, Nucleosil	DCA	3.88[b]	0.207[b] 0.200[a]	39 min, 2.07[b]
	TFA		1.97[b] 3.19[a]	
Diol, 300 Å, 15 m^2, Nucleosil	DCA	11.60[b]	4.23[b]	70 min, 7.69
		13.69[b]	5.91[b]	
Diol, 4000 Å, 3.0 m^2, Nucleosil	Citric acid	3.05[b]	1.60[b]	50 min, 2.07, 120 min, 2.16[b]
	DCA	5.10[b]	2.52[b]	
	TFA	4.88[b]	1.63[b]	36 min, 1.99[b]; overnight, 4.44[b]

[a] 4% methanol containing 0.1% additive.
[b] 6% methanol containing 0.1% additive.

silanols, but was higher than some estimates of surface coverages of "reactive" silanols (0.1–0.3%) [19–21] on uncoated silica. The surface coverage on a cyanopropyl (CN) stationary phase was the same as on the MOS column. On the SA column, surface coverages were 4–8 times higher. The 300 Å Diol column had up to a 30 times higher surface coverage than the MOS and CN columns. The right-hand column in Table I indicates that even very long (2–24 h) methanol washes did not wash off as much additive as a base wash (some of the additive is difficult to remove). The 4000 Å Diol column has a surface coverage about twice that on the 300 Å Diol column. Both Diol columns showed a substantial difference between methanol and base washes (possibly owing to two forms of retention).

From the least to the most retentive column, the surface coverage varied more than 50-fold, from 0.4% to 21%, from a $4 \cdot 10^{-4}$ *M* additive solution. As the MOS and CN columns did not retain much additive, the population of active sites must be

TABLE II

DATA FROM TABLE I FOR DCA ADDITIVE CONVERTED TO LOADING FACTORS AND SURFACE COVERAGE

Column	After base wash		After methanol wash	
	Loading factor (μmol/m^2)	Surface coverage (%)	Loading factor (μmol/m^2)	Surface coverage (%)
MOS			0.041	0.5[a]
			0.033	0.4[b]
CN	0.033	0.4[b]	0.033	0.4,0.6[a]
			0.048	
			0.040	0.5[b]
SA	0.26	3.4[b]	0.13	1.6[b]
Diol (300 Å)	0.84	12[b]	0.76	4.3[b]
Diol (4000 Å)	1.70	21[b]	0.76	10[b]

[a] 4% methanol.
[b] 6% methanol.

small, or the additives must not interact with active sites. The large differences in surface coverage between MOS and CN on the one hand, and Diol and SA columns on the other, indicate that additives are retained on the Diol and SA columns by some mechanism in addition to coverage of active sites.

The surface coverage by additive appeared to be independent of the additive concentration in the mobile phase, as shown in Fig. 3. If the concentration on the stationary phase is fixed while the mobile phase concentration changes, then the additive distribution constant (K_D) changes and the additive does not partition like a solute. An adsorption isotherm relating surface coverage to additive concentration could not be generated either. In contrast, additive surface coverage was inversely proportional to modifier concentration. Stepwise increases in the concentration of the polar modifier (additive concentration also increases) produce step changes in background absorbance, with an additional peak or maximum (absorbance due to additive) superimposed on the step change, as shown in Fig. 4a. The areas of the peaks are measures of the amount of additive washed off the column by the increased concentration of the modifier. In Fig. 4a, the mobile fluid initially contained 4% of methanol in carbon dioxide, which was increased to 8% of methanol at 4 min and to 12% at 12 min.

Stepwise decreases in the concentration of modifier confirmed the inverse relationship between the modifier concentration and surface coverage. The effect was clearly seen when modifier concentration was decreased from 4% to 2%, as in Fig. 4b. Between 17 and 20 min (in Fig. 4b) the background absorbance was characteristic of 4% of modifier containing the additive. At 20 min, the modifier concentration was decreased to 2%. After a short delay, the background absorbance decreased but to a value substantially below that expected for 2% of modifier containing the additive.

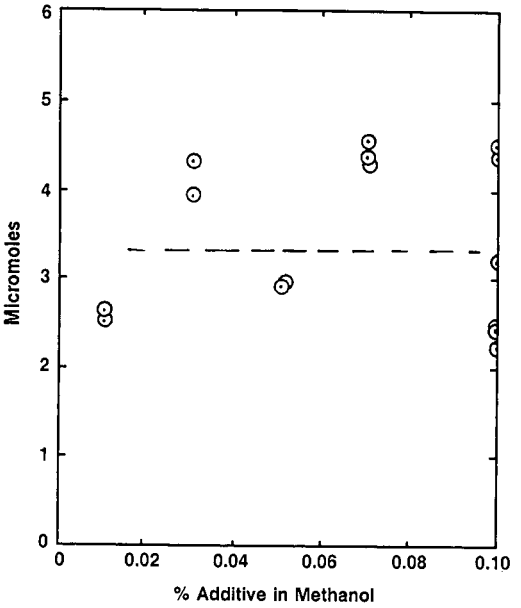

Fig. 3. Effect of additive concentration on the amount of additive retained. Dichloroacetic acid in 6% methanol after methanol washes; 40°C, 207 bar outlet pressure, a 100 mm × 2 mm I.D., 7-μm Nucleosil, 300 Å Diol column.

At about 39 min, the baseline increased to the expected value. The decrease in absorbance between 20 and 39 min indicates that most of the additive was being removed from the mobile phase and was being retained by the column. The depth and duration of the decrease in absorbance and the flow-rate provide a measure of the change in the amount of additive retained. The concentration of additive emerging from the column was calibrated against the absorbance of additive–modifier–carbon dioxide mixtures with the column removed. Table I gives the absolute amount retained at one modifier concentration. Table I and measurements on Fig. 4b produced the relationship between modifier concentration and amount of retained additive shown in Fig. 5.

Chromatographic experiments

Additive polarity. The additives and stationary phases used to measure surface coverage were also used to collect chromatograms of benzoic acid, 1,2-benzenedicarboxylic (phthalic) acid and 1,3,5-benzenetricarboxylic (trimellitic) acid. The solutes were separated on five stationary phases using five additives of increasing polarity. The columns were exposed to additives, then washed overnight with methanol at 80°C before equilibration with the mobile phases containing the additive. The methanol concentration was adjusted to obtain roughly the same retention times on all the columns. The concentration of additive was fixed at 0.2% in methanol. If the methanol concentration in the mobile phase is changed, the additive concentration also changes proportionally. Chromatograms obtained with MOS, Phenyl and CN columns are shown in Fig. 6. The Diol and SA columns are considered separately below.

The weakest acids (acetic and chloroacetic acid) were ineffective in improving

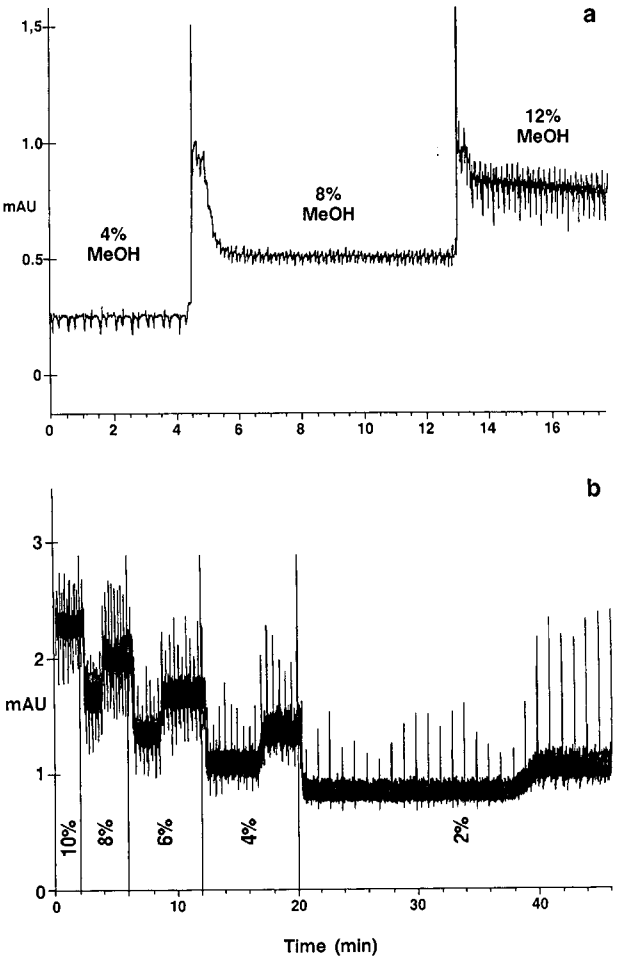

Fig. 4. Effect of step changes in modifier concentration. (a) Typical step up in concentration: 0.1% TFA additive in methanol (MeOH); total flow-rate = 1 ml/min, 40°C, 130 bar. A 100 mm × 2 mm I.D., 5-μm Nucleosil SA column. (b) Typical step down in concentration: 1.00 g/l citric acid in methanol; flow-rate = 1 ml/min, 40°C, 207 bar; a 100 mm × 2 mm I.D., 7-μm Nucleosil, 4000 Å Diol column.

peak shapes when used as additives. Dichloroacetic acid improved peak shapes on the CN column but not on the MOS or Phenyl columns. According to Tables I and II, the MOS and CN columns retain the same, small amount of additive. The poor peak shapes on the MOS column and the symmetrical peaks on the CN column, under identical conditions, suggest that there is a substantial difference in additive behavior on the two column types. The additive is easily washed off with a methanol wash so it is not strongly adsorbed.

Significantly higher modifier concentrations were required to obtain the same retention times on a sulfonic acid column as on the CN column, as can be seen by comparing Figs. 6 and 7. As on the CN column, only the more acidic additives

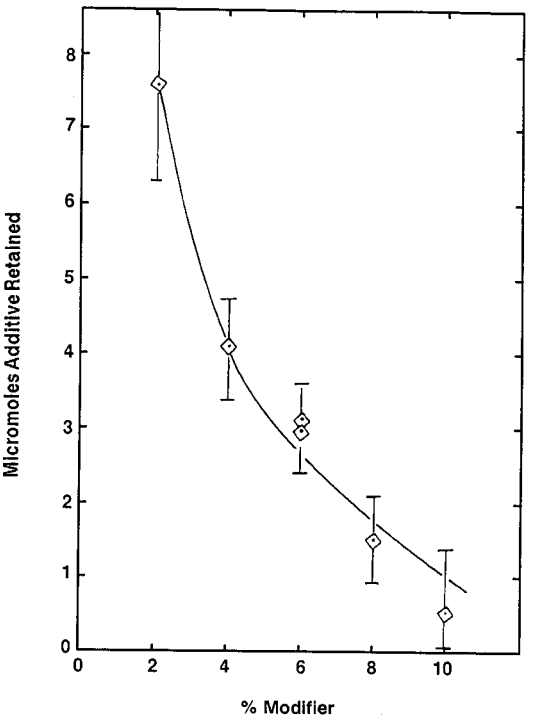

Fig. 5. Effect of modifier concentration on the amount of additive retained. Conditions as in Fig. 4b.

improved peak shapes. Sulfonic acids are strong acids, whereas silanols have a surface pH between 4 and 7 [20,21]. If the sulfonic acid functional groups are substantially more acidic, and are present in greater numbers than even the most "reactive" active sites, there should be only one dominant (solute) retention mechanism and polar solutes should not tail. However, the peak shapes were poor on the SA column, when no additive or a low polarity additive was used. This suggests a tailing mechanism other than interaction with active sites.

The chromatographic behavior of Diol phases is different from that on the other column types. On the 300 Å Diol column, phthalic acid and trimellitic acids were strongly retained, with poor peak shapes (not shown in Fig. 8) when acetic acid was used as the additive. The retention decreased dramatically, peak shapes improved and the elution order even reversed, with stronger acid additives, as shown in Fig. 8. Such dramatic changes in retention and selectivity are usually not associated with a simple coverage of active sites, and imply a major change in the chemical characteristics of one or both chromatographic phases.

Additive concentration. The retention of benzoic, hydroxybenzoic and benzenedicarboxylic acids was measured as a function of additive (citric acid) concentration, as shown in Fig. 9. Some citric acid was probably present on the column even when the mobile phase contained no added citric acid, as the column was prepared by washing overnight with pure methanol. The breakthrough experiments showed that additives produced high surface coverages on Diol columns but, once established, the

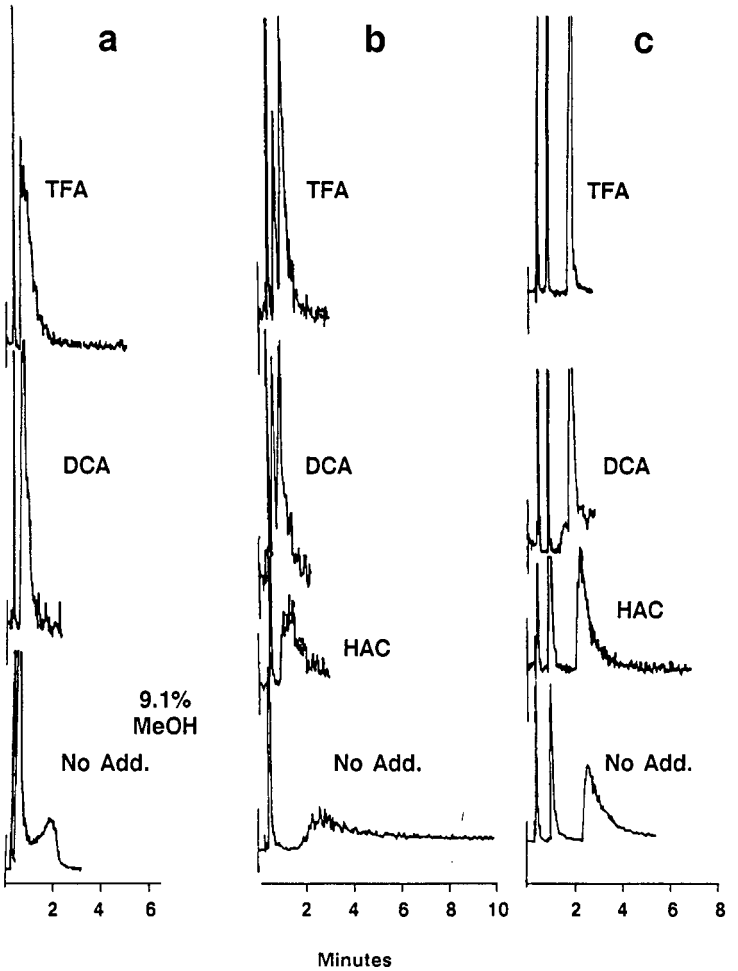

Fig. 6. (a) 1.2% methanol on MOS column; (b) 0.8% methanol on Phenyl column; (c) 1.6% methanol on CN column. Solute elution order: benzoic acid, phthalic acid and trimellitic acid. Additives: HAc = acetic acid; CA = chloroacetic acid; DCA = dichloroacetic acid; TCA = trichloroacetic acid; TFA = trifluoroacetic acid. Methanol (MeOH) contains 0.2% additive; in carbon dioxide. A 100 mm × 2 mm I.D. column; flow-rate = 3 ml/min, 40°C, 130 bar outlet pressure.

amount of additive present on the stationary phase is independent of its concentration in the mobile phase. The retention of the three hydroxybenzoic acids changed dramatically with the first small additions (from 0 to <0.1–0.2%) of citric acid to the mobile phase, whereas the retention of 1,3- and 1,4-benzenedicarboxylic acid changed only modestly. The retention and peak shapes of both 1,2-substituted solutes (salicylic and phthalic acids) changed most dramatically with the first addition of citric acid. More important, the retention of these two solutes continued to change as the additive concentration was increased. Solute separation factors ($\alpha = k'_2/k'_1$) *vs.* additive concentration, as shown in Fig. 10, indicate that the additive has an even larger

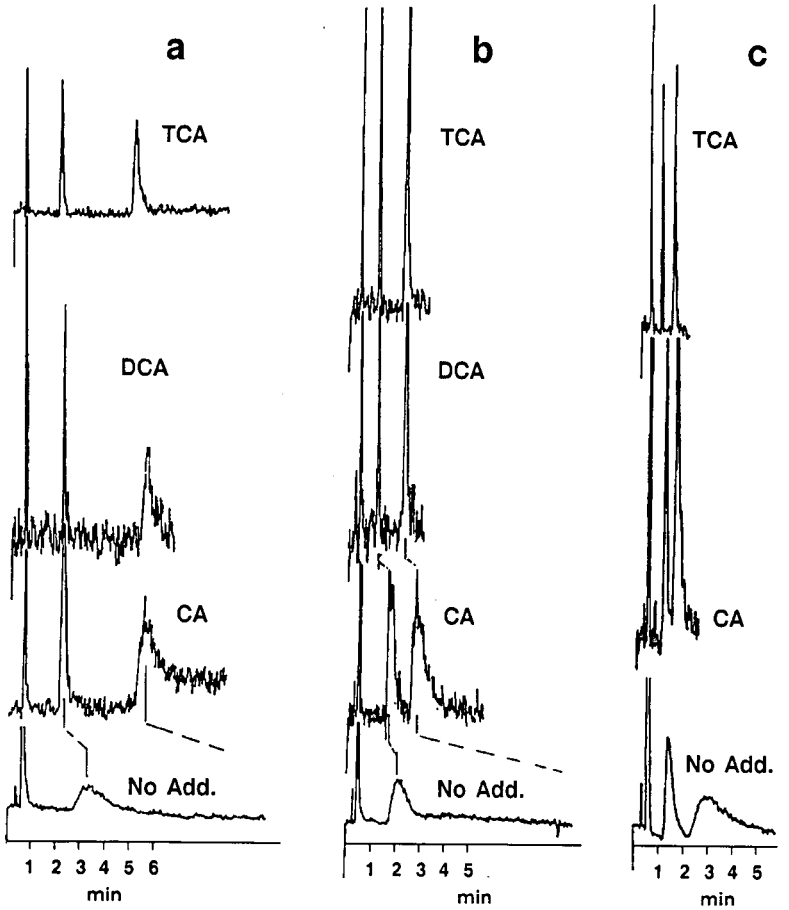

Fig. 7. Chromatograms as in Fig. 6, except obtained on an SA column. (a) 3.0% methanol plus additive; (b) 4.8% methanol plus additive; (c) 6.3% methanol plus additive.

impact on selectivity than is evident from Fig. 9. The smallest changes in selectivity occurred between similar compounds (*i.e.*, pairs of dicarboxylic acids). Some peaks were symmetrical even when there was no additive in the mobile phase (see Fig. 11). For those solutes, the first addition of the additive dramatically shifted the retention but did not change peak shapes. Phthalic acid did not elute without additive, and was severely tailed, using 0.05% citric acid in methanol ($2 \cdot 10^{-4}$ *M*) in the mobile phase. The peak shape improved as the additive concentration was increased.

Correlation with acid strength

A possible explanation for the poor peak shapes of carboxylic acids using modified fluids, and the improvements attributable to additives, involves partial ionization of such solutes. Several reports [8,10], have discussed ion-pair separations in supercritical fluids, so the concepts of ionization and ion-pair formation in supercritical fluids is not new. In LC, ion-pairing agents improve the peak shapes of some

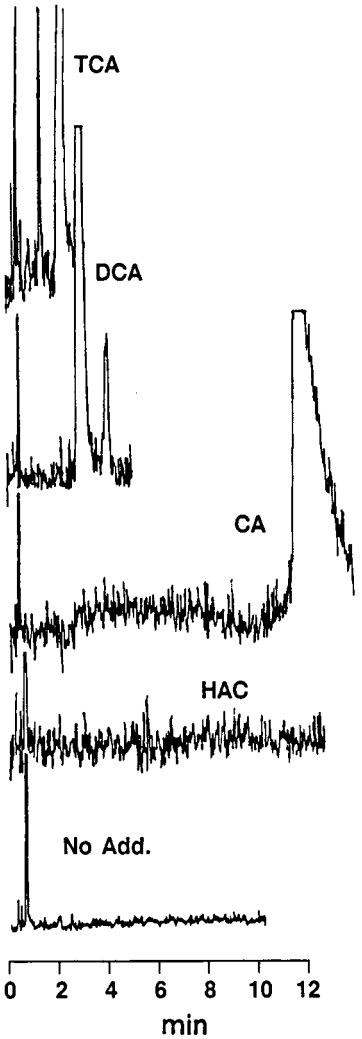

Fig. 8. Chromatograms as in Fig. 6, except obtained on a Diol column. 4.8% methanol plus additive.

aromatic carboxylic acids [27]. In this work, however, stronger acids were used to improve the peak shapes of less acidic solutes through ionization suppression. Such suppression also has precedents in LC [28,29].

In the absence of measured values in methanol–carbon dioxide mixtures, dissociation constants of acids in water [30,31] can be used to indicate at least a relative tendency for acids to ionize. Some dissociation constants in water and methanol are presented in Table III.

As shown in Figs. 6–8, the peak shapes of phthalic and trimellitic acid were always poor on all the stationary phases when no additive was present in the mobile phase. Only additives more acidic (lower pK_a values) than the solute improved the peak shapes. Acetic acid was ineffective, chloroacetic acid was partially successful and

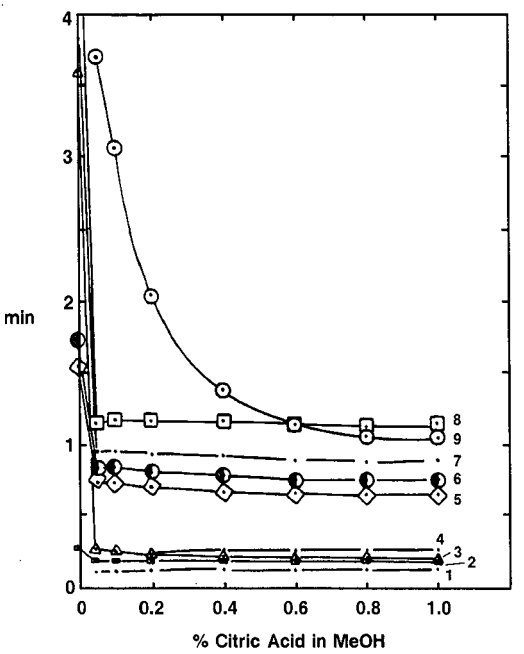

Fig. 9. Retention time *vs.* additive concentration. Lines 1 and 4 = trace contaminants; 2 = benzoic acid; 3 = 2-hydroxybenzoic acid; 5 = 1,4-benzenedicarboxylic acid; 6 = 1,3-benzenedicarboxylic acid; 7 = 3-hydroxybenzoic acid; 8 = 4-hydroxybenzoic acid; 9 = 1,2-benzenedicarboxylic acid. Mobile phase: 5.7% (v/v) methanol in carbon dioxide at 40°C; flow-rate = 3 ml/min, outlet pressure = 200 bar. Column: 100 mm × 2 mm I.D., 7-μm Nucleosil 300 Å Diol.

dichloroacetic acid dramatically improved the peak shapes on the SA column. According to Table III, acetic acid is much weaker ($pK_a = 4.75$), chloroacetic acid is of similar acid strength (2.85), while dichloroacetic acid is a stronger (1.48) acid than phthalic acid ($pK_{a,1} = 2.89$).

In Figs. 9–11, the retention of *ortho*-(1,2-)substituted solutes changed dramatically with citric acid concentration. The retention of the other solutes ceased to shift after the first small additions of citric acid. The first dissociation constant of the citric acid additive ($pK_{a,1} = 3.14$) is about the same as those of the *ortho*-substituted solutes [2-hydroxybenzoic acid ($pK_a = 2.97$) and 1,2-benzenedicarboxylic acid ($pK_a = 2.89$)], but more acidic than the other solutes ($pK_a = 3.51$–4.48). This suggests that additives suppress the ionization of less acidic solutes, but are only partially effective in suppressing the ionization of acids of similar strength.

CONCLUSIONS

Solute ionization is a major cause of peak tailing of carboxylic acid solutes in SFC. Such ionization can be suppressed by the common ion effect using additives that are more easily ionized than the solutes (*i.e.*, that are stronger acids). Tailing could not be suppressed simply by increasing the polarity of the mobile phase or by decreasing the polarity or activity of the stationary phase. Modifiers, such as methanol, were

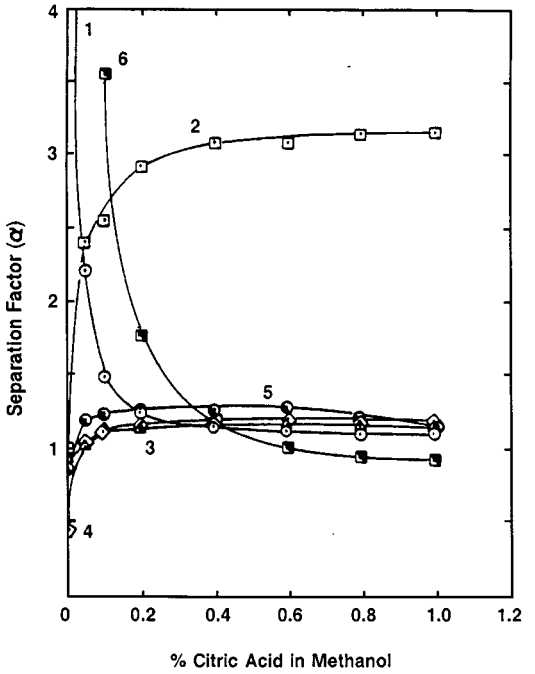

Fig. 10. Separation factors (α) *vs.* citric acid concentration for data in Fig. 9. Key: 1 = 3/2 in Fig. 9; 2 = 5/3 in Fig. 9; 3 = 6/5 in Fig. 9; 4 = 7/6 in Fig. 9; 5 = 8/7 in Fig. 9; 6 = 9/8 in Fig. 9.

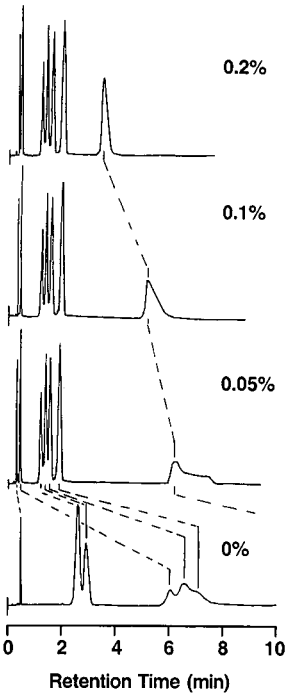

Fig. 11. Chromatograms obtained at a constant modifier concentration but with various additive concentrations. Conditions and elution order as in Fig. 9.

TABLE III

REPRESENTATIVE pK_a VALUES IN WATER AND METHANOL FOR VARIOUS ADDITIVES AND SOLUTES [30,31] INDICATING THE RELATIVE TENDENCY OF ACIDS TO IONIZE

	pK	pK_2	pK_3	pK_a (methanol)
Additive				
Acetic acid	4.75			9.52
Chloroacetic acid	2.85			
Dichloroacetic acid	1.48			
Trichloroacetic acid	0.70			
Trifluoroacetic acid	0.50			
Octanoic acid	4.89			
Citric acid	3.14	4.77	6.39	
Solute				
Benzoic acid	4.19			10.72 (ethanol)
2-Hydroxybenzoic acid	2.97	13.4		8.7
3-Hydroxybenzoic acid	4.06	9.92		
4-Hydroxybenzoic acid	4.48	9.32		
1,2-Benzenedicarboxylic acid	2.89	5.51		11.65 (pK_2)
1,3-Benzenedicarboxylic acid	3.54	4.60		
1,4-Benzenedicarboxylic acid	3.51	4.82		
2,3-Dihydroxybenzoic acid	2.94			
2,5-Dihydroxybenzoic acid	2.97			
3,4-Dihydroxybenzoic acid	4.48			
3,5-Dihydroxybenzoic acid	4.04			

not effective in suppressing tailing. Additives were only effective when they were stronger acids than the acidic solutes. However, even very acidic additives were ineffective in improving peak shapes on low-polarity columns such as C_8 (MOS). This implies that the column surface needs to be hydrophilic for additives to be effective. On polar columns, such as sulfonic acid or Diol, most of the additive retained appears to interact with the stationary phase, not the bare silica surface.

Polar columns exhibit as much as a 50-fold higher additive surface coverage than non-polar columns. However, both moderate- (CN) and high-polarity (SA or Diol) columns can produce symmetrical peaks for polar solutes. On the less polar columns, less than 1% of the surface is covered by "reactive" or "active" sites. These sites cannot be very polar as the additive can be washed off by a relatively mild methanol wash. Polar columns are unlikely to have 50-fold more active sites, so most of the additive retained must interact with the stationary phase, not active sites. Part of the retained additive is much more difficult to wash off, indicating a stronger interaction between the additive and the stationary phase than between the additive and "active" sites. In some instances, retention changes with additive concentration even through the surface coverage on the column apparently does not. Subtle differences in acid strength between additives and solutes appear to have a significant effect on solute peak shapes and retention.

ACKNOWLEDGEMENT

The authors thank Professor Jon Parcher, Department of Chemistry, University of Mississippi, for measuring the *in situ* surface areas of the columns.

REFERENCES

1 C. R. Yonker, S. L. Frye, D. R. Kalkwarf and R. D. Smith, *J. Phys. Chem.*, 90 (1986) 3022.
2 S. L. Frye, C. R. Yonker, D. R. Kalkwarf and R. D. Smith, in T. G. Squires and M. E. Paulaitis (Editors), *Supercritical Fluids: Chemical and Engineering Principles and Applications* (*ACS Symposium Series*, No. 329), American Chemical Society, Washington, DC, 1987, Ch. 3.
3 J. F. Deye, T. A. Berger and A. G. Anderson, *Anal. Chem.*, 62 (1990) 615.
4 L. R. Snyder, *J. Chromatogr.*, 92 (1974) 223.
5 L. R. Snyder and J. J. Kirkland, *Introduction to Modern Liquid Chromatography*, Wiley, New York, 2nd. ed., 1979, Ch. 6.
6 T. A. Berger and J. F. Deye, *Anal. Chem.*, submitted for publication.
7 M. Ashraf-Khorassani, M. G. Fessahaie, L. T. Taylor, T. A. Berger and J. F. Deye, *J. High. Resolut. Chromatogr. Chromatogr. Commun.*, 11 (1988) 352.
8 W. Steuer, M. Schindler, G. Schill and F. Erni, *J. Chromatogr.*, 447 (1988) 287.
9 T. A. Berger, J. F. Deye, M. Ashraf-Khorassani and L. T. Taylor, *J. Chromatogr. Sci.*, 27 (1989) 105.
10 W. Steuer, J. Baumann and F. Erni, *J. Chromatogr.*, 500 (1990) 469.
11 T. M. Engel and S. V. Olesik, in P. Sandra and G. Redant (Editors), *Eleventh International Symposium on Capillary Chromatography*, Hüthig, Heidelberg, 1990, pp. 736–746.
12 K. K. Unger, *Porous Silica*, Elsevier, Amsterdam, 1979.
13 L. R. Snyder and H. Poppe, *J. Chromatogr.*, 184 (1980) 363.
14 R. K. Iler, *J. Chromatogr.*, 209 (1981) 341.
15 M. L. Hair and W. Hertl, *J. Phys. Chem.*, 74 (1970) 91.
16 D. N. Strazhesko, V. B. Strelko, V. N. Belyakov and S. C. Rubanik, *J. Chromatogr.*, 102 (1974) 191.
17 H. Muller and H. Engelhardt, in I. Molnar (Editor), *Practical Aspects of Modern HPLC*, Walter de Gruyter, Berlin and New York, 1985, p. 25.
18 D. B. Marshal, C. L. Cole and A. D. Norman, *J. Chromatogr. Sci.*, 25 (1987) 262.
19 J. Nawrocki, *J. Chromatogr.*, 407 (1987) 171.
20 M. Verzele and C. Dewaele, *J. Chromatogr.*, 217 (1981) 399.
21 P. C. Sadek, C. J. Koester and L. D. Bowers, *J. Chromatogr. Sci.*, 25 (1987) 489.
22 K. K. Unger, N. Becker and P. Roumeliotis, *J. Chromatogr.*, 125 (1976) 115.
23 J. J. Kirkland, *Chromatographia*, 8 (1975) 661.
24 L. Boksanyi, O. Liardon and E. Kováts, *J. Adv. Colloid Interface Sci.*, 6 (1976) 95.
25 J. R. Strubringer, H. Song and J. F. Parcher, *Anal. Chem.*, 63 (1991) 104–108.
26 J. F. Parcher and M. I. Selim, *Anal. Chem.*, 51 (1979) 2154.
27 A. Tilly-Melin, Y. Askemark, K.-G. Wahlund and G. Schill, *Anal. Chem.*, 51 (1979) 976.
28 R. M. Cassidy and C. M. Niro, *J. Chromatogr.*, 126 (1976) 787.
29 R. Schwarzenbach, *J. Chromatogr.*, 251 (1982) 339.
30 J. A. Dean (Editor), *Lange's Handbook of Chemistry*, MacGraw-Hill, New York, 13th ed., 1985, Tables 5-8 and 5-11.
31 R. C. Weast (Editor), *CRC Handbook of Chemistry and Physics*, CRC Press, Boca Raton, FL, 69th ed., 1988, pp. D-161–D-162.

Journal of Chromatography, 547 (1991) 393–401
Elsevier Science Publishers B.V., Amsterdam

CHROM. 23 126

Analysis of lipids in aging seed using capillary supercritical fluid chromatography

R. M. HANNAN*
USDA-ARS, Regional Plant Introduction Station, 59 Johnson Hall, Washington State University, Pullman, WA 99164 (USA)
and
H. H. HILL, Jr.
Department of Chemistry, Washington State University, Pullman, WA 99164 (USA)
(First received August 7th, 1990; revised manuscript received January 24th, 1991)

ABSTRACT

Because of separation or detection problems associated with non-volatility and the non-chromophoric nature of lipids, capillary supercritical fluid chromatography (cSFC) was chosen over gas chromatography or high-performance liquid chromatography for the analysis of seed lipids. cSFC and flame ionization detection (FID) enabled more complete and accurate analysis of lipids extracted from onion seed. Replicated chromatography of triglyceride standards showed that retention times and quantitative chromatographic response was very reproducible. Analysis of cSFC–FID chromatograms of artificially aged and fresh onion seed lipids showed that significant changes occur in the lipid component of seed during aging. As the seed aged, there was a relative decrease of some of the larger molecular weight fractions and of the peak identified as vitamin E, tocopherol, while an increase was found in free palmitic and linoleic acids.

INTRODUCTION

Something occurs in a seed during its period of quiescence that results in premature senescence and death prior to or during the germination process. The importance of quality seed to agriculture and to the economic value of the seed industry provide reason enough to further understand the seed aging process. The quiescent seed represents life in a state of suspended animation, and thus provides a means of studying the organism in an orderly manner, unobscured by a high level of metabolism.

Previous studies have indicated that seed deterioration could be a result of genetic damage [1,2], degradation of the lipids and proteins of membranes [3,4] or degradation of other cellular organelles [5]. Free radicals, resulting from peroxidation reactions, have been implicated [6]. Although free radical reactions due to peroxidation of lipids is often mentioned in the literature, complete evaluation, quantification, and characterization of the changes in seed lipids due to this process have not been reported.

The peroxidation of seed lipids has been proposed as a fundamental mechanism

0021-9673/91/$03.50

of seed storage deterioration [3,4,7]. Lipid peroxidation is a free radical chain reaction between fatty acids and oxygen leading initially to hydroperoxides. Methylene interrupted pairs of double bonds in polyunsaturated fatty acids are especially prone to autoxidation. These same fatty acids serve as substrates for lipoxygenases which are found almost universally in plant tissues [8]. Lipoxygenase accelerates the rate of peroxidation of polyunsaturated fatty acids [9].

Also present in dicot seeds and seedlings are lyases which split hydroperoxides into aldehydes, hydrocarbons and smaller oxo-acids [9,10]. Volatile products comprise a characteristic volatile chemical signature amenable to analysis by gas chromatography (GC) [11]. Less volatile products such as large aldehydes, unsaturated aldehydes and ketones and products bearing glyceride residues have been poorly studied. Oxygenated fatty acids may accumulate during aging via autoxidation and break down to toxic aldehydes during seed hydration.

In order to study changes in the seed as it ages, accelerated aging techniques are often employed. It has been shown that the use of an elevated temperature and oxygen concentration regime sufficiently simulates natural aging [12,13]. To study seed lipids after seeds have undergone accelerated aging, many investigators have transesterified the entire lipid fraction and looked for changes in the fatty acid complement. This approach is simple and well established, but has not shed much light on causes of quality loss because whole lipid changes are obscured in the transesterification process. Less volatile compounds of complex mixtures are insufficiently volatile or stable to separate by GC at GC temperatures, and the mixtures are too complex for adequate resolution and identification using retention time in high-performance liquid chromatography (HPLC). Further, the lack of chromophoric groups limits detection after HPLC. These compounds are ideal candidates for the separation and detection by capillary supercritical fluid chromatography (cSFC) with flame ionization detection (FID). In addition, high-pressure liquefied gas extraction (HPLGE) is an attractive method for the study of seed aging because it combines low temperature and an inert atmosphere.

Since this combination of analytical methods is uniquely suited to extraction, separation and detection of lipid molecular species and their oxidation products, the objective of this study was to determine if changes occurred over time in the lipid content of onion seeds exposed to two different storage conditions. Changes were measured by monitoring seed viability (germination), seedling vigor, and making a critical comparison of lipid profiles obtained by cSFC–FID from pure, chemically unaltered extracted seed lipids.

MATERIALS AND METHODS

Seed storage treatment

Onion (*Allium cepa*) seed, breeding line MSU 2399B Lot 537879, was obtained from Dr. R. Watson, ARCO Seed Co. (El Centro, CA, USA). Until used, the seed was stored in plastic containers at 4°C, 28–30% relative humidity (%RH) at the USDA-ARS, Western Regional Plant Introduction Station (WRPIS) seed storage facility in Pullman, WA, USA.

Storage treatment conditions for the seed were: (1) the control was held in standard seed storage at 4°C, 28–30% RH in the WRPIS facility. Samples of seeds

were put into small coin envelopes and stored in drawers, the same as normal procedure for the Plant Introduction germplasm. (2) Seed exposed to heat treatment with elevated oxygen (accelerated aging) was removed from the conventional seed storage and 6–7 g seed/replicate was put into 250-ml erlenmeyer flasks. These were placed into a warm water bath (4 cm deep) maintained at constant 40–41°C. The flasks were then flooded with pure oxygen (O_2) for 2–3 min, and stoppered with rubber stoppers. A 95–99% oxygen atmosphere at 40–41°C was maintained by reflooding the flasks with oxygen every 14 days. Three replications were made for each aging time interval.

Treatment environments were monitored regularly by sampling the head space over the seed in each flask of the elevated oxygen temperature treatment for oxygen, nitrogen and carbon dioxide concentrations using GC–thermal conductivity detection (TDC). To separate the oxygen and nitrogen, injections were made into a GS-Q, 30 m × 0.53 mm I.D. capillary column (J & W Scientific, Folsom, CA, USA) which was valved in tandem to a 10 m × 0.53 mm I.D. Chrompack molecular sieve 5 A capillary column in a HP 5890A GC–TDC system. Chromatographic conditions were: 50-μl injections, using a gas-tight syringe, into the columns held at constant oven temperature of 30°C, and a helium carrier gas flow-rate of 15–20 ml/min. Air standards were run before and between sets of samples. For the first four weeks samples were taken every 48 h over the 12–14-day interval between oxygen flooding. Later, samples were taken just prior to oxygen flooding to verify the 95–99% oxygen concentration.

Germination and vigor tests

Seed was tested at regular intervals using the standard AOSA [14] methods. Seeds were germinated for viability data by plating 2 replicates of 50 seeds on blotter paper set in 15 cm diameter plastic petri plates. Plates were moistened and placed in environators (Puffer-Hubbard Environator, Grand Haven, MI, USA) set at the recommended regime of constant 20°C and constant dark. At each germination testing date, cold storage controls were also germinated. In these studies, successful germination was defined as when the seed had uniform imbibition and at least a 2 mm radical emerged. Vigor was evaluated based on comparative growth rates of the radical and hypocotyl between the treated samples and the control. Chlorosis, deformation and stunting of the radical were also considered in the vigor evaluations. Measurement of seedling vigor was based on a 1–5 scale where 5 was best vigor and 1 was very poor. Seeds that did not germinate where not rated for vigor. Germination data were analyzed with a standard analysis of variance and comparisons between treatments were made using the least significant difference (LSD) test at $P=0.05$.

Extraction

Extractions were conducted using a high-pressure Soxhlet extractor (J & W Scientific) and liquid carbon dioxide (CO_2) as the extraction solvent. A liquid CO_2 tank with an eductor tube was used as the solvent source. Seed was ground dry in a 37-ml stainless-steel container on a standard laboratory Waring blender for 20 s. Extractions were run for 48 h at 650–700 p.s.i. with a temperature differential of 38–41°C at the base of the chamber to 4°C on the cold finger. Blanks were run periodically to test for system contaminants. For each sample treatment three replicate extractions were made. Three aliquots for each extract were diluted 1:10 and 1:100 (v/v) in methylene chloride and chromatographed.

Capillary supercritical fluid chromatography

The cSFC was performed on a Lee Scientific Model 501 SFC with a flame ionization detector (Lee Scientific, Salt Lake City, UT, USA). Injection volume was 100 μl and split 12–15:1. A 20 $m \times 0.05$ mm I.D., SB-Methyl-100 capillary column (Lee Scientific) was used. In all of the separations the mobile phase was SFC-grade carbon dioxide (Matheson Gas Products), and the following pressure program was used at 150°C isothermally: 100 atm held for 3 min then increased to 275 atm at 25 atm/min, 300 atm at 5 atm/min, 320 atm at 2 atm/min, and finally to 400 atm at 40 atm/min which was held for 5 min. The column was thermally conditioned 14 h at 280°C, and was rinsed with pentane and then with supercritical carbon dioxide by cycling between densities of 0.19 and 0.845 g/cm^3 for 12 h at 75°C. Three replicate chromatograms per dilution per extraction per treatment were made, and adjusted peak areas and retention times were statistically analyzed.

Component identification by mass spectrometry

The 70-eV electron impact mass spectra were obtained on a VG 7070E spectrometer with a source temperature of 200°C and 6000-V ion acceleration. An aliquot of 2 μl of oil was put into a melting point capillary and heated by the solids probe in 25°C increments to 400°C. Scans were made between 30–750 mass/charge (m/e) at 1.5 s/decade. Spectra were obtained and selected scans were compared to the National Bureau of Standards Library of standard spectra.

RESULTS AND DISCUSSION

Germination and vigor tests

Initial germination upon receipt of the onion seed was 99.5%. At the beginning of the aging experiments the germination was 96%. There was no significant change in germination in the cold treatment over the duration of the experiment (Table I). There was a significant loss of viability in response to the heat (41°C) and elevated oxygen treatment as compared to the control, 14% and 99% respectively over 11

TABLE I

GERMINATION AND VIGOR OF ONION SEEDS STORED AT CONSTANT 4°C, OR AT 41°C IN ELEVATED OXYGEN ATMOSPHERE

Crop	Treatment			Mean percent[a] germination					Mean vigor[a]				
	Temp. (°C)	$\%O_2$	%RH	T_0	T_3	T_6	T_9	T_{11}	T_0	T_3	T_6	T_9	T_{11}
Onion	4	21	28	96	97	98	98	99a[b]	5.0	4.7	5.0	4.8	4.8a[b]
	41	97	22	95	65	28	19	14b	4.7	2.5	1.0	1.0	0.8b

[a] Values represent mean percent germination or mean vigor from 2 replications of 50 seeds. T subscripts represent the number of months from the beginning of the aging treatment to the time sampled for testing.

[b] Comparisons among treatments followed by the same letter do not differ significantly from each other according to Duncan's new multiple range test, $P = 0.05$.

months. Vigor data indicated that 41°C and under the elevated oxygen environment, tested seed quickly lost seedling vigor when compared to the control.

Extraction and chromatography

The onion seed had an extractable lipid content within the normal range for its species. The average lipid component on a dry weight basis for the onion seed was 10–12%.

In replicated studies of the chromatography of lipids from onion seed stored under the two aging environments, significant differences were found in the quantitative comparisons of peaks from the chromatograms. Degradation of the triglyceride peaks in the aged seed lipids and an increase in the smaller components free fatty acids were found. In addition, there was a quantitative increase in the last few peaks. Statistical analysis showed no significant differences for the retention times of corresponding peaks in chromatograms of replicate sub-samples from either within or between sample treatments.

At the 1:100 dilution of seed lipids from onion seed which underwent accelerated aging there was a significant decrease in two of the triglyceride peaks (peaks 5 and 7) of 3.8 and 19.5%, respectively compared to the 4°C control, and increases in peaks 1, 2 and 3. As shown in Fig. 1, new peaks, numbered 1 and 2, appeared after 11 months of accelerated aging. There was a three fold increase of peaks 8 and 9 in the aged seed over the control. As shown in Table II, all but one of the peaks from the aging treatments were significantly different from those of the cold storage control.

As seen in Table III these differences were further amplified in the chromatography of the 1:10 dilutions of the same onion seed lipid samples. Of 20 integrated peaks from the oxygen treated aged sample, all but 2 (peaks 3 and 10) were significantly different from the room temperature treatment. There were large relative decreases in the two major peaks 11 and 12 of 4.7 and 22.1% respectively. Degradation in these

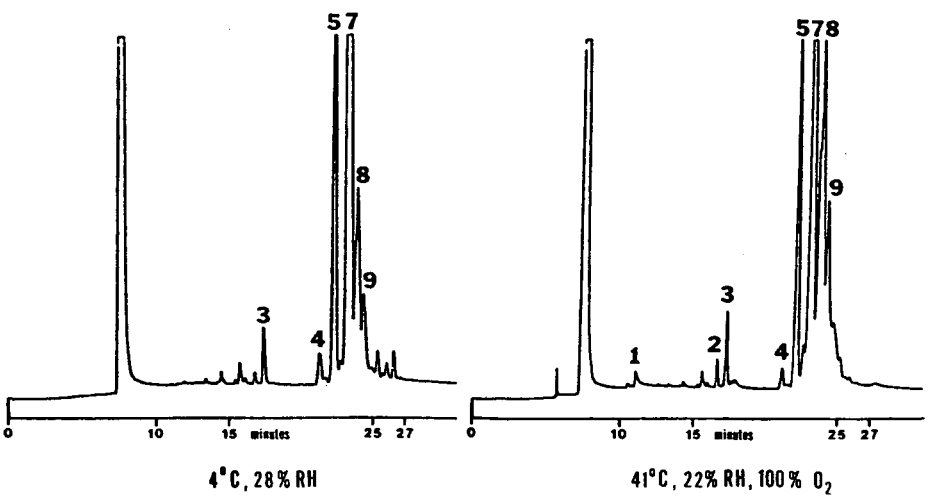

Fig. 1. cSFC–FID chromatograms of lipids from onion seeds which had been stored in different environments at 1:100 dilution in methylene chloride.

TABLE II

COMPARISON OF LIPIDS CHROMATOGRAPHED WITH cSFC–FID in 1:100 DILUTION OF SEED LIPID IN METHYLENE CHLORIDE

Allium cepa seeds were stored at 4°C in ambient atmosphere or 41°C in elevated oxygen atmosphere.

Peak No.	Relative areas[a]	
	Treatment temperature (°C)	
	4°C	41°C and O_2
1	NP	0.919 ± 0.083*
2	NI	0.636 ± 0.020*
3	1.068 ± 0.016	1.805 ± 0.089*
4	0.766 ± 0.130	0.621 ± 0.025*
5	16.181 ± 0.311	12.336 ± 0.202**
6	NI	1.297 ± 0.096*
7	72.554 ± 0.132	52.988 ± 1.31*
8	7.084 ± 0.274	21.015 ± 0.360*
9	2.771 ± 0.073	10.100 ± 0.916*

[a] Relative areas = (peak area) (total area of lipid components) (100%). Data are followed by the standard deviation. Data calculated from 3 runs per 3 replicate extractions. Treatment comparison where * = significantly different at $P = 0.05$, and ** = significantly different at the $P = 0.01$ level using Student's paired t-test. NP = no peak in chromatogram. NI = Peak is in chromatogram but not large enough to be integrated.

TABLE III

COMPARISON OF LIPIDS CHROMATOGRAPHED WITH cSFC–FID IN 1:10 DILUTIONS OF SEED LIPID IN METHYLENE CHLORIDE

Allium cepa seeds stored at 4°C in ambient atmosphere or 41°C in oxygen atmosphere.

Peak No.	Retention time	Normalized peak areas[a]		
		Treatment temperature (°C)		Ratio 41°C/4°C
		4°C	41°C & O_2	
1	10.89	–	0.590 ± 0.054	–
2	11.25	0.366 ± 0.024	3.043 ± 0.338	8.319
3	14.49	0.509 ± 0.025	0.285 ± 0.036	0.561
4	15.71	1.000	1.000	1.000
5	16.71	0.614 ± 0.030	1.685 ± 0.132	2.743
6	17.32	3.054 ± 0.169	5.000 ± 0.421	1.637
7	17.71	–	0.437 ± 0.085	–
8	18.12	–	0.953 ± 0.206	–
10	21.65	2.751 ± 0.235	2.133 ± 0.255	0.755
11	22.74	44.356 ± 2.41	30.963 ± 0.418	0.698
12	24.11	196.959 ± 8.89	136.810 ± 9.11	0.694
13	24.37	19.832 ± 2.10	18.786 ± 1.16	0.947
14	24.88	9.951 ± 0.505	38.037 ± 3.03	3.822
15	25.22	2.188 ± 0.188	28.320 ± 2.05	12.943
15′	25.41	–	10.245 ± 2.12	–
16	25.62	1.781 ± 0.189	5.211 ± 0.427	2.895
17	25.94	0.273 ± 0.023	0.597 ± 0.121	2.197
18	26.22	0.663 ± 0.238	0.895 ± 0.022	1.350
19	26.67	1.171 ± 0.039	–	–
20	27.84	–	2.544 ± 0.613	–

[a] All peaks were normalized to peak 4 since relative peak areas were equivalent for this peak. Data are followed by the standard deviation. Data calculated from 3 runs per 3 replicate extractions.

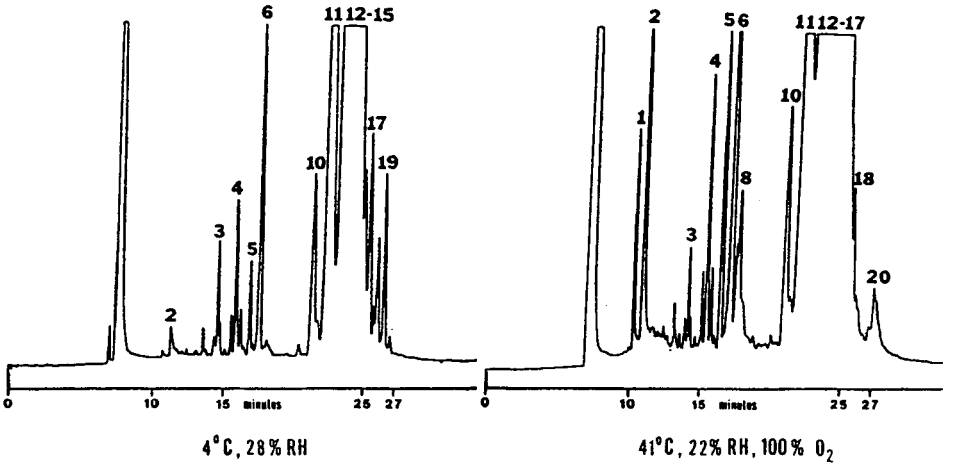

Fig. 2. cSFC–FID chromatograms of lipids from onion seeds which had been stored in different environments at 1:10 dilution in methylene chloride. Peaks: 1 = palmitic acid, 2 = linoleic acid, 3 = tocopherol, and 4 = sitosterol.

peaks was reflected in significant increases in the lower-molecular-weight fractions at peaks 1, 2, 5 and 7–9, and the larger-molecular-weight peaks at 14, 15, 16 and 17. In the control and room temperature treatments there was one small, non-integrated coalesced peak at a retention time which would span the retention times for peaks 7–9 of the oxygen treatment. Although there was not good separation for peaks 7–9 in the oxygen treatment, they can be seen in the chromatogram (Fig. 2).

Results from electron impact (EI) mass spectrometry gave a very clear spectra at scan 400 between 250 and 700 mass units. Using a cut of this scan in the mass range of 370–460 the spectra matched the NBS library spectra for α-tocopherol (vitamin E) and γ-sitosterol. In a comparison of standards for these two compounds and the 4°C control onion lipid sample run on cSFC–FID there was a match for retention times for both compounds (Fig. 3). These peaks are represented by peaks 3 and 4 in the onion lipid chromatogram (Fig. 2).

CONCLUSIONS

These studies represent the first time that the seed lipid components have been compared in fresh and artificially aged seed using capillary supercritical fluid chromatography and flame ionization detection to generate chromatographic pictures and data for intact lipid molecular species reflecting the aging process. Results from these studies show that under less than optimal storage conditions there are significant changes in the lipid component of normal, healthy onion seed. During the aging process, compounds are either fragmented or chemically redistributed. Therefore, when the lipid components are chemically hydrolysed and prepared for fatty acid analysis, changes in the larger triglyceride species are not readily evident. As has been found previously by many others, there was a corresponding loss in seed viability and vigor during the aging process [12]. Under high-temperature and oxidative conditions the change of seed lipid components was accelerated, and the patterns of these chang-

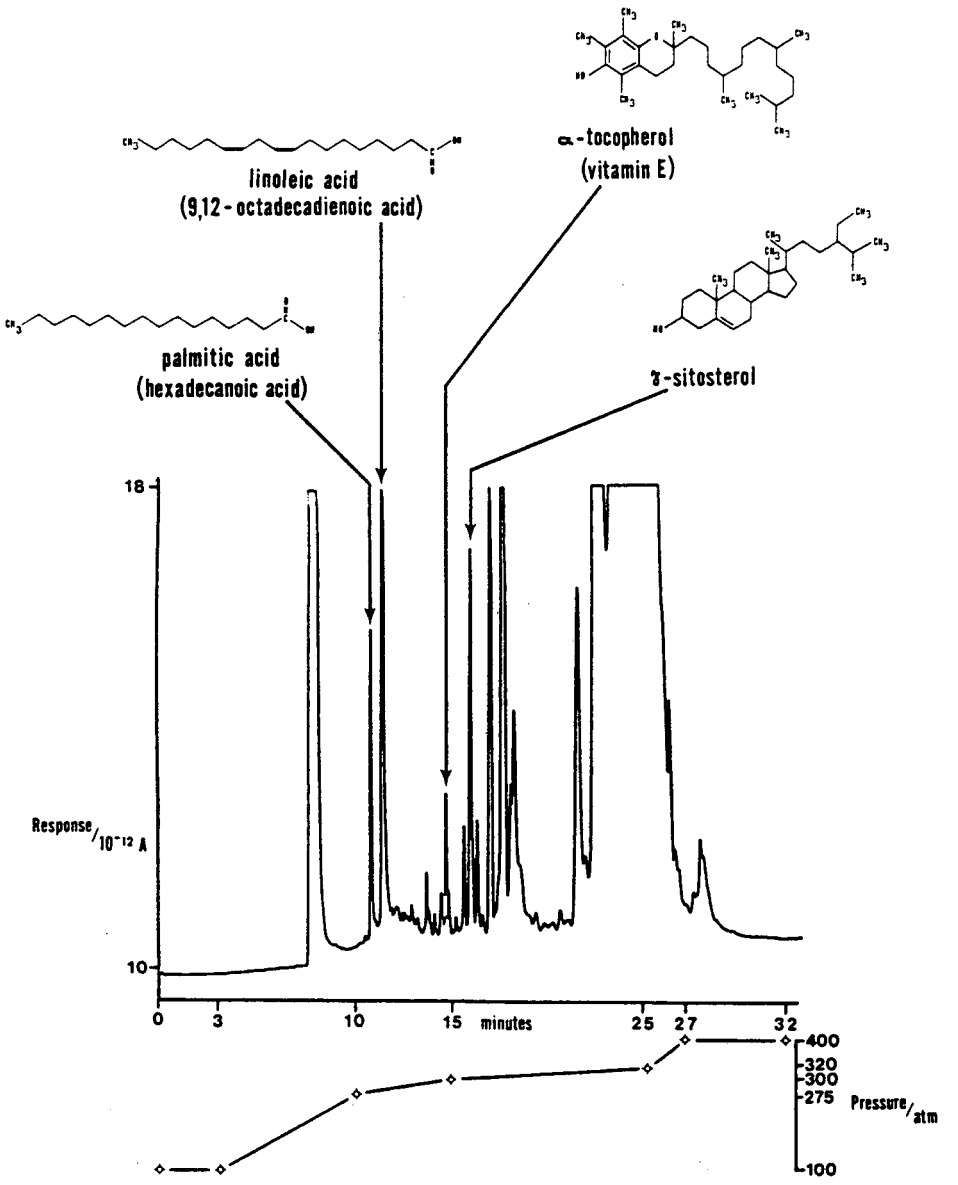

Fig. 3. Combination of mass spectrometry and cSFC retention time matching of standards indicated that two products of accelerated aging were palmitic and linoleic acid. Also, tocopherol and sitosterol were identified in both the control and aged seed lipid samples.

es was similar to what has been found in naturally aged seed [15]. The gradual loss in germination and appearance of seedlings with poor vigor was similar to what is found when testing a broad selection of genotypes from the same species from naturally aged germplasm. There was a general chlorosis, slow growth of the radical, and often

deformation of the primary leaves found in the seedlings from accelerated aged seeds. This was a similar response to what is often found in seeds of the same species which have been stored under optimal maintenance storage conditions for a long period of time.

Mention of a trademark or proprietary product does not constitute a guarantee or warranty of the product by the U.S. Department of Agriculture and does not imply its approval to the exclusion of other products that may also be suitable.

REFERENCES

1 E. H. Roberts, *Viability of Seeds*, Syracuse University Press, Syracuse, NY, 1972, pp. 253–306.
2 E. E. Roos, *HortScience*, 15 (1980) 781–784.
3 P. T. Koostra and J. F. Harrington, *Proc. Int. Seed Test. Assoc.*, 34 (1969) 329–340.
4 D. O. Wilson, Jr. and M. B. McDonald, Jr., *Seed Sci. Technol.*, 14 (1986) 269–300.
5 A. A. Abdul-Baki and J. E. Baker, *Seed Sci. Technol.* 1 (1973) 89–125.
6 A. D. Knapp, *Ph.D. Thesis*, Washington State University, Pullman, WA, 1981.
7 R. R. C. Stewart and J. D. Bewley, *Plant Physiol.*, 65 (1980) 245–248.
8 R. Tressl, D. Bahri and K. H. Engel, (*ACS Symposium Series*, No. 170), American Chemical Society, Washington, DC, 1981, pp. 213–232.
9 J. Sekiya, T. Kajiwara, K. Munechika and A. Hatanaka, *Phytochemistry*, 22 (1983) 1867–1870.
10 B. A. Vick and D. C. Zimmerman, *Plant Physiol.*, 57 (1976) 780–788.
11 E. N. Frankel, W. E. Neff and E. Selke, *Lipids*, 26 (1981) 279–285.
12 R. M. Hannan, *Ph.D. Thesis*, Washington State University, Pullman, WA, 1989.
13 J. B. Ohlrogge and T. P. Kernan, *Plant Physiol.*, 70 (1982) 791–794.
14 Association of Official Seed Analysts, *J. Seed Technol.*, 6 (1981) 1–125.
15 D. A. Priestley, *Seed Aging Implications for Seed Storage and Persistence into the Soil*, Cornell University Press, Ithaca, NY, 1986, Ch. 7.

Journal of Chromatography, 547 (1991) 403–409
Elsevier Science Publishers B.V., Amsterdam

CHROM. 23 180

Direct use of Empore sheets in overpressured thin-layer chromatography

C. REGNAULT, P. DELVORDRE and E. POSTAIRE*
Laboratory of Analytical Development, Central Pharmacy for Paris Hospitals, 7 Rue du Fer à Moulin, 75221 Paris Cedex 05 (France)
(First received October 26th, 1990; revised manuscript received February 5th, 1991)

ABSTRACT

The impregnation of the edges of plates before carrying out forced-flow thin-layer chromatography (TLC) as overpressured TLC is time consuming. This paper reports the optimisation of analytical parameters and the direct use of a new separation medium, Empore TLC sheets, for forced-flow TLC. The pressure of the water pump (P) and the flow-rate of the eluent (F) were studied and optimum values of P = 2–4 bar and F = 0.4–0.6 ml/min were determined. The separation of a mixture of dyes and a bergamot oil was investigated and the results demonstrated that the direct utilisation of Empore TLC sheets in forced-flow TLC gave performances similar to pre-impregnated high-performance TLC plates.

INTRODUCTION

One of the major advantages of the use of forced-flow thin-layer chromatography (TLC) as overpressured TLC (OPLC) over other planar chromatography techniques is the decrease in migration time resulting from the absence of a vapour phase and no capillary flow. The distance of the front, Z, is a linear function of development time, t: $Z = kt$ [1–4]. However, the overpressured chromatographic separation technique requires that the edges of the chromatographic plate are sealed by a polymer solution, which prevents the eluent from flowing off the chromatographic plate in an unwanted direction. This procedure, called impregnation, is time consuming and needs careful attention and skill.

Empore TLC sheets were recently introduced in the USA as a new separation medium [5]; they are prepared from 8 μm diameter and 60 Å pore size particles entrapped in a matrix of poly(tetrafluoroethylene) (PTFE) microfibrils. Their flexibility suggests an interesting means of eliminating the impregnation step.

Poole *et al.* [6] have recently demonstrated the successful use of forced-flow development with an Empore sheet, but pretreatment of the edges of the plate was still needed. To improve the analytical conditions, preliminary tests without pretreatment have been performed to check the performance of these plates under OPLC conditions.

To assess their performances in OPLC, these plates were compared, after pa-

0021-9673/91/$03.50

rameter optimisation, to those most commonly used for the separation of dyes and bergamot oils.

EXPERIMENTAL

Characteristics of the Empore plates

The Empore plates (also called sheets) were from 3M Labs. (Analytichem International Harbor City, CA, USA). They consist of 90 ± 2% silica entrapped in a matrix of PTFE, which gives great flexibility and allows the sheet to be cut easily in the laboratory (using, for instance a pair of scissors). The sheets consist of a 0.5 mm thick layer with 60 Å diameter silica pores and 8 μm diameter silica particles. The absorption capacity of the particles is greater than that of similar plates. The tests were performed with untreated Empore sheets.

Preliminary tests

Seven streaks of 1 μl of dye solution containing violet 1, butter yellow, red, sudan red G and indophenol blue (Labor MIM, Budapest, Hungary), mixed with heptane, were placed in a 4-mm band on an Empore 10 × 20 cm silica plate without fluorescence indicator (Analytichem International) using an automatic applicator (Linomat IV, Camag, Muttenz, Switzerland).

The dyes were eluted by toluene using a Chrompres 25 (Labor MIM) over a migration distance of about 8 cm. The conditions were as follows: water pump pressure, 25 bar; eluent pump pressure, 6 bar; initial volume used to fill the trough and form a uniform solvent front, 1.2 ml; and flow-rate, 0.3 ml/min.

Influence of the water cushion pressure

The tests were carried out on an Empore 10 × 10 cm silica plate (without fluorescence indicator). The selected solvent was ethanol, which allows the observation of potential leaks on the press base, the study of the linearity of the solvent front and the calculation of migration distance. The initial conditions were as follows: eluent pump pressure, 6 bar; solvent volume, 0.7 ml; flow-rate, 1 ml/min; and migration distance, 7 cm.

The cushion pressure was then varied from 0 to 20 bar in steps of 1 bar; the appearance of potential leaks, and the time and migration distance of the α and β fronts were observed. Each test was carried out in duplicate.

Influence of the eluent flow-rate

The operating conditions were as described for the influence of water cushion pressure. The cushion pressure was 4 bar and the eluent pump flow-rate varied from 0.1 to 2 ml/min.

Separation of a dye mixture after optimisation

The dye mixture was re-used to test the optimisation of the utilisation parameters of the Empore plates in OPLC.

Volumes of 1 μl of dye mixture were manually applied to an Empore 10 × 10 cm silica plate (without fluorescence indicator). The conditions were as follows: water cushion pressure, 2 bar; flow-rate, 0.6 ml/min; initial volume, 0.7 ml; and eluent pump pressure, 6 bar. The elution was performed with toluene.

Separation of bergamot oil

A comparative study of bergamot oil (Man C^{ie}, Bar sur loup France) separation in chamber and by OPLC was carried out using the Empore silica F_{254} 10 × 10 cm plates and HPTLC silica F_{254} 10 × 10 cm plates (Merck, Darmstadt, Germany) on a glass support (chamber) and an aluminium support (OPLC).

Streaks of 6 μl of bergamot oil were added to the plates in a 6-mm band using Linomat IV. The eluting phase was chloroform–methanol–1 *M* sodium hydroxide solution (95:5:0.1, v/v/v).

The operating conditions in the OPLC were the same as those used for optimising the parameters for the Empore plates. For standard plates, the water cushion pressure was 25 bar, the eluent pump pressure 6 bar, the initial volume 0.7 ml and the flow-rate 0.25 ml/min.

Readings were taken using a Desaga CD 60 densitometer (Desaga, Heidelberg, Germany) at 254 nm in the reflectance mode.

RESULTS AND DISCUSSION

Optimisation of parameters

During the preliminary tests, the elution was not linear, but followed a radial path (Fig. 1). This phenomenon is a result of applying too high a pressure to the Empore plate. The distortion is imprinted on the inlet as well as on the cushion membrane groove, which is obstructed, and therefore the solvent no longer has free access to the whole length of the plate. The eluent moves centrifugally away from the inlet. An optimisation of the utilisation parameters of the Empore plate in OPLC [water cushion pressure (*P*) and solvent flow-rate (*F*)] was therefore necessary.

The results of pressure optimisation study (Fig. 2a) show that (1) the leaks are proportional to pressure; (2) the migration time remains very similar; and (3) the α and β fronts are altered. The migration time is unacceptable for high pressures (> 4 bar) and for low pressures (< 2 bar) as there are numerous leaks and the solvent fronts are non-linear. However, these phenomena are considerably reduced and the solvent front is almost linear for pressure from 2 to 4 bar.

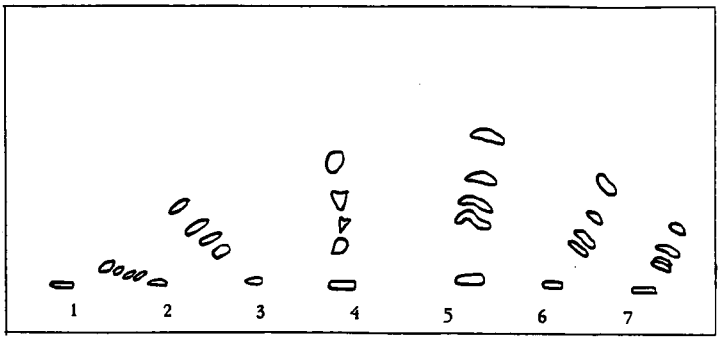

Fig. 1. Overpressured thin-layer chromatography of dyes. Elution order: violet 1, sudan red G, indophenol blue, red, butter yellow. Seven streaks of the same solution were applied. Conditions: eluent, toluene; water pump pressure, 25 bar; eluent pump pressure, 6 bar; initial volume, 1.2 ml; flow-rate, 0.3 ml/min.

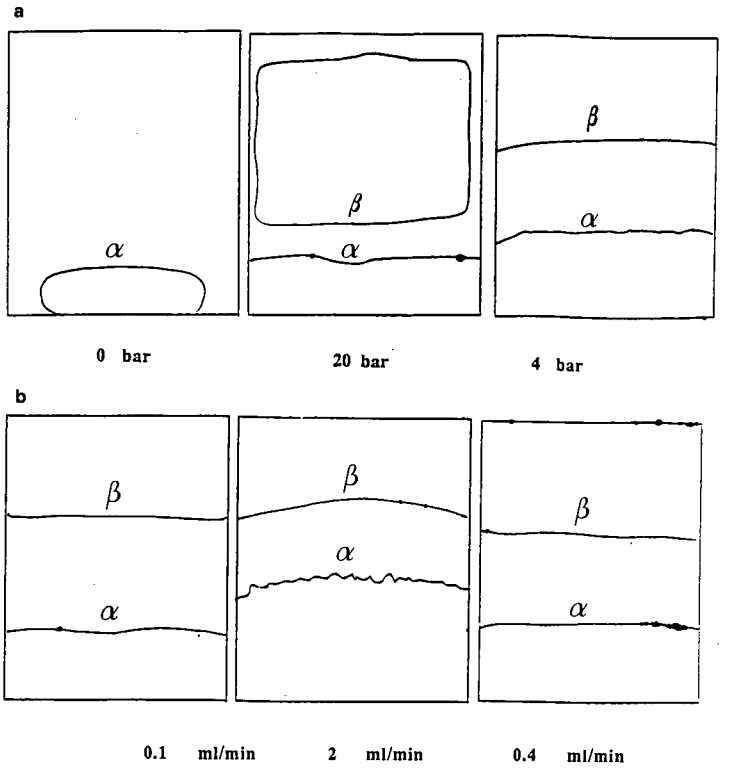

Fig. 2. (a) Optimisation of pressure. Conditions: eluent pump pressure, 6 bar; initial volume, 0.7 ml; flow-rate, 1 ml/min. α and β fronts can be observed for a pressure of 4 bar. (b) Flow optimisation. Conditions: eluent pump pressure, 6 bar; initial volume, 0.7 ml; water pump pressure, 4 bar. α and β fronts can be observed.

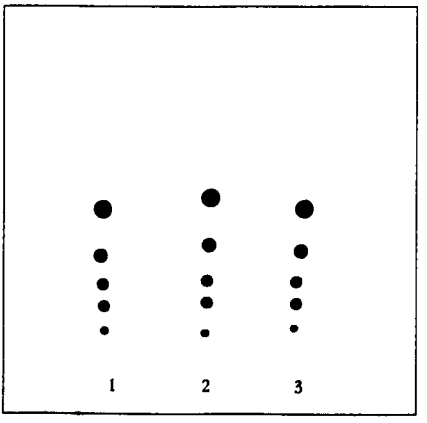

Fig. 3. Overpressured thin-layer chromatography of dyes. Three streaks of the same solution were applied. Conditions: eluent pump pressure, 6 bar; water pump pressure, 2 bar; initial volume, 0.7 ml; flow-rate, 0.6 ml/min. For elution order of dyes, see Fig. 1.

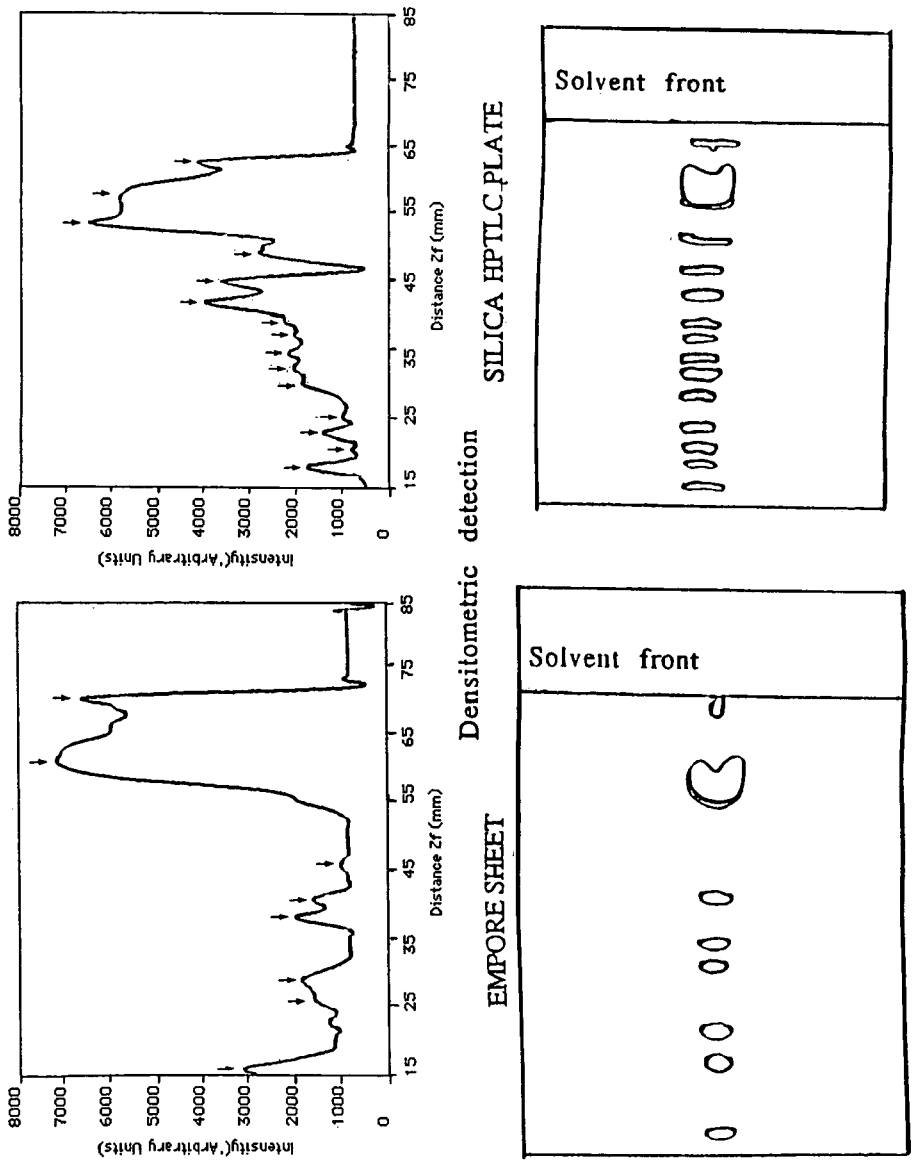

Fig. 4. Planar chromatography of bergamot oil in a tank using a silica high-performance TLC (HPTLC) plate and an Empore sheet. Arrows indicate that the integrated compounds are visually detectable. Z_f is the elution distance.

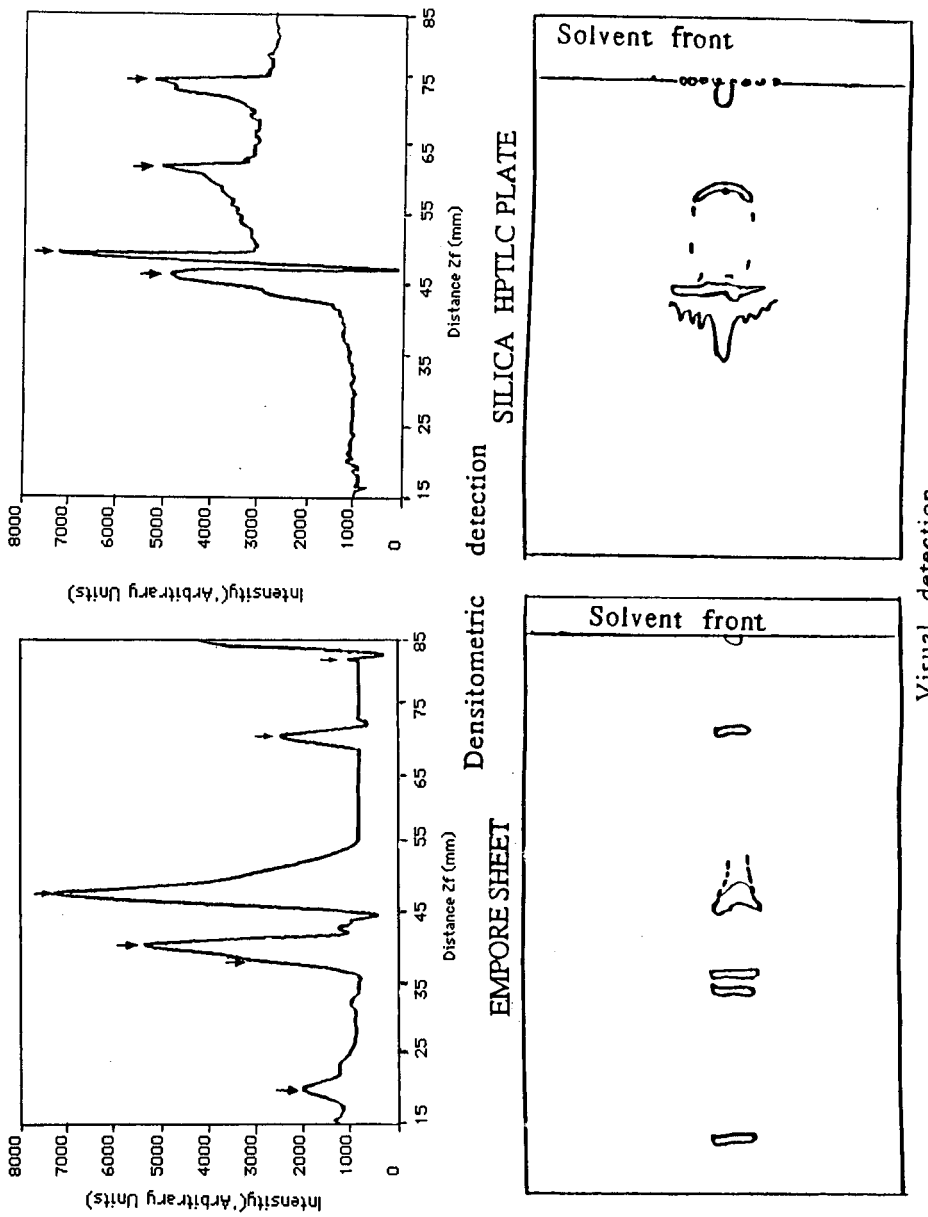

Fig. 5. Overpressured thin-layer chromatography of bergamot oil using a silica HPTLC plate and an Empore sheer. Arrows as in Fig. 4. Z_f is the elution distance.

The results of the flow-rate optimisation (Fig. 2b) show that the migration time is inversely proportional to the flow-rate. In contrast, the number of leaks is proportional to the flow-rate and a modification of the linearity of the α and β fronts is observed for flow-rates >0.75 ml/min. The maximum flow-rate therefore lies between 0.4 and 0.6 ml/min for ethanol.

Application to specific cases

*Separation of a dye mixture.*The migration of the dyes is similar to that observed with conventional plates and leaks are almost non-existent (Fig. 3). The lower pressure of the water cushion no longer distorts the plate, allowing the solvent to migrate freely.

*Separation of bergamot oil.*The results observed do not show any correlation between separation in tank and by OPLC. This is because in a tank the solvents migrate together, whereas in OPLC each solvent migrates independently as a result of their different physicochemical properties [7].

In a first analysis, the results in the chamber with Empore sheets are therefore more favourable than a separation on conventional plates; it enables the display of fifteen spots compared to the eight on the Empore plates, and these have a higher peak intensity (Fig. 4). In addition, these results confirm the work of Poole *et al.* [8], which showed the inferior performance of these new plates. However, these results are reversed in OPLC; the number of compounds detected densitometrically is greater on the Empore plate and the intensity of the common peaks is higher with a better resolution. The baseline is perfectly linear (Fig. 5).

CONCLUSION

The direct utilisation of the new Empore plates in OPLC is possible. Parameter optimisation was necessary, although the results are encouraging and suggest that further development may allow this product to become of much more use in the future.

ACKNOWLEDGEMENTS

The authors thank J. M. Newmann (Newmann Howells Associated Limited, Winchester, UK) for the supply of the 20 × 20 cm Empore TLC sheets.

REFERENCES

1 E. Tyihák, E. Mincsovics and H. Kalász, *J. Chromatogr.*, 174 (1979) 75.
2 E. Tyihák, E. Mincsovics, H. Kalász and J. Nagy, *J. Chromatogr.*, 211 (1981) 4.
3 Z. Witkiewicz and J. Bladek, *J. Chromatogr.*, 373 (1986) 3.
4 S. Hara, T. Uchimaru, Y. Hoshi and G. Szepesi, *J. Planar Chromatogr.*, 2 (1989) 430.
5 *Empore Thin Layer Chromatography Sheets; Data Sheet*, Analytichem International, Harbor City, CA, 1988.
6 S. K. Poole, W. P. N. Fernando and C. F. Poole, *J. Planar Chromatogr.*, 3 (1990) 331.
7 Sz. Nyiredi, S. Y. Mèszaros, K. Dallenbach-Toelke, K. Nyiredi-Mikita and O. Sticher, *J. High Resolut. Chromatogr., Chromatogr. Commun.*, 10 (1987) 352.
8 S. K. Poole and C. F. Poole, *J. Planar Chromatogr.*, 2 (1989) 478.

Journal of Chromatography, 547 (1991) 411–418
Elsevier Science Publishers B.V., Amsterdam

CHROM. 23 248

Separation and determination of polyether carboxylic antibiotics from *Streptomyces hygroscopicus* NRRL B 1865 by thin-layer chromatography with flame ionization detection

S. AUBOIRON and D. BAUCHART*
U.R. Métabolismes Energétique et Lipidique, INRA, Centre Clermont-Theix, 63122 Saint-Genès Champanelle (France)
and
L. DAVID
Laboratoire de Chimie Organique Biologique, BP 86, 63172 Aubière Cedex (France)
(First received January 14th, 1991; revised manuscript received February 26th, 1991)

ABSTRACT

Thin-layer chromatography coupled with flame ionization detection was used to develop a method to separate and to determine simultaneously three polyether carboxylic ionophore antibiotics (abierixin, nigericin and grisorixin) produced by *Streptomyces hygroscopicus* NRRL B 1865. Various proportions of chloroform, methanol and formic acid (or acetic acid as a substitute for formic acid) were used in the developing solvent to determine changes in R_F values of the antibiotics and to allow conditions for maximum resolution to be obtained. Development on Chromarods SII with chloroform–methanol–formic acid (97:4:0.6, v/v/v) gave satisfactory and reliable separations of the three polyether antibiotics. Under these conditions, the internal standard methyl desoxycholate was found to be suitable for their simultaneous determination in the lipid extracts of *Streptomyces hygroscopicus* NRRL B 1865.

INTRODUCTION

Carboxylic polyether ionophore antibiotics constitute a family of metabolites mainly produced by *Streptomyces* spp. Owing their anticoccidial and antimicrobial properties, they are used as feed additives to prevent coccidiosis in poultry [1] and to improve food efficiency and growth rate in sheep [2] and beef cattle [3].

These antibiotics have also been subjected to biosynthetic experiments [4]. In the course of our study on the biosynthesis of the carboxylic polyether ionophore antibiotic nigericin, produced by *Streptomyces hygroscopicus* NRRL B 1865 (Fig. 1), the addition of methyl oleate in the original fermentation culture increased the titre of the antibiotic pool [5]. Under these conditions, we isolated two nigericin closed-structural antibiotics which were produced at low levels, abierixin [5] and grisorixin [6] (Fig. 1); grisorixin was first isolated from *Streptomyces griseus* LAB 2142 [7].

In order to determine precisely the concentration of these three antibiotics in lipid extracts of *Streptomyces hygroscopicus* NRRL B 1865 and to measure the effects of the addition of effectors, a reliable and rapid method of analysis was required.

0021-9673/91/$03.50

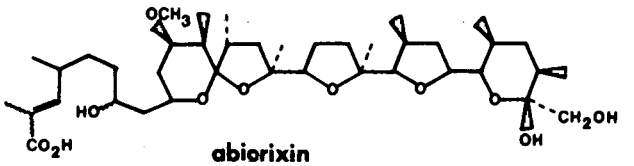

abierixin

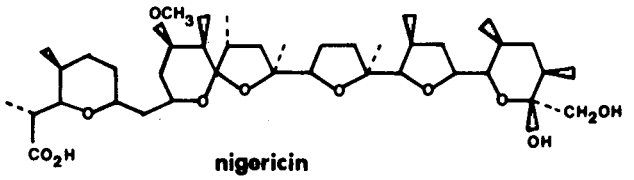

nigericin

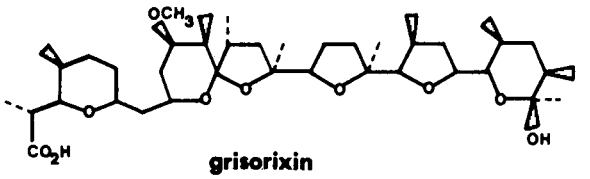

grisorixin

Fig. 1. Structures of three polyether carboxylic antibiotics produced by *Streptomyces hydroscopicus* NRRL B 1865.

Isolation by thin-layer chromatography (TLC) and detection with a vanillin–sulphuric spray [8] or by bioautography [9] were unsuitable for low levels of antibiotics. Complete separation and subsequent analysis of antibiotics has been achieved by high-performance liquid chromatography (HPLC), but this method is expensive and usually needs the preparation of fluorescent derivatives [10,11].

Separation on silica gel-coated quartz rods (Chromarods) by thin-layer chromatography and flame ionization detection (FID) was largely developed for qualitative analysis and the determination of plasma and tissue lipids [12]. The TLC–FID method appeared to be rapid, selective and sensitive, but had not previously been applied to antibiotic analysis, excepted for β-lactams and tetracycline [13], mainly because of the absence of an appropriate developing solvent. Therefore, the aim of this work was to establish the experimental conditions for analysis by TLC–FID to allow the accurate and reproducible separation and determination of abierixin, nigericin and grisorixin in lipid extracts of *Streptomyces hygroscopicus* NRRL B 1865.

EXPERIMENTAL

Antibiotic production

The three polyether carboxylic antibiotics abierixin, grisorixin and nigericin were produced by a strain of *Streptomyces hygroscopicus* NRRL B 1865. Cultures

were grown at 27°C for 7 days in a basal medium [5] with or without methyl oleate (1 g in 100 ml of medium) (Fluka, Buchs, Switzerland).

Antibiotic purification

A 15-l volume of the culture broth was filtered, yielding *ca.* 300 g of mycelial cake. After acidification at pH 4.0 with 1 *M* hydrochloric acid, the mycelial cake was homogenized in ethanol for 2 h in an Ultra-Turrax homogenizer. After 2 h, mycelium was removed by filtration and ethanol was eliminated by evaporation under vacuum, then the residual syrup which contained the antibiotics was solubilized in ethyl acetate–water (50:50, v/v). After drying over anhydrous sodium sulphate, the ethyl acetate extract was concentrated under reduced pressure and the residue was solubilized in chloroform. Antibiotics were fractionally separated by column liquid chromatography on a silica gel Type 60 (0.063–0.200 mm) (Merck, Darmstadt, Germany) column using cyclohexane–ethyl acetate with increasing amounts of ethyl acetate as eluting solvent [5].

Antibiotic analysis by TLC–FID

Antibiotic samples were chromatographed on silica gel Chromarods S-II and then analysed on an Iatroscan TH 10 Analyser, Mark III (Iatron Labs., Tokyo, Japan; French distributor, Delsi Instruments, Argenteuil, France) equipped with a flame ionization detector and connected to an Enica-10 electronic integrator (Delsi Instruments). The hydrogen flow-rate was 160 ml min^{-1} and the air flow-rate was 2 l min^{-1}. The scanning speed was 0.42 cm s^{-1}.

Chromarods were cleaned before use by soaking overnight in 5 *M* sulphuric acid, rinsed with distilled water, then dried at 110°C for 5 min and finally scanned twice in the Iatroscan just before use.

A chloroform solution containing equal amounts by weight (2μg/μl) of abierixin (A), nigericin (N) and grisorixin (G) was prepared to determine the effect of solvents on the resolution of antibiotics of Chromarods. For the purpose of standardization, a number of compounds including different antibiotics purified in our laboratory and lipids (Sigma, St. Louis, MO, USA) were tested. For the calculation of the response correction factors, three chloroform solutions were prepared; they contained a similar amount of methyl desoxycholate (5 μg/ml) (Sigma), which was used as the internal standard, and increasing amounts of each of the three antibiotics (2, 6 and 10 μg/ml).

For the determination of antibiotics from *Streptomyces hygroscopicus* NRRL B 1865, total lipids were extracted from 0.5 g of mycelia with chloroform–methanol (2:1, v/v) according the method of Folch *et al.* [14]. Methyl desoxycholate (1.25 mg) was added to the lipid extracts for the determination of the antibiotics in mycelia. Lipid solution in chloroform (20 mg/ml) was finally prepared for antibiotic analysis using TLC–FID.

For each of the aliquots, 0.5–1 μl of the chloroform solution was spotted on each of ten Chromarods held in an appropriate frame and transferred to the developing tank lined with filter-paper. Each antibiotic sample was analysed on 7–10 rods, the procedure being repeated at least once for each sample.

All solvent mixtures used for development were prepared by mixing x volumes of methanol with $100 - x$ (first trial, Fig. 2) or with $97 - x$ (second trial, Fig. 3)

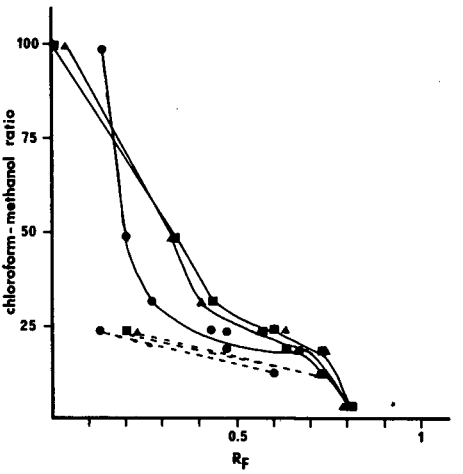

Fig. 2. R_F values of (●) abierixin, (■) nigericin and (▲) grisorixin plotted at various concentrations of chloroform, methanol and acetic acid (———, 0.5 vol.; ---, 1 vol.) in the developing solvent keeping the sum of the levels of chloroform and methanol constant (100) [chloroform–methanol–acetic acid = 100 − x : x : 0.5 (———) or 100 − x : x : 1 (----)].

volumes of chloroform. The organic acids (acetic and formic acids) were added to the 100 ml (Fig. 2) or 97 ml (Fig. 3) of solutions containing chloroform and methanol in amounts of 0.5–1 ml.

For the determination of antibiotics from *Streptomyces hygroscopicus* NRRL B 1865, the Chromarods were developed in chloroform–methanol–formic acid (97:4:0.6, v/v/v). The rods were then dried at 110°C for 5 min and transferred to the Iatroscan analyser for subsequent scanning.

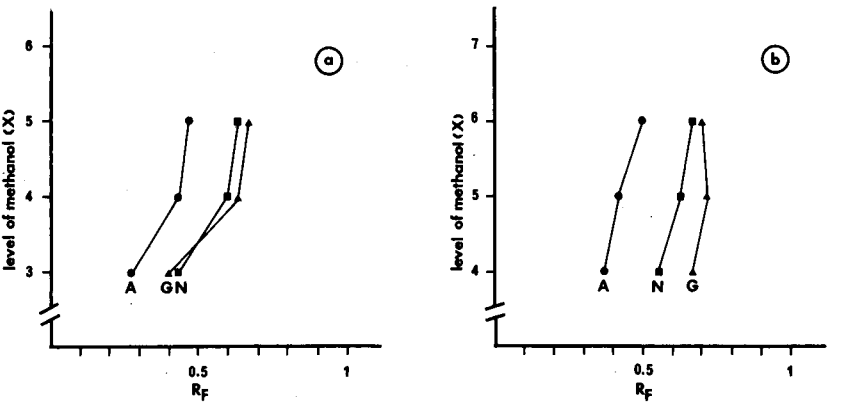

Fig. 3. R_F values of (■) nigericin (N), (●) abierixin (A) and (▲) grisorixin (G) plotted at various concentrations of chloroform, methanol and (a) acetic acid or (b) formic acid in the developing solvent. (a) The level of methanol (x) was varied while the level of acetic acid was kept constant (chloroform–methanol–acetic acid = 97:x:0.5). (b) The level of methanol (x) varied while the level of formic acid was kept constant (chloroform–methanol–formic acid = 97:x:0.5).

RESULTS AND DISCUSSION

Effects of solvents on the resolution of antibiotics

The chromatographic behaviour of a three-component standard mixture of antibiotics (grisorixin, abierixin and nigericin) on Chromarods was studied in order to determine suitable conditions for their separation and determination in biological samples by TLC–FID. Preliminary studies using chloroform–methanol as eluting solvent in different ratios such as that used in absorption TLC (95:5, v/v) [5] gave an inadequate separation of grisorixin and nigericin. Addition of a constant volume of acetic acid (0.5 vol.) improved the separation of the three antibiotics, especially with chloroform-to-methanol ratios between 20:1 and 30:1 (Fig. 2 and 3a), but no separation was observed with a larger proportion of acetic acid (1 vol.) whatever the chloroform-to-methanol ratio used (Fig. 2).

A developing solvent containing small amounts of methanol with formic acid (Fig. 3b) instead of acetic acid (Fig. 3a) [chloroform–methanol–formic acid (97:4:0.5, v/v/v)] increased specifically the relative mobility of grisorixin on Chromarods and therefore allowed a complete separation of the three antibiotics (Fig. 3b).

Concerning the analysis of biological lipid samples prepared from *Streptomyces hygroscopicus* NRRL B 1865, no interferences between the three antibiotics and the other lipid compounds were observed if the separation sequence was conducted with a developing solvent slightly enriched in formic acid (0.6 vol. rather than 0.5 vol.) [developing solvent:chloroform–methanol–formic acid (97:4:0.6, v/v/v)].

Internal standard for antibiotic determination

For the determination of antibiotics using the internal standardization procedure, relative mobilities of different lipid molecules were determined in order to select an appropriate internal standard with regard to its stability and solubility properties in both the extraction mixture and the chromatographic solvent and also its chromatographic behaviour.

Among the compounds tested, ionophore antibiotics (not produced by *Streptomyces hygroscopicus* NRRL B 1865) such as cezomicin [15], alborixin [16] and calcimycin [17], whose R_F value is similar to that of grisorixin (R_F = 0.67), and monensin [18], which overlaps with abierixin (R_F = 0.30), were not considered.

Similarly, phospholipids (phosphatidylethanolamine, phosphatidyl- and lysophosphatidylcholine) and glycolipids (mono- and digalactosyldiacylglycerols), which do not migrate from the origin, and non-phosphorus lipids (as free fatty acids, di- and triacylglycerols, fatty acid methyl esters, cholesterol esters, waxes), which migrate at the top with the developing solvent, (R_F >0.90), would interfere with endogenous bacterial lipids. Monoacylglycerol (1-monoheptadecanoin), which is virtually absent in lipid extracts of our strain, do not separate from nigericin (R_F = 0.56).

However, among the lipid biliary compounds tested, which included cholic acid, sodium tauro- and glycocholate (R_F = 0.10) and sodium desoxycholate (R_F = 0.30), methyl desoxycholate (MeDOC), which migrates (R_F = 0.47) between abierixin (R_F = 0.33) and nigericin (R_F = 0.57) (Fig. 4), was the most suitable internal standard for the determination of the antibiotics by TLC–FID. Moreover, no bacterial compounds were observed to display a similar R_F value to that of MeDOC.

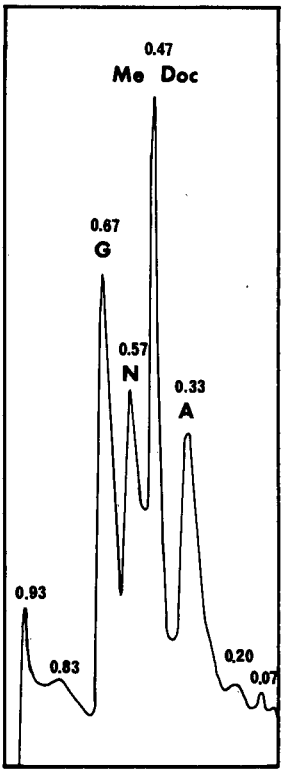

Fig. 4. TLC–FID of abierixin (A, 3 μg), nigerixin (N, 3 μg) and grisorixin (G, 3 μg) in chloroform solution (0.5 μl) with methyl desoxycholate (MeDoc, 1 μg) as internal standard. Separation was achieved on Chromarods SII with chloroform–methanol–formic acid (97:4:0.6, v/v/v) as the developing solvent.

Antibiotic calibration graphs

In order to calculate the amounts of individual antibiotics produced by *Streptomyces hygroscopicus* NRRL B 1865 in the mycelium or in the medium, standard solutions containing from 1 to 10 μg of antibiotic were analysed with the Iatroscan TH 10 analyser. Straight lines for peak-area ratio *versus* the weight ratio of the individual antibiotics to methyl desoxycholate wer obtained for abierixin, nigericin and grisorixin over the range considered (Fig. 5). Each point shown is the mean of five replicate analyses. The reproducibility of peak-area measurements depends on the amount of antibiotics applied. The relative standard deviation (R.S.D.) ranged from 2.3 to 6.1% intra-assay, and from 3.5 to 6.9% inter-assay when 2–10 μg of individual antibiotics were applied. In the same range of applied antibiotic, the reproducibility of the relative mobilities of the antibiotics was fairly constant and the R.S.D. averaged 0.5–1.5% for both intra- and inter-assay.

Determinations of FID responses using different amounts of antibiotics and normalized to that of 5 μg of methyl desoxycholate showed that, with 2–10 μg as the working range, the response factor was fairly constant (R.S.D. 2.1–5.6%) and similar for abierixin and grisorixin (0.4–0.5), which had the largest FID response, and the

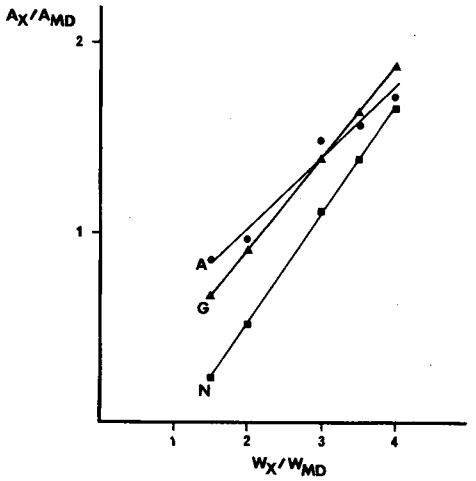

Fig. 5. Calibration lines of Iatroscan TLC–FID peak area (*A*) ratio *vs.* weight (*W*) ratio on the Chromarods SII for (●) abierixin, (■) nigericin and (▲) grisorixin as compared with methyl desoxycholate (MD) internal standard. Rods were developed in chloroform–methanol–formic acid (97:4:0.6, v/v/v).

yield was satisfactory (96.8 ± 3.5%). However, the response factor increased 1.5-fold with the amount of nigericin analysed (R.S.D. 3.1–8.5%) in the range 2–6 μg (yield 89.5 ± 8.6%) (Fig. 6). As for nigericin, similar correlations between response and amount of sample have been reported previously for neutral lipids (cholesterol, triacylglycerols) [19,20] and for phospholipids [20]. Hence, in order to improve the usefulness of TLC–FID for determination of the three antibiotics produced by *Streptomyces hygroscopicus* NRRL B 1865, it is recommended to limit the working range from 5 to 10 μg.

Determination of antibiotics in Streptomyces hygroscopicus NRRL B 1865

Determinations of antibiotics were performed on the lipid extracts of the mycelium of *Streptomyces hygroscopicus* NRRL B 1865 grown for 7 days on a basal medium with 1% methyl oleate. Only traces of grisorixin were observed in the myceli-

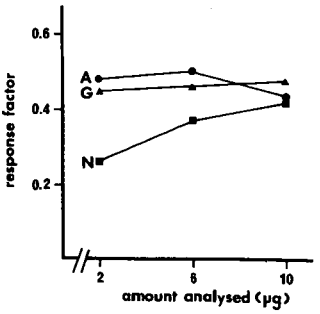

Fig. 6. Influence of amount of sample spotted on chromarods on response factor. Response factors for (●) abierixin, (■) nigericin and (▲) grisorixin were calculated as peak area/amount analysed and normalized to that of 5 μg of methyl desoxycholate.

um of our strain when the abierixin content is higher (84 mg per 100 g of dry matter (DM) mycelium). Nigericin was found to be the major antibiotic produced by the strain (527 mg per 100 g of DM mycelium). With the basal medium (without methyl oleate), the nigericin content of the mycelium was dramatically lowed (13 mg per 100 g of DM mycelium) as previously observed with the same strain grown under the same culture conditions [5]. A similar increase in antibiotic synthesis by sodium oleate was reported previously by Arima *et al.* [21] in the formation of neomycin by *Streptomyces fradiae*. In both instances, esters or soaps derived from oleic acid would stimulate the biosynthesis of branched-chain fatty acids from exogenous amino acids, which are known to be direct precursors of nigericin in *Streptomyces hygroscopicus* [22] and of neomycin in *Streptomyes fradiae* [21].

REFERENCES

1 J. M. Westley, *Polyether Antibiotics: Carboxylic Ionophores, Vol. 1, Biology*, Marcel Dekker, New York, 1982, Ch. 6, p. 58.
2 R. D. Hedde, *Pharmacologie et Toxicologie Vétérinaire*, Colloques de l'INRA, Éd. INRA publications, Versailles, 1982, Ch. 8, p. 391.
3 P. Thivend and J. P. Jouany, *Reprod. Nutr. Dev.*, 23 (1983) 817.
4 D. E. Cane, W. D. Celmer and J. W. Westley, *J. Am. Chem. Soc.*, 105 (1983) 3594.
5 L. David, H. Leal Ayala and J. C. Tabet, *J. Antibiot.*, 38 (1985) 1655.
6 L. David and J. Mouslim, *J. Antibiot.*, (1991) submitted for publication.
7 P. Gachon, A. Kergomard, H. Veschambre, C. Esteve and T. Staron, *Chem. Commun.*, (1970) 1421.
8 R. L. Brown, *J. Assoc. Off. Anal. Chem.*, 62 (1979) 266.
9 G. P. Dimenna, B. E. Walker, L. B. Turnbull and G. J. Wright, *J. Agric. Food Chem.*, 34 (1986) 472.
10 E. E. Martinez and W. Shimoda, *J. Assoc. Off. Anal. Chem.*, 69 (1986) 637.
11 H. Asukabe, H. Yoneyama, Y. Mori, K. I. Harada, M. Suzuki and H. Oka, *J. Chromatogr.*, 396 (1987) 261.
12 J. K. G. Kramer, R. C. Fouchard and E. R. Farnworth, *J. Chromatogr.*, 198 (1980) 279.
13 M. Ranny, in J. Janak (Editor), *Thin-Layer Chromatography with Flame Ionization Detection*, Reidel, Dordrecht, 1987, p. 134.
14 J. Folch, M. Lees and G. H. Sloane Stanley, *J. Biol. Chem.*, 226 (1957) 497.
15 L. David and S. Emadzadeh, *J. Antibiot.*, 11 (1982) 1616.
16 M. Alleaume, B. Busetta, C. Farges, P. Gachon, A. Kergomard and T. Staron, *J. Chem. Soc., Chem. Commun.*, (1975) 411.
17 M. O. Chaney, P. V. Demarco, N. D. Jones and J. L. Occolowitz, *J. Am. Chem. Soc.*, 96 (1974) 1932.
18 A. Agtarap, J. W. Chamberlin, M. Pinkerton and L. Steinrauf, *J. Am. Chem. Soc.*, 89 (1967) 5737.
19 E. R. Farnworth, B. K. Thompson and J. K. G. Kramer, *J. Chromatogr.*, 240 (1982) 463.
20 R. T. Crane, S. C. Goheen, E. C. Larkin and G. Amanda, *Lipids*, 18 (1983) 74.
21 K. Arima, H. Okasaki, H. Ono, K. Yamada and T. Beppu, *Agric. Biol. Chem.*, 37 (1973) 2313.
22 L. David, P. Lhoutellier, S. Auboiron, D. Bauchart and J. Asselineau, *Agric. Biol. Chem.*, (1991) submitted for publication.

Journal of Chromatography, 547 (1991) 419–428
Elsevier Science Publishers B.V., Amsterdam

CHROM. 23 167

Separation of water- and fat-soluble vitamins by micellar electrokinetic chromatography

C. P. ONG, C. L. NG, H. K. LEE and S. F. Y. LI*
Department of Chemistry, National University of Singapore, Kent Ridge 0511 (Singapore)
(First received November 2nd, 1990; revised manuscript received January 16th, 1991)

ABSTRACT

A mixture of seven water- and two fat-soluble vitamins was successfully separated simultaneously using micellar electrokinetic capillary chromatography. In addition to sodium dodecyl sulphate, modifiers such as γ-cyclodextrin, β-cyclodextrin, and isopropyl alcohol were introduced into the electrophoretic media to investigate their effect on the overall separation of the nine vitamins. Amongst these modifiers, the combination of γ-cyclodextrin with sodium dodecyl sulphate in the electrophoretic medium was found to provide the best selectivity for separating vitamins.

INTRODUCTION

The separation of vitamins by chromatographic methods has been known for many years [1,2]. Amongst the chromatographic techniques, high-performance liquid chromatography (HPLC) has been one of the most popular choices [3,4]. However, the use of HPLC for the separation of this group of compounds has been found to suffer from a number of problems. In the case of isocratic elution, the main problem is usually due to the broadening and tailing of some of the vitamin peaks [5,6]. Consequently it is often difficult to achieve complete separation of these compounds by this method [7]. Thus it is common to implement gradient elution to achieve satisfactory results [6]. Furthermore the analysis of the fat- and water-soluble vitamins can only be achieved with sequential elution employing mobile phases of different polarity. To date the simultaneous separation of both groups of vitamins in a single analysis has not been reported.

High-performance capillary electrophoresis (CE) is a fairly new techniques and interest in this area has been growing rapidly in recent years. One of the reasons for its popularity is the exceptionally high separation efficiency achievable with this techniques, which is based on a simple instrumental set-up. In the case of capillary zone electrophoresis, separation of charged compounds can be achieved relatively easily.

The introduction of micelles into the electrophoretic medium by Terabe *et al.* [8] in 1984 has given another new dimension to this mode of separation. Since then, there have been numerous papers reporting the usefulness of this new technique,

0021-9673/91/$03.50

referred to as micellar electrokinetic chromatography (MEKC) [9–17]. The success of the MEKC technique could largely be due to the additional partition mechanism between the solutes and the micellar pseuco-stationary phase. Consequently the selectivity and peak shape are considerably improved, especially for the separation of neutral species.

The separation of water-soluble vitamins has been previously investigated by MEKC [9,11]. In this work, besides the water-soluble vitamins, fat-soluble vitamins were also examined. One of the objectives of this investigation is to attempt to simultaneously separate the two groups of vitamins in a single analysis by MEKC. The migration behavior of the vitamins under different pH and sodium dodecyl sulphate (SDS) concentrations was studied. In addition, the effects of modifiers including γ-cyclodextrin, β-cyclodextrin and organic modifiers on the separation of the two groups of vitamins were examined.

EXPERIMENTAL

The experiments were performed using the instrumental set-up described elsewhere [12]. A Spellman (Plainview, NY, USA) Model RHR30AN10/RCA power supply, capable of delivering up to a maximum of 30 kV was used. A fused-silica capillary (50 cm effective length × 50 μm I.D.) obtained from Polymicro Technologies (AZ, USA) was used as the separation tube. The detection of peaks was carried out on a Micro-UVis detector (Carlo Erba, Milan, Italy) with wavelength set at 210 nm. The window for the on-column detection cell was made by removing a small section of the polyimide coating on the fused silica capillary. A Linear Instruments (Irvine, USA) Model 252A/MM chart recorder was used to record the chromatograms. Sample solution was introduced by gravity feed. An injection time of 5 s at a height difference of 5 cm between the reservoirs was used for sample introduction.

All chemicals used were of analytical grade or better. The buffer solution was prepared by dissolving sodium dihydrogen phosphate dihydrate and sodium tetraborate in Millipore water. The electrophoretic media containing SDS and the modifiers were prepared as previously described [8]. In this work, the seven water-soluble vitamins are vitamins B, B_1, B_2, B_6, B_{12}, C and H, and the two fat-soluble vitamins investigated are A and E. A standard solution containing the vitamins and Sudan III at a concentration of 1000 ppm for each species was prepared. All these chemicals are of the purest grade and were supplied by Fluka (Buchs, Switzerland).

RESULTS AND DISCUSSION

In Fig. 1, the migration times for the vitamins obtained at different pH values are shown. From the results it can be seen that the migration time of each vitamin increased with increasing pH. This observation is consistent with previous investigation [9]. At the same time, it was noted that the migration order for all the vitamins remained unchanged throughout the range of pH values examined. This observation seems to suggest that there are no major changes in the extent of ionization for the two groups of vitamins at all the pH values investigated. The water-soluble vitamins were found to migrate much faster than the fat-soluble vitamins. This is in agreement

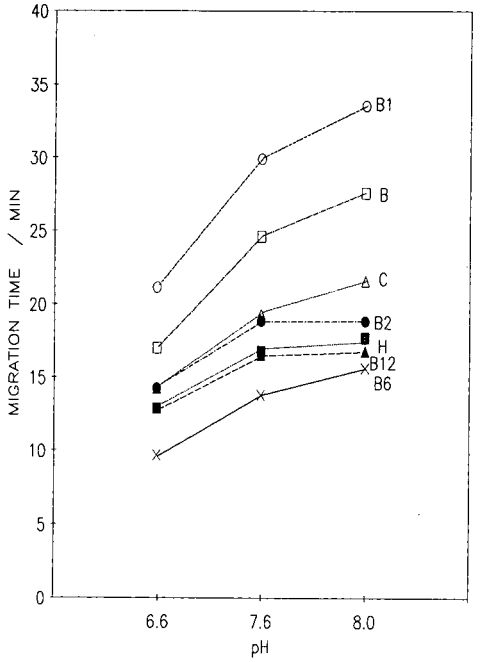

Fig. 1. Plot of migration times *versus* pH. All these experiments are conducted at a voltage of 15 kV across the 50 cm × 50 μm I.D. separating tube filled with 0.1 *M* borate–0.05 *M* phosphate buffer with 30 m*M* SDS. Note that the curves for the fat-soluble vitamins are not plotted since their capacity factors are very large. Vitamins: ○ = B_1; □ = B; △ = C; ● = B_2; ■ = H; ▲ = B_{12}; × = B_6.

with the fact that since the water-soluble vitamins are less lipophilic than the fat-soluble vitamins, they will not be influenced by the micelles and therefore would migrate earlier. On the other hand, the fat-soluble vitamins, A and E, co-eluted with Sudan III at lower pH. At a higher pH, vitamin A was found to migrate out faster than Sudan III. The main reason for these species having a similar migration time as that of Sudan III is that they are highly hydrophobic (*i.e.* they have very similar log P values to Sudan III). However at pH 8, the higher pH would have resulted in the dissociation of the carboxylate group of the vitamin A. Thus the decrease in the migration time in this case would presumably be due to the repulsive ionic interaction between the negatively-charged vitamin A and the anionic micelles.

The results obtained for the investigation on the effect of different SDS concentrations on the separation of the vitamins are illustrated in Fig. 2. From the figure, it can be seen that a similar migration pattern is observed, *i.e.* the water-soluble vitamins migrated out earlier and the two fat-soluble vitamins again have a similar migration time to that of Sudan III. It should be recognised that in the case of MEKC, when the solutes are electrically neutral the migration time is proportional to the SDS concentration. If the migration time is independent of the SDS concentration, one may conclude that the solute is totally exluded from the SDS micelles. On the other hand, if the migration of a solute is influenced by changes in the SDS concentration, then interaction between the solute and the micelles is expected. In the case of charged solutes, their migration due to electrophoretic interaction must be considered.

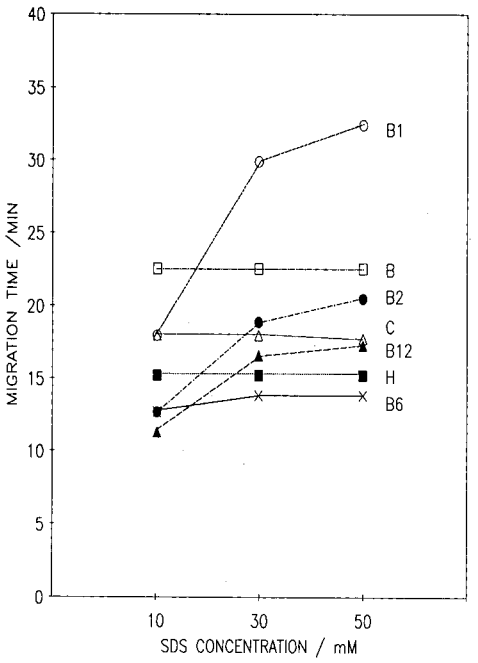

Fig. 2. Plot of migration times *versus* SDS concentration. All these experiments are conducted at a voltage of 15 kV across the 50 cm × 50 μm I.D. separating tube filled with 0.1 *M* borate–0.05 *M* phosphate buffer at pH 7.6. Note that the curves for the fat-soluble vitamins are not plotted since their capacity factors are very large. Symbols as in Fig. 1.

From the migration order observed, it seems that the vitamins can be categorised into the following groups:

(1) group I consisting of vitamins B_6, H, B and C;

(2) group II consisting of vitamins B_1 and B_{12}; and

(3) group III consisting of the vitamins B_2, A and E.

The vitamins in group I are generally the more hydrophilic species. Therefore they would be least solubilised by the micelles, and are expected to migrate out earlier than the vitamins in the other groups. Within this group, the migration times can be arranged in the following order: vitamins $B_6 < H < C < B$. The reason for this order observed can be explained mainly by the number of hydrophilic substituent groups present in each species. At the same time, the presence of any intra-molecular interaction (*i.e.* hydrogen bonding), which render the species less polar would also need to be considered. For example in the case of vitamin C, due to the orientation of the oxygen of the carbonyl group and hydroxyl groups, intra-molecular hydrogen bonding between these groups are very favourable. With the possibility of formation of this type of bonding, the hydrophobicity of vitamin C would be increased since the polar groups are now "caged up". Consequently, vitamin C, inspite of having more polar substituent grousp than most of the water-soluble vitamins, is less hydrophilic. Therefore because of these "caging" effect, vitamin C has a migration time longer than expected.

For vitamin B, the carboxylate hydrogen should be fairly acidic in the presence of the pyridine ring. Therefore, vitamin B would probably be assuming a negative charge at the pH investigated. Consequently vitamin B would migrate more slowly than the rest of the vitamins in this group because of the negative electrophoretic effect (ionic attraction to the positive electrode). In contrast to vitamin B, vitamin H has a small migration time despite the presence of a carboxylate group. This is because of the presence of the long alkyl chain which makes the carboxylate hydrogen less acidic to effect ionisation. Therefore, vitamin H is expected to be in the "neutral" form. At the same time, the presence of other polar groups in vitamin H would have hinder effective solubilisation by the micelles, hence resulting in the observed shorter migration time.

As for the group II vitamins, both vitamins B_1 and B_{12} are expected to assume positive charges (N^+ and Co^{2+} respectively). These vitamins are prone to the formation of an ion pair between its cationic group and the polar groups of the anionic micelles. This ionic interaction could have resulted in the large migration time for vitamin B_1 observed in Fig. 2. However for B_{12}, the migration times were much shorter. It seems that the electron-rich nitrogen atoms surrounding the metal centre could have neutralised the positive charge on the CO^{2+}. Consequently formation of the ion pair is more difficult. At the same time, its bulky substituent groups would have rendered effective solubilisation of the "neutral" B_{12} molecules by the SDS. Hence, vitamin B_{12} is found to migrate out much earlier than anticipated.

The migration order for the vitamins in group III is primarily governed by the extent of solubilisation by the micelles. In the case of vitamin B_2, despite the presence of the numerous polar substituent groups in this molecule, its apparent high hydrophilicity is somewhat reduced by its bulky size. Consequently the solubilisation of this molecules by the micelle was observed. As for the fat-soluble vitamins (A and E), since they are very lipophilic, they would be completely solubilised by the micelles. Hence they would migrate out together with the micelles.

It was noted that with the exception of B_1, B_2 and B_{12}, the migration times for the water-soluble vitamins remained fairly constant with the increase in the SDS concentration in the electrophoretic media. Although the trend was not observed in previous investigations [10, 12], this observation seems to be characteristic of compounds in Group I. A possible reason could be that the majority of the water-soluble vitamins, especially for those in group I, are highly hydrophilic. It is expected that their interaction with the micelles is minimum. Consequently, changes in the SDS concentration would not have caused any significant influence on the migration behaviour of these compounds. On the contrary, the other three water-soluble vitamins; vitamins B_1, B_2 and B_{12}, exhibit an entirely different trend. Because of stronger interaction with the micelles, the usual trend of increasing migration times with an increase in SDS concentration was observed. In other words, for these three species, the increase in SDS concentration would mean that there would be a higher probability of interaction with the micelles. Due to this increment in the concentration of micelles, a corresponding increase in the migration times would be observed. As a result of these two different trends, cross-over of peaks for the water-soluble vitamins are observed as shown in Fig. 2. Another point to note from Fig. 2 is that the increase in migration time is more pronounced in vitamin B_1 than in vitamins B_2 and B_{12}. The behaviour could be attributed to the fact that the ion-pair formation in B_1 would

result in stronger electrostatic attraction with the micelles compared to the mere Van der Waals type of interaction experienced by the other two vitamins. Furthermore, the bulky sizes of these two vitamins would prevent effective solubilisation into the micelles. Consequently, their migration times are much smaller than those of vitamin B_1.

So far our attempts to optimize the separation of both fat- and water-soluble vitamins by changing pH and SDS concentration in the electrophoretic media failed to achieve satisfactory results. The main difficulty lies in the separation of the two fat-soluble vitamins. This could be largely attributed to the fact that large molecules

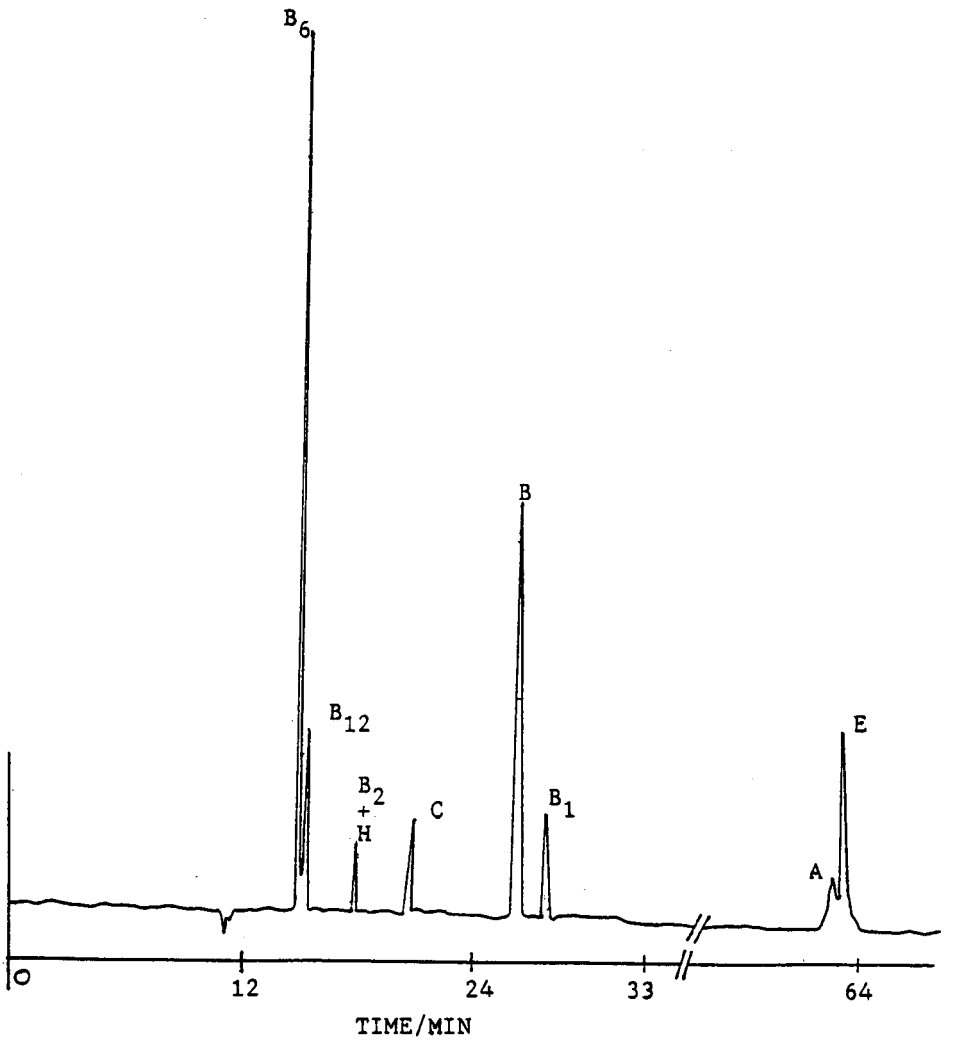

Fig. 3. Electrokinetic chromatogram of the vitamins with IPA. Electrophoretic solution: 30 m*M* SDS in 0.1 *M* borate–0.05 *M* phosphate with 1% IPA; pH 7.6; separation tube: 50 cm × 50 μm I.D. fused-silica capillary; voltage 15 kV; amount injected: 0.75 nl.

like vitamins A and E have strong hydrophobic interaction which would result in these molecules migrating together with the micelles.

It has been shown that a small percentage of organic modifiers can improve the separation efficiency in MEKC [14,15]. Upon addition of isopropanol (IPA) to the electrophoretic media, a marked improvement in the resolution of some peaks was observed, especially for the fat-soluble vitamins as these two compounds are no longer co-eluting. Typical chromatograms obtained using IPA as an organic modifier are given in Figs. 3 and 4. The improvement in the separation of some of the vitamins can be explained by the increase in the elution range provided as a result of the addition of

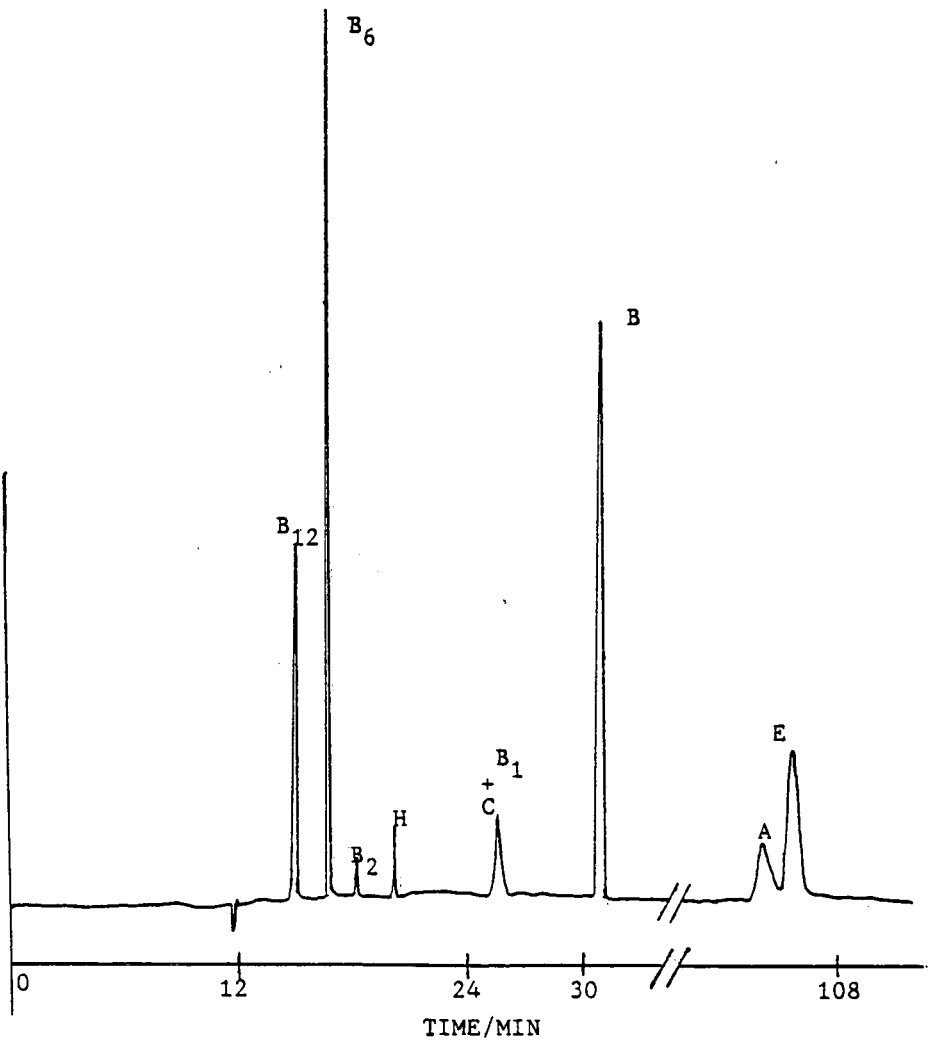

Fig. 4. Electrokinetic chromatogram of the vitamins with IPA. Electrophoretic solution: 30 *M* SDS in 0.1 *M* borate–0.05 *M* phosphate with 3% IPA; pH 7.6; separation tube: 50 cm × 50 μm I.D. fused-silica capillary; voltage 15 kV; amount injected: 0.75 nl.

the modifiers [14]. However, at the same time, it was noted that some of the water-soluble vitamin peaks are found to have overlapped with each other. Even though the two fat-soluble vitamin peaks are resolved to a certain extent, however, vitamin E is till migrating out together with Sudan III. Furthermore, it was found that after prolonged analysis using IPA, regeneration of the surface of the capillary tubing is required to give reproducible migration times. Taking into account these negative effects resulting from the use of IPA, it was considered an unsuitable modifier for the separation of the vitamins.

In previous investigations on the analysis of some polyaromatic hydrocarbons (PAH), γ-cyclodextrin was successfully adopted to separate this group of neutral compounds [16,17]. From the encouraging results obtained using cyclodextrin as modifiers, β-cyclodextrin was employed in this investigation to study its effect on the separation of the vitamins. The results obtained are shown in Fig. 5A en B. An important observation was that in all three sets of experiments, all the vitamins, including the two fat-soluble vitamins, are resolved. The migration times for the water-soluble vitamins, B_6, H, B_2, C and B are not affected by β-cyclodextrin. Their migration times remained fairly constant with varying β-cyclodextrin concentration. However for vitamins B_1, B_2 and B_{12}, there was a reduction in migration times. With

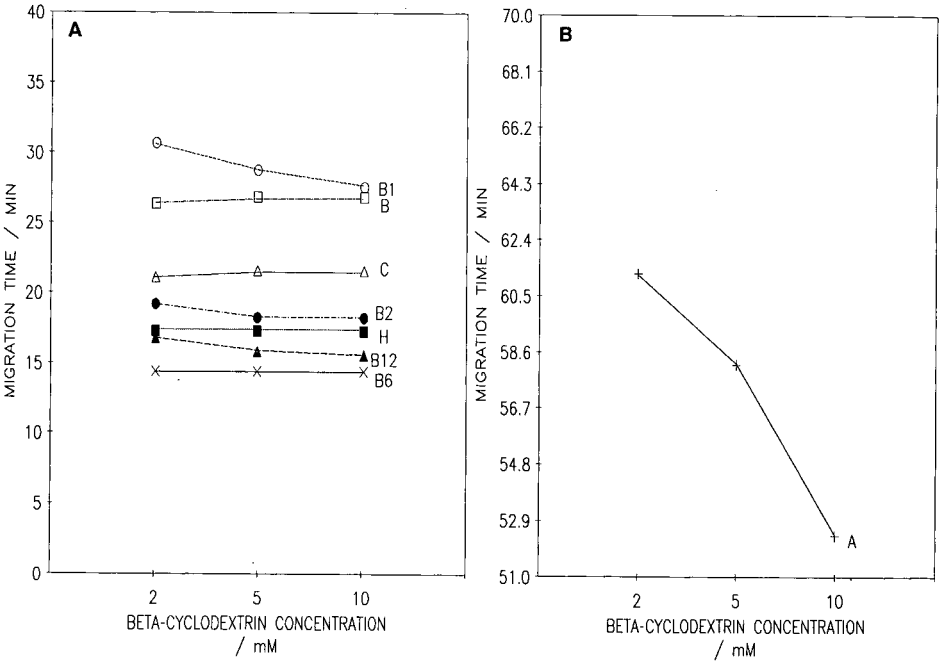

Fig. 5. (A) Plot of migration times *versus* β-cyclodextrin concentration. All these experiments are conducted at a voltage of 15 kV across the 50 cm × 50 μm I.D. separating tube filled with 0.1 *M* borate–0.05 *M* phosphate buffer at pH 7.6 with 30 m*M* SDS. Symbols as in Fig. 1. (B) Plot of migration times *versus* β-cyclodextrin concentration. All these experiments were conducted at a voltage of 15 kV across the 50 cm × 50 μm I.D. separating tube filled with 0.1 *M* borate–0.05 *M* phosphate buffer at pH 7.6 with 30 m*M* SDS. Note that the curve for the vitamin E is not plotted since its capacity factors are very large. + = Vitamin A.

further increment in the β-cyclodextrin concentration, the decrease in the migration times was even more apparent. This observation seems to suggest that there was keen competition between the micelles and β-cyclodextrin for these species. It is expected that for B_1 and B_{12}, unlike B_2, there would not be actual solubilisation of these positively charged vitamins into the neutral cavity of β-cyclodextrin. However, the presence of the electrically neutral β-cyclodextrin in the electrophoretic media seems to be able to lessen the interaction (ion-pair formation) between the positively charged solutes and the micelles. Consequently, a decrease in the migration times is observed for B_1 and B_{12}.

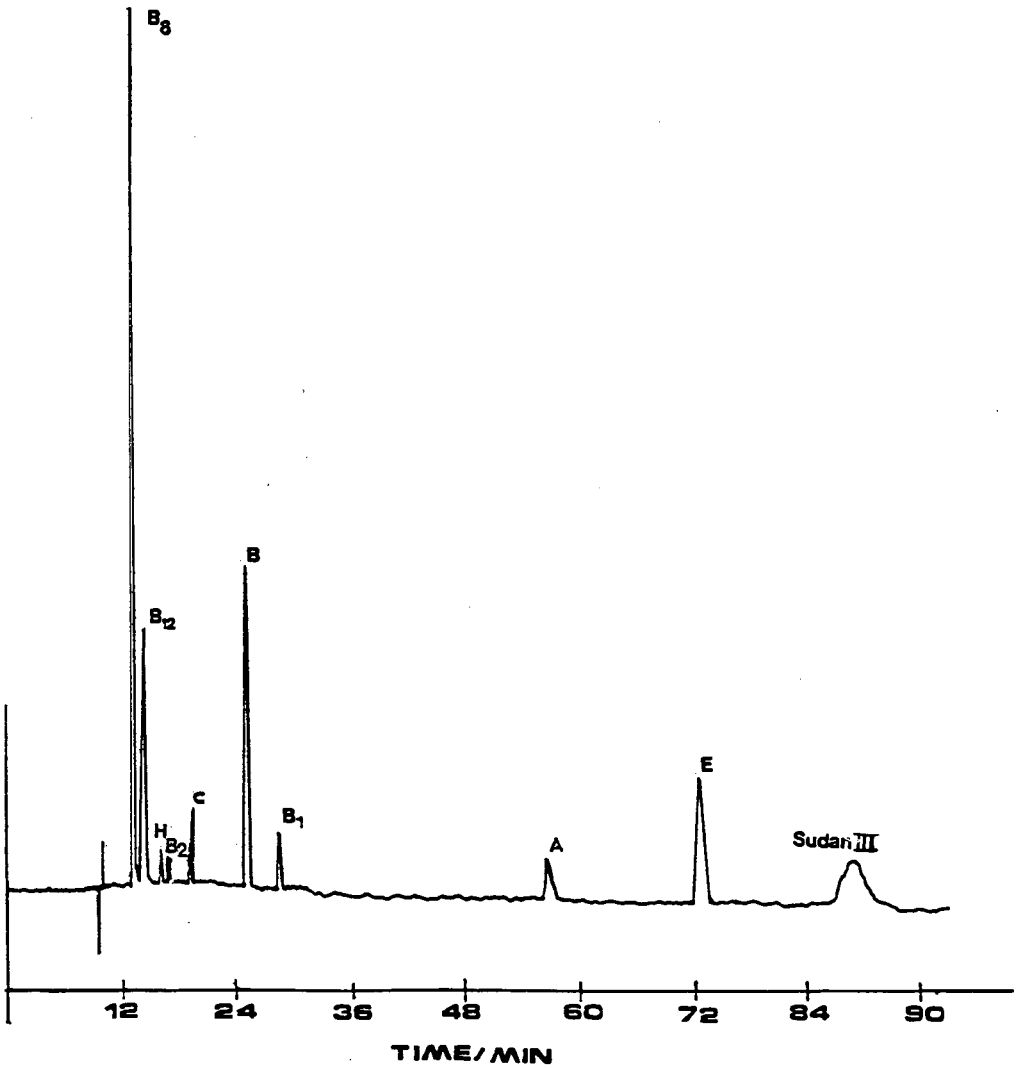

Fig. 6. Electrokinetic chromatogram of the vitamins with γ-cyclodextrin. Electrophoretic solution: 3 m*M* γ-cyclodextrin and 30 m*M* SDS in 0.1 *M* borate–0.05 *M* phosphate; pH 7.6; separation tube: 50 cm × 50 μm I.D. fused-silica capillary; Voltage 20 kV; amount injected: 0.75 nl.

Amongst the fat-soluble vitamins, only vitamin A is affected by the addition of β-cyclodextrin. It seems that the neutral vitamin A molecules can be solubilised into the β-cyclodextrin cavity much more readily than vitamin E. Since these neutral β-cyclodextrin molecules are not influenced by the electrophoretic attraction as much as the anionic micelles, they are expected to migrate faster than Sudan III. Therefore with the increment in the amount of β-cyclodextrin in the electrophoretic media, a corresponding decrease in the migration times for the affected species would be observed. On the other hand, the migration of vitamin E did not seem to be significantly influenced by β-cyclodextrin. This can be accounted for by the fact that its bulky size could have prevented its entry into the cavity of β-cyclodextrin. To demonstrate this fact, an additional experiment was carried out by replacing β-cyclodextrin with γ-cyclodextrin. With the increase in the size of the cavity due to the addition of another pyranose ring provided by γ-cyclodextrin, vitamin E can now be incorporated into the cavity. In this case, vitamin E is no longer eluting out together with the micelles, as shown in the chromatogram given in Fig. 6. From the chromatogram, it can be noted that all the peaks are satisfactorily separated. The usual tailing and broadening of peaks observed during analysis by HPLC were not observed in the present study.

This investigation is, to our best knowledge, the first ever reported separation of both fat- and water-soluble vitamins in a single analysis by CE. By the use of a simple instrumental set-up, separation of complex mixtures can be readily achieved by optimizing parameters such as pH and the concentration of SDS in the electrophoretic media or by the addition of modifiers such as β- and γ-cyclodextrins. The MEKC technique offers great flexibility and further investigations on its potential for the separation of other types of compounds should be considered.

ACKNOWLEDGEMENTS

The authors would like to thank the National University of Singapore for their financial assistance, and staff in the Physics Workshop for their help in fabricating some parts of the instrument.

REFERENCES

1 R. C. Williams, D. R. Bakar and J. A. Schmit, *J. Chromatogr. Sci.*, 11 (1973) 618.
2 D. P. Wittmer and W. G. Harvey, *J. Pharm. Sci.*, 63 (1974) 588.
3 W. T. Wahyuni and K. Jinno, *Chromatographia*, 23 (1987) 320.
4 E. Wang and W. Hou, *J. Chromatogr.*, 447 (1988) 256.
5 F. L. Lam, I. J. Holcomb and S. A. Fusari, *J. Assoc. Off. Anal. Chem.*, 67 (1984) 1007.
6 R. M. Kothari and M. W. Taylor, *J. Chromatogr.*, 247 (1982) 205.
7 T. Cannella and G. Bichi, *Bull. Chim. Farm.*, 122 (1983) 205.
8 S. Terabe, K. Otsuka, K. Ichikawa, A. Tsuchiya and T. Ando, *Anal. Chem.*, 56 (1984) 111.
9 S. Fujiwara, S. Iwasa and S. Honda, *J. Chromatogr.*, 447 (1988) 133.
10 H. Nishi, T. Fukuyama, M. Matsuo and S. Terabe, *J. Chromatogr.*, 498 (1990) 313.
11 H. Nishi, N. Tsumagari, T. Kakimoto and S. Terabe, *J. Chromatogr.*, 465 (1989) 331.
12 C. P. Ong, C. L. Ng, N. C. Chong, H. K. Lee and S. F. Y. Li, *J. Chromatogr.*, 516 (1990) 263.
13 K. Otsuka, S. Terabe and T. Ando, *J. Chromatogr.*, 348 (1985) 39.
14 A. T. Balchunas, M. J. Sepaniak, *Anal. Chem.*, 59 (1987) 1466.
15 J. Gorse, A. T. Balchunas, D. F. Swaile, M. J. Sepaniak, *J. High Resolut. Chromatogr. Chromatogr. Commun.*, 11 (1988) 554.
16 S. Terabe, Y. Miyashita, O. Shibata, E. R. Barnhart, L. R. Alexander, D. G. Patterson, B. L. Karger, K. Hosoya and N. Tanaka, *J. Chromatogr.*, 516 (1990) 23.
17 Y. F. Yik, C. P. Ong, H. K. Lee and S. F. Y. Li, *Environ. Monitor. Asses.*, in press.

Journal of Chromatography, 547 (1991) 429–433
Elsevier Science Publishers B.V., Amsterdam

CHROM. 23 189

Short Communication

Sample remaining in an ODS column after compositional fractionation of copolymers by high-performance liquid chromatography

SHINYA TERAMACHI*, AKIRA HASEGAWA and TATSUYA MATSUMOTO
Department of Industrial Chemistry, Kogakuin University, Nakano-cho 2665-1, Hachioji, Tokyo 192 (Japan)
(First received November 5th, 1990; revised manuscript received February 8th, 1991)

ABSTRACT

High-performance liquid chromatography is very effective for the compositional fractionation of copolymers. Octadecyl-modified silica gel (ODS) has been used as a packing material for fractionation in the reversed-phase (RP) adsorption mode. In the compositional fractionation of the samples of copoly(methyl methacrylate–styrene) by RP gradient elution through ODS column, it was found that small peaks were observed with blank elution just after the sample measurement and a perfect baseline was recovered after several blank elutions.

INTRODUCTION

High-performance liquid chromatography (HPLC) has been widely used for the compositional fractionation of copolymers in both adsorption [1] and phase-separation (selective precipitation and dissolution) [2] modes. In the compositional fractionation of copolymers by the adsorption mechanism, both normal-phase (NP) and reversed-phase (RP) modes [3–6] have been used succesfully. Octadecyl-modified silica gel (ODS) has commonly been used as a packing material for the RP fractionation.

Although no mention of any sample remaining after elution was made in the papers cited, we observed small peaks with blank elution just after sample measurement in the compositional fractionation of the samples of statistical and graft copoly(methyl methacrylate–styrene) using ODS columns. As this is a serious problem for the accurate determination of the chemical composition distribution of copolymers using ODS columns, we present here a brief of the phenomenon.

0021-9673/91/$03.50

EXPERIMENTAL

Statistical and graft copolymers of methyl methacrylate (MMA) and styrene (S) were used as samples. The former samples were prepared by radical copolymerization in bulk using benzoyl peroxide as the initiator. Styrene contents determined by elemental analysis and number-average molecular weights determined by osmometry are given in Table I. The conversions of the samples were low, so that the chemical composition distributions of the samples should be sharp. The graft copolymer samples, which were supplied by T. Tsukahara of Nagoya University, were prepared by radical copolymerization of ω-methacryloyl polystyrene macromonomer with MMA [7]. Styrene contents of the samples determined by ^{1}H NMR spectroscopy are shown in Table II.

TABLE I

SAMPLES OF STATISTICAL COPOLYMERS

Code	Styrene content (mol%)	$M_n \times 10^{-5}$
SMMA-81-25(2)	21.0	1.22
-87-30	29.0	2.01
-81-50(2)	48.7	1.27
-88-61	60.8	2.23
-88-73	72.5	2.41
-81-75(1)	84.9	1.40
PS (Tosoh)	100	1.86

Tetrahydrofuran (THF) and acetonitrile (ACN), used as eluents for HPLC, were of chromatographic grade from Wako (Tokyo, Japan) and Nacalai Tesque (Kyoto, Japan), respectively.

Two sets of HPLC instruments were used. One (A) was composed of two Model-510 pummps and a Model-680 controller (Waters Assoc., Milford, MA, USA), a CO-8000 column oven (Tosoh, Tokyo, Japan) and a Model ERC-7211 UV detector (Erma, Tokyo, Japan). The other (B) was composed of two LC-6A pumps, an SCL-6A controller, an SPD-6A UV detector (Shimadzu, Tokyo, Japan) and an SSC-3510 column oven (Senshu Scientific, Tokyo, Japan). In both sets, Rheodyne Model 7010 injectors were used.

TABLE II

SAMPLES OF GRAFT COPOLYMERS

Code	Styrene content (wt.%)
PMMA-g-PS-A	27.0
-B	46.3
-C	74.4

TABLE III

GRADIENT PROTOCOLS

Gradient No.	Time (min)	THF (vol.%)	ACN (vol.%)
1	0–15	10–60	90–40
	15–20	60	40
	20	60–100	40–0
	20–30	100	0
	30–45	100–10	0–90
2	0–15	15–60	85–40
	15–18	60	40
	18	60–95	40–5
	18–28	95	5
	28–43	95–15	5–85

Two ODS columns and also a phenyl-modified silica gel column (phenyl column) were used: ODS-1251-K (Senshu Scientific) (25 cm × 4.6 mm I.D., particle diameter $d = 5$ μm, micropore size of starting silica gel, $d_p = 10$ nm); ODS-120T (Tosoh) (25 cm × 4.6 mm I.D., $d = 5$ μm, $d_p = 12$ nm) and μBondasphere 5 μm Phenyl-100A (Waters Assoc.) (15 cm × 3.9 mm I.D., $d = 5$ μm, $d_p = 10$ nm).

HPLC measurements were carried out on two samples. One was an equi-weight mixture of six samples of statistical copolymers and a polystyrene (Table I) dissolved in THF at a total concentration of 1.05 mg/cm^3 (STAT) and the other was an equi-weight mixture of three samples of the graft copolymers (Table II) dissolved in THF at a total concentration of 1.5 mg/cm^3 (GRAFT). In all measurements, the injection volume was 0.1 cm^3, the flow-rate was 1.0 cm^3/min, the column temperature was 30°C and the wavelength of the UV detectors was 254 nm. The gradient protocols of the eluents are given in Table III, in which the samples were separated by a linear gradient from 10 or 15 to 60 vol.% THF. The combinations of the HPLC instrument, the column, the gradient protocol and the sample are given in Table IV.

RESULTS AND DISCUSSION

The chromatograms of the STAT sample mixture obtained by a combination of HPLC set A, ODS-1251-K column and gradient protocol No. 1 are shown in Fig. 1. Chromatogram (a) obtained by the sample injection has seven clearly separated

TABLE IV

COMBINATION OF EXPERIMENTAL CONDITIONS

No.	HPLC set	Column	Sample	Gradient No.
1	A	ODS-1251-K	STAT	1
2	A	ODS-120T	STAT	1
3	A	Phenyl	STAT	1
4	B	ODS-1251-K	GRAFT	2

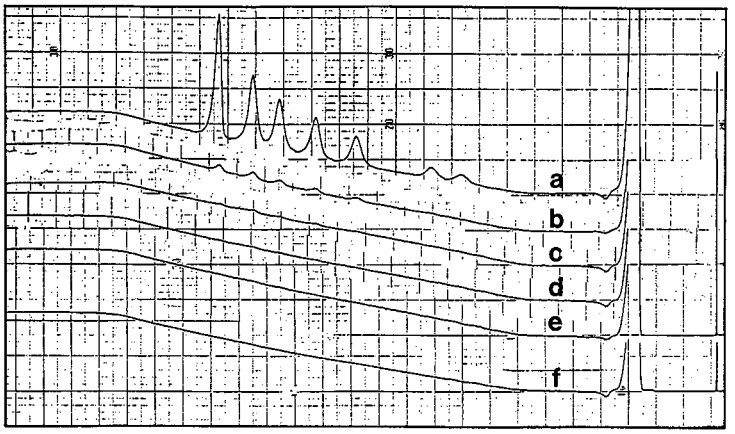

Fig. 1. Chromatograms of a mixture of statistical copolymers (Table I) and blank elutions obtained by combination No. 1. (Table IV). (a) Sample elution; (b)–(e) 1st–4th blank elutions after the sample elution; (f) baseline obtained by blank elution just before the sample elution. For further details, see text.

peaks, which correspond to the respective samples in order from low to high styrene content in accordance with the mechanism of reversed-phase adsorption. The peak assignment was made by single injections of the respective samples. Chromatograms (b)–(e) were obtained by consecutive blank elutions with the same gradient and pure solvent injection just after the sample elution. Curve (f) is the baseline obtained with the same gradient just before the sample measurement. In the first and second blank elutions, clear, small peaks for the respective components were observed at the same positions as in the sample measurement. Even in the third blank elution, the peaks were not completely eliminated, although the peak heights gradually decreases as the

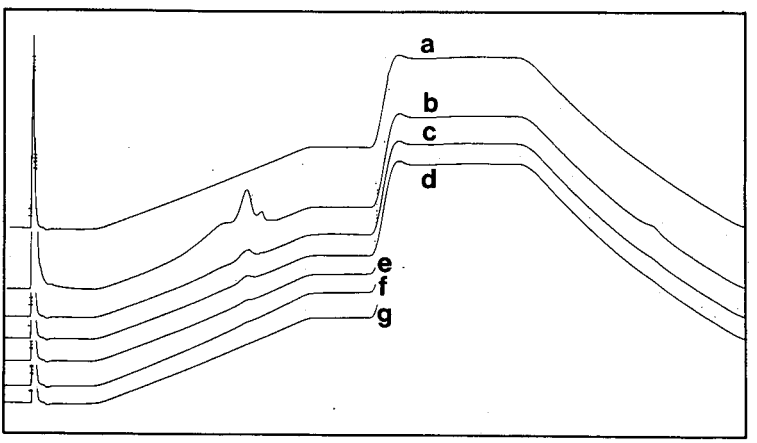

Fig. 2. Chromatograms of a mixture of graft copolymers (Table II) and blank elutions obtained by combination No. 4 (Table IV). (a) Baseline obtained by blank elution just before the sample elution; (b) sample elution; (c) 1st, (d) 2nd, (e) 4th, (f) 7th and (g) 10th blank elutions just after the sample elution. For further details, see text.

blank elution was repeated. The fourth blank elution (e) finally exhibited the complete baseline as in (f).

The same experiments were carried out changing the column from ODS-1251-K to ODS-120T and also to the phenyl column. The results with the ODS-120T column (not shown) were the same as those with the ODS-1251-K column, whereas no peak was observed with blank elution through the phenyl column.

The chromatograms shown in Fig. 2 are for the GRAFT sample, obtained by a combination of HPLC set B, ODS-1251-K column and gradient protocol No. 2. Chromatogram (a) is the baseline obtained just before the sample measurements. Chromatogram (b) obtained by sample injection appears to contain three peaks, but they do not correspond to the respective original samples. As shown elsewhere [7], the first peak corresponds to the mixture of samples A and B, the second is sample C and the last is homopolystyrene. Chromatograms (c)–(g) were obtained by blank elutions. For the graft copolymer, it was more difficult than for the statistical copolymer to remove the small peaks by repeated blank elutions. As shown in Fig. 2, the tenth blank elution finally exhibited the perfect baseline (g). Further, during the return to the starting composition, a peak was observed at an eluent composition near to that of the main peak not only with the sample elution but also with the first and the second blank elutions, although no peak on the returning gradient was found for the statistical copolymer.

In these experiments, the injectors of the HPLC instruments were carefully rinsed with pure THF before the blank elutions, and the injection syringe used for the pure solvent in blank elutions was carefully rinsed and was not also used for injection of sample solutions. Therefore, it is clear that the small peaks on the chromatograms obtained by blank elutions are not due to samples injected accidentally, but represent sample components remaining in the ODS columns. It is also obvious that the sample remaining is particular to an ODS column, as the phenomenon was not observed with the phenyl column. As shown in a previous paper [6], both adsorption and phase-separation mechanisms coexist in the compositional fractionation of the statistical copolymer by the present combination of column and eluent. However, it is difficult to explain the phenomena reported here by these mechanisms. Although partitioning is regarded as the main mechanism for the separation of low-molecular-weight compounds by ODS columns, it is not clear whether the mechanism can explain the present phenomena.

REFERENCES

1 S. Teramachi, A. Hasegawa, Y. Shima, M. Akatsuka and M. Nakajima, *Macromolecules*, 12 (1979) 992.
2 G. Glöckner, H. Kroschwitz and Ch. Meissner, *Acta Polym.*, 33 (1982) 614.
3 G. Glöckner and J. H. M. van den Berg, *J. Chromatogr.*, 384 (1987) 135.
4 G. Glöckner, *J. Chromatogr.*, 403 (1987) 280.
5 H. Sato, K. Mitsutani, I. Shimizu and Y. Tanaka, *J. Chromatogr.*, 447 (1988) 387.
6 S. Teramachi, A. Hasegawa and K. Motoyama, *Polym. J.*, 22 (1990) 489.
7 S. Teramachi, A. Hasegawa, T. Matsumoto, Y. Tsukahara and Y. Yamashita, *Polym. Prepr. Jpn.*, 39 (1990) 4058.

Journal of Chromatography, 547 (1991) 434–438
Elsevier Science Publishers B.V., Amsterdam

CHROM. 23 330

Short Communication

Study of polystyrene–poly(ethylene oxide) block copolymer micelles in aqueous solution by size-exclusion chromatography

RENLIANG XU, YONGZHONG HU and MITCHELL A. WINNIK*
Department of Chemistry and Erindale College, University of Toronto, Toronto, Ontario M5S 1A1 (Canada)
GERARD RIESS
École Nationale Superieure de Chimie, 3 Rue Alfred-Werner, 68093 Mulhouse Cedex (France)
and
MELVIN D. CROUCHER
Xerox Research Center of Canada, 2660 Speakman Drive, Mississauga, Ontario L5K 2L1 (Canada)
(First received November 26th, 1990; revised manuscript received March 22nd, 1991)

ABSTRACT

Size-exclusion chromatography experiments are reported for aqueous solutions of polystyrene–poly(ethylene oxide) (PS–PEO) diblock and triblock copolymers. These samples show two peaks: the first peak elutes due to polymer micelles (characterized independently by light scattering), and the second due to individual polymer molecules. Sharp micelle peaks imply slow dynamic exchange. By collecting fractions and examining them by Fourier transform infrared spectrometry we were able to establish that the single-molecule peak contained more PEO and less PS than the micelle.

INTRODUCTION

Size-exclusion chromatography (SEC) is a powerful method for characterizing polymer molecules in solution. It also has a tremendous potential for the study of colloidal systems [1], but these applications have been much slower to develop, either because of technical problems, or because of the complexity of the behaviour of the systems themselves.

The major limitation for using porous gel columns in the separation of colloidal particles in aqueous media comes from the adsorption of particles onto the packing materials or from plugging of the column by aggregated particles. In both instances, the injected materials will either be lost in the column or take a very long time to elute. In the case of micelles, the micelle–single molecule (unimer) association and dis-

0021-9673/91/$03.50

sociation processes during elution represent an additional complication which can become particularly severe if the single molecules adsorb strongly onto the packing material. However, if adsorption can be avoided by choosing a proper SEC column and correct experimental conditions, the complications which arise from the micelle–unimer dynamic equilibrium can be utilized to study the association–dissociation behaviour of such systems. Theoretical models to describe these effects have recently been proposed [2–4].

There have been several reports on the use of SEC for the characterization of block copolymer micelles in non-aqueous systems or in organic solvent–aqueous mixtures [5–9]. Berlinova *et al.* [5] investigated the SEC of polystyrene–poly(ethylene oxide) (PS–PEO) block copolymers in water–methanol (1:1). For diblock copolymers they observed two peaks, one of which was assigned to the micelle, and a second peak at longer retention time which was attributed to a PEO homopolymer impurity. From the sharpness of the micelle peak they inferred that the relaxation of these micelles to free chains was very slow. This point of view was originally proposed by Price and co-workers [7,8], who studied several block copolymer micelles in organic solvents and found that the successful elution of copolymer micelles as a single narrow peak in a time period of a few hours was the result of the even slower dissociation process of the copolymer micelles. On the other hand, Spacek and Kubin [9] found that the elution volume and elution concentration of micelles and unimers depended on the solvent composition and measurement temperature for their systems (kraton in dioxane–heptane), and that the shape of the chromatograms was influenced by the disruption and reestablishment of the association equilibrium during the separation.

In this paper, we wish to report results on the SEC of polystyrene–poly(ethylene oxide) diblock (PS–PEO) and triblock (PEO–PS–PEO) copolymers in water. In both systems we observe that micelles and unimers are eluted as well-separated peaks from a conventional aqueous SEC column. The analysis is rapid and convenient. Perhaps the most interesting conclusion from our experiments is that when the block copolymer has a somewhat broad molecular weight distribution [*e.g.*, weight-average molecular weight (M_w)/number-average molecular weight (M_n) = 1.5], the unimer peak derives from material enriched in the component (here PEO) forming the soluble block.

TABLE I

COPOLYMER SAMPLE PROPERTIES AND THE SEC RETENTION TIMES (t)

Sample	M_n (total) (g/mol)	PEO (%, w/w)	M_w/M_n	R_h (nm)	$t_{micelle}$ (min)	t_{unimer} (min)
Diblock						
Jlm5	8500	80	1.6	10	3.55	6.78
DB40	14100	72	1.2	15	3.55	6.72
Triblock						
Jlm6	18000	79	1.1	11	3.50	6.70
Jlm11	25900	80	1.5	18	3.47	6.55

EXPERIMENTAL

The PEO–PS–PEO triblock and PS–PEO samples were prepared in Mulhouse by standard anionic polymerization methods. The details have been reported elsewhere [10,11], and the characteristics of these polymers are listed in Table I.

Solutions for SEC analysis were prepared by weighing sufficient sample to give a final concentration of 1 mg/ml, adding sufficient doubly distilled deionized (Millipore Milli-Q grade) water, and heating the solution at $\approx$ 65°C for 2 h to complete dissolution of the samples. The solutions were then allowed to cool to room temperature (22°C) prior to the SEC analysis.

The SEC measurements were performed using a Micropak TSK-Gel G5000 PW column (Toyo Soda, purchased from Varian; packing material, polyether type; average pore size, $\approx$ 1000 Å)[a] and a Waters Model 510 pump, with a flow-rate of 1.5 ml/min. Deionized water (Millipore Milli-Q water system) was used as the eluent. Two detectors were used: a Waters R401 differential refractometer (RI) and a Kratos fluorometer (FL). As the fluorescence excitation wavelength 268 nm was chosen. The wavelength range (emission wavelength = 310–410 nm) corresponding to that of polystyrene excimer emission, the main emission from polystyrene, particularly in the bulk state, was chosen as the fluorescence emission band. Solutions were introduced onto the column by a Rheodyne six-way injector. The detected refractive index and fluorescence signals were recorded by a PC-XT-type microprocessor through a home-made interface card. The Fourier transform in infrared (FT-IR) measurements were made on a Nicolet Analytical Instruments 5DX FT-IR spectrometer.

RESULTS AND DISCUSSION

Fig. 1 shows a typical SEC trace from injection of an aqueous solution of our block copolymers onto the TSK-Gel G5000 PW polyether type column. In independent studies using quasi-elastic light scattering (QELS) and static light scattering (SALS), this particular sample was shown to form a narrow distribution of spherical micelles with a hydrodynamic radius R_h = 18 nm and a mean aggregation number N = 43 [12].

We assign the peak at a retention time of 3.5 min, which has both strong RI and FL signals, to eluting micelles. We found, as shown in Table I, that the measured retention time, $t_{micelle}$, is insensitive to the sample composition and to the overall hydrodynamic radius (R_h) of the micelles. This is a curious result, particularly since the micelles of Jlm5 have an R_h value (9 nm) half that of the micelles of Jlm11 (18 nm), and independent experiments on surfactant-stabilized latex samples [13] have shown that the elution volume of the micelles is well within the separation range of the column. Although details are not presented, Berlinova *et al.* [5] reported identical elution times for a series of micelles of diblock copolymers of different molecular weights.

---

[a] Our SEC column has been exposed repeatedly to dilute aqueous solutions of sodium dodecyl sulphate. The manufacturer's data sheet indicates that this kind of treatment can modify the column characteristics from that of a new column exposed only to water. Nevertheless, we always obtain reproducible results with this column.

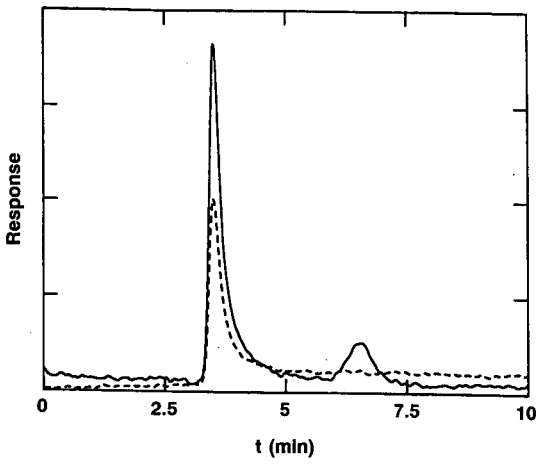

Fig. 1. The SEC trace of Jlm11 in aqueous solution, using a Micropak TSK-Gel G5000 PW size-exclusion column at a flow-rate of 1.5 ml/min. The solid line is the response from the refractive index detector and the dashed line is the fluorescence signal (excitation wavelength 268 nm and emission wavelength 310–410 nm).

Eluent samples containing the substances eluted at 3.5 min and 6.7 min were collected, concentrated and analyzed by FT-IR spectroscopy. Both contain block copolymer. The spectra are shown in Fig. 2. One notes the presence in both samples of a peak at 698 cm^{-1} characteristic of the C–H deformation vibration of PS and a peak at 1115 cm^{-1} characteristic of the C–O stretching vibration of PEO. We assign the SEC peak at 6.7 min to individual block copolymer molecules (unimers). The data in Table I indicate that the retention times for unimers decrease with increasing molecular weight. There is no fluorescence signal observed for the unimers. This important observation indicates that the aqueous medium is able to quench the PS

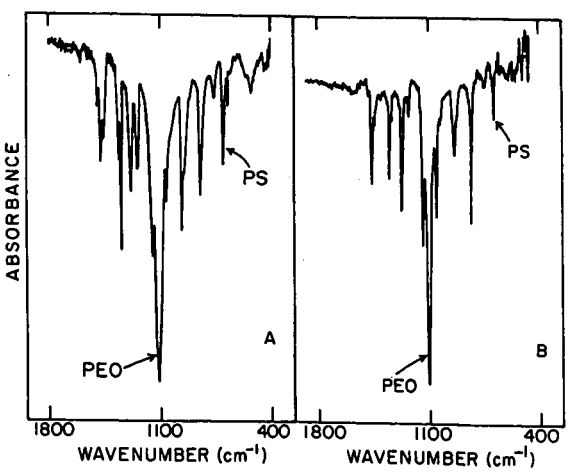

Fig. 2. FT-IR spectra from (A) Jlm11 and (B) substance collected from the monomer peak (the right peak in Fig. 1). The ratio of the two characteristic peaks (PS wavenumber = 698 cm^{-1} and PEO wavenumber = 1115 cm^{-1}) was used as an indicator for the relative PS content in the copolymer molecules.

fluorescence in the unimer, whereas in the larger micelle, the excited groups are protected from quenching.

By using the ratio of the characteristic FT-IR absorbance (A) of PS (wavenumber 698 cm^{-1}) to that of PEO (wavenumber 1115 cm^{-1}) as a measure of composition, we calculated that $(A_{PS}/A_{PEO})_{unimer}/(A_{PS}/A_{PEO})_{original} \approx 0.71$, *i.e.*, there is about 30% less PS in the unimer than in the original sample. The FT-IR analysis indicates that the micelles are formed preferentially from polymer enriched in the insoluble compound due to fractionation during micelle formation. This particular block copolymer sample has a large molecular weight distribution and is also likely to have a significant compositional heterogeneity. We know from independent studies that the critical micelle concentration (CMC) of the block copolymer in water depends critically on the size of the PS block [12,14]. These values are of the order 1–5 mg/l for the samples listed in Table I. Thus, those molecules enriched in styrene units stay in micelle form and those with a lower PS content remain as unimers. Consequently, both the unimer molecules and the molecules in micelles have a different composition distribution when compared with the original block copolymer material. The result suggests that preparative SEC experiments in selective solvents may provide a means of fractionating the block copolymer samples [15].

ACKNOWLEDGEMENTS

The authors thank NSERC Canada and the Province of Ontario for their support of this research. R.X. is a recipient of a Postdoctoral Fellowship awarded by the National Science and Engineering Research Council of Canada.

REFERENCES

1 A. Penlidis, A. E. Hamielec and J. F. MacGregor, *J. Liq. Chromatogr.*, 6(s-2) (1983) 179.
2 G. A. Gilbert, *Proc. R. Soc. London, Ser. A.*, 250 (1959) 377.
3 H. Coll, *Sep. Sci.*, 6 (1971) 207.
4 K. Prochazka, T. Mandak, M. Kocirik, B. Bednar and Z. Tuzar, *J. Chem. Soc. Faraday Trans.*, 86 (1990) 1103.
5 I. V. Berlinova, N. G. Vladimirov and I. M. Panayotov, *Makromol. Chem. Rapid Commun.*, 10 (1989) 163.
6 C. Price, A. L. Hudd and C. Booth, *Polym. Commun.*, 23 (1982) 650.
7 C. Price, *Pure Appl. Chem.*, 55 (1983) 1563.
8 P. K. Das, J. Hoover, R. J. Dodson, T. C. Ward and J. E. McGrath, *Polym. Prep. Am. Chem. Soc., Div. Polym. Chem.*, 25 (1984) 96.
9 P. Spacek and M. Kubin, *J. Appl. Polym. Sci.*, 30 (1985) 143.
10 S. Marti, J. Nervo and G. Riess, *Prog. Colloid Polym. Sci.*, 58 (1975) 114.
11 G. Riess, J. Nervo and D. Rogez, *Polym. Eng. Sci.*, 17 (1977) 634.
12 M. Wilhelm, C. Zhao, Y. Wang, R. Xu, M. A. Winnik, J. Mura, G. Riess and M. Croucher, *Macromolecules*, 24 (1991) 1033.
13 R. Xu, Y. Hu, M. A. Winnik, S. Mohanraj and G. Riess, *Langmuir*, 7 (1991) 831.
14 C. Zhao and M. A. Winnik, *Langmuir*, 6 (1990) 514.
15 G. Riess, G. Hurtrez and P. Bahadur, in H. F. Mark and J. I. Kroschwitz (Editors), *Encyclopedia of Polymer Science and Engineering*, Vol. 2, Wiley, New York, 1985, p. 324.

Journal of Chromatography, 547 (1991) 439–442
Elsevier Science Publishers B.V., Amsterdam

CHROM. 23 244

Short Communication

High-performance liquid chromatography with diode-array ultraviolet detection of methoxylated flavones in *Orthosiphon* leaves

P. G. PIETTA*, P. L. MAURI, C. GARDANA and A. BRUNO
Università degli Studi di Milano, via Celoria 2, 20133 Milan (Italy)
(First received October 22nd, 1990; revised manuscript received February 13th, 1991)

ABSTRACT

A rapid method for the determination of polymethoxylated flavones present in *Orthosiphon* leaves is described. Sinensetin, tetramethylscutellarein and 3′-hydroxy-4′,5,6,7-tetramethoxyflavone were separated on a C_{18} 3-μm Microsorb column using 2-propanol–tetrahydrofuran–water (22:4:74) as the eluent, followed by diode-array UV detection. The procedure was also applicable to the determination of polymethoxylated flavones from orange peel.

INTRODUCTION

Flavonoids have been shown to be ubiquitous in plants [1] and their chemistry and pharmacology are well documented [2,3]. Among them the polymethoxylated flavones are notable because they constitute a special group found in *Orthosiphon spicatus* (Thunb.) leaves [4,5] and in some citrus species [6].

Polymethoxylated flavones have often been examined in the past by spectrophotometric [7] or liquid chromatographic methods [8]. Several high-performance liquid chromatographic (HPLC) methods, mainly based on gradient elution, have been described for their determination in citrus and orange juices. So far no report has appeared on the HPLC of the polymethoxylated flavones present in *Orthosiphon* leaves. In this study, a rapid method for the determination of these flavones is described. Separation was achieved by reversed-phase isocratic elution with 2-propanol–tetrahydrofuran–water (22:4:74), followed by diode-array UV detection (DAD).

0021-9673/91/$03.50

EXPERIMENTAL

Materials

Orthosiphon spicatus leaves were obtained from Milanfarma (Milan, Italy). 3′,4′,5,6,7-pentamethoxyflavone (sinensetin, **I**), 3′,5-dihydroxy-4′,6,7-trimethoxyflavone (eupatorin, **IV**) and 4′,5,6,7,8-pentamethoxyflavone (tangeretin, **VII**) were purchased from Extrasynthese (Genay, France). 4′,5,6,7-Tetramethoxyflavone (tetramethylscutellarein, **III**), 3′,4′,5,6,7,8-hexamethoxyflavone (nobiletin, **V**) and 3′,4′,3,5,6,7,8-heptamethoxyflavone (**VI**) were already available in our laboratory [9].

Chromatographic conditions

The HPLC system consisted of a Model 510 pump, equipped with a Model U6K universal injector and a Model 1040 photodiode-array detector (Hewlett-Packard, Waldbronn, Germany). Chromatographic runs were performed on a 3-μm C_{18} Microsorb column (100 mm × 4.6 mm I.D.) (Rainin, Woburn, MA, USA). The mobile phase was 2-propanol–tetrahydrofuran–water (22:4:74) at a flow-rate of 0.5 ml/min (*Orthosiphon*) or 0.6 ml/min (orange peel).

Sample preparation

A 1-g amount of powdered *Orthosiphon* leaves was extracted by shaking for 10 min with 10 ml of methylene chloride. The clear filtrate (Schleicher and Schüll, folded filters) was evaporated to dryness *in vacuo* and the residue was dissolved in 1 ml of methanol. The solution was filtered through Spartan 13 filters (0.45 μm) and 10–20 μl were injected.

A 1-g amount of orange peel was extracted by shaking for 15 min with 10 ml of methanol. The clear filtrate was evaporated to dryness and the residue was dissolved in 2 ml of 30% methanol and percolated under positive pressure through a Sep-Pak C_{18} cartridge (Waters Assoc.) previously activated with methanol (3 ml) and water (5 ml). After washing with 3 ml of 50% methanol, the polymethoxylated flavones fraction was eluted with 3 ml of 70% methanol. Volumes of 100–200 μl were injected.

Evaluation of peak purity

To check peak purity, the eluates were monitored with the photodiode-array detector (200–400 nm). The three spectra corresponding to the upslope, apex and downslope of each peak were normalized and superimposed. Peaks were considered pure when there was exact coincidence between the three spectra (match factor >995).

RESULTS AND DISCUSSION

A number of lipophilic flavonoids are present in *Orthosiphon* leaves, sinensetin and tetramethylscutellarein being the most abundant. In addition to these two components, orange peel contains nobiletin, 3′,4′,3,5,6,7,8-heptamethoxyflavone and tangeretin [10] (Fig. 1). It should be noted that polymethoxylated flavones differ only in the position and the number of methoxy groups. Owing to the hydrophobic nature of these compounds and the small difference in polarity, C_{18} columns were used with eluents containing 2-propanol and tetrahydrofuran, whose suitability in resolving

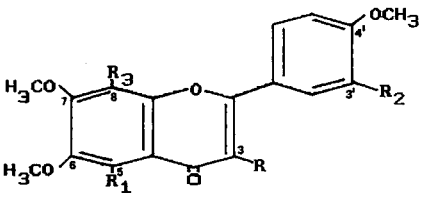

Fig. 1. Polymethoxylated flavones of *Orthosiphon spicatus* leaves and orange peel. R_1, R_2 = OCH_3; R, R_3 = H: sinensetin (**I**). R_1 = OCH_3; R, R_2, R_3 = H: tetramethylscutellarein (**II**). R_1 = OCH_3; R_2 = OH; R, R_3 = H: 3'-hydroxy-4',5,6,7-tetramethoxyflavone (**III**). R_1, R_2 = OH; R, R_3 = H: eupatorin (**IV**). R_1, R_2 = OH; R, R_3 = H: nobiletin (**V**). R, R_1, R_2, R_3 = OCH_3: 3',4',3,5,6,7,8-heptamethoxyflavone (**VI**). R_1, R_3 = OCH_3; R, R_2 = H: tangeretin (**VII**).

flavonoids has already been ascertained [11]. The isocratic mobile phase composition was 2-propanol–tetrahydrofuran–water (22:4:74), giving a sharp baseline resolution in less than 25 min (Fig. 2).

Different apolar solvents were evaluated for their ability to extract selectively polymethoxylated flavonoids from *Orthosiphon* leaves. Methylene chloride was selected, as the flavonoids were extracted with a very small amount of relatively polar compounds, which did not interfere with the early portion of the chromatogram. For this reason, further purification using Sep-Pak C_{18} was unnecessary. The UV spectra scanned from the peaks of eluting standards were in agreement with those from the peaks eluting at the corresponding times in the leaves sample.

Linearity between polymethoxylated flavone concentration and peaks area was found between 10 and 50 μg/ml, the correlation coefficients being 0.997 and 0.995 for sinensetin and tetramethylscutellarein, respectively. Recovery tests with known

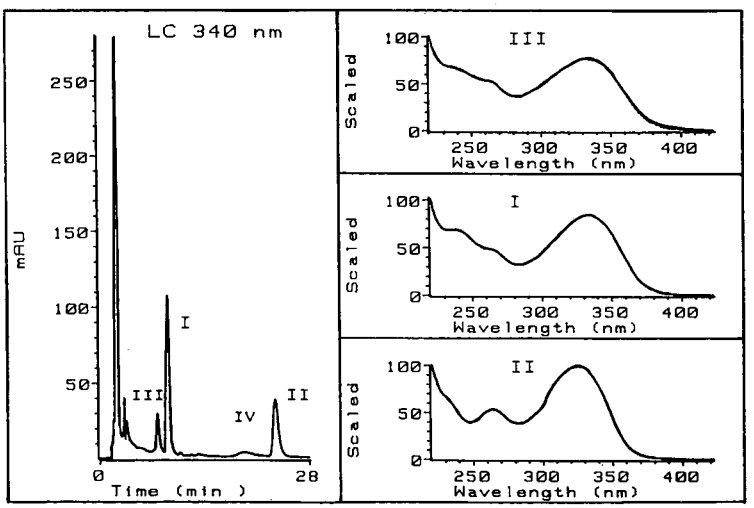

Fig. 2. Chromatogram obtained from *Orthosiphon* leaves. Chromatographic conditions: column, 3-μm C_{18} Microsorb; eluent, 2-propanol–tetrahydrofuran–water (22:4:74); flow-rate, 0.5 ml/min; UV detection at 340 nm. For peaks, see Fig. 1.

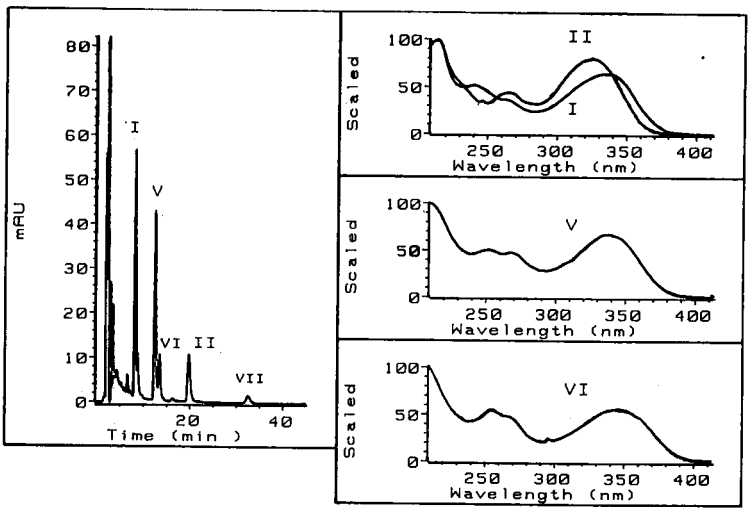

Fig. 3. Chromatogram obtained from orange peel. Chromatographic conditions as in Fig. 2. Flow-rate, 0.6 ml/min. For peaks, see Fig. 1.

amounts of standards added to a sample were performed, and the recoveries were in the range 92–108% (n = 6; S.D. = 4.9%).

This HPLC procedure was also applied to the determination of polymethoxylated flavones in orange peel. Prepurification of the sample through a Sep-Pak C_{18} cartridge was essential in this instance to obtain a satisfactory separation of sinensetin, heptamethoxyflavone, tetramethylscutellarein and tangeretin (Fig. 3).

The presence of chlorophylls and carotenoids in *Orthosiphon* leaves and orange peel was excluded on the basis of both sample purification and diode-array analysis.

In conclusion, the described method for the determination of polymethoxylated flavones in *Orthosiphon* leaves offers several advantages over existing thin-layer chromatographic methods. Moreover, it can be applied satisfactorily to the determination of analogues flavonoids in other matrices, such as orange peel.

ACKNOWLEDGEMENTS

The authors are grateful to Annamaria Pietta for technical assistance and to CNR-P.S. "Innovazione Produttiva nella P&MI" for providing funds.

REFERENCES

1 J. B. Harborne, *The Flavonoids: Advances in Research*, Chapman & Hall, New York, 1988.
2 T. A. Geissmann, *The Chemistry of Flavonoid Compounds*, Pergamon Press, Oxford, 1962.
3 V. Cody, E. Middleton, Jr., J. B. Harborne and A. Beretz, *Plant Flavonoids in Biology and Medicine, II: Biochemical, Cellular and Medicinal Properties*, Alan R. Liss, New York, 1988.
4 E. Wollenweber and K. Mann, *Planta Med.*, 51 (1985) 459.
5 K. E. Malterud, I. M. Hanche-Olsen and I. Smith-Kielland, *Planta Med.*, 55 (1989) 569.
6 S. Magy, P. E. Shaw and H. K. Veldhuis, *Citrus Science and Technology*, Vol. 1, Avi, New York, 1977.
7 L. F. Swift, *J. Agric. Food Chem.*, 15 (1967) 99.
8 R. Roussef and S. V. Ting, in G. Charalambous (Editor), *Liquid Chromatographic Analysis of Food and Beverages*, Vol. 2, Academic Press, London, 1979, p. 537.
9 J. P. Bianchini and E. M. Gaydou, *J. Chromatogr.*, 190 (1980) 233.
10 B. Heimhuber, R. Galensa and K. Herrmann, *J. Chromatogr.*, 439 (1988) 481.
11 P. G. Pietta, P. L. Mauri, E. Manera and P. L. Ceva, *J. Chromatogr.*, 513 (1990) 391.

Journal of Chromatography, 547 (1991) 443–446
Elsevier Science Publishers B.V., Amsterdam

CHROM. 23 139

Short Communication

Reversed-phase high-performance liquid chromatographic separation of 5β,20-dihydroxyecdysone and 20-hydroxyecdysone on a β-cyclodextrin-bonded stationary phase

T. VAISAR* and T. VANEK

Institute of Organic Chemistry and Biochemistry, Czechoslovak Academy of Sciences, Flemingovo namesti 2, 166 10 Prague (Czechoslovakia)

(First received June 13th, 1990; revised manuscript received January 29th, 1991)

ABSTRACT

For the high-performance liquid chromatographic separation of two ecdysteroids, 20-dihydroxyecdysone and 5β,20-dihydroxyecdysone which are hardly or not at all resolved on classical normal or reversed stationary phases, we have used a β-cyclodextrin stationary phase, prepared in our laboratory. Easy preparation was obtained in reversed-phase mode, either with methanol or with acetonitrile as an organic modifier in the aqueous mobile phase. The separation of these two ecdysteroids in mixture with two other ecdysteroids by gradient elution is also shown.

INTRODUCTION

The ecdysteroids control a number of important physiological functions, *i.e.* periodic moulting, interruption of larval or pupal diapause, or they can influence control of embryonic development in insects [1]. In the late 1960s the first analogues of these compounds were found in some plants (phytoecdysones), and among others also in the fern species *Polypodium vulgare* and *Pteridium aqulinium* [2].

During our experiments on the production of ecdysteroids by plant tissue cultures [3] we aimed to develop a suitable method for their separation. As we needed to inject the liquid media without any further purification, a reversed-phase system with C_{18} stationary phase and aqueous methanol or acetonitrile mobile phase was shown to be suitable [4]. Behavior of ecdysteroids under reversed-phase conditions was extensively studied from a structural point of view [5]. It was established that the position of hydroxy groups is more important for their retention than their number, *e.g.* a hydroxy group in the aliphatic chain has greater effect compared with C-2 or C-11 hydroxy groups. A hydroxy group in the 5β position has the least effect on retention

0021-9673/91/$03.50

and the separation of 20-hydroxyecdysone from 5β,20-dihydroxyecdysone is therefore a difficult one. However, separation of these two ecdysteroids with supercritical fluid chromatography has been described previously [6].

Recently many applications of cyclodextrin-bonded stationary phase to reversed-phase liquid chromatography have emerged [7,8]. In these papers many separations of isomeric or closely related compounds have been shown. We applied our prepared cyclodextrin stationary phase 7CDSIL [9] to the separation of ecdysteroids to achieve a more selective separation than on common C_{18} reversed-phase.

EXPERIMENTAL

Chemicals

Methanol and acetonitrile (Lachema, Brno, Czechoslovakia) were redistilled from glass, water was twice deionized and redistilled from glass. Standards of ecdysteroids were obtained from The Department of Natural Compounds in our Institute.

Apparatus

Chromatographic experiments were performed on Gilson liquid chromatograph (France) comprising two Model 303 pumps, a Model 802C manometric module, a Model 811 dynamic mixer and a Holochrome UV-detector. The system was controlled by an IBM PC-AT via a Gilson data module Model 621 Data Master. Samples were injected through a Rheodyne 7125 (USA) sampling valve.

Chromatographic conditions

The cyclodextrin-bonded stationary phase (7CDSIL) was slurry packed into a stainless-steel column (250 × 4 mm I.D.). The mobile phases were mixtures of acetonitrile or methanol with water. The flow-rate was 1.0 ml/min and detection was UV at 245 nm.

RESULTS AND DISCUSSION

Separations on 7CDSIL were at first performed in an aqueous methanol mobile phase. Retention of solutes in 80% methanol was low, resembling on a C_{18} reversed phase in similar mobile phase. A remarkable increase in retention, however, was observed with increasing polarity of mobile phase, and with 50% methanol separation of solutes was observed. Further decrease in the methanol portion improved separation such that at 35% methanol almost baseline separation was obtained (resolution, $R_s = 1.56$) (Fig. 1). Decreasing the amount of methanol below 30% did not bring about any remarkable improvement of resolution; on the contrary, peak broadening was observed. These results suggest a strong dependence of host–guest interaction on the amount of water in the mobile phase. The elution order 20-hydroxyecdysone (B) > 5β,20-dihydroxyecdysone (A) was determined from the retention times of pure solutes.

It has been noted elsewhere [5] that better results in separations of ecdysteroids on reversed phase were obtained with acetonitrile as the organic modifier in the mobile phase, so we performed experiments with this solvent using the same methods as with methanol. A reasonable separation was observed with 40% acetonitrile be-

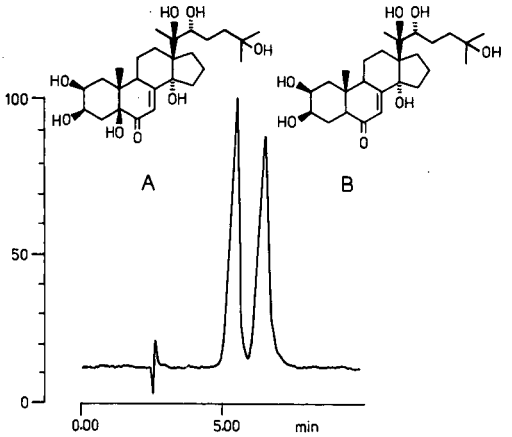

Fig. 1. Separation of 20-hydroxyecdysone (B) and 5β,20-dihydroxyecdysone (A) in a methanol–water (35:65) mobile phase. Flow-rate, 1.0 ml/min; detection, UV at 245 nm; injection, 10 μl of methanolic solution, approximately 1 μg of each compound.

cause of the greater elution strength of this mobile phase, and baseline separation with 15% acetonitrile (R_s = 1.87) was achieved. A further decrease of the acetonitrile portion again caused peak broadening. However, observed resolution and peak shape were better with acetonitrile than with methanol, and, moreover, a lower amount of organic modifier was necessary for baseline separation.

Separation of these two ecdysteroids in mixture with two other ecdysteroids (ecdysone and ponasterone B) under gradient elution conditions, as indicated in the figure legend, is shown in Fig. 2.

These investigations have shown that a cyclodextrin-bonded stationary phase

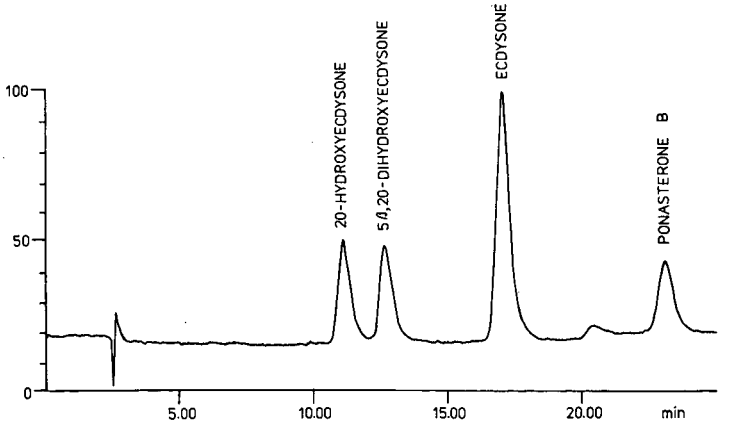

Fig. 2. Gradient separation of four ecdysteroids: 0–25 min, 15–50% methanol in water. Flow-rate, 1.0 ml/min; detection, UV at 245 nm; injection, 10 μl of methanolic solution, approximately 1 μg of 20-hydroxyecdysone, 5β,20-dihydroxyecdysone and ponasterone B and 2 μg of ecdysone.

with aqueous acetonitrile and aqueous methanol mobile phases can be recommended for separations of 20-hydroxyecdysone and 5β,20-dihydroxyecdysone. Further use of this methodology in the analysis of ecdysteroids is under investigation.

ACKNOWLEDGEMENT

The authors gratefully acknowledge J. Pis for the gift of ecdysteroids standards.

REFERENCES

1 K. Slama, M. Romanuk and F. Sorm, in *Insect Hormones and Bioanalogues*, Springer Verlag, New York, Vienna, 1974, pp. 303–387.
2 R. Bergamosco and D. H. S. Horn, in R. G. H. Dewner and H. Laufer (Editors), *Endocrinology of Insects*, Allan R. Liss, New York, pp. 627–654.
3 T. Vanek, T. Macek, T. Vaisar and A. Bereznovits, *Biotechnol. Lett.*, 10 (1990) 727.
4 R. Lafont, J.-L. Pennetier, M. Andiranjafintrimo, J. Claret, J.-F. Modde and C. Blais, *J. Chromatogr.*, 236 (1982) 137.
5 D. Wilson, C. R. Bielby and E. D. Morgan, *J. Chromatogr.*, 238 (1982) 97.
6 E. D. Morgan, S. J. Murphy, D. E. Games and I. C. Mylchreest, *J. Chromatogr.*, 441 (1988) 165.
7 D. W. Armstrong, W. DeMond, A. Alak, W. L. Hinze, R. E. Riehl and K. H. Bui, *Anal. Chem.*, 57 (1985) 234.
8 W. L. Hinze, T. E. Riehl, D. W. Armstrong, W. DeMond, A. Alak and T. J. Ward, *Anal. Chem.*, 57 (1985) 237.
9 T. Vaisar, T. Vanek and E. Smolkova-Keulemansova, *Eur. Pat.*, 89121526.1 (1989).

Journal of Chromatography, 547 (1991) 447–451
Elsevier Science Publishers B.V., Amsterdam

CHROM. 23 279

Short Communication

High-performance liquid chromatographic determination of low levels of primary and secondary amines in aqueous solutions including 2-amino-2-methylpropanol by pre-column derivatisation to sulphonamides

JOHN R. LINDSAY SMITH and ALISON U. SMART
Department of Chemistry, University of York, York, YO1 5DD (UK)
and
FRED E. HANCOCK and MARTYN V. TWIGG*
ICI Chemicals and Polymers Ltd., Research and Technology Department, Billingham, Cleveland, TS23 1LB (UK)

(First received July 25th, 1990; revised manuscript received February 20th, 1991)

ABSTRACT

Pre-column derivatisation of primary and secondary amines to sulphonamides, by reaction with 5-dimethylamino-1-naphthalenesulphonyl chloride (dansyl chloride) has advantages over the corresponding derivatisation with 1,2-naphthoquinone-4-sulphonate (NQS) because the reaction is less susceptible to steric effects, and the resultant sulphonamides are readily extracted from the derivatising solution. A procedure employing a relatively high reaction temperature and chloroform extraction followed by reversed-phase high-performance liquid chromatography using ultraviolet detection at 340 nm provides a robust method for determining primary and secondary amines. The method was used to analyse samples of industrial waters containing various mixtures (0–2 m*M*) of ammonia, hexamethyleneimine, hydrazine, methylamine and piperidine, as well as 2-amino-2-methylpropanol and 1,6-hexanediamine that could not be analysed via NQS derivatisation.

INTRODUCTION

Previously we reported [1] a convenient high-performance liquid chromatographic (HPLC) method for determining low levels of primary and secondary amines in industrial waters based on pre-column derivatisation with 1,2-naphthoquinone-4-sulphonate (NQS). Although useful for some routine work it has been found to have some serious disadvantages. Derivatisation of hindered amines is slow, and derivatives with hydrophilic groups such as hydroxyl do not partition favourably with organic solvents to such an extent they may not be extracted from the aqueous derivatising solution. For example, it was not possible to analyse dilute aqueous solutions for

0021-9673/91/$03.50

2-amino-2-methylpropanol, an amine of particular interest. We therefore devised a derivatisation procedure that does not suffer these deficiencies. For practical reasons we wished to employ UV detection and use a fairly high wavelength to minimize possible background interference by strongly UV-absorbing contaminants that were often present. Of the possible derivatisation reagents 2,4-dinitrofluorobenzene was rejected because it causes contact hypersensitivity [2], and some of its derivatives are known to be very toxic [3]. In contrast formation of sulphonamides from 5-dimethylamino-1-naphthalenesulphonyl chloride (dansyl chloride) appeared not to present such potential problems, and fluorescence detection could be employed should extra sensitivity be required.

Derivatisation of amines by dansyl chloride to form sulphonamides was originally developed as a thin-layer chromatographic (TLC) technique by Seiler and Wiechmann [4] and has since been modified [5–7] for use with HPLC. In the reversed-phase procedure described here problems associated with NQS were overcome, and it has been successfully used for estimating a wide range of primary and secondary amines in industrial waters over an extended period.

EXPERIMENTAL

Equipment

A Waters 840 HPLC system equipped with 510 pumps, a WISP 710B autosampler, an M490 UV detector and an 840 data module was used throughout the work described here. The reversed-phase column was a 25 cm × 4.6 mm I.D., 5-μm Spherisorb ODS2 column supplied by HiChrom (Reading, UK).

Chemicals

HPLC-grade acetonitrile (Rathburns, UK), chloroform (Aldrich, UK) and water were used. Potassium carbonate came from BDH (Poole, UK), dansyl chloride and all other chemicals were of the highest purity available from Aldrich or Fluka.

Derivatisation

All calibration solutions were prepared using HPLC-grade water. Reactions were carried out in screw-top glass vials, capable of holding a minimum of 15 ml liquid. To the analyte solution (3 ml; amine concentration in the range 0.01–5 mM) were added aqueous potassium carbonate solution (0.5 ml; 0.7 M) and dansyl chloride solution in acetone (6 ml; 18.5 mM). Solutions were incubated at 55°C for 90 min. After cooling to 50°C (acetone boils at 56°C) aqueous proline (3 ml; 1.3 M) was added to each vial, and the samples were maintained at 55°C for a further 20 min to remove excess dansyl chloride by forming the ionised proline derivative. After cooling the solutions to 50°C, water (5 ml) was added, and the samples were allowed to cool to ambient temperature. Each solution was extracted with chloroform (2 ml), and the organic phase collected by filtering through silicone-treated phase separator filter papers (Whatman 1PS). The organic phase (1 ml) was diluted with acetonitrile (1 ml) and the solution used for HPLC analysis.

HPLC analysis methodology

An injection volume of 10 μl was used. The mobile phase was a mixture of

17.5 m*M* pH 7.2 phosphate buffer and acetonitrile. The phosphate buffer was prepared by titrating an aqueous solution of disodium hydrogenphosphate with orthophosphoric acid. This was preferred to titration with glacial acetic acid described by Hayman *et al.* [5], which was found to give a cloudy solution on standing for a day. When orthophosphoric acid was used no turbidity was observed. For optimal HPLC separation the flow-rates and solvent composition used depended on the amines to be separated, and typically the amount of aqueous buffer in the mobile phase was in the range 30–40% with flow-rates of 1.0–1.5 ml min^{-1}. The eluting peaks were monitored at 340 nm. Table I shows the conditions employed for analysis of ammonia with a variety of other amines including 2-amino-2-methylpropanol. Calibration graphs prepared using six to ten samples of pure amine solutions up to 2.0 m*M* (0.5 m*M* for ammonia) were linear with correlation coefficients better than 0.998.

TABLE I

TYPICAL EXAMPLES OF SOLVENT COMPOSITIONS AND FLOW-RATES FOR HPLC SEPARATION OF SULPHONAMIDE AND ITS N-SUBSTITUTED DERIVATIVES

Parent amines	Solvent composition (acetonitrile–buffer)	Flow-rate (ml min^{-1})
NH_3/hydrazine	60:40	1.0
NH_3/2-amino-2-methylpropanol	60:40	1.0
NH_3/2-amino-2-methylpropanol/piperidine	70:30	1.3
NH_3/2-amino-2-methylpropanol/morpholine	65:35	1.0
NH_3/2-amino-2-methylpropanol/hexamethyleneimine/1,6-hexanediamine	62:38	1.5

RESULTS AND DISCUSSION

In order to reduce derivatisation times and optimise conversion a relatively high reaction temperature (55°C for 90 min) was chosen. Temperatures much in excess of this are detrimental, possibly due to side-reactions between the co-solvent acetone and the analyte amine. After derivatisation proline was reacted with the excess dansyl chloride that otherwise would cause interference in the HPLC analysis. Of the organic solvents used to extract, and if necessary concentrate the sulphonamide, chloroform was chosen for routine work because it separated readily from the aqueous layer and was more selective than commonly employed ethyl acetate [5,6,8]. Moreover, chloroform is less likely than ethyl acetate or aromatic solvents [4–8] to hamper UV detection. Extraction with chloroform combined with the use of phase-separating filters made the extraction process straightforward.

Monitoring eluting peaks due to dansylated derivatives at 340 nm minimised interference by acetone encountered by others [8] as well as by highly absorbing species in the original samples, and afforded detection limits (twice the average baseline noise) of less than 10 μM for all the amines analysed. Relative standard deviations for six repeat determinations were generally better than 5%. If required higher sensitivity can be obtained by using a lower detection wavelength (monitoring at 254 nm rather than

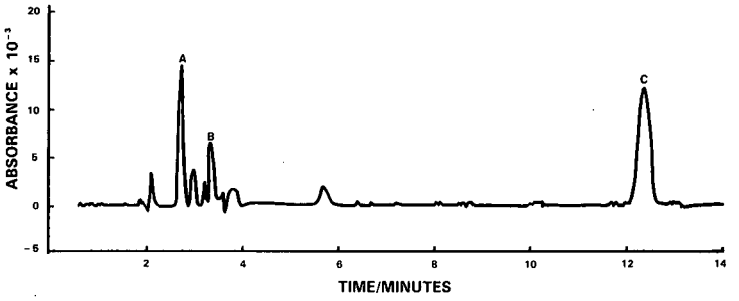

Fig. 1. Chromatogram showing the separation of three amines in an industrial liquor: (A) ammonia, 346 μM; (B) 2-amino-2-methylpropanol, 232 μM; (C) hexamethyleneimine, 237 μM. Chromatographic conditions: mobile phase, acetonitrile–17.5 mM pH 7.2 phosphate buffer (62:38); flow-rate, 1.5 ml min^{-1}; column, Spherisorb ODS2, 5 μm (25 cm × 4.6 mm I.D.), injection size, 10 μl; monitoring wavelength, 340 nm.

at 340 nm increased sensitivity five-fold), but baseline interference was more common. Alternatively, a fluorescence [9] detector could be used.

Dansyl chloride itself has negligible solubility in water, so it was added to the derivatisation mixture as an acetone solution, and surprisingly the amount of acetone used was found to determine the linearity range of the method. This was particularly important for 1,6-hexanediamine where, when 3 ml of a 18.5 mM solution of dansyl chloride in acetone was used, the linearity range was only 0–0.25 mM, whereas, when 6 ml of a 9.25 mM derivatising solution was used, the linearity range increased more than an order of magnitude. Similar patterns were observed with other amines: for example, the linear range with hexamethyleneimine increased from 0–1 mM to 0–10 mM under the same conditions. This may be a consequence of higher chloroform solubility of sulphonamides in the presence of acetone (some was extracted into the chloroform layer), or acetone may assist transferring the sulphonamides from the aqueous phase to the organic phase. However, tests with dansylamide showed it is readily and completely extracted into chloroform in the absence of acetone, suggesting other effects may be operating. It is known that acetone inhibits first-order neutral hydrolysis of some sulphonyl chlorides [10], but insufficient data are available about second-order reactions to comment meaningfully about solvent effects in kinetic terms; we did not pursue this point experimentally.

There was no problem in estimating ammonia [11] in the presence of any of the amines we examined, and methylamine and hydrazine could similarly be analysed. In addition 1,6-hexanediamine and 2-amino-2-methylpropanol, which could not be determined via NQS derivatisation, were readily estimated and Fig. 1 is a typical routine chromatogram showing the separation of ammonia, hexamethyleneimine and 2-amino-2-methylpropanol in an industrial liquor.

CONCLUSIONS

The reversed-phase HPLC procedure reported here involving pre-column sulphonamide derivatisation is a reliable and sensitive method for the determination of a wide range of primary and secondary amines. Problems with NQS derivatives of

sterically hindered and/or hydroxyl-containing amines were successfully circumvented by forming sulphonamide derivatives. Nucleophilic substitution at sulphur in dansyl chloride appears at least as facile and less susceptible to steric effects than at the carbon centre of NQS. For the hydrophilic amine 2-amino-2-methylpropanol, which is sterically crowded around the nitrogen, it provides a ready means for its routine analysis. The NQS methodology failed to detect it mainly because the derivative is too hydrophilic to extract into non-polar solvent [1]. Linearity of the calibration graphs with UV detection was excellent and enabled less than 10 μM amine to be measured. Low-molecular-weight amines, including ammonia, can be analysed in the presence of a variety of other amines and, if necessary, significantly lower detection levels could no doubt be achieved using more sensitive detection systems.

ACKNOWLEDGEMENT

A.U.S. thanks ICI Chemicals & Polymers Ltd. for a research studentship.

REFERENCES

1 J. R. Lindsay-Smith, A. U. Smart, F. E. Hancock and M. V. Twigg, *J. Chromatogr.*, 483 (1989) 341.
2 J. W. Streilein, S. Suluvan and S. Thompson, *J. Immunol.*, 124 (1980) 577.
3 N. I. Sax and R. J. Lewis, *Dangerous Properties of Industrial Materials*, Van Nostrand Reinhold, New York, 7th ed., 1989.
4 N. Seiler and M. Wiechmann, *J. Physiol. Chem.*, 348 (1967) 1285.
5 A. R. Hayman, D. O. Gray and S. V. Evans, *J. Chromatogr.*, 325 (1985) 462.
6 N. D. Brown, R. B. Sweet, J. A. Kintzios, H. D. Cox and B. P. Doctor, *J. Chromatogr.*, 164 (1979) 35.
7 Y. Saeki, N. Uehara and S. Shirakawa, *J. Chromatogr.*, 145 (1978) 221.
8 T. Kremmer, L. Holozinger, M. Boldiszar, L. Semeci and S. Bardocz, *J. Chromatogr.*, 286 (1984) 371.
9 N. Seiler and L. Demisch, in K. Blau and G. S. King (Editors), *Handbook of Derivatives for Chromatography*, Heyden Press, London, 1977, pp. 349–363.
10 A. Arcoria, F. P. Ballistreri, E. Spina, G. A. Tomaselli and E. Maccarone, *J. Chem. Soc., Perkin Trans. II*, (1988) 1793.
11 J. R. Lindsay-Smith, A. U. Smart, F. E. Hancock and M. V. Twigg, *Chem. Ind.*, (1989) 353.

Journal of Chromatography, 547 (1991) 452–456
Elsevier Science Publishers B.V., Amsterdam

CHROM. 23 310

Short Communication

Very high speed separation of proteins with a 20-μm reversed-phase sorbent

S. P. FULTON*, N. B. AFEYAN and N. F. GORDON
PerSeptive Biosystems, 38 Sidney Street, Cambridge, MA 02139 (USA)
and
F. E. REGNIER
Department of Chemistry, Purdue University, West Lafayette, IN 47907 (USA)
(First received January 24th, 1991; revised manuscript received March 19th, 1991)

ABSTRACT

A five-protein mixture was successfully separated in less than 15 s by reversed-phase gradient elution on a 20-μm polymeric flow-through type chromatographic packing material (POROS R/M). The same mixture could also be separated with far better resolution in less than 60 s on the same column by simply extending the gradient volume. Pressure drop across the column was less than 130 bar, despite a superficial linear velocity of nearly 9000 cm/h. Frontal chromatography at different flow-rates was used to demonstrate that the ability to separate at high speed was due to greatly enhanced mass transport within the particles due to the flow-through (perfusion chromatography) effect.

INTRODUCTION

It has been recognized for half a century that stagnant mobile phase mass transfer is a dominant limitation in liquid chromatography [1]. Although the development of microparticulate, macroporous supports substantially diminished this problem, resolution was still seriously compromised at high mobile phase velocity [2–4].

Recent work has shown that the stagnant mobile phase mass transfer problem in porous sorbents may be dealt with in several ways. One approach is to eliminate the pores. Through the use of 1–2 μm non-porous particles it has been possible to carry out protein separations an order of magnitude faster, albeit at the expense of diminished loading capacity and high operating pressure [5–7]. A second alternative is to cause liquid to flow or perfuse through the particles. An initial report indicates that 6000–8000 Å diameter, particle-transecting pores allow convective transport into the interior of supports [8,9]. Because convective transport is much more rapid than that achieved by diffusion, these materials can also be used at an order of magnitude

0021-9673/91/$03.50

higher mobile phase velocity in protein separations. This raises the question of whether the facilitation of transport provided by intraparticle convective flow will allow the use of larger particles in rapid separations.

Although 20 μm porous particles are easy to prepare and pack, provide high loading capacity, operate at low pressure and are generally less expensive to produce than microparticulate materials, they are never considered for high speed protein separations because of the mass transfer restrictions outlined above. This note reports the behavior of 20 μm perfusable reversed-phase sorbent at 30–60 times greater mobile phase velocity than is conventional.

MATERIALS AND METHODS

Reagents

All proteins used in this work were obtained from Sigma (St. Louis, MO, USA).

Chromatography

Gradient separations were carried out on an HP 1090 liquid chromatograph (Hewlett-Packard, Avondale, PA, USA) equipped with a diode array detector operated at 220 nm. The column used was a 30 × 2.1 mm POROS R/M (PerSeptive Biosystems, Cambridge, MA, USA). This packing consists of highly cross-linked styrene–divinyl benzene with no surface derivatization (nominal particle diameter, 20 μm).

The protein mixture used in the gradient separation consisted of ribonuclease A (6 mg/ml), cytochrome *c* (4 mg/ml), lysozyme (3 mg/ml) β-lactoglobulin (4 mg/ml) and ovalbumin (6 mg/ml) dissolved in 0.1% trifluoroacetic acid (TFA). A sample volume of 2 μl and flow-rate of 5 ml/min were used in all cases. Elution was achieved with a linear gradient from 0.1% TFA in 20% aqueous acetonitrile (ACN) to 0.1% TFA in 50% aqueous ACN. Gradient times are specified in the captions.

Frontal uptake studies were carried out on a Waters Delta Prep System (Waters Associates, Milford, MA, USA) equipped with a UV–VIS detector operated at 220 nm. The same column was used as in the gradient separation study.

The sample for the frontal uptake consisted of lysozyme (1 mg/ml) dissolved in 0.1% TFA in 1% aqueous ACN.

The column was equilibrated in 0.1% TFA in 1% aqueous ACN. A 2.0-ml injection was made at 0.1, 1.0 and 4.0 ml/min, which fully saturated the column. Following the injection, the column was washed with 0.1% TFA in ACN to remove all bound protein and reequilibrated in the starting mobile phase.

The superficial linear velocity (u in ml/h · cm^2 or cm/h) of mobile phase through the columns was calculated using the equation $u = 60\ vL/V$, where v is the flow-rate in ml/min, L is the column length in cm and V is the column volume in ml (0.104 ml for the column used in this study). Superficial linear velocity (flow-rate divided by column cross-sectional area) is often used because it is a simple method of comparing columns without regard to the type of packing material or packing density. It should be noted that true linear velocity is a function of both packing density and the specific interstitial volume of the sorbent.

RESULTS AND DISCUSSION

A separation of five proteins in 12 s on a POROS R/M column packed with 20 μm particles and operated at a superficial mobile phase linear velocity of 8700 cm/h is shown in Fig. 1. Peaks 1–5 in this figure are ribonuclease A, cytochrome *c*, lysozyme, β-lactoglobulin and ovalbumin, respectively. Since the pore volume is approximately 45% of the particle volume and the interstitial volume is approximately 38% of the column volume, it may be calculated that the liquid volume in the column is about 69 μl. With a flow-rate of 5 ml/min (8700 cm/h) the entire 69 μl liquid volume is displaced in 0.82 s. The five proteins standards were eluted within 15 column liquid volumes of the 30 column liquid volume gradient. The column pressure drop in these runs averaged around 120 bar.

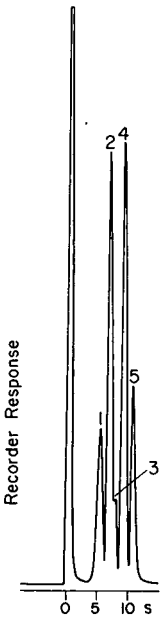

Fig. 1. A high speed reversed-phase separation of proteins with a steep gradient. Sample, operating parameters and peak identification were as specified in the text. Elution was achieved with a 24-s gradient.

In an effort to improve the resolution, the gradient time was extended to 1.5 min (110 column liquid volumes). It will be seen in Fig. 2 that this five-fold decrease in gradient slope substantially increased the resolution. (Peak identification is the same as in Fig. 1). All major protein species were fully resolved in less than 60 s (73 column liquid volumes). In addition, β-lactoglobulin (peak 4) was partially resolved into its A and B variants.

Because the mobile phase velocity in these separations is approximately 30–60 times higher than that generally used in high-performance liquid chromatography (HPLC), especially with larger particles, it could be argued that the proteins do not actually penetrate into the pores of the sorbent. This possibility was examined by

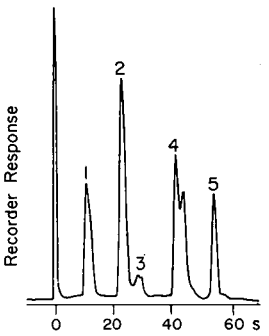

Fig. 2. A high speed reversed-phase separation of proteins with a shallow gradient. Sample, operating parameters and peak identification were as specified in the text. Elution was achieved with a 90-s gradient.

measuring the loading capacity of the column at 170, 1700 and 7000 cm/h superficial linear velocity (0.1, 1.0 and 4.0 ml/min). The results are shown in Fig. 3. Frontal loading curves at these low and high velocities show that the loading capacity (approximately 7 mg/ml for lysozyme under these conditions) is independent of the flow-rate. Thus the proteins actually can penetrate into the particles, even at these very short residence times.

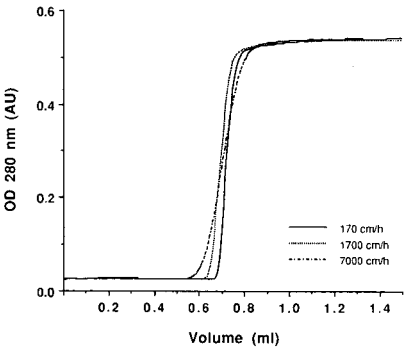

Fig. 3. Frontal loading of the column as a function of mobile phase superficial linear velocity. Study carried out with lysozyme on the 30 × 2.1 mm POROS R/M column as described in the text.

Based on the data presented above with a 20-μm perfusable reversed-phase sorbent it may be concluded that: (i) rapid separations of macromolecules may be achieved with 20-μm perfusable sorbents at very high mobile phase velocity; (ii) proteins have complete access to the interior of larger perfusable packings at superficial mobile phase velocities up to at least 7000 cm/h; and (iii) the ability of these materials to retain resolution at 30–60 times greater mobile phase velocity than normal in HPLC is the result of large particle transecting pores that allow convective transport within the particles.

The obvious advantages of 20-μm perfusable particles over 1–3 μm sorbents are that they are easier to pack, more difficult to plug and operate at much lower pressure. Similar high resolution analytical performance has been obtained using perfusable supports with other surface chemistries including ion exchange, hydrophobic interaction and affinity [10].

REFERENCES

1 A. J. P. Martin and R. L. M. Synge, *Biochem. J.*, 35 (1941) 1358.
2 R. E. Majors, *Anal. Chem.*, 44 (1972) 1722.
3 K. K. Unger, R. Kern, M. C. Ninov and K.-F. Krebs, *J. Chromatogr.*, 99 (1974) 435.
4 F. D. Antia and Cs. Horváth, *J. Chromatogr.*, 435 (1988) 1.
5 K. K. Unger, G. Jilge, J. N. Kinkel and M. T. W. Hearn, *J. Chromatogr.*, 359 (1986) 61.
6 K. Kalghatgi and Cs. Horváth, *J. Chromatogr.*, 398 (1987) 335.
7 K. Kalghatgi and Cs. Horváth, *J. Chromatogr.*, 443 (1988) 343.
8 N. B. Afeyan, N. F. Gordon, I. Mazsaroff, L. Varady, S. P. Fulton, Y. B. Yang and F. E. Regnier, *J. Chromatogr.*, 519 (1990)1.
9 N. B. Afeyan, S. P. Fulton and F. E. Regnier, *J. Chromatogr.*, 544 (1991) 267.
10 N. B. Afeyan, S. P. Fulton, N. F. Gordon, L. Varady and F. E. Regnier, presented at *Anabiotech 1990, Burlingame, CA, October 1990.*

Journal of Chromatography, 547 (1991) 457–461
Elsevier Science Publishers B.V., Amsterdam

CHROM. 23 293

Short Communication

Purification to homogeneity of bovine prolactin by high-performance ion-exchange chromatography

ANNA BERRINI, VITALIANO BORROMEO and CAMILLO SECCHI*
Istituto di Fisiologia Veterinaria e Biochimica, Università di Milano, Via Celoria 10, I-20133 Milan (Italy)
(First received November 19th, 1990; revised manuscript received February 25th, 1991)

ABSTRACT

Homogeneous bovine prolactin (bPRL) has been obtained using a procedure based on high-performance anion-exchange chromatography. The procedure enables up to 6 mg of 99.4% pure bPRL to be obtained per hour, with a recovery of 32.4%. The purity of the protein was checked by N-terminal sequencing and sodium dodecyl sulphate–polyacrylamide gel electrophoresis. The highly purified bPRL obtained with this method is suitable for complete structural and immunochemical studies.

INTRODUCTION

Prolactin (PRL) is a polypeptide hormone of molecular weight 23 000 which is secreted by the acydophil cells of the anterior pituitary. The single chain of 199 residues has three disulphide-bonded loops, two of which are located near the two termini of the molecule. It is secreted in the form of a prohormone with a sequence of 229 amino acids. An enzymatic cleavage occurs at position 30 giving the native form of PRL [1]. Belonging to the same hormonal family as growth hormone, it shares a number of biological, immunological and structural features with this molecule [2], as well as with mammalian placental lactogen and proliferin [3].

Pituitary PRL preparations always contain a certain degree of heterogeneity because of the presence of various post-translational modified forms of the molecule [4–6]. Using traditional chromatographic systems, it is difficult and time consuming to remove the heterogeneous forms from the native PRL preparation.

This paper describes the application of a high-performance liquid chromatography (HPLC) system with an anion-exchange column for the purification to homogeneity of pituitary bovine PRL (bPRL).

0021-9673/91/$03.50

EXPERIMENTAL

Purification of bPRL

The starting material was prepared by following the first steps of the procedure described by Reichert [7]. The ethanolic precipitate obtained (bPRL 1) was chromatographed (100 mg per 10 ml per run) on a Sephacryl S-200 (Pharmacia LKB, Uppsala, Sweden) column (70 × 2.6 cm) in a 25 m*M* phosphate buffer solution, pH 7.5. Eluate fractions (10 ml) were collected and aliquots were assayed by sodium dodecyl sulphate–polyacrylamide gel electrophoresis (SDS-PAGE). The bPRL peak (bPRL S-200) was concentrated and further purified by anion-exchange HPLC.

The HPLC apparatus used was a Waters 625 LC system equipped with a Waters tunable absorbance detector (Waters Millipore, Milan, Italy). A TSK-DEAE 5PW column (10 μm; 75 × 7.5 mm) (Toyo Soda, Japan) was used, which was operated at a flow-rate of 1 ml/min in phosphate buffer solution (25 m*M*, pH 7.5). The eluate was recorded at 280 nm. The sample (2–10 mg per injection) was eluted with a 16 min linear gradient to 0.9 *M* NaCl in the phosphate buffer. The fraction containing bPRL was identified by SDS-PAGE, assayed for protein content [8] and stored in a lyophilized form at −20°C (bPRL-DEAE).

Sodium dodecyl sulphate–polyacrylamide gel electrophoresis

The SDS-PAGE was performed in polyacrylamide gradient gels (7–20%) overlain with 5% stacking gel [9], using a Minigel apparatus (Biometra, Göttingen, Germany). The electrophoresis was performed at a constant current of 10 mA for 15 min and successively at constant voltage (200 V) for about 1 h. The gels were stained with Coomassie Brilliant Blue R250 and with silver nitrate [9]. The stained bands were quantified by scanning the electrophoretic patterns at 595 nm using a Quick Scan R & D densitometer (Helena Labs, Beaumont, TX, USA).

Amino acid sequence

A sample of 2.7 nmol of bPRL-DEAE was submitted to 10 cycles of sequence analysis using an automatic amino acid sequencer (Applied Biosystems, Milan, Italy).

RESULTS AND DISCUSSION

The yields and purification rate at each stage of the purification procedure are given in Table I. The total protein concentration was determined using the method of Lowry *et al.* [8]. The amount of bPRL in the fractions was determined by SDS-PAGE, comparing the integrated intensity of the hormone band with the integrated intensity of known amounts of the purified hormone migrated on the same gel [10]. The total yield of homogeneous native bPRL was about 20 mg per 100 g wet weight of pituitaries. The recovery was 32.4% and the purification was 99.4%.

Fig. 1 shows the elution profile obtained after the application of 2 mg of bPRL S-200 to the anion-exchange column. Homogeneous bPRL eluted in the first peak (6.36 min after the injection) at a sodium chloride concentration of 0.21 *M*. Using HPLC it was possible to purify large amounts of bPRL in a short time. To isolate less than 20 mg/h, an analytical column (75 × 7.5 mm) was chosen, but it is possible to scale-up the method for preparative separations.

TABLE I

SEQUENCE OF PURIFICATION OF bPRL

Stage	Total protein (mg)	bPRL (mg)	Yield (%)	Purification (%)
bPRL 1	185.25	59.09	100	31.9
bPRL S-200	62.06	42.09	71.2	67.8
bPRL-DEAE	19.25	19.13	32.4	99.4

The purification rate during the bPRL preparation was monitored by SDS-PAGE and the Coomassie-stained bands were quantified by densitometry. The electrophoretic patterns of bPRL after each stage of the purification are shown in Fig. 2. The bPRL-DEAE formed (samples 3 and 4) was homogeneous with a purity of more than 95%, also when the gel was stained with silver nitrate.

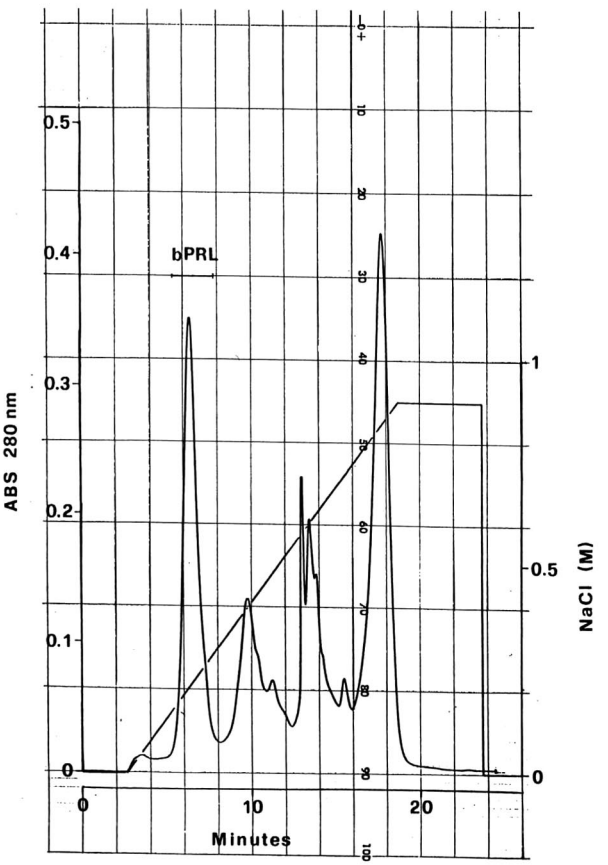

Fig. 1. High-performance liquid chromatogram obtained after the application of 2 mg of bPRL S-200 to the anion-exchange column. The sodium chloride concentration gradient used for the elution is shown on the graph.

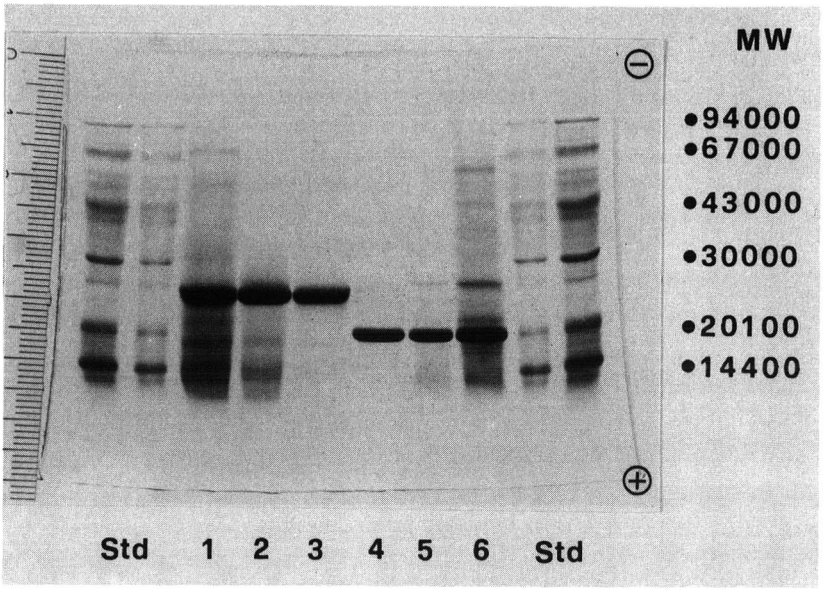

Fig. 2. Gradient SDS-PAGE of bPRL during the purification procedure. Std = standard proteins for molecular weight (MW); 1, 6 = bPRL 1; 2, 5 = bPRL S-200; 3, 4 = bPRL-DEAE. Samples 1–3 were dissolved in the presence of the reducing agent 2-mercaptoethanol (5%). Samples 4–6 were in the oxidized form.

Samples were analysed under reducing (samples 1–3) and non-reducing (samples 4–6) conditions. As the figure shows, bPRL has a mobility which is related to the reduced or oxidized state of its disulphide bridges. This phenomenon has already been observed for rat [5] and human PRL [11]. It has been suggested [11] that these proteins in their S–S bonded form have a more compact structure which results in lower apparent molecular weight.

The first ten amino acid residues of purified bPRL obtained from sequence analysis were: H_2N–Thr–Pro–Val–Cys–Pro–Asn–Gly–Pro–Gly–Asn. This sequence was obtained free of contamination by other amino acids and corresponds exactly to the bPRL sequence [1].

Using the procedure described here, bPRL can be purified from a crude extract to homogeneity with only two chromatographic steps, one of which exploits the resolving power of HPLC. The bPRL purification procedures described previously involve the use of preparative electrophoresis, which is useful in minimizing microheterogeneity in the protein preparation [10]. This kind of methodology offers the advantage of a high resolution separation, but it is not very reproducible and requires a very long time to obtain the separation and elution of the protein bands [9]. In comparison, the method reported in this paper gives a fast and reproducible recovery of highly homogeneous bPRL, which is readily available for structural and immunochemical characterization.

REFERENCES

1 W. L. Miller, D. Coit, J. D. Baxter and J. A. Martial, *DNA*, 1 (1981) 37.
2 C. S. Nicoll, G. L. Mayer and S. M. Russel, *Endocrine Rev.*, 7 (1986) 169.
3 N. Paris, F. Rentier-Delrue, A. Defontaine, V. Goffin, J. J. Lebrun, L. Mercier and J. A. Martial, *Biotech. Appl. Biochem.*, 12 (1990) 436.
4 U. J. Lewis, R. N. P. Singh, L. J. Lewis, B. K. Seavey and Y. N. Sinha, *Proc. Natl. Acad. Sci. U.S.A.*, 81 (1984) 385.
5 F. Bollengier, B. Velkeniers, E. Hooghe-Peters, A. Mahler and L. Vanhaelst, *J. Endocrinol.*, 120 (1989) 201.
6 U. J. Lewis, R. N. P. Singh and L. J. Lewis, *Endocrinology*, 124 (1989) 1558.
7 L. E. Reichert, Jr., *Methods Enzymol.*, 37 (1975) 360.
8 O. H. Lowry, N. J. Rosebrough, A. L. Farr and R. J. Randall, *J. Biol. Chem.*, 193 (1951) 265.
9 C. Secchi, P. A. Biondi, A. Berrini and S. Ronchi, *Experientia*, 39 (1983) 1052.
10 J. A. Bell, K. Moffat, B. K. Vonderhaar and D. W. Golde, *J. Biol. Chem.*, 260 (1985) 8520.
11 S. Meuris, M. Svoboda, J. Christophe and C. Robyn, *Anal. Biochem.*, 143 (1984) 163.

Journal of Chromatography, 547 (1991) 462–467
Elsevier Science Publishers B.V., Amsterdam

CHROM. 23 292

Short Communication

Enrichment of biologically active U1 small nuclear RNAs by ion-exchange high-performance liquid chromatography

VICKY LEFF, JIAN-PING GAO, LETICIA R. VEGA and RENE J. HERRERA*
Department of Biological Sciences, Florida International University, Miami, FL 33199 (USA)
(First received July 30th, 1990; revised manuscript received February 26th, 1991)

ABSTRACT

The use of ion-exchange high-performance liquid chromatography in conjunction with preparative electrophoresis to facilitate the purification of biologically active snRNAs is described. Separation of total nuclear RNA from a *Bombyx mori* cell line was done with a Bio-Rad MA7 plasmid column in a HRLC 500 system. Individual fractions were subjected to electrophoresis through 14% polyacrylamide gels for identification. High levels of U1 RNA were confirmed by Northern analysis with a human U1 probe. Biological activity of RNAs from the column was demonstrated by their ability to incorporate ^{32}P-AMP at the 3′ end. Ion-exchange chromatography provides a rapid, automated method for purifying large amounts of RNAs that can then be utilized in further studies.

INTRODUCTION

This paper describes a method for separating small nuclear RNAs (snRNAs) by ion-exchange high-performance liquid chromatography (HPLC) in conjunction with preparative electrophoresis and aims at providing a rapid automated method for purifying specific snRNA species. The snRNAs are relatively short (*ca.* 80–300 nucleotides), non-ribosomal, non-transfer RNAs. These uracil-rich molecules (thus the name U series snRNAs) exist associated with at least seven proteins as small nuclear ribonucleoprotein particles (snRNPs). Each snRNP is composed of one molecule or U1, U2, or U5 snRNA [1]. U4 and U6 exist together in the same snRNA [2]. Peptides B, B′, D, D′, E, F and G are common to all U snRNPs. Some U snRNPs contain specific proteins, for example, the proteins 70K, A and C are found only associated with U1s. The snRNP complexes have been shown to participate in crucial cellular processes which include splicing of pre-mRNA precursors by U1, U2, U4, U5 and U6 [3–6]; 3′ editing of most histone mRNA precursors by U7 [7]; cleavage/polyadenylation of mRNA by U11 [8]; and ribosome biogenesis by U3, U8 and U13 [9].

Of particular interest are the recent preparative electrophoretic isolations of U1

0021-9673/91/$03.50

snRNA which revealed the existence of U1 isoforms; this was established in *Xenopus laevis* by Forbes *et al.* [10], in mouse by Kato and Harada [11], in chicken by Roop *et al.* [12] and in the silkmoth *Bombyx mori* by Adams and coworkers [13,14]. In addition, experimental evidence shows that U1 isoforms are tissue-specific and developmentally expressed [10, 13–16]. This may be indicative of their possible involvement in the regulation of gene expression at the RNA splicing level. Since most biochemical studies that could be performed to study structure–function relationships of these U1 variants require nano-and microgram quantities of individual isoforms, it is impractical to purify these RNAs by just preparative acrylamide electrophoresis. It is therefore advantageous to use HPLC for the enrichment of U1 isoforms in order to provide an efficient method to start purifying them and further study their involvement in pre-mRNA splicing *in vivo* and *in vitro*.

EXPERIMENTAL

Instrumentation

A Bio-Rad HRLC 500 series system consisting of two series 1350 soft start pumps, a Model 7125 injector, an HRLC system interface, and a 100-μl fixed-volume titanium steel loop was used. The column was a Bio-Rad MA7, 50 × 7.8 mm plasmid column, and detection was accomplished using a Bio-Rad monitor set at 260 nm. The Acer 900 personal computer system and Bio-Rad HRLC software were interfaced for data collection and analysis [17].

Mobile phase

Eluent A consisted of 5 *M* urea and 20 m*M* $NaPO_4$, pH 6.7 (283.5 ml of 40 m*M* NaH_2PO_3, 216.5 ml of 40 m*M* Na_2HPO_3/l). Eluent B consisted of eluent A with 1.5 *M* KCl, pH 6.7. The eluents were autoclaved, filtered through a 0.22-μm membrane and degassed by vacuum.

Sample preparation

Bm-N, a *Bombyx mori* ovarian-derived permanent cell line, was grown and subcultured in TC-100 medium as previously described [18]. Total nuclear RNA was extracted [19]. Nuclear RNA samples were dissolved in 99 μl distilled water and 1 μl 1 *M* Tris–HCl, pH 8.0. Each sample was injected into the loop at 23°C using a 1-ml syringe. After collecting the fractions, the samples were precipitated twice in three volumes of 100.0% ethanol at room temperature followed by centrifugation at 12 000 × *g* for 15 min to remove the KCl and urea. Prior to acrylamide gel analysis the samples were dissolved in 1 × TBE loading buffer (0.089 *M* Tris, 0.089 *M* boric acid, 0.05 *M* EDTA and trace amounts of the bromophenol blue and xylene cyanol electrophoretic marker dyes in 50% formamide, 20% glycerol, pH 8.3), heated at 65°C for 4 min, immediately chilled in ice water and loaded onto acrylamide gels for analysis.

Gel electrophoresis

The presence of snRNAs was established for each fraction by running each one through 14% polyacrylamide gels (8 *M* urea; 1 × TBE, 0.089 *M* Tris, 0.089 *M* boric acid, 0.05 *M* EDTA and trace amounts of bromophenol blue and xylene cyanol, pH 8.3). Electrophoresis was typically 2.5 h at 100 V constant power, until the xylene

cyanol marker migrated to the bottom of the gels. Gels were stained with ethidium bromide (10 μg/μl in water) for 5 min, destained twice in distilled water for 15 min and viewed under UV light. The gels were subsequently photographed.

Electrotransfer of nuclear RNA

The filters were cut to size, soaked in 1 × TBE and placed on the gels. Gels and filters were then placed between two pieces of Whatman No. 1 paper and set up on a Hoefer Model TE52 electroblotting apparatus with the filter side facing the positive electrode. The apparatus was placed in ice water and allowed to run for 2 h. The buffer was kept in circulation using a magnetic stir bar. The filter was then removed and baked at 80°C for 2 h under vacuum to fix the nucleic acid onto 0.1-μm Nytran membrane (Schleicher & Schuell).

Nucleic acid hybridization

The probe, a human U1 clone in the pSP6-64 [20] plasmid was radioactively labeled by random priming [21] using ^{32}P α-deoxy ATP. The filters were prehybridized in hybridization buffer [50% formamide, 10% Denhart's solution, 20% sodium dodecyl sulfate (SDS), 20× SSC (3 *M* NaCl, 0.3 *M* sodium citrate · $2H_2O$, pH adjusted to 7.0 with 1 *M* HCl) and 13 μg/μl *E. coli* DNA] at 42°C overnight. The human U1 radioactive probe was denatured by boiling for 10 min, immediately placed in ice water and added to the hybridization buffer. This solution was then used for hybridization under the same conditions for 24 h. The filter was washed in a 1 × SSC, 0.1% SDS solution and exposed to Kodak XAR-5 film overnight at −135°C with two intensifying screens.

Addition of poly(A) chains to the 3'-ends of snRNAs

The addition of poly(A) tracts was done as described by Devos *et al.* [22] utilizing 1.7 μg of peak 3 (Fig. 1) RNA per reaction and ^{32}P α-ATP. Autoradiography was done for two days at room temperature with Kodak XAR-5 film.

RESULTS AND DISCUSSION

The gradient profile of eluent B used for the separation and analysis of Bm-N

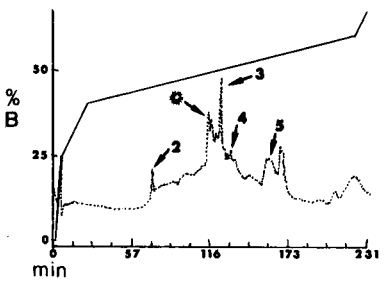

Fig. 1. Representative ion-exchange chromatography of total nuclear RNA from the Bm-N cell line. (Quantity of total nuclear RNA injected was 105 μg.) The abscissa represents the time in minutes. The *y*-axis is percent eluent B. Numbered arrows point to peaks collected. Their RNAs were loaded into wells 2, 3, 4 and 5 of Fig. 2, respectively. Peak No. 3 was eluted at 120 min at 50.4% eluent B. Peak marked with an asterisk contained mainly mature and precursor tRNA.

snRNAs was: 0–3 min, 100.0% A/0% B; 3–8 min, 100.0–75.0% A/0–25.0% B; 8–26 min, 75.0–59.8% A/25.0–40.2% B; 26–223 min, 59.8–40.0% A/40.2–60.0% B and 223–232 min, 40.0–32.8% A/60.0–67.2% B. A linear gradient that starts at a low salt concentration and ends at a high salt concentration was used. Although other gradient profiles were employed, the parameters represented above proved to be the method of choice for optimizing the sharpness and separation of the peaks.

Eluent peaks from nuclear extracts were identified by collecting each corresponding fraction and separating them by polyacrylamide gel electrophoresis. Peak 3 in Fig. 1, eluted from the column at a concentration of 50.4% eluent B (0.76 *M* KCl), was identified as a fraction enriched in U1 snRNA (Fig. 2, lane 3). Fig. 2 also shows the composition of some of the other eluent peaks after gel electrophoresis, and shows that peak 4 (lane 4) was enriched in U2 and U3 snRNAs. Peak 5 in Fig. 1 (lane 5) was mainly composed of high-molecular-weight RNA. The additional peaks to the right of peak 5 that were eluted at higher salt concentrations contained high-molecular-weight RNA that failed to penetrate the 14% polyacrylamide gel and remained at the origin (data not shown). Peak number 2 in Fig. 1 was composed of small-molecular-weight RNAs that migrated out of the gel into the reservoir buffer while the peak marked with an asterisk contained mainly mature and precursor tRNA (data not shown).

The high level of U1 snRNA in fraction 3 was confirmed by electrotransfer of the RNA in the gels onto 0.1 μm Nytran filters and hybridization with the human U1 clone. This is illustrated by Fig. 3, lane 3, which shows an autoradiogram displaying a strong signal in the area of U1 snRNA.

Former work in this area by Adams *et al.* [13], has shown the area of U1 snRNA to be between 5.8S and 5S RNAs, very close to 5.8S RNA. This area can be easily identified by using RNA markers during gel electrophoresis as shown in Fig. 2,

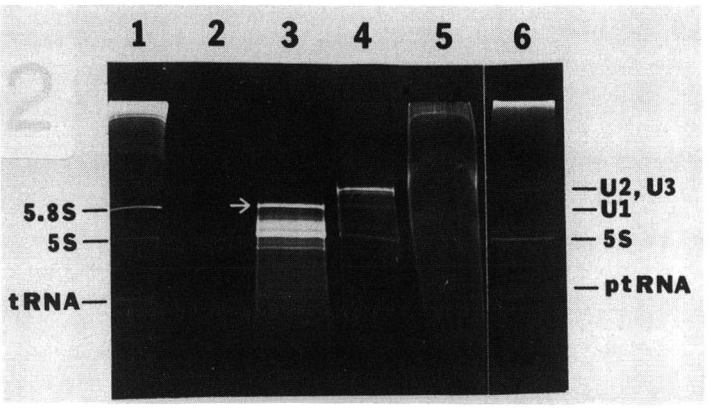

Fig. 2. Electrophoretic separation of fractions collected during the HPLC fractionation represented in Fig. 1. Well 1, total cytoplasmic RNA as a marker; mature tRNA is shown in this fraction. Well 6, total nuclear RNA (total nuclear RNA was run on a separate gel, but under the same conditions as the gel used for this experiment). Precursor tRNA (ptRNA) can be seen in this fraction. RNA in well 3 is enriched for U1, U4, 5S, U5 and U6 while well 4 contains mainly U2 and U3 snRNAs. White arrow points to U1 snRNA. RNAs were visualized by ethidium bromide staining.

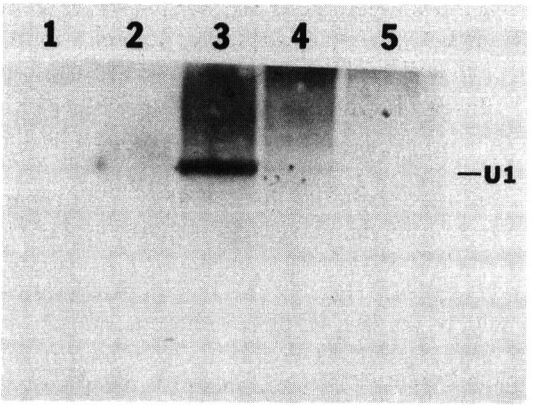

Fig. 3. Autoradiogram of gel in Fig. 2 after electroblotting and probing with a cloned human U1 gene. Notice the strong signal from the U1 area identified in Fig. 2, lane 3. The slow-moving smear in wells 3 and 4 represents high-molecular-weight DNA.

lanes 1 and 6. U1 snRNA was found to be about 0.5 mm below 5.8S RNA after electrophoresis as described in the Experimental section.

In order to determine the usefulness of this HPLC enrichment technique in some molecular biology studies, the biological activity of fraction 3 was tested by determining the snRNAs' capacity to incorporate, consecutively, 5′-adenosine ribonucleotide monophosphate (AMP) at its 3′-hydroxyl end by poly(A) polymerase (RNA adenyltransferase). Since snRNAs lack a poly(A) tail, it is essential to polyadenylate them before cDNA production and cloning. Fig. 4 shows the polyadenylation of this fraction. The snRNAs present in greater mass (*e.g.*, 5S) exhibit greater AMP

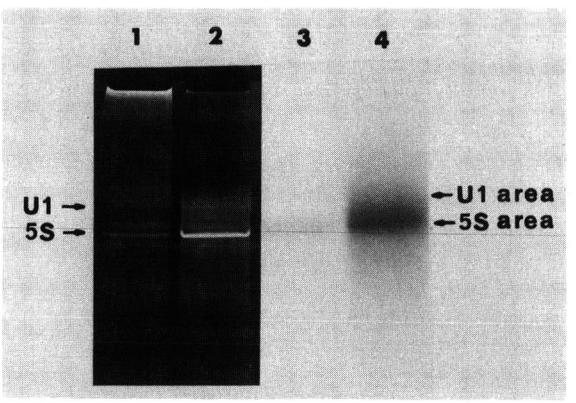

Fig. 4. Electrophoretic separation and autoradiography of fraction 3 (Fig. 2, lane 3) at different times during poly(A) tract addition. snRNAs in wells 1 and 2 were visualized by ethidium bromide staining while wells 3 and 4 represent an autoradiograph of the ^{32}P-labelled RNA. Well 1, total nuclear RNA as a marker; wells 2–4, fraction 3 at reaction incubation times of 0, 5 and 20 min, respectively. Wells 1 and 2 were run on a separate gel, but under the same conditions as the autoradiographed gel used in this experiment.

incorporation. Notice that there was an overall increase in radioactive signal as incubation time augmented from 5 to 20 min. As expected, due to the different sizes of poly(A) tracts incorporated into individual snRNAs [poly(A) polymerase ceases polyadenylation irregularly subsequent to initiation], the bands and radioacitivy became more diffuse with reaction time.

This study demonstrates some potential for ion-exchange HPLC in conjunction with electrophoresis to facilitate the purification of specific species of biologically active snRNAs. These purified biologically active snRNAs, in turn, can be utilized in experiments probing their structure and function.

ACKNOWLEDGEMENT

This research was supported by US Public Health Service Grant RR08205.

REFERENCES

1 R. Luhrmann, in M. Birnstiel (Editor), *Structure and Function of Major and Minor Small Nuclear Ribonucleoprotein Particles*, Springer, Berlin, 1988, p. 71.
2 S. W. Ruby and J. Abelson, *Science (Washington, D.C.)*, 242 (1988) 1028.
3 D. S. McPheeters, P. Fabrizio and J. Abelson, *Genes Dev.*, 3 (1989) 2124.
4 G. M. Winkelman and R. Luhrmann, *EMBO J.*, 8 (1989) 3105.
5 A. Binderelf, W. Thorsten and M. R. Green, *EMBO J.*, 9 (1990) 251.
6 V. Heinrichs, M. Bach, G. Winkelman and R. Luhrmann, *Science (Washington, D.C.)*, 247 (1990) 69.
7 A. L. Kirsch, M. Groudine and P. B. Challoner, *Genes Dev.*, 3 (1989) 2172.
8 G. Christofori and W. Keller, *Cell*, 26 (1988) 363.
9 K. Tye and J. A. Steitz, *EMBO J.*, 8 (1989) 3113.
10 D. J. Forbes, M. W. Kirshner, D. Caput, J. E. Dahlberg and E. Lund, *Cell*, 38 (1984) 681.
11 N. Kato and F. Harada, *J. Biol. Chem.*, 260 (1985) 7775.
12 D. R. Roop, P. Kristo, W. E. Stumph, M. J. Tsai and B. M. O'Malley, *Cell*, 23 (1981) 671.
13 D. S. Adams, R. J. Herrera, R. Luhrmann and P. M. Lizardi, *Biochemistry*, 24 (1985) 117.
14 D. S. Adams and R. J. Herrera, *Comp. Biochem. Physiol.*, 88B (1987) 415.
15 E. Lund, C. J. Bostock and J. E. Dahlberg, *Genes Dev.*, 1 (1987) 47.
16 E. Lund and J. E. Dahlberg, *Genes Dev.*, 1 (1987) 39.
17 *HRLC Software User's Manual*, Bio-Rad Labs., Richmond, CA, 1989.
18 R. J. Herrera and A. B. Mukherjee, *Comp. Biochem. Physiol.*, 72B (1982) 359.
19 T. Maniatis, E. F. Fritsch and J. Sambrook, *Molecular Cloning*, Cold Spring Harbor Laboratory Press, 1990, p. 7.3–7.20.
20 E. Lund and J. E. Dahlberg, *J. Biol. Chem.*, 259 (1984) 2013.
21 A. P. Feinberg and B. Vogelstein, *Anal. Biochem.*, 137 (1984) 266.
22 R. Devos, E. Gillis and W. Fiers, *Eur. J. Biochem.*, 62 (1976) 401.

Journal of Chromatography, 547 (1991) 468–471
Elsevier Science Publishers B.V., Amsterdam

CHROM. 23 254

Short Communication

Analysis of some tropane alkaloids in plants by mixed-column high-performance liquid chromatography[a]

S. MANDAL, A. A. NAQVI* and R. S. THAKUR
Central Institute of Medicinal and Aromatic Plants, Lucknow-226016 (India)
(First received September 3rd, 1990; revised manuscript received February 25th, 1991)

ABSTRACT

A simple and rapid high-performance liquid chromatographic method for the determination of atropine and scopolamine in plants using the combination of two different polarity columns in series and direct injection of plant extract is described. Application of the method to the analysis of two species of solanaceous plants is reported.

INTRODUCTION

The analysis of tropane alkaloids in solanaceous plants is of interest because of the extensive use of atropine and scopolamine in pharmaceutical preparations. Using an ion-pair technique, the analysis of tropane alkaloids by high-performance liquid chromatography (HPLC) has been reported [1–7]. Anetai and Yamagishi [8] applied an HPLC method which was not an ion-pair technique to analyse crude drugs from plants, but the method is only suitable for atropine because the scopolamine peak overlaps the impurities peak. A combination of columns using sodium acetate buffer has been applied for the analysis of atropine and its degradation products [9].

The aim of the present study was to explore the chromatographic possibilities of using a combination of two different polarity columns and a non-ion-pair technique in an attempt to overcome difficulties associated with co-elution of scopolamine and impurities in the analysis of plant extracts. The use of buffer was avoided, as constant use of salts when there is a large number of samples to be analysed creates the problem of corrosion and excessive wear of the pump piston and seal, which can cause leaks [10]. A simple method for determination of atropine and scopolamine in solanaceous plants using a combination of HPLC columns employing acetonitrile–water, containing 0.5% triethylamine as the mobile phase, was determined.

[a] CIMAP publication No. 1011.

0021-9673/91/$03.50

EXPERIMENTAL

Reagents

The reagents used were HPLC-grade acetonitrile and triethylamine. Water was deionized and double-distilled in glass. All the solvents and solutions were filtered through a Millipore filter. Atropine and scopolamine hydrobromide were obtained from Sigma (St. Louis, MO, USA).

Apparatus

A Waters modular HPLC system, consisting of a U6K injector, M-6000A pump, M-450 variable-wavelength detector and M-730 data system, was used. Analyses were performed on RP-C_{18} and RP-CN columns (150 × 3.9 mm; particle size 5 μm) obtained from Waters (Division of Millipore, Milford, MA, USA). The combination was made by connecting the outlet of RP-CN to the inlet of RP-C_{18}.

HPLC conditions

The composition of the mobile phase was optimized by varying the percentage of acetonitrile to give the operating conditions as follows: acetonitrile–water (35:65) containing 0.5% triethylamine, flow-rate 0.8 ml/min, column temperature 30°C, detector wavelength 254 nm and detector sensitivity 0.04 a.u.f.s.

Calibration graphs

Known amounts of atropine and scopolamine free bases were dissolved in methanol to give corresponding standard solutions of concentration 2 mg/ml. Different volumes of these standards were processed using the HPLC conditions described above. The area counts of peaks and the corresponding concentrations were used to construct the calibration graphs. The graphs followed Beer's law in the range 1–50 μg. The regression equations for atropine and scopolamine are $y = 0.3190\,x + 0.0099$ ($r = 0.998$) and $y = 0.4480\,x + 0.1599$ ($r = 0.999$), respectively.

Extraction procedure

Extraction of crude alkaloids from different parts (inflorescence, leaf and stem) of *Hyoscyamus muticus* and *Hyoscyamus niger* was carried out using the following method [11]. Dried powder (10 g) of plant material was extracted with 200 ml of solvent (dichloromethane–methanol–ammonium hydroxide, 70:25:5, v/v/v) for 2 h and filtered. The filtrate was extracted with 100 ml of 0.5 *M* sulphuric acid. The aqueous layer was separated and basified with ammonium hydroxide. The basified solution was extracted with dichloromethane (4 × 80 ml) and evaporated to dryness to give crude alkaloids, which were dissolved in 10 ml of methanol. Samples were filtered through a Millipore sample filtration kit. A 2–10 μl sample of this extract was used for injection into the HPLC column.

RESULTS AND DISCUSSION

The number of theoretical plates (N) calculated for atropine and scopolamine on different columns and their combinations is given in Table I. The maximum value of N for scopolamine was achieved only on the combination RP-CN + RP-C_{18}. In

TABLE I

NUMBER OF THEORETICAL PLATES (N) OF DIFFERENT COLUMNS AND COMBINATIONS

Dimension of columns: 150 × 3.9 mm; particle size 5 μm.

Alkaloid	N			
	C_{18}	CN	C_{18} + CN	CN + C_{18}
Atropine	1524	1542	4045	2896
Scopolamine	506	360	747	1304

fact it is the scopolamine peak that needs higher resolution to overcome the problem of co-elution with impurities in plant extract, and atropine has no such difficulties. This combination provided reproducible and accurate results with good resolution of atropine and scopolamine in plant extract without interference from impurities. The order of the columns is very significant because reversal of the sequence results in very poor resolution and overlapping of the scopolamine peak with impurities. The graph in Fig. 1 shows the capacity factor (k') *versus* percentage of acetonitrile in the mobile phase. The resulting chromatogram of atropine and scopolamine using the HPLC conditions given above is shown in Fig. 2. Quantitative results of individual alkaloids in various parts of *Hyoscyamus muticus* and *Hyoscyamus niger* are reported in Table II. The standard deviation and coefficient of variation for atropine are 0.57 and 2.94,

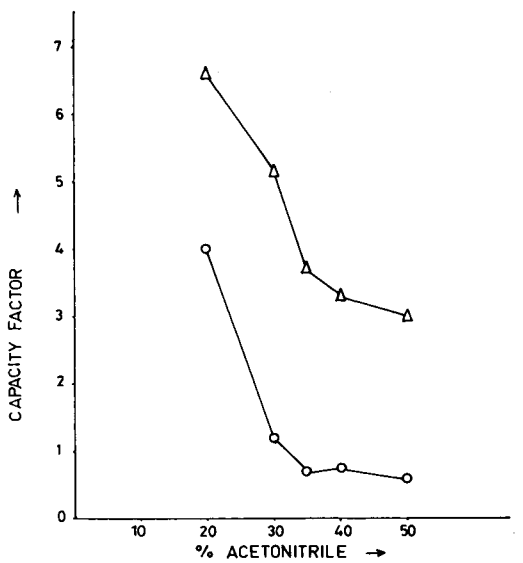

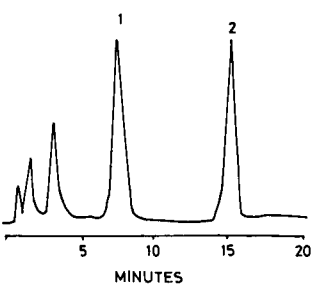

Fig. 1. Effect of acetonitrile concentration in the mobile phase on capacity factor. Column combination: RP-CN and RP-C_{18}. ○ = Scopolamine; △ = atropine.

Fig. 2. Resolution of atropine and scopolamine. Column combination: RP-CN and RP-C_{18}. Mobile phase: acetonitrile–water (35:65) + 0.5% triethylamine; amount of alkaloid 10 μg each. Peaks: 1 = scopolamine; 2 = atropine.

TABLE II

CONTENT OF ATROPINE AND SCOPOLAMINE IN DIFFERENT PARTS OF PLANTS

Sample	Atropine			Scopolamine		
	Content (%)	S.D. (%)	C.V. (%)	Content (%)	S.D. (%)	C.V. (%)
Hyoscyamus muticus						
Inflorescence	0.720	2.5	3.4	0.043	0.20	4.6
Leaf	0.615	1.6	2.6	0.002	0.02	8.0
Stem	0.341	1.0	2.9	–	–	–
Hyoscyamus niger						
Inflorescence	0.025	0.10	4.0	0.040	0.20	5.0
Leaf	0.010	0.06	6.0	0.035	0.12	3.5
Stem	0.020	0.11	5.5	0.032	0.15	4.7

respectively, and for scopolamine are 0.39 and 1.97, respectively.

Because of its simplicity, selectivity and accuracy, the HPLC assay described here is suitable for the analyse of tropane alkaloids in plants extracts.

REFERENCES

1 M. J. Walters, *J. Assoc. Off. Anal. Chem.*, 61 (1978) 1428.
2 L. J. Pennington and W. F. Schmidt, *J. Pharm. Sci.*, 71 (1982) 951.
3 T. Oshima, Sagara, Yu-Yi Tong, Guande Zhang and Yu-Heng Chen, *Chem. Pharm. Bull.*, 37 (1989) 2456.
4 H. Morimasa, *Shimadzu Hyoron*, 45 (1988) 171.
5 R. Verpoorte, J. M. Verzijl and A. Baerheim Svendsen, *J. Chromatogr.*, 283 (1984) 401.
6 T. Fujita, *Shimadzu Hyoron*, 43 (1986) 89.
7 H. Li-Yi, Z. Guande, T. Yu-Yi, K. Sagara, T. Oshima and T. Yoshida, *J. Chromatogr.*, 481 (1989) 428.
8 M. Anetai and T. Yamagishi, *Hokkaidouritu Eiscikenkyushoho*, 35 (1985) 371.
9 U. Lund and S. H. Hansen, *J. Chromatogr.*, 161 (1978) 371.
10 E. L. Johnson and R. Stevenson, *Basic Liquid Chromatography*, Varian Assoc., Palo Alto, CA, 1978.
11 Tai-Hui Chiu and T. Okamoto, *J. Taiwan Pharm. Assoc.*, 39 (1987) 247.

Journal of Chromatography, 547 (1991) 472–477
Elsevier Science Publishers B.V., Amsterdam

CHROM. 23 263

Short Communication

High-performance liquid chromatography of two derivatives of vitamin B_6, the carbamoyl derivatives of pyridoxal 5′-phosphate and pyridoxamine 5′-phosphate

L. TERZUOLI, R. PAGANI, R. LEONCINI, D. VANNONI and E. MARINELLO*
Istituto Chimica Biologica, Università di Siena, Piano dei Mantellini 44, I-53100 Siena (Italy)
(First received August 1st, 1990; revised manuscript received March 5th, 1991)

ABSTRACT

We present the results of a study of the high-performance liquid chromatography of two vitamin B_6 derivatives: the carbamoyl derivatives of pyridoxal 5′-phosphate and pyridoxamine 5′-phosphate. These compounds, obtained by condensation of either pyridoxal 5′-phosphate or pyridoxamine 5′-phosphate with either carbamoyl phosphate or potassium cyanate, were separated on an octadecyl silica column with a mobile phase consisting of 0.01 *M* potassium phosphate (pH 5.0)–methanol (98:2); detection was at 254 nm. The method was sensitive, fast and precise.

INTRODUCTION

In previous studies [1–4] we have observed that L-threonine deaminase (EC 4.2.1.16), a pyridoxal 5′-phosphate (PLP)-dependent enzyme, is inhibited by both carbamoyl phosphate (CP) and potassium cyanate, a decomposition product of carbamoyl phosphate [5]. We have demonstrated [6] (1) that CP and potassium cyanate inhibit the enzyme essentially by an interaction with the coenzyme, and (2) that this chemical reaction occurs more easily with free PLP. In fact, when CP was added to incubation mixtures containing the holoenzyme, the inhibition was appreciable only at the final 50 m*M* (K_1 = 42 m*M*) concentration of the inhibitor. On the other hand, when the dialyzed enzyme was incubated with increasing amounts of PLP, the inhibition was highest at a final inhibitor concentration of only 0.1 m*M* (K_1 = 30 μM). When free PLP was added to incubation mixtures containing the holoenzyme, activity was enhanced, but the activation was no longer evident when the PLP was preincubated with CP. Moreover, when free PLP was preincubated either with CP or

0021-9673/91/$03.50

potassium cyanate, it failed to restore the activity of the dialyzed enzyme. This indicates that inhibition affected the association reaction

apoenzyme + PLP → holoenzyme

The occurrence of a chemical reaction between free PLP and either CP or potassium cyanate was confirmed when free PLP was incubated with either CP or potassium cyanate under physiological conditions (pH 7) and even at pH 5. Characteristic changes in PLP spectra were observed, and a new compound was crystallized which, by means of chemical tests and spectra (UV, IR and NMR), was identified as 3,4-dihydro-2H-pyrido[3,4-*e*]1-1,3-oxazin-2-one, which we have called "carbamoyl pyridoxal 5'-phospate" (C-PLP). Its structure is shown in Fig. 1.

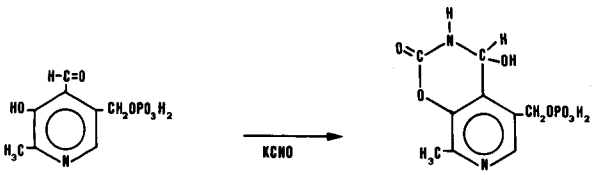

Fig. 1. Formation of 4'-carbamoyl pyridoxal 5'-phosphate.

Under analogous conditions, we obtained another derivative of vitamin B_6: 4'-carbamoyl pyridoxamine 5'-phosphate (C-PMP) (unpublished results). Its structure is shown in Fig. 2.

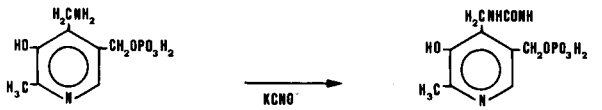

Fig. 2. Formation of 4'-carbamoyl pyridoxamine 5'-phosphate.

We were interested in investigating the biological properties of these new compounds, and for this purpose a satisfactory procedure of separation and determination of C-PLP, C-PMP, pyridoxamine 5'-phosphate (PMP) and PLP, also suitable for tissue extracts, was imperative. This procedure is presented in the Experimental section.

EXPERIMENTAL

Chemicals

PLP, PMP, potassium cyanate, potassium dihydrogenphosphate, and dipotassium hydrogenphosphate were obtained from Merck (Darmstadt, Germany). CP and Norit A were purchased from Sigma (St. Louis, MO, USA). Methanol [high-performance liquid chromatography (HPLC) grade] was obtained from Baker (Phillipsburg, NJ, USA).

Preparation of C-PLP and C-PMP

In preliminary experiments, we found that the reaction either between PLP and CP or between PMP and CP produced two derivatives, C-PLP and C-PMP, respectively, which could be obtained more rapidly by using potassium cyanate; therefore, all subsequent syntheses were carried out with potassium cyanate instead of CP.

A 1-g sample of PLP or 1.12 g of PMP was dissolved in a few milliliters of water and mixed slowly with 0.6 g of potassium cyanate: the condensation product precipitated at pH 4.0. Recovery was 1.05 g of C-PLP (90%) and 0.86 g of C-PMP (80%).

As previously demonstrated [7], desiccated products were very stable; in solution both C-PLP and C-PMP were in equilibrium with their starting compounds: CP or potassium cyanate, PLP or PMP. Their equilibrium differed according to the pH and temperature of the solution.

Preparation and utilization of rat liver supernatant

We used a rat liver supernatant prepared as previously reported [8]. Male albino rats, 9 weeks old, 250 g bodyweight, were decapitated and the livers rapidly removed. A 10% homogenate (in 50 m*M* potassium phosphate, pH 7.5) was prepared and centrifuged at 260 000 *g* for 1 h at 4°C; 10 ml of supernatant were treated with 1.5 ml of 50% Norit A (v/v) for 15 min and centrifuged at 1000 *g* for 15 min.

A 2-μmol sample of the C-PLP or C-PMP was added to 0.5 ml of supernatant, immediately deproteinized with 2 *M* hydrochloridric acid (0.5 *M* final concentration), centrifuged at 8000 *g* and diluted with a 50 m*M* potassium phosphate buffer (pH 7.5) until the C-PLP or C-PMP reached a final concentration of 0.1 m*M*. The blank was obtained by replacement of the supernatant with 0.5 ml of the same buffer, and 20 μl of this solution (2 nmol) were injected into HPLC system.

Apparatus and chromatographic conditions

A Vista 5500 high-performance liquid chromatograph (Varian, Sunnyvale, CA, USA) equipped with a Model 2550 variable-wavelength UV detector (Varian) and Model 4290 electronic integrator (Varian) was used. A ready-for-use, prepacked (250 × 4.6 mm) Supelcosil LC-18, 5-μm column (Supelco, Bellefonte, PA, USA), protected by a precolumn (20 × 4.6 mm) filled with the same packing (Supelguard, Supelco), completed the analytical system. The mobile phase consisted of 0.01 *M* potassium phosphate buffer (adjusted to pH 5.0 with 0.5 *M* potassium hydroxide) and 2% methanol, at a flow-rate of 1 ml/min. Detection was performed at 254 nm.

RESULTS AND DISCUSSION

After HPLC separation, the compounds were detected at 254 nm, to minimize the non-specific interferences either of the buffer or of the samples at lower wavelengths. Moreover, at this wavelength, CP and potassium cyanate did not show any significant absorption (molar absorptivity of potassium cyanate 0.001 $mmol^{-1}\ cm^{-1}$ and CP 0.059 $mmol^{-1}\ cm^{-1}$). These compounds can be detected at 204 nm (molar absorptivity of potassium cyanate 0.180 $mmol^{-1}\ cm^{-1}$ and CP 0.211 $mmol^{-1}\ cm^{-1}$ at 204 nm), with retention times for potassium cyanate and CP of 2.74 and 2.36 min, respectively.

A preliminary study involving the separation of PMP, C-PMP, PLP and C-PLP

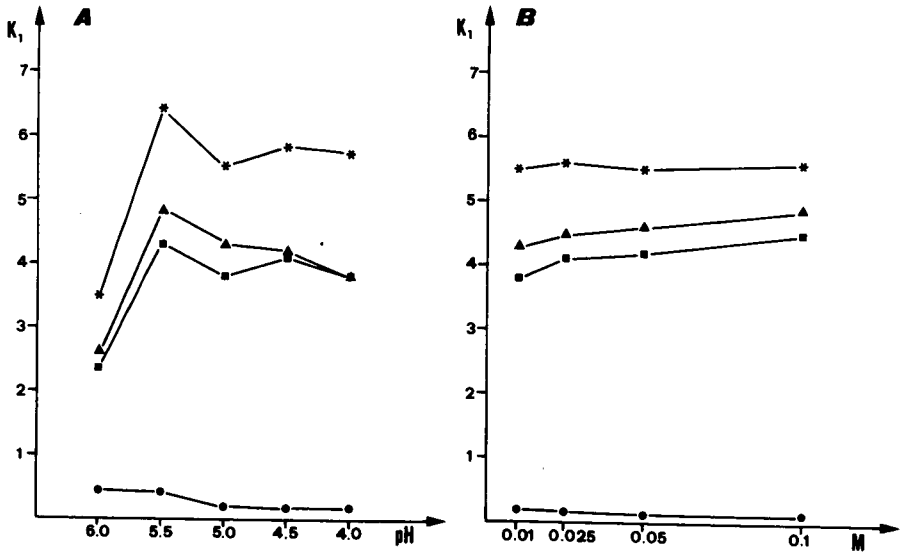

Fig. 3. Effect of (A) pH and (B) ionic strength buffer at pH 5.0 on K_1 value of (●) PMP, (▲) C-PLP, (■) PLP and (∗) C-PMP.

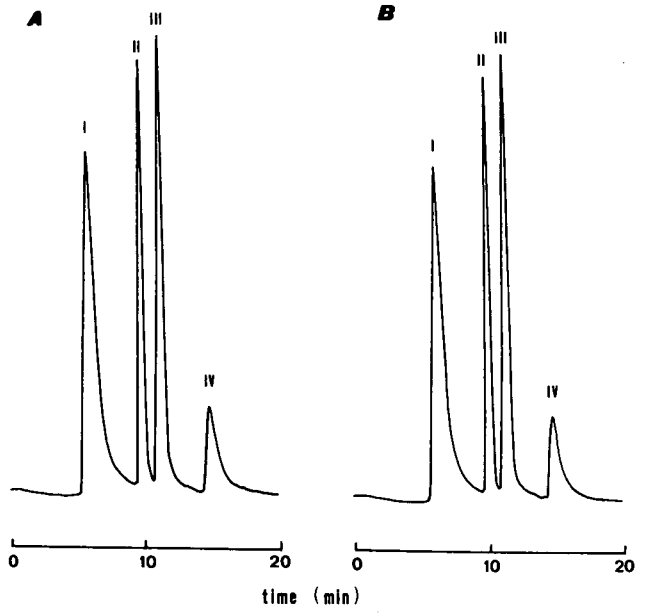

Fig. 4. Separation of (I) PMP, (II) C-PLP, (III) PLP and (IV) C-PMP (A) in the absence and (B) in the presence of rat liver supernatant. Injection volume: 20 μl of 1 mM solution of each standard.

TABLE I

REGRESSION EQUATIONS AND CORRELATION COEFFICIENTS FOR PMP, C-PLP, PLP, PMP

Compound	Regression equation[a]	Correlation coefficient
PMP	$A = 282617\ C - 35922$	0.998
C-PLP	$A = 115818\ C - 5671$	0.996
PLP	$A = 144900\ C + 237$	0.999
C-PMP	$A = 61632\ C - 14854$	0.998

[a] A = peak area; C (nmol) = amount of reagent.

led us to study the effect of (A) different pH and (B) ionic strength buffer at pH 5.0 in the mobile phase (Fig. 3).

Fig. 4 shows a satisfactory separation of the four compounds obtained by isocratic elution at pH 5.0. Linearity was obtained for all amounts of PMP, C-PMP, PLP and C-PLP used in this study (2–20 nmol). The minimum amount of these compounds detectable in our mixtures was 0.5 nmol.

Correlation coefficients and the regression equations of the calibration curve are reported in Table I.

The overall precision of the retention times and peak areas was assessed by determination of run-to-run and day-to-day precision (Table II).

Effect of rat liver extract on C-PLP and C-PMP solutions

We also wanted to ascertain if the determination of these substances was possible in presence of rat liver extracts. We prepared a rat liver supernatant, to which we added C-PLP and C-PMP: the final solutions were chromatographed as reported in the Experimental section.

The elution patterns were not influenced by the addition of the supernatant, as

TABLE II

REPRODUCIBILITY AND ACCURACY OF RETENTION TIMES AND PEAK AREAS OF PMP, C-PLP, PLP, C-PMP

Compound	Retention time (min)	S.D. ($n=5$) (min)	C.V. (%)	Area (arbitrary units)	S.D. ($n=5$)	C.V. (%)
Run-to-run precision (within 1 day)						
PMP	5.74	0.02	0.35	1393947	56769	4.07
C-PLP	9.90	0.06	0.61	552373	6054	1.10
PLP	11.37	0.05	0.44	729938	4181	0.57
C-PMP	15.48	0.02	0.13	275147	9297	3.38
Day-to-day precision (7 days)						
PMP	5.58	0.13	2.33	1370303	52561	3.84
C-PLP	9.99	0.15	1.50	531595	22382	4.21
PLP	11.42	0.14	1.23	723601	18757	2.59
C-PMP	15.25	0.17	1.11	294121	13971	4.75

demonstrated by Fig. 4A and B, which shows that the area of peaks of C-PLP (II, Fig. 4B) and C-PMP (IV, Fig. 4B) were almost identical under differing conditions.

The experiment was repeated with different final concentrations of C-PLP and C-PMP (2, 1.5 and 0.5 m*M*; 20 μl of these solutions were injected into the HPLC system) with good proportionality and recovery.

We conclude that tissue extracts do not interfere with chromatographic runs and permit the determination of these substances also under various biological conditions.

CONCLUSIONS

Our results show that the carbamoyl derivatives of PLP and PMP can easily be separated from each other and from their starting compounds through HPLC. In certain conditions, the tested compounds were stable. The procedure is easily reproducible even when two compounds are added to tissue extracts and it is expected that it will be useful in clarifying the biological role of C-PLP and C-PMP.

REFERENCES

1 R. Pagani, R. Leoncini and E. Marinello, *Biol. Chem. Hoppe-Seyler*, 367 (1986) 339.
2 R. Pagani, R. Leoncini, L. Terzuoli and E. Marinello, *Boll. Soc. It. Biol. Sper.*, LXII (1986) 295.
3 E. Marinello, R. Pagani and R. Leoncini, *It. J. Biochem.*, 35 (1986) 443.
4 R. Pagani, R. Leoncini, L. Terzuoli, R. Guerranti and E. Marinello, *Enzyme*, 43 (1990) 122.
5 C. M. Allen and H. E. Jones, *Biochemistry*, 3 (1964) 1238.
6 R. Pagani, F. Ponticelli, L. Terzuoli, R. Leoncini and E. Marinello, *Biochim. Biophys. Acta*, in press.
7 L. Terzuoli, F. Ponticelli, R. Leoncini and E. Marinello, *Communication I.110, Abstract book, 34th Congresso Soc. It. Bioc.*, CLUEP, Padova, 1988, p. 126.
8 L. Terzuoli, R. Pagani, R. Leoncini, D. Vannoni and E. Marinello, *J. Chromatogr.*, 514 (1990) 80.

Journal of Chromatography, 547 (1991) 478–483
Elsevier Science Publishers B.V., Amsterdam

CHROM. 23 278

Short Communication

Determination of phenoxyacid herbicides in water

RENÉ B. GEERDINK*, ANITA M. B. C. GRAUMANS and JOHN VIVEEN
Institute for Inland Water Management and Waste Water Treatment, P.O. Box 17, 8200 AA Lelystad (Netherlands)

(First received July 24th, 1990; revised manuscript received February 15th, 1991)

ABSTRACT

Novel clean-up techniques for a polymeric precolumn (PLRP-S) for the subsequent determination of bentazone and eight phenoxy acid herbicides in surface water samples are described. After preconcentration of the components at pH 3 on a 10 × 2 mm I.D. precolumn, the technique consists of a clean-up with 1000 μl of 0.1 mol/l sodium hydroxide solution (pH 12.5) and of a heartcut consisting of four precolumn bed volumes of eluent directed to waste followed by ten precolumn bed volumes of eluent directed to the analytical column. Analytical separation is performed with acetonitrile–water (30:70) containing 0.005 mol/l of tetrabutylammonium hydrogensulphate (pH 8.3) (which is also the desorption eluent during heartcutting) on a polymeric analytical column (PLRP-S). With 25 ml of surface water, spiked at 0.25 and 1 μg/l, applied to the precolumn, recoveries for all components were over 85% with a relative standard deviation ($n = 5$) of *ca.* 9% at 0.25 μg/l and *ca.* 2% at 1 μg/l. Detection limits in surface water samples are 0.05–0.1 μg/l. Owing to automation, the total analysis time is *ca.* 30 min.

INTRODUCTION

Trace enrichment of (medium) polar pesticides on porous polymeric sorbents [1–4] such as PRP-1 and PLRP-S, in order to isolate and concentrate them prior to their separation and detection, has become a widely used approach. These hydrophobic porous polymers, compared with other hydrophobic sorbents such as C_{18} types, show better retention of the analytes and also a greater sorption capacity. Their poor selectivity, however, remains a major disadvantage, *i.e.*, part of the sample matrix may also be adsorbed. In natural waters this matrix consists of DOC (dissolved organic carbon), 30–50% of which is generally composed of humic acids, fulvic acids and hydrophobic low-molecular-weight acids [5], and the concentration of which is often in the mg/l range. Breakthrough volumes of surface water samples therefore depend on the sample matrix constituents rather than on the concentration of the analytes.

In a previous paper [1] the preconcentration and separation of five phenoxy acids by a fully automated method with a total analysis time of *ca.* 20 min were

0021-9673/91/$03.50

reported. Detection limits in surface water were 0.1–0.5 μg/l and those in tap water were 0.01–0.05 μg/l. The clean-up procedure in this method, consisting of delivering to waste four precolumn bed volumes of acetonitrile–water (30:70) (pH 3), was not sufficient to eliminate interfering chromatographic peaks with surface water samples.

In this study alternative procedures for scavenging the precolumn and to eliminate the interference of the large matrix peak were investigated. Washing the precolumn with 0.1 mol/l sodium hydroxide solution and heartcutting (transferring to the analytical column the fraction that contains the solutes of interest) turned out to be reliable and effective in removing the humic matrix constituents. A fully automated method applicable to bentazone, 4-chloro-2-methylphenoxyacetic acid (MCPA), (2,4-dichlorophenoxy)acetic acid (2,4-D), 2-(4-chloro-2-methylphenoxy)propionic acid (MCPP), 2-(2,4-dichlorophenoxy)propionic acid (2,4-DP), (2,4,5-trichlorophenoxy)acetic acid (2,4,5-T), 4-(dichlorophenoxy)butyric acid (2,4-DB), 4-(4-chloro-2-methylphenoxy)butyric acid (MCPB) and (2,4,5-trichlorophenoxy)propionic acid (2,4,5-TP), including data on repeatability, is described here and the scope of the method is discussed.

EXPERIMENTAL

Reagents

High-performance liquid chromatographic (HPLC)-grade acetonitrile and water were obtained from Mallinckrodt (St. Louis, MO, USA), HPLC-grade methanol and dichloromethane, sodium hydroxide, ethyl acetate and perchloric acid from Baker (Deventer, Netherlands), buffer solutions of pH of 7.0 and 10.0 from Merck (Darmstadt, Germany) and low-UV PIC A reagent (a buffered solution of tetrabutylammonium hydrogensulphate) from Millipore (Bedford, MA, USA). Chlorophenoxy carboxylic acids were obtained from Riedel-de Haën (Hannover, Germany) and Promochem (Wesel, Germany) and bentazone from Promochem.

Apparatus

The HPLC apparatus consisted of a Waters Assoc. (Millipore, Bedford, MA, USA) Model 600E pump to deliver the wetting, conditioning and washing solvents, two LKB (Bromma, Sweden) Model 2150 pumps and an LKB Model 2152 system controller to deliver the mobile phase and the aqueous samples. A Pye Unicam Model 4110 variable-wavelength UV absorbance detector obtained from Philips (Eindhoven, Netherlands) was set at 230 nm. Model SPH 99 a column thermostat was obtained from Spark (Emmen, Netherlands). PROSPEKT fully automated cartridge exchange system (Spark) with two additional valves was used to control the flow scheme during analysis. Chromatograms were recorded and integrated by a data station (Millipore) with Baseline 810 software.

Procedures

Stock solutions of the chlorophenoxy acids and bentazone were prepared by weighing *ca.* 5 mg of each component followed by dissolution in 50 ml of methanol. These solutions were diluted with tap water to obtain standard solutions and mixed standard solutions (tap water is relatively pure except for the presence of some natural humic substances, in this respect the matrix is already very much like surface water, which is an advantage for these experiments).

Sample solutions were prepared by diluting the stock solutions with tap water or surface water and acidified to pH 3 with 0.1 mol/l perchloric acid.

Precolumns (10 × 2 mm I.D.) were prepacked with 15–25-μm PLRP-S (Polymer Labs., Shropshire, UK), wetted with 2 ml of methanol (2 ml/min) and activated with 2 ml of 0.001 mol/l perchloric acid (1 ml/min) prior to preconcentration of the samples.

Separations were carried out at 50°C on a 250 × 4.6 mm I.D. column, prepacked with 5-μm, 100 Å PLRP-S, using acetonitrile–water (30:70) containing 0.005 mol/l of tetrabutylammonium hydrogensulphate (TBA) (pH 8.3) [in practice one bottle of low-UV PIC A was added to 1 l of acetonitrile–water (30:70)] at a flow-rate of 1.0 ml/min as the mobile phase, which also served as the desorption eluent for the precolumn. Conditions during sample concentration, heartcutting and precolumn washing are described below.

RESULTS AND DISCUSSION

Heartcut technique

Heartcutting in liquid chromatography is not a common technique, probably because additional microprocessor-controlled valves are required. Several years ago [6,7], the so-called "venting-technique" was introduced; 10 μl of untreated blood plasma were injected into a precolumn, and by carefully regulating the precolumn eluent with the aid of a three-port valve and a back-pressure regulator, interfering matrix components could be vented to waste. Goewie and Hogendoorn [8] transferred the analytes of interest in a small volume of mobile phase to the analytical column after a washing procedure with a solvent of low eluotropic strength [9]. Both techniques are known as heartcutting.

In our laboratory, we investigated the possibility of taking a heartcut from the precolumn eluent that exclusively and instantaneously is desorbed by the mobile phase. To do so we used the set-up in Fig. 1, which is the basis of the PROSPEKT apparatus. With switch moments of valve 2 at 10, 20 or 40 s with mobile phase flow-rates of 1, 0.5 and 0.25 ml/min, respectively, the recoveries are still very good ($\geqslant$85%) for all components. These results indicate that the first five bed volumes (*ca.* 170 μl) can be directed to waste without significant loss. The end-point (switching valve 1 again) is between 20 and 30 s. This means that the analytes of interest are desorbed from the precolumn in a narrow band of *ca.* 300 μl (*ca.* 10 bed volumes).

Desorption and heartcutting of the precolumn, to which a surface water sample had been applied, resulted in a decrease of the interfering matrix peak, now becoming relatively small and sharp. A humic peak, however, remained in the middle of the chromatogram coming from humic substances, which was confirmed by LC with diode-array detection. Therefore, although the large interfering matrix peak can be removed or decreased, other clean-up techniques are still required to remove all interfering humic substances.

Clean-up procedure

As outlined above and previously [1], it was not possible to remove the surface water matrix constituents from the precolumn with the "normal" washing procedures, *i.e.*, even 30% acetonitrile at pH 3 did not eliminate the interfering matrix

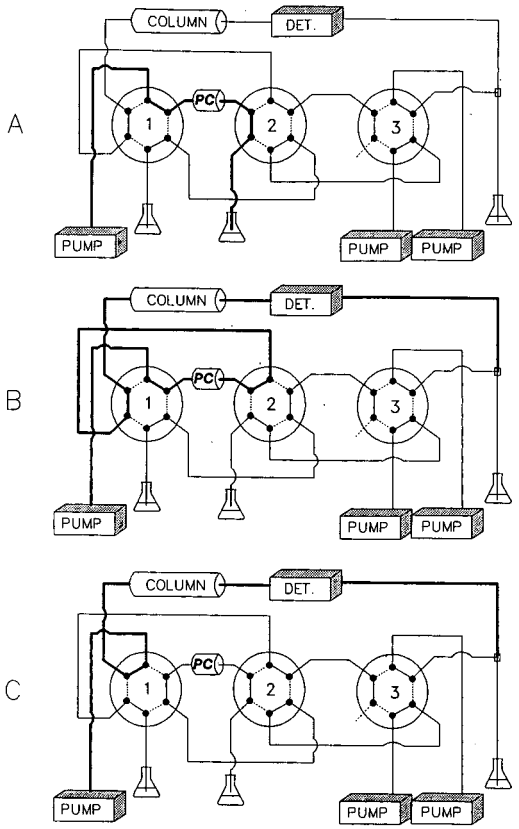

Fig. 1. Flow diagram of the heartcutting set-up. (A) Desorption from precolumn to waste; (B) first point of heartcut is reached; desorption to analytical column; (C) second point of heartcut is reached; end desorption, start of separation.

peak. During desorption at higher pH, however, the matrix components causing this interfering peak mostly elute prior to the analytes of interest. This suggested the development of an extraneous washing procedure with solvents of high pH.

Initial experiments indicated that washing with HPLC-grade water of pH 9.7 and 11.3 gave better results with increasing pH. Clean-up with 7 ml of 0.1 mol/l sodium hydroxide solution (pH 12.5), however, showed no breakthrough of the phenoxy acids. Also, interfering matrix peak decreased considerably and became sharp, and moreover the humic peak in the middle of the chromatogram disappeared completely. Increasing the volume of washing solvent, however, did not result in a continuous decrease in the remaining interfering matrix peak, *i.e.*, after 1 ml of washing solvent there was no further improvement in the chromatogram. Bentazone, however, will elute (breakthrough) with *ca.* 2 ml of washing solvent. At pH 12.5 bentazone is a neutral component ($pK_B \approx 10$). The difference in behaviour of the phenoxy acids and the apparently "similar" humic substances might be explained in the following way.

At very high pH values the humic substances, which can be imagined as "large

complex spheres", substituted with acidic (CO_2H) and phenolic (OH) groups, are negatively charged not only on the outside but also on the inside. They are wholly polar phases now and, consequently, will elute easily from the precolumn without dragging along the analytes of interest. The phenoxy acids, being carboxylic acids, will also be negatively charged at this pH. The major part of their molecules, however, still remains apolar and will be attracted by the polymer. At this pH bentazone is a neutral component, being attracted by the polymer, yet still fairly polar.

Apparently a high pH value is necessary to charge the whole humic "phase" negatively, *i.e.*, to make it wholly polar. At lower pH there is apparently still available an apolar humic "phase", being contained in the mobile phase, which is why the analytes of interest show an earlier breakthrough.

Optimization and repeatability

Using surface water spiked at 1 μg/l with all components of interest, we now combined both techniques and determined the optimum conditions for automated measurements. These optimum conditions turned out to be a washing volume of 1000 μl of 0.1 mol/l sodium hydroxide solution and a switching moment for valve 2 of 8 s. Chromatograms obtained from spiked surface water, tap water and HPLC-grade water are shown in Fig. 2.

Under these optimum conditions, the repeatability of the method was tested using spiked surface water samples at 0.25 μg/l and 1 μg/l for all components. The repeatability at both levels is excellent, *i.e.*, the relative standard deviation (R.S.D.) at the 1 μg/l level was *ca.* 2% (2,4,5-TP 8%) and at the 0.25 μg/l level *ca.* 9% (2,4,5-TP 16%) (n = 5). Detection limits for surface water samples were calculated to be 0.05–0.1 μg/l (signal-to-noise ratio = 3).

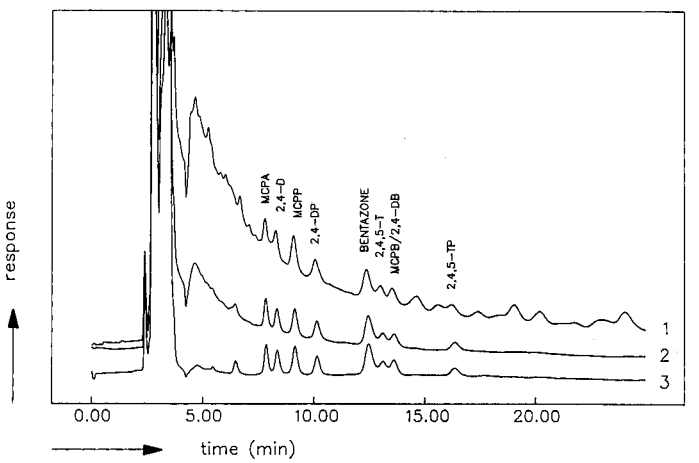

Fig. 2. Chromatograms for 25 ml of spiked water samples (1 μg/l) under optimum conditions. (1) Surface water; (2) tap water; (3) HPLC-grade water. Mobile phase, acetonitrile–water (30:70) containing 0.005 mol/l TBA (pH 8.3); flow-rate, 1 ml/min; analytical columns, 250 × 4.6 mm I.D. PLRP-S (50°C); precolumn, 10 × 2 mm I.D. PLRP-S; 0.1 mol/l NaOH (pH 12.5) wash volume, 1000 μl; heartcut first 130 μl to waste, second 300 μl to analytical column; UV detection at 230 nm, 0.1 a.u.f.s.

Scope

As outlined above humic acid constituents elute easily from the precolumn at very high pH without dragging along the analytes of interest. The phenoxy carboxylic acids were retained even after applying 10 ml of 0.1 mol/l sodium hydroxide washing solvent. The basic component bentazone also elutes slowly. From these results we concluded that, in principal, all basic, neutral and acidic components having an apolar part in their molecule can be applied with this method.

We are currently investigating another approach, namely preconcentration of a broad range of components (acidic, basic and neutral pesticides) from alkaline surface water samples.

CONCLUSION

Clean-up procedures using a polymeric precolumn (PLRP-S) in the determination of bentazone and phenoxy acid herbicides in surface water samples have been studied. Combining both clean-up techniques, *i.e.*, washing of the precolumn with 0.1 mol/l sodium hydroxide solution at pH 12.5 followed by heartcutting, resulted in a considerable decrease in the interfering matrix peak and consequently reliable integration of the chromatogram.

Surface water samples spiked at 0.25 and 1 μg/l showed excellent recoveries (>85%) with R.S.D.s at 1 μg/l of *ca.* 2% and 0.25 μg/l of *ca.* 9% ($n = 5$). Detection limits for surface water samples were calculated to be 0.05–0.1 μg/l. Owing to the automation, the total analysis time was only 30 min, indicating promising potential for this technique.

REFERENCES

1 R. B. Geerdink, C. A. A. van Balkom and H.-J. Brouwer, *J. Chromatogr.*, 481 (1989) 275.
2 R. L. Smith and D. J. Pietrzyk, *J. Chromatogr. Sci.*, 21 (1983) 282.
3 M. Åkerblom, *J. Chromatogr.*, 319 (1985) 427.
4 R. B. Geerdink, *J. Chromatogr.*, 445 (1988) 273.
5 E. M. Thurman and R. L. Malcolm, *Environ. Sci. Technol.*, 15 (1981) 463.
6 K.-G. Wahlund and U. Lund, *J. Chromatogr.*, 122 (1976) 269.
7 T. Arvidsson, K.-G. Wahlund and N. Daoud, *J. Chromatogr.*, 317 (1984) 213.
8 C. E. Goewie and E. A. Hogendoorn, *J. Chromatogr.*, 410 (1987) 211.
9 P. J. Schoenmakers, *Optimization of Chromatographic Selectivity*, (*Journal of Chromatography Library*, Vol. 35), Elsevier, Amsterdam, 1986.

Journal of Chromatography, 547 (1991) 484–487
Elsevier Science Publishers B.V., Amsterdam

CHROM. 23 266

Short Communication

Separation of cations in buffered 1-methyl-3-ethylimidazolium chloride–aluminum chloride ionic liquids by ion chromatography

JOHN R. STUFF
The Frank J. Seiler Research Laboratory, U.S.A.F. Academy, Colorado Springs, CO 80840-6528 (USA)
(First received June 28th, 1990; revised manuscript received March 5th, 1991)

ABSTRACT

Ion chromatography was used to separate sodium and 1-methyl-3-ethylimidazolium cations in the buffered 1-methyl-3-ethylimidazolium chloride–aluminum chloride room-temperature molten salt system. The calibration curves for the two species were linear over three decades and the accuracy of the method was ± 2.8% relative error.

INTRODUCTION

The addition of aluminum chloride to 1-methyl-3-ethylimidazolium chloride (MEIC) results in the formation of an ionic liquid (melt) at room temperature [1]. The liquids are described in terms of the apparent mole fraction, N, of aluminum chloride used to make them. Melts with $N<0.5$ are termed 'basic' because of the presence of the Lewis base, Cl^-. Melts with $N>0.5$ are termed 'acidic' because of the presence of the Lewis acid, $Al_2Cl_7^-$, and melts with $N=0.5$ are termed 'neutral' because the only anion present is the Lewis neutral $AlCl_4^-$.

These ionic liquids are of interest to our laboratory as battery electrolytes because of their wide electrochemical window, high specific conductance and good thermal properties [2,3]. Their application as battery electrolytes has been demonstrated [4,5]. The neutral composition has the widest electrochemical window (over 4 V), but is difficult to maintain because small changes in ion concentrations alter the electrochemistry, closing the electrochemical window by as much as 2 V. Recently, we have discovered that the addition of sodium chloride to acidic melts results in the formation of neutral buffered ionic liquids [6]. The resulting ionic liquid has the wide electrochemical window associated with the neutral composition and is still liquid at

room temperature over a wide composition range. It is buffered against addition of the Lewis base, Cl^-, by the presence of Na^+ by the reaction

$$Na^+ + Cl^- \rightarrow NaCl(s)$$

and is buffered against the addition of the Lewis acid, $Al_2Cl_7^-$, by the presence of excess NaCl(s) by the reaction

$$NaCl(s) + Al_2Cl_7^- \rightarrow Na^+ + 2AlCl_4^-$$

A parameter of particular interest in battery applications is the transport number for the various ions in the electrolyte of choice. The transport number for an ion defines the fraction of current carried by that particular ion across a separator when charge is passed in an electrochemical cell. Previous experiments in the unbuffered MEIC–aluminum chloride system have shown that the bulk of the current, approximately 70%, is carried by MEI [7]. The addition of sodium chloride to this system should affect the transport numbers of the various species involved.

The aim of the present study was to develop a method by ion chromatography to monitor changes in the concentrations of Na^+ and MEI^+ in the neutral buffered ionic liquids. The method can then be used to help determine transport number for the new system.

EXPERIMENTAL

The ion chromatograph was a Dionex (Sunnyvale, CA, USA) Model 4500i, with an IonPac CS3G guard column, IonPac CS3 column, cation micromembrane suppressor and conductivity detector. Chromatographs were recorded and integrated on a Dionex 4400 integrator.

The starting materials and room-temperature molten salts were made as described previously [6,8]. Tetrabutylammonium hydroxide (40, w/w), 2,3-diaminopropionic acid monohydrochloride (DAP) (99%), hydrochloric acid (ACS reagent grade) and sodium chloride (99.999%) were obtained from Aldrich (Milwaukee, WI, USA). All dilutions were made with 18.3 M Ω cm water from a Barnstead (Boston, MA, USA) Nanopure II still. Ultrex nitric acid was obtained from J. T. Baker (Phillipsburg, NJ, USA). Disposable 10-ml B–D brand syringes and Gelman Acrodisc 0.45-μm PTFE syringe filters were obtained from Fisher Scientific (Denver, CO, USA).

Acidic melts were made in the range $N = 0.50$–0.60. They were then buffered to neutrality with a 10% excess of sodium chloride and allowed to equilibrate for 24 h prior to use. All glassware was stored under 1:3 ultrex nitric acid–deionized water for a minimum of 48 h before use. The melt samples were filtered through a 0.45-μm PTFE syringe filter prior to weighing. The melts were then weighed (2.0–2.5 g samples) into a 25-ml volumetric flask in a dry box, removed from the box, cooled in a dry ice–acetone bath, slowly hydrolyzed with deionized water and diluted to volume. Na^+ and MEI^+ were quantitated with a calibration curve. A standard stock solution of MEI^+ was prepared from MEIC. A standard stock solution of Na^+ was prepared from 99.999% sodium chloride.

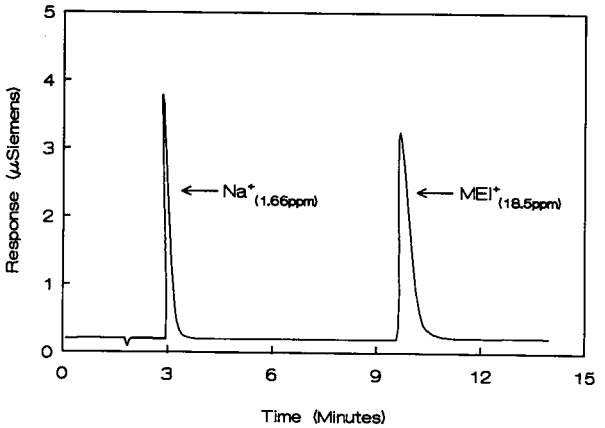

Fig. 1. Separation of Na^+ and MEI^+ by ion chromatography.

RESULTS AND DISCUSSION

The optimum mobile phase composition for the separation of the two ions was found to be a solution of 25 m*M* hydrocloric acid and 0.35 m*M* DAP in deionized water delivered isocratically at 1.0 ml/min. With this mobile phase and the column described, the cations from the melt could be separated in a 12-min run. The MEI^+ elutes at retention time 10.2 min. Fig. 1 shows the separation of the two ions. The regenerant for the chemical suppressor was 50 m*M* tetrabutylammonium hydroxide delivered at a rate of 3.0 ml/min to the suppressor column. The resulting capacity factors for the ions are $k'_{Na+} = 0.65$ $k'_{MEI+} = 4.10$.

The calibration curves for the two ions are linear over three decades. Standards and sample dilutions were chosen so as to fall near the center of the calibration curves (0.2–2 ppm for Na^+ and 10–40 ppm for MEI^+). Samples included buffered melts over the composition range 0.52–0.60 apparent mole fraction, *N*, of aluminum chloride. The Na^+ and MEI^+ peaks were quantitated and the weight percentage of sodium chloride and MEIC calculated. The results are summarized in Table I. The accuracy

TABLE I

ANALYTICAL DATA FOR MEIC AND NaCl DETERMINATION

N	MEIC			NaCl		
	Theoretical (%)	Experimental[a] (%)	Relative error (%)	Theoretical (%)	Experimental[a] (%)	Relative error (%)
52	49.40	50.77	+2.80	1.70	1.77	+2.30
54	46.06	46.36	+0.65	3.08	3.01	−2.27
56	44.26	44.68	+0.95	4.73	4.66	−1.50
58	41.75	41.62	−0.31	6.18	6.09	−1.46
60	38.14	39.14	+0.13	7.73	7.78	+0.65

[a] Average of three trials.

of the method (worst case + 2.8%) for determination of Na^+ and MEI^+ is sufficient to distinguish between melts over the composition range studied and therefore could be used to monitor changes in the concentrations of these ions during a transport number experiment.

Ion chromatography provides a convenient method for the quantitation of Na^+ and MEI^+ from the buffered aluminum chloride–MEIC ionic liquid. Other group 1A metal ions could also be separated and quantitated using this method. The solvent strength and flow may require further optimization depending on the ions of interest. Divalent cations would not elute under the given conditions and time frame of the experiment described.

REFERENCES

1 A. A. Fannin, Jr., L. A. King, J. A. Levisky and J. S. Wilkes, *J. Phys. Chem.*, 88 (1984) 2609.
2 A. A. Fannin, Jr., D. A. Floreani, L. A. King, J. S. Landers, B. J. Piersma, D. J. Stech, R. L. Vaughn, J. S. Wilkes and J. L. Williams, *J. Phys. Chem.*, 88 (1984) 2614.
3 J. R. Stuff, *Thermochim. Acta*, 152 (1989) 421.
4 G. F. Reynolds and C. J. Dymek, Jr., *J. Power Sources*, 15 (1985) 109.
5 C. J. Dymek, Jr., G. F. Reynolds and J. S. Wilkes. *J. Electrochem. Soc.*, 134 (1987) 1658.
6 T. J. Melton, J. Joyce, J. T. Maloy, J. A. Boon and J. S. Wilkes, *J. Electrochem. Soc.*, 137 (1990) 3865.
7 C. J. Dymek, Jr. and L. A. King, *J. Electrochem. Soc.*, 132 (1985) 1375.
8 J. S. Wilkes, J. A. Levisky, R. A. Wilson and C. L. Hussey, *Inorg. Chem.*, 21 (1982) 1263.

Journal of Chromatography, 547 (1991) 488–493
Elsevier Science Publishers B.V., Amsterdam

CHROM. 23 354

Short Communication

Gas phase retention volume behavior of organic compounds on Carbotrap graphitized carbon

JAMES F. PANKOW

Department of Environmental Science and Engineering, Oregon Graduate Institute, 19600 N.W. Von Neumann Dr., Beaverton, OR 97006 (USA)

(First received October 31st, 1990; revised manuscript received April 9th, 1991)

ABSTRACT

The graphitized carbon material Carbotrap is often used for sampling gaseous organic compounds. Knowledge of the retention volumes of the compounds of interest on Carbotrap is required to design sampling protocols. Published data are examined here to develop correlation equations between retention volume and both vapor pressure and boiling point. The 38 compounds considered included ethane, butane, 1,2-dichloroethane, benzene, trichloroethene, 1,1,2-trichloroethane, phenol, toluene, chlorobenzene, *n*-butylamine, 4-heptanone, *p*-dichlorobenzene, decane, *n*-butylbenzene, biphenyl, *n*-dodecane, *n*-tetradecane. The correlation equations are examined in terms of gas–solid adsorption theory. They allow prediction of retention behavior for compounds for which experimental retention data are not yet available.

INTRODUCTION

Interest is increasing in using the graphitized carbon material Carbotrap for sampling gas phase organic compounds. Recently, retention volumes on Carbotrap at 293 K were released by Supelco [1] for a wide range of compounds. However, that work did not examine how those data may be used to predict retention values for other compounds of interest. As Pankow [2] has discussed for the sorbent Tenax-GC, useful correlation equations can be developed in gas–solid chromatography between retention volumes and physical constants such as vapor pressure and boiling point.

THEORY

The specific gas phase retention volume ($V_{g,T}$) of a compound on a sorbent at a given temperature T (K) is defined as

$$V_{g,T} = V_{R,T}/w \tag{1}$$

0021-9673/91/$03.50

where $V_{R,T}$ is the actual net gas phase retention volume at temperature T, and w is the weight of sorbent (g). The standard units for $V_{R,T}$ and $V_{g,T}$ are l and l/g, respectively. Both $V_{R,T}$ and $V_{g,T}$ depend on T as well as the enthalpy of desorption ΔH_s (kcal/mol) from the sorbent surface [3].

When the number of sites for sorption is limited, the sorption process is Langmuirian in character. When the system is not being overloaded chromatographically, such sorption occurs in a "linear" manner, and Pankow [2] obtains

$$\log V_{g,T} = 5.79 + \log fN_sAT + (\Delta H_s - \Delta H_v)/0.0046T - \log p_T^0 \quad (2)$$

where f is a dimensionless constant that depends on the difference between the compound's entropy of desorption from the surface and the entropy of vaporization of the pure compound, N_s is the moles of sites per cm^2 of surface, A is the specific surface area of the sorbent (m^2/g), ΔH_v is the enthalpy of vaporization of the pure compound (kcal/mol), and p_T^0 is the vapor pressure (Torr) of the pure compound at temperature T.

The value of f is often assumed to be equal to ≈ 1, though in many cases that may not in fact be the case [4]. Using an equation described by Pankow [5], one can show that $N_s \approx 5 \cdot 10^{-10}$ mol/cm^2 for the types of compounds for which Carbotrap is suited. The value of A released by Supelco [1] for Carbotrap is about 100 m^2/g. Taking these values and assuming that f is in fact equal to 1, at $T = 293$ K, eqn. 3 becomes

$$\log V_{g,293} = 0.96 + 0.745\,(\Delta H_s - \Delta H_v) - \log p_{293}^0 \quad (3)$$

For Tenax-GC, the corresponding equation ($T = 293$ K) is

$$\log V_{g,293} = -0.15 + 0.745\,(\Delta H_s - \Delta H_v) - \log p_{293}^0 \quad (4)$$

The smaller constant in eqn. 4 *vs.* that in eqn. 3 is due to the comparatively small value of A for Tenax-GC (≈ 6.4 m^2/g, Pankow [2]). On Carbotrap at $T = 293$ K, for "liquid-like" sorption (*i.e.*, $f = 1.0$ and $\Delta H_s - \Delta H_v$), eqn. 3 becomes

$$\log V_{g,293} = 0.96 - \log p_{293}^0 \quad (5)$$

To the extent that fN_s and $(\Delta H_s - \Delta H_v)$ remain constant from compound to compound, eqn. 2 indicates that at a given value of T, a correlation of $\log V_{g,T}$ data *vs.* $\log p_T^0$ should yield a straight line with a slope of -1.00. For a compound that is normally a solid at the temperature of interest, the value of the vapor pressure in eqns. 2–5 should be that of the sub-cooled liquid, *i.e.*, $p_{L,T}^0$. The reason is that the sorbed state is likely to be more similar to the liquid state than it is to the ordered crystalline solid state [6]. Bidleman [6] describes how to calculate $p_{L,T}^0$ values.

Application of Trouton's rule as described by Pankow [2] transforms eqns. 2 and 5 into

$$\log V_{g,T} = -1.91 + \log fN_sAT + (\Delta H_s - \Delta H_v)/0.0046T + 0.016\,T_b \quad (6)$$

$$\log V_{g,293} = -6.74 + 0.016\,T_b \quad (7)$$

TABLE I

SPECIFIC RETENTION VOLUME VALUES ($V_{g,293}$, l/g) FOR ORGANIC COMPOUNDS ON CARBOTRAP AT 293 K ALONG WITH BOILING POINTS AND LOG p^0_{293} VALUES

Compound	Boiling point (°C)	log p^0_{293} (Torr)	log $V_{g,293}$[a] (l/g)
Ethane	−88	4.47	−1.76
Propane	−42	3.81	−1.26
Butane	−0.5	3.18	−0.39
Ethanol	78	1.64	−0.31
Acetic acid	118	1.07	−0.15
Propionic acid	141	0.46	0.22
1,2-Dichloroethane	84	1.78	0.29
2-Butanone	80	1.88	0.58
Pentane	36	2.63	0.77
tert.-Butanol	83	1.49	0.81
Benzene	80	1.88	1.07
Trichloroethane	87	1.78	1.10
n-Butanol	118	0.64	1.28
1,1,2-Trichloroethane	114	1.28	1.39
Hexane	69	2.08	1.90
n-Pentanoic acid	187	−0.82	2.63
Phenol	182	−0.70	2.79
Toluene	111	1.34	2.81
Chlorobenzene	132	0.94	3.20
Cyclohexanone	157	0.60	3.31
n-Butylamine	78	1.86	3.32
4-Heptanone	149	−0.08	3.39
p-Dichlorobenzene	173	−0.22	4.13
Octane	126	1.04	4.21
Ethylbenzene	136	0.85	4.31
p-Cresol	202	−1.40	4.31
Benzylamine	184	−0.24	4.35
p-Xylene	138	0.81	4.63
Acetophenone	202	−0.46	4.81
Isopropylbenzene	153	0.51	5.23
n-Propylbenzene	159	0.40	6.24
Decane	174	0.43	6.68
n-Butylbenzene	183	−0.05	6.77
Biphenyl	258	−1.41	9.57
n-Hexylbenzene	226	NA[b]	9.85
n-Dodecane	216	−0.52	11.21
n-Octylbenzene	262	NA	12.12
n-Tetradecane	252	−1.57	13.92

[a] Data from Supelco [1].
[b] Not available.

where T_b (K) is the boiling point at 1 atm pressure. Thus, when fN_s and $(\Delta H_s - \Delta H_v)$ remain constant log $V_{g,293}$ will correlate with T_b as well as log p^0_{293}.

RESULTS AND DISCUSSION

The available gas phase retention data for Carbotrap are summarized in Table I

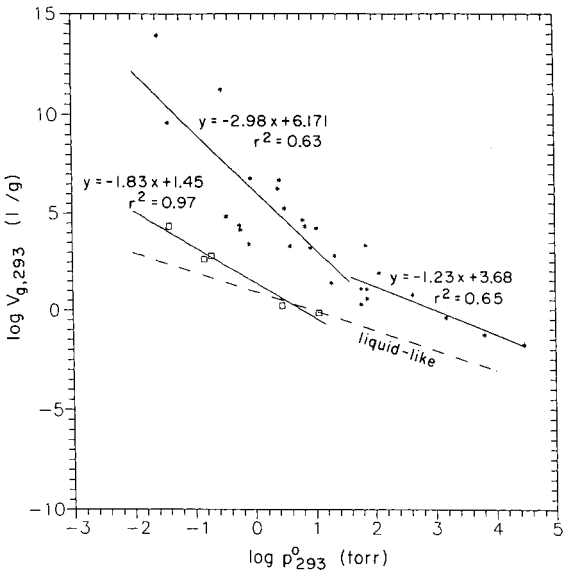

Fig. 1. Plots of log $V_{g,293}$ *vs.* log p^0_{293} for Table I data. Squares are for the acids and phenols. Dashed line is for liquid-like sorption (eqn. 5).

along with boiling points (in °C) and log p^0_{293} values. It should be pointed out that in obtaining the data for the strongly retained compounds, it was apparently necessary to extrapolate the retention data [as log $(V_{g,T}/T)$ *vs.* $1/T$, see ref. 3] from relatively high temperatures down to 293 K. If a given ΔH_s is not relatively constant over such a wide temperature range, the extrapolation will lead to an incorrect retention volume.

The Table I data (except for the alcohols) are plotted *vs.* log p^0_{293} in Fig. 1 and *vs.* T_b in Fig. 2. For the few compounds that are solids at 293 K, there is little difference between the vapor pressures of the solids and that of the corresponding sub-cooled liquids, and so the former were used. Excluding the alcohols, acids and phenols from consideration for the moment, a break in behavior seems to occur at a log p^0_{293} value of ≈ 1.6 and at a T_b value of ≈ 373 K. The group of compounds for which log $p^0_{293} < 1.6$ is the same group for which $T_b > 373$ K. It is not known whether this break is real, or a result of artifacts due to obtaining the large $V_{g,293}$ values by extrapolation from high temperatures.

The four correlation lines that the two groups give *vs.* log p^0_{293} and *vs.* T_b are included in the figures. There is a fair amount of scatter around some of these correlation lines, more than was found in some cases by Pankow [2] for Tenax-GC. Therefore, in the case of the group for which log $p^0_{293} < 1.6$ and $T_b > 373$ K, it will not be possible to use the corresponding correlation lines to predict retention volume to better than perhaps ± 1.5 orders of magnitude. That degree of prediction will, nevertheless, still be useful. In the case of the acids and phenols, however, the degree of correlation is quite high, both when log p^0_{293} and T_b are used as the correlating parameters. Although not included in Figs. 1 and 2, the data for the alcohols are not out of line with the other data; the points deviate slightly negatively from the four correlation lines discussed above. An overall comparison of the Table I data with the

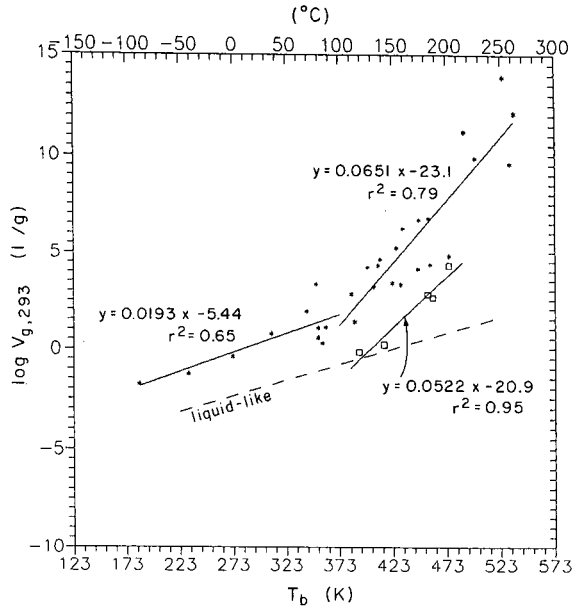

Fig. 2. Plots of log $V_{g,293}$ *vs.* T_b for Table I data. Squares are for the acids and phenols. Dashed line is for liquid-like sorption (eqn. 7).

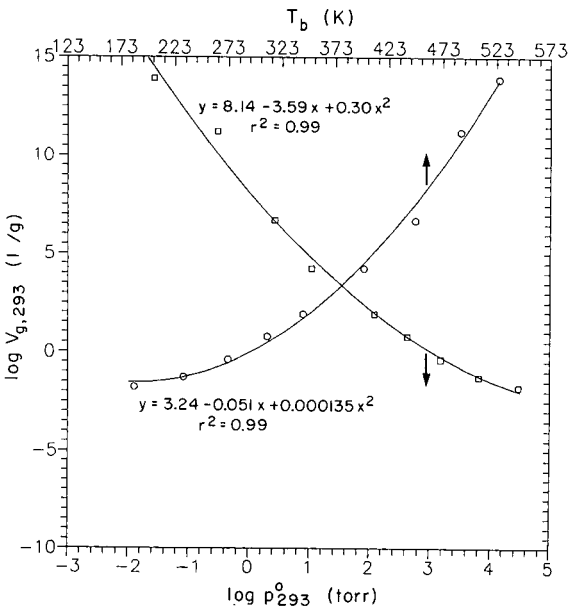

Fig. 3. Plots of log $V_{g,293}$ *vs.* log p^0_{293} and log $V_{g,293}$ *vs.* T_b for Table I alkanes.

plots of eqns. 5 and 7 given in the figures lead to the conclusion that sorption on Carbotrap is *not* very liquid-like for most compounds. Some of the correlation lines, however, have slopes approaching the theoretical values.

Fig. 3 presents the data for the alkanes alone. There is a definate curvature when $\log p^0_{293}$ and when T_b is used as the independent variable. As above, it is not known whether this curvature is real, or is an artifact of the extrapolations. The correlation parameters for the best-fit second order polynomial curves are given in the figure.

CONCLUSIONS

Gas–solid partitioning theory provides a useful framework in which to consider the gas phase retention volume behavior of organic compounds on Carbotrap. Correlation equations between specific retention volume and compound vapor pressure and boiling point with fair to very good r^2 values have been obtained. It is likely that these equations will be useful in predicting retention behavior for compounds for which experimental retention data are not yet available.

REFERENCES

1 Supelco, *The Supelco Reporter*, 7 (1988) 1.
2 J. F. Pankow, *Anal. Chem.*, 60 (1988) 950–958.
3 A. V. Kiselev and Ya. I. Yashin, *Gas-Adsorption Chromatography*, Plenum, New York, 1969.
4 S. Brunauer, L. E. Copeland and D. L. Kantro, in E. Alison Flood (Editor), *The Solid–Gas Interface*, Marcel Dekker, New York, pp. 77–103.
5 J. F. Pankow, *Atmos. Environ.*, 21 (1987) 2275–2283.
6 T. F. Bidleman, *Environ. Sci. Technol.*, 22 (1988) 361–367.

Journal of Chromatography, 547 (1991) 494–500
Elsevier Science Publishers B.V., Amsterdam

CHROM. 23 109

Short Communication

Study of large sample volume injection in a capillary gas chromatographic–Fourier transform infrared system using a retention gap column

HUILIAN HU*, MINGHUA ZHU, YIHUA HE and KEFU SUN

Analysis and Research Centre, East China University of Chemical Technology, P.O. Box 426, Shanghai 200237 (China)

(First received August 5th, 1990; revised manuscript received January 7th, 1991)

ABSTRACT

In the work reported here, the technique of large sample volume injection based on the retention gap method proposed by Grob (*J. Chromatogr.*, 237 (1982) 15) has been applied successfully to increase the relative sensitivity of a gas chromatography–Fourier transform infrared (GC–FTIR) system. By regulating the make-up gas in the lightpipe (the interface which connects the GC system with the FTIR system) and the flow-rate of the carrier gas, the interference from the large volume of solvent is resolved and the sensitivity of the system is retained. Using this method, a sample as large as 100 μl can be injected with excellent results. By using this method the relative sensitivity was increased by 100 times and therefore the detection range of the GC–FTIR system is expanded.

INTRODUCTION

As a result of the limited sensitivity of infrared detection, it is often difficult to determine trace amounts of analytes by gas chromatographic–Fourier transform infrared (GC–FTIR) techniques. To solve this problem, the technique of capillary column chromatography with large sample volume injection has recently been developed. Fehl and Marcott [1] used an injection trapping technique to inject a 100-μl volume [1]; Chow *et al.* [2], with the aid of an injection–Cu^{2+} pre-column technique, have expanded the injection range. It is therefore possible to obtain satisfactory detection results for trace amounts of some analytes.

In this study, the more simple retention gap technique [3] was used to inject a large sample volume in capillary GC–FTIR. The results showed that the method allowed the efficient removal of solvent vapours, such that the large sample volumes had no negative effect on the GC–FTIR resolution and sensitivity. When the injection begins, the lightpipe make-up gas is added; when the solvent peak has decreased sufficiently, the make-up gas is no longer required.

0021-9673/91/$03.50

EXPERIMENTAL

A Model 9A gas chromatograph (Shimadzu) was used, coupled with a Model 5SXC Fourier transform infrared spectrometer (Nicolet). Fig. 1 shows a schematic diagram of GC–FTIR system. The gold-coated lightpipe was 15 cm × 1 cm I.D. The separation column was a cross-linked quartz capillary column (9 m × 0.32 mm I.D.) coated with a 0.5-μm OV-1 film. The retention gap column was a soft glass capillary column (37 m × 0.32 mm I.D.) deactivated by silylanization with hexamethyldisilazane. The separation column and the retention gap column were connected by a stainless-steel butt connector. The separation column outlet stretched into the lightpipe inlet.

The following conditions of analysis were used: carrier gas, nitrogen; flame ionization detector temperature, 200°C; lightpipe and transfer line temperature, 190°C; on-column injection.

A test mixture of decane, octanol, 2,6-dimethylphenol, 2,6-xylidine, 2,4,6-trimethylphenol, dodecane, decanol, diphenyl, 2,6-dimethylnaphthalene, dicyclohexylamine, acenaphthene, methyl dodecanoate, hexadecane and fluorenone was used. The solvent was *n*-pentane.

RESULTS AND DISCUSSION

When a large sample volume is injected, a long section of the capillary column is flooded by the solvent; the length of the flooded zone is proportional to the volume of injection (about 15–30 cm/μl [4]). The resultant broadening of the initial solute bands causes a loss of resolution from the separation column. Fig. 2 shows the gas chromatogram obtained by the on-column injection of a 100-μl volume of *n*-pentane solution

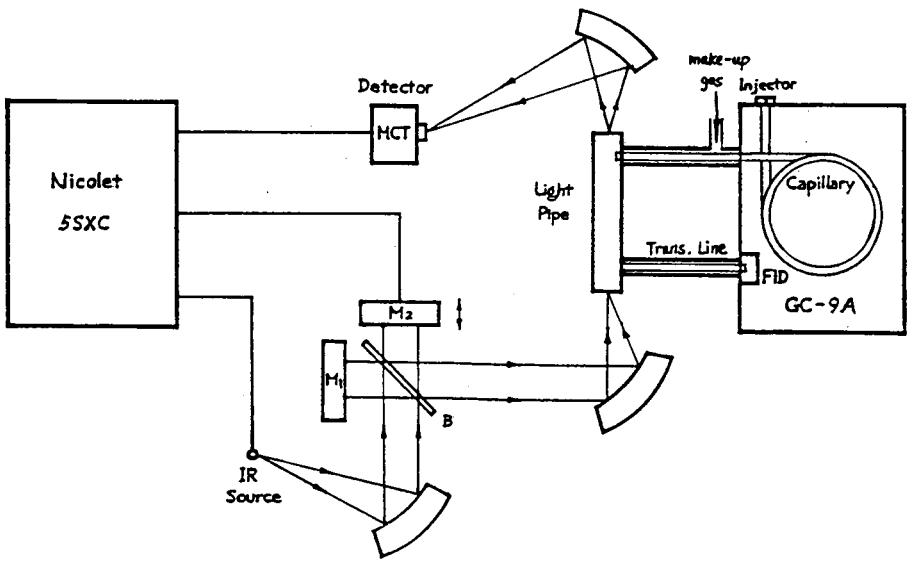

Fig. 1. Schematic diagram of the GC–FTIR system.

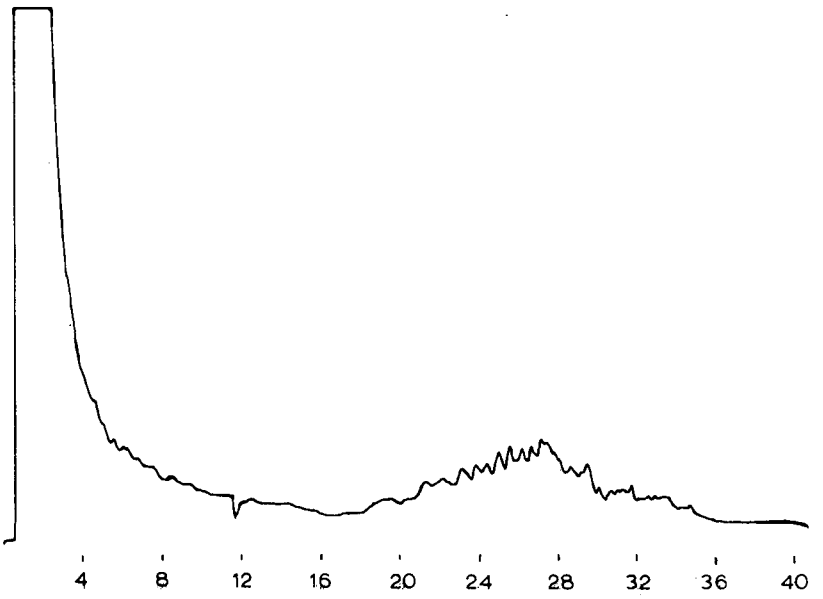

Fig. 2. On-column injection of a 100-μl volume without using a retention gap column. *n*-Pentane solution, 38°C for 17 min, then 6°C/min up to 170°C.

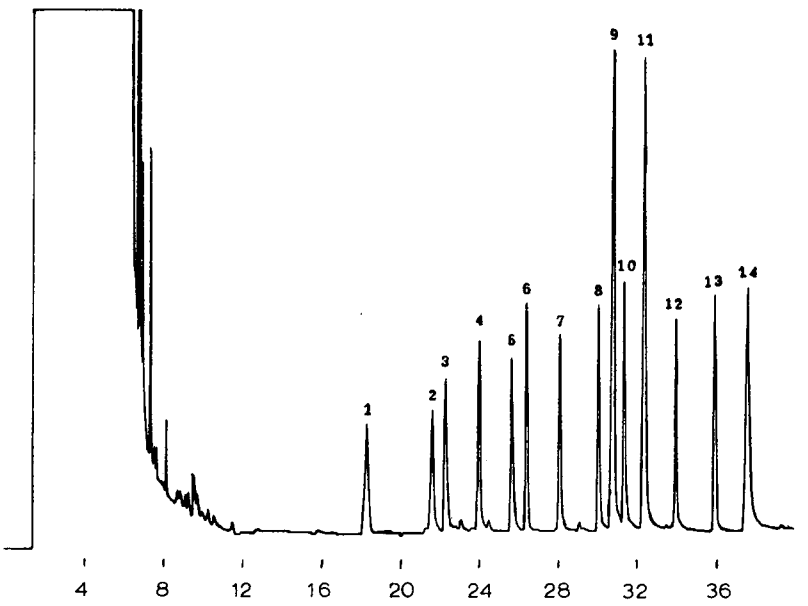

Fig. 3. Injection as in Fig. 2, but using a retention gap column. A 37-m retention gap column was connected to a 9-m separation column at 38°C for 17 min, then 6°C/min up to 170°C. On-column injection, injection volume, 100 μl; carrier gas flow-rate, 2.4 ml/min. Peaks: 1 = decane; 2 = octanol; 3 = 2,6-dimethylphenol; 4 = 2,6-xylidine; 5 = 2,4,6-trimethylphenol; 6 = dodecane; 7 = decanol; 8 = diphenyl; 9 = 2,6-dimethylnaphthalene; 10 = dicyclohexylamine; 11 = acenaphthene; 12 = methyl dodecanoate; 13 = hexadecane; 14 = fluorenone.

without the use of an uncoated pre-column. The peaks cannot be clearly seen. However, when a retention gap column without any separation ability is fitted to the head of the separation column satisfactory results were obtained with the same injection volume and separation column (Fig. 3).

Effect of carrier gas flow-rate on solute peak separation

In GC–FTIR, the carrier gas flow-rate affects the resolution and sensitivity of the system. Fig. 4 shows the Gram–Schmidt reconstruction chromatograms for a 1-μl sample at various carrier gas flow-rates. When the carrier gas flow-rate is less than or equal to 2.4 ml/min, the system maintains the higher sensitivity. However, when the rate is increased, the signal-to-noise ratio decreases. Therefore a lower carrier gas

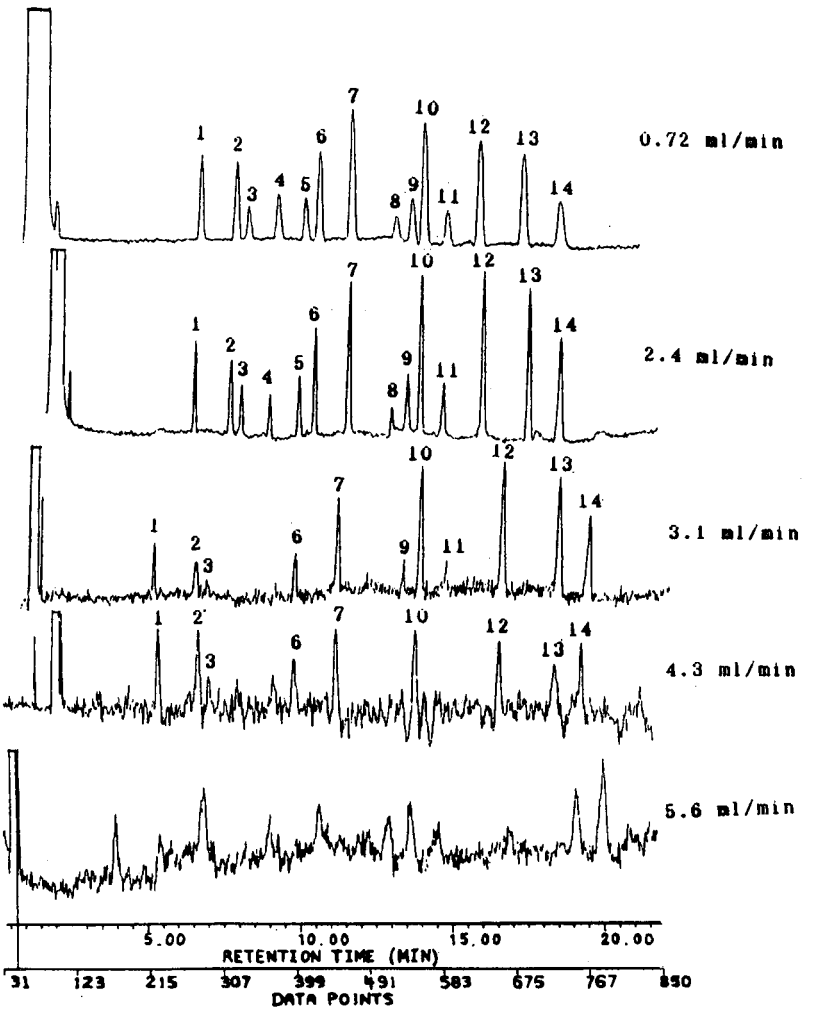

Fig. 4. Gram–Schmidt reconstruction chromatograms with different carrier gas flow-rates. *n*-Pentane solution, 27°C for 1 min then 6°C/min up to 180°C; injection volume, 1 μl. Peak identification as in Fig. 3.

flow-rate increases the sensitivity of the system. In addition, the evaporation rate of the solvent in the column inlet is proportional to the carrier gas flow-rate [5]. As a higher solvent evaporation rate will decrease the analysis time, a carrier gas volume flow-rate of 2.4 ml/min was used in this experiment.

Effect of the make-up gas of the lightpipe on a large volume of solvent

Fig. 5 shows that the injection of large volumes may cause distorted solvent peaks when using FTIR as a detection method. The internal diameter of the capillary column of the GC–FTIR system was 0.32 mm, but that of the lightpipe was 1 mm. When the carrier gas passes from the capillary column into the FTIR lightpipe, the average linear velocity decreases ten times as a result of the change in pipe diameter. At these low gas velocities, longitudinal diffusion, *i.e.* broadening of the solvent band, becomes important. To improve the shape of the solvent peak, it is necessary to add a make-up carrier gas at the connection between the chromatography column and the lightpipe. Fig. 5c shows the gas chromatogram of a 100-μl injection after adding a 40 ml/min make-up gas to the lightpipe. The shape of the solvent peak is substantially improved.

Effect of the make-up gas of the lightpipe on the solute peak

Griffiths [6] studied the problem of matching the chromatography fraction half-peak width volume ($V_{1/2}$) to the volume of the lightpipe (V_L). He concluded that only when the average value of the carrier sample half-width volume is greater than or

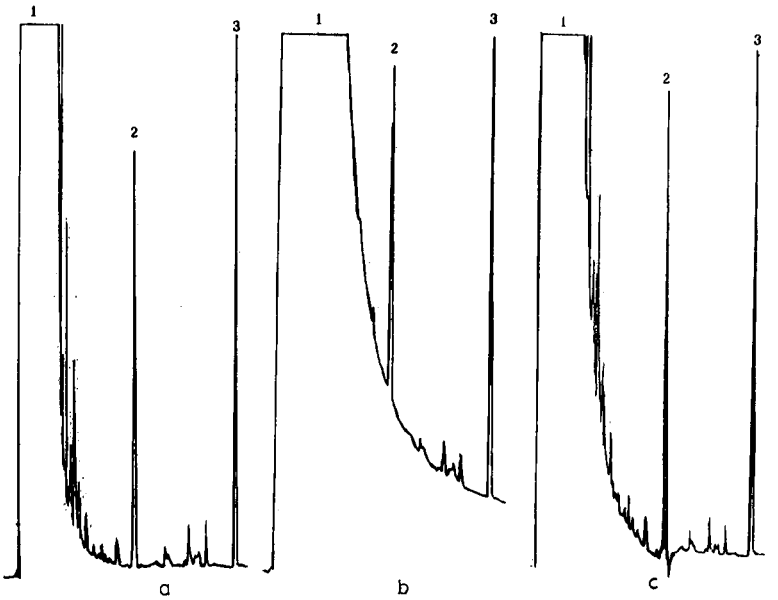

Fig. 5. Chromatograms for 100-μl on-column injection. (a) Capillary column outlet connected to flame ionization detector; (b) capillary column outlet connected to lightpipe (without make-up gas); (c) with 40 ml/min make-up gas to the lightpipe. Temperature, 40°C for 17 min then 5°C/min up to 130°C. Peaks: 1 = *n*-pentane solvent; 2 = decane; 3 = dodecane.

TABLE I

AVERAGE CHROMATOGRAPHIC FRACTION HALF-PEAK WIDTH VOLUMES AT DIFFERENT MAKE-UP GAS FLOW-RATES THROUGH THE LIGHTPIPE

V_L = 0.117 ml; Carrier gas flow-rate = 2.4 ml/min.

Make-up carrier gas flow-rate (ml/min)	Total carrier volume flow-rate (ml/min) (F)	Experimental average half-peak width ($\bar{Y}_{1/2}$) (min)	$\bar{V}_{1/2} = F\bar{Y}_{1/2}$ (ml)
0	2.4	0.160	0.38
10	12.4	0.155	1.92
20	22.4	0.152	3.40
30	32.4	0.151	4.89
40	42.4	0.149	6.32

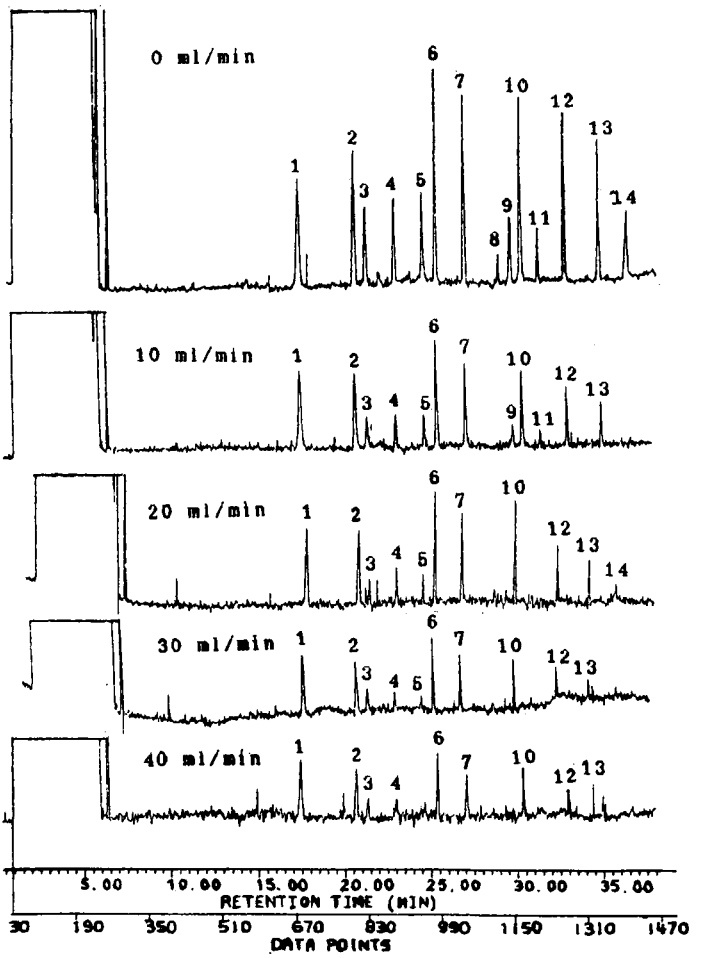

Fig. 6. Gram–Schmidt reconstruction chromatogram with make-up gas flow-rates to the lightpipe. *n*-Pentane solution, 100 μl; 38°C for 17 min then 6°C/min up to 170°C; carrier gas flow-rate, 2.4 ml/min. Peak identification as in Fig. 3.

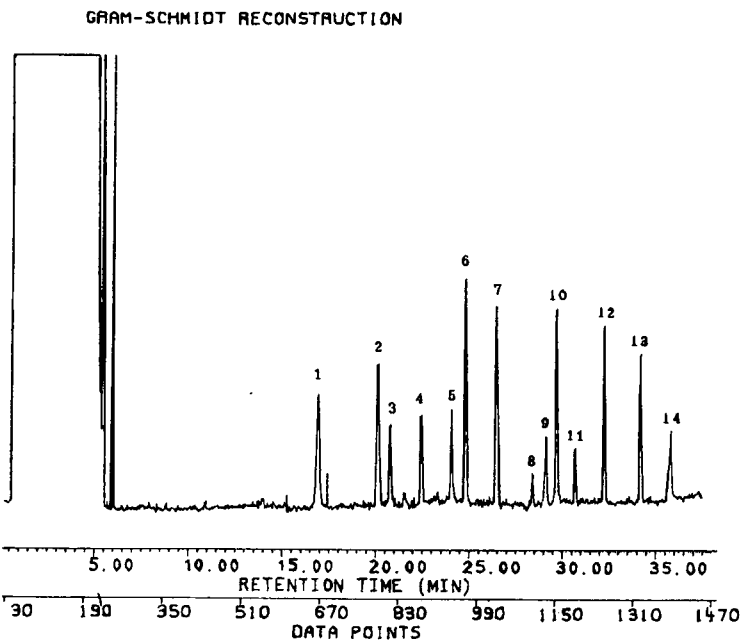

Fig. 7. Gram–Schmidt reconstruction chromatogram for *n*-pentane solution. Chromatographic conditions as in Fig. 6; on-column injection of 100 μl of the *n*-pentane solution. Lightpipe make-up gas flow-rate, 40 ml/min for 12.5 min, then closed. Peak identification as in Fig. 3.

equal to that of the lightpipe *i.e.* $\bar{V}_{1/2} \geqslant \bar{V}_L$, is the best resolution and sensitivity achieved. This may require the introduction of a make-up gas. Table I shows the average value of the half-peak width of the sample volume ($\bar{V}_{1/2}$) obtained by fourteen chromatographic fractions with different make-up gas flow-rates to the lightpipe.

It can be seen from Table I that when the make-up gas flow-rate to the lightpipe is zero, the calculated value $\bar{V}_{1/2}$ is closest to V_L, where the system has the best sensitivity. The experimental results confirmed this. Fig. 6 shows the Gram–Schmidt reconstruction chromatograms for samples obtained at various make-up gas flow-rates into the lightpipe. In fact, with increasing make-up gas flow-rates into the lightpipe, the sensitivity of the system decreases. To obtain well shaped solvent peaks and the optimum sensitivity, a make-up gas flow-rate of 40 ml/min is required during the elution of the solvent. This additional gas flow must be stopped during the analysis. Fig. 7 shows the Gram-Schmidt chromatogram for a 100-μl *n*-pentane solution using the retention gap technique.

Good results were also obtained using solvents of various boiling points and polarity, such as diethyl ether, acetone, dichloromethane, chloroform and *n*-hexane.

REFERENCES

1 A. J. Fehl and C. Marcott, *Anal. Chem.*, 58 (1986) 2578.
2 W.-M. Chow, H.-H. Pheng, Z.-X. Sun and Y.-H. Wang, *Chin. Bull. Anal. Test.*, 1 (1989) 23.
3 K. Grob, Jr., *J. Chromatogr.*, 237 (1982) 15.
4 K. Grob and B. Schilling, *J. High. Resolut. Chromatogr. Chromatogr. Commun.*, 7 (1984) 532.
5 K. Grob, Jr., *J. Chromatogr.*, 334 (1985) 129.
6 P. R. Griffiths, *Appl. Spectrosc.*, 31 (1977) 284.

Journal of Chromatography, 547 (1991) 501–508
Elsevier Science Publishers B.V., Amsterdam

CHROM. 23 297

Short Communication

Determination of nor-nitrogen mustard hydrochloride using gas chromatography with flame ionization detection

H. THULIN
Kabi Pharmacia Therapeutics AB, Box 941, S-251 09 Helsingborg (Sweden)
(First received December 27th, 1990; revised manuscript received March 13th, 1991)

ABSTRACT

A megabore gas chromatographic method with flame ionization detection was developed for the determination of nor-nitrogen mustard hydrochloride (C.A. No. 821-48-7) in toluene. The method is based on a derivatization procedure with trifluoroacetic anhydride. Benzylmethylamine was used as an internal standard. The calibration graph was linear within the range investigated (2–1050 μg/ml in toluene) with a correlation coefficient of 0.9999. The relative overall recovery was 96 ± 1.5% for a concentration of 20 μg of nor-nitrogen mustard hydrochloride per ml of toluene and 100 ± 3% for 200 μg/ml. The minimum detectable concentration in toluene was less than 0.5 μg/ml. The method is applicable to the determination of nor-nitrogen mustard hydrochloride in industrial working environments to establish occupational exposure to the compound.

INTRODUCTION

Nor-nitrogen mustard hydrochloride [bis-(2-chloroethyl)amine hydrochloride] is a commercially important amine used as a raw material in the production of various cytostatic drugs such as cyclophosphamide [1] and estramustine disodium phosphate.

Nor-nitrogen mustard is a mutagenic substance and its genetic toxicology has been reviewed in detail by Fox and Scott [2]. The compound has been shown to induce mutations in *Salmonella his* [3] and chromosomal damage in Chinese hamster cells [4]. Cytogenetic experiments with human lymphocytes have revealed that nor-nitrogen mustard induces a dose-dependent increase in chromosomal aberrations and sister chromatic exchanges [5].

Nor-nitrogen mustard hydrochloride is a white crystalline powder. In the production of cytostatic drugs it is manually handled during weighing and charging operations. Occupational exposure can arise from airborn dust or contaminated surfaces and therefore the monitoring of this substance in working environments is of

0021-9673/91/$03.50

major importance. The monitoring consists both of sampling and analytical procedures. The sampling procedures will be described in a separate paper [6].

The direct gas chromatographic (GC) analysis of free nor-nitrogen mustard in a solvent is impaired by peak taling. To overcome this tailing effect, trifluoroacetic anhydride (TFAA) derivatizations have been used in gas–liquid chromatography [7]. This method has been used to determine nor-nitrogen mustard in human serum and urine using gas chromatography–mass spectrometry (GC–MS) in the chemical ionization mode with tetradeuterated nor-nitrogen mustard as the internal standard [8,9].

The aim of this study was to develop an accessible and simple method for the determination of nor-nitrogen mustard hydrochloride which is applicable for the levels found in industrial working environments.

EXPERIMENTAL

Apparatus

A Varian 3400 gas chromatograph equipped with an on-column injector and a flame ionization detector was used. The column temperature was maintained at 120°C, the injection port and detector temperatures were 230°C. Nitrogen was used as the carrier gas at a flow-rate of 15 ml/min and as the make-up gas at a flow-rate of 20 ml/min. The gas chromatograph was equipped with a recorder and an integrator, which was used for peak evaluation. A 0.5-μl volume was injected using a Hamilton syringe.

A Finnigan MAT TSQ 70 mass spectrometer connected to a Hewlett-Packard 5890 A gas chromatograph was used for the identification of the derivatives. The mass spectrometer was used in the electron-impact mode with the ionization energy set at 70 eV.

^{1}H and ^{13}C nuclear magnetic resonance (NMR) spectra were recorded on a Bruker AC-250 NMR instrument with tetramethylsilane as the internal standard deuterochloroform ($C^{2}HCl_3$) solution.

A Rotavapor R (Büchi) was used for the evaporation of toluene containing the synthesis standards of TFAA derivatives of nor-nitrogen mustard and benzylmethylamine (BMA). For the enrichment of samples the toluene, containing trifluoroacetic anhydride derivatives, was evaporated in a stream of nitrogen.

Columns

A fused-silica megabore column with a chemically bonded stationary phase, DB-1 (J&W Scientific), 30 m × 0.53 mm I.D., with a film thickness of 1.5 μm was used.

For the GC–MS determinations a capillary column with cross-linked methylsilicone gum, HP 1 (Hewlett-Packard), 12 m × 0.2 mm I.D., with a film thickness of 0.33 μm was used.

Chemicals

The chemicals used were nor-nitrogen mustard hydrochloride (synthesized at Kabi Pharmacia (Helsingborg, Sweden), and acetone, chloroform, ethyl acetate and toluene from BDH (Poole, UK). Phosphate buffer (pH 7.0), diisobutylamine and

TFAA from Merck (Darmstadt, Germany), BMA, di-*n*-butylamine and thionyl chloride from Janssen (Beerse, Belgium), diethanolamine from Aldrich (Steinheim, Germany), ethanol from Kemetyl (Stockholm, Sweden) and diethyl ether from Lab-Scan (Dublin, Ireland) were also used.

Synthesis of nor-nitrogen mustard hydrochloride

In a 250-ml three necked, round-bottomed flask equipped with a stirrer, reflux condenser and a dropping funnel, 10.5 g (0.1 mol) of diethanolamine were dissolved in 50 ml of chloroform.

The mixture was heated to near reflux and a solution of 28.3 ml (0.4 mol) of thionyl chloride in 50 ml of chloroform was added dropwise with stirring. Reflux was maintained during the addition and for another 2 h. After reflux, about 50 ml of the chloroform were distilled off. The reaction mixture was cooled, transferred into a glass beaker and diethyl ether was added to precipitate the hydrochloride.

The precipitate was filtered off, washed with diethyl ether and suspended in 200 ml of acetone. The mixture was heated and ethanol was added cautiously until a clear solution was obtained. The nor-nitrogen mustard hydrochloride crystallized on cooling and was filtered, washed with acetone and dried under vacuum at room temperature.

Synthesis of TFAA derivatives of nor-nitrogen mustard and BMA

A 1-ml (7 mmol) volume of TFAA was slowly added to a solution containing 0.5 g (2.8 mmol) of nor-nitrogen mustard hydrochloride in 50 ml of toluene. The mixture was heated to 70°C for 20 min and then extracted with phosphate buffer (pH 7.0) to remove any excess of the reagent and acid formed. The organic phase was separated and the toluene was evaporated on a Rotavapor evaporator. The TFAA derivative of the internal standard (BMA) was synthesized in a similar manner. The two derivatives are liquid at room temperature.

Preparation of standard solutions

Standard solutions of the derivatives of TFAA were prepared by dissolving accurately weighed amounts of each derivative in toluene. The solutions were further diluted in toluene to the appropriate concentrations. Standard solutions of the derivatives of TFAA were also prepared using the work-up procedure.

The stability of the standard in light is good and they may be kept in the laboratory at room temperature for months without degradation. The recovery after 2 months for the investigated concentration range (2–300 μg/ml) was 97.6 ± 1.9% (n = 9). The values are given with a 95% confidence limit (Student's t-distribution [10]).

The internal standard used was BMA.

Work-up procedure

To a 25-ml Erlenmeyer flask 5 ml of toluene, 6 mg of nor-nitrogen mustard hydrochloride, 1 μl of BMA and 0.2 ml of TFAA were added. The mixture was immediately shaken for 5 min. The excess of anhydride reagent and acid formed were removed by extraction with 5 ml of phosphate buffer solution (pH 7.0). The toluene layer containing the derivatives was then transferred into a calibrated flask and further diluted with toluene to the appropriate concentrations.

Enrichment

For enrichment the solvent was evaporated under a low flow-rate of nitrogen. The volume was reduced from 1 ml to *ca.* 100 μl or to dryness. The dry residue was dissolved in 100 μl of ethyl acetate.

RESULTS AND DISCUSSION

Standards

The identity of the nor-nitrogen mustard hydrochloride was confirmed by NMR and the purity by titration with perchloric acid. The purity was 99%.

The identities of the TFAA derivatives prepared were confirmed by GC–MS (Fig. 1 and 2) and NMR. The purity was determined using megabore GC–flame ionization detection (FID). The purity was greater than 99%. The purity was further examined by elemental analysis and the percentage composition of carbon, hydrogen and nitrogen are shown in Table I.

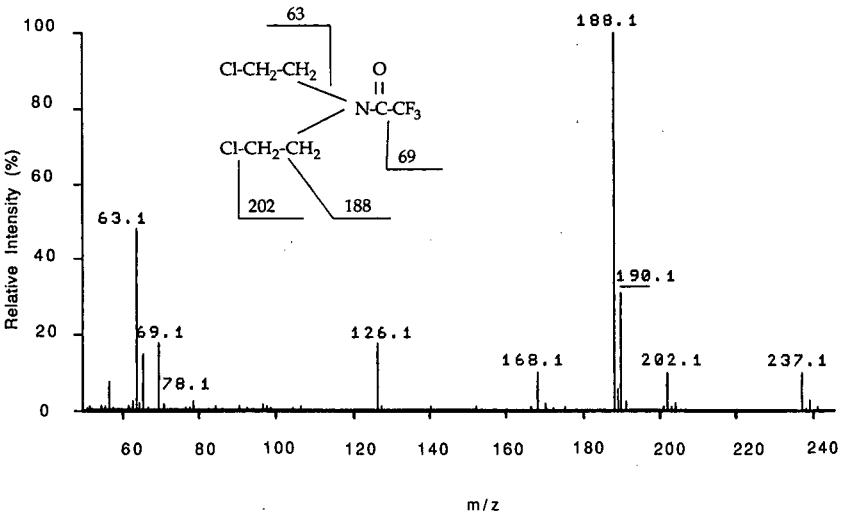

Fig. 1. Mass spectrum of TFAA derivative of nor-nitrogen mustard obtained in the electron-impact mode at an ionization potential of 70 eV.

Internal standard. BMA, di-isobutylamine and di-*n*-butylamine were tested for their suitability as internal standards. Di-isobutylamine and di-*n*-butylamine gave unsatisfactory results. The di-isobutylamine derivative performed differently to nor-nitrogen mustard during the enrichment procedure and the di-*n*-butylamine derivative was not separated from the nor-nitrogen mustard derivative in the GC analysis.

BMA was the best choice as it gave a similar performance to nor-nitrogen mustard hydrochloride during the work-up procedure. In addition, it is not expected to be present in the same working environment as the compound under investigation.

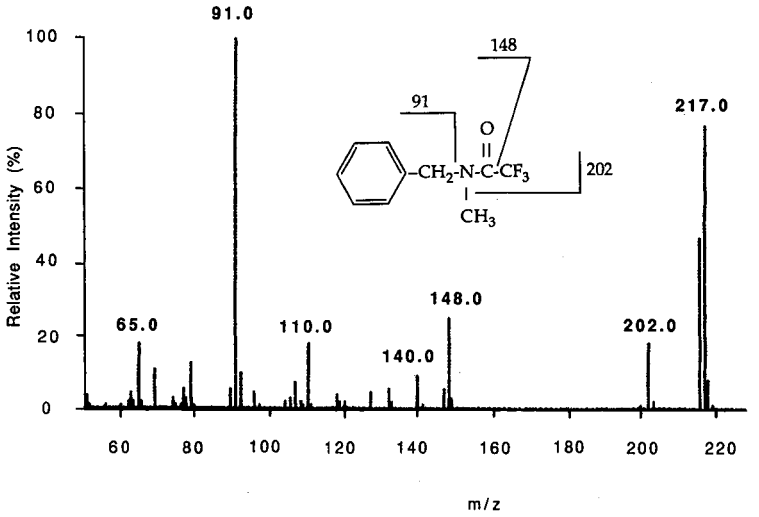

Fig. 2. Mass spectrum of TFAA derivative of BMA obtained in the electron-impact mode at an ionization potential of 70 eV.

TABLE I

ELEMENTAL ANALYSIS OF THE TFAA DERIVATIVES

Agent		C (%)	H (%)	N (%)
Nor-nitrogen mustard derivative	Found	29.77	3.38	5.44
	Calculated	30.27	3.39	5.88
BMA derivative	Found	54.53	4.64	6.20
	Calculated	55.30	4.64	6.45

Work-up procedure

Derivatization. The derivatization reactions with TFAA in toluene were completed within 2 min at room temperature.

Extraction. Excess reagent and liberated acid were removed by extraction with phosphate buffer (pH 7.0). The removal of the excess reagent and acid in the sample increased the lifetime of the megabore column.

The losses during the extraction procedure were studied by comparing the amount of derivatives in toluene before and after the extraction of 1-ml toluene solutions with 1 ml of phosphate buffer. The results at a 95% degree of confidence (Student's *t*-distribution [10]) are shown in Table II.

Enrichment. The derivatives were enriched ten-fold. Evaporation of the solvent to dryness with a gentle flow of nitrogen gave losses of 5–35%. The losses of the nor-nitrogen mustard derivative were the same as for the BMA derivative. To decrease losses, especially for low concentrations, it is better to only reduce the volume, not to evaporate to dryness.

TABLE II

CONCENTRATION OF DERIVATIVES IN TOLUENE BEFORE AND AFTER EXTRACTION WITH PHOSPHATE BUFFER (pH 7.0) AT A 95% DEGREE OF CONFIDENCE

In all cases, $n = 6$.

Agent	Before phopshate buffer extraction (μg/ml)	After phosphate buffer extraction μm/ml)
Nor-nitrogen mustard	1.32 ± 0.04	1.29 ± 0.02
BMA	0.94 ± 0.02	0.92 ± 0.01
Nor-nitrogen mustard	16.8 ± 0.4	16.5 ± 0.3
BMA	7.6 ± 0.1	7.4 ± 0.1
Nor-nitrogen mustard	168.4 ± 0.7	168.5 ± 1.0
BMA	75.6 ± 0.5	75.5 ± 0.5

The accuracy was good after correction for losses with the aid of the internal standard (BMA). For a concentration of 168.4 ± 0.7 μg of nor-nitrogen mustard hydrochloride per ml, a result of 166.6 ± 0.5 μg/ml ($n = 6$) was obtained; for 16.8 ± 0.4 μg/ml, 16.6 ± 0.4 μg/ml ($n = 5$) was obtained; and for 1.32 ± 0.04 μg/ml, 1.49 ± 0.02 μg/ml ($n = 6$) was obtained. The values are given with a 95% confidence range (Student's t-distribution [10]).

Chromatography

The TFAA dervatives of nor-nitrogen mustard and BMA were studied. Both compounds showed excellent chromatographic behaviour using GC–FID. Baseline separation of the two derivatives was evident (Fig. 3). Peaks from impurities in the

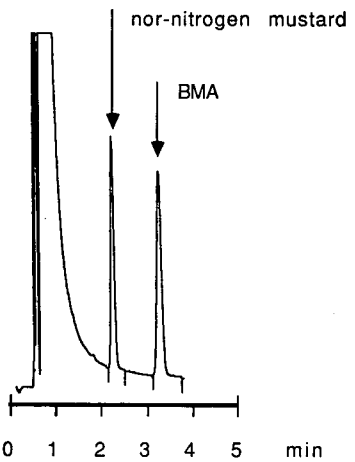

Fig. 3. Gas chromatogram of TFAA derivatives of nor-nitrogen mustard and BMA (injected amounts: nor-nitrogen mustard, 85 ng; BMA, 40 ng). The chromatogram was performed using GC–FID with the on-column injection of 0.5 μl of toluene solution. Megabore column: J&W fused silica coated with DB-1 bonded stationary phase (30 m × 0.53 mm I.D.), film thickness 1.5 μm. Isothermal at 120°C. Carrier gas (nitrogen) at a flow-rate of 15 ml/min. Make-up gas (nitrogen) at a flow-rate of 20 ml/min.

toluene interfered in the determination of low concentrations after the enrichment procedure.

Quantitative analysis

Recovery. The relative overall recovery was studied by spiking toluene solutions and performing the derivatization and work-up procedures as described. The peak areas were corrected with the aid of the internal standard and compared to those of standards using GC–FID. The relative recovery was 96 ± 1.5% (n = 5) for a concentration of 20 μg/ml nor-nitrogen mustard hydrochloride and 100 ± 3% (n = 6) for 200 μg/ml). The values are given with a 95% confidence range (Student's t-distribution [10]).

Calibration graphs. The calibration graph for the nor-nitrogen mustard derivative of TFAA for the concentration range 2–1050 μg/ml in toluene was linear and gave a correlation coefficient of 0.9999 (n = 10 ; y = 2.0863x + 3.627) for a plot of the peak area ratio for ten concentrations.

Detection limit. Using GC–FID the detection limit, calculated as three times the noise level, for the derivative of nor-nitrogen mustard in ethyl acetate where the chromatograms were free from interfering peaks, was less than 0.05 ng of the injected amount. This corresponds to a concentration of 0.1 μg/ml. Small interfering peaks appeared in toluene, giving a detection limit of the order of 0.4 μg/ml.

Preliminary studies have shown that GC with nitrogen–phosphorus detection gives a detection limit in toluene of less than 0.0025 ng of the injected amount. This corresponds to a concentration of 0.005 μg/ml.

The detection limit can be lowered further by enrichment, and an enrichment factor of up to 10 is possible.

Precision. When calculating the precision of procedures involving extraction and enrichment, the addition of an internal standard to the samples before the analysis is strongly recommended. In this study, the internal standard chosen behaves in a similar manner to nor-nitrogen mustard throughout the analytical procedure. The overall precision (relative standard deviation) with the work-up procedure (including weighing, derivatization, extraction and the enrichment procedure) and GC analysis, using BMA as the internal standard, was 1.3% (n = 5) for 20 μg/ml nor-nitrogen mustard hydrochloride spiked in toluene, and 2.8% (n = 6) for 200 μg/ml.

CONCLUSIONS

A GC–FID method has been demonstrated for the determination of nor-nitrogen mustard in toluene or ethyl acetate. The method is based on a derivatization procedure with TFAA. The internal standard (BMA) has the same performance during the analytical procedure as the nor-nitrogen mustard, which results in accurate and precise determinations. The method is sensitive enough for the determination of nor-nitrogen mustard hydrochloride in industrial working environments, *e.g.* in air using a filter sample technique and on surfaces using a wipe sample technique. Further details about the sampling procedures and workplace monitoring are described in a separate paper [6].

ACKNOWLEDGEMENTS

The author thanks Sten Kristensson (Kabi Pharmacia Therapeutics, Helsingborg, Sweden) for the synthesis of nor-nitrogen mustard hydrochloride, Leif Svensson, (Kabi Pharmacia) for the GC–MS analysis and Dr. Jiri Polacek (Kabi Pharmacia) for the NMR and elemental analysis. Professor Roland Akselsson, Department of Working Environment (University of Lund), Dr. Lennart Mathiasson, Department of Analytical Chemistry (University of Lund), Dr. Rolf Lundgren and Dr. Torbjörn Brorson (Kabi Pharmacia) are thanked for valuable discussions and great interest in this work.

REFERENCES

1 M. Sorsa, L. Pyy, S. Salomaa, L. Nylund and J. W. Yager, *Mut. Res.*, 204 (1988) 465.
2 M. Fox and D. Scott, *Mut. Res.*, 75 (1980) 131.
3 E. Balbinder, C. I. Reich, D. Shugarts, J. Keogh, R. Fibiger, T. Jones and A. Banks, *Cancer Res.*, 41 (1981) 2967.
4 W. Au, O. I. Sokova, B. Kopnin and F. E. Arrighi, *Cytogenet. Cel Genet.*, 26 (1980) 108.
5 B. Hartley-Asp and F. Hyldig-Nielsen, *Carcinogenesis*, 5 (1984) 1637.
6 H. Thulin, *Am. Ind. Hyg. Assoc. J.*, submitted for publication.
7 W. J. Irvine and M. J. Saxby, *J. Chromatogr.*, 43 (1969) 129.
8 I. Jardine, R. Brundrett, M. Colvin and C. Fenselau, *Cancer Treat. Rep.*, 60 (1976) 403.
9 I. Jardine, C. Fenselau, M. Appler, M.-N. Kan, R. B. Brundrett and M. Colvin, *Cancer Res.*, 38 (1978) 408.
10 J. C. Miller and J. N. Miller, *Statistics for Analytical Chemistry*, Ellis Horwood, Chichester, 1984, p. 191.

Journal of Chromatography, 547 (1991) 509–515
Elsevier Science Publishers B.V., Amsterdam

CHROM. 23 195

Short Communication

Determination of diclofop-methyl and diclofop residues in soil and crops by gas chromatography

WEIPING LIU*,[a], ZIWEN CHEN, HUIQING XU and YINGYO SHI
Department of Chemistry, Zhejiang University, Hangzhou 310027 (China)
and
YAOZU CHEN
Department of Chemistry, Lanzhou University, Lanzhou 730001 (China)
(First received January 18th, 1990; revised manuscript received February 11th, 1991)

ABSTRACT

A method is described for the determination of residues of the herbicide diclofop-methyl and its metabolite, diclofop, in soil and crops. The residues were extracted with acetone–light petroleum and extracts were concentrated (diclofop was derivatized to its pentafluorobenzyl derivative), and then the products were purified on a chromatographic column containing alumina, silver–alumina and Florisil. Finally, they were determined by gas chromatography using an electron-capture detector. The detection limits of diclofop-methyl and diclofop were between 0.01 and 0.05 mg/kg. The average recoveries were 76.4–97.2% and 72.8–105.2%, respectively, making the method suitable for statutory residue testing purposes.

INTRODUCTION

The selective grass herbicide diclofop-methyl (I), methyl 2-[4-(2,4-dichlorophenoxy)phenoxy]propionate, is the active ingredient of the product Illoxan [1–4]. It is rapidly hydrolysed in the environment to the corresponding acid, diclofop (II), 2-[4-(2,4-dichlorophenoxy)phenoxy]propionic acid [5,6].

Most methods for the determination of diclofop-methyl and diclofop have been developed for water, soil and plant analyses or for formulations, and gas chromatography (GC) and high-performance liquid chromatography (HPLC) are most often used. Diclofop-methyl in formulations can be determined by HPLC [7], but if residue levels are to be detected, *e.g.*, in waters, soils and plants, several GC and HPLC methods [8,9] have been reported. Analysis of soil for diclofop-butyl and diclofop by

[a] Present address: Istituto di Chimica Agraria, Università di Sassari, Via E. De Nicola 10, I-07100 Sassari, Italy.

0021-9673/91/$03.50

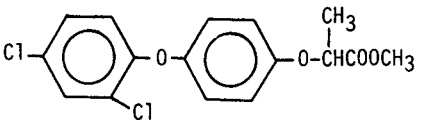

I

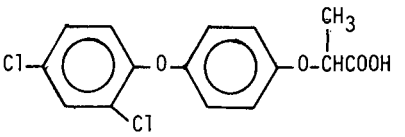

II

GC using electron-capture detection (ECD) has also been reported [10]. The determination of diclofop residues in plants has not been reported. As diclofop-methyl undergoes relatively rapid hydrolysis to the free acid, it is necessary to have methods available for the determination of Diclofop residues in plant and grain.

The procedure developed here for the determination of diclofop-butyl and diclofop residues in soil, leaves of wheat and sugar beet, wheat grain and sugar beet root involves (a) acetone–light petroleum extraction; (b) filtration and concentration; (c) derivatization of diclofop to its pentafluorobenzyl derivative; (d) clean-up on a chromatographic column containing alumina, silver–alumina and Florisil; and (e) GC–ECD. This work is part of a wider study on the movement and degradation of diclofop-methyl and diclofop in Chinese agrosystems [11].

EXPERIMENTAL

Reagents and materials

Light petroleum (b.p. 68–70°C) and other solvents used were of analytical-reagent grade (Hangzhou Oil Refining Plant and Shanghai Chemical Reagent Plant). A pure standard of diclofop-methyl (99.0%) was supplied by Hoechst (Frankfurt/M, Germany). Diclofop was obtained by refluxing Diclofop-methyl for 3 h in 3 *M* sodium hydroxide solution containing sufficient acetonitrile to dissolve the compound. The purity of diclofop was checked by thin-layer chromatography (TLC) and UV and IR spectroscopy. Pentafluorobenzyl bromide was kindly supplied by PCR Research.

Neutral alumina, (200–300 mesh) (Shanghai Wu Si Chemical Reagent Plant) was heated at 500°C for 3 h, cooled to 50°C, mixed with 8 g of water per 100 g and stored in air-tight containers overnight. Silver–alumina was obtained by adding 10 g of neutral alumina (containing 8% of water) a mixture of silver nitrate (0.75 g), water (0.75 g) and acetone (4 ml) and shaking until no smell of acetone remained. Florisil (120–160 mesh) (Floridin, Berkeley Springs, WV, USA) was heated at 650°C for 3 h, cooled to 50°C, mixed with 2 g of water per 100 g and stored in a desiccator overnight.

The samples of soil, leaves of wheat and sugar beet, wheat grain and sugar beet root were obtained by Zhejiang Agricultural University.

Apparatus

A chopper, ultrasonic bath, shaker, water-bath, vacuum pump, 500-ml separating funnels, Kuderna–Danish evaporators and chromatographic columns (15 cm × 1 cm I.D.) for clean-up were used for the sample pretreatment. The GC system consisted of a Shimadzu Model GC-7A gas chromatograph, an ECD-7 nickel-63 electron-capture detector and a C-R1B integration system.

Standard solutions

Stock standard solutions (0.1 g/l) of diclofop-methyl and diclofop in light petroleum were prepared. Working standard solutions were obtained by suitable dilution with light petroleum and stored at 0°C. Fresh solution were prepared every 3 months.

Procedure

After chopping, a representative sample of 10 g was weighed into a 250-ml conical flask.

Extraction of diclofop-methyl. Add 100 ml of acetone–light petroleum (1:1) and 2 g of Celite, place the flask in an ultrasonic bath filled with sufficient water and sonicate for 30 min.

Extraction of diclofop. Add 10 ml of 4 *M* hydrochloric acid and 60 ml of acetone–light petroleum (2:1), place the flask in an ultrasonic bath filled with sufficient water and sonicate for 30 min.

Filtration. Filter the extract through a Büchner funnel fitted with a filter-paper (prewashed with 10 ml of acetone) and transfer the filtrate into a 500-ml separating funnel. Add 100 ml 2% sodium sulphate solution and 50 ml of light petroleum (for extraction of diclofop, add 60 ml of chloroform) and shake. Discard the aqueous layer and wash the organic layer with 50 ml of 2% sodium sulphate solution and 40 ml of 2% sodium carbonate solution.

Dry the organic layer by filtration through 10 g of anhydrous sodium sulphate into a Kuderna–Danish evaporator and concentrate the extract to 5 ml (for the determination of diclofop, concentrate the extract to dryness).

Derivatization of diclofop. Add 2 ml of 2% pentafuorobenzyl bromide in acetone and three drops of triethylamine to the dry residue. Mix and heat at 35°C in waterbath for 1 h in the dark. The reaction is as follows:

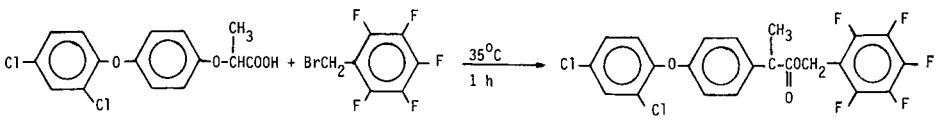

After cooling in ice, add 50 ml of light petroleum and transfer the mixture into a 500-ml separating funnel. Wash the product with 50 ml of 1% hydrochloric acid and then 70 ml of 2% sodium sulphate solution. Transfer the organic phase into a Kuderna–Danish evaporator and concentrate it to 50 ml at 40°C.

Clean-up. Prepack a chromatographic column as described in Tables I and II and prewash the column with 10 ml of light petroleum. Add the sample extract and allow the solvent to settle and run off at the rate of 90–100 drops/min. Elute the

TABLE I

COLUMNS AND ELUENTS FOR CLEAN-UP OF DICLOFOP-METHYL

Sample	Column	Eluent	Volume collected (ml)
Soil	2 g anhydrous Na_2SO_4, 15 g neutral Al_2O_3	50 ml acetone–light petroleum (1:99)	40
Leaves of wheat and sugar beet	2 g anhydrous Na_2SO_4, 15 g neutral Al_2O_3, 2g Ag–Al_2O_3	80 ml acetone–light petroleum (1:99)	50
Wheat grain and sugar beet root	2 g anhydrous Na_2SO_4, 10 g neutral Al_2O_3, 5 g Florisil	80 ml acetone–light petroleum (0.7:99.3)	50

products from the column using the solvents and collecting volumes listed in Tables I and II. Finally, concentrate the collected liquid to 10–50 ml using a Kuderna–Danish evaporator at 40°C.

Determination by GLC–ECD. A glass column (1.6 m × 7.0 mm O.D. × 3.2 mm I.D.) packed with 2% OV-17 on Chromosorb W DMCS (60–80 mesh) was used. The oven temperature was 215°C and the injector and detector temperatures 260°C. The carrier gas was nitrogen at a flow-rate of 60 ml/min and the injection volume was 1 μl.

RESULTS AND DISCUSSION

Under the above chromatographic conditions the chromatograms shown in Figs. 1 and 2 were obtained.

The linearity of ECD was checked by injecting 2-μl aliquots of diclofop-methyl and diclofop (pentafluorobenzyl ester) standard solutions with concentrations ranging from 0.01 to 21.0 mg/l and 0.008 to 46.0 mg/l, respectively. The regression equations for peak area *vs.* amount injected were C (mg/l) $= 0.0041 + 8.59 \cdot 10^{-6} A$ (μV s) ($r = 0.9997$) and C(mg/l) $= 0.0029 + 7.51 \cdot 10^{-6} A$($\mu$V s) ($r = 0.9984$), respectively. The minimum detectable amount of both standards (signals-to-noise ratio = 4) was 0.02–0.016 ng per injection.

TABLE II

COLUMNS AND ELUENTS FOR CLEAN-UP OF DICLOFOP

Sample	Column	Eluent	Volume collected (ml)
Soil	2 g anhydrous Na_2SO_4, 10 g Florisil	70 ml acetone–light petroleum (2:98)	60
Leaves of wheat and sugar beet	2 g anhydrous Na_2SO_4, 2 g neutral Al_2O_3, 8 g Florisil	30 ml acetone–light petroleum (2:98) and 60 ml (1:99)	70
Wheat grain and sugar beet root	2 g anhydrous Na_2SO_4, 4 g neutral Al_2O_3, 8 g Florisil	120 ml acetone–light petroleum (2:98)	80

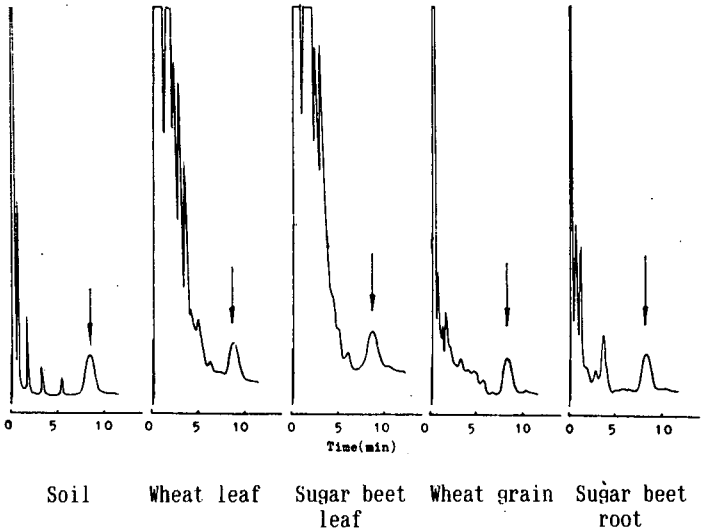

Fig. 1. Chromatograms of diclofop-methyl residues in soil and crops. Residual level in samples, 0.10 mg/kg; final volume, 20 ml; injection volume, 1 μl; detection current, 2.0 nA; range, 10; attenuation, 4.

The detection limits (for real samples) were calculated by using the following equation:

$$\text{Detection limit (mg/kg)} = \frac{\text{minimum detectable amount (ng)}}{\text{injection volume } (\mu\text{l})} \cdot \frac{\text{final volume (ml)}}{\text{sample weight (g)}}$$

The results for various samples are given Table III.

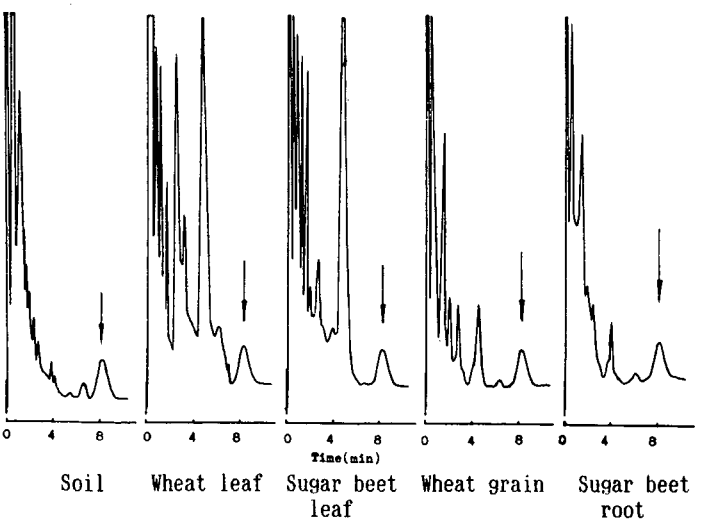

Fig. 2. Chromatograms of diclofop (pentafluorobenzyl ester) residues in soil and crops. Conditions as in Fig. 1.

TABLE III

DETECTION LIMITS FOR VARIOUS SAMPLES

Sample	Detection limit (mg/kg)	
	Diclofop-methyl	Diclofop
Soil	0.01	0.02
Wheat leaf	0.05	0.05
Sugar beet leaf	0.05	0.05
Wheat grain	0.03	0.04
Sugar beet root	0.04	0.04

The recoveries and precisions for diclofop-methyl and diclofop in various samples at three residual levels appeared to be satisfactory (Table IV).

In the study, the detection limit of diclofop as its pentafluorobenzyl ester in soil was 0.02 mg/kg compared with 0.05 mg/kg obtained by Johnstone *et al.* [10] for the methyl ester. The efficiency of conversion of diclofop to its pentafluorobenzyl ester at the 0.10-, 0.36- and 0.72-μg levels was more than 90%.

The average recoveries for diclofop-methyl and diclofop in soil were 88.8% and 76.2%, respectively, which is consistent with the results cited by Schwalbe *et al.* [12] and Johnstone *et al.* [11]. The precisions of the procedure for various samples were satisfactory, the standard deviations being less then 15%.

In conclusion, the described method has high sensitivity and gives high recoveries. It is now used routinely in our laboratory for studies on the movement and degradation of diclofop-methyl and diclofop in Chinese agrosystems and for statutory chemical confirmation of their residue levels in wheat grains and sugar beet. We have found it to be equally suitable for other vegetables and soybean samples.

TABLE IV

RECOVERIES FOR VARIOUS SAMPLES IN A STANDARD ADDITION TEST

Sample	Amount added (mg/kg)	Recovery ± S.D. (%) ($n=5$)	
		Diclofop-methyl	Diclofop
Soil	0.10	86.9 ± 12.7	77.2 ± 7.6
	0.36	95.5 ± 7.1	76.4 ± 10.1
	0.72	83.9 ± 5.4	75.1 ± 9.7
Wheat leaf	0.10	84.8 ± 11.2	78.9 ± 7.0
	0.36	86.5 ± 8.3	79.2 ± 15.5
	0.72	93.3 ± 4.1	90.7 ± 9.8
Sugar beet leaf	0.10	76.4 ± 5.7	78.9 ± 7.2
	0.36	84.6 ± 6.8	80.1 ± 8.1
	0.72	89.3 ± 4.6	81.1 ± 16.9
Wheat grain	0.10	79.2 ± 10.4	72.8 ± 6.6
	0.36	81.0 ± 2.8	103.4 ± 8.8
	0.72	84.6 ± 9.3	105.2 ± 7.7
Sugar beet root	0.10	97.2 ± 8.6	78.5 ± 14.9
	0.36	87.5 ± 6.4	75.8 ± 9.0
	0.72	79.3 ± 7.0	77.3 ± 8.2

ACKNOWLEDGEMENT

This research was supported in part by a grant from Hoechst (Frankfurt/M, Germany).

REFERENCES

1 S. G. Gorbach, K. Kuenzler and J. Asshauer, *J. Agric. Food Chem.*, 25 (1977) 507.
2 J. D. Gaynor, *Can. J. Soil Sci.*, 64 (1984) 283.
3 W. W. Donald and R. H. Shimabukuro, *Physiol. Plant*, 49 (1980) 45.
4 J. A. Dusky, R. H. Davis and R. H. Shimabukuro, *Physiol. Plant.*, 49 (1980) 151.
5 A. E. Smith, R. Grover, A. J. Cessna, S. R. Shewchuk and J. H. Hunter, *J. Environ. Qual.*, 3, 15 (1986) 234.
6 A. Jacobson and R. H. Shimabukuro, *J. Agric. Food Chem.*, 32 (1984) 742.
7 R. W. Stringham and B. R. Bennett, *J. Assoc. Off. Anal. Chem.*, 66 (1983) 1207.
8 T. V. Novitskaya, V. F. Novitskii and A. L. Pensovskii, *Gig. Sanit.*, 10 (1984) 51; *Anal. Abstr.*, (1985) 7D126.
9 W. Liu and Z. Chen, *Huanjing Huaxue*, 7, No. 2 (1988) 42.
10 P. K. Johnstone, I. R. Minchinton and R. J. W. Trucott, *Pestic. Sci.*, 16 (1985) 159.
11 W. Liu, Z. Chen, H. Xu, K. Yu, K. Tang and C. Qiu, *Huanjing Huaxue*, 10, No. 2 (1991) 48.
12 M. Schwalbe, E. Dorn and K. Beyermann, *J. Agric. Food Chem.*, 32 (1984) 734.

Journal of Chromatography, 547 (1991) 516–522
Elsevier Science Publishers B.V., Amsterdam

CHROM. 23 283

Short Communication

Thermal desorption– and sniffing–mass spectrometric monitoring of enriched trace compounds by means of a "live total transfer system"

SIEGFRIED NITZ*, HUBERT KOLLMANNSBERGER, MICHAEL ALBRECHT and FRIEDRICH DRAWERT

Institut für Lebensmitteltechnologie und Analytische Chemie, Technische Universität München, W-8050 Freising-Weihenstephan (Germany)

(First received December 28th, 1990; revised manuscript received March 10th, 1991)

ABSTRACT

A system for thermal desorption of samples obtained by enrichment of airborne chemicals or column effluents is described. The enriched components from the adsorption traps are transferred to the capillary column by a valveless switching system originally developed for multi-dimensional gas chromatography. When applied to flavour analysis (*e.g.* passion fruit), the additional sniffing–mass spectrometry monitoring facility proved to be useful for the detection of sensorially active trace compounds (*e.g.* 7,8-dihydro-β-ionone, β-damascenone). The ease of changing between multi-dimensional gas chromatography operation and thermal desorption allows a maximum of flexibility with regard to different analytical tasks.

INTRODUCTION

The identification of sensorially active trace compounds in complex mixtures such as fruit flavours requires appropriate gas chromatographic (GC) systems and procedures suitable for solving different analytical problems [1]. Multi-dimensional GC (MDGC) in combination with simultaneous sniffing–mass spectrometric (MS) monitoring [2] and different sampling techniques (*e.g.*, liquid injection, dynamic headspace, thermal desorption of samples obtained by enrichment of substances on adsorption traps) have proved to be suitable tools for structure elucidation of sensorially active compounds [1,3,4].

Frequently, when dealing with flavour extracts which, apart from the main constituents, contain numerous compounds at trace levels, enrichment steps are necessary to obtain sufficient amounts for the determination of spectroscopic data (*e.g.*, MS, IR and NMR). Therefore, GC systems for micropreparative enrichment of the effluents from GC capillary columns have been developed in recent years [5–9]. Maxi-

0021-9673/91/$03.50

mum analytical information is obtained if these enriched substances can be analysed in undiluted form, which, in the case of combined GC–spectroscopic systems such as GC–sniffing–MS or GC–Fourier transform IR, is achieved by direct thermal desorption [3] of the sample. When direct sampling of sorption traps is used with capillary columns, special desorption devices are required [3].

This paper describes a thermal desorption facility obtained after minor modifications of a multi-dimensional double-oven system for coupled packed capillary columns. Apart from a flow regulator, no additional equipment is required and, owing to the modular type of construction, multi-dimensional analysis with packed or capillary columns and also direct splitless sampling of sorption traps, containing trapped airborne chemicals or enriched column effluents, into a capillary column can be performed.

SYSTEM DESCRIPTION AND OPERATION

Micropreparative enrichment of sensorially active components

This was performed on a Siemens SiChromat 2 double-oven gas chromatograph equipped with an automatic injection device, sniffing facilities for both column effluents and a micropreparative module for enrichment of capillary GC effluents as described [5].

Preseparation was achieved by splitless injection of 4 μl of passion fruit extract on an SE-54 fused-silica capillary column (20 m × 0.53 mm I.D., film thickness 1.5 μm) programmed from 120 to 200°C at 4°C/min, at a helium flow-rate of 2 ml/min (column I). By means of a valveless Live-T column-switching device, only the peak group of interest (retention range 20–35 min) was entirely transferred into an FFAP fused-silica capillary column (20 m × 0.53 mm I.D., film thickness 1.5 μm) programmed from 100°C (maintained for 20 min) to 190°C at 2°C/min, at a helium flow-rate of 3 ml/min (column II). Cuts into two different precooled sorption traps (packed with 3% OV-101 on Chromosorb W-AW) at retention ranges corresponding to the elution of two compounds of sensorial interest (cut A, 39.8–40.2 min; cut B 41.4–41.7 min) were performed as described (trapping efficiency >90%) [5]. After 34 injection cycles (total analysis time 42.5 h), both traps were analysed by thermal desorption (see below).

Thermal desorption

Thermal desorption was carried out on a Siemens SiChromat 2 double-oven gas chromatograph by replacement of the precolumn in the first oven with a sorption trap (Fig. 1). A constant desorption flow-rate of 20 ml/min through the sorption trap is achieved by means of an orifice-type flow regulator adjusted to a specific helium pressure with pressure regulator PR1. Thermal desorption of enriched volatiles in the sorption trap is achieved by heating the first oven from 30 to 205°C (10 min). The direction of substance flow eluting from the sorption trap depends on the direction of flow in the transfer tube, which is controlled by solenoid valve SV_2 (Fig. 1). The direction of flow in the transfer tube is determined by the differential pressure set on the total transfer system by adjustment of NV1+, NV1− and NV-Dos as described [10,11]. A positive differential pressure (trapping) diverts the substance flow from the sorption tube into the precooled transfer tube (−150°C), whereas a negative differ-

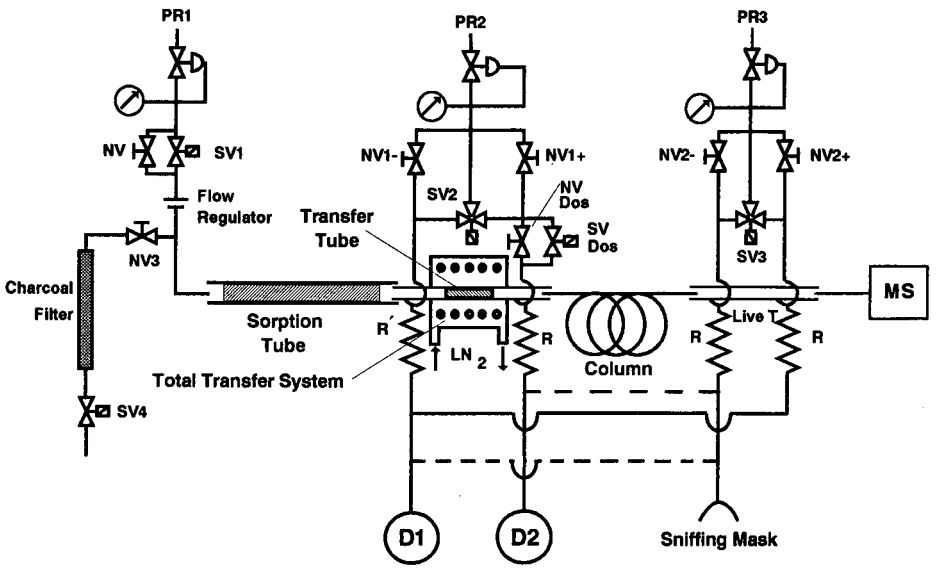

Fig. 1. Schematic diagram of the "live total transfer" system adapted for thermal desorption and GC–sniffing–MS monitoring of sorption tubes containing enriched airborne chemicals or column effluents. PR = Pressure regulator; SV = solenoid valve; NV = needle valve; R = restriction; D = flame ionization detector; LN2 = liquid nitrogen; MS = mass spectrometer.

ential pressure diverts the substance flow to flame ionization detector D1 and the "sniffing mask" via restriction R′ (Fig 1).

After cryofocusing of the volatiles, the transfer tube is heated to 200°C (2 min) in order to "inject" the sample quantitatively into the analytical capillary column. The differential pressure necessary for quantitative transfer (ejection) into the capillary is obtained by opening solenoid valve "Dos". After "injection", the gas flow in the transfer tube is reversed by actuating SV_2 and the sorption tube is backflushed by closing SV1 and opening SV4 (see Fig. 1). During GC separation, the volatiles can be sniffed and simultaneously monitored by the directly coupled mass spectrometer using a Live-T switching device as described [2].

Total transfer system

The transfer tube (1/8-in. glass-lined stainless steel) was packed with 5% SE-30 on Chromosorb G (10 mm packing length). The trapping flow-rate was 20 ml/min, ejection flow-rate 1 ml/min and backflush flow-rate 30 ml/min. Differential pressures were set to +10 mbar for trapping, +1,5 mbar for ejection and −35 mbar for monitoring the substance flow on the flame ionization detector (D1) or backflushing of the sorption tube.

Analytical column

A Carbowax 20M glass capillary column (25 m × 0.3 mm I.D., film thickness 0.3 μm) was used, programmed from 100 to 200°C at 4°C/min. The carrier gas was helium at 1.3 ml/min.

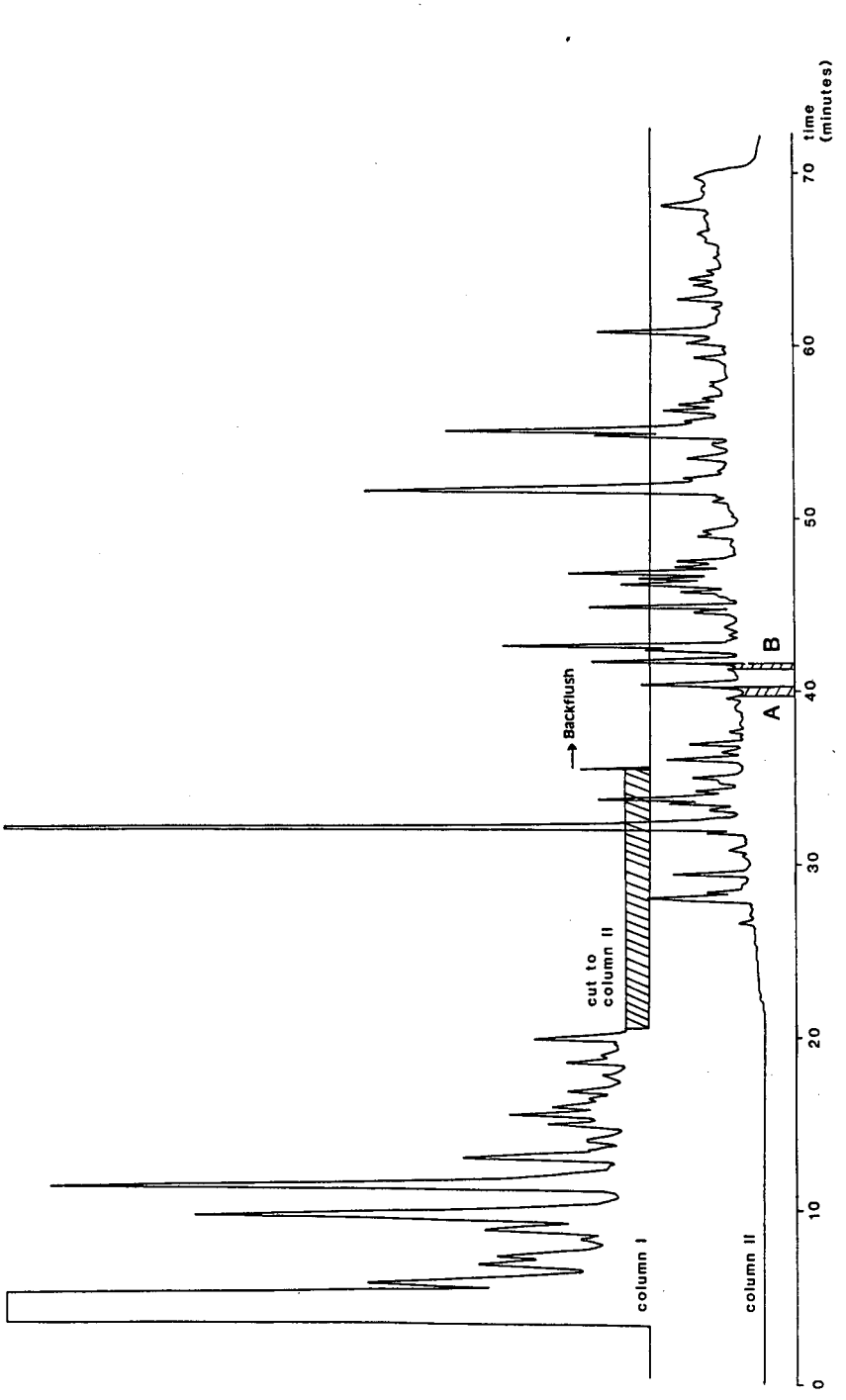

Fig. 2. Gas chromatograms of a passion fruit extract on column I and of the selected cut on column II. Marked areas A and B correspond to the elution ranges of compounds with typical fruity odour impressions (see text).

Mass spectrometer

A Finnigan Model 4021 C quadrupole mass spectrometer operated at 70 eV ionization energy and an ionization chamber temperature of 250°C was used. A mass range from 33 to 400 a.m.u. with a scan cycle time of 0.55 s was recorded.

APPLICATION

An application in the flavour field is given as an example.

GC sniffing analysis of a pentane–diethylether extract from fresh yellow passion fruits, carried out on a Carbowax 20M column, showed "fruity-tropical passion fruit-like" flavour impressions eluting after phenylethyl acetate (retention index *I* 1795–1815), but no positive identification of compounds responsible for these odours could be achieved by GC–MS analysis of the extract. On an SE-54 column (column I), the

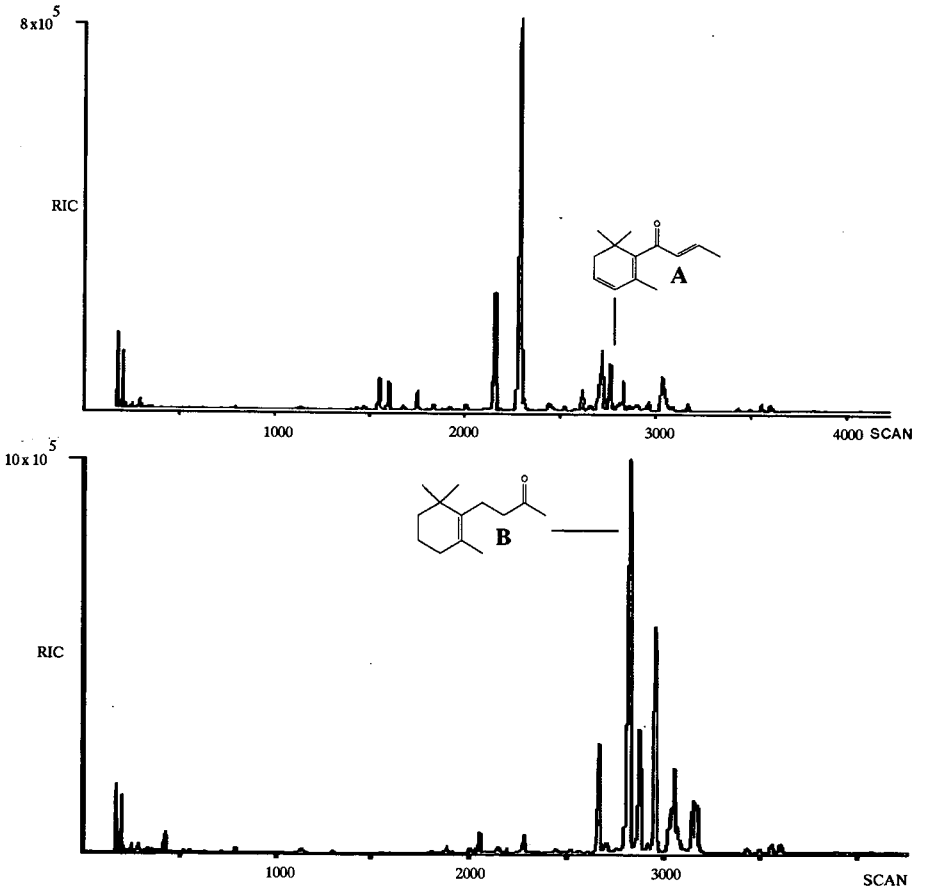

Fig. 3. Reconstructed ion chromatograms (RIC) of thermally desorbed volatiles from sorption tube A (upper trace) and sorption tube B (lower trace). Odorous compounds identified by simultaneous sniffing–MS monitoring: (A) β-damascenone and (B) 7,8-dihydro-β-ionone.

typical odour impressions resembling tropical fruits were recorded near the retention of the major component hexyl hexanoate (*I* 1375–1435). The effluents in this retention range were cut into a FFAP column (column II) and two regions of sensorial interest (A, "fresh fruity, gooseberry-like"; B, "powerful fruity, apricot-like"; see Fig. 2) were enriched on two different sorption traps using the micropreparative system described previously [5].

Thermal desorption of the enriched volatiles and subsequent MS analysis revealed that β-damascenone (A) (see Fig. 3, $R_{I\ CW\ 20\ M}$ 1797, $R_{I\ SE\text{-}54}$ 1380, *m/z* 69, 121, 41, 105, 91, M^+ 190) and 7,8-dihydro-β-ionone (B) (see Fig. 3, $R_{I\ CW\ 20\ M}$ 1807, $R_{I\ SE\text{-}54}$ 1431, *m/z* 43, 121, 41, 93, 161, M^+ 194) were responsible for these flavour impressions. Both volatiles are known ingredients of yellow passion fruit flavour, but could not be detected in our study by direct GC–MS analysis of an extract from nearly 1 kg of passion fruit because of its low concentration level.

Compound B was identified by Winter and Klöti [12] in an extract of 539 kg of yellow passion fruit juice; compound A was detected in yellow passion fruits after distillation for 2 h at pH 3 by Tressl and Engel [13]. Liberation of both C_{13}-norterpenoids from glycosidically bound precursors was presumed [13]. In contrast to our findings, the odour of compound A has been described as "fruity, rose-like" [14]. A "fruity-berry" odour comparable to that detected in the passion fruit extract was also observed during the investigation of cape gooseberry [15]. After micropreparative enrichment, thermal desorption and sniffing–MS monitoring, β-damascenone could also be identified.

CONCLUSIONS

The arrangement described has proved to be invaluable in the GC–MS analysis of compounds present at trace levels, especially in biological systems. A 500–1000-fold increase in the signal-to-noise ratio can be obtained with thermal desorption and splitless transfer on the capillary column as compared with solvent elution of sorption traps containing enriched substances and subsequent splitless liquid sample injection. When applied to the analysis of sensorially relevant components at trace levels, MS monitoring of the eluate in addition to the sniffing facilities is indispensable for identification purposes. If a deliberately unbalanced total transfer system is used, sniffing of the whole eluate and of each separated component can also be performed. In this instance an additional connection of the sniffing mask to D1 or D2 as indicated with dashed lines in Fig. 1 is necessary.

The ease of changing between multi-dimensional operation and thermal desorption allows maximum flexibility with regard to different analytical tasks.

REFERENCES

1 S. Nitz, H. Kollmannsberger and F. Drawert, *J. Chromatogr.*, 471 (1989) 173.
2 S. Nitz, F. Drawert and U. Gellert, *Chromatographia*, 22 (1986) 51.
3 S. Nitz and E. Jülich, in P. Schreier (Editor), *Analysis of Volatiles*, Walter de Gruyter, Berlin and New York, 1984, p. 151.
4 S. Nitz, H. Kollmannsberger and F. Drawert, in P. Schreier (Editor), *Bioflavour'87*, Walter de Gruyter, Berlin and New York, 1988, p. 123.
5 S. Nitz, F. Drawert, M. Albrecht and U. Gellert, *J. High Resolut. Chromatogr. Chromatogr. Commun.*, 11 (1988) 322.

6 J. Roeraade, S. Blomberg and H. D. J. Pietersma, *J. Chromatogr.*, 356 (1986) 271.
7 F. Etzweiler, *J. High Resolut. Chromatogr. Chromatogr. Commun.*, 11 (1988) 449.
8 P. Werkhoff, W. Bretschneider and S. Brennecke, *Gerstel Aktuell*, 12 (1991).
9 J. P. E. M. Rijks and J. A. Rijks, *J. High Resolut. Chromatogr.*, 13 (1990) 261.
10 M. Oreans, F. Müller, D. Leonhard and A. Heim, in P. Schreier (Editor), *Analysis of Volatiles*, Walter de Gruyter, Berlin and New York, 1984, p. 171.
11 S. Nitz, in R. G. Berger, S. Nitz and P. Schreier (Editors), *Topics in Flavour Reasearch*, Eichhorn, Hangenham, 1985, p. 43.
12 M. Winter and R. Klöti, *Helv. Chim. Acta*, 55 (1972) 1916.
13 R. Tressl and K. H. Engel, in G. Charalambous and G. Inglett (Editors), *Instrumental Analysis of Foods*, Vol. 1, Academic Press, New York, 1983, p. 153.
14 R. Kaiser and D. Lamparsky, *Helv. Chim. Acta*, 61 (1978) 2328.
15 R. G. Berger, F. Drawert and H. Kollmannsberger, *Z. Lebensm.-Unters.-Forsch.*, 188 (1989) 122.

Journal of Chromatography, 547 (1991) 523–530
Elsevier Science Publishers B.V., Amsterdam

CHROM. 23 267

Short Communication

Lipophilic character of cardiac glycosides: correlation between R_M values and acute toxicity data in different animal species

G. L. BIAGI*, M. C. GUERRA, A. M. BARBARO and A. SAPONE
Istituto di Farmacologia, Università di Bologna, Bologna (Italy)
and
M. RECANATINI
Dipartimento di Scienze Farmaceutiche, Università di Bologna, Bologna (Italy)
(First received December 10th, 1990; revised manuscript received February 26th, 1991)

ABSTRACT

The R_M for a new series of cardiac glycosides were calculated by means of some of the ΔR_M values previously derived from another series of compounds. The experimental or calculated R_M values of both series of derivatives were correlated with the acute toxicity data (log $1/C$). The slopes of the linear equations for cats, dogs, guinea-pigs and frogs are very close, showing that the dependence of toxicity on the lipophilic character is the same in these animal species.

INTRODUCTION

The R_M values of cardiac steroids have been shown to represent a reliable measure of their lipophilicity [1–3]. In a previous paper [3] we reported the experimental and calculated R_M values for a series of cardiac steroids. The existence of good correlations between chromatographic parameters and *n*-octanol–water partition coefficients has been demonstrated [1–3]. In particular, a number of ΔR_M values were calculated, accounting for the lipophilic contribution of substituent groups either in the steroid skeleton or in the sugar side-chain. The ΔR_M values allowed the calculation of the R_M values of several compounds, which were included in the above correlations. The aim of that work was to collect a set of lipophilicity indices with a view to performing a quantitative structure–activity relationship (QSAR) study of cardiac steroids, as such studies are scarce.

Davydov *et al.* [4], Jinno [5] and Davydov [6] showed a linear relationship between reversed-phase high-performance liquid chromatographic (HPLC) retention

0021-9673/91/$03.50

data of cardiac glycosides and acute toxicity in cats. More recently, Dzimiri and co-workers [2,7] pointed out the influence of the lipophilic character, as expressed by chromatographic parameters, on the ATPase inhibition and the inotropic action on guinea-pig isolated left atria. The purpose of this work was to extend the set of available R_M values of cardiac glycosides in order to study the relationships between R_M values and acute toxicity data [4–6].

EXPERIMENTAL

The thin-layer chromatographic technique has been described previously [3]. Glass plates were coated with silica gel G (E. Merck, Darmstadt, Germany). A slurry of silica gel G was prepared with 0.09 *M* sodium hydroxide solution. A non-polar stationary phase was obtained by impregnating the silica gel layer with silicone DC 200 (Applied Science Labs., State College, PA, USA). The mobile phase was aqueous buffer (sodium acetate–Veronal buffer, 1/7 *M* at pH 7.2), alone or mixed with various amounts of acetone.

The previously reported ΔR_M values [3] were used in order to calculate the R_M values of the compounds listed in Table I. The lipophilic character of the parent structures is expressed by experimental R_M values and the ΔR_M values were used only for the substituent groups. The previously published R_M values of cardiac glycosides and the newly calculated values are reported in Table II. The acute toxicity of cardiac glycosides is due to their arrhythmogenic action causing cardiac arrest.

The classical method for determining the toxicity of cardiac glycosides is based on the continuation of intravenous infusion until cardiac systolic arrest occurs in anaesthetized cats, guinea-pigs, dogs, rabbits or pigs [8]. The smallest dose necessary to produce cardiac arrest in 60–90 min in 100% of the population is determined and the so-called MLD (minimum lethal dose) is calculated per kilogram body weight.

Different kinds of assay methods are used for the determination of lethal doses in non-anaesthetized frogs, mice and rats [8]. In frogs the principle of the assay method depends on the occurrence of cardiac systolic arrest in 1 h, brought about by the cumulative effect of successive increasing doses injected into the lymphatic sac. In mice and rats individual increasing doses are administered i.v. or i.p. After an observation period of 3–14 days, the median lethal dose (LD_{50}) is calculated statistically.

In this work we used the cat MLDs listed by Gisvold [9], Baumgarten [10] and Davydov *et al.* [4,6] or in the NIOSH registry [11]. They are reported in Table II as $\log(1/C)$ values, where C is the MLD expressed in 10^{-6} *M*/kg. In a similar way, Table II reports the $\log(1/C)$ values calculated from the lethal doses measured in guinea-pigs, dogs, frogs, mice and rats by means of the above assay methods [8,10–16].

RESULTS AND DISCUSSION

Jinno [5] examined the data of Davydov *et al.* [4] and showed a good linear relationship between the lipophilic character of sixteen out of a series of seventeen cardiac glycosides and their acute toxicity in cats. The equation was recalculated using the original HPLC $\ln V$ values of Davydov *et al.* [4] and their biological data transformed into log $1/C$ values:

$$\log(1/C) = 1.103\ (\pm 0.042) - 0.161\ (\pm 0.013)\ \ln V \quad (1)$$
$$(n = 16;\ r = 0.958;\ s = 0.060;\ F = 156.0;\ P < 0.005)$$

TABLE I

CALCULATION OF R_M VALUES OF CARDIAC GLYCOSIDES

No.	Compound			Calculation of R_M value: parent structure $(R_M)^a$ ± substituent group(s) $(\Delta R_M)^b$
	Generic name	Genin	Side-chain at C-3-β-OH	
1	Digoxigenin monoglucoside	Digoxigenin	D-Glucose	Digoxigenin (0.98) + glucosyl (−0.18)
17	Acetylneriifolin	Digitoxigenin	L-Thevetose + acetyl	Neriifolin (2.14) + acetyl (0.35)
19	Somalin	Digitoxigenin	D-Cymarose	Digitoxigenin (1.93) + cymarosyl (0.43)
20	Echubioside	Digitoxigenin	D-Cymarose + D-glucose	Digitoxigenin (1.93) + cymarosyl (0.43) + glucosyl (−0.18)
21	Echujin	Digitoxigenin	D-Cymarose + 2 D-glucose	Digitoxigenin (1.93) + cymarosyl (0.43) + 2 glucosyl (−0.36)
18	Diacetylneriifolin	Digitoxigenin	L-Thevetose + 2 acetyl	Neriifolin (2.14) + 2 acetyl (0.70)
8	Digitoxigenin monoglucoside	Digitoxigenin	D-Glucose	Digitoxigenin (1.93) + glucosyl (−0.18)
26	Deslanoside B	Gitoxigenin	3 D-Digitoxose + D-glucose	Lanatoside B (3.12) − acetyl (0.35)
30	Lanatoside E	16-Formylgitoxigenin	3 D-Digitoxose + D-glucose + acetyl	16-Formylgitoxin (2.50) + glucosyl (−0.18) + acetyl (0.35)
34	Hongheloside A	Oleandrigenin	D-Cymarose	Oleandrigenin (1.58) + cymarosil (0.43)
35	Hongheloside C	Oleandrigenin	D-Cymarose + D-glucose	Oleandrigenin (1.58) + cymarosyl (0.43) + glucosyl (−0.18)
36	Honghelin	Oleandrigenin	L-Thevetose	Oleandrigenin (1.58) + thevetosyl (0.21)
32	Urechitoxin	Oleandrigenin	L-Oleandrose + D-glucose	Oleandrin (2.34) + glucosyl (−0.18)
47	Strophanthidin monoglucoside	Strophanthidin	D-Glucose	Strophanthidin (0.94) + glucosyl (−0.18)
41	Convalloside	Strophanthidin	L-Rhamnose + D-glucose	Convallatoxin (1.29) + glucosyl (−0.18)
43	Cheirotoxin	Strophanthidin	D-Gulomethylose + D-glucose	Strophanthidin (0.94) + gulomethylosyl (0.35)[c] + glucosyl (−0.18)
53	Glucoscillaren A	Scillarenin	L-Rhamnose + 2 D-glucose	Proscillaridin (2.15) + 2 glucosoyl (−0.36)
55	Lanatoside D	Gitaloxigenin	3 D-Digitoxose + D-glucose + acetyl	Lanatoside A (3.38) + 16-OH(−0.19) + 12-OH(−1.03)

[a] Experimental R_M values; see ref. 3.

[b] See ref. 3.

[c] As gulomethylose is an isomeric form of rhamnose, the ΔR_M value of the latter was used; see ref. 3.

TABLE II

R_M VALUES AND ACUTE TOXICITY DATA FOR CARDIAC GLYCOSIDES

No.	Compound	R_M	Acute toxicity [log (1/C)[a]]					
			Cat	Dog	Guinea-pig	Frog[h]	Mouse (i.p.)[j]	Rat (i.v.)[j]
1	Digoxigenin monoglucoside	0.80	0.74[b]	–	–	–	–	–
2	Digoxin	2.01	0.53[b]	0.59[g]	−0.01[i]	–	−0.84	−1.50
3	α-Acetyldigoxin	2.27	0.36[c]	–	−0.22[g]	–	–	–
4	β-Acetyldigoxin	2.38	0.35[c]	–	−0.23[i]	–	–	–
5	Lanatoside C	2.19	0.63[b]	–	−0.02[i]	–	−0.85	−1.48
6	Deslanoside C	1.86	0.62[b]	–	–	–	–	–
7	β-Methyldigoxin	2.48	0.48[d]	–	–	–	–	–
8	Digitoxigenin monoglucoside	1.75	0.65[b]	–	–	–	–	–
9	Digitoxigenin monodigitoxoside	2.23	0.27[e]	–	–	–	–	–
10	Digitoxigenin bisdigitoxoside	2.65	0.26[e]	–	–	–	–	–
11	Digitoxin	3.18	0.36[b]	0.18[g]	−0.33[i]	−0.76	−0.71	−0.74
12	α-Acetyldigitoxin	3.54	0.26[b]	–	−0.45[i]	–	–	–
13	β-Acetyldigitoxin	3.53	0.22[c]	–	–	–	–	–
14	Lanatoside A	3.38	0.43[b]	–	−0.05[g]	–	−1.31	−1.22
15	Evomonoside	2.28	0.27[c]	–	–	–	–	–
16	Neriifolin	2.14	0.43[c]	–	–	–	–	–
17	Acetylneriifolin	2.49	0.58[c]	–	–	–	–	–
18	Diacetylneriifolin	2.84	0.02[c]	–	–	–	–	–
19	Somalin	2.36	0.25[b]	–	–	–	–	–
20	Echubioside	2.18	0.37[c]	–	–	–	–	–
21	Echujin	2.00	0.45[c]	–	–	–	–	–
22	Gitoxin	3.00	0.29[b]	–	−0.31[c]	−1.04	–	–
23	α-Acetylgitoxin	3.35	0.20[c]	–	–	–	–	–
24	β-Acetylgitoxin	3.33	0.13[c]	–	–	–	–	–
25	Lanatoside B	3.12	0.40[b]	–	−0.57[g]	–	–	–
26	Deslanoside B	2.77	0.23[b]	–	–	–	–	–
27	Pentaacetylgitoxin	4.59	–	–	–	–	−0.81	−1.33
28	16-Acetylgitoxin	2.93	0.19[b]	–	–	–	−0.92	−1.30
29	16-Formylgitoxin	2.50	0.05[c]	–	–	–	–	–
30	Lanatoside E	2.67	0.23[c]	–	–	–	–	–

31	Oleandrin	2.34	0.46[c]	–	–	−0.59	–	–
32	16-Desacetyloleandrin	2.44	0.25[b]	–	–	–	–	–
33	Urechitoxin	2.16	0.31[c]	–	–	–	–	–
34	Hongheloside A	2.01	0.17[c]	–	–	–	–	–
35	Hongheloside C	1.83	0.31[c]	–	–	–	–	–
36	Honghelin	1.79	0.40[b]	–	–	–	–	–
37	Cymarin	1.34	0.62[b]	0.41[h]	–	−0.33	−1.34	−1.56
38	K-Strophanthin-β	1.02	0.74[b]	0.81[h]	0.03[c]	−0.08	−0.69	−1.29
39	K-Strophanthoside	0.99	0.67[b]	–	0.23[c]	–	–	–
40	Convallatoxin	1.29	0.84[b]	–	0.12[c]	–	−1.26	−1.46
41	Convalloside	1.11	0.51[b]	–	–	–	–	–
42	Desglucocheirotoxin	1.29	0.74[c]	–	–	–	–	–
43	Cheirotoxin	1.11	0.77[b]	–	–	–	–	–
44	Olitoriside	1.28	0.71[f]	–	–	–	–	–
45	Helveticoside	1.21	0.74[g]	–	−0.18[g]	–	−1.16	−2.00
46	Erysimoside	1.03	0.64[c]	–	–	–	–	–
47	Strophanthidin monoglucoside	0.76	0.99[b]	–	–	–	–	–
48	Cymarol	1.19	0.74[b]	–	–	–	–	–
49	Convallatoxol	1.11	0.79[c]	–	–	–	−1.73	−2.00
50	Ouabain	0.53	0.81[c]	1.07[g]	0.36[i]	−0.20	−1.27	−1.53
51	Proscillaridin	2.15	0.53[b]	–	−0.08[i]	–	–	–
52	Scillaren A	1.97	0.54[g]	0.12[h]	0.21[c]	–	–	–
53	Glucoscillaren A	1.79	0.70[c]	–	–	–	–	–
54	Peruvoside	1.68	0.56[c]	–	−0.11[g]	–	–	–
55	Lanatoside	2.16	0.39[c]	–	–	–	–	

[a] where $C = M \times 10^{-6}$/kg.
[b] Ref. 9.
[c] Ref. 10.
[d] Ref. 8.
[e] Ref. 12.
[f] Ref. 4.
[g] Ref. 11.
[h] Ref. 15.
[i] Ref. 13.
[j] Ref. 16.

For the same series of compounds, the R_M values in Table II allowed the calculation of a similar equation:

$$\log(1/C) = 1.010\ (\pm 0.044) - 0.211\ (\pm 0.020)\ R_M \quad (2)$$
$$(n = 15;\ r = 0.945;\ s = 0.069;\ F = 108.0;\ P < 0.005)$$

As the R_M value of corelborin-π was not available in the present chromatographic system, eqn. 2 is based on only 15 compounds.

When considering a larger series of cardiac glycosides and different animal species (Table II), eqns. 3–6 were calculated:

Cat:
$$\log(1/C) = 0.951\ (\pm 0.053) - 0.234\ (\pm 0.024)\ R_M \quad (3)$$
$$(n = 54;\ r = 0.805;\ s = 0.136;\ F = 96.0;\ P < 0.005)$$

Guinea-pig:
$$\log(1/C) = 0.346\ (\pm 0.102) - 0.209\ (\pm 0.044)\ R_M \quad (4)$$
$$(n = 17;\ r = 0.771;\ s = 0.162;\ F = 22.0;\ P < 0.005)$$

Dog:
$$\log(1/C) = 1.069\ (\pm 0.217) - 0.322\ (\pm 0.116)\ R_M \quad (5)$$
$$(n = 6;\ r = 0.812;\ s = 0.241;\ F = 7.72;\ P < 0.05)$$

Frog (*Rana temporaria*):
$$\log(1/C) = 0.083\ (\pm 0.137) - 0.307\ (\pm 0.064)\ R_M \quad (6)$$
$$(n = 6;\ r = 0.923;\ s = 0.156;\ F = 23.1;\ P < 0.01)$$

Although the correlation coefficient in eqn. 3, calculated with 54 compounds, is lower than that in eqn. 2, based on only 15 compounds, it is remarkable that the intercept and slope are similar in the two equations. The exclusion of the four most deviating compounds, *i.e.*, 14, 18, 29 and 34, would increase the correlation coefficient to 0.853. In a similar way, on excluding compounds 14, 45 and 52 from eqn. 4 the correlation coefficient increases to 0.935. In any event, the correlation coefficients in eqns. 3–6 are reasonable when it is considered that one is dealing with data from different laboratories for intact animals.

However, rather than the correlation coefficient for each equation it is more interesting here that the slopes of eqns. 2–6 are very similar. Although great care must be taken in discussing eqns. 5 and 6 on the basis of only six compounds, the similarity of the slopes of eqns. 3–6 shows that the dependence on the lipophilic character is very similar for the four animal species. The closeness of the slope of eqn. 6 to those of eqns. 3–5 is probably due to the fact that the assay method for the frog closely resembles the classical i.v. procedure used in cats, guinea-pigs and dogs. It can be noted that the slopes are negative. As it is well known that generally the relationship between biological activity and lipophilicity is parabolic, one must conclude that in the present instance one is dealing with the descending branch of a parabola. On the other hand, less lipophilic cardiac glycosides are not known.

As regards the intercepts, eqns. 3–6 show that the cat and dog are equally more

susceptible than the guinea-pig and the frog is much less sensitive to this kind of drug. The toxicity data used in calculating eqns. 2–6 were taken from several compilations. Therefore, one could argue that strain and seasonal differences, state of health, diet, etc., might influence the acute toxicity. However, the fact that similar linear relationships were found seems to indicate that lipophilicity plays a basic role, which is not masked by the above sources of variation.

Mice and rats are generally considered to be of little use for measuring the effects of cardiac glycosides because it is always uncertain whether death is due to cardiac arrest or to some extracardiac action, and paralyses and/or convulsions may occur [8]. The only set of homogeneous data on the effects of cardiac steroids in mice and rats seems to be that reported by Foerster *et al.* [16]. However, the acute toxicity data listed in Table II did not show any significant correlation with the R_M values (r = 0.433 in mice; r = 0.570 in rats). Here one should consider also the lipophilic requirements necessary for penetration into the central nervous system.

CONCLUSIONS

The role of lipophilic character in determining the biological activity of cardiac glycosides was questioned by Repke [17]. On the other hand, experimental evidence for a relationship between lipophilicity and *in vivo* and *in vitro* activity has been presented [2,4–7]. The present results confirm that lipophilicity significantly affects the acute toxicity of these compounds, as previously found by Davydov *et al.* [4,6] and Jinno [5]. It is interesting that eqn. 2, calculated with only fifteen compounds, is very similar to eqn. 3 with 54 derivatives. Another important point is that the same relationship holds also for other animal species, such as the guinea-pig, dog and frog, strongly suggesting a similar mechanism leading to the toxic effect. This aspect shows the importance of comparative studies, where the QSAR approach can be very useful in ascertaining the mechanism of action [18]. The lack of any significant relationship for mice and rats depends on the fact that in these animals the acute toxicity of cardiac glycosides is also due to their action on the central nervous system. Finally, this work shows again the usefulness of R_M and ΔR_M values in QSAR studies.

REFERENCES

1 E. Cohnen, H. Flasch, N. Heinz and F. W. Hempelmann, *Arzneim.-Forsch.*, 28 (1978) 2179.
2 N. Dzimiri, U. Fricke and W. Klaus, *Br. J. Pharmacol.*, 91 (1987) 31.
3 G. L. Biagi, A. M. Barbaro, M. C. Guerra, P. A. Borea and M. Recanatini, *J. Chromatogr.*, 504 (1990) 163.
4 V. Ya. Davydov, M. Elizalde Gonzales and A. V. Kiselev, *J. Chromatogr.*, 248 (1982) 49.
5 K. Jinno, *J. Chromatogr.*, 264 (1983) 485.
6 V. Ya. Davydov, *J. Chromatogr.*, 365 (1986) 123.
7 N. Dzimiri and U. Fricke, *Br. J. Pharmacol.*, 93 (1988) 281.
8 H. Bahrmann and K. Greeff, in K. Greeff (Editor), *Cardiac Glycosides: Part I: Experimental Pharmacology*, Springer, Berlin, Heidelberg, New York, 1981, pp. 117–152.
9 O. Gisvold, in C. O. Wilson, O. Gisvold and R. F. Doerge (Editors), *Textbook of Organic Medicinal and Pharmaceutical Chemistry*, Lippincott, Philadelphia, PA, 1966, pp. 693–776.
10 G. Baumgarten, *Die Herzwirksamen Glykosiden*, Georg Thieme, Leipzig, 1963.
11 *Registry of Toxic Effects of Chemical Substances*, NIOSH, Cincinnati, OH, 1985–86.
12 G. Kroneberg, *Naunyn-Schmiedeberg's Arch. Pharmacol.*, 237 (1959) 222.
13 W. Kobinger, B. Wenzel and H. Klupp, *Arzneim.-Forsch.*, 20 (1970) 1862.

14 W. S. Spector (Editor), *Handbook of Toxicology*, Vol. 1, Saunders, Philadelphia, PA, 1956.
15 L. Lendle, in A. Hefter (Editor), *Handbuch der Experimentellen Pharmakologie*, Suppl., Vol. 1, Springer, Berlin, 1935, pp. 11–265.
16 W. Foerster, W. Sziegoleit and I. Guhlke, *Arch. Int. Pharmacodyn.*, 155 (1965) 165.
17 K. Repke, *Trends Pharmacol. Sci.*, 6 (1985) 275.
18 C. Hansch, D. Kim, A. J. Leo, E. Novellino, C. Silipo and A. Vittoria, *CRC Crit. Rev. Toxicol.*, 19 (1989) 185.

Journal of Chromatography, 547 (1991) 531–537
Elsevier Science Publishers B.V., Amsterdam

CHROM. 23 226

Short Communication

Thin-layer chromatographic method for the simultaneous determination of physiological aromatic amino acids

L. SENTIER* and J. MARCHAL
Laboratoire de Microbiologie Industrielle, ENSAIA, 2 Avenue de la Forêt de Haye, 54500 Vandoeuvre-les-Nancy (France)
J. BOUDRANT
CNRS–ENSAIA, 2 Avenue de la Forêt de Haye, 54500 Vandoeuvre-les-Nancy (France)
and
P. GERMAIN
Laboratoire de Microbiologie Industrielle, ENSAIA, 2 Avenue de la Forêt de Haye, 54500 Vandoeuvre-les-Nancy (France)
(First received December 6th, 1990; revised manuscript received February 18th, 1991)

ABSTRACT

A method for the determination of phenylalanine, tryptophan and tyrosine has been adapted from a published method based on thin-layer chromatographic separation on cellulose. The proposed method uses sodium sulphate solution as the migration solvent, which avoids the complete plate coloration that occurs with ninhydrin and leaves only stained spots where amino acids are present. Quantification is performed by densitometry. A linear relationship between amino acid concentration and peak area is obtained for amounts in the range 0.1–1 μg of each amino acid. The method is rapid (25 samples within 6 h), it is specific for aromatic amino acids and it is economical. The main disadvantages are that three standards per plate are needed and that the geometry of the spots is influenced by the ionic strength of the solution, necessitating the preparation of the further standard amino acid solution at a similar ionic strength.

INTRODUCTION

The identification and determination of amino acids and protein sequencing have remained important aspects of biology [1] This group of molecules is also of great importance in clinical biology and pharmacology [2]. Within the nutrition field, essential amino acids play an important role [3] and are considered as industrially interesting metabolites [4]. They include tryptophan, which interposes in brain functioning [5] and which is expensive [4]. Phenylalanine and tyrosine are also of importance and are related. In fact, their biosynthesis is cross-regulated in both prokaryotic

0021-9673/91/$03.50

and eukaryotic cells [6]. This makes the simultaneous determination of these three aromatic amino acids of considerable interest.

The aim of this work was to improve the sensitivity of the thin-layer chromatographic (TLC) method published by Kuhn and Lederer [7] and to adapt it to densitometric determination.

EXPERIMENTAL

Materials

Glass TLC plates (20 × 20 cm) with a cellulose layer 0.1 mm thick were obtained from Merck (Darmstadt, Germany) and tryptophan, tyronsine, phenylalanine and ninhydrin from Fluka (Buchs, Switzerland). The densitometer used was a Shimadzu CS 9000 from Roucaire (Vélizy-Villacoublay, France).

Procedures

A standard solution was prepared dissolving 100 mg of each amino acid in 1 l of distilled water. Volumes of 1–10 μl of the standard or the sample solution were placed with a 20-μl micropipette 2 cm from the edge of the plate every 1.5 cm. Each deposit was performed using small amounts, separated by drying periods. The plates were then placed in a developing tank that had been saturated 1 day before with sodium sulphate solution in distilled water. The ascending mode was used and the migration was stopped when the solvent line reached 12 cm from the sample deposit line. The migration time was about 60–90 min. After drying in an oven at 110°C for 10 min, the spots were revealed by spraying with a 0.3 g in 100 ml solution of ninhydrin in acetone in such a way that the plate was completely wetted. The volume sprayed was about 20 ml. The plates were then incubated at 110°C for 15 min. When the plate had cooled to room temperature, the absorbance of the spots was immediately measured using the densitometric analyser under the following conditions: photo mode, absorbance reflection; scan mode, zig-zag; wavelength, 565 nm; zero set mode; background correction; swing width, 12.0 mm; δy, 0.04 (δy is a parameter of the swing, as noted by the constructor); peak filter, 2; drift line, 0; minimum width, 5.0; minimum area, 5000.0.

RESULTS

Optimization of migration solvent

Because of the reaction of the ammonium sulphate used in the original procedure [7] with ninhydrin, we proposed to replace it with sodium sulphate solution. However, a 1.3 *M* concentration did not give a good separation. Table I shows the R_F values of tryptophan, tyrosine and phenylalanine on plates where the migration step was achieved with sodium sulphate solutions of different concentrations. The optimum value is assumed to give the best separation and to give R_F values below 0.8, in order to avoid interactions between the spots and the solvent front. The optimum sodium sulphate concentration was 0.7 *M*. Fig. 1 shows a plate on which tryptohan, tyronsine and phenylalanine were separated with 0.7 *M* sodium sulphate solution and developed with ninhydrin.

TABLE I

OPTIMIZATION OF THE SODIUM SULPHATE CONCENTRATION OF THE MIGRATION SOLVENT

Other conditions as indicated under Experimental.

Sodium sulphate concentration (M)	R_F values		
	Trp	Tyr	Phe
0	0.5	0.77	0.86
0.5	0.47	0.76	0.83
0.7	0.43	0.71	0.78
0.9	0.38	0.67	0.74
1.3	0.33	0.64	0.68

Densitometric analysis

Fig. 2 shows a chromatogram given by the densitometer under the optimum conditions.

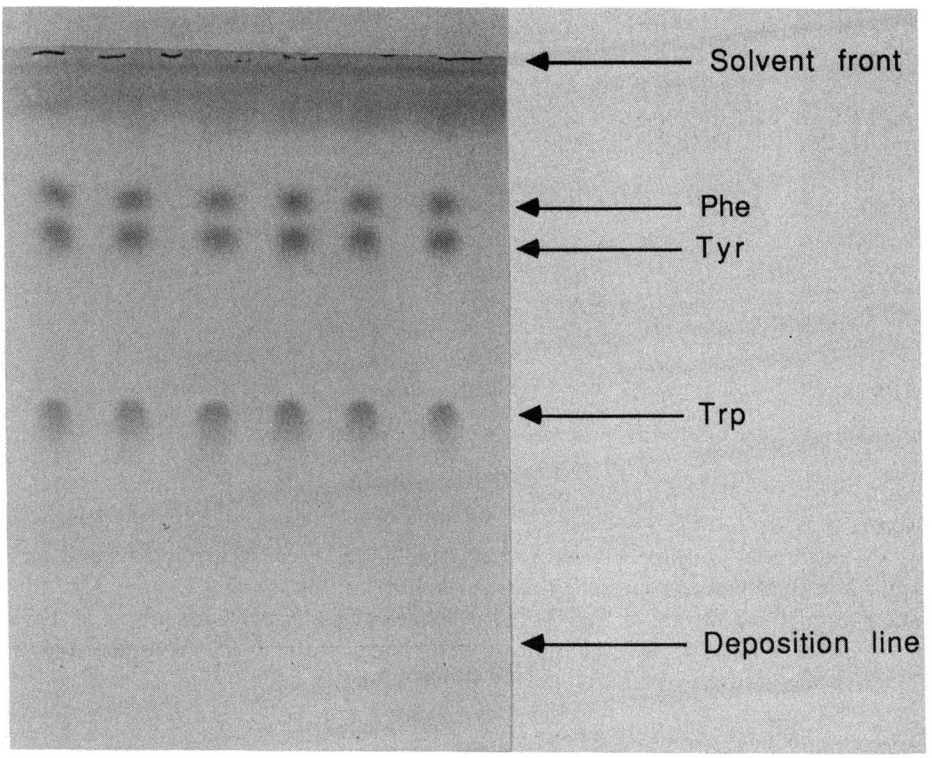

Fig. 1. Separation of phenylalanine, tyrosine and tryptophan in a mixture containing 0.3, 0.4, 0.5, 0.6, 0.7 and 0.8 μg of each amino acid on a cellulose thin-layer plate. Assays were performed as indicated under Experimental.

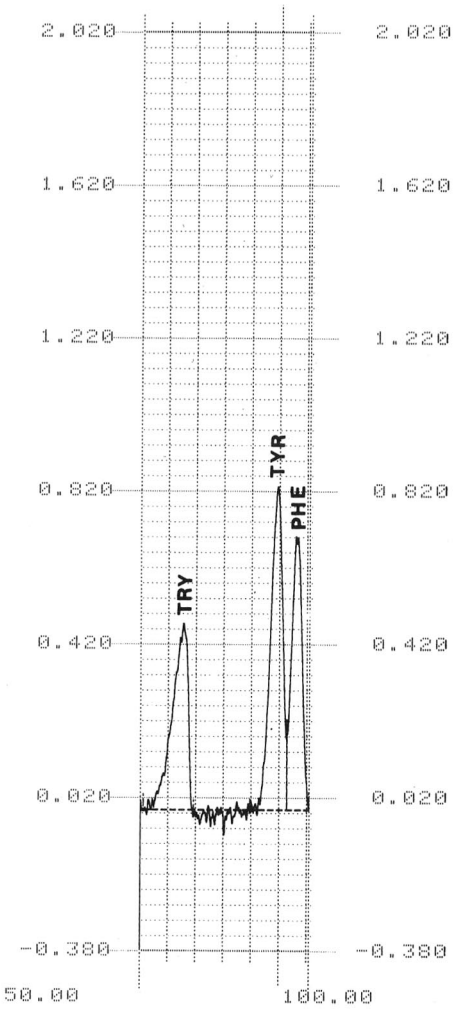

Fig. 2. Example of a chromatogram given by the Shimadzu CS 9000 densitometric analyser.

Linearity

A linear relationship between the amount of each amino acid and the corresponding peak integrated surface area was obtained in the range 0.1–1 μg. The calibration graphs are shown in Fig. 3. Error bars which are arbitrarily fixed at 10% around the integrated area value indicate that the accuracy of the method is below 10% when the amount of amino acids is above 0.2 μg.

Sensitivity and accuracy

The method is able to detect amino acids in amounts down to *ca.* 0.1 μg. As the maximum recommended volume is 10 μl, tryptophan, tyrosine, and phenylalanine can be determined in solutions in concentration down to 10 mg/l.

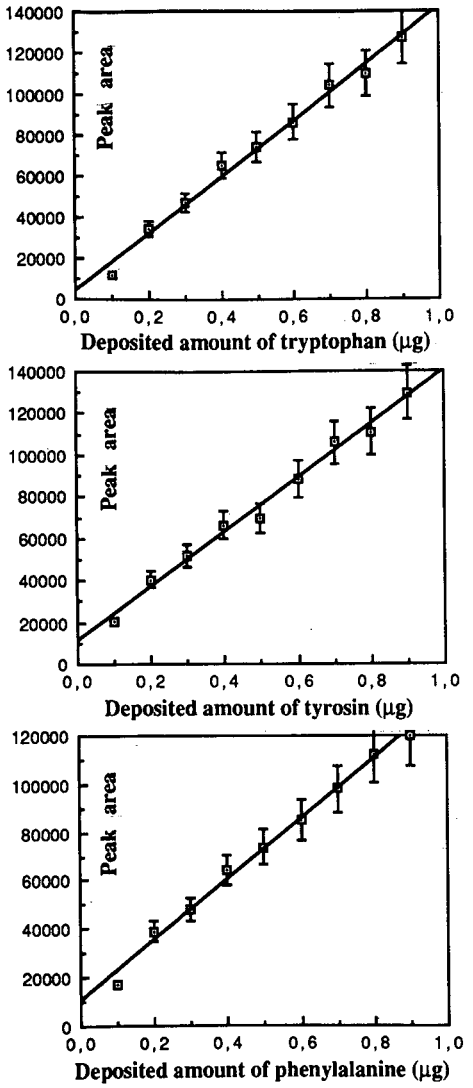

Fig. 3. Calibration graphs obtained for each amino acid. Assays were performed as indicated under Experimental. Error bars around area values are arbitrarily fixed at 10%.

Solutions containing 0.1, 0.4, 0.6 and 1 μg of a mixture of the three aromatic amino acids were spotted four times on a plate and analysed. The average, standard deviation and relative standard deviation of the integrated areas were calculated and the results are given in Table II.

The standard deviation, which is the absolute error, does not depend on the amount of amino acid applied.Thus the relative standard deviation, which is the relative error, increases strongly when the amount decreases. The relative error is below 10% when the amount deposited is up to 0.1 μg, except for tryptophan, because the geometry of the spots increases the integration errors.

TABLE II

STATISTICAL ANALYSIS OF THE RESULTS FOR DIFFERENT AMOUNTS OF EACH AMINO ACID APLLIED

The calculations were made with four deposits for each amount. Assays were performed as described under Experimental.

Amino acid	Statistical parameters[a]	Amount applied (μg)			
		0.1	0.4	0.6	1.0
Tryptophan	μ	18057	55223	73088	132670
	Σ	2547	4304	3669	1175
	Σ/μ (%)	14.1	7.6	5.0	0.9
Tyrosine	μ	26143	65893	86601	131035
	Σ	2939	2393	3834	3460
	Σ/μ (%)	11.2	3.6	4.4	2.6
Phenylalanine	μ	18386	48800	69837	118298
	Σ	1744	1673	1459	1234
	Σ/μ (%)	9.4	3.4	2.1	1.0

[a] μ = Average of the integrated area; Σ = standard deviation; Σ/μ = relative standard deviation.

DISCUSSION

Advantages

In addition of the accuracy and sensitivity which were indicated above, the technique has the following advantages: no treatments are necessary before the chromatographic analysis; only aromatic amino acids are separated because the others remain in the solvent front; the materials that are needed are inexpensive so that this method can be used in routine applications; and is rapid, since two plates (24 samples) can be treated in 6 h. In addition, the densitometer has an automatic analysis function.

Selectivity

The support–solvent system used and the ninhydrin reaction decrease interference problems. However, some molecules from biogenic amines such as dopamine or tyramine have R_F values between those of tyrosine and phenylalanine [2] and could interact in a quantitative determination.

Limitations

Ninhydrin development can differ from one plate to another. Therefore, it is necessary to include three standard solutions at different concentration on each plate, which decreases the number of samples that can be treated per plate. Moreover, ionic strenght can influence the geometry of the spots, particularly for phenylalanine and tyrosine. This requires standard solutions to be prepared at the same ionic strength as the samples.

REFERENCES

1 M. Friedman, in M. Friedman (Editor), *Proteins Nutritional Quality of Foods and Feeds*, Part 1, Marcel Dekker, New York, 1975, p. 423.
2 B. Spring, in R. J. Wurtman and J. J. Wurtman (Editors), *Nutrition and the Brain*, Vol. 6, Raven Press, New York, 1983, p. 232.
3 J. C. Cheftel, J. L. Cuq and D. Lorient, in O. R. Fennema (Editor), *Food Chemistry*, Marcel Dekker, New York, Basle, 2nd ed., 1985, p. 245.
4 B. Tork and Ph. Renault, *Ann. Mines*, Nos. 10–11 (1988) 73.
5 S. G. Potkin, E. Cannoni-Spoor, L. E. Delisi, L. M. Neckers and R. J. Wyatt, *Arch. Gen. Psychiatry*, 40 (1983) 749.
6 E. W. Jones and G. R. Fink, in J. N. Strather, E. W. Jones and J. R. Broach (Editors), *The Molecular Biology of the Yeast Saccharomyces: Metabolism and Gene Expression*, Cold Spring Harbor Laboratory, 1982, Cold Spring Harbor, p. 181.
7 A. O. Kuhn and M. Lederer, *J. Chromatogr.*, 440 (1988) 165.

Journal of Chromatography, 547 (1991) 538–543
Elsevier Science Publishers B.V., Amsterdam

CHROM. 23 255

Short Communication

Separation of opium alkaloids by thin-layer chromatography combined with flame ionization detection using the peak pyrolysis method[a]

NAGARAJ R. AYYANGAR*, SUJATA S. BISWAS and AMRUTA S. TAMBE
National Chemical Laboratory, Pune 411 008 (India)
(First received July 19th, 1990; revised manuscript received February 26th, 1991)

ABSTRACT

A fast, efficient and reproducible method for the separation of the five major opium alkaloids by thin-layer chromatography coupled to flame ionization detection is reported. The alkaloids were separated without derivatization on silica rods of type SII using the partial scanning or peak pyrolysis method —where organic matter separated on the rods are burnt when they pass through the hydrogen flame— between the stages of a two-step development system. The first development, in benzene–acetonitrile–ethyl acetate (60:20:20, v/v) separated narcotine and papaverine. Morphine, codeine and thebaine were separated during the second development in ethyl acetate–benzene–acetonitrile–ammonium hydroxide (25:30:40:5, v/v). The best binary solvent system was benzene–ethanol (9.5:0.5, v/v) and (9:1, v/v) which separated all the five alkaloids simultaneously.

INTRODUCTION

The separation of opium alkaloids is of prime importance in toxicology and forensic and pharmaceutical chemistry. Separations of alkaloids by different chromatographic methods were reviewed by Giplin and Pachla [1,2]. Borke and Kirsch [3] were the first to report the separation of opium alkaloids by thin-layer chromatography (TLC). Misra *et al.* [4] used glass-fibre sheets to separate morphine, codeine and thebaine and some of their metabolites and congeners. Two-dimensional TLC was used by Munier and Meunier [5] to separate five alkaloids on a silica gel plate. Okumura *et al.* [6] separated some opium alkaloids on silica gel sintered sticks, but the sticks had to be rechromatographed to remove excess of diethylamine, which was used as one of the solvents. Recently, Patzch *et al.* [7] have used high-performance

[a] NCL Communication No. 4959.

0021-9673/91/$03.50

TLC to determine morphine, codeine and heroin on silica gel plates with post-column derivatization.

This paper reports a rapid, relatively simple and reproducible method for the separation of the five major opium alkaloids, *viz.*, morphine, codeine, thebaine, papaverine and narcotine (noscapine). TLC coupled with flame ionization detection (FID) combines the efficiency of TLC and the sensitivity of FID. It has the added facility allowing the use of the partial scanning or peak pyrolysis method [8]. Analysis by TLC–FID does not require derivatization of samples and high operating temperatures as in gas chromatography or the use of large volumes of solvent and maintenance of pH as in high-performance liquid chromatography. As little as 2–3 μg of each compound is needed for detection without derivatization.

EXPERIMENTAL

Apparatus

An Iactroscan TH-10 MK III analyser (Iatron Labs., Tokyo, Japan) was equipped with a flame ionization detector and connected to a two-pen linear recorder (National).

Materials

The alkaloids morphine, codeine, thebaine, papaverine and narcotine were obtained from Government Opium and Alkaloids Works Undertaking (Neemmuch, M.P., India).

Procedure

The detector was operated with a hydrogen flow-rate of 160 ml/min and an air flow-rate of 2000 ml/min. The recorder was used at 50–100 mV full-scale deflection. The chart speed was kept at 12 cm/min and the scanning speed at 35 s per scan. A new set of Chromarod SII silica rods (particle size 5 μm) (Newman–Howells, UK) was used throughout.

The alkaloids were dissolved in methanol–dichloromethane (2:1, v/v). Spotting was done in aliquots of 0.25 μl to prevent spreading of the sample on the rod. Calibration was done by spotting different volumes (0.5–3 μl) of standard samples of the same concentration (2 mg/ml). Absolute calibration graphs were drawn for each standard sample as the peak area (abscissa) *versus* spot weight (ordinate). The calibration graphs were linear and the slope was determined using the equation $y = mx$ (y = spot weight in mg; x = peak area and m = slope). The slopes were thebaine = 1, morphine = 0.99, codeine = 0.99 and narcotine = 1.2. The graphs were linear from 1 to 7 μg. As long as analysis and calibration are performed under identical conditions, the calibration graphs can be used to determine directly the weights (in μg) of the components provided that the peak areas of the components are known. When 1 μl of a sample containing a mixture of the alkaloids of concentration12.4 mg/ml was spotted and the peak areas for the different components were determined, the amounts (in μg) could be read directly from the calibration graph.

The alkaloids were separated using the partial scanning method between the stages of a two-step development system; details are given under *Results and Discussion*. Narcotine and papaverine were separated using benzene–acetonitrile–ethyl

TABLE I

R_F VALUES OF OPIUM ALKALOIDS ON CHROMAROD SII SILICA RODS

Solvent system	Composition (%, v/v)	Mode of development	R_F value				
			Morphine	Codeine	Thebaine	Papaverine	Narcotine
Benzene–acetonitrile–ethyl acetate	60:20:20	Two-step development system with peak pyrolysis in between	0.13	0.15	0.18	0.41	0.56
Ethyl acetate–benzene–acetonitrile–ammonia solution	25:30:40:5	As above	0.24	0.33	0.49	–[a]	–[a]
Benzene–ethanol	9.5:0.5 then 9:1	Dual development	0.16	0.23	0.38	0.63	0.70

[a] Burnt during peak pyrolysis.

acetate (60:20:20, v/v) as solvent system in the first step and morphine, codeine and thebaine using ethyl acetate–benzene–acetonitrile–ammonia solution (25:30:40:5, v/v) in the second step.

Dual development with benzene–ethanol (9.5:0.5 and 9:1, v/v) effected the simultaneous separation of the five opium alkaloids.

RESULTS AND DISCUSSION

The R_F values of five major alkaloids on Chromarod SII silica rods are given in Table I. Binary and multi-component solvent systems involving one- or two-step development systems were employed. The best multi-component solvent system involving peak pyrolysis between two-step development and a binary system which effects the separation of all five opium alkaloids simultaneously is reported. Results obtained by quantitative analysis are given in Table II.

TABLE II

QUANTITATIVE ANALYSIS OF A MIXTURE OF OPIUM ALKALOIDS

Alkaloid	Peak area[a]	Amount applied (μg)	Amount found (μg)[b]	Recovery (%)	Standard deviation of peak area[a]
Narcotine	52.4	3.77	3.75	99.4	3.0
Thebaine	41.1	2.12	2.10	99.05	4.7
Codeine	68.7	3.01	3.00	99.6	4.3
Morphine	77.9	3.51	3.50	99.7	1.8

[a] Mean of six determinations.
[b] From calibration graph.

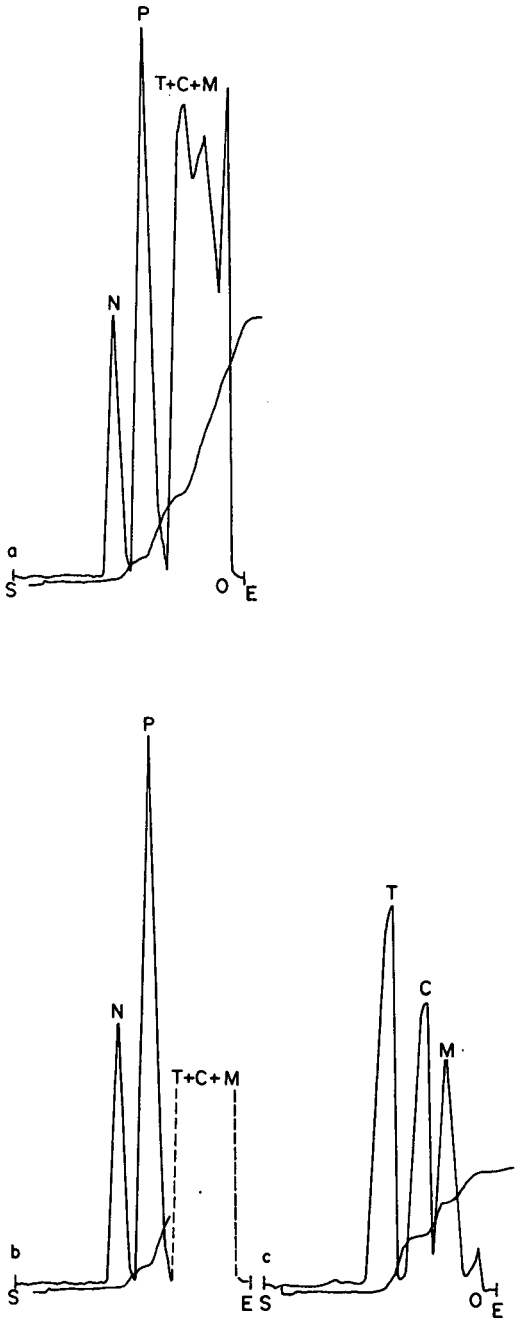

Fig. 1. Two-step development for separation of opium alkaloids on Chromarods SII. (a) Complete scan of the five opium alkaloids developed with benzene–acetonitrile–ethyl acetate (60:20:20, v/v); (b) partial scan; (c) development with ethyl acetate–benzene–acetonitrile–ammonia solution (25:30:40:5, v/v) resolved the forked peak into morphine, codeine and thebaine. P = Papaverine; N = narcotine; T = thebaine; C = codeine; M = morphine.

The fastest migrating alkaloid was narcotine, followed by papaverine, thebaine, codeine and morphine. This pattern of elution was constant for both binary and multi-component systems. It should be noted that in the figures the direction of development is from right to left and the scanning direction is from left to right. Hence, narcotine, which is the fastest moving compound, elutes as the first peak and morphine, which is very sluggish, elutes as the last peak. S and E denote the start and end of the scans, respectively, and **O** is the point of sample application.

The quaternary system suggested by Steele [9] was investigated. This system consists of ethyl acetate–benzene–acetonitrile–ammonia solution in different ratios such as (a) (50:30:15:15, v/v) and (b) (25:30:40:5, v/v). System (a) gave only a moderate separation of morphine, codeine and thebaine and no separation of narcotine and papaverine. However, system (b) resolved the peaks of morphine, codeine and thebaine well, but there was no change in the separation of papaverine and narcotine. We therefore concluded that a less polar system such as benzene–acetonitrile–ethyl acetate (60:20:20, v/v), might give a clean separation of narcotine and papaverine. Hence, a two-step development sequence with the partial scanning or peak pyrolysis method could be a successful approach to this problem.

The first development was done with benzene–acetonitrile–ethyl acetate (60:20:20, v/v). This resulted in the fastest migrating compounds, *i.e.*, narcotine and papaverine, to migrate into the upper part of the rod, morphine, codeine and thebaine remaining near the point of application and appearing as a forked peak, as can be seen in Fig. 1a. The scan stop screw was then set at a point between the resolved and unresolved compounds and the remaining rods were partially scanned, as shown in Fig. 1b. In this way, narcotine and papaverine were determined and this part of the rod was reactivated so that a second development could be performed with a more

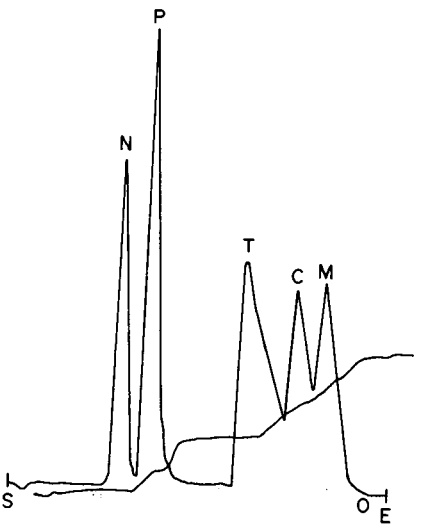

Fig. 2. Simultaneous separation of the five major alkaloids of opium on Chromarods SII developed twice with benzene–ethanol (9.5:0.5 and 9:1, v/v). P = papaverine; N = narcotine; T = thebaine; C = codeine; M = morphine.

polar solvent system, taking the unresolved compounds (morphine, codeine and thebaine) as the new origin. The second development of the rods was done with ethyl acetate–benzene–acetonitrile–ammonia solution (25:30:40:5, v/v), which gave a good separation of morphine, codeine and thebaine (Fig. 1c). The rods in both these systems were developed up to 10 cm for a period of 35 min each and scanned at 35 s per scan. A dual development with a binary system consisting of benzene–ethanol (9.5:0.5 and 9:1, v/v) effected the simultaneous separation of all the five alkaloids (Fig. 2).

CONCLUSION

All five major opium alkaloids could be separated without derivatization on Chromarod SII silica rods using partial scanning or peak pyrolysis between the stages of a two-step development system. The first development with benzene–acetonitrile–ethyl acetate (60:20:20, v/v) helps to move the less polar compounds away from the point of application. The remaining unresolved compounds are then separated with a more polar solvent system, ethyl acetate–benzene–acetonitrile–ammonia solution (25:30:40:5, v/v). The best binary solvent system was benzene–ethanol (9.5:0.5 and 9:1, v/v), which could separate all five alkaloids simultaneously.

REFERENCES

1 R. K. Gilpin and L. A. Pachla, *Anal. Chem.*, 57 (1985) 29R.
2 R. K. Gilpin and L. A. Pachla, *Anal. Chem.*, 61 (1989) 191R.
3 M. L. Borke and E. R. Kirsch, *J. Am. Pharm. Assoc.*, 42 (1953) 627.
4 A. L. Misra, R. B. Pontani and S. J. Mule, *J. Chromatogr.*, 71 (1972) 554.
5 R. L. Munier and S. Meunier, *Chromatographia*, 13 (1980) 259.
6 T. Okumura, T. Kadano and A. Iso'o, *J. Chromatogr.*, 108 (1975) 329.
7 K. Patzsch, W. Funk and H. Schuetz, *GIT, Suppl.*, 3 (1988) 85 and 88.
8 R. G. Ackman and A. D. Woyewoda, *J. Chromatogr. Sci.*, 17 (1979) 514.
9 J. A. Steele, *J. Chromatogr.*, 19 (1965) 300.

Journal of Chromatography, 547 (1991) 544–550
Elsevier Science Publishers B.V., Amsterdam

CHROM. 23 359

Short Communication

Improved capillary zone electrophoretic separation of basic proteins, using a fluorosurfactant buffer additive[a]

ÅSA EMMER, MÅRTEN JANSSON and JOHAN ROERAADE*
Royal Institute of Technology, Department of Analytical Chemistry, S-100 44 Stockholm (Sweden)
(First received February 8th, 1991; revised manuscript received April 9th, 1991)

ABSTRACT

In this paper, a new method to reduce the adsorption of basic proteins in capillary zone electrophoresis is described. Small amounts of a cationic fluorosurfactant are added to the running buffer. This leads to a surface charge reversal. Consequently, proteins at a pH below their p*I* are repelled from the wall. High efficiencies and symmetrical peaks were obtained for a number of model proteins, even when running buffer solutions with a low ionic strength were employed. Reproducibility was excellent. It is believed that the extreme hydrophobic nature of the fluorocarbon chain of the surfactant is a significant factor for the improved performance.

INTRODUCTION

Capillary zone electrophoresis (CZE) is rapidly becoming an important tool for the separation of biomolecules like peptides and proteins. During the last few years, intensified research has scored impressive results in terms of speed, resolution and detectability. A key problem in protein separation, which was already pointed out by Jorgenson *et al.* in one of their early reports [1], is the tendency of these molecules to adsorb on the surface of the capillary tubing. The often employed fused-silica tubing has a negatively charged surface due to the presence of silanol groups, which attract the positively charged sites of proteins by electrostatic force. This seriously impairs the separation efficiency.

Several solutions have been proposed to circumvent this problem. Lauer and McManigill [2] suggested the use of a carrier medium with a pH above the p*I* of the proteins. Under such conditions, proteins have a net negative charge and are then repulsed from the wall by coulombic forces. Other approaches have been to increase

[a] Presented as a last-minute poster at the *3rd International Symposium on High Performance Capillary Electrophoresis, San Diego, CA, February 3–6, 1991.*

0021-9673/91/$03.50

the ionic strength of the buffer, using conventional salts [3] or zwitterions [4]. A different route to reduce the adsorption of proteins is by the action of suitable hydrophilic surface modifiers, such as polyacrylamide [5], polyvinylpyrrolidone [6], polyethylene glycol or maltose [7], which are covalently linked to the surface silanol groups via an organosilane coupling agent. Also a modifier with a terminal arylpentafluoro ligand [8] has been reported for surface deactivation. Recently Gordon *et al.* [9] have proposed an alternative method involving adding ethylene glycol to the protein samples.

Although some workers have demonstrated that it is possible to obtain high efficiencies (in excess of 500 000 theoretical plates/m), such results have been obtained under restrained conditions (such as extreme pH or by using a separation media with a high ionic strength). Swedberg for example [8] used high buffer concentrations, (in some cases also with additional salt). This leads to an extended analysis time (decreased electroosmotic flow) and an increased joule heat generation. The latter necessitates the use of very narrow bore tubing, which, in its turn, demands high analyte concentrations, due to a decreased detectability.

The possibility of being able to use buffers with a low ionic strength, at a freely adjusted pH, is very desirable since this would allow us to match the running conditions to the practical situation, and thus enable us to reduce the risk of protein denaturation, while keeping the necessary degree of freedom to tune selectivity. In order to achieve the best possible result, the coulombic interactions with the surface must be reduced to an absolute minimum.

In the present report, we describe a simple method, where we propose the use of a fluorinated cationic surfactant as an additive. Due to a surface charge reversal as well as a charge interaction with the analytes, basic proteins are repelled by the silica surface, even in neutral pH solutions of low ionic strength. This is demonstrated with some model compounds.

EXPERIMENTAL

Apparatus

The apparatus used consisted of a high voltage d.c. power supply (Model 225, Bertan Assoc., Hicksville, NY, USA) delivering up to +/− 30 kV, and a UV detector (Model 206, Linear Instruments, Reno, NV, USA). The other parts were custom made: a plexiglass box with a safety interlock and an injection device, comprising an electronic timer for controlled electromigration injection. Provisions were also made to allow an *in situ* flushing of the capillaries by action of pressurized air (0.5–1.0 bar). Electropherograms were recorded on a Chromatointegrator (Hitachi, Tokyo, Japan).

Materials and reagents

Fused-silica capillary tubing (360 μm O.D. and 50 μm I.D.) was obtained from Polymicro Technologies (Phoenix, AZ, USA). The total length of the capillaries used was 100 cm and the length from the injector to the detector was 90 cm. The fluorosurfactant Fluorad FC 134 was obtained from 3M Company (St. Paul, MN, USA). The chemical structure of this material is shown in Fig. 1. Buffer solutions were prepared from boiled, de-ionized water, that was passed through a Milli-Q system (Millipore, Bedford, MA, USA), and were filtered before use. Myoglobin, ribonuclease and

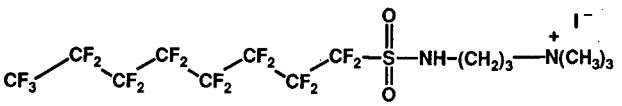

Fig. 1. General structure of Fluorad FC 134.

lysozyme were purchased from Sigma (St. Louis, MO, USA). Cytochrome *c*3 was a gift from the Department of Biochemistry and Biotechnology, Royal Institute of Technology (Stockholm, Sweden).

Stock protein solutions were prepared for each protein in 0.05 *M* phosphate buffer with a protein concentration of 10 mg/ml, except for cytochrome *c*3, which was prepared in 0.02 *M* (pH 7) 3-(N-morpholino)propanesulphonic acid (MOPS) buffer at a concentration of 1.0 mg/ml [10]. All solutions were stored in a freezer. The protein samples for the analyses were freshly prepared from the stock solutions in running buffer, containing FC 134 additive. Protein concentrations ranged from 0.12 to 0.22 mg/ml.

Sample injection was accomplished by electromigration. A reversed polarity setup was employed, where the capillary inlet was kept at negative potential, while the detector side of the capillary was grounded.

RESULTS AND DISCUSSION

When basic proteins are separated at a pH below their isoelectric points, they obtain a net positive charge, and are then strongly adsorbed onto the wall of silica tubing. When an anionic surfactant like sodium dodecyl sulphate (SDS), is added to the buffer solution, adsorption is suppressed due to a competing interaction with the cationic sites of the protein, and also by interaction between the hydrophobic parts of surfactant and the protein [11]. Unfortunately, the effectiveness of this approach seems to be rather modest. It has proven to be more suitable when dealing with smaller molecules like peptides, particularly in the form of micellar chromatography, where both charged and uncharged solutes can be separated, *e.g.* [12–14].

Also cationic surfactants like dodecyl and hexadecylmethylammonium salts have been used in micellar chromatography [14–16]. These compounds adsorb on the silicious surface and cause a drastic change in electroosmotic behavior [17–19]. This is initiated by an electrostatic attraction between the positively charged head groups and the negatively charged $Si-O^-$ groups [20]. Thus, the non-polar chains of the surfactant will form a hydrophobic layer. The chains will eventually be oriented in a perpendicular position at some saturation concentration, and the negative surface charge will be completely neutralized. The Stern potential is thereby reduced to zero and the electroosmotic flow is inhibited.

At still higher surfactant concentrations, an admicellar structure, consisting of a bilayer is formed by hydrophobic interaction between the non-polar chains. The cationic sites of the second adhering surfactant molecules are now faced towards the buffer solution, resulting in a positive surface charge, and a reversal of the electroosmotic flow direction (*cf.* Fig. 2). At the same time, electrophoretic migration of the proteins will occur in the opposite direction.

An important advantage of the charge reversal is that proteins at a pH below

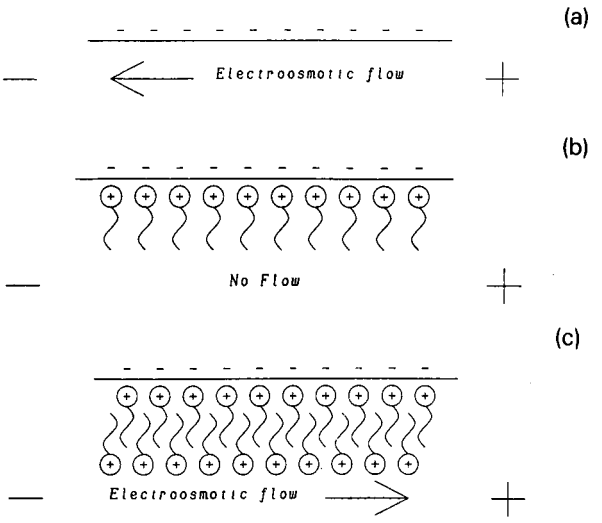

Fig. 2. (a) No surfactant added. Electroosmotic flow in normal direction. (b) Electrostatic adsorption of the positively charged surfactant headgroups to the negative silanol groups on the silica surface of the capillary inner wall. (c) Admicellar bilayer formation by hydrophobic interaction between the apolar chains, resulting in a reversal of the electroosmotic flow.

their p*I* will be repelled from the surface. Interactions between the surfactant and the proteins can enhance this effect. Addition of a suitable cationic surfactant to the running buffer may therefore be an effective approach to improve the separation of basic proteins at physiological pH values. This was experienced in our experiments. Fig. 3 shows an example of an electropherogram of four basic proteins. High efficiencies (Table I) were obtained for all compounds. Additionally, the reproducibility of the electrophoresis, in spite of the fact that a non-thermostated system was employed, is excellent (Table II), which is a further indication of the suppressed adsorption.

The migration order of the proteins is reversed compared to what is commonly observed. The most positively charged protein (lysozyme) appears as the last peak in the electropherogram. This is due to the fact that the transport rate of the proteins is dominated by the reversed electroosmotic flow towards the anode, while they migrate in the opposite direction by electrophoresis.

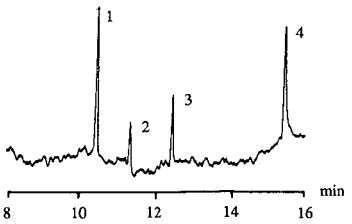

Fig. 3. Electropherogram of four model proteins. 1 = Myoglobin, 2 = ribonuclease A, 3 = cytochrome *c*3, 4 = lysozyme. Running buffer: 0.05 *M* phosphate (pH 7) with 100 μg/ml FC 134 added. Separation voltage: −30 kV. Current: 70 μA. Protein concentration: 0.22 mg/ml except for cytochrome *c*3 which is 0.13 mg/ml. Injection: electromigration at −15 kV for 10 s. UV detection: 230 nm.

TABLE I

EFFICIENCY FOR FOUR PROTEINS RUN IN BUFFER SOLUTION CONTAINING FC 134, BUFFER STRENGTH 0.05 *M*

Protein	Efficiency (plate number, *N*)	Mol. wt.	p*I*
Myoglobin (horse heart)	240 000	17 500	7.3
Ribonuclease A (bovine pancreas)	287 000	13 500	9.3
Cytochrome *c*3 (ref. 20)	542 000	14 300	9.5
Lysozyme (egg white)	372 000	14 000	11

The electroosmotic flow was rather large, as determined from the migration time of mesityl oxide, which passed the detector almost at the same time as myoglobin. The magnitude of the electroosmotic flow is of course dependent on several parameters, like pH, type of buffer, etc. We are presently investigating the influence of these parameters on the separation performance.

The moderate buffer strength and the surfactant concentration, used in the separation, shown in Fig. 3 can be further reduced, without any adverse effects on the separation and with maintained efficiency and excellent peak symmetry (Fig. 4 and Table III).

We believe that the observed effectiveness of deactivation is to an important extent due to the particular chemical nature of the surfactant. The hydrophobic chain of our additive has an extremely non-polar character, due to the presence of the fluorine atoms. This will enhance the stability of the bilayer. Compared to surfactants with a hydrocarbon chain, a more dense layer can be expected, since fluorinated chains pack more tightly [21].

A well known aspect of surfactants, when added to protein solutions, is their tendency to cause denaturation. In fact, a compound like SDS is used for this purpose in gel electrophoresis. Denaturing, induced by detergents is a complicated interplay, and is dependent on the character of the surfactant, the protein and the environment. The surfactants influence the protein conformation either by disrupting ion–ion bindings or by hydrophobic associations. This usually leads to a loss in biological activity, which is undesirable if subsequent bioassays are to be carried out with the separated materials.

TABLE II

REPRODUCIBILITY OF MIGRATION TIMES

$\bar{t}$ = mean time of migration; R.S.D. = relative standard deviation.

Protein	Within day		Day-to-day	
	$\bar{t}^a$ (min)	R.S.D. (%)	$\bar{t}^a$ (min)	R.S.D. (%)
Myoglobin	10.4	0.43	10.2	1.7
Ribonuclease A	11.2	0.45	11.1	1.5
Cytochrome *c*3	12.3	0.45	12.4	1.7
Lysozyme	15.1	0.67	15.5	2.4

[a] $n = 7$.

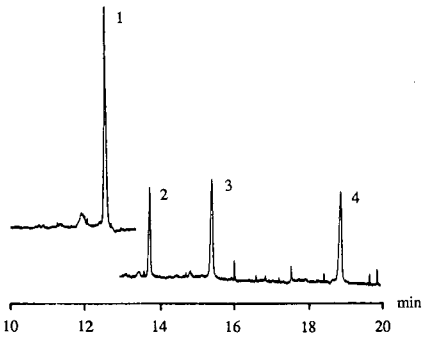

Fig. 4. Electropherogram of four model proteins (myoglobin run separately). 1 = Myoglobin, 2 = ribonuclease A, 3 = cytochrome *c*3, 4 = lysozyme. Running buffer: 0.01 *M* phosphate (pH 7) with 50 μg/ml FC 134 added. Separation voltage: −30 kV. Current: 11 μA. Protein concentration: 1.7 mg/ml for myoglobin, 0.20 mg/ml for ribonuclease A and lysozyme, 0.12 mg/ml for cytochrome *c*3. Injection: electromigration at −20 kV for 10 s and at −5 kV for 5 s for myoglobin. UV detection: 230 nm.

In this context, our additive has several favorable properties. It has been shown that the chemistry of the surfactant head group is very important for the ability to denaturate [22,23]. Some cationic surfactants do denature proteins [24], while surfactants with sterically hindered head groups, (like the nitrogen with the surrounding three methyl groups in FC 134) act by no means as potent as those with less bulky ligands. Also, on the whole, the denaturating behavior of cationic surfactants is usually lower than that of anionic compounds [24]. Finally, the fluorinated chain of the surfactant is very important. Fluorocarbons are well known for their biocompatibility. In fact, certain fluorocarbon liquids have been used as blood substitutes [25]. Due to the lipophobic behavior of the fluorinated chain, interaction with the hydrophobic part of proteins should be minimal. Instead, the excess surfactant will form non-interacting ("neutral") micelles. This occurs already at very low concentrations [the critical micellar concentration (CMC) in water is about 10 ppm according to the manufacturer]. It is therefore not unrealistic to assume, that the biological activity of proteins may be relatively unaffected in our proposed separation method. We are presently investigating this, as well as the applicability of other fluorinated surfactants.

TABLE III

EFFICIENCY FOR FOUR PROTEINS RUN IN BUFFER SOLUTION CONTAINING FC 134, BUFFER CONCENTRATION 0.01 *M*

Protein	Efficiency (*N*)
Myoglobin	352 000
Ribonuclease A	337 000
Cytochrome *c*3	283 000
Lysozyme	370 000

CONCLUSIONS

(1) Capillary zone electrophoretic separation of basic proteins, at a pH below their p*I*, can be significantly improved by adding a small amount of fluorinated cationic surfactant to the running buffer.

(2) A buffer, having a low ionic strength can be employed, while efficiency and resolution are maintained.

(3) Short and long term reproducibility is excellent.

(4) The method described is simple. Cheap, non-treated capillary tubing can be used (which can be rinsed with aggressive media if necessary). No complicated pre-treatments of the capillary tubing are necessary. Therefore, there should be a potential in clinical applications for the proposed concept.

ACKNOWLEDGEMENTS

This work was supported financially by the Swedish Natural Science Research Council and the Swedish Board for Technical Development.

REFERENCES

1 J. W. Jorgenson and K. D. Lukacs, *Science (Washington, D.C.)*, 222 (1983) 266.
2 H. H. Lauer and D. McManigill, *Anal. Chem.*, 58 (1986) 166.
3 J. S. Green and J. W. Jorgenson, *J. Chromatogr.*, 478 (1989) 63.
4 M. M. Bushey and J. W. Jorgenson, *J. Chromatogr.*, 480 (1989) 301.
5 S. Hjertén, *J. Chromatogr.*, 347 (1985) 191.
6 R. M. McCormick, *Anal. Chem.*, 60 (1988) 2322.
7 G. J. M. Bruin, R. Huisden, J. C. Kraak and H. Poppe, *J. Chromatogr.*, 480 (1989) 339.
8 S. A. Swedberg, *Anal. Biochem.*, 185 (1990) 51.
9 M. J. Gordon, K.-L. Lee, A. A. Arias and R. N. Zare, *Anal. Chem.*, 63 (1991) 69.
10 L. H. Eng and H. Y. Neujahr, *Arch. Microbiol.*, 153 (1989) 60.
11 S. E. Moring and J. A. Nolan, *Applied Biosystems Research News*, 2 (1990) 2.
12 S. Terabe, K. Otsuka, K. Ichikawa, A. Tsuchiya and T. Ando, *Anal. Chem.*, 56 (1984) 111.
13 S. Terabe, K. Otsuka and T. Ando, *Anal. Chem.*, 57 (1985) 834.
14 J. Liu, K. A. Cobb and M. Novotny, *J. Chromatogr.*, 519 (1990) 189.
15 K. Otsuka, S. Terabe and T. Ando, *J. Chromatogr.*, 332 (1985) 219.
16 J. Liu, J. F. Banks, Jr. and M. Novotny, *J. Microcolumn Sep.*, 1 (1989) 136.
17 K. D. Altria and C. F. Simpson, *Anal. Proc. (London)*, 23 (1986) 453.
18 T. Tsuda, *HRC & CC*, 10 (1987) 622.
19 J. E. Wiktorowicz and J. C. Colburn, *Electrophoresis*, 11 (1990) 769.
20 B. H. Bijsterbosch, *J. Colloid Interface Sci.*, 47 (1974) 186.
21 A. Haas, J. Köhler and H. Hemetsberger, *Chromatographia*, (1981) 341.
22 C. Blinkhorn and M. N. Jones, *Biochem. J.*, 135 (1973) 547.
23 M. N. Jones, H. A. Skinner, E. Tipping and A. Wilkinson, *Biochem. J.*, 135 (1973) 231.
24 Y. Nozaki, J. A. Reynolds and C. Tanford, *J. Biol. Chem.*, 249 (1974) 4452.
25 L. C. Clark, Jr., E. P. Wesseler, M. L. Miller and S. Kaplan, *Microvasc. Res.*, 8 (1974) 320.

Journal of Chromatography, 547 (1991) 551–553
Elsevier Science Publishers B.V., Amsterdam

CHROM. 23 358

Short Communication

Capillary electrophoretic separation in both H_2O- and ^2H_2O-based electrolytes can provide more information on tryptic digests

G. N. OKAFO and P. CAMILLERI
SmithKline Beecham, The Frythe, Welwyn, Herts. AL6 9AR (UK)
(First received January 25th, 1991; revised manuscript received April 9th, 1991)

ABSTRACT

Capillary electrophoresis of a tryptic digest of cytochrome *c* in ^2H_2O-based buffer solutions has been shown to give complementary information to that obtained in H_2O-based electrolytes of the same acidity.

We recently [1] introduced the use of ^2H_2O-based buffer solutions in capillary electrophoresis (CE). We found that a higher resolution can be obtained if H_2O is replaced by ^2H_2O in the electrolyte solutions. The increase in resolution is thought [1] to be due to a lowering of electroosmotic flow in ^2H_2O-compared to H_2O-based buffer solutions.

Electroosmotic effects mainly occur due to negative charges arising from the ionisation of the surface silanol groups on the inside wall of the capillary [2]. Control of electroosmotic flow can have a beneficial effect on both the separation efficiency and the resolution in CE.

As the magnitude of electroosmotic flow is greatly dependent on the pH of the electrolyte in CE (electroosmosis is suppressed in acidic pH values) we have analysed the tryptic fragments of cytochrome *c* at a pH close to neutral (pH 7.81) and in an acidic medium (pH 2.95), and have carried out measurements in buffer solutions of similar acidity ($p^2H = 7.83$ and 2.95), but replacing H_2O by ^2H_2O. Results (including experimental details) are summarised in Figs. 1 and 2. CE instrumentation described in ref. 1 was used to obtain these data.

The tryptic digest maps of cytochrome *c* are very different when CE is run in ^2H_2O or H_2O solution at a a^2H or pH around 7.8. In agreement with our previous observations [1,3], migration times in ^2H_2O are longer than the corresponding values in H_2O-based buffer solutions. A striking feature of the comparison shown in Fig. 1 is the considerable improvement that occurs in ^2H_2O, especially before the negative

0021-9673/91/$03.50

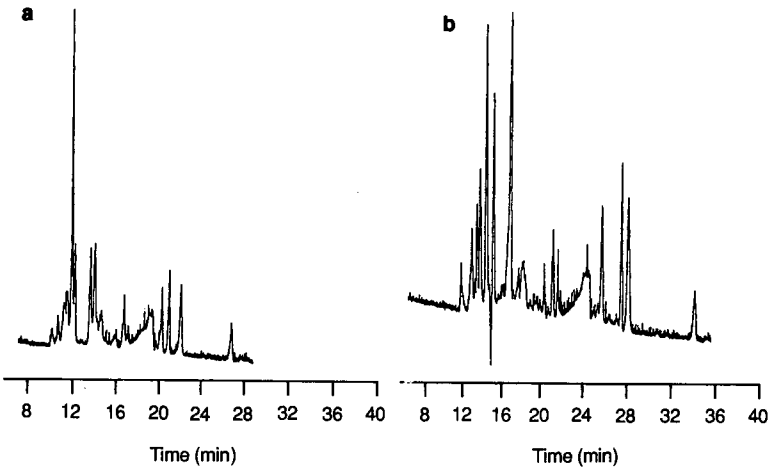

Fig. 1. CE separation of fragments from the tryptic digest of bovine cytochrome *c*. (a) pH 7.81; (b) p^2H 7.83. Buffer, 20 m*M* NaH_2PO_4/Na_2HPO_4 in H_2O (a) or ^2H_2O (b); capillary, 95 cm (effective length 70 cm) × 50 μm I.D., separation voltage, 20 kV; current, < 50 μA; injection voltage, 3 kV for 1 s; detection, UV at 200 nm; temperature, ambient.

peak. The latter signal is due to H_2O as samples were electrokinetically [4] withdrawn from H_2O-based buffer solutions in all experiments. The occurrence of this negative peak is convenient as it marks the point of migration of uncharged (or neutral) peptide fragments. Positively and negatively charged fragments are expected to migrate before and after this signal, respectively.

The tryptic digest maps in Fig. 2 show that differences between electropherograms in H_2O- and ^2H_2O-based buffer solutions at an acidic pH are not as significant as those observed at higher pH values. Although electroosmotic flow is largely suppressed in acidic pH values, migration times in ^2H_2O are still about 15% longer

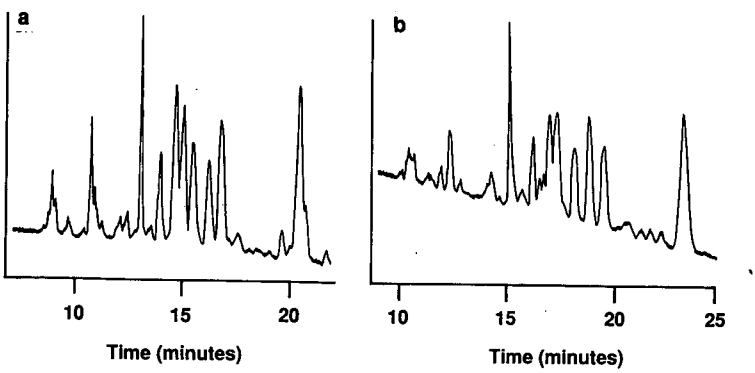

Fig. 2. CE separation of fragments from the tryptic digest of bovine cytochrome *c*. (a) pH 2.95; (b) p^2H = 2.95. Buffer, 20 m*M* NaH_2PO_4/HCl in H_2O (a) or ^2H_2O (b); capillary, 72 (effective length 50 cm) × 50 μm I.D.; separation voltage, 15 kV; injection voltage, 20 kV for 3 s; detection, UV at 200 nm; temperature, ambient.

than in H_2O-based electrolytes. The pattern of the digest maps in Fig. 2a and b are very similar. However, new peaks previously unresolved in the H_2O-based buffer are clearly visible in ^2H_2O. This may be largely due to the different pI values that can arise in H_2O and ^2H_2O solution [5].

In conclusion, we have again shown that CE separation of peptides in ^2H_2O solution can provide analytical information not provided by similar experiments carried out in H_2O-based electrolytes. We think that CE experiments carried out in both ^2H_2O and H_2O can give a more complete picture of the fragmentation pattern of a tryptic digest than in CE experiments in H_2O alone.

REFERENCES

1 P. Camilleri and G. N. Okafo, *J. Chem. Soc., Chem. Commun.*, (1991) 196.
2 E. Heftmann, *Chromatography*, Reinhold, New York, 1976, 2nd ed., Ch. 10.
3 P. Camilleri and G. N. Okafo, *J. Chromatogr.*, 541 (1991) 481.
4 X. Huang, M. J. Gordon and R. N. Zare, *Anal. Chem.*, 60 (1988) 375.
5 W. P. Jencks, *Catalysis in Chemistry and Enzymology*, McGraw-Hill, New York, 1969, Ch. 4.

Journal of Chromatography, 547 (1991) 554–559
Elsevier Science Publishers B.V., Amsterdam

CHROM. 23 243

Short Communication

Study of chelating tendency of sulphur-containing amino acids by electrophoresis

B. B. TIWARI*, R. K. P. SINGH, V. KUMAR and K. L. YADAVA
Electrochemical Laboratories, Department of Chemistry, University of Allahabad, Allahabad-211 002 (India)
(First received October 9th, 1990; revised manuscript received February 26th, 1991)

ABSTRACT

The stability constants of different complex species of some metal ions, *viz.*, Zn^{2+} and Cd^{2+} with methylcysteine, were determined electrophoretically at an ionic strength of 0.1 *M* perchloric acid and at 30°C. The stability constant of metal–nitrilotriacetate–methylcysteine complexes were found to be 3.72 and 3.54 (log *K* values) for Zn(II) and Cd(II) complexes, respectively.

INTRODUCTION

A significant development in the determination of stability constants of complexes was made by Jokl [1] in 1964. A theoretical treatment similar to that of Jokl was adopted by Biernat [2] for the study of stepwise complex formation [3]. We have previously described [4,5] a method for the study of mixed complexes. This work is an extension of that technique and reports observations on mixed systems, *viz.*, Zn^{2+}/Cd^{2+}–nitrilotriacetate–methylcysteine.

EXPERIMENTAL

Apparatus

A Systronics Model 604 electrophoresis system was been used. It has a built-in power supply (a.c.–d.c.) which is directly fed to paper electrophoretic tanks. In order to maintain the temperature constant, two hollow metallic plates coated with thin plastic paper on the outside were used for sandwiching paper strips, and thermostated water (35°C) was circulated through these plates.

pH measurements were made with an Elico Model L_{1-10} pH meter using a glass electrode.

0021-9673/91/$03.50

Chemicals

Zinc and cadmium perchlorate solutions were prepared from the nitrates (analytical-reagent grade) via the carbonates. The solutions were standardized and diluted to $5.0 \cdot 10^{-3}$ M.

Metal spots were detected with dithizone in carbon tetrachloride (for Zn^{2+}) and 1-(2-pyridylazo)-2-naphthol (PAN) (for Cd^{2+}). A saturated aqueous solution (0.9 ml) of silver nitrate was diluted with acetone to 20 ml. Glucose was detected by spraying with this solution and then with 2% ethanolic sodium hydroxide, when a black spot was formed.

Background electrolyte

The background electrolyte in the study of binary complexes was 0.1 *M* perchloric acid and $1.0 \cdot 10^{-2}$ *M* methylcysteine. For the study of the ternary system the background electrolyte was of 0.1 *M* perchloric acid, $1.0 \cdot 10^{-2}$ *M* nitrilotriacetate (NTA) and various amounts of 0.01 *M* methylcysteine. It was maintained at pH 8.5 by addition of sodium hydroxide for the study of mixed systems.

Stock solutions of 9.0 *M* perchloric acid, 2.0 *M* sodium hydroxide and 0.5 *M* methylcysteine were prepared from AnalaR chemicals (BDH, Poole, UK); 0.01 *M* nitrilotriacetic acid was prepared from the compound obtained from E. Merck (Darmstadt, Germany).

Procedure

The level of the hollow base plate in the instrument was made horizontal with a spirit level. A 150-ml volume of background electrolyte was placed in each tank of the electrophoretic apparatus. The paper strips (Whatman No. 1, 30×1 cm^2) in triplicate were then spotted with metal ions and glucose in the centre with a micropipette and were subsequently placed on the base plate and sandwiched under the upper hollow metallic plate with the ends of the strips lying in the two sides of the tank solutions. Then a 200 V potential difference was applied between the tank solutions and electrophoresis was carried out for 60 min. Subsequently the strips were removed and the spots were detected. The averages of triplicate strips were noted for calculations and movement of the glucose spot was used as a correction factor. It was found that the variation in the movement was about $\pm 5\%$. The mobilities were calculated by dividing the movement by the potential gradient and expressed in cm^{2}V^{-1}.

RESULTS AND DISCUSSION

M(II)–methylcysteine binary system

The plot of the overall mobility of a metal spot against pH gives a curve with a number of plateaus, as shown in Fig. 1. The first, at the beginning, corresponds to a region in which metal ions are uncomplexed. A second plateau in each instance with positive mobility indicates the formation of 1:1 complex of a cationic nature. A further increase of pH results in a third plateau with zero mobility, which indicates the formation of an electrically neutral metal complex. The literature also assigns prominent liganding properties to unprotonated anionic species of methylcysteine, ruling out any such property to the zwitterion [6]. In view of the above observation, the

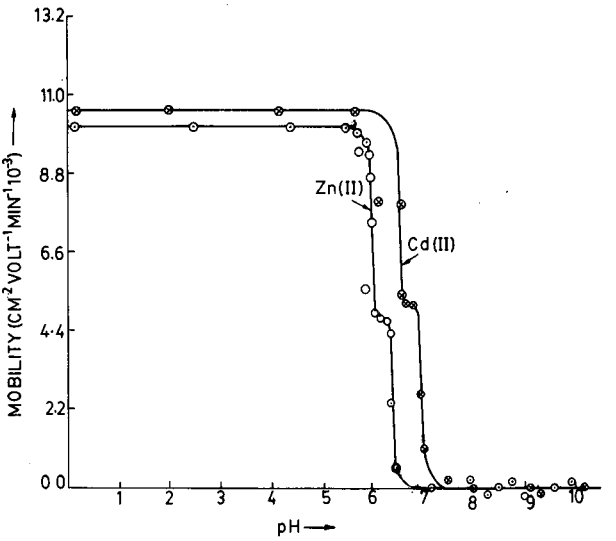

Fig. 1. Mobility curves for M–methylcysteine systems. ⊙, Zn(II)–methylcysteine; ⊗, Cd(II)–methylcysteine. Temperature, 35°C; ionic strength, 0.1.

complexation of a metal ion with the methylcysteine anion L^- may be represented by

$$M^{2+} + L^- \overset{K_1}{\rightleftharpoons} ML^+ \tag{1}$$

$$ML^+ + L^- \overset{K_2}{\rightleftharpoons} ML_2 \tag{2}$$

where M represents Zn or Cd and ML^+ and ML_2 are their complexes with methylcysteine.

The metal spot on the paper is thus a conglomeration of uncomplexed metal ions and 1:1 and 1:2 complexes. The overall mobility, U, is given by

$$U = \frac{u_0 + u_1K_1[L^-] + u_2K_1K_2[L^-]^2}{1 + K_1\,[L^-] + K_1K_2[L^-]^2} \tag{3}$$

where u_0, u_1 and u_2 are the mobilities of the uncomplexed metal ion, 1:1 complex and 1:2 complex, respectively.

For calculating the first stability constant, K_1, the region between the first and second plateaux is pertinent. The overall mobility U will be equal to the arithmetic mean of the mobility of the uncomplexed metal ion, u_0, and that of the first complex, u_1, at a pH where $K_1 = 1/[L^-]$ with the help of dissociation constants of methylcysteine ($k_1 = 10^{2.55}$, $k_2 = 10^{8.55}$) [7,8].

The concentration of liganding methylcysteine, L^-, is calculated with the equation

$$[L^-] = \frac{[L_T]}{1 + \frac{[H]}{k_2} + \frac{[H]^2}{k_1 k_2}} \tag{4}$$

where $[L_T]$ = total concentration.

The stability constant K_2 of the second complex can be calculated by taking into consideration the region between the second and third plateaus of the mobility curve. These calculated values are given in Table I.

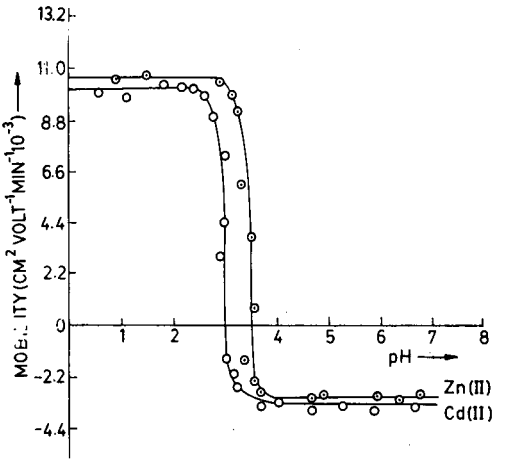

Fig. 2. Mobility curves for M–NTA systems. ○, Zn(II)–NTA; ⊙, Cd(II)–NTA. Temperature, 35°C; ionic strength, 0.1.

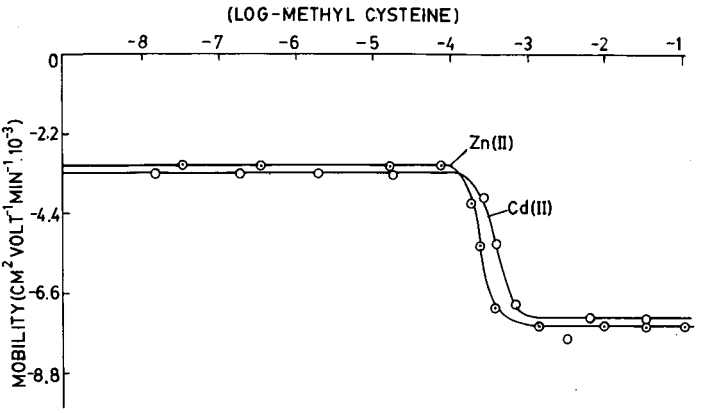

Fig. 3. Mobility curves for M–NTA–methylcysteine. ⊙, Zn(II)–NTA–methylcysteine; ○, Cd(II)–NTA–methylcysteine. Temperature, 35°C; ionic strength, 0.1.

TABLE I

STABILITY CONSTANTS OF BINARY AND TERNARY COMPLEXES OF Zn(II) AND Cd(II)

Ionic strength = 0.1; temperature = 35°C; NTA anion = $N(CH_2COO)_3^{3-}$; methylcysteine anion = $CH_3SCH_2CH(NH_2)COO^-$.

Metal ion	Calculated values of stability constants[a]				Literature values of stability constants[a]			
	$Log K^M_{1_{ML}}$	$Log K^M_{2_{ML_2}}$	$Log K^M_{M-NTA}$	$Log K^{M-NTA}_{M-NTA-L}$	$Log K^M_{1_{ML}}$	$Log K^M_{2_{ML_2}}$	$Log K^M_{M-NTA}$	$Log K^{M-NTA}_{M-NTA-L}$
Zn(II)	4.55	4.15	10.66	3.72	4.46 [7] 4.46 [9]	4.06 [7] 4.06 [9]	10.66 [7] 10.00 [8]	–
Cd(II)	3.95	3.55	9.78	3.54	3.77 [7] 3.77 [9]	3.32 [7] 3.32 [9]	9.78 [7] 9.40 [8]	–

[a] $K^M_{1_{ML}} = \frac{[ML]}{[M][L]}$; $Log K^M_{2_{ML_2}} = \frac{[ML_2]}{[ML][L]}$; $K^M_{M-NTA} = \frac{[M-NTA]}{[M][NTA]}$; $K^{M-NTA}_{M-NTA-L} = \frac{[M-NTA-L]}{[M-NTA][L]}$.

Metal(II)–NTA binary system

The overall mobilities of the metal ion spots were plotted against the pH of the background electrolyte containing NTA (Fig. 2). As the mobility of the second plateau is in the negative range, the complex formed with a bivalent metal ion should have a 1:1 composition with a net negative charge. The stability constants of these complexes were calculated in the same manner as for complexes with other amino acids. These values are recorded in Table I.

Metal–NTA–methylcysteine system

The study of this system was done at pH 8.5 for a purpose. It is observed from the mobility curves for M–methylcysteine and M–NTA binary systems that binary complexes are formed at pH <8.5. Therefore, it would be preferable to study the transformation of the M–NTA complex into the M–NTA–methylcysteine complex at pH 8.5 in order to avoid any side interactions.

On the plot of mobility *versus* log (concentration of added amino acid) a curve is obtained, as shown in Fig. 3. The first constant value of the mobility obviously corresponds to the mobility of the M–NTA complex, whereas the second constant mobility corresponds to the mobility of a second complex. This new complex cannot be a 1:1 or 1:2 metal–amino acid complex as the mobilities of such complex species are different from that of the new complex. The interaction may be represented by

$$ML' + L \overset{K'}{\rightleftharpoons} ML'L \tag{5}$$

Under these conditions, the overall mobility can be given by the expression

$$U = \frac{u_0 + u_1 K'[L]}{1 + K'[L]} \tag{6}$$

where u_0 and u_1 are the mobilities of M–NTA and mixed ML'L complexes, respectively. These mobilities pertain to the two-plateau region of the curve; using again the principle of average mobility, K' can be determined to be equal to $1/[L^-]$. All these values of K' are given in Table I.

REFERENCES

1 V. Jokl, *J. Chromatogr.*, 14 (1964) 71.
2 J. Biernat, *Rocz. Chem.*, 38 (1964) 343.
3 R. K. P. Singh, J. K. Sirkar, J. R. Yadava, P. C. Yadava and K. L. Yadava, *Electrochim. Acta*, 26 (1981) 395.
4 P. C. Yadava, A. K. Ghose, K. L. Yadava and A. K. Dey, *J. Chromatogr.*, 119 (1976) 563.
5 J. R. Yadava, J. K. Sirkar and K. L. Yadava, *Electrochim. Acta*, 26 (1982) 391.
6 J. R. Blackburn and M. M. Jones, *J. Inorg. Nucl. Chem.*, 35 (1973) 1605.
7 A. E. Martell and R. M. Smith, *Critical Stability Constants, Vol. 1, Amino Acids*, Plenum Press, New York, London, 1977, p. 49.
8 D. D. Perrin, *Stability Constants of Metal Ion Complexes, Part B, Organic Ligands (IUPAC Chemical Series*, No. 22), Pergamon Press, Oxford, 1979.
9 L. G. Sillen and A. E. Martell, *Stability Constants of Metal Ion Complexes (Special Publication*, No. 17), Chemical Society London, 1964.

Journal of Chromatography, 547 (1991) 560
Elsevier Science Publishers B.V., Amsterdam

CHROM. 23 291

Book Review

Countercurrent chromatography: apparatus, theory and applications, by W. D. Conway, VCH, Weinheim, 1990, XIV + 475 pp., price DM 138.00, £ 51.00, ISBN 0-89573-331-5.

Pure liquid–liquid partition chromatography (absence of a solid support) has attracted increasing interest over the last 20 years. Numerous new instruments have been developed and applied to the preparative separation of a large variety of compounds, mainly in the field of natural products. They all derive from the Craig counter-current distribution apparatus. The term "counter-current" used in the modern versions of instrumentation using centrifugal force is misleading. In fact, one liquid phase is stationary and the other is the mobile phase. Most developments of efficient instruments for fast separations have been made by Dr. Yoichiro Ito of the National Institute of Health, Bethesda, MD, USA.

The present book has arrived at a timely moment and complements the volume "Countercurrent chromatography: Theory and practice" by N. B. Mandava and Y. Ito (Marcel Dekker, New York, 1988), although there are some unavoidable overlaps. The first part of the volume is devoted to a description of the different types of instruments available and to basic theoretical aspects. Chapter 7 is of particular interest as it deals with the problem facing each counter-current chromatography (CCC) practitioner, namely to find a solvent system providing partition coefficients in an optimum range. For the commonly employed chloroform–methanol–water mixtures, ternary phase diagrams are given. The last part of the book describes various applications of the different CCC techniques, including rotation locular CCC and centrifugal CCC. Curiously, there is almost no mention of applications of droplet CCC, which is certainly the most widely used technique. Examples of separations of various natural products of plant origin, peptides and antibiotics and of resolutions of enantiomeric mixtures by centrifugal CCC are presented and explained. The application of centrifugal CCC to the determination of partition coefficients is also described.

The volume ends with a very useful bibliographic outline with 422 references. Unfortunately, some significant recent applications of centrifugal CCC are missing. Despite this, the book should find a place in any laboratory involved in separation science. It will be especially useful to all researchers who are considering entering the highly promising field of centrifugal partition chromatography.

Lausanne (Switzerland) K. HOSTETTMANN

Author Index

Errata

J. Chromatogr., 521 (1990) 71–87 corrected 26 nov 34

Page 83, first line below eqn. 81, "... and hence $d\sigma^2$ = ..." should read "... and hence $d\sigma^2/dz$ = ...".

Page 85, eqn. 93, "R^2v^{72}" should read "$R^2\bar{v}^2$".

J. Chromatogr., 539 (1991) 83–90 corrected 26 nov 34

Page 86, Table I, the last two lines at compound 7:

R	20:80	7.1	8.9	1.10
S	20:80	7.1	5.4	1.09

These values belong to compound 8.

J. Chromatogr., 540 (1991) 293–310 corrected 26 nov 34

Page 296, top right, "2910 − 1174 + 31 = 1705" should read "2848 − 1174 + 31 = 1705".

Page 297, line 14, "(see Table III)" should read "(see Table II)".

Page 297, line 38, "octabromodibenzo-*p*-dioxane" should read "octabromodibenzo-*p*-dioxin".

Page 300, Table I, 4th column , 2nd line, "2,3-Br_3" should read "2,3-Br_2".

Page 300, Table I, 2nd column, 12th line, "2133–2070" should read "2123–2070".

Page 301, line 22, "one single brominated" should read "one single ring brominated".

Page 302, Table III, 3rd column, line 28, "2686" should read "2586".

J. Chromatogr., 543 (1991) 17–38 corrected 26 nov 34

Page 23, 2nd line from the bottom, "[43]" should read "[42]".

Page 24, 15th line from the bottom, "[50,51]" should read "[51,52]".

Page 38, reference 42 should read "D. J. Winzo, in C. R. Lowe and D. G. Dean (Editors), *Affinity Chromatography*, Wiley, London, 1985, p. 149."

Page 38, reference 53 should read "R. P. Singhal and S. S. M. DeSilva, *Adv. Chromatogr. (N.Y.)*, 31 (1991) 293."

Page 38, reference 58 should read "N. Heinrich and B. Wrackmeyer, in P. Diehl, E. Fluck and R. Kosfeld (Editors), *NMR:Basic Principles and Progress*, Vol. 14, Springer, New York, 1978, pp. 16 and 74."

Page 38, reference 66 should read "D. W. Newton and R. B. Kluza, in W. O. Foye (Editor), *Principles of Medicinal Chemistry*, Lea and Febiger, Philadelphia, 3rd ed., 1989, p. 861."

J. Chromatogr., 543 (1991) 327–343 corrected 26 nov 34

Page 327, Introduction, 5th line, "[5,6]" should read "[4–6]".

Page 329, 1st paragraph, 13th line and thereafter, wherever CH_3CN appears as a constituent in complex aqueous media designations, it should be enclosed in parentheses, i.e. "CH_3CN" should read "(CH_3CN)".

Page 329, 2nd paragraph, 5th line, "[3]" should read "[2]".

Page 332, Figure 1 legend, 2nd line, lane 4 designations should read "'B-B'".

Page 335, 2nd paragraph, 10th line "$SDS_{0.07}$" should read "SDS_{70}".
Page 339, 2nd paragraph, 3rd and 4th lines, "except that elution times for corresponding peaks are shorter." should be deleted.

J. Chromatogr., 545 (1991) 196–200 corrected 26 nov 34
Page 197, section Experimental, 5th line, "melanocyte-stimulating hormone" should read "mercaptoethanol".

PUBLICATION SCHEDULE FOR 1991

Journal of Chromatography and Journal of Chromatography, Biomedical Applications

MONTH	D 1990–F 1991	M	A	M	J	J	A	S
Journal of Chromatography	Vols. 535–539	540/1 + 2 541/1 + 2 542/1	542/2 543/1	543/2 544/1 + 2 545/1	545/2 546/1 + 2 547/1 + 2	548/1 + 2 549/1 + 2 550/1 + 2	552/1 + 2 553/1 + 2 554/1 + 2 555/1 + 2	556/1 + 2
Cumulative Indexes, Vols. 501–550							551/1 + 2	
Bibliography Section		560/1			560/2			561/1
Biomedical Applications	Vols. 562, 563	564/1	564/2 565/1 + 2	566/1 566/2	567/1	567/2 568/1	568/2	569/1 + 2

The publication schedule for further issues will be published later

INFORMATION FOR AUTHORS

(Detailed *Instructions to Authors* were published in Vol. 522, pp. 351–354. A free reprint can be obtained by application to the publisher, Elsevier Science Publishers B.V., P.O. Box 330, 1000 AH Amsterdam, The Netherlands.)

Types of Contributions. The following types of papers are published in the *Journal of Chromatography* and the section on *Biomedical Applications:* Regular research papers (Full-length papers), Review articles and Short Communications. Short Communmications are usually descriptions of short investigations, or they can report minor technical improvements of previously published procedures; they reflect the same quality of research as Full-length papers, but should preferably not exceed six printed pages. For Review articles, see inside front cover under Submission of Papers.

Submission. Every paper must be accompanied by a letter from the senior author, stating that he/she is submitting the paper for publication in the *Journal of Chromatography*.

Manuscripts. Manuscripts should be typed in double spacing on consecutively numbered pages of uniform size. The manuscript should be preceded by a sheet of manuscript paper carrying the title of the paper and the name and full postal address of the person to whom the proofs are to be sent. As a rule, papers should be divided into sections, headed by a caption (*e.g.*, Abstract, Introduction, Experimental, Results, Discussion, etc.). All illustrations, photographs, tables, etc., should be on separate sheets.

Introduction. Every paper must have a concise introduction mentioning what has been done before on the topic described, and stating clearly what is new in the paper now submitted.

Abstract. All articles should have an abstract of 50–100 words which clearly and briefly indicates what is new, different and significant.

Illustrations. The figures should be submitted in a form suitable for reproduction, drawn in Indian ink on drawing or tracing paper. Each illustration should have a legend, all the *legends* being typed (with double spacing) together on a *separate sheet*. If structures are given in the text, the original drawings should be supplied. Coloured illustrations are reproduced at the author's expense, the cost being determined by the number of pages and by the number of colours needed. The written permission of the author and publisher must be obtained for the use of any figure already published. Its source must be indicated in the legend.

References. References should be numbered in the order in which they are cited in the text, and listed in numerical sequence on a separate sheet at the end of the article. Please check a recent issue for the layout of the reference list. Abbreviations for the titles of journals should follow the system used by *Chemical Abstracts*. Articles not yet published should be given as "in press" (journal should be specified), "submitted for publication" (journal should be specified), "in preparation" or "personal communication".

Dispatch. Before sending the manuscript to the Editor please check that the envelope contains four copies of the paper complete with references, legends and figures. One of the sets of figures must be the originals suitable for direct reproduction. Please also ensure that permission to publish has been obtained from your institute.

Proofs. One set of proofs will be sent to the author to be carefully checked for printer's errors. Corrections must be restricted to instances in which the proof is at variance with the manuscript. "Extra corrections" will be inserted at the author's expense.

Reprints. Fifty reprints of Full-length papers and Short Communications will be supplied free of charge. Additional reprints can be ordered by the authors. An order form containing price quotations will be sent to the authors together with the proofs of their article.

Advertisements. Advertisement rates are available from the publisher on request. The Editors of the journal accept no responsibility for the contents of the advertisements.

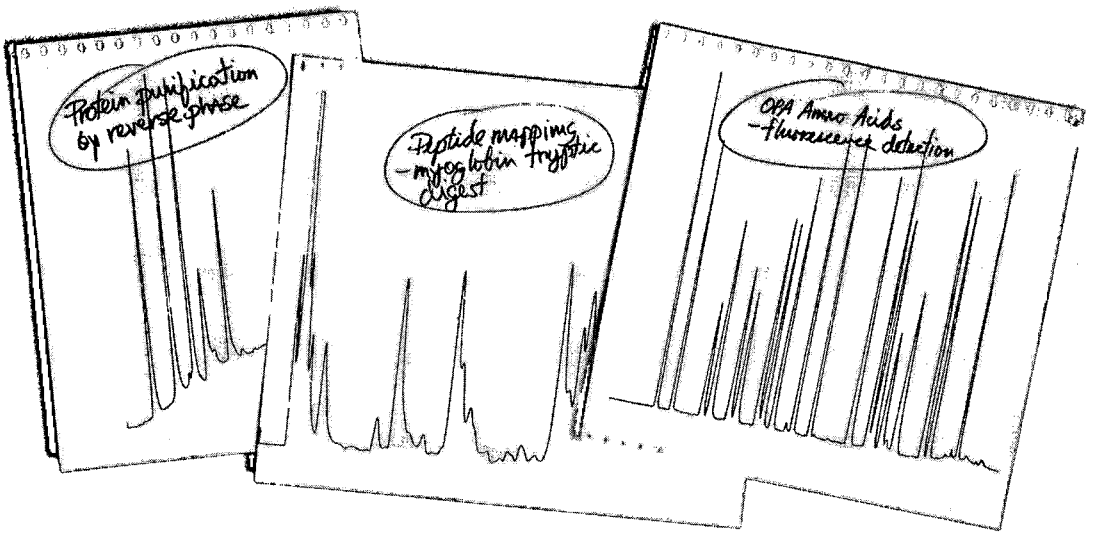

Here are three ways to record success in your biochromatography

Proteins

Isco ProTeam™ LC with proven high-performance macroporous columns offers outstanding speed and flexibility for your protein separations. Choose from a comprehensive selection of columns for SEC, ion exchange, reverse phase, and hydrophobic interaction modes. ProTeam SynChropak columns are available for any separation scale and any molecular size, with a broad range of phases for optimum selectivity. And for added assurance of active protein recovery, Isco ProTeam LC systems are available with fully biocompatible inert construction.

Peptides

For high-resolution peptide mapping by reverse-phase LC, you need precise gradient elution and the right bonded phase for optimum selectivity. ProTeam LC gives you both, with a choice of binary and ternary solvent delivery and packings from C1 to C18. And for sample-limited analyses such as synthetic peptides, you can get the same packings in Isco 2 mm and 1 mm columns.

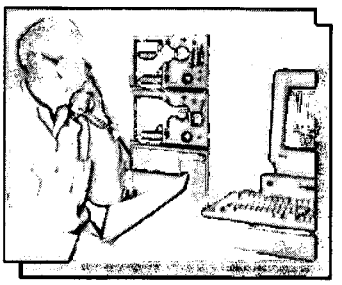

Amino acids

The same ProTeam LC system can also handle your amino acid analyses—in hydrolysates, physiological fluids, media, or for sequencing. Modular system design makes it easy to incorporate automated pre-column derivatization. Choose absorbance detection for picomole sensitivity with PITC, dabsyl, or OPA derivatives; or fluorescence for trace analysis with OPA and dansyl derivatives.

Ask today for details.

Isco, Inc., P.O. Box 5347,
Lincoln NE 68505, U.S.A.
Tel: **(800)228-4250**
Isco Europe AG, Brüschstr. 17
CH8708 Männedorf, Switzerland
Fax **(41-1)920 62 08**

ISCO

Distributors • **Australia:** Australian Chromatography Co. • **Austria:** INULA • **Belgium:** N.V. Mettler-Toledo S.A. • **Canada:** Canberra Packard Canada, Ltd.• **Denmark:** Mikrolab Aarhus • **Finland:** ETEK OY • **France:** Bts. Roucaire, S.A. • **Germany:** Colora Messtechnik GmbH • **Italy:** Analytical Control Italia S.p.A. • **Japan:** JSI Co. Ltd. • **Korea:** Sang Chung, Ltd. • **The Netherlands:** Beun-de Ronde B.V. • **Norway:** Dipl. Ing. Houm A.S. • **Spain:** CHEMICONTROL, S.L. • **Sweden:** Spectrochrom AB • **Switzerland:** IG Instrumenten-Gesellschaft AG • **U.K.:** Jones Chromatography Ltd. •